ZooKeys 1209: 1–17 (2024)
DOI: 10.3897/zookeys.1209.128944

Research Article

First report of albinism for *Achalinus sheni* (Serpentes, Xenodermidae), with extended diagnosis of the species

Yu-Hao Xu[1], Shuai Wang[1], Shun Ma[2,3], Frank T. Burbrink[4], Li-Fang Peng[1], Song Huang[5]

1 *State Key Laboratory of Plateau Ecology and Agriculture, Qinghai University, Xining 810016, China*
2 *Chengdu Institute of Biology, Chinese Academy of Sciences, Chengdu 610041, China*
3 *University of Chinese Academy of Science, Beijing 100049, China*
4 *Department of Herpetology, The American Museum of Natural History, New York NY 10024, USA*
5 *Anhui Province Key Laboratory of the Conservation and Exploitation of Biological Resource, College of Life Sciences, Anhui Normal University, Wuhu 241000, China*
Corresponding author: Li-Fang Peng (lifang@qhu.edu.cn)

Abstract

Albinism is an uncommon phenomenon and inherited condition in animals characterized by a partial or complete lack of melanin. The family Xenodermidae Gray, 1849, is a group of caenophidian snakes widely distributed in South, East, and Southeast Asia, including five recognized genera and 36 species. However, there are currently no reports of albinism in any species in Xenodermidae. *Achalinus sheni* Ma, Xu, Qi, Wang, Tang, Huang & Jiang, 2023 was first described based on five male specimens from Loudi City and Nanyue District, Hunan Province, China. At the time, there were no descriptions on female individuals. In this study, we report in detail a collected albinistic specimen of *A. sheni*, which is the first discovery of wild albinism in the family Xenodermidae. We also provide photographs and descriptions of the first three female specimens of *A. sheni* and extend the diagnosis of this species.

Key words: Hunan Province, morphological characters, phylogeny, Shen's Odd-scale Snake, Xenodermidae

OPEN ACCESS

Academic editor: Robert Jadin
Received: 4 June 2024
Accepted: 5 July 2024
Published: 6 August 2024

ZooBank: https://zoobank.org/923C8E76-D352-42AC-A752-1257B7A562D1

Citation: Xu Y-H, Wang S, Ma S, Burbrink FT, Peng L-F, Huang S (2024) First report of albinism for *Achalinus sheni* (Serpentes, Xenodermidae), with extended diagnosis of the species. ZooKeys 1209: 1–17. https://doi.org/10.3897/zookeys.1209.128944

Introduction

Coloration in most organisms evolved to respond to the background environment (Bechtel 1978; Krecsák 2008; Bruni 2017; Lu et al. 2024; Sun et al. 2024), and melanocytes that function to produce and store melanin play a crucial role in physiological color adaptations. However, the variation of melanocytes can also lead to corresponding chromatic anomalies, like the occurrence of albinism, which is usually characterized by a partial or complete lack of melanin. This condition is usually has been the result of tyrosinase inactivation caused by autosomal recessive mutations (Griffiths et al. 1998; Alberts et al. 2004; Krecsák 2008; Abegg et al. 2015).

In squamate reptiles, albinism is one of the most striking aberrations of body color pattern, which is usually divided into two types: 1) complete albinism showing the complete absence of melanin in the entire body with the red eyes and a pastel yellow, yellow, or white body coloration; and 2) partial albinism manifested as reduction in melanism across the whole body, rather than complete disappearance, resulting in a lighter body coloration (Sazima and Pombal 1986; Sazima and Di-Bernardo 1991; Hoshing and Mahabal 2013; Abegg et al. 2015). Often under artificial conditions, albino reptiles have been well documented, and many species with albino variants have been bred in large numbers for the pet market (Bechtel 1991; Bechtel 1995; Broghammer 2000). However, the wild albino phenomenon is usually extremely rare, due to the high probability of stillborns or malformations, such as linked anatomical abnormalities affecting eyesight, communications, and sexual selection, difficulty thermoregulating, and easy detection by prey and predators (Roulin and Bize 2007; Dutta et al. 2022).

The family Xenodermidae Gray, 1849 is a group of caenophidian snakes widely distributed in South, East, and Southeast Asia and including five recognized genera and 36 species (Deepak et al. 2021). Among them, *Achalinus* Peters, 1869 has the most species in this family, with 28 recognized species. Due to their cryptic lifestyle, small body size, and inconspicuous body color, they are hard to detect in the wild (Zhao et al. 1998; Zhao 2006; Ziegler et al. 2019). At present, there have been no cases of albinism in any species of Xenodermidae. *Achalinu sheni* was first described from Loudi City and Nanyue District, Hunan Province, China in 2023 based on five male specimens (Ma et al. 2023a). During a recent herpetological survey in Yangshi Town, Hunan Province, China in July 2023, we collected one male and three female specimens of *A. sheni*. However, one of the adult females displayed a distinct pastel-yellow body coloration and red eyes, which is considered to be a completely albino individual. In addition, the newly collected female specimens also showed certain sex differences in morphology. Herein, we first report details of the specimen displaying albinism, provide photographs of the first female specimens of *A. sheni*, and present an extended diagnosis of this species.

Materials and methods

Morphometrics

Four snake specimens were collected from Yangshi Town, Lianyuan City, Hunan Province, China (specimen vouchers LFR2023008–LFR2023010 and LFR2024015). Specimens were humanely euthanized using lethal injection with 0.7% tricaine methanesulfonate (MS222) solution, and liver tissues were taken and preserved in 95% alcohol. Then the specimens were directly preserved in 75% ethanol and deposited in Qinghai University Museum. Sampling procedures involving live snakes were in accordance with the Wild Animals Protection Law of China and approved by the Institutional Ethics Committee of Qinghai University (protocol code SL-2023028). The sex of all specimens was determined by tail dissection.

Measurements and scale counts followed Zhao (2006) and Ma et al. (2023a). Three measurement characters were measured with Deli Stainless Ruler (No. 8462) to the nearest 1 mm: snout–vent length (**SVL**), tail length (**TAL**) and total length (**TL**). All other measurements were performed using Deli digital calipers (DL312200) to the nearest 0.1 mm: loreal height (**LorH**): measured from the highest part to the lowest part of the loreal in lateral view; loreal length (**LorL**):

measured from the most anterior loreal to the most posterior loreal in lateral view; length of the suture between internasals (**LSBI**); length of the suture between prefrontals (**LSBP**); head length (**HL**): taken from the tip of snout to the posterior margin of mandible; head width (**HW**): measured around the widest part of the head in dorsal view; eye diameter (**ED**): taken from the most anterior corner of the eye to the most posterior corner, length of supraocular (**SPOL**): horizontal distance between anterior and posterior tip of supraocular, and length of upper anterior temporal (**ATUL**): horizontal distance between anterior and posterior tip of upper anterior temporal. The scale characters and their abbreviations are as follows: supralabials (**SL**); infralabials (**IL**); infralabials touching the first pair of chin shields (**IL-1st Chin**); loreals (**Lor**); preoculars (**PRO**); postoculars (**PO**); temporals (**TEMP**); supraoculars (**SPO**); dorsal scale rows (**DSR**) (counted at one-head-length behind the head, at midbody, at one-head-length before the cloacal plate); ventral scales (**VS**), cloacal plate (**CP**), and subcaudals (**SC**).

Molecular phylogenetic analyses

Genomic DNA was extracted from liver tissue using a Qiagin DNEasy Blood and Tissue Extraction Kit (Qiagen Inc., Valencia, CA). The partial mitochondrial DNA gene encoding cytochrome c oxidase subunit 1 (*CO1*) was obtained by polymerase chain reaction (PCR) using primer Chmf4 (5'-TYT CWA CWA AYC AYA AAG AYA TCG G-3') and Chmr4 (5'-ACY TCR GGR TGR CCR AAR AAT CA-3') (Che et al. 2012). PCR products were sequenced by Shanghai Map Biotech Co., Ltd. The raw sequences were stitched using SeqMan in the DNASTAR software package (Burland 2000) and the newly generated sequences were submitted to GenBank (Table 1).

Except for the newly generated sequence, 32 sequences of 25 recognized species and one unnamed of genus *Achalinus*, and three outgroups (selected as Ma et al. 2023a): *Fimbrios klossi* Smith, 1921, *Parafimbrios lao* Teynié, David, Lottier, Le, Vidal & Nguyen, 2015, and *Stoliczkia vanhnuailianai* Lalronunga, Lalhmangaiha, Zosangliana, Lalhmingliani, Gower, Das & Deepak, 2021 were downloaded from the National Center for Biotechnology Information (NCBI) (Accession numbers listed in Table 1). The *CO1* sequences (624 bp) were input in MEGA X software (Kumar et al. 2018) and aligned by MUSCLE (Edgar 2004). Maximum likelihood (ML) was used to infer tree structure with IQ-TREE v. 1.6.12 (Nguyen et al. 2015). The best-fit model, TN+F+I+G4, was inferred using a Bayesian Information Criterion (BIC) with the program ModelFinder (Kalyaanamoorthy et al. 2017). Ultrafast Bootstrap Approximation (UFB) node support was assessed by using 5000 ultrafast bootstrap replicates, and SH-like approximate likelihood ratio test (SH-aLRT) was conducted to the single branch tests by 1000 replicates. In addition, we calculated the uncorrected pairwise distances (*p*-distances) using the MEGA X software (Kumar et al. 2018).

Results

The phylogeny inferred using the mitochondrial fragment *CO1* (624 bp) demonstrated that the newly collected specimens from Yangshi Town, Hunan Province, China were clustered together with selected *A. sheni* type series (SH 100

Table 1. Localities, voucher information, GenBank numbers and references for all samples used in this study.

NO.	Species name	Locality	Voucher NO.	Genbank No.	References
1	*Achalinus sheni*	Lianyuan, Hunan, China	LFR2023008	PP725554	This study
2	*A. sheni*	Lianyuan, Hunan, China	LFR2023009	PP725555	This study
3	*A. sheni*	Lianyuan, Hunan, China	LFR2023010	PP725556	This study
4	*A. sheni*	Lianyuan, Hunan, China	LFR2024015	PP725559	This study
5	*A. sheni*	Lianyuan, Hunan, China	ANU20230012	OR178145	Ma et al. 2023a
6	*A. sheni*	Lianyuan, Hunan, China	ANU20230013	OR178146	Ma et al. 2023a
7	*A. yunkaiensis*	Dawuling Forestry Station, Guangdong, China	SYS r001443	MN380329	Wang et al. 2019
8	*A. yunkaiensis*	Dawuling Forestry Station, Guangdong, China	SYS r001502	MN380330	Wang et al. 2019
9	*A. yunkaiensis*	Maoershan Nature Reserve, Guangxi, China	YBU 14612	MT365525	Yu et al. 2020
10	*A. yunkaiensis*	Xinning, Hunan, China	CIB 119041	OQ978852	Ma et al. 2023b
11	*A. ater*	Huaping Nature Reserve, Guangxi, China	SYS r00852	MN380334	Wang et al. 2019
12	*A. dabieshanensis*	Yaoluoping Nature Reserve, Anhui, China	AHU2018EE0710	MW316598	Zhang et al. 2023
13	*A. damingensis*	Nanning, Guangxi, China	ANU20220009	OP644487	Yang et al. 2023
14	*A. dehuaensis*	Dehua, Fujian, China	YBU 13013	MZ442662	Li et al. 2021
15	*A. emilyae*	Hoanh Bo, Vietnam	IEBR 4465	MK330857	Ziegler et al. 2019
16	*A. formosanus*	Taiwan, China	RN2002	KU529452	Unpublished
17	*A. hunanensis*	Huaihua, Hunan, China	CIB 119039	OQ848425	Ma et al. 2023c
18	*A. huangjietangi*	Huangshan, Anhui, China	HSR18030	MT380191	Huang et al. 2020
19	*A. juliani*	Ha Lang, Cao Bang, Vietnam	IEBR A.2018.8	MK330854	Ziegler et al. 2019
20	*A. meiguensis*	Mianyang, Sichuan, China	GP835	MZ442641	Li et al, 2021
21	*A. nanshanensis*	Huaihua, Hunan Province, China	HNNU230901	OR523368	Li et al. 2024
22	*A. niger*	Taiwan, China	RN0667	KU529433	Unpublished
23	*A. ningshanensis*	Ningshan, Shaanxi, China	ANU 20220006	ON548422	Yang et al. 2022
24	*A. panzhihuaensis*	Yanbian, Sichuan, China	KIZ 040189	MW664862	Hou et al. 2021
25	*A. pingbianensis*	Honghe, Yunnan, China	YBU 18273	MT365521	Li et al. 2020b
26	*A. quangi*	Phu Yen, Son La, Vietnam	ZVNU.2022.08	OQ197471	Pham et al. 2023
27	*A. rufescens*	Hongkong, China	SYS r001866	MN380339	Wang et al. 2019
28	*A.* sp1	Ningshan, Shaanxi, China	LFR2023038	PP725557	This study
29	*A.* sp1	Ningshan, Shaanxi, China	LFR2023039	PP725558	This study
30	*A.* sp2	Taibai, Shaanxi, China	CHS007	MK064591	Li et al. 2020a
31	*A. spinalis*	Badagong Mountains, Hunan, China	SYS r001327	MN380340	Wang et al. 2019
32	*A. timi*	Thuan Chau, Son La, Vietnam	IEBR A.2018.10	MK330856	Ziegler et al. 2019
33	*A. tranganensis*	Ninh Binh, Vietnam	VNUF R.2018.21	MW023086	Luu et al. 2020
34	*A. vanhoensis*	Van Ho, Son La, Vietnam	VNUF R.2019.13	ON677935	Ha et al. 2022
35	*A. yangdatongi*	Wenshan Nature Reserve, Yunnan, China	KIZ 034327	MW664865	Hou et al. 2021
36	*A. zugorum*	Bac Me, Ha Giang, Vietnam	IEBR 4698	MT502775	Miller et al. 2020
	Out group				
37	*Fimbrios klossi*	Quang Ngai, Vietnam	IEBR 3275	KP410744	Teynié et al. 2015
38	*Parafimbrios lao*	Louangphabang, Laos	MNHN 2013.1002	KP410746	Teynié et al. 2015
39	*Stoliczkia vanhnuailianai*	Mizoram, India	BNHS 3656	OL422476	Deepak et al. 2021

/ UFB 100) (Fig. 1). We also show that intraspecific generic divergence ranged from 0.0%–0.8% was detected (Table 2), which is less than the minimum interspecific uncorrected *p*-distance among other recognized species of *Achalinus*, indicating that the newly collected *Achalinus* specimens should be identified as *A. sheni*.

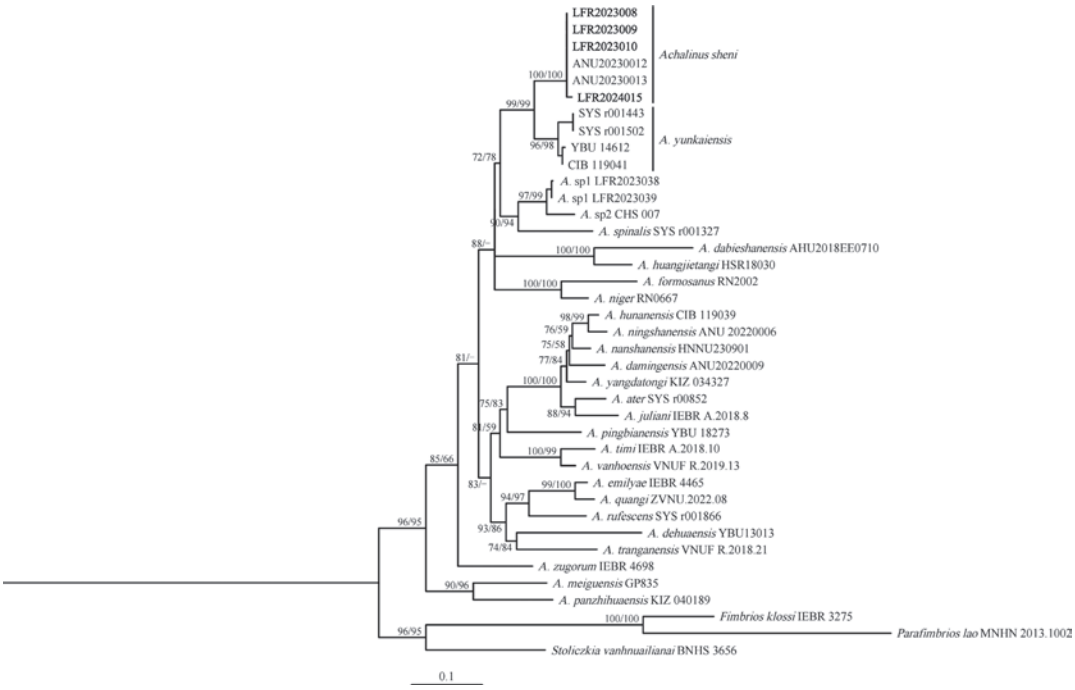

Figure 1. Maximum-likelihood tree of the genus *Achalinus* inferred from the *CO1* gene fragment. The nodes supporting values on branches are presented as SH-like approximate likelihood ratio test (SH) / Ultrafast Bootstrap Approximation (UFB), the ones lower than 50 are displayed as "–".

Table 2. Uncorrected *p*-distances (%) among the *Achalinus* species based on partial mitochondrial *CO1* gene for species compared in this study.

ID	Species	1–6	7	8	9	10	11	12	13	14
1–6	*A. sheni*	0–0.8								
7	*A. ater*	13.1–13.4	–							
8	*A. dabieshanensis*	15.3–15.9	14.8	–						
9	*A. damingensis*	13.3–13.6	7.4	15.9	–					
10	*A. dehuaensis*	13.8	16.1	18.6	15.2	–				
11	*A. emilyae*	13.6–14.2	11.2	18.0	12.9	15.3	–			
12	*A. formosanus*	12.7–12.9	13.3	18.8	14.2	15.7	13.6	–		
13	*A. huangjietangi*	12.9	13.1	11.0	15.2	15.3	15.5	16.1	–	
14	*A. hunanensis*	12.7–13.1	7.6	17.0	5.7	15.3	13.8	13.6	15.0	–
15	*A. juliani*	13.6–14.0	6.6	15.9	8.3	14.8	12.9	11.4	14.4	9.1
16	*A. meiguensis*	14.2–14.8	15.3	18.0	16.5	18.4	15.3	15.5	16.9	16.3
17	*A. niger*	12.9–13.1	12.9	16.1	13.3	16.3	12.7	8.5	15.7	13.3
18	*A. ningshanensis*	13.6–14.0	7.4	17.2	7.4	15.5	13.8	14.2	15.5	3.4
19–20	*A.* sp1	9.8–10.4	12.7–12.9	14.4–14.6	11.9–12.1	13.8–14.0	12.9–13.1	12.7–12.9	13.6–13.8	13.1–13.3
21	*A. nanshanensis*	13.6–14.0	6.8	16.1	5.1	13.4	13.3	13.6	14.6	4.9
22	*A. panzhihuaensis*	14.8	16.5	16.5	15.5	15.5	16.5	16.1	15.7	16.5
23	*A. pingbianensis*	11.2	11.0	15.3	10.2	14.6	13.1	14.2	14.0	11.0
24	*A. quangi*	14.2–14.8	11.4	18.4	12.7	15.5	2.8	13.6	15.9	13.6
25	*A. rufescens*	13.1	11.7	15.9	12.1	12.9	9.7	13.8	14.6	11.7
26	*A. spinalis*	11.7–12.3	14.6	16.5	14.6	14.2	14.4	14.2	14.4	14.0
27	*A.* sp2	11.0	14.0	14.8	13.4	15.3	13.3	14.2	13.6	15.0
28	*A. timi*	13.3–13.6	12.7	16.5	12.5	15.0	12.9	13.3	15.9	12.1
29	*A. tranganensis*	14.2–14.6	12.5	15.3	13.8	14.0	12.3	16.9	13.4	14.8
30	*A. vanhoensis*	12.7–13.1	11.9	15.5	11.7	14.8	11.7	13.6	15.2	11.4
31	*A. yangdatongi*	14.0–14.4	6.4	16.7	5.7	14.4	12.7	14.2	14.8	5.1
32–35	*A. yunkaiensis*	6.4–7.2	11.9–12.9	15.0–15.9	12.3–12.9	14.4–14.8	12.7–13.1	11.9–12.5	14.0–14.2	11.7–12.3
36	*A. zugorum*	10.4	13.3	15.3	12.3	14.2	12.9	13.4	15.0	12.1

Table 2. Continued.

ID	Species	15	16	17	18	19–20	21	22	23	24
1–6	*A. sheni*									
7	*A. ater*									
8	*A. dabieshanensis*									
9	*A. damingensis*									
10	*A. dehuaensis*									
11	*A. emilyae*									
12	*A. formosanus*									
13	*A. huangjietangi*									
14	*A. hunanensis*									
15	*A. juliani*	–								
16	*A. meiguensis*	16.7	–							
17	*A. niger*	11.7	13.8	–						
18	*A. ningshanensis*	9.5	16.9	14.0	–					
19–20	*A.* sp1	12.1–12.3	15.0–15.2	9.8–10.0	13.8–14.0	0.2				
21	*A. nanshanensis*	8.1	17.6	12.1	5.7	12.5–12.7	–			
22	*A. panzhihuaensis*	15.7	11.4	14.0	17.4	14.4–14.6	15.3	–		
23	*A. pingbianensis*	11.6	16.7	11.9	11.6	10.0–10.2	11.0	14.8	–	
24	*A. quangi*	12.5	15.2	12.1	13.1	12.3–12.5	12.7	16.9	13.6	–
25	*A. rufescens*	11.2	18.6	13.8	11.9	13.4–13.6	11.4	15.9	12.7	10.0
26	*A. spinalis*	14.0	15.9	13.8	15.2	8.9–9.1	14.4	16.1	13.3	13.6
27	*A.* sp2	13.8	15.7	11.9	15.7	3.2–3.4	13.8	15.5	12.3	13.1
28	*A. timi*	13.4	15.9	11.6	12.9	11.4–11.6	13.1	15.3	11.9	12.5
29	*A. tranganensis*	14.2	16.3	14.6	15.0	13.1–13.3	13.4	16.5	13.4	11.7
30	*A. vanhoensis*	12.7	15.7	11.7	11.7	11.2–11.4	11.9	15.3	10.6	11.6
31	*A. yangdatongi*	7.6	17.2	13.4	5.9	12.1–12.3	4.5	15.7	10.8	12.5
32–35	*A. yunkaiensis*	12.3–12.9	15.3–15.9	10.4–11.9	12.7–13.3	9.3–10.0	11.6–12.5	15.7–16.1	10.8–11.4	12.7–13.6
36	*A. zugorum*	13.3	15.0	13.1	12.5	11.6–11.7	12.7	15.2	10.2	13.1

Table 2. Continued.

ID	Species	25	26	27	28	29	30	31	32–35
1–6	*A. sheni*								
7	*A. ater*								
8	*A. dabieshanensis*								
9	*A. damingensis*								
10	*A. dehuaensis*								
11	*A. emilyae*								
12	*A. formosanus*								
13	*A. huangjietangi*								
14	*A. hunanensis*								
15	*A. juliani*								
16	*A. meiguensis*								
17	*A. niger*								
18	*A. ningshanensis*								
19–20	*A.* sp1								
21	*A. nanshanensis*								
22	*A. panzhihuaensis*								
23	*A. pingbianensis*								
24	*A. quangi*								
25	*A. rufescens*	–							
26	*A. spinalis*	12.7	–						
27	*A.* sp2	14.8	10.4	–					
28	*A. timi*	14.0	14.0	12.9	–				
29	*A. tranganensis*	12.7	15.5	13.6	13.4	–			
30	*A. vanhoensis*	12.9	12.3	12.7	4.5	11.9	–		
31	*A. yangdatongi*	11.6	14.2	13.6	12.7	12.9	10.8	–	
32–35	*A. yunkaiensis*	12.1–13.4	11.7–11.9	10.0–11.0	12.7–13.3	13.1–14.0	11.7–12.3	12.3–12.5	0.0–3.0
36	*A. zugorum*	13.8	13.4	13.6	13.4	11.7	11.7	12.1	10.4–11.9

Taxonomic account

Reptilia
Serpentes
Xenodermidae
Achalinus

Achalinus sheni **Ma, Xu, Qi, Wang, Tang, Huang & Jiang, 2023**
Figs 2–6
Common name: Shen's Odd-scale Snake / Shěn Shì Jǐ Shé (沈氏脊蛇)

Specimens examined. Three typical specimens: LFR2023008 (adult female), LFR2023009 (adult male), LFR2023010 (adult female); and one albinistic specimen: LFR2024015 (adult female), collected in July, 2023 from Yangshi Town, Lianyuan City, Loudi City, Hunan Province (27°32'07.08"N, 111°48'31.68", 370 m a. s. l.) ; coll. by Shu Li and Ziyuan Feng.

Description of the albinistic specimen. ***Measurements and scalation*****.** An adult female specimen (field number LFR2024015) with SVL 354 mm (TL 416 mm and TAL 62 mm); tail relatively short, TAl/TL ratio 0.149; body slender and cylindrical; head slightly distinct from the neck; HW 5.8 mm; HL 10.8 mm; eye small; ED 1.1 mm; rostrum small, triangular, slightly visible from above; length of the suture between the internasals (LSBI 1.25 mm) subequal to the length of the suture between the prefrontals (LSBP 1.32 mm), LSBI/LSBP ratio 0.95; nostril in the anterior part of the nasal; prefrontals paired; frontal single, pentagonal, pointing to the rear, the width and length close; loreal one, subrectangular, LorL 1.6 mm, LorH 0.9 mm, LorH/LorL ratio 0.56; supraocular one, pentagonal, SPOL 1.9 mm; TEMP 7/8, arranged in three rows (2+1+4 in left and 2+2+4 in right), the anterior two contact the eye, ATUL 1.7 mm, SPOL/ATUL ratio 1.1; SL 6, the 4th–5th contact the eye, the last one much elongated; two pairs of chin shields, the anterior pairs longer than the posterior pairs, followed by preventrals; one mental; IL 5, the first one contact with each other after the mental and before the 1st chin-shields, 1st–3rd touch the first pair of chin-shields.

Dorsal scales strongly keeled, lanceolate, 23 rows throughout the body, the outmost row smooth and significantly enlarged. VS 164; anal entire; SC 46, not paired.

Coloration**.** The comparison of color pattern between the albinistic specimen and the typical specimen are shown in Fig. 4. In life, dorsum (head, body, and tail) predominantly pastel yellow or paster orange owning to the lack of melanophoric pigments, and the iridescence on the body surface also disappears. Head scales in dorsal view same as dorsum, interstitial skin of dorsal and sutures of head scales milk star white. The iris was blood-red, with a reddish pupil. Supralabials, mental, and infralabials were pastel orange. The ventral ground color of body and tail were milk star white, darker on both sides than in the middle, and with free margins of ventral scales and subcaudals almost transparent with a slight hint of pastel orange (Figs 2, 3).

Expanded description of the females. Measurements and scalation data of the newly collected specimens (1 male and 3 females) are presented in Table 3. Based on three newly collected female specimens (field number: LFR2023008, LFR2023010, LFR2024015), an expanded description of the females is provided as below.

Figure 2. Adult female albinistic specimen of *Achalinus sheni* in life (LFR2024015) **A** dorsal view **B** ventral view. Photos by Yu-Hao Xu.

***Measurements and scalation*.** Tail relatively short, TAL/TL ratio 0.149–0.164; body slender and cylindrical, the maximal TL 416 mm with SVL 354 mm and TAL 62 mm; head relatively narrow, slightly distinct from the neck, HL 10.8–11.5 mm; HW 5.5–6.6 mm; rostrum small, triangular, slightly visible from above; eye small, pupil round, ED 1.1 mm; LSBI subequal to LSBP; nostril in the anterior part of the nasal; prefrontals 2, elongated; frontal 1, pentagonal, pointing to the rear, the width and length close; loreal one, subrectangular, LorL 1.6–1.7 mm, LorH 0.9–1.3 mm, LorH/LorL ratio 0.56–0.76; supraocular one, pentagonal,

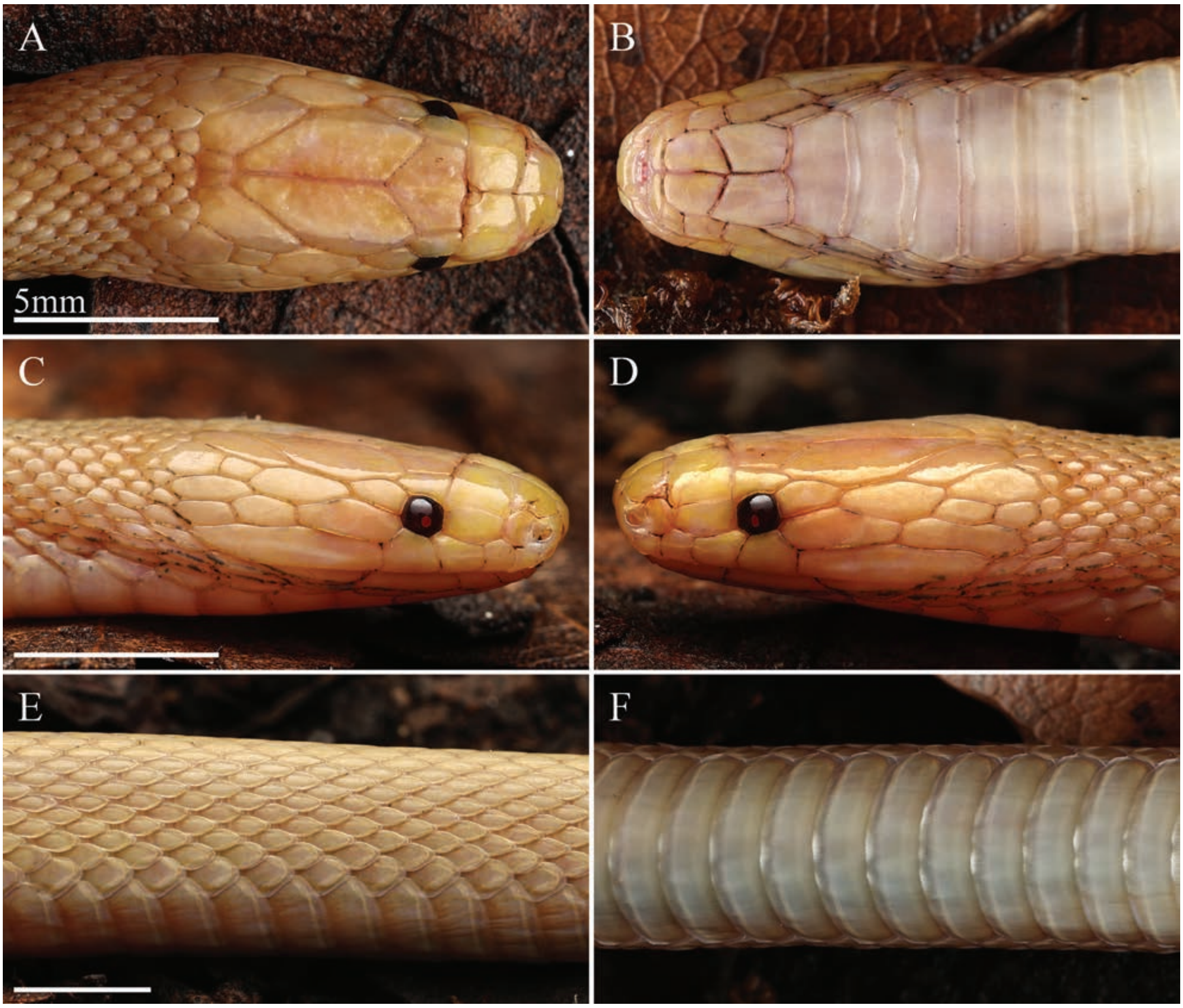

Figure 3. Close-up view of the adult female albinistic specimen of *Achalinus sheni* in life (LFR2024015) **A** dorsal view of the head **B** ventral view of the head **C** right view of the head **D** left view of the head **E** lateral view of the middle body **F** venter view of the middle body. Photos by Yu-Hao Xu.

SPOL 1.6–1.9 mm; temporals long, arranged in three rows, TEMP 2+1+4, 2+2+3 or 2+2+4, the anterior two contact the eye, ATUL 1.7 mm, SPOL/ATUL ratio 0.94–1.12; SL 6, the 4th–5th contact the eye, the last one much elongated; two pairs of chin shields, the anterior pairs longer than the posterior pairs, followed by preventrals; one mental; IL 5, the first one contact with each other after the mental and before the 1st chin-shields, 1st–3rd touch the first pair of chin-shields.

Dorsal scales 23-23-23, lanceolate and strongly keeled, the outmost row smooth and significantly enlarged. VS 172–174; CP entire; SC 46–49, unpaired.

***Coloration in life*.** In life, the dorsum (head, body, and tail) is predominantly brownish black and slightly tinged with iridescence. Head scales in dorsal view are the same as the dorsum, and with the middle darker than the sides. Dorsum brownish black and the five innermost dorsal scale rows a little darker, forming an inconspicuous longitudinal vertebral line. Eyes pure black. Mental, infralabials, and chin shields light grayish brown. Ventral ground color of body and tail generally light grey or light taupe and darker on the sides. The free margins of ventral scales are greyish white (Fig. 4).

Figure 4. Comparisons between the albinistic specimen and typical specimen of *Achalinus sheni* in life **A1–A2** LFR2024015 **B1–B2** LFR2023010 **A1**, **B1** dorsal view **A2**, **B2** ventral view. Photos by Yu-Hao Xu.

Coloration in preservation. In preservation, coloration still resembles the specimen in life, except that the coloration of dorsum further deepening, and the background color of the venter becomes light brownish grey (Fig. 5).

Variation. The female specimens have a similar color pattern as male specimens, but in measurement and scalation features, there is variation by sex: females have a relatively large body size (TL 355–408 mm vs 149–371 mm in male); a significantly short tail, TAL/TL ratio 0.149–0.164 (vs 0.183–0.224 in male) (Fig. 6); more ventral scales (172–174 vs 161–170 in male); and fewer subcaudals (46–49 vs 55–61 in male) (Table 4).

Revision of diagnostic characters. (1) dorsal scales strongly keeled, 23 rows throughout the body, the outmost row smooth and significantly enlarged; (2) tail relatively short, TAL/TL ratio 0.183–0.224 in males, and 0.140–0.164 in females; (3) the suture between internasals subequal to the suture between prefrontals; (4) loreal one, subrectangular, LorH/LorL 0.53–0.76; (5) ventrals 161–170 in males and 172–174 in females; (6) cloacal plate entire; (7) subcaudals 55–61 in males and 46–49 in females, not paired; (8) the length of supraocular almost equal to the length of upper anterior temporal; (9) vertebral line inconspicuous and subcaudal streak absent.

Natural history notes. *Achalinus sheni* is currently known from Hunan Province, China: Lianyuan City, Nanyue District and Nanshan National Park, Shaoyang City (350–410 m a.s.l.). The known activity period of *A. sheni* is from March to October but activity peaks in early summer. The species usually prefers to hide under rocks, decaying wood, or fallen leaves, but it has sometimes been found on cement roads in the mountains after rain or on high-humidity nights. Through dissection, it was found that there were undigested earthworms in the intestine of specimen LFR2023009. Therefore, we speculate that *A. sheni* feeds mainlyon worms in the wild.

Figure 5. Preserved specimen of the typical female specimen of *A. sheni* (LFR2023008). Photos by Yu-Hao Xu.

Table 3. Morphological variation characters in the newly collected *Achalinus sheni* specimens.

Voucher number	LFR2023008	LFR2023009	LFR2023010	LFR2024015
Sex	♀	♂	♀	♀
SVL	341	257	298	354
TL	408	324	355	416
TAL	67	67	57	62
TAL/TL	0.164	0.207	0.160	0.149
HL	11.4	9.6	11.5	10.8
HW	6.6	5.1	5.5	5.8
SL	3+2+1	3+2+1	3+2+1	3+2+1
IL	5/5	5/5	5/5	5/5
Chin	2	2	2	2
IFL–1stChin	1th–3rd	1th–3rd	1th–3rd	1th–3rd
Lor	1	1	1	1
LorH	1.2	1.0	1.3	0.9
LorL	1.7	1.6	1.7	1.6
LorH/LorL	0.71	0.63	0.76	0.56
LSBI	1.8	1.3	1.5	1.23
LSBP	1.6	1.1	1.6	1.32
LSBI/LSBP	=	=	=	=
ED	1.1	0.9	1.1	1.1
PrO	0	0	0	0
PO	0	0	0	0
TEMP	2+2+3/2+2+3	2+2+3/2+2+4	2+2+3/2+2+3	2+1+4/2+2+4
ATUL	1.7	1.3	1.7	1.7
SPO	1	1	1	1
SPOL	1.6	1.3	1.6	1.9
SPOL/ATUL	0.94	1.00	0.94	1.12
DSR	23-23-23	23-23-23	23-23-23	23-23-23
VS	172	167	172	174
CP	entire	entire	entire	entire
SC	49	59	47	46

Table 4. Comparison of the key morphological characters between *Achalinus sheni* and *A. yunkaiensis* obtained from specimens examined in this study, Wang et al. (2019), and Ma et al. (2023a).

Sex	*A. sheni*		*A. yunkaiensis*	
	♂	♀	♂	♀
N	6	3	4	3
SVL	122–292	298–354	189–359	204–386
TL	149–371	355–416	232–418	256–488(+)
TAL	27–80	57–67	43–63	52–73
TAL/TL	**0.183–0.224**	**0.149–0.164**	**0.185–0.200**	**0.156–0.204**
SL	3+2+1	3+2+1	3+2+1	3+2+1
IL	**5 (rarely 6)**	**5**	**6**	**6**
Chin	2	2	2	2
IFL–1stChin	1th–3rd	1th–3rd	1th–3rd	1th–3rd
Lor	1	1	1	1
LorH	0.7–1	0.9–1.3	0.8–1.3	0.7–1.2
LorL	1.3–1.7	1.6–1.7	1.3–2.2	1.5–2.2
LorH/LorL	0.53–0.93	0.56–0.76	0.56–0.64	0.49–0.55
LSBI vs LSBP	=	=	=	=
TEMP	2+2+3	2+2+3 or 2+2+4 or 2+1+4	2+2+3 or 2+2+4	2+2+3 or 2+2+4
ATUL	1.3–1.5	1.7	1.2–2.2	1.9–2.9
SPO	1	1	1	1
SPOL	1.1–1.6	1.6–1.9	1–1.6	1.3–1.6
SPOL/ATUL	**0.99–1.16**	**0.94–1.12**	**0.66–0.83**	**0.55–0.65**
DSR	23-23-23	23-23-23	23-23-23	23-23-23
VS	**161–170**	**172–174**	**151–162**	**144–156**
CP	1	1	1	1
SC	**55–61**	**46–49**	**49–56**	**51–55**
VS+SC	**220–226**	**219–221**	**200–212**	**195–205**

Figure 6. Comparisons of the tails between males and females of *Achalinus sheni* **A1** specimen ANU20230013, paratype, adult male **A2** specimen ANU20230012, paratype, adult male **A3** specimen LFR2023009, adult male **B1** specimen LFR2023010, adult female **B2** specimen LFR2024015, adult female **B3** specimen LFR2023008, adult female. Photos by Yu-Hao Xu.

Discussion

The genus *Achalinus* is widely distributed in Vietnam, China, and Japan (Zhao et al. 1998; Zhao 2006), with 28 currently recognized species, and lately it has attracted much attention in scientific literature (Wang et al. 2019; Ziegler et al. 2019; Li et al. 2020b; Luu et al. 2020; Hou et al. 2021; Huang et al. 2021; Li et al. 2021; Ha et al. 2022; Yang et al. 2022; Ma et al. 2023a, 2023b, 2023c; Pham et al. 2023; Yang et al. 2023; Zhang et al. 2023; Li et al. 2024). However, no cases of albinism have been described to our knowledge. Therefore, this first report of albinism in *A. sheni* sheds light on this rare phenomenon in the genus and family.

Species of *Achalinus* typically exhibit a rainbow-colored iridescence on their body surface especially when exposed to sunlight or camera flash. However, when observing the albino individual, we found that the rainbow color on their body surface almost completely disappeared. It is currently unclear whether the lack of iridescence is entirely caused by the disappearance of melanin. In the future, we will further examine microstructure of albinism and examine the genetic underpinnings of this phenomenon.

In this study, we provide the first detailed description and photographs of the female of *A. sheni* and compare the morphological differences between males and females. We demonstrate intersexual differences such as the total length, the tail length, and the number of venter scales and subcaudals, which will help distinguish this species from other closely related species, especially its sister species *A. yunkaiensis* (Table 4), which is sympatric in distribution with *A. sheni* in the Nanshan National Park (Li et al. 2024).

Moreover, in this study, we provide two partial *CO1* sequences of two *Achalinus* specimens from Ningshan County, Shaanxi Province, China, which cluster with the Taibai specimen (considered as *Achalinus* sp. by Yang et al. (2023)) (Table 1) with high support values (SH 97 / UFB 99) (Fig. 1). Interestingly, the uncorrected *p*-distance was 3.2–3.4%, indicating substantial genetic differences between the two populations, but further population genomic investigation is needed to properly understand biogeographic causes of this putative population structure. However, the morphological examination indicated that these two specimens from Ningshan County are consistent with the original descriptions of *A. ningshanensis*. Therefore, broad sampling of morphological and genomic data is required to better understand population or species structuring within *A. ningshanensis*.

Acknowledgements

We are very grateful to Shu Li and Ziyuan Feng for their help fieldwork.

Additional information

Conflict of interest

The authors have declared that no competing interests exist.

Ethical statement

All sampling and procedures involving live snakes were performed in accordance with the Wild Animals Protection Law of the People's Republic of China, approved by the Institutional Ethics Committee of Qinghai University (protocol code SL-2023028 and date of approval 15 March 2023).

Funding

This work was supported by the Project of Qinghai Science & Technology Department (2024-ZJ-965), the National Natural Science Foundation of China [32301325] and the Open Project of State Key Laboratory of Plateau Ecology and Agriculture, Qinghai University [2023-ZZ-08].

Author contributions

YHX, SW, SM, measured the specimens, analyzed the data, constructed the phylogenetic tree, and prepared the manuscript; LFP and SH provided the funding for the field survey; LFP, SH and FTB conceived and designed the study and reviewed the manuscript before submission. All authors have read and agreed to the published version of the manuscript.

Author ORCIDs

Yu-Hao Xu https://orcid.org/0000-0001-6094-6680
Li-Fang Peng https://orcid.org/0000-0001-9325-7048

Data availability

All of the data that support the findings of this study are available in the main text.

References

Abegg AD, Entiauspe-Neto OM, Lema T (2015) First record of albinism in the *Elapomorphini* tribe (Serpentes: Dipsadidae). Herpetology Notes 8: 503–505.

Alberts B, Johnson A, Lewis J, Raff M, Roberts K, Walter P (2004) Biologia Molecular da Célula. 4th edn. Artmed, Biologia Molecular da Célula. 4th edn. Artmed, Artmed, Porto Alegre, Brazil, 1464 pp.

Bechtel HB (1978) Colour and pattern in snakes (Reptilia, Serpentes). Journal of Herpetology 12(4): 521–532. https://doi.org/10.2307/1563357

Bechtel HB (1991) Inherited color defects. Comparison between humans and snakes. International Journal of Dermatology 30(4): 243–246. https://doi.org/10.1111/j.1365-4362.1991.tb04628.x

Bechtel HB (1995) Reptile and Amphibian Variants: Colors, Patterns, and Scales. Krieger Publishing, Malabar, 224 pp.

Broghammer S (2000) Albinos, Color and Pattern Mutations of Snakes and Other Reptiles. M&S Verlag, Münster, Germany, 96 pp.

Bruni G (2017) A leucistic grass snake *Natrix natrix* (Linnaeus, 1758) (Serpentes: Natricidae) from Tuscany, central Italy. Herpetology Notes 10: 313–316.

Burland TG (2000) DNASTAR's Lasergene sequence analysis software. Methods in Molecular Biology (Clifton, N.J.) 132: 71–91. https://doi.org/10.1385/1-59259-192-2:71

Che J, Chen HM, Yang JX, Jin JQ, Jiang K, Yuan ZY, Murphy RW, Zhang YP (2012) Universal *COI* primers for DNA barcoding amphibians. Molecular Ecology Resources 12(2): 247–258. https://doi.org/10.1111/j.1755-0998.2011.03090.x

Deepak V, Lalronunga S, Lalhmingliani E, Das A, Narayanan S, Das I, Gower DJ (2021) Phylogenetic relationships of xenodermid snakes (Squamata: Serpentes: Xenodermidae), with the description of a new genus. Vertebrate Zoology 71: 747–762. https://doi.org/10.3897/vz.71.e75967

Dutta S, Pareek PS, Singh A, Riedle JD, Singh S (2022) First record of albinism in the Crowned River Turtle, *Hardella thurjii*, Gray, 1831 (Reptilia: Testudines, Geoemydidae). Zootaxa 5091(1): 197–200. https://doi.org/10.11646/zootaxa.5091.1.10

Edgar RC (2004) MUSCLE: Multiple sequence alignment with high accuracy and high throughput. Nucleic Acids Research 32(5): 1792–1797. https://doi.org/10.1093/nar/gkh340

Griffiths AJF, Miller JH, Suzuki DT, Lewontin RC, Gelbart WM (1998) Introdução à Genética. 6th Edition. Guanabara-Koogan, Rio de Janeiro, Brazil, 507 pp.

Ha NV, Ziegler T, Sy TD, Le MD, Nguyen TQ, Luu VQ (2022) A new species of the genus *Achalinus* (Squamata: Xenodermidae) from Son La Province, Vietnam. Zootaxa 5168(3): 375–387. https://doi.org/10.11646/zootaxa.5168.3.8

Hoshing V, Mahabal STA (2013) Cases of total albinism in Green Keelback *Macropisthodon plumbicolor* and Common Wolf Snake *Lycodon aulicus* (Colubridae). Reptile Rap 15: 46–47.

Hou SB, Wang K, Guo P, Chen JM, Yuan ZY, Che J (2021) Two new species and a new country record of the genus *Achalinus* (Reptilia: Squamata: Xenodermidae) from China. Zootaxa 4950(3): 528–546. https://doi.org/10.11646/zootaxa.4950.3.6

Huang RY, Peng LF, Yu L, Huang TQ, Jiang K, Ding L, Chang JK, Yang DC, Xu YH, Huang S (2021) A new species of the genus *Achalinus* from Huangshan, Anhui, China (Squamata: Xenodermidae). Asian Herpetological Research 12(2): 178–187. https://doi.org/10.16373/j.cnki.ahr.200075

Kalyaanamoorthy S, Minh BQ, Wong TKF, Haeseler AV, Jermiin LS (2017) ModelFinder: Fast model selection for accurate phylogenetic estimates. Nature Methods 14(6): 587–589. https://doi.org/10.1038/nmeth.4285

Krecsák L (2008) Albinism and leucism among European Viperinae: A review. Russian Journal of Herpetology 15(2): 97–102.

Kumar S, Stecher G, Li M, Knyaz C, Tamura K (2018) MEGA X: Molecular evolutionary genetics analysis across computing platforms. Molecular Biology and Evolution 35(6): 1547–1549. https://doi.org/10.1093/molbev/msy096

Li JN, Liang D, Wang YY, Guo P, Huang S, Zhang P (2020a) A large-scale systematic framework of Chinese snakes based on a unified multilocus marker system. Molecular Phylogenetics and Evolution 148: 106807. https://doi.org/10.1016/j.ympev.2020.106807

Li K, Yu M, Wu YY, Liao LH, Tang K, Liu Q, Guo P (2020b) A new species of the genus *Achalinus* (Squamata: Xenodermatidae) from southeastern Yunnan Province, China. Zootaxa 4860(1): 116–128. https://doi.org/10.11646/zootaxa.4860.1.6

Li K, Wu YY, Xu RY, Zhu F, Ren JL, Guo P, Dong BJ (2021) A new species of the *Achalinus rufescens* complex (Xenodermidae: *Achalinus*) from Fujian Province, China. Zootaxa 5026(2): 239–254. https://doi.org/10.11646/zootaxa.5026.2.5

Li H, Zhu LQ, Xiao B, Huang J, Wu SW, Yang LX, Zhang ZQ, Mo XY (2024) A new species of the genus *Achalinus* (Squamata, Xenodermatidae) from southwest Hunan Province, China. ZooKeys 1189: 257–273. https://doi.org/10.3897/zookeys.1189.112784

Lu B, Qiu X, Yang WZ, Yao ZY, Ma XF, Deng SY, Zhang Q, Fu JZ, Qi Y (2024) Genetic Basis and Evolutionary Forces of Sexually Dimorphic Color Variation in a Toad-Headed Agamid Lizard. Molecular Biology and Evolution 41(3): msae054. https://doi.org/10.1093/molbev/msae054

Luu VQ, Ziegler T, Van HN, Van LO, Hoang TT, Ngo HT, Le MD, Tran DH, Nguyen TQ (2020) A new species of *Achalinus* (Squamata: Xenodermidae) from Trang An Landscape Complex, Ninh Binh Province, Vietnam. Zootaxa 4877(1): 174–184. https://doi.org/10.11646/zootaxa.4877.1.8

Ma S, Xu YH, Qi S, Wang YY, Tang SS, Huang S, Jiang JP (2023a) Discovery of a new cryptic *Achalinus* Peters, 1869 (Serpentes, Xenodermidae) species from Hunan Province, China. ZooKeys 1181: 9–27. https://doi.org/10.3897/zookeys.1181.109462

Ma S, Shi SC, Jiang JP (2023b) *Achalinus yunkaiensis*, a new provincial record of Hunan Province, China, with description of an additional topotype of *A. rufescens*. Dongwuxue Zazhi 58(5): 760–771. [In Chinese with English abstract]

Ma S, Shi SC, Xiang SJ, Shu F, Jiang JP (2023c) A new species of *Achalinus* Peters, 1869 (Squamata, Xenodermidae) from Hunan Province, China. ZooKeys 1166: 315–331. https://doi.org/10.3897/zookeys.1166.103055

Miller AH, Davis HR, Luong AM, Do QH, Pham CT, Ziegler T, Lee JL, Queiroz KD, Reynolds RG, Nguyen TQ (2020) Discovery of a new species of enigmatic odd-scaled snake (Serpentes: Xenodermidae: *Achalinus*) from Ha Giang Province, Vietnam. Copeia 108(4): 796–808. https://doi.org/10.1643/CH2020060

Nguyen LT, Schmidt HA, Haeseler AV, Minh BQ (2015) IQ-TREE: A fast and effective stochastic algorithm for estimating maximum likelihood phylogenies. Molecular Biology and Evolution 32(1): 268–274. https://doi.org/10.1093/molbev/msu300

Pham AV, Pham CT, Le MD, Ngo HT, Ong AV, Ziegler T, Nguyen TQ (2023) *Achalinus quangi*, a new odd-scaled snake species from Vietnam. Zootaxa 5270(1): 48–66. https://doi.org/10.11646/zootaxa.5270.1.2

Roulin A, Bize P (2007) Sexual selection in genetic colour-polymorphic species: A review of experimental studies and perspectives. Journal of Ethology 25(2): 99–105. https://doi.org/10.1007/s10164-006-0006-z

Sazima I, Di-Bernardo M (1991) Albinismo em serpentes neotropicais. Memorias do Instituto Butantan 53: 167–173.

Sazima I, Pombal JP (1986) Um albino de *Rhamdella minuta*, com notas sobre comportamento (Osteichthyes, Pimelodidae). Revista Brasileira de Biologia 46(2): 377–381.

Sun BJ, Li WM, Lv P, Wen GN, Wu DY, Tao SA, Liao ML, Yu CQ, Jiang ZW, Wang Y, Xie HX, Wang XF, Chen ZQ, Liu F, Du WG (2024) Genetically encoded lizard color divergence for camouflage and thermoregulation. Molecular Biology and Evolution 41(2): 1–18. https://doi.org/10.1093/molbev/msae009

Teynié A, David P, Lottier A, Le MD, Vidal N, Nguyen TQ (2015) A new genus and species of xenodermatid snake (Squamata: Caenophidia: Xenodermatidae) from northern Lao People's Democratic Republic. Zootaxa 3926(4): 523–540. https://doi.org/10.11646/zootaxa.3926.4.4

Wang J, Li Y, Zeng ZC, Lyu ZT, Sung YH, Li YY, Lin CY, Wang YY (2019) A new species of the genus *Achalinus* from southwestern Guangdong Province, China (Squamata: Xenodermatidae). Zootaxa 4674(4): 471–481. https://doi.org/10.11646/zootaxa.4674.4.6

Yang DC, Huang RY, Jiang K, Burbrink FT, Gong YN, Yu J, Zhang Y, Huang TQ, Huang S (2022) A new species of the genus *Achalinus* (Squamata: Xenodermidae) from Ningshan County, Shaanxi Province, China. Zootaxa 5190(1): 127–140. https://doi.org/10.11646/zootaxa.5190.1.5

Yang DC, Xu YH, Wu JX, Gong YA, Huang RY, Xiang J, Feng ZL, Huang TQ, Huang S (2023) A new species of the genus *Achalinus* (Squamata: Xenodermidae) from Nanning, Guangxi, China. Zootaxa 5319(3): 389–402. https://doi.org/10.11646/zootaxa.5319.3.5

Yu M, Li K, Liu Q, Yang K, Wu YY, Guo P (2020) First record of the *Achalinus yunkaiensis* from Maoershan National Nature Reserve, Guangxi, China. Dongwuxue Zazhi 55(6): 793–796. [In Chinese with English abstract]

Zhang CW, Liu K, Huang RY, Hu TL, Yu L, Sun RL, Zhang YC, Wen J, Zhang BW (2023) A new species of the genus *Achalinus* (Squamata: Xenodermidae) from the Dabie Mountains, Anhui, China. Animals (Basel) 13(4): 708. https://doi.org/10.3390/ani13040708

Zhao EM (2006) Snakes of China. Anhui Science and Technology Publishing House, Hefei, 669 pp. [in Chinese]

Zhao EM, Huang MH, Zong Y (1998) Fauna Sinica: Reptilia. Vol. 3. Squamata, Serpentes. Science Press, Beijing, 522pp. [in Chinese] [ISBN 978-7030065605]

Ziegler T, Nguyen TQ, Pham CT, Nguyen TT, Pham AV, Schingen MV, Nguyen TT, Le MD (2019) Three new species of the snake genus *Achalinus* from Vietnam (Squamata: Xenodermatidae). Zootaxa 4590(2): 249–269. https://doi.org/10.11646/zootaxa.4590.2.3

ZooKeys 1209: 19–42 (2024)
DOI: 10.3897/zookeys.1209.125838

Research Article

A description of a new species of *Mongolodiaptomus* Kiefer, 1937 (Copepoda, Calanoida, Diaptomidae) from Thailand with an up-to-date key to the genus

Laorsri Sanoamuang[1,2], Kamonwan Koompoot[2]

1 *Laboratory of Biodiversity and Environmental Management, International College, Khon Kaen University, Khon Kaen 40002, Thailand*
2 *Applied Taxonomic Research Center, Faculty of Science, Khon Kaen University, Khon Kaen 40002, Thailand*
Corresponding author: Laorsri Sanoamuang (la_orsri@kku.ac.th)

Abstract

The genus *Mongolodiaptomus* is widely distributed in stagnant water bodies in Southeast Asia. During a comprehensive collection of freshwater copepods from different areas in Thailand, a previously unknown species of calanoid copepod, *Mongolodiaptomus phutakaensis* **sp. nov.**, was recorded. Representatives were found in a natural swamp located in the Kok Phutaka community forest in Khon Kaen Province, northeastern Thailand. The new species belongs to the "*M. loeiensis* species group" and most closely resembles *M. loeiensis* and *M. mekongensis* by having a distinct shape of the second exopodal segment of the male right P5, with enlarged proximal and distal parts of the outer margin as well as a bent and twisted principal lateral spine. The new species can be distinguished from its congeners by various characters in the males. The ventral surface of the right caudal ramus has two chitinous teeth and two knobs. The intercoxal plate is slightly produced distally and without any spine. The right P5 basis lacks a hyaline membrane on the inner margin but has a distinct spur-like chitinous process at the mid-distal margin on the posterior surface. The left P5 basis has a thin, longer hyaline lamella on the inner margin. The new species is rare, having been observed in only one out of approximately 5,000 surveyed locations in Thailand. A detailed morphological comparison and an up-to-date key to the *Mongolodiaptomus* species are presented. Their taxonomic characters, interspecies relationships, and biogeography are discussed.

Key words: Aquatic habitats, biodiversity, distribution, endemic, *Mongolodiaptomus phutakaensis*, Southeast Asia, taxonomy

OPEN ACCESS

Academic editor: Maria Cristina Bruno
Received: 20 April 2024
Accepted: 1 July 2024
Published: 6 August 2024

ZooBank: https://zoobank.org/2440735C-827B-4446-9463-757DF90C034A

Citation: Sanoamuang L, Koompoot K (2024) A description of a new species of *Mongolodiaptomus* Kiefer, 1937 (Copepoda, Calanoida, Diaptomidae) from Thailand with an up-to-date key to the genus. ZooKeys 1209: 19–42. https://doi.org/10.3897/zookeys.1209.125838

Introduction

In 1937, Kiefer created the genus *Mongolodiaptomus* to include a group of Asian freshwater diaptomid copepods, with *Mongolodiaptomus formosanus* Kiefer, 1937 as the type taxon (Kiefer 1937; Walter and Boxshall 2024). Ranga Reddy et al. (2000) recommended to use the ornamentation of the right second exopod of the male P5 as an important character to distinguish between diaptomid copepods, especially those from the three closely related genera *Neodiaptomus* Kiefer, 1932, *Allodiaptomus* Kiefer, 1936, and *Mongolodiaptomus* Kiefer,

1937. Thus, the characters used to distinguish the males of *Mongolodiaptomus* from related genera is the presence of at least two lateral spines on the second exopod of the right P5, one principal spine in the middle of the segment, and one or two accessory spines proximally or distally on the outer margin.

At present, the genus *Mongolodiaptomus* consists of 11 valid species, distributed across Asia, with countries in the lower Mekong River Basin as the epicenter (Sanoamuang and Watiroyram 2018). However, this is not the final number, since there are two more species with doubtful identities. Ranga Reddy et al. (1998) observed some morphological variabilities in *M. botulifer* (Kiefer, 1974) from Thailand, leading to serious doubt about the validity of the closely allied *M. malaindosinensis* (Lai & Fernando, 1978). Despite the similarities in morphological features, Sanoamuang and Dabseepai (2021: 20) provide detailed explanations that distinguish the two congeners from each other. The validity was confirmed in the previously mentioned paper. Ranga Reddy et al. (1998) originally described *M. rarus* (Ranga Reddy, Sanoamuang & Dumont, 1998) as *Allodiaptomus rarus*, based on a single male specimen from Thailand. This species was later transferred to the genus *Mongolodiaptomus* by Sanoamuang (2001). Since there are no type specimens of *M. malaindosinensis* available and no description of the female morphology of *M. rarus*, it would be advisable to redescribe *M. malaindosinensis* and *M. rarus*, pending the collection of new specimens.

Thailand is the most species-rich country of the *Mongolodiaptomus* species, with nine already known taxa plus one new species reported (Ranga Reddy et al. 1998, 2000; Sanoamuang 1999, 2001; Watiroyram and Sanoamuang 2017; Sanoamuang and Watiroyram 2018; Sanoamuang and Dabseepai 2021; this study). Recently, Watiroyram and Sanoamuang (2017) provided a key to the identification of both sexes of the valid *Mongolodiaptomus* species.

During the study of copepod diversity in the forest area of the Plant Genetics Conservation Project in Khon Kaen province, northeast Thailand, we came across a new species of the genus *Mongolodiaptomus*. As a result, this paper deals with the following: i) an illustrated description of *M. phutakaensis* sp. nov.; ii) a review and detailed morphological characteristics comparison of the genus *Mongolodiaptomus*; iii) the interspecies relationships; iv) the biogeography of the genus; and v) the updated key to the genus.

Materials and methods

The study area, Kok Phutaka community forest, is located in Wiang Kao District, 78 kilometers from the center of Khon Kaen Province in northeastern Thailand. Her Royal Highness Princess Maha Chakri Sirindhorn of Thailand initiated the Plant Genetics Conservation Project in 1992, which encompasses an area of approximately 1,150 square kilometers. This protected area is a dry dipterocarp forest that provides a source for researchers to study the biodiversity and utilization of plants, animals, and microorganisms. There is one natural swamp and four small artificial ponds in the forest.

Monthly sampling campaigns were conducted from January to December 2007 in all the five above-mentioned habitats using a plankton net with a mesh size of 60 μm. All samples were preserved in 70% ethanol immediately after collection. Specimens were put in a mixture of glycerol and 70% ethanol (ratio 1:10 v/v) and pure glycerol, respectively, just before dissection. Specimens were dissected and mounted at 40–100× magnification under an Olympus SZ51 stereomicroscope. An Olympus compound microscope (CX31) was used to examine all appendages and body ornamentation at 1,000× magnification. All the drawings were created using an Olympus U-DA drawing tube and a compound microscope configured for 100× magnification. Final versions of the drawings were made using the CorelDRAW® 12.0 graphic program. Specimens for scanning electron microscopy (SEM) were dehydrated in an ethanol series (50%, 70%, 80%, 90%, 95%, 100%), for 15 min at each concentration. Specimens were dried in a critical point dryer and coated with gold in a sputter coater. The SEM photographs were taken using a scanning electron microscope (LEO, 1450VP).

The following abbreviations can be found in both the text and the figures: **ae**, aesthetasc; **Enp**, endopod; **Exp**, exopod; **Exp/Enp-n**, exopodal segment n/endopodal segment n; **Pdg1–Pdg5**, pedigers 1–5; **P1–P5**, legs 1–5; **sp**, spine. The nomenclature and descriptive terminology follow Huys and Boxshall (1991), including the analysis of caudal setae (**I–VII**). Type specimens were placed at the Thailand Natural History Museum (**THNHM**) and the Applied Taxonomic Research Center at Khon Kaen University, Thailand (**KKU**).

Taxonomic section

Order Calanoida Sars, 1903
Infraorder Neocopepoda Huys & Boxshall, 1991
Family Diaptomidae Baird, 1850
Sub-family Diaptominae Kiefer, 1932
Genus *Mongolodiaptomus* Kiefer, 1937

Mongolodiaptomus phutakaensis **sp. nov.**

https://zoobank.org/9B4A5018-E0E5-45C6-9701-A299D8301A81
Figs 1–8

Mongolodiaptomus sp. Sanoamuang and Dabseepai (2021): 7, 18, 20.

Type locality. A natural swamp in Kok Phutaka community forest, Muang Kao Phatthana Subdistrict, Wiang Kao District, Khon Kaen Province, northeast Thailand (16°38'43.77"N, 102°18'11.90"E); elevation 220 m a.s.l., water temperature 31.2 °C, pH 8.2, conductivity 299 µS cm^{-1}.

Type material. ***Holotype*:** adult male (THNHM-1V-19371), dissected and mounted in glycerol on one slide. ***Allotype*:** adult female (THNHM-1V-19372), dissected and mounted in glycerol on one slide. ***Paratypes*:** three adult males and three adult females (THNHM-1V-19373), undissected and preserved in 4% formalin; collected from the type locality on the same date as the holotype. All specimens were collected on 16 August 2007, by P. Dabseepai and K. Koompoot.

Description of adult male. Total body length, measured from anterior margin of rostrum to posterior margin of caudal rami, 1.3–1.4 mm (mean = 1.37 mm, *n* = 10), (Figs 1A, 2A). Body smaller and slender than in female. Prosome ~ 2.2 × as long as urosome (Fig. 2A). Rostrum (Fig. 1B) well developed, with two spiniform processes. Pedigers 4 and 5 fused except at lateral margins. Lateral wings of Pdg 5 asymmetrical; right postero-lateral wing shorter than left one; each wing with one thin postero-lateral spine (Fig. 2A).

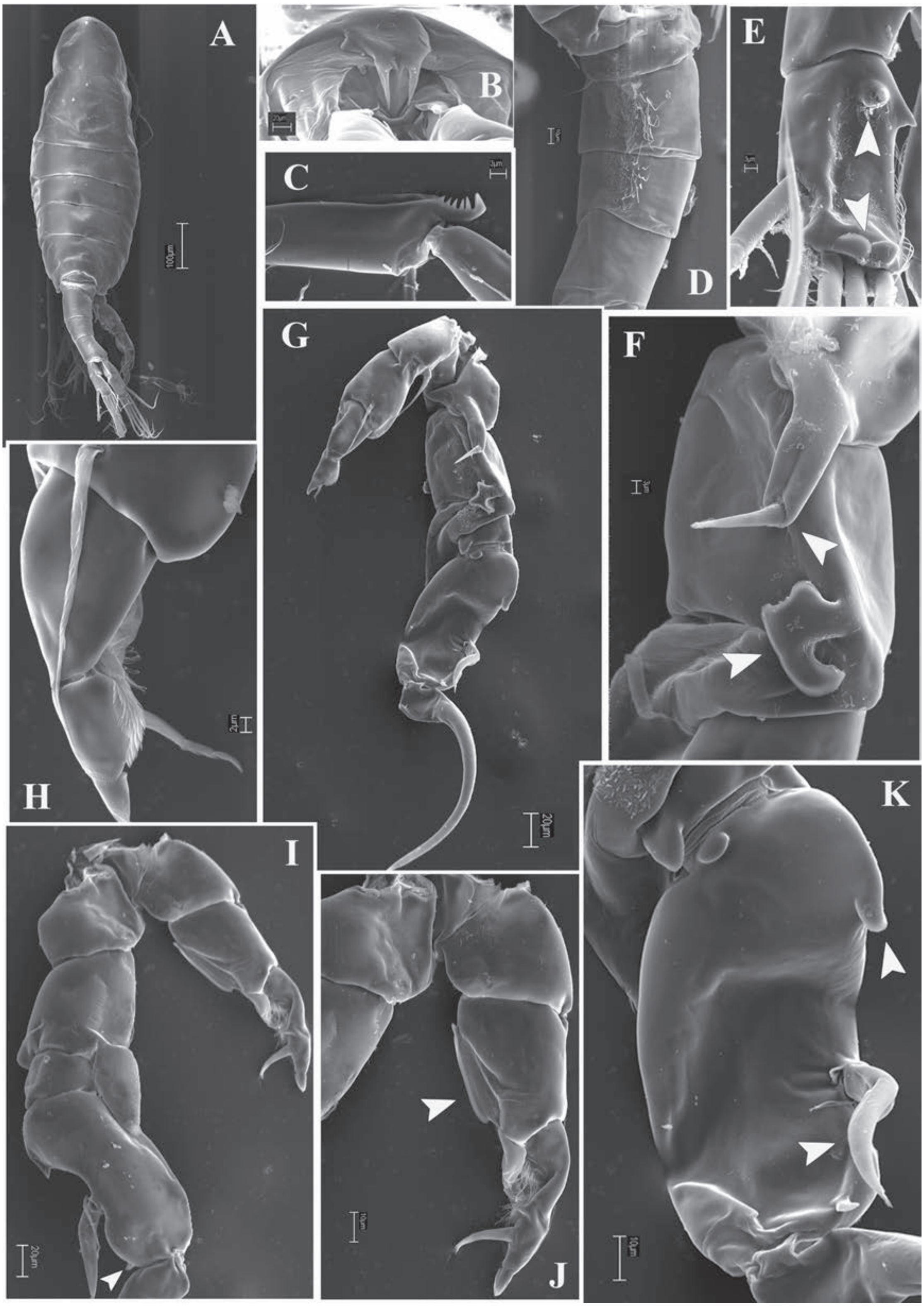

Figure 1. *Mongolodiaptomus phutakaensis* sp. nov., SEM photographs of male **A** habitus, dorsal view **B** rostrum **C** comb-like process on the antepenultimate segment of the right antennule **D** genital somite, and urosomites 2 and 3 **E** right caudal ramus, ventral view (white arrows indicate proximal chitinous spine and distal knob) **F** right P5 coxa and basis, posterior view (white arrows point to the coxal spine and spur-like hyaline membrane) **G** P5 in posterior view **H** distal part of left P5, posterior view **I** P5, anterior view (without end claw, white arrow points to the distal accessory spine) **J** left P5, anterior view (white arrow points to the hyaline membrane) **K** right P5 Exp-1 and 2, posterior view (white arrows point to the proximal accessory spine and twisted principal lateral spine).

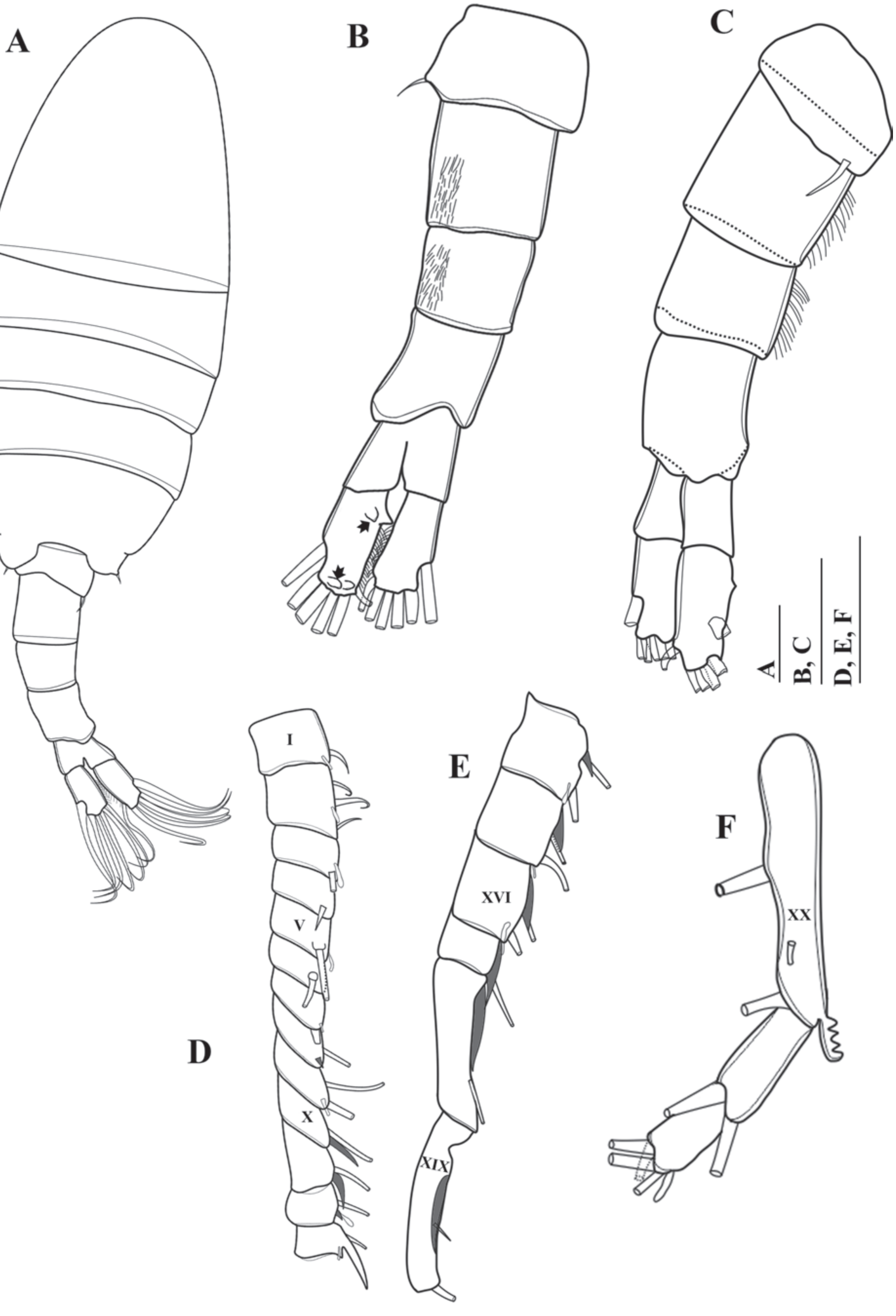

Figure 2. *Mongolodiaptomus phutakaensis* sp. nov., male **A** habitus, dorsal view **B** urosome and caudal rami, ventral view (black arrows indicate chitinous spine and knob on right caudal ramus) **C** urosome and caudal rami, lateral view **D–F** right antennule **D** segments 1–13 **E** segments 14–19 **F** segments 20–22. Scale bar: 100 µm.

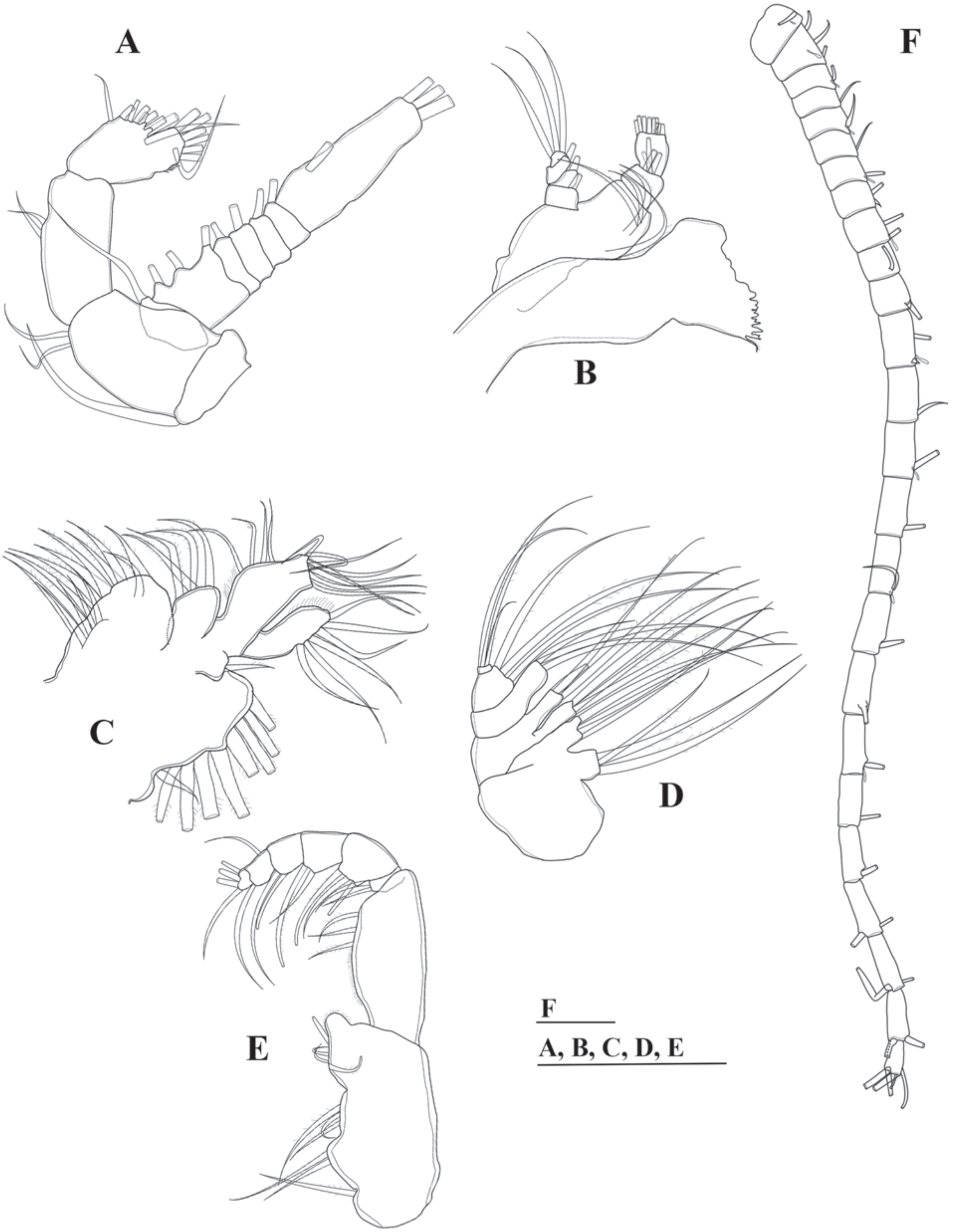

Figure 3. *Mongolodiaptomus phutakaensis* sp. nov., male **A** antenna **B** mandible **C** maxillule **D** maxilla **E** maxilliped **F** left antennule. Scale bar: 100 µm.

Urosome (Figs 1D, 2A–C) with five somites. Genital somite dilated postero-laterally on right side, shorter than wide, with a curved spine on the right posterolateral corner. Urosomites 2–4 approximately as long as wide each.

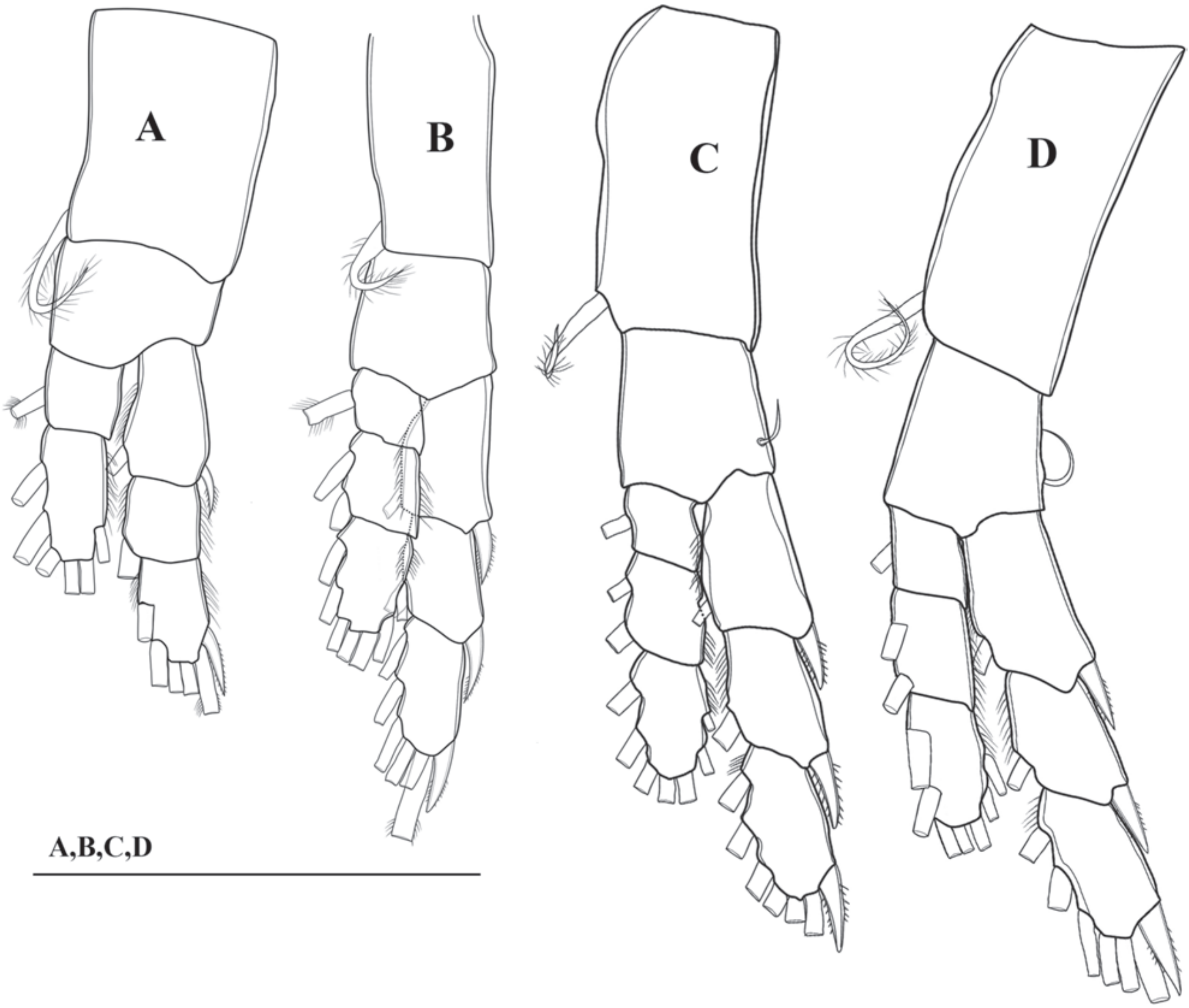

Figure 4. *Mongolodiaptomus phutakaensis* sp. nov., male **A** P1 **B** P2 **C** P3 **D** P4. Scale bar: 100 μm.

Urosomites 2–3 (Figs 1D, 2B, C) with a patch of hairs on right ventral side. Urosomite 4 with expanded right dorso-posterior margin. Anal somite asymmetrical, right side slightly longer than left side (Fig. 2A, C). Caudal rami asymmetrical (Figs 1E, 2A–C), each ramus ~ 2.3 × as long as wide, inner right margin hairy (Figs 1E, 2B). Right ramus armed with four chitinous structures on ventral surface; two sharp tips situated proximally and two semicircular knobs distally (Figs 1E, 2B). Each ramus with six setae (setae II–VII): setae II–VI plumose, anterolateral (II) seta with smooth region on outer margin proximally; terminal setae (setae IV and V) without fracture plane; dorsal seta (VII) articulated, bare, longest.

Antennule: asymmetrical, extending beyond the end of caudal setae. Left antennule (Fig. 3F): 25-segmented. Armature formula as in Table 1. Right antennule (Figs 1C, 2D–F) 22-segmented. Armature formula as in Table 2. External extension on antepenultimate segment (segment XX) short, comb-like, with five or six teeth (Figs 1C, 2F).

Antenna (Fig. 3A): coxa and basis with one and two bare setae on inner distal corner, respectively. Enp two-segmented; Enp-1 with two setae along inner margin; Enp-2 with nine setae along inner margin, seven setae apically; all setae bare. Exp seven-segmented: Exp-1–6 with 1, 3, 1, 1, 1, 1 setae along

Table 1. Armature formula of the left male antennule of *Mongolodiaptomus phutakaensis* sp. nov. The number of setae (Arabic numerals), aesthetascs (ae), and spines (sp) is given. The Roman numerals refer to segment numbers.

	Segment number												
	I	**II**	**III**	**IV**	**V**	**VI**	**VII**	**VIII**	**IX**	**X**	**XI**	**XII**	**XIII**
Number of elements	1+ae	3+ae	1+ae	1	1+ae	1	1+ae	1+sp	2+ae	1	1	1+ae+sp	1
	XIV	**XV**	**XVI**	**XVII**	**XVIII**	**XIX**	**XX**	**XXI**	**XXII**	**XXIII**	**XXIV**	**XXV**	
Number of elements	1+ae	1	1+ae	1	1	1+ae	1	1	2	2	2	4+ae	

Table 2. Armature formula of the right male antennule of *Mongolodiaptomus phutakaensis* sp. nov. The number of setae (Arabic numerals), aesthetascs (ae), and spines (sp) is given. The Roman numerals refer to segment numbers.

	Segment number										
	I	**II**	**III**	**IV**	**V**	**VI**	**VII**	**VIII**	**IX**	**X**	**XI**
Number of elements	1+ae	3+ae	1+ae	1	1+ae	1	1+ae	1+sp	2+ae	1+sp	1+sp
	XII	**XIII**	**XIV**	**XV**	**XVI**	**XVII**	**XVIII**	**XIX**	**XX**	**XXI**	**XXII**
Number of elements	1+ae+sp	1+ae+sp	2+ae+sp	2+ae+sp	2+ae+sp	1+sp	1+sp	2+sp	3+sp	2	4+ae

inner margin; Exp-7 with one seta on inner margin and three setae apically; all setae bare.

Mandible (Fig. 3B): ~ 6 cuspidate teeth dorsally and one seta on coxal gnathobase dorsally. Basis with four bare setae: one proximally and three distally along inner margin. Enp-1 with four setae on inner distal corner. Enp-2 with nine setae apically; two oblique rows of spinules along outer margin. Exp-1–3 each with one seta on inner margin; Exp-4 with three setae apically; all setae bare.

Maxillule (Fig. 3C): praecoxal arthrite with nine strong setae laterally and four slender submarginal setae. Coxal endite with four setae; coxal epipodite with nine setae; two proximal-most setae smaller than others. Two basal endites fused to segment bearing them: proximal and distal endite, each with four setae apically; basal exopodite with one short seta. Enp-1 and Enp-2 each with four setae apically, proximal segment fused to basis. Exp with six bare setae apically.

Maxilla (Fig. 3D): praecoxa fused to coxa. Proximal and distal endites on praecoxa with three setae apically each. Two coxal endites with three setae apically each. Allobasis with three setae apically. Enp two-segmented; with three setae each.

Maxilliped (Fig. 3E): four medial lobes on syncoxa: setal formula 1, 2, 3, 4, respectively; subdistal inner margin produced into a spherical lobe with a patch of tiny spinules. Basis with three setae along medial inner margin, with a row of tiny spinules proximately. Enp six-segmented, with 2, 3, 2, 2, 2, and 4 bare setae, respectively.

P1–P4 (Fig. 4A–D): coxa with a pinnate seta at innermost distal corner. P1 and P2 basis without setae; a reduced bare seta on outer distal margin of P3 and P4. Exp longer than Enp; two-segmented Enp and three-segmented Exp on P1, three-segmented Enp and Exp on P2–P4. Armature formula of P1–P4 as in Table 3.

P5 (Figs 1F–K, 5A, B): intercoxal sclerite trapezoidal, inner distal margin not produced, without any projection. Right P5: coxa with an acute, robust spine on extension on posterior surface, its tip bent inward (Figs 1F, 5A), inner distal margin slightly produced into a rounded lobe. Basis rectangular, ~ 1.5 × as long as wide; with prominent irregular-shaped chitinous process at mid-distal

Table 3. Armature formula of the swimming legs of *Mongolodiaptomus phutakaensis* sp. nov. The number of setae (Arabic numerals) and spines (Roman numerals) is given in the following sequence: outer-inner margin or outer-apical-inner margin.

	Coxa	Basis	Exp			Enp		
			1	2	3	1	2	3
P1	0–1	0–0	I–1	0–1	I–3–2	0–1	1–2–3	----
P2	0–1	0–0	I–1	I–1	I–3–3	0–1	0–2	2–2–3
P3	0–1	1–0	I–1	I–1	I–3–3	0–1	0–2	2–2–3
P4	0–1	1–0	I–1	I–1	I–3–3	0–1	0–2	2–2–3

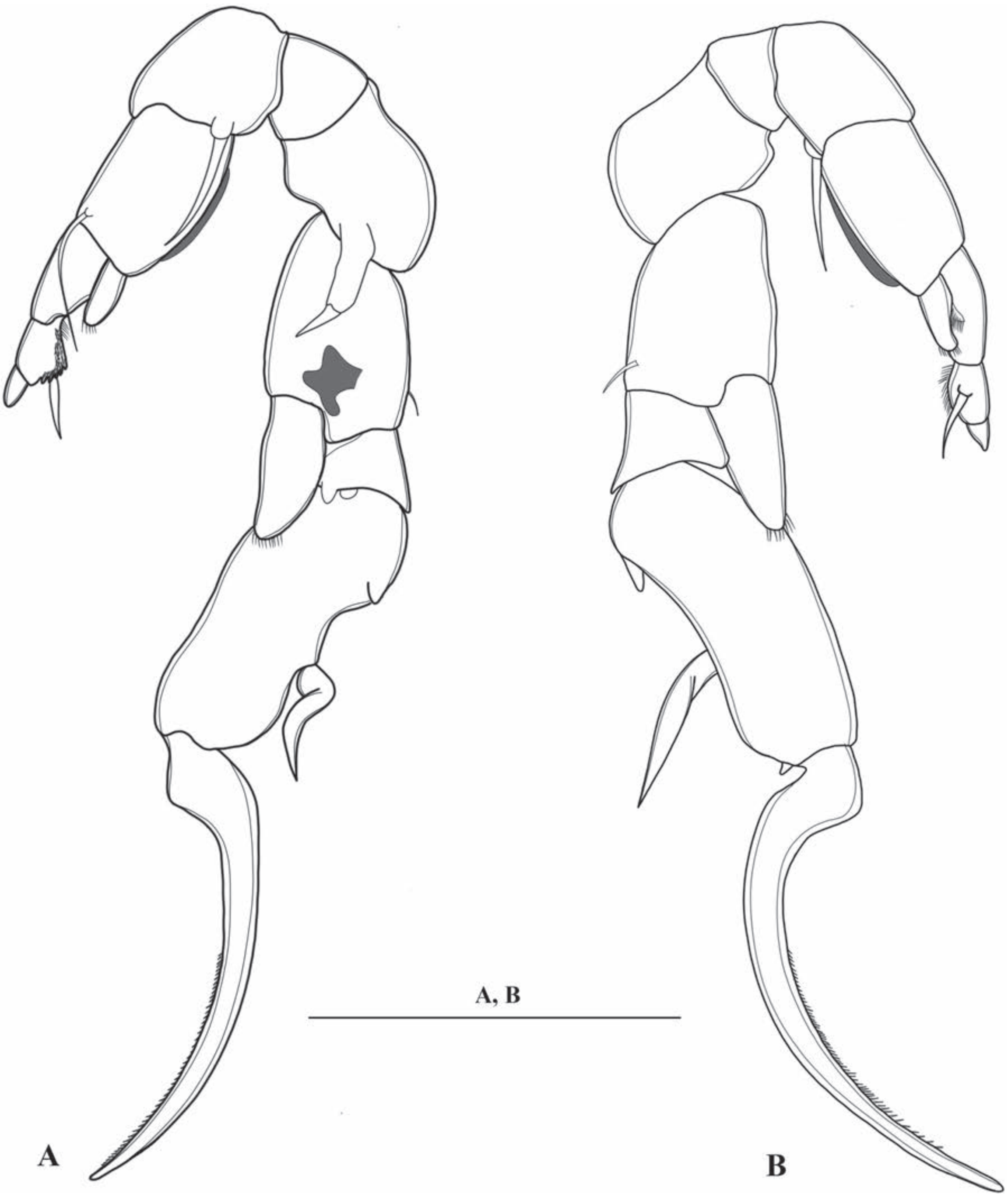

Figure 5. *Mongolodiaptomus phutakaensis* sp. nov., male **A** P5, posterior view **B** P5, anterior view. Scale bar: 200 μm.

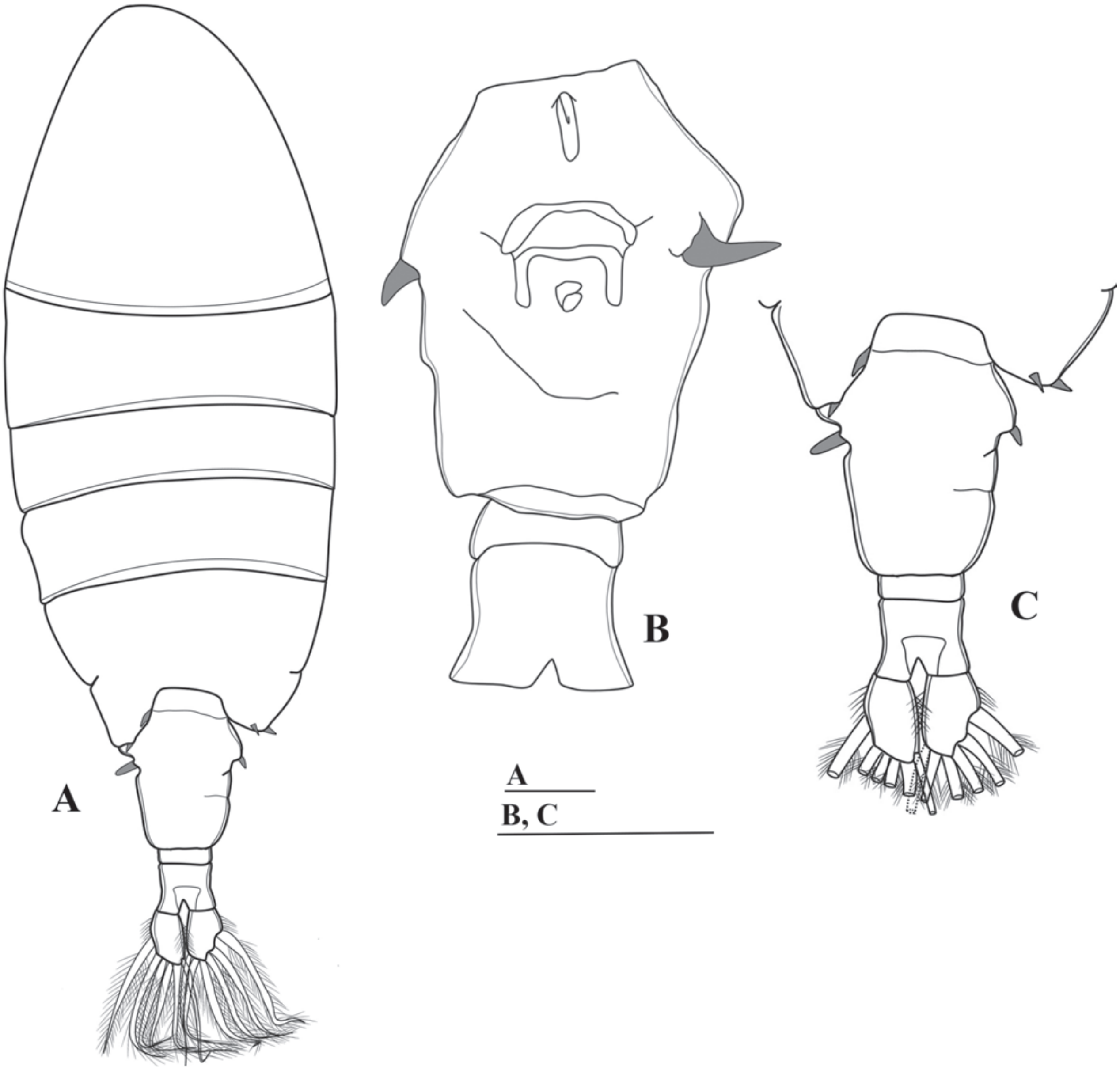

Figure 6. *Mongolodiaptomus phutakaensis* sp. nov., female **A** habitus, dorsal view **B** urosome, ventral view (without caudal rami) **C** pediger 5, urosome, and caudal rami, dorsal view. Scale bar: 100 µm.

length on posterior surface (Figs 1F, 5A); a small seta on distal outer margin; without any hyaline structure. Enp one-segmented, gradually tapering to distal end, tipped with tiny spinules distally; reaching beyond 1/3 of Exp-2. Exp-1 shorter than wide, with two chitinous knobs at distal inner corner; outer distal margin produced into acute tip (Figs 1I, 5A, B). Exp-2 slightly incurved, inner margin convex, outer margin concave, ~ 2.5 × as long as wide, with two small processes proximally and distally; principal lateral spine inserted slightly posterior to mid-length of outer margin. Principal lateral spine (Figs 1K, 5A, B) somewhat slightly curved, robust, ~ 1/2 length of segment. Accessory lateral spine (Figs 1K, 5A, B) minute, distal spine situated close to insertion of end-claw (Figs 1I, 5B), distal accessory spine smaller than proximal one. End-claw sickle-shaped, long, and slender, with a serrate inner margin, with blunt tip; ~ 1.5 × as long as Exp-2.

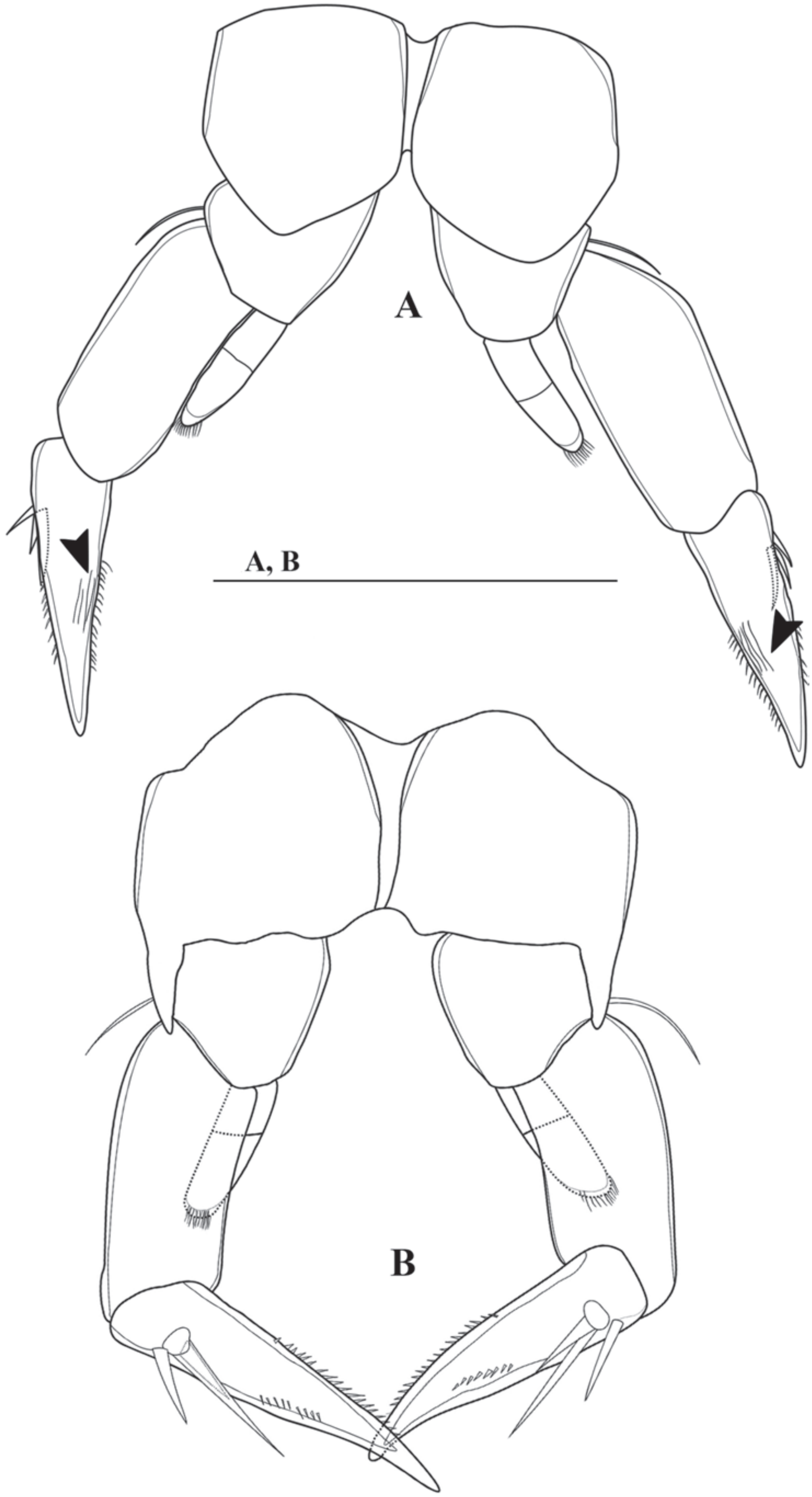

Figure 7. *Mongolodiaptomus phutakaensis* sp. nov., female. P5 **A** P5, posterior view (black arrows indicate longitudinal ridges) **B** P5, anterior view. Scale bar: 100 μm.

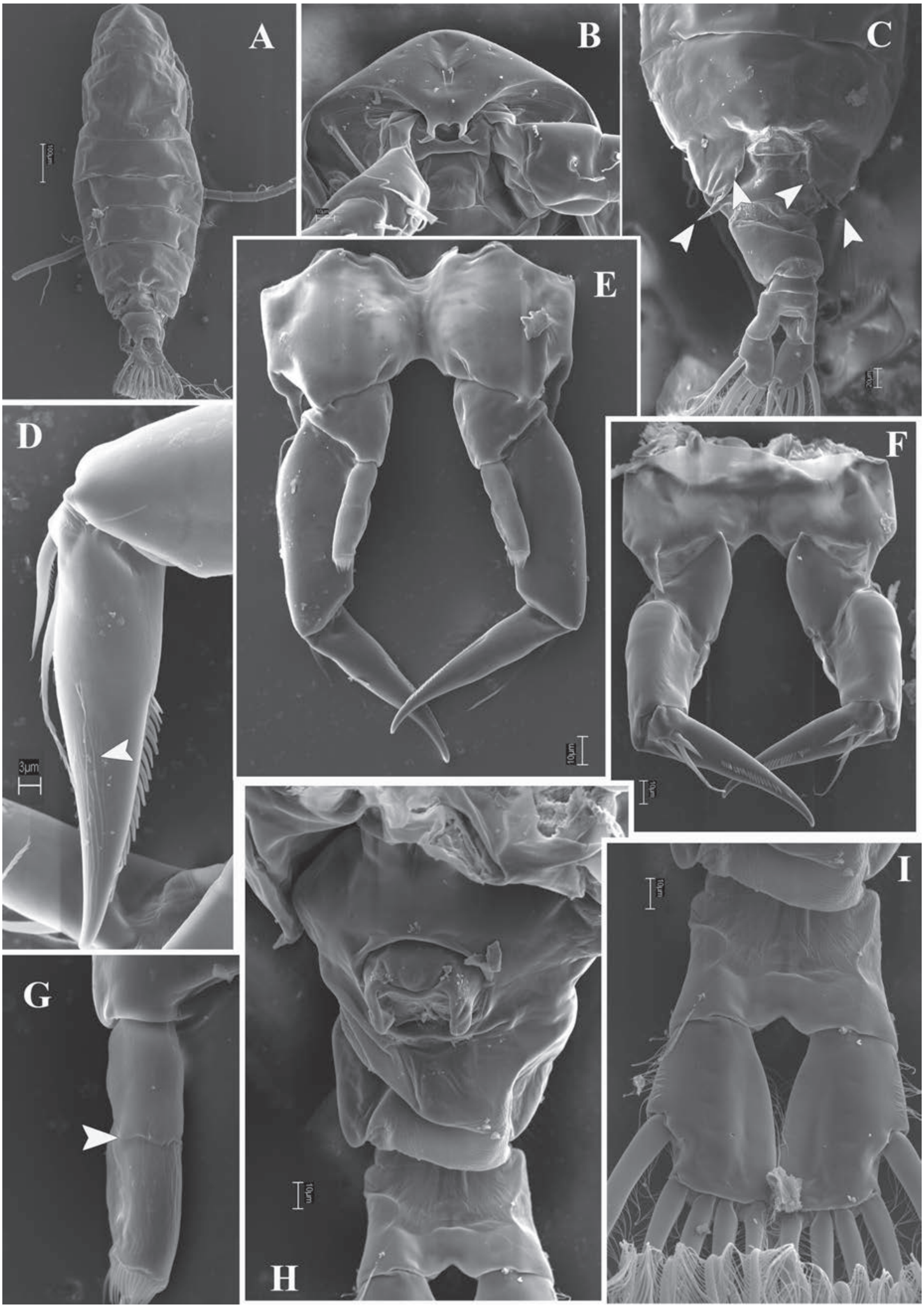

Figure 8. *Mongolodiaptomus phutakaensis* sp. nov., SEM photographs of female **A** habitus, dorsal view **B** rostrum **C** pediger 5 and urosome, dorsal view (white arrows point to spines) **D** P5 Exp-1–2, posterior view (white arrow indicates longitudinal ridges) **E** P5, posterior view **F** P5, anterior view **G** P5 Enp, anterior view (white arrow indicates the border of the two segments) **H** urosome, ventral view **I** caudal rami, ventral view.

Left P5 (Figs 1G–J, 5A, B): coxa with long bare seta on posterior lobe near distal inner corner; longer and slender than spine on right coxal segment. Basis with long narrow hyaline lamella along inner margin (Figs 1J, 5A, B); slender, long posterolateral seta on posterior surface, reaching to middle of Exp-2 segment (Figs 1H, 5A, B). Exp-1 trapezoidal, tapering towards distal end, medial margin concave with a field of setules (Figs 1H, 5A, B). Exp-2 smaller than Exp-1, with inner robust seta, longer than Exp-2; with inner strongly serrate margin (Figs 1H, 5A, B). Exp-3 reduced to thumb-like segment. Enp one-segmented, shorter than Exp-1, with spinulated tip.

Description of adult female. Total body length, measured from anterior margin of rostrum to posterior margin of caudal rami, 1.5–1.7 mm (mean = 1.6 mm, *n* = 10) (Figs 6A, 8A). Prosome: urosome ratio ~ 2.4:1. Prosome similar to that of male. Rostrum fused, symmetrical, acutely pointed (Fig. 8B). Fourth and fifth pedigerous somites incompletely fused. Fifth pediger with sub-asymmetrical posterolateral wings (Figs 6A, C, 8C); right wing rounded, left wing triangular and longer than right wing. Urosome 3-segmented, with asymmetrical genital double-somite (Fig. 6A–C). Genital double-somite longer than urosomite 2, anal somite, and caudal rami combined (Figs 6B, C, 8C); right proximal region slightly curved with small spine. Left side with large dorsolateral spine on sub-proximal region. A pair of gonopores and copulatory pores located centrally at ~ 1/2 length of genital double-somite (Figs 6B, 8H). Urosomite 2 symmetrical, shorter than wide. Anal somite symmetrical, as long as length of caudal rami (Figs 6C, 8I); anal operculum small with convex free margin. Caudal rami parallel, symmetrical; both rami with hairy inner and outer margins (Figs 6C, 8I). All principal caudal setae slightly dilated anteriorly; dorsal seta approximately as long as principal setae.

Antennule symmetrical; left antennule, antenna, mouthparts, and P1–P4 as in male.

P5 symmetrical (Figs 7A, B, 8D–G). Intercoxal sclerite narrow, triangular. Distal outer margin of coxa extended on anterior side into spiniform apophysis reaching distal part of Exp-1 (Fig. 7B). Basis with thin, bare seta on outer margin, reaching ~ 1/4 of Exp-1 length. Exp three-segmented (Figs 7A, B, 8E, F). Exp-1 sub-rectangular, ~ 2.3 × as long as wide. Exp-2 triangular, with a row of strong spinules along both margins; with longitudinal grooves (conveyor canals) on posterior view (Figs 7A, 8D), small outer spine proximally. Exp-3 reduced, represented by a small segment on proximal outer margin of Exp-2, armed with two unequal spiniform setae apically. Enp two-segmented (Fig. 8G), subconical, ~ 2/3 as long as Exp-1; with obliquely truncate and finely spinulose apex.

Etymology. The specific epithet is derived from Kok Phutaka, reflecting the name of the area in which the type locality is located. The name is an adjective in the nominative singular, gender feminine.

Distribution. At present, the new species has been found only in the type locality, a natural swamp in Kok Phutaka community forest in Khon Kaen Province, northeast Thailand. It co-exists with other calanoids, *Phyllodiaptomus praedictus* Ranga Reddy & Dumont, 1994 and *Mongolodiaptomus rarus* (Ranga Reddy, Dumont, & Sanoamuang, 1998). The other artificial ponds nearby also contained *M. botulifer* (Kiefer, 1974). Representatives of the new species were observed only once out of approximately 5,000 sampled sites throughout Thailand. Currently, this species is endemic to Thailand. The new species is present in only one locality throughout the year, and ecological parameters varied in a temperature range of 25.0–32.5 °C (mean = 29.13 °C), conductivity 74–495 µS cm^{-1} (mean = 201.25 µS cm^{-1}), and pH 5.16–10.03 (mean = 7.66).

Key to the species of *Mongolodiaptomus* Kiefer, 1937

Males:

1 Spinous process on antepenultimate segment of right antennule is slender and smooth **2**
– Spinous process on antepenultimate segment of right antennule is serrated or comb-like **4**
2 Right P5 Enp conical, proximal part very broad and swollen, distal part tapering, extended to 1/3 length of inner margin of Exp-2 .... ***M. birulai***
– Right P5 Enp large, conical, reaching to nearly 3/4 length of inner margin of Exp-2 .... **3**
3 Right P5 basis with triangular hyaline membrane on inner margin .... ***M. malaindosinensis***
– Right P5 basis with spherical hyaline membrane on inner margin .... ***M. botulifer***
4 P5 intercoxal plate with outgrowth on distal margin **5**
– P5 intercoxal plate without outgrowth on distal margin **8**
5 Principal lateral spine on right P5 Exp-2 straight **6**
– Principal lateral spine on right P5 Exp-2 curved and twisted **7**
6 P5 intercoxal plate with rounded lobe on distal margin .... ***M. pectinidactylus***
– P5 intercoxal plate with spine-like lobe on distal margin .... ***M. uenoi***
7 Spine-like process on P5 intercoxal plate with 1 strong spine .... ***M. mekongensis***
– Spine-like process on P5 intercoxal plate with 2 strong spines .... ***M. loeiensis***
8 Right P5 basis with hyaline membrane on inner margin ... ***M. mephistopheles***
– Right P5 basis without hyaline membrane on inner margin **9**
9 Left P5 basis with hyaline membrane on inner margin **10**
– Left P5 basis without hyaline membrane on inner margin **11**
10 Principal lateral spine on right P5 Exp-2 straight .... ***M. dumonti***
– Principal lateral spine on right P5 Exp-2 bent .... ***M. calcarus***
– Principal lateral spine on right P5 Exp-2 bent and twisted .... ***M. phutakaensis* sp. nov.**
11 Right P5 basis with chitinous spur on posterior surface .... ***M. rarus***
– Right P5 basis without any process on posterior surface .... ***M. gladiolus***

Females:

1 P5 Enp 1-segmented **2**
– P5 Enp 2-segmented **7**
2 Genital double-somite with postero-laterally oriented conical outgrowth on proximal right side **3**
– Genital double-somite without postero-laterally oriented outgrowth on proximal right side **6**

3 Left spine inserted on lobe-like process of genital double-somite .... ***M. gladiolus***
– Left spine inserted directly on genital double-somite................................**4**
4 Genital double-somite with expanded right distal corner..........................**5**
– Genital double-somite without expanded right distal corner .... ***M. uenoi***
5 P5 with long Enp, reaching beyond distal end of Exp-1... ***M. malaindosinensis***
– P5 with short Enp, not reaching distal end of Exp-1 (2/3 of Exp-1 length) .. .. ***M. botulifer***
6 Genital double-somite with longer spine on left side compared to right side... ***M. mephistopheles***
7 P5 Exp-3 absent.. ***M. birulai***
– P5 Exp-3 present **8**
8 Genital double-somite with postero-laterally oriented outgrowth on proximal right side **9**
– Genital double-somite without postero-laterally oriented outgrowth on proximal right side..**11**
9 Genital double-somite with hyaline membrane along inner margin on right side... ***M. rarus***
– Genital double-somite without hyaline membrane along inner margin on right side **10**
10 Lateral wings on Pdg 5 (left: right) symmetrical .... ***M. loeiensis***
– Lateral wings on Pdg 5 (left: right) asymmetrical .... ***M. mekongensis***
11 Spine on left side of genital double-somite similar in size to spine on right side.. ***M. pectinidactylus***
– Spine on left side of genital double-somite larger than spine on right side **12**
12 Genital double-somite somewhat rectangular in shape .... ***M. dumonti***
– Genital double-somite with swollen proximal part and distal part tapering to end **13**
13 Lateral wings on Pdg 5 (left: right) sub-symmetrical .... ***M. calcarus***
– Lateral wings on Pdg 5 (left: right) asymmetrical.... ***M. phutakaensis* sp. nov.**

Discussion

Mongolodiaptomus phutakaensis sp. nov. exhibits the distinguishing features of the genus, as described in the updated generic traits outlined by Ranga Reddy et al. (2000). For the males, the right P5 Exp-2 carries the characteristic three lateral spines, one principal spine inserted at the middle of the segment on the outer margin, and two accessory spines located proximally and distally. A comparison with its congeners shows that *M. phutakaensis* sp. nov. resembles the two recently described taxa from the Mekong region: *M. loeiensis* Watiroyram & Sanoamuang, 2017 and *M. mekongensis* Sanoamuang & Watiroyram, 2018, respectively. These three closely related species can be distinguished from the other congeners by the unique shape of the male right P5 Exp-2; the inner margin is slightly incurved, the proximal and distal parts of the outer margin are enlarged, and the principal lateral spine is bent and twisted. The antepenultimate segment of the male right antennule of all three related species has a comb-like process. Other similarities among the three closely related species are the male right P5 has a spur-like or irregular process on the basis, the coxa has a strong spine, the Exp-1 has an acute process on the outer distal margin, the left P5 has a hyaline lamella on the inner margin of the basis, and the strong spinules along the inner margin of the Exp-2. The female of the new species shares similarities with *M. loeiensis* and *M. mekongensis* by having two-segmented P1 Enp.

The new species can be differentiated from *M. mekongensis* and *M. loeiensis* by the characteristics of the male caudal rami and P5 (Table 4): the right caudal ramus of *M. phutakaensis* sp. nov. has four ventral chitinous processes (two proximal spine-like processes and two distal semi-circular knobs), while *M. mekongensis* has one spine-like process and one semi-circular knob, and *M. loeiensis* has two spine-like processes and one semi-circular knob. The intercoxal plate of the new species is slightly produced distally and without any spine, but it is well-produced with one strong spine and two spines on its distal margin in *M. mekongensis* and *M. loeiensis*, respectively. The right P5 basis in males lacks a hyaline membrane on the inner margin in the new species, which is present in *M. mekongensis* and *M. loeiensis*. The male P5 has a distinct mid-distal spur-like chitinous process on the posterior surface in the new species versus a small chitinous prominence on the same position in *M. mekongensis* and *M. loeiensis*. The left P5 basis has a thin, longer hyaline lamella on the inner margin in the new species but is somewhat shorter in *M. mekongensis* and *M. loeiensis*. Only *M. mekongensis* has an obviously longitudinal chitinous ridge on the posterior side of this segment.

In the females, the left wing of Pdg 5 is longer than the right one in the new species and *M. mekongensis*, whereas both wings are symmetrical in *M. loeiensis*. The genital double-somite is only slightly asymmetrical in the new species but pronounced in *M. mekongensis* and *M. loeiensis*, with well-developed posterolateral outgrowth on the right side. The P5 Exp-2 has longitudinal grooves (conveyor canals) on the posterior view in the new species and *M. mekongensis*, but these grooves are absent in *M. loeiensis*.

Table 4. The morphological characteristics and distribution of the closely related *Mongolodiaptomus* species: *M. loeiensis*, *M. mekongensis*, and *M. phutakaensis* sp. nov.

Characters and distribution	***M. loeiensis***	***M. mekongensis***	***M. phutakaensis* sp. nov.**
MALE			
Chitinous teeth on ventral surface of the right caudal ramus	Two	One	Two
Chitinous (semicircular) knob on ventral surface of the right caudal ramus	One	One	Two
Spine-like process on the P5 intercoxal plate	Two strong spines	One strong spine	Absent
Right P5 basis with inner hyaline membrane	Yes	Yes	No
Left P5 basis with longitudinal chitinous ridge	No	Yes	No
Left P5 basis with extra-long posterolateral seta on posterior surface (longer than Exp-1 segment)	No	No	Yes
FEMALE			
Lateral wings on Pdg 5 (left: right)	Symmetrical	Asymmetrical	Asymmetrical
Right side of genital double-somite with well-developed posterolateral process	Yes	Yes	No
P5 Exp-2 with longitudinal grooves (conveyor canals) on posterior view	No	Yes	Yes
DISTRIBUTION	Thailand endemic (a temporary pond in Loei Province, northeast Thailand)	Mekong region (temporary-water habitats in northeast Thailand, Laos, Cambodia, Vietnam, and South China)	Thailand endemic (a natural swamp in Khon Kaen Province, northeast Thailand)

Review of taxonomic characters of *Mongolodiaptomus* species

Currently, 13 species of the genus *Mongolodiaptomus* have been reported worldwide (see Table 2 in Sanoamuang and Watiroyram 2018; Sanoamuang and Dabseepai 2021; this study). This number does not include *Mongolodiaptomus mariadvigae* (Brehm, 1921) and *M. formosanus* Kiefer, 1937. According to Li et al. (2018) and Walter and Boxshall (2024), *M. mariadvigae* has been transferred to *Neutrodiaptomus mariadvigae* (Brehm, 1921). For the status of *M. formosanus*, several scientists from China (Shen et al. 1979; Li et al. 2018), Taiwan (Young and Shih 2011; Young et al. 2013), and Vietnam (Tran et al. 2016) considered it a synonym of *M. birulai*. Thus, in this paper, we treat *M. mariadvigae* as a member of *Neutrodiaptomus* and *M. formosanus* as a synonym of *M. birulai.* Another doubtful taxon, *M. malaindosinensis*, is considered a synonym of *M. botulifer* by Ranga Reddy et al. (2000), but after detailed examinations of specimens from Thailand, Cambodia, and Vietnam, we considered *M. malaindosinensis* as a distinct species (Sanoamuang 2002; Watiroyram and Sanoamuang 2017; Boonmak et al. 2018; Sanoamuang and Watiroyram 2018, 2023; Sanoamuang and Dabseepai 2021; Boonmak and Sanoamuang 2022; Chaicharoen and Sanoamuang 2022).

A comparison of male and female morphological characters of the *Mongolodiaptomus* species is presented in Tables 5–6. The prominent morphological characteristics of this genus are reviewed briefly hereafter.

Antennule

While the setal armature of the female antennules remains conservative among species, the characteristics of the male grasping antennules serve to identify species. The degree of spine development on segments 8 and 15 is important at the species level; segment 16 bears a spinous projection in eight species but is absent in five species (Table 5). The spinous process on the antepenultimate segment of most species is comb-like, but it is long and slender in three species (*M. birulai*, *M. botulifer*, and *M. malaindosinensis*). However, the shape and size of the comb-like projections are different across the species (Table 5).

Lateral wings of fifth pediger

In the female, the shape and size of the lateral wings and the position of the inner (posterior) spine on either wing are of significant taxonomic value. In most species, both left and right wings are moderate in size and moderately asymmetrical, only four (*M. calcarus*, *M. dumonti*, *M. loeiensis*, and *M. pectinidactylus*) have symmetrical wings (Table 6).

Urosome

The relative lengths of urosomites and caudal rami, as well as the structural details of the female's genital double-somite, are highly diagnostic. The genital double-somite's relative length varies greatly between species. It is strikingly asymmetrical. In five species (*M. birulai*, *M. botulifer*, *M. loeiensis*, *M. mekongensis*, and *M. uenoi*), the right proximal region has a well-developed posterolat-

Table 5. Comparison of male morphological characters of *Mongolodiaptomus* species (? means unknown or doubtful).

Male characters	*M. birulai*	*M. botulifer*	*M. malaindosinensis*	*M. gladiolus*	*M. calcarus*	*M. rarus*	*M. dumonti*	*M. mephistopheles*	*M. uenoi*	*M. pectinidactylus*	*M. loeiensis*	*M. mekongensis*	*M. phutakaensis*
Right antennule													
- segment 16 with spine		+		+	+		+	+	+			+	+
- segment 16 without spine	+		+			+				+	+		
- spinous process on antepenultimate segment long and slender	+	+	+										
- spinous process on antepenultimate segment comb-like				+	+	+	+	+	+	+	+	+	+
Urosomites 2 and 3													
- with ventral hairs	+	+	+	?	+		+		+	+	+	+	+
- without ventral hairs				?		+		+					
Right caudal ramus													
- with chitinous structure ventrally	+	+	+		+	+	+	+	+		+	+	+
- without chitinous structures ventrally				+						+			
Right P5													
- intercoxal plate produced	+	+	+						+	+	+	+	
- intercoxal plate unproduced				+	+	+	+	+					+
- basis with inner hyaline lamella	+	+	+			+		+	+	+	+	+	
- basis without inner hyaline lamella				+	+		+						+
- basis with spurlike process					+	+	+			+	+	+	+
- basis without spurlike process	+	+	+	+				+	+				
- Exp-1 with pointed spinous process at distal outer corner		+	+					+	+		+	+	+
- Exp-1 with blunt spinous process at distal outer corner	+			+	+	+	+			+			
- principal lateral spine of Exp-2 located at or close to mid-length of outer margin	+	+	+	+	+	+		+	+	+	+	+	+
- principal lateral spine of Exp-2 located at ¾ length of outer margin							+						
- principal lateral spine of Exp-2 straight				+		+	+		+	+			
- principal lateral spine of Exp-2 curved	+	+	+		+			+					
- principal lateral spine of Exp-2 curved and twisted											+	+	+
- Enp: obovate shaped, ~ ¾ length of Exp-2 segment		+	+										
- Enp: conical shaped, ≤ ½ length of Exp-2 segment	+			+	+	+	+	+	+	+	+	+	+
Left P5													
- basis with inner hyaline lamella or knoblike outgrowth	+	+	+		+	+	+	+	+	+	+	+	+
- basis without inner hyaline lamella				+									
- Enp one-segmented	+			+	+	+	+	+	+	+	+		+
- Enp two-segmented		+	+									+	

eral process, while in the other five species (*M. gladiolus*, *M. malaindosinensis*, *M. pectinidactylus*, *M. phutakaensis* sp. nov., and *M. rarus*), it has a moderately developed posterolateral process. In the male, most species have ventral hairs on urosomites 2 and 3, but only *M. mephistopheles* and *M. rarus* do not have ventral hairs on those segments. In general, the male right caudal ramus of most species is armed with one or two chitinous structures and sometimes with two minute semicircular knobs ventrally; only *M. gladiolus* and *M. pectinidactylus* do not have such structures.

Table 6. Comparison of female morphological characters of *Mongolodiaptomus* species (? means unknown or doubtful).

Female characters	***M. birulai***	***M. botulifer***	***M. malaindosinensis***	***M. gladiolus***	***M. calcarus***	***M. rarus***	***M. dumonti***	***M. mephistopheles***	***M. uenoi***	***M. pectinidactylus***	***M. loeiensis***	***M. mekongensis***	***M. phutakaensis***
Lateral wings on Pdg 5 (left: right)													
- symmetrical					+		+			+	+		
- asymmetrical	+	+	+	+		+		+	+			+	+
Genital double-somite													
- right proximal region with well-developed posterolateral process	+	+							+		+	+	
- right proximal region with moderately developed posterolateral process			+	+		+				+			+
- right proximal region without posterolateral process					+		+	+					
- right distal corner expanded		+	+				+						
- right distal corner not expanded	+			+	+	+		+	+	+	+	+	+
P5													
- seta on basis longer than ½ length of Exp-1		+	+		+	+	+	+	+	+	+	+	
- seta on basis shorter than ½ length of Exp-1	+			+									+
- Exp-3 inarticulate (fused with Exp-2)		+		+					+				
- Exp-3 distinct	?		+		+	+	+	?		+	+	+	+
- Enp one-segmented		+	+	+				+	+				
- Enp two-segmented	+				+	+	+			+	+	+	+

Male fifth leg (P5)

The interspecific differences in the male P5 are well pronounced in this genus. On the right and left P5, the shape and structure of the Exp-2 and of the Enp are different in most species (Table 5). On the right P5, the inner coxal plate is uniquely produced in six species, particularly with one and two strong spines in *M. mekongensis* and *M. loeiensis*, respectively. The basis in most species has inner hyaline lamella, except in *M. calcarus*, *M. dumonti*, *M. gladiolus*, and *M. phutakaensis* sp. nov. Furthermore, another distinctive characteristic of the genus is the presence of a spur-like process at the mid-distal margin of the posterior surface of the basis in seven species (Table 5). In seven species, the Exp-1 of the right P5 has a pointed spinous process in the distal outer corner. The principal lateral spine of Exp-2 is located at or close to mid-length of the outer margin in all species except *M. dumonti*, where such a spine is located at 3/4 length of the outer margin. The principal lateral spine of Exp-2 is either straight, curved, or twisted. On the left P5, the basis has either inner hyaline lamella or knoblike outgrowth in all but *M. gladiolus*. The Enp is one-segmented except for *M. botulifer*, *M. malaindosinensis*, and *M. mekongensis*.

Female fifth leg

The seta on basis is longer than ½ length of Exp-1 in most species except *M. birulai*, *M. gladiolus*, and *M. phutakaensis* sp. nov. The Exp-3 is distinct in all but *M. botulifer*, *M. gladiolus*, and *M. uenoi*. The Enp are two-segmented except for *M. botulifer*, *M. gladiolus*, *M. malaindosinensis*, *M. mephistopheles*, and *M. uenoi*.

Interspecies relationships

Recently, Sanoamuang and Watiroyram (2018) divided the known species of *Mongolodiaptomus* based on the male characters into three species groups. Hereafter, an amended proposal is presented to include all known species of *Mongolodiaptomus* in four groups:

1. The *birulai* species group includes *M. botulifer*, *M. birulai*, and *M. malaindosinensis* and exhibits the following characteristics: (1) the spinous process on the antepenultimate segment of the right antennule is slender and smooth; (2) the right P5 basis has hyaline lamella on the inner margin but without chitinous prominence; (3) the inner distal margin of the P5 intercoxal sclerite is produced into a protruded plate; and (4) the right caudal ramus has ventral chitinous processes.
2. The *gladiolus* species group includes *M. calcarus*, *M. dumonti*, *M. gladiolus*, and *M. rarus* and exhibits the following characteristics: (1) the spinous process on the antepenultimate segment of the right antennule is comb-like; (2) the right P5 basis has no inner hyaline membrane; (3) the inner distal margin of the P5 intercoxal plate is not produced into a protruded plate; and (4) the right P5 Exp-1 has no acute process on the outer distal margin.
3. The *mephistopheles* species group includes *M. mephistopheles*, *M. uenoi*, and *M. pectinidactylus* and exhibits the following characteristics: (1) the spinous process on the antepenultimate segment of the right antennule is comb-like; (2) the male right P5 Exp-2 has a straight or bent principal lateral spine; and (3) both the right and left basis have an inner hyaline membrane.
4. The *loeiensis* species group includes *M. loeiensis*, *M. mekongensis*, and *M. phutakaensis* sp. nov. and exhibits the following characteristics: (1) the spinous process on the antepenultimate segment of the right antennule is comb-like; (2) the male right P5 Exp-2 has enlarged proximal and distal parts of the outer margin and a bent and twisted principal lateral spine; (3) the right P5 coxa has a strong spine; (4) the left P5 basis has an inner hyaline lamella; and (5) the right P5 Exp-1 has an acute process on the outer distal margin.

Biogeography

Regarding distribution records of *Mongolodiaptomus* species, *M. phutakaensis* sp. nov. is the 13th member of the genus and the 10th taxon recorded in Thailand. Only three species (*M. birulai*, *M. gladiolus*, and *M. mephistopheles*) among the 13 species recorded across Asia remain unrecorded in Thailand (Sanoamuang and Dabseepai 2021). Previous records of *M. mephistopheles* by Bricker et al. (1978) and Boonsom (1984) from Thailand were actually misidentified specimens of *M. calcarus* (Ranga Reddy et al. 2000). Thailand is the most species-rich country with *Mongolodiaptomus* in Southeast Asia. From Vietnam are known seven valid species (Boonmak and Sanoamuang 2022), plus two unnamed species (Tran et al. 2016). China has six species (Li et al. 2018), including a newly recorded taxon, *M. mekongensis*, from Hainan Island by Wei et al. (2023). Cambodia, and Malaysia have five species each (Sanoamuang and

Watiroyram 2018; Chaicharoen and Sanoamuang 2022). Laos has four species, while Indonesia and Taiwan have three species each, whereas Singapore and the Philippines both have only one species each (Lopez et al. 2017; Sanoamuang and Watiroyram 2018).

Most species are currently restricted to Southeast Asia; only six species have also been recorded outside the area, including *M. birulai*, *M. calcarus*, *M. gladiolus*, *M. mekongensis*, *M. pectinidactylus*, and *M. uenoi* (Ranga Reddy et al. 1998, 2000; Sanoamuang 2001; Alekseev et al. 2013; Tran et al. 2016; Lopez et al. 2017). Therefore, the distribution of these six species extends from Southeast Asia to South China. *M. birulai* has the widest distribution, occurring from Vietnam upwards to North China, including Taiwan (Young and Shih 2011; Tran et al. 2016; Li et al. 2018). *M. mekongensis* is a common species in the Mekong region and has been found in Thailand, Laos, Cambodia, Vietnam, and South China (Table 4). *M. botulifer* and *M. malaindosinensis* have been found only in Southeast Asia (Boonmak et al. 2018). *M. dumonti*, and *M. mephistopheles*, are confined in distribution to the Mekong region, and Malay Archipelago, respectively. Three species (*M. loeiensis*, and *M. phutakaensis* sp. nov., and *M. rarus*) are currently endemic to Thailand; for more details see also Table 2 in Sanoamuang and Watiroyram (2018).

In Thailand, the most widespread *Mongolodiaptomus* species are *M. botulifer* and *M. calcarus*. Both species live in both temporary and permanent water bodies throughout the country and occur throughout the year. *M. malaindosinensis* is moderately common and has been recorded throughout the country. *M. mekongensis* is widely distributed in the Mun River Basin, a tributary of the Mekong River, and mostly occurs in temporary water bodies. *M. dumonti*, *M. rarus*, and *M. uenoi*, are uncommon. *M. rarus* has been found only in temporary water bodies. In contrast, *M. pectinidactylus* is rare and has been reported only at two temporary water bodies (Sanoamuang 2002). *M. loeiensis* and *M. phutakaensis* sp. nov. are extremely rare and, to date, have been found only in a single locality each (Watiroyram and Sanoamuang 2017; this study).

Acknowledgements

The authors highly appreciate Anton Brancelj, Manuel Elías Gutierrez, and Maria Cristina Bruno for their constructive comments and suggestions. We would like to thank Prapatsorn Dabseepai for collecting samples in the field.

Additional information

Conflict of interest

The authors have declared that no competing interests exist.

Ethical statement

No ethical statement was reported.

Funding

This research is funded by National Research Council of Thailand (NRCT) (N34E670115), and Centre of Excellence on Biodiversity (MHESI) (BDC-PG1-167005).

Author contributions

LS organized and provided funding for the sampling trips, conceptualization, methodology, identifying specimens, reviewing literature, writing, and editing the final manuscript, and revising the manuscript. KK reviews the literature, photographs, and figures' preparation and writes the first draft of the manuscript.

Author ORCIDs

Laorsri Sanoamuang https://orcid.org/0000-0003-0377-1225
Kamonwan Koompoot https://orcid.org/0009-0005-2116-5191

Data availability

All of the data that support the findings of this study are available in the main text.

References

Alekseev VR, Haffner DG, Vaillant JJ, Yusoff FM (2013) Cyclopoid and calanoid copepod biodiversity in Indonesia. Journal of Limnology 72(s2): 245–274. https://doi.org/10.4081/jlimnol.2013.s2.e12

Baird W (1850) The natural history of the British Entomostraca: I–VII. The Ray Society, London, 364 pp. https://doi.org/10.5962/bhl.title.1807

Boonmak P, Sanoamuang L (2022) Diversity of freshwater calanoid copepods (Crustacea: Copepoda: Calanoida) in Southern Vietnam with an updated checklist for the country. Diversity 14(7): 523. https://doi.org/10.3390/d14070523

Boonmak P, Liu X, Ban S, Sanoamuang L (2018) Effects of different algal diets and carbon supplies on larval development, growth and survival in the freshwater copepod *Mongolodiaptomus malaindosinensis* (Copepoda: Calanoida). Plankton & Benthos Research 13(4): 163–172. https://doi.org/10.3800/pbr.13.163

Boonsom J (1984) The freshwater zooplankton of Thailand (Rotifera and Crustacea). Hydrobiologia 113(1): 223–229. https://doi.org/10.1007/BF00026610

Brehm V (1921) Diagnose neuer Entomostraken. Sitzungsberichte der Akademie der Wissenschaften Wien (Mathematisch-naturwissenschaftliche Klasse) 20: 194–196.

Bricker KS, Wongrat L, Gannon JE (1978) Composition and distribution of Crustacean plankton in twelve inland water bodies of Thailand. Journal of Fisheries and Environment 10: 1–14.

Chaicharoen C, Sanoamuang L (2022) Distribution and diversity of diaptomid copepods in freshwater habitats of Cambodia (Crustacea: Copepoda: Calanoida: Diaptomidae). Diversity 14(11): 903. https://doi.org/10.3390/d14110903

Huys R, Boxshall GA (1991) Copepod evolution. The Ray Society, London, 468 pp.

Kiefer F (1932) Zwei neue Diaptomiden (Copepoda, Calanoida) aus Indien. Zoologischer Anzeiger 100: 265–270.

Kiefer F (1936) Indische Ruderfusskrebse (Crustacea, Copepoda). III. Zoologischer Anzeiger 113(11/12): 321–325.

Kiefer F (1937) Süsswassercopepoden aus Ostasien. II. Neue Diaptomiden und Cyclopiden von der Insel Formosa. Zoologischer Anzeiger 119: 58–64.

Kiefer F (1974) Eine neue Diaptomidenart aus Malaysia (Crustacea, Copepoda, Calanoida). Zoologischer Anzeiger 192(5/6): 420–424.

Lai HC, Fernando CH (1978) Redescription of *Neodiaptomus botulifer* Kiefer and one of its related species (Calanoida, Copepoda). Hydrobiologia 59(3): 229–235. https://doi.org/10.1007/BF00036502

Li H, Dumont HJ, Han BP, Lin Q (2018) Updated checklist and distribution of the diaptomid copepods (Copepoda, Calanoida, Diaptomidae) of China. Crustaceana 91(3): 335–352. https://doi.org/10.1163/15685403-00003752

Lopez MLD, Pascual JAF, Dela Paz ESP, Rizo EZC, Tordesillas DT, Guinto SK, Han B, Dumont HJ, Mamaril AC, Papa RDS (2017) Annotated checklist and insular distribution of freshwater microcrustaceans (Copepoda: Calanoida and Cyclopoida; Cladocera: Anomopoda & Ctenopoda in the Philippines. The Raffles Bulletin of Zoology 65: 623–654.

Ranga Reddy Y, Sanoamuang L, Dumont HJ (1998) A note on the Diaptomidae of Thailand, including redescription of three species and description of a new species (Copepoda, Calanoida). Hydrobiologia 361(1/3): 201–223. https://doi.org/10.1023/A:1003135200559

Ranga Reddy Y, Sanoamuang L, Dumont HJ (2000) Amended delimitation of *Mongolodiaptomus* against *Neodiaptomus* and *Allodiaptomus* and redescription of the little known *Mongolodiaptomus uenoi* (Kikuchi, 1936) from Thailand (Copepoda: Calanoida: Diaptomidae). Hydrobiologia 418(1): 99–109. https://doi.org/10.1023/A:1003859908612

Sanoamuang L (1999) Species composition and distribution of freshwater Calanoida and Cyclopoida (Copepoda) of north-east Thailand. In: Schram FR, Klein JVC (Eds) Crustaceans and Biodiversity Crisis. Brill Academic Publishers, Leiden, 217–230. https://doi.org/10.1163/9789004630543_018

Sanoamuang L (2001) *Mongolodiaptomus dumonti* n. sp., a new freshwater copepod (Calanoida, Diaptomidae) from Thailand. Hydrobiologia 448(1/3): 41–52. https://doi.org/10.1023/A:1017526018189

Sanoamuang L (2002) Freshwater Zooplankton: Calanoid Copepods in Thailand. Klangnanatham Publishers (Khon Kaen), Thailand, 159 pp.

Sanoamuang L, Dabseepai P (2021) Diversity, distribution, and habitat occurrence of the diaptomid copepods (Crustacea: Copepoda: Diaptomidae) in freshwater ecosystems of Thailand. Water 13(17): 2381. https://doi.org/10.3390/w13172381

Sanoamuang L, Watiroyram S (2018) *Mongolodiaptomus mekongensis*, a new species of copepod (Copepoda, Calanoida, Diaptomidae) from temporary waters in the floodplain of the lower Mekong River Basin. The Raffles Bulletin of Zoology 66: 782–796.

Sanoamuang L, Watiroyram S (2023) *Phyllodiaptomus parachristineae*, a new species of copepod (Copepoda, Calanoida, Diaptomidae) from the floodplain of the lower Mekong River Basin in Thailand and Cambodia. ZooKeys 1168: 403–424. https://doi.org/10.3897/zookeys.1168.104636

Sars GO (1903) An account of the Crustacea of Norway, with short descriptions and figures of all the species: IV. Copepoda Calanoida. Bergens Museum: Bergen. 171 pp.

Shen CJ, Tai AY, Zhang ZC, Li ZY, Song DX, Song YC, Chen GX (1979) Fauna Sinica. Crustacea, Freshwater Copepoda. Science Press, Beijing 450 pp.

Tran DL, Dang NT, Ho TH (2016) An annotated checklist of the family Diaptomidae Sars, 1903 (Copepoda, Calanoida) in Vietnam. Tap Chi Sinh Hoc 38: 384–399.

Walter TC, Boxshall G (2024) World of Copepods Database. *Mongolodiaptomus* Kiefer, 1937. https://www.marinespecies.org/copepoda/aphia.php?p=taxdetails&id=347524 on 2024-04-17

Watiroyram S, Sanoamuang L (2017) A new species of *Mongolodiaptomus* Kiefer, 1938 from northeast Thailand and a key to the species (Crustacea: Copepoda, Calanoida, Diaptomidae). ZooKeys 710: 15–32. https://doi.org/10.3897/zookeys.710.13941

Wei C-J, Xiong D-N, Wang Y-L, Feng W-S, Miao R-L, Gong Y-C (2023) First record of *Mongolodiaptomus mekongensis* in China and its phylogenetic analysis. Acta Hydrobiologica Sinica 47(10): 1640–1648. https://doi.org/10.7541/2023.2022.0309

Young SS, Shih CT (2011) Freshwater calanoids (Copepoda, Calanoida) of Taiwan, with some comments on the morphology of *Neutrodiaptomus tumidus* Kiefer, 1937 observed by SEM. In: Defaye D, Suarez-Morales E and Vaupel Klein JC (Eds) Studies on Freshwater Copepoda: A Volume in Honour of Bernard Dussart. Crustaceana Monographs, Volume 16. Brill, 2011, 545–566.

Young SS, Lin SC, Liu MY (2013) Genetic Diversity and Population Structure of Two Freshwater Copepods (Copepoda: Diaptomidae), *Neodiaptomus schmackeri* (Poppe and Richard, 1892) and *Mongolodiaptomus birulai* (Rylov, 1922) from Taiwan. Diversity 5(4): 796–810. https://doi.org/10.3390/d5040796

ZooKeys 1209: 43–68 (2024)
DOI: 10.3897/zookeys.1209.120812

Research Article

Caligus selenecola sp. nov. (Siphonostomatoida, Caligidae) parasitic on the hairfin lookdown *Selene brevoortii* (Gill) from the Gulf of California, Mexico, with some comments on *Caritus tolii* Rangnekar, 1984

Francisco Neptalí Morales-Serna[1], Beatriz Yáñez-Rivera[1], Samuel Gómez[1]

1 *Universidad Nacional Autónoma de México, Instituto de Ciencias del Mar y Limnología, Unidad Académica Mazatlán, Joel Montes Camarena s/n, Mazatlán, 82040, Sinaloa, Mexico*

Corresponding author: Samuel Gómez (samuelgomez@ola.icmyl.unam.mx)

Abstract

Specimens of a caligid copepod (Siphonostomatoida) were found on the gills of the hairfin lookdown *Selene brevoortii* (Gill) (Carangidae) from off Mazatlán, Sinaloa (north-western Mexico). This material represents a new species of *Caligus*, *C. selenecola* **sp. nov.**, and is assigned to the *diaphanus* species group. Within this group, only *C. kapuhili* Lewis, 1967, *C. laticaudus* Shiino, 1960, *C. macrurus* Heller, 1865, and *C. selenecola* **sp. nov.**, have been described with a reduced outer spine 1 on the second exopodal segment of leg 1. These four species can be readily separated by the relative length of the abdomen, and the presence/absence of a process on the myxal area of the female maxilliped, the sternal furca, the postantennal process, and the spiniform process on the basal antennary segment. A full description of the new species is given with some comments on *Caritus tolii* Rangnekar, 1984.

Key words: Biodiversity, Carangidae, Copepoda, Crustacea, parasite, taxonomy

Academic editor: Kai Horst George
Received: 13 February 2024
Accepted: 21 May 2024
Published: 7 August 2024

ZooBank: https://zoobank.org/C34EF793-F819-4FDE-B66F-31DE9F9C4D51

Citation: Morales-Serna FN, Yáñez-Rivera B, Gómez S (2024) *Caligus selenecola* sp. nov. (Siphonostomatoida, Caligidae) parasitic on the hairfin lookdown *Selene brevoortii* (Gill) from the Gulf of California, Mexico, with some comments on *Caritus tolii* Rangnekar, 1984. ZooKeys 1209: 43–68. https://doi.org/10.3897/zookeys.1209.120812

Introduction

Parasitic copepods of the family Caligidae Burmeister, 1835 (Copepoda: Siphonostomatoida) are commonly found on marine fishes, and are of importance in aquaculture due to the considerable economic losses they can cause to the aquaculture industry (Johnson et al. 2004). Currently, this family includes 29 valid genera (Walter and Boxshall 2024a), of which the most species-rich are *Caligus* Müller, 1785 and *Lepeophtheirus* Nordmann, 1832, with 269 and 123 species, respectively (Walter and Boxshall 2024b, 2024c). On the other hand, several genera contain only a few species. One of these genera is *Caritus* Cressey, 1967 with only two valid species so far, *C. serratus* Cressey, 1967 and *C. tolii* Rangnekar, 1984. Since its discovery, for unknown reasons, *C. tolii* has never been mentioned again: it does not appear in the most relevant and comprehensive literature on the subject (e.g., Dojiri and Ho 2013 and Boxshall and Halsey 2004), and there is no evidence of new records or discussions on it (Geoff Boxshall in litt.), or of any nomenclatural act upon which the species was placed into synonymy or transferred to another genus, or relegated to taxon inquirendum or invalidated. The morphological characteristics of the female of *Caritus* resemble those of *Caligus*, and these two genera have been hypothesized to be closely related (Dojiri and Ho 2013). The major differences between *Caritus* and *Caligus* are the strong reduction of the second and third distal exopodal segments of leg 3, the lamelliform, unarmed endopod of the same leg, and the shape and ornamentation of the exopodal spines of leg 2 (Dojiri and Ho 2013). These three character states are considered herein as probable autapomorphies for *Caritus*. Dojiri and Ho (2013) argued that *Caritus* differs from *Caligus* in the combined lack of the posteriorly directed spiniform process on the basal antennary segment, the postantennal process, and the sternal furca. These structures are present in nearly all the species of *Caligus* and one of these structures may be absent in some species of that genus, but none lacks all these structures (see Dojiri and Ho 2013: 41, table III). They (Dojiri and Ho 2013) purportedly consider the combined lack of these structures as one single character state defining *Caritus*, but the lack of these structures are independent character states. Indeed, the reduction of one or more of these structures seem to have occurred randomly within the *Caligus* group sensu Dojiri and Ho (2013), with a gradual trend towards the reduction of the sternal furca, the postantennal process, and the process on the second antennary segment, and their complete loss in *Caritus*.

Twenty-nine species of *Caligus* and their hosts had been reported from Mexico by 2016 (Morales-Serna et al. 2016: 144–150, app. 1). Since then, four additional, already known, species of *Caligus* have been recorded from Mexican waters: *C. asperimanus* Pearse, 1951 and *C. curtus* Müller, 1785 were found attached to individuals of the spotted rose snapper *Lutjanus guttatus* (Steindachner) (Perciformes: Lutjanidae) from off Michoacan and Guerrero states in south-western Mexico (Villalba-Vasquez et al. 2022); *C. dasyaticus* Rangnekar, 1957 was reported attached to the spotted eagle ray *Aetobatus narinari* (Euphrasen) (Myliobatiformes: Aetobatidae) and to the southern stingray *Hypanus americanus* (Hildebrand & Schroeder) (Myliobatiformes: Dasyatidae) from the southern Gulf of Mexico (Rodríguez-Santiago et al. 2016); *C. xystercus* Cressey, 1991 was found attached to the schoolmaster *Lutjanus apodus* (Walbaum) (Eupercaria: Lutjanidae) from the Caribbean (Hernández-Olascoaga et al. 2022). Additionally, another species, *Caligus fajerae* Morales-Serna, Oceguera-Figueroa & Tang, 2017 was described parasitizing the Pacific sierra *Scomberomorus sierra* Jordan & Starks (Scombriformes: Scombridae) from off Mazatlán (Sinaloa state, north-western Mexico) (Morales-Serna et al. 2017). Several species have been placed into synonymy since 2016 (e.g., *C. aesopus* Wilson, 1921 and *C. bennetti* Causey, 1953 are currently considered synonyms of *C. lichiae* Brian, 1906 and *C. macrurus* Heller, 1865, respectively), and an updated table of the species of *Caligus* reported from Mexico is presented.

This contribution deals with the description of a new species of *Caligus* found during a recent survey of the metazoan parasites of the marine fish *Selene brevoortii* (Gill) (Carangidae) from the southeastern Gulf of California. The new species lacks the spinelike process on the basal segment of the antenna, the postantennal process, and the sternal furca, and—most interestingly—spine 1 of the second exopodal segment of the first swimming leg is reduced, and spines 2 and 4 lack the accessory process. The new species is attributable to the *diaphanus* species group of Boxshall (2018), and share the reduced outer spine 1 on the second exopodal segment of leg 1 with *C. kapuhili* Lewis, 1967, *C. laticaudus* Shiino, 1960, and *C. macrurus*. However, these species are readily separated by several characters mentioned below.

Materials and methods

A total of 57 individuals of the hairfin lookdown, *Selene brevoortii* (mean total length = 23.5 cm) caught off Mazatlán, Sinaloa, Mexico, were directly purchased from local fishermen and subjected to a parasitological examination between June and November 2021. Copepod specimens recovered from the gills of the fish were fixed and preserved in 70% ethanol. The specimens were cleared in 85% lactic acid. Drawings were made using a Leica DMLB microscope equipped with a drawing tube.

Abbreviations used through the text, figures, and tables are: **P1–P6**, leg 1–leg 6; **EXP**, exopod; **ENP**, endopod; **EXP (ENP)1 (2, 3)**, first (second, third) segment of the exopod (endopod). Morphological terminology follows Kabata (1979), Boxshall (1990), and Huys and Boxshall (1991). Fish classification and names used herein conform to Froese and Pauly (2023). Nomenclature of the apical elements on the second exopodal segment of the first swimming leg follows Ho and Lin (2004) and Dojiri and Ho (2013).

The type-material was deposited in the Copepoda collection of the Instituto de Ciencias del Mar y Limnología, Unidad Académica Mazatlán (**ICML-EMUCOP**), in Sinaloa, Mexico.

Systematics

Order Siphonostomatoida Thorell, 1859
Family Caligidae Burmeister, 1835
Genus *Caligus* Müller, 1785

***Caligus selenecola* sp. nov.**
https://zoobank.org/BAD3A0A2-EA0B-47FE-82A6-FF39C115D12B
Figs 1–12

Type host. Hairfin lookdown *Selene brevoortii* (Gill) (Carangidae).

Type locality. Mexican Pacific, off Mazatlán Port (23°12'N, 106°26'W), Sinaloa, Mexico.

Prevalence. 15% (9/57).

Type material. ***Holotype***, adult female preserved in ethanol (ICML-EMUCOP-090621-01), collected on 9 June 2021. ***Allotype***, adult male preserved in ethanol (ICML-EMUCOP-081121-01), collected on 8 November 2021. ***Paratypes***, 1 adult female preserved in ethanol (ICML-EMUCOP-090621-02) from the same host individual as the holotype; 1 adult female preserved in ethanol (ICML-EMUCOP-120921-01) from which pair of antennules and P1 a were dissected and mounted onto two slides, and 1 adult female dissected and mounted onto ten slides (ICML-EMUCOP-120921-02), collected on 12 September 2021; and 1 adult female and 1 adult male preserved in ethanol (ICML-EMUCOP-221121-01) from a single host individual collected on 22 November 2021.

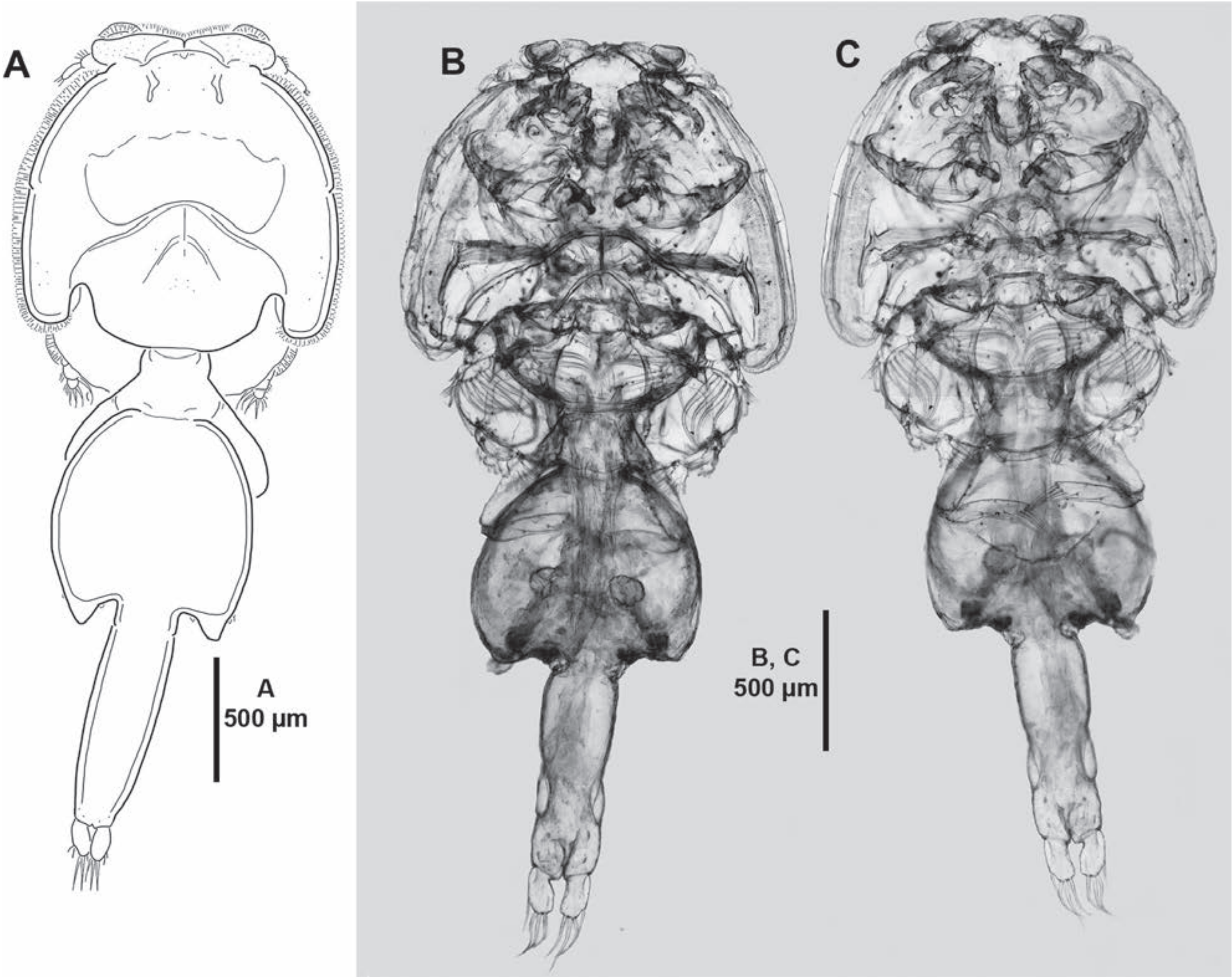

Figure 1. *Caligus selenecola* sp. nov., adult female, holotype **A** habitus, dorsal **B** light microscopy image, habitus, dorsal **C** light microscopy image, habitus, ventral.

Site on host. Gills.

Etymology. The specific name comes from the host genus name *Selene*, and the Latin suffix -*cola*, inhabitor. It is in the nominative singular, gender masculine.

Differential diagnosis. Caligidae. Female: cephalothoracic shield subcircular, with well-developed distinct paired frontal plates, the latter with large ventral lunules. Genital complex nearly as long as wide, slightly shorter than abdomen. Abdomen indistinctly separated from genital complex. Caudal rami twice as long as wide; armed with six setae. Antennule two-segmented; proximal segment with 27 plumose anterior setae; second segment with 13 naked setae and one aesthetasc. Antenna indistinctly four-segmented; second segment without process; without postantennal process; postantennal area with three setule-bearing papillae. Maxilliped with tiny denticle process in myxal area. Sternal furca absent. P1 biramous; P1 ENP vestigial; P1 EXP two-segmented; P1 EXP2 with three plumose setae on posterior margin, distally with lateral spine 1 minute, elements 2 and 4 spiniform without accessory process, element 3 longest with membranous inner flange. P2 biramous; ENP and EXP tree-segmented; endopodal segments with patch of surface setules anteriorly. P3 biramous; ENP two-segmented; EXP three-segmented. P4 uniramous; EXP three-segmented; outer spines of EXP3 with transverse strip of membrane (modified pecten) close to insertion of spines.

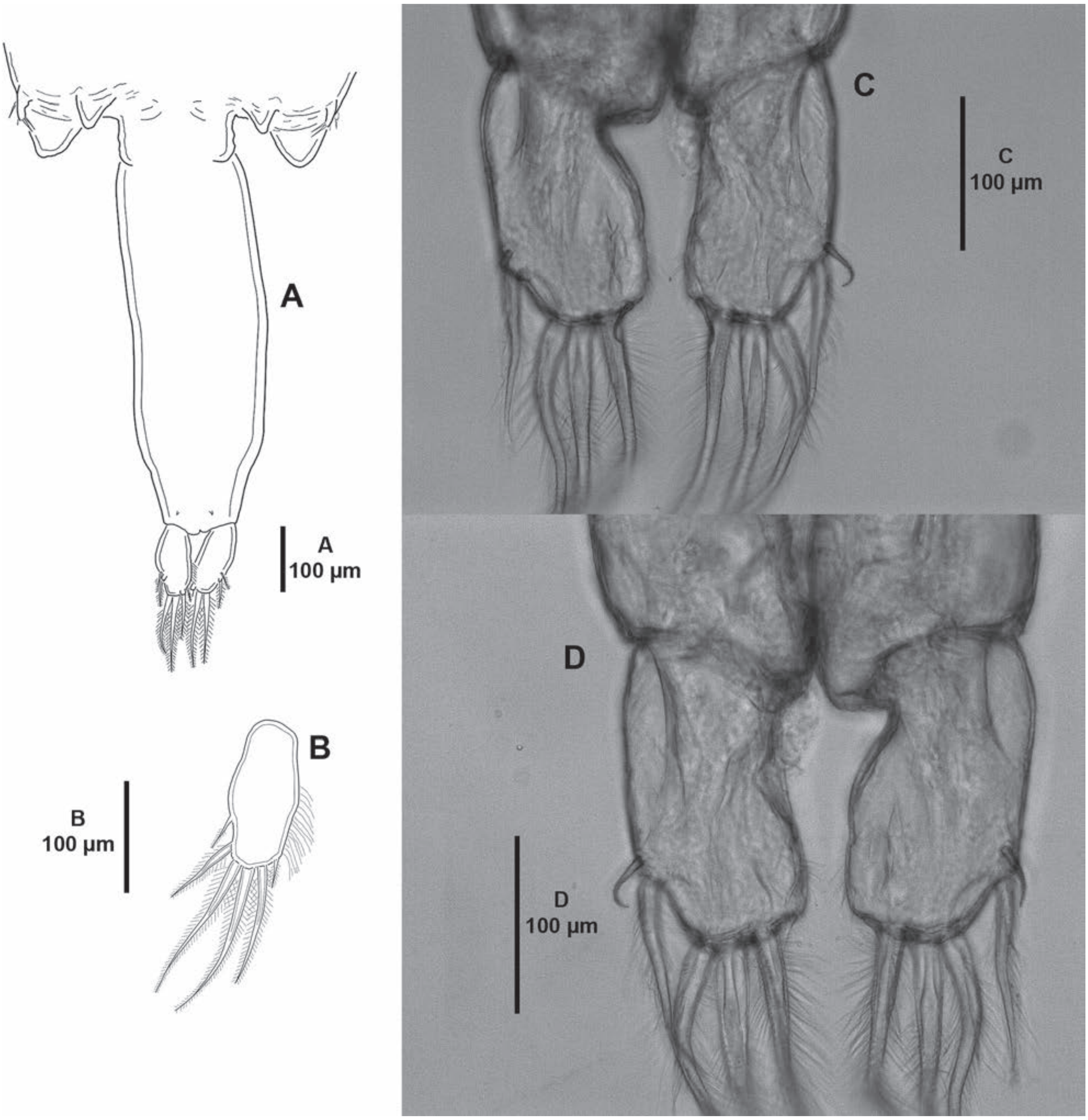

Figure 2. *Caligus selenecola* sp. nov., adult female, holotype **A** posterior region of genital complex, abdomen, and caudal rami, ventral **B** caudal ramus, ventral **C** light microscopy image, caudal ramus, dorsal **D** light microscopy image, caudal ramus, ventral.

Female P5 vestigial, comprised of small lobe with one seta, and larger elongate lobe with three elements. Male: abdomen with two free somites. Antenna three-segmented; middle segment with two corrugated pads and anterior rows of fine striations; distal segment forming long claw with one accessory process and one tiny seta. Maxillule as in female except for dentiform process with blunt distal process. Maxilliped three-segmented; with two conical projections on myxal area of proximal segment. P5 with three setae. P6 represented by two plumose setae.

Description. Adult female (Figs 1–9). Mean total body length measured from anterior margin of frontal plate to posterior margin of caudal rami, 3.1 mm (ranging from 2.8 to 3.4 mm; n = 6). Cephalothoracic shield (Fig. 1A–C) subcircular, slightly longer than wide; with well-developed distinct paired frontal plates, the latter with large ventral lunules; with posterior sinuses as shown; medial posterior margin of thoracic zone extending beyond posterolateral margins of cephalothoracic shield; with hyaline membrane along distal margin of frontal plates and laterally. Free fourth pedigerous somite (Fig. 1A–C) slightly wider than long, indistinctly separated from genital complex. Genital complex (Fig. 1A–C) nearly as long as wide, slightly shorter than abdomen, genital complex: cephalothoracic shield length radio 0.7; with posterolateral processes. Abdomen (Figs 1A–C, 2A) indistinctly separated from genital complex; ~ 3.5 × as long as wide; with a slight constriction anteriorly. Caudal rami (Figs 1A–C, 2A–D) twice as long as wide; armed with six setae of which two short and four long plumose, ornamented with inner row of setules. Egg sacs (not figured) uniseriate.

Antennule (Fig. 3A, B) two-segmented. Proximal segment longer than distal, the former with 27 plumose anterior setae. Second segment cylindrical, bearing 13 naked setae and one aesthetasc.

Antenna (Fig. 3C–E) indistinctly four-segmented. First segment unornamented, second segment without process, third segment unornamented, terminal segment a curved claw with one minute seta. Without postantennal process; postantennal area with three setule-bearing papillae (arrowed in Fig. 3F).

Mandible (Fig. 4A, B) of typical stylet-like structure; with twelve marginal teeth.

Maxillule (Fig. 4C) comprising anterior papilla bearing three unequal naked setae; with posterior moderately long dentiform process.

Maxilla (Fig. 5A–C) two-segmented, brachiform, comprising elongate unarmed lacertus and slender brachium, the latter with flabellum (Fig. 5C) slightly above halfway inner margin and with long calamus and shorter canna; calamus with strips of serrated membrane arranged obliquely around surface; canna with bilateral strips of serrated membrane.

Maxilliped (Fig. 5D–G) subchelate; corpus concave proximally, with tiny denticle process in myxal area; claw with naked seta on posterior surface (arrowed in Fig. 5G).

Sternal furca absent.

P1 (Fig. 6A–E) biramous, with slender, naked intercoxal sclerite. Sympod with one inner and one outer plumose seta, and one proximolateral seta. Endopod vestigial, represented by unarmed process bearing one tiny apical element. Exopod two-segmented. P1 EXP1 with inner row of setules and one small spine at outer distal corner; P1 EXP2 with three plumose setae on posterior margin, and four distal elements as follows: spine 1 minute, arising on outer lateral margin of segment (arrowed in Fig. 6B, C, E); elements 2 and 4 spiniform, seemingly without accessory process, the former slightly longer than the latter, both visibly shorter than element 3; the latter longest, with membranous inner flange.

P2 (Fig. 7A–C) biramous, with subquadrate intercoxal sclerite bearing distal hyaline membrane. Coxa with one inner plumose seta and one anterior sensillum. Basis with one outer small seta, one inner sensillum, and with inner hyaline membrane. Exopod three-segmented; first segment as long as second and third segments combined, with one plumose inner seta, one outer stout spine, and with dorsally flexed membrane along outer margin; second segment smallest, with one inner long plumose seta, one small outer spine, and ornamented with inner row of setules; third segment with five plumose inner setae, and two outer spines of which proximal shortest and one outer subdistal seta, the latter stout and with

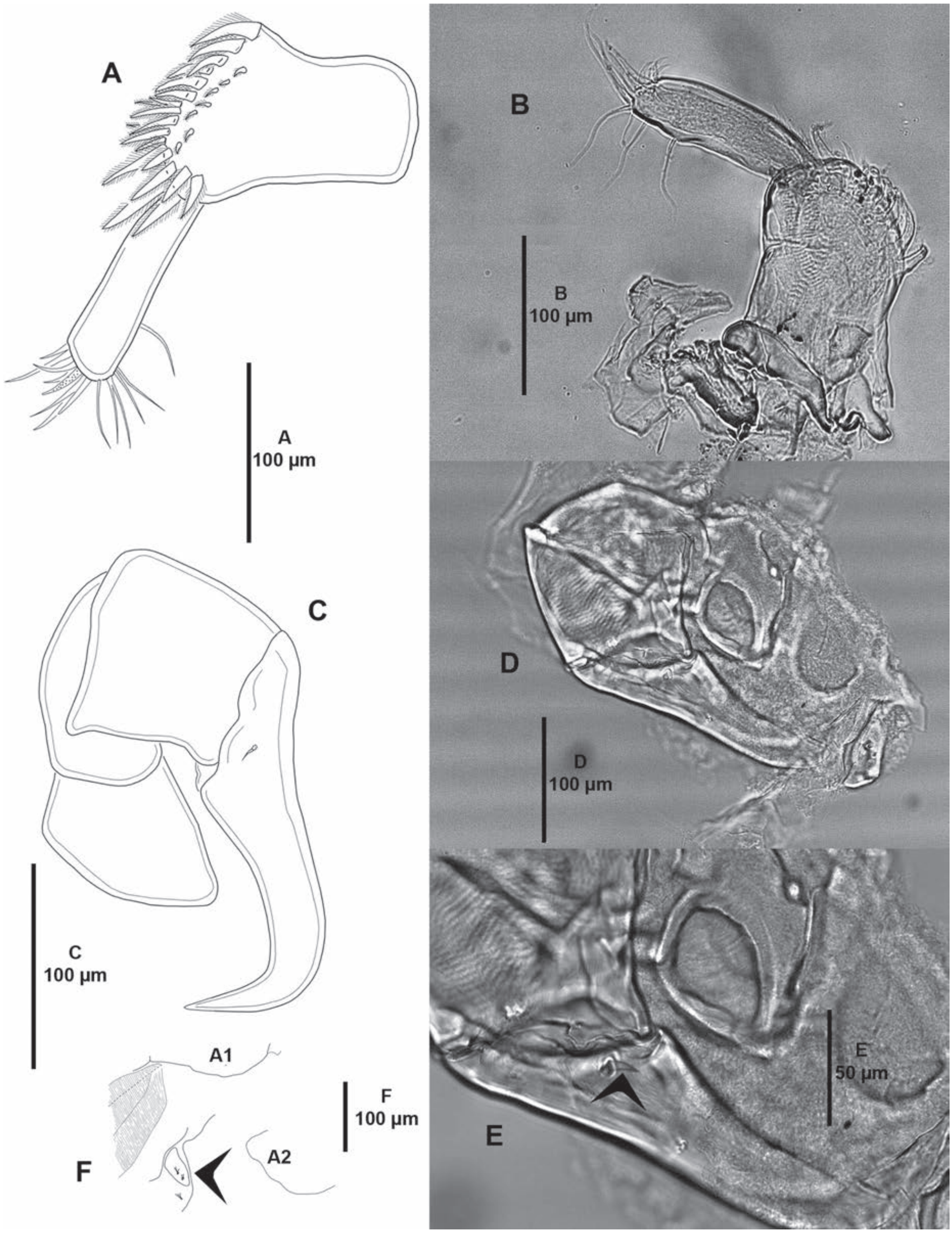

Figure 3. *Caligus selenecola* sp. nov., adult female, holotype (**A, E, F**), paratype ICML-EMUCOP-120921-02 (**B, D, E**) **A** antennule, ventral **B** light microscopy image, antennule, dorsal **C** antenna, ventral **D** light microscopy image, antenna **E** light microscopy image, antenna, showing seta on claw **F** postantennal area showing bases of antennule (a1) and antenna (a2).

inner hyaline membrane. Endopod three-segmented; first segment with one inner plumose seta, with patch of surface setules anteriorly; second segment with two inner plumose setae and ornamented with anterior patch of setules; third segment with six plumose setae and ornamented with anterior patch of setules.

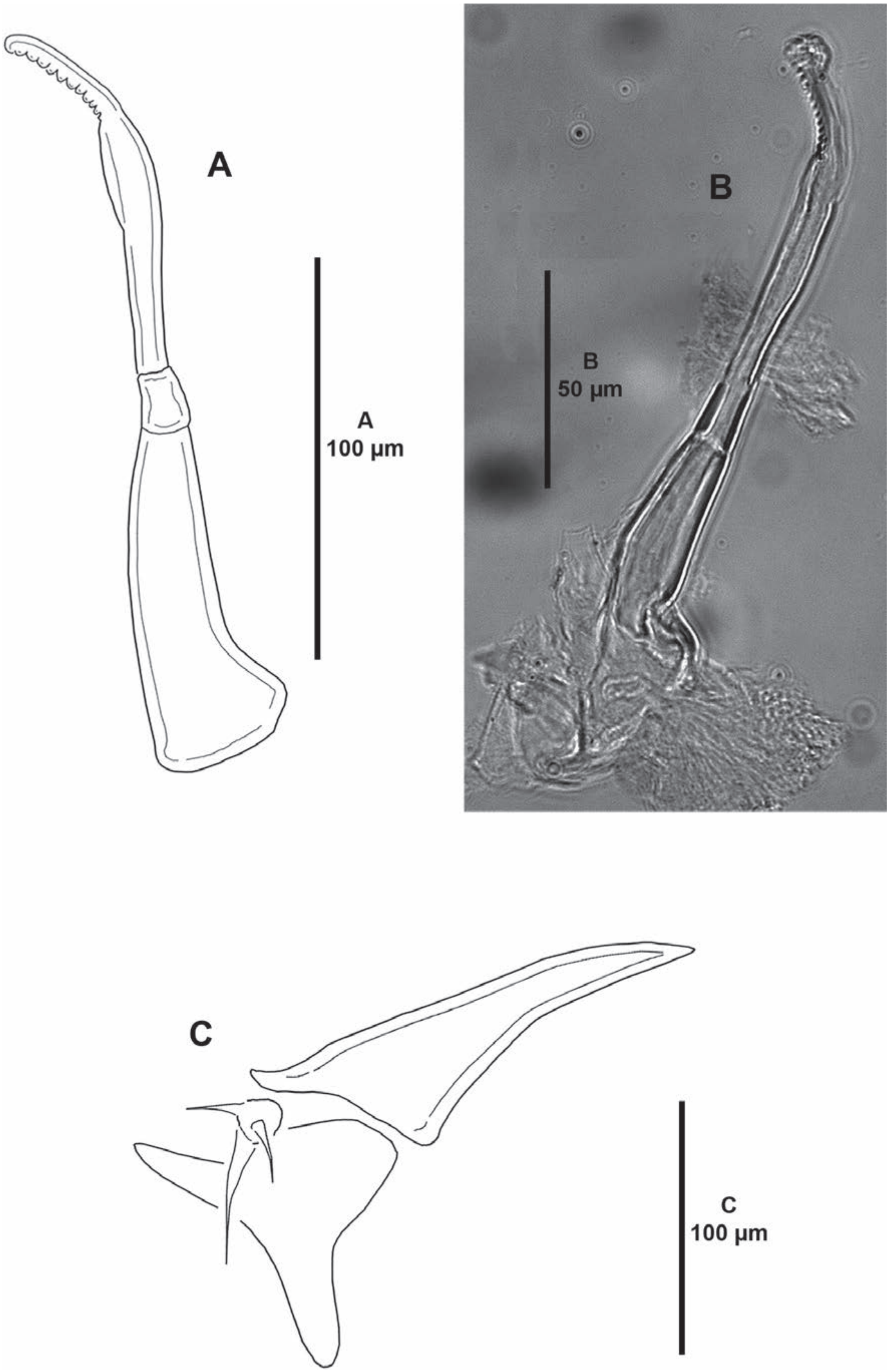

Figure 4. *Caligus selenecola* sp. nov., adult female, paratype ICML-EMUCOP-120921-02 **A** mandible, posterior **B** light microscopy image, mandible **C** maxillule, anterior.

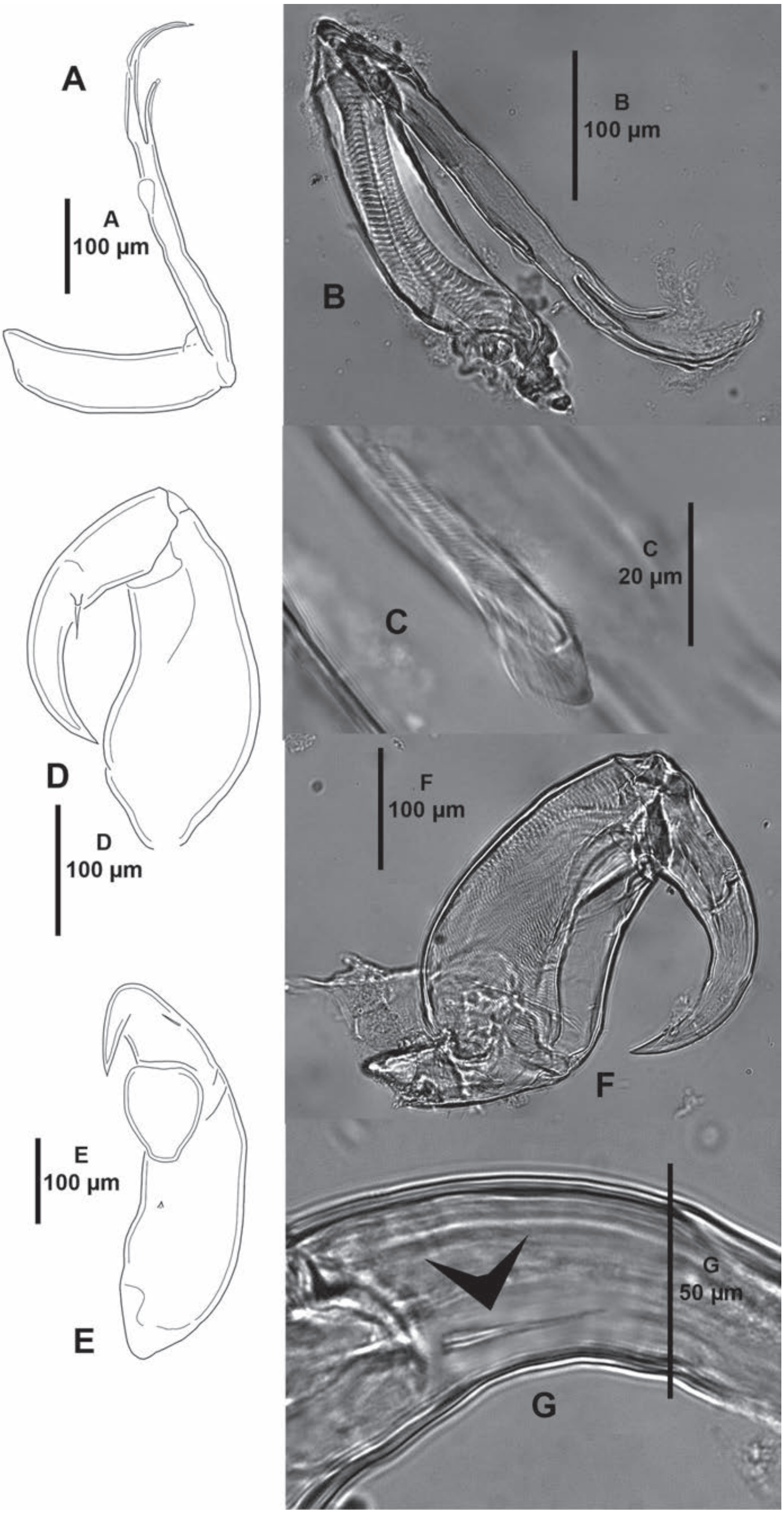

Figure 5. *Caligus selenecola* sp. nov., adult female, paratype ICML-EMUCOP-120921-02 **A** maxilla, anterior **B** light microscopy image, maxilla **C** flabellum of maxilla **D** maxilliped, posterior **E** maxilliped, posteroventral **F** light microscopy image, maxilliped **G** light microscopy image, middle part of claw of maxilliped showing small seta.

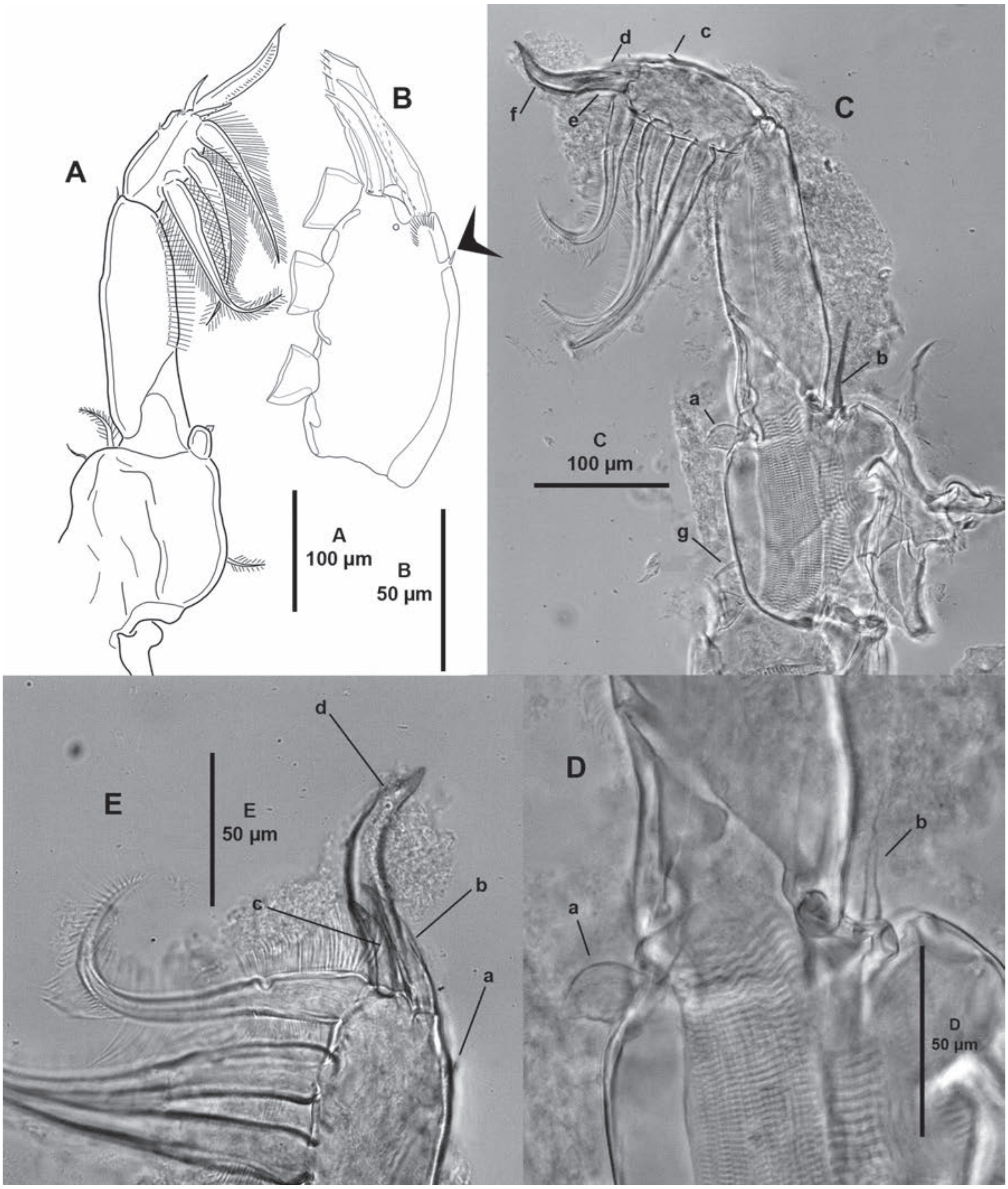

Figure 6. *Caligus selenecola* sp. nov., adult female, paratype ICML-EMUCOP-120921-02 (**A, C–E**), paratype ICML-EMUCOP-120921-01 (**B**) **A** P1, anterior **B** second exopodal segment (spine 1 arrowed), anterior **C** light microscopy image, P1, showing (**a**) endopod (**b**) outer seta of sympod (**c**) spine 1 (**d**) spine 2 (**e**) spine 4 (**f**) seta 3 (**g**) inner seta of sympod **D** light microscopy image, sympod showing (**a**) endopod and (**b**) outer seta **E** light microscopy image, second exopodal segment showing (**a**) spine 1 (**b**) spine 2, (**c**) spine 4, (**d**) seta 3.

P3 (Fig. 7D–G) with coxa and basis fused into flattened apron-like sympod, with one small outer plumose seta near insertion of exopod, one inner long plumose seta near intercoxal sclerite, and two widely separated sensilla along posterior margin. Sympod and intercoxal sclerite with extended strips of hyaline membrane along lateral and free posterior margins. Exopod three-segmented; first segment with one apical spine longer than segment and reaching slightly beyond articulation between second and third exopodal segments;

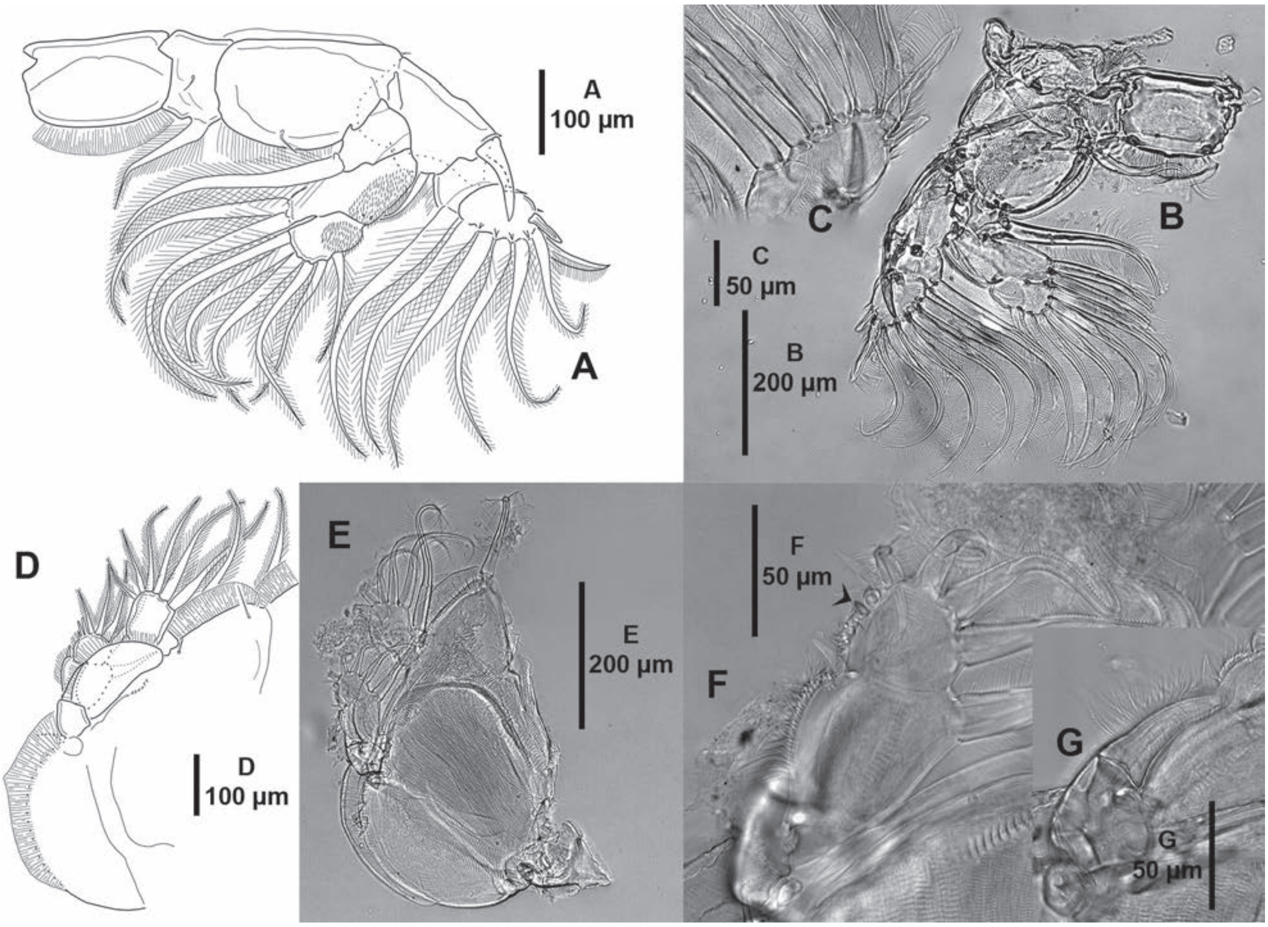

Figure 7. *Caligus selenecola* sp. nov., adult female, paratype ICML-EMUCOP-120921-02 **A** P2, anterior **B** light microscopy image, P2, anterior **C** light microscopy image, third exopodal segment, anterior **D** P3, ventral **E** light microscopy image, P3, anterior **F** light microscopy image, P3 EXP showing reduced proximal outer spine **G** light microscopy image, P3 EXP1 showing length of outer spine relative to length of supporting segment.

second segment with one outer spine and one inner plumose seta, ornamented with outer row of setules; third exopodal segment with three outer spines (proximal outer smallest), and four plumose setae, ornamented with outer setules. Endopod two-segmented; first segment extended laterally for form velum, and armed with long inner plumose seta; second segment with six plumose setae.

P4 (Fig. 8A–F) uniramous. Protopodal segment with 1 distal seta. Exopod three-segmented; first and second segments with one outer spine each; third segment with three outer spines, with transverse strip of membrane (modified pecten) close to insertion of spines. All spines subequal in length.

P5 (Fig. 9A, B) vestigial, situated on ventral surface, near outer margin of posterolateral lobe of genital complex; comprised of small lobe with one plumose seta, and larger elongate lobe with three plumose setae.

Armature formula of P1–P4 as follows (Roman numerals for spines; Arabic numerals for setae):

	EXP	ENP
P1	I-0; I,III,3	vestigial
P2	I-1; I-1; II,1,5	0–1; 0–2; 6
P3	I-0; I-1; III,4	0–1; 5
P4	I; I; III	absent

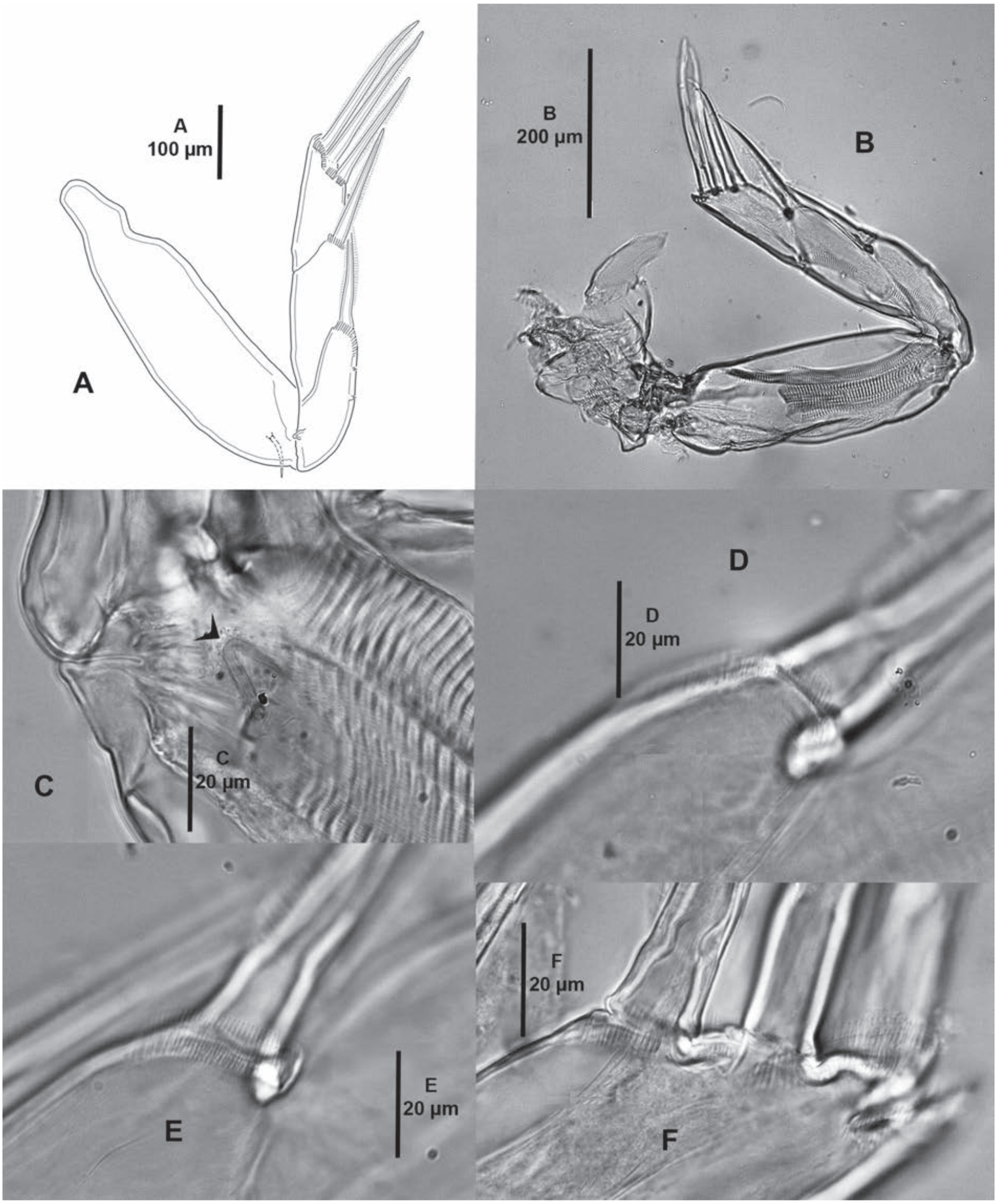

Figure 8. *Caligus selenecola* sp. nov., adult female, paratype ICML-EMUCOP-120921-02 **A** P4, anterior **B** light microscopy image, P4, anterior **C** light microscopy image, protopod of P4 showing seta, anterior **D** outer spine of first exopodal segment showing modified pecten, anterior **E** outer spine of second exopodal segment showing modified pecten, anterior **F** distal spines of third exopodal segment showing modified pectines, anterior.

P6 possibly represented by pair of protuberances located posteromedial to P5 (Figs 1A–C, 2A).

Adult male (Figs 10–12). Total body length measured from anterior margin of frontal plate to posterior margin of caudal rami 1.9 mm long (*n* = 1). Cephalothoracic shield (Fig. 10A, B) as in female but with narrower anterior region, slightly

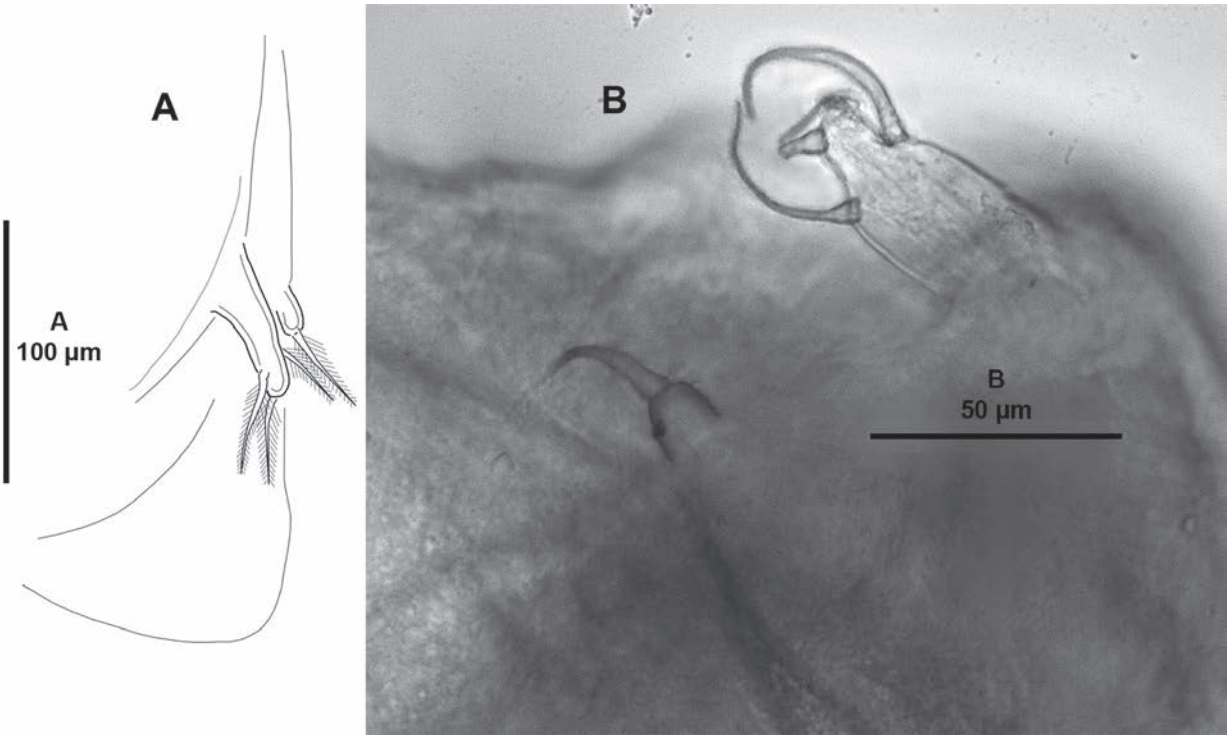

Figure 9. *Caligus selenecola* sp. nov., adult female, holotype (**A**), paratype ICML-EMUCOP-120921-02 (**B**) **A** P5, ventral **B** light microscopy image, P5 ventral.

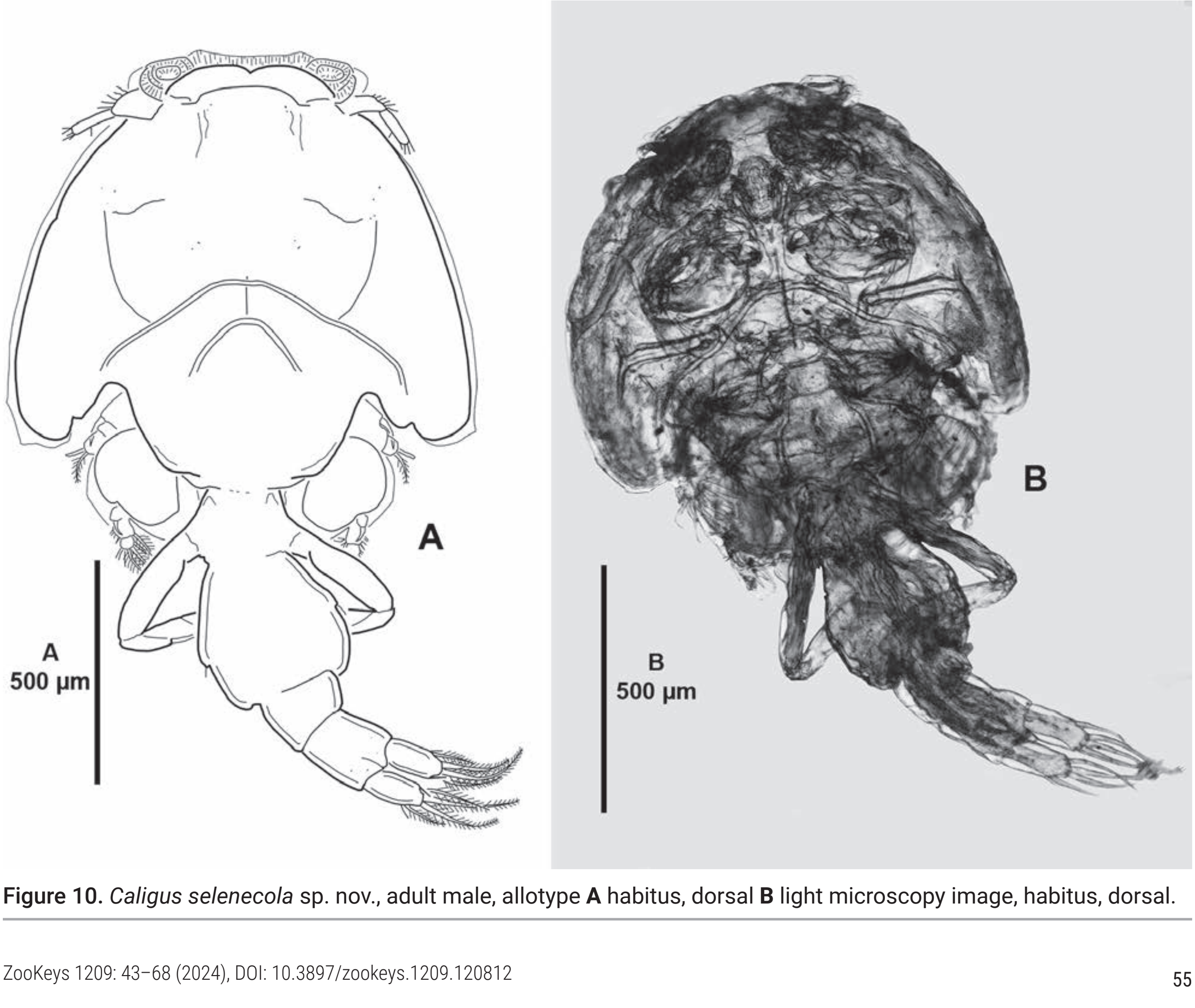

Figure 10. *Caligus selenecola* sp. nov., adult male, allotype **A** habitus, dorsal **B** light microscopy image, habitus, dorsal.

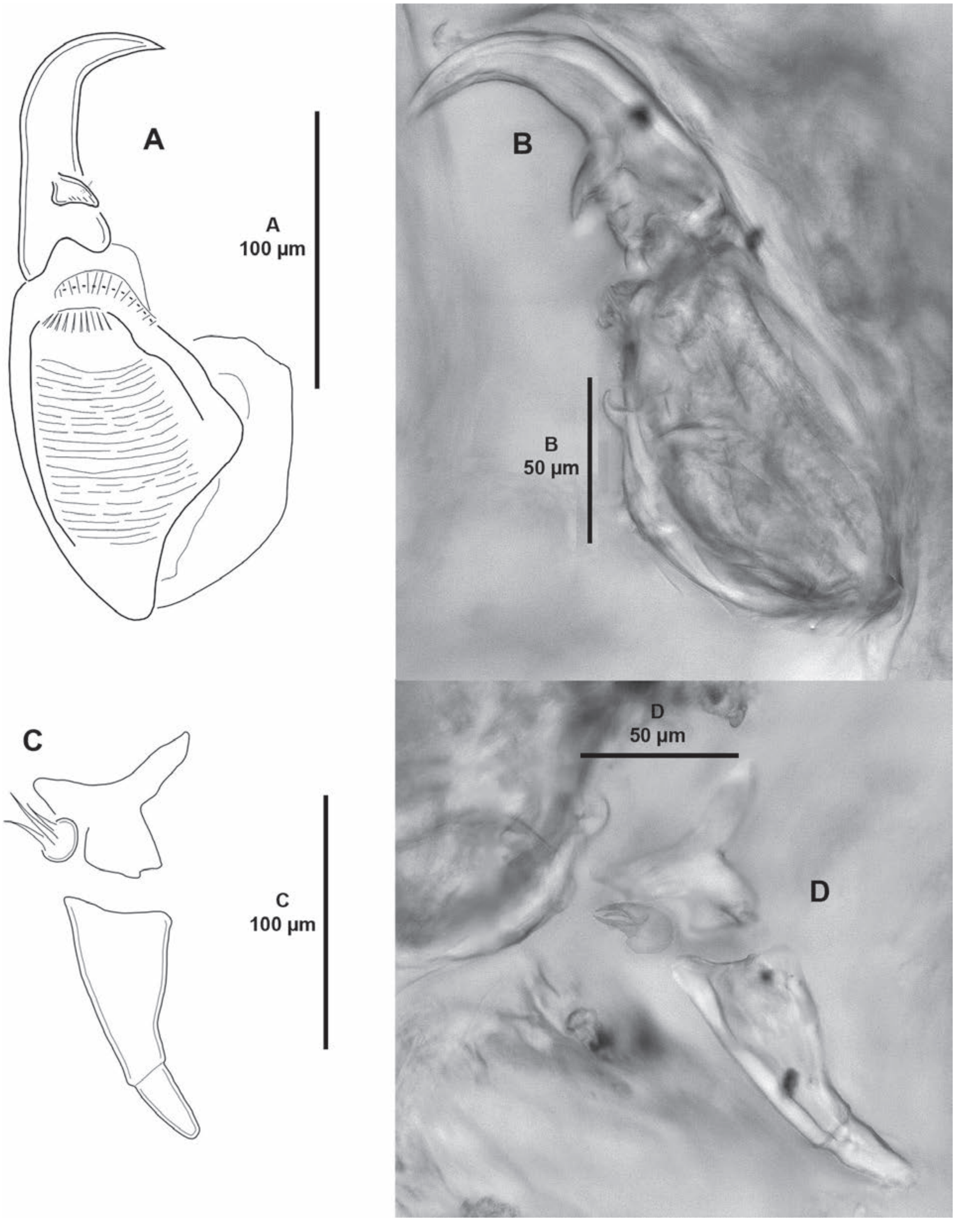

Figure 11. *Caligus selenecola* sp. nov., adult male, allotype **A** antenna, posterior **B** light microscopy image, antenna, anterior **C** maxillule, anterior **D** light microscopy image, maxillule, anterior.

wider than long. Free fourth pedigerous somite (Fig. 10A, B) slightly wider than long, indistinctly separated from genital complex. Genital complex (Fig. 10A, B) as long as wide. Abdomen (Fig. 10A, B) with two free somites; first somite slightly wider than long, second somite slightly longer than wide. Caudal rami

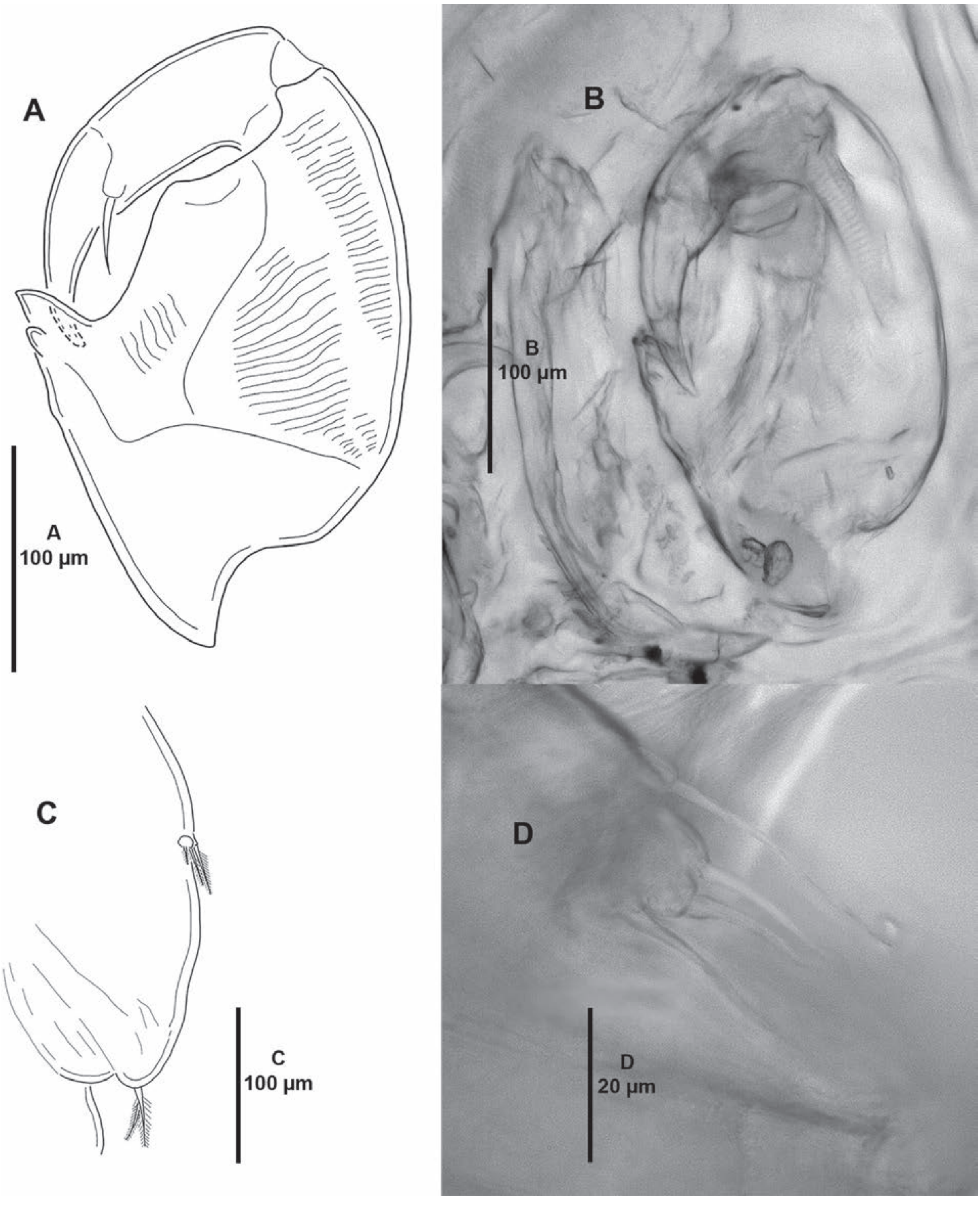

Figure 12. *Caligus selenecola* sp. nov., adult male, allotype **A** maxilliped, posterior **B** light microscopy image, maxilliped, anterior **C** posterolateral margin of genital complex showing P5 and P6 **D** light microscopy image, P5, anterior.

(Fig. 10A, B) ~ 2 × as long as wide, with two short and four long plumose setae. All appendages as in female, except for antenna, maxillule, and maxilliped.

Antenna (Fig. 11A, B) three-segmented; proximal segment small and unarmed; middle segment with two corrugated pads and anterior rows of fine striations; distal segment forming long curved pointed claw with one accessory process and one tiny seta near its base. Postantennal area (not shown) as in female.

Maxillule (Fig. 11C, D) as in female except for dentiform process with blunt distal process.

Maxilliped (Fig. 12A, B) three-segmented; myxal area of proximal segment with two conical projections bearing subterminal tooth; subchela as in female.

P5 (Fig. 12C, D) located at approximately midway along lateral margin of genital complex; composed of small lobe bearing three plumose setae.

P6 (Fig. 12C) represented by two plumose setae at tip of a posteroventral protuberance on genital complex.

Discussion

Taxonomic position of *Caritus tolii* Rangnekar, 1984

The genus name *Caritus* was coined by Cressey (1967) for *C. serratus* found attached to specimens of the milk fish, *Chanos chanos* (Forsskål) from Nosy Be, Madagascar. Amongst other characters, the genus was diagnosed by the one-segmented abdomen, by the presence of lunules, by the two-segmented P3 ENP, and by the lack of dorsal plates, postantennal process and sternal furca. Since the discovery of the type species of the genus, *C. serratus*, in 1967, only one species, *C. tolii* (erroneously synonymized with *C. serratus* in Soler-Jiménez et al. (2019: 95)) found on the inner wall of the operculum of some specimens of the herring, *Tenualosa toli* (Valenciennes) (Dorosomatidae) from Bombay (Rangnekar 1984), had been added. Rangnekar (1984) thought that the one-segmented condition of the abdomen of *C. serratus* observed by Cressey (1967) could be a misinterpretation since he (Cressey 1967: 6, 8; figs 1, 14) showed the female and male abdomen with a slight constriction probably suggesting its two-segmented condition. Rangnekar (1984) wrote that, following Cressey (1967), *C. serratus* lacked the maxillules. This is obviously erroneous (Cressey (1967) clearly described and showed the maxillule of his species) as is Rangnekar's (1984) written description of this appendage (compare Rangnekar (1984: 345) and his fig. 1 in the same page). More important are the differences in the armature of the P3 ENP noticed by Rangnekar (1984), being unarmed in *C. serratus*, but with one seta on P3 ENP1 and six elements in P3 ENP2 in *C. tolii*. Rangnekar (1984: 348) expressed some doubts regarding the phylogenetic importance of the absence of the sternal furca in *Caritus* as a character to justify that genus and believed that *Caritus* might well be placed as a subgenus of *Caligus*. Because of the close resemblance between the females of *Caritus* and *Caligus*, these two genera have been hypothesized to be closely related (Dojiri and Ho 2013), being the major differences between them i) the strong reduction of the second and third distal exopodal segment of P3, ii) the lamelliform, unarmed endopod of the same leg, and iii) the shape and ornamentation of the exopodal spines of P2 (Dojiri and Ho 2013), which are regarded here as potential autapomorphies for *Caritus*. That the combined lack of the posteriorly directed spiniform process on the basal antennary segment, the postantennal process, and the sternal furca is one of the major differences between *Caritus* and *Caligus* as argued by Dojiri and Ho (2013) is, in our opinion, not entirely correct. Indeed, these structures are present in nearly all the species of *Caligus*, or one of these structures may be absent in some species, but none lacks all these structures (see Dojiri and Ho (2013: 41, table III)). However, the reduction of one or more of these structures seems to have occurred randomly within the *Caligus* group *sensu* Dojiri and Ho (2013: 402), and a gradual trend towards the reduction of the sternal furca, the postantennal process, and the process on the second antennary segment, seems to be in progress, with their complete loss in *Caritus*. For example, the sternal furca of *Anchicaligus nautili* Stebbing, 1900 —the only species of that genus—is reduced to posteriorly directed sclerotized protrusions, it lacks the postantennal process, and the spinelike projection on the second antennary process is reduced to a rounded protrusion; the sternal furca may be present or absent in the species previously allocated in the former *Sciaenophilus* Beneden, 1852 (= *Caligus* after Özak et al. 2017), and the postantennal process is present, but lacks the posteriorly directed process on the second antennary segment; *Metacaligus* Thomsen, 1949 lacks the sternal furca, and the postantennal process is pointed but reduced in size, and the spinelike projection on the second antennary process is missing in *Metacaligus trichiuri* Krøyer, 1863; *Echetus* Krøyer, 1864, with its type and only species, *E. typicus* Krøyer, 1864, lacks the sternal furca and the process of the postantennal process, and the posteriorly directed process on the second antennary process is reduced in size; *Caligodes* Heller, 1865 possesses the sternal furca and posteriorly directed spinelike process on the second antennary segment, but lacks the postantennal process.

Recent advances showed that i) *C. bennetti* is a junior synonym of *C. macrurus*, and *Sciaenophilus* is a synonym of *Caligus* (Özak et al. 2017), ii) that *Caligodes alatus* Heegaard, 1945 and *Parapetalus spinosus* Byrnes, 1986 belong to *Caligus* but required replacement names, *Caligus seriolicolus* Boxshall, 2018 and *Caligus alepicolus* Boxshall, 2018, respectively (Boxshall 2018), and iii) that *Sinocaligus* Shen, 1957 is synonym of *Caligus* (Boxshall and Barton 2023). Besides regarding some species of *Caligus* as *species inquirendae* and *nomina nuda*, the proposal of several synonymies between some species of *Caligus* and between some species of *Caligus* and *Euryphorus* Milne Edwards, 1840, the reallocation of *Chalimus tenuis* Leidy, 1889 to that, currently, invalid genus, and the partial redescription of several poorly-known species, Özak et al. (2017), Boxshall (2018), Boxshall and Bernot (2023), and Boxshall and Barton (2023) contributed importantly to the taxonomy and systematics of *Caligus*. However, being the largest genus within the entire family, and given the inherent complexity of making comparisons to establish new species (Boxshall 2018) it is not clear to what extent the generic diagnosis of *Caligus* has been expanded. The genus could eventually be divided into two or more genera, but a revision of the genus must be conducted first (Dojiri and Ho 2013).

Rangnekar (1984) believed that *C. tolii* was the second species of *Caritus* based on the simultaneous lack of the posteriorly directed spiniform process on the basal antennary segment, the postantennal process, and the sternal furca. The drawings of Rangnekar (1984) are not detailed enough, but *C. tolii* departs from the general scheme of *Caritus* in the shape of the spines of the P2 EXP (which look of the normal caligid type), and armature of P3 EXP2–3 (normal, relatively well-developed, and of the caligid type in *C. tolii*, but extremely reduced in *C. serratus*) and P3 ENP (well-developed in *C. tolii* but absent in *C. serratus*). Based on the available literature and evidence, it seems that *C. tolii* does not belong to *Caritus*, and is herein proposed to be removed from that genus and reallocated into *Caligus* as *Caligus tolii* (Rangnekar, 1984), comb. nov. The original description of the species by Rangnekar (1984) lacks the necessary detail and some characteristics of the *diaphanus* group cannot be verified.

Pending its redescription, *C. tolii* comb. nov. is attributed here to the *diaphanus* species group by the combination of i) the armature of the three-segmented P3 EXP with I, I, and III spines¸ ii) the presence of three plumose setae on the posterior margin of P1 EXP2, iii) the apparent lack of an accessory process on spines 2 and 3 of P1 EXP2, and iv) lack of the posterior process on the proximal segment of the antenna, and lack of the postantennal process.

Taxonomic position of *Caligus selenecola* sp. nov.

Boxshall and Gurney (1980) proposed the *macarovi* group for 28 species. More recently, Boxshall (2018) listed 44 species in that group and, aiming at facilitating the identification process, establishment of new species, and comparison of the species of *Caligus*, he proposed four additional species groups of *Caligus* based on the combination of several morphological character states, the *bonito*, *confusus*, *diaphanus*, and *productus* groups. More recently, Ohtsuka and Boxshall (2019) proposed the *pseudorhombi* species group, and Ohtsuka et al. (2020) grouped some species of *Caligus* in their *undulatus* species group. Of interest here is the *diaphanus* group characterized by i) three-segmented P4 EXP with I, I, III spines and ornamented with a modified pecten at the base of each spine, ii) P1 EXP2 with three plumose setae on the posterior margin, iii) spines 2 and 3 on the distal exopodal segment of P1 apparently lacking the accessory processes, iv) P2 ENP2–3 ornamented with surface fine setules, v) outer spines of P2 EXP1–2 aligned close to longitudinal axis of ramus, vi) antenna without posterior process on proximal segment, and vii) tine on post-antennal process vestigial or weakly developed (Boxshall 2018). To this group belong *C. auriolus* Boxshall & Barton, 2023, *C. cybii* Bassett-Smith, 1898c, *C. diaphanus* Nordmann, 1832, *C. fajerae*, *C. kanagurta* Pillai, 1961, *C. kapuhili*, *C. laticaudus*, *C. macrurus*, *C. pagelli* Delamare Deboutteville & Nunes-Ruivo, 1958, *C. pagri* Capart, 1941, *C. pelamydis* Krøyer, 1863, *C. platytarsis* Basset-Smith, 1898a, *C. robustus* Bassett-Smith, 1898b, *C. seriolae* Yamaguti, 1936, *C. stromatei* Krøyer, 1863, *C. tanago* Yamaguti, 1939, *C. tenuis* (Beneden, 1852), *C. tolii* comb. nov., and *C. torpedinis* Heller, 1865 (Boxshall 2018; Boxshall and Barton 2023; Boxshall and Bernot 2023), and Boxshall and Barton (2023) provided a key to the species of this group.

The new species is attributable to the *diaphanus* species group of Boxshall (2018), and following Boxshall and Barton's (2023) key to the species of that species group, the new species keys out as an intermediate form between *C. torpedinis* (= *C. rotundigenitalis* Yü, 1933 after Boxshall and Bernot (2023)) and *C. pagri*, with the lateral margins of the genital complex slightly convex and with the outer spine of P3 EXP1 reaching slightly beyond the articulation between EXP2 and EXP3. On the other hand, in addition to *C. selenecola* sp. nov., a very small outer spine 1 of P1 EXP2 has been documented for several species of the genus, i.e., *C. balistae* Steenstrup & Lütken, 1861, *C. creyessorum* Kabata, 1992, *C. cookeoli* Ho & Lin, 2010, *C. dactylopteni* Uma Devi & Shyamasundari, 1981, *C. kapuhili*, *C. laticaudus*, *C. macrurus*, *C. nataliae* Boxshall, 2018, *C. praecinctorius* Hayes, Justine & Boxshall, 2012, *C. pseudorhombi* Boxshall, 2018, *C. sclerotinosus* Roubal, Armitage & Rohde, 1983, and *C. seriolae*, and it has not been observed in many others, i.e., *C. calotomi* Shiino, 1954b, *C. diaphanus*, *C. hamatus* Heegaard, 1955 (recently, Boxshall and Bernot (2023: 562) announced the submission of a case to the International Commission of Zoological Nomenclature (ICZN) to propose that *C. undulatus* Shen & Li, 1959 be given precedence over *C. hamatus*, but the case has not yet been resolved), *C. hobsoni* Cressey, 1969, *C. longicaudus* Bassett-Smith, 1898b, *C. robustus*, *C. sensorius* Heegaard, 1962, *C. sepetibensis* Luque & Takemoto, 1996, and *C. suffuscus* Wilson, 1913. Rangnekar (1984) described the P1 EXP2 of *C. tolii* with three plumose setae on the posterior margin, and four well-developed distal elements. The description of an additional outer minute spine on the outer distal corner of P1 EXP2 needs to be verified, but it is probably a pectinate membrane at the base of spine 1 also observed in *C. serratus* (see Dojiri and Ho 2013: 163, fig. 58f), and other caligids.

Within the first group of species above, only *C. cresseyorum*, *C. macrurus*, *C. nataliae*, *C. praecinctorius*, *C. pseudorhombi*, and *C. sclerotinosus* have been observed possessing an accessory process on spines 2 and 3 of P1 EXP2, but it is highly probable that such processes may be evident under electron microscopy (Boxshall 2018), as recently shown for *C. macrurus* (Özak et al. 2017). Also, within that group of species for which a small spine 1 of P1 EXP2 has been unequivocally observed, only a few species besides *C. selenecola* sp. nov., belong to the *diaphanus* species group, i.e., *C. kapuhili*, *C. laticaudus*, and *C. macrurus*. *Caligus selenecola* sp. nov. can be readily separated from the other three species by i) the relative length of the abdomen (extremely elongate, ~ 1.5 × as long as the cephalothorax, P4-bearing somite, and genital complex combined in *C. macrurus*, shorter than genital complex in *C. kapuhili* and *C. laticaudus*, but as long as genital complex in the new species); ii) shape of the female maxilliped (with process on the myxal margin in *C. kapuhili* and *C. laticaudus*, but with smooth myxal margin in *C. macrurus* and in the new species), iii) presence/absence of the sternal furca (present in *C. macrurus*, *C. kapuhili*, and *C. laticaudus*, but absent in *C. selenecola* sp. nov.), iv) presence/absence of postantennal process (present in present in *C. macrurus*, *C. kapuhili*, and *C. laticaudus*, but absent in *C. selenecola* sp. nov.), v) presence/absence of the spiniform process on the basal antennary segment (present in *C. macrurus* and *C. kapuhili*, but absent in *C. laticaudus* and *C. selenecola* sp. nov.).

With the addition of *C. selenecola* sp. nov., there are currently 35 species of *Caligus* parasitizing teleosts and elasmobranchs from Mexican waters (Table 1).

Table 1. Updated list of the species of *Caligus* reported from Atlantic (A) and Pacific (P) coastal waters of Mexico.

Species	Host	Locality	References
C. asperimanus Pearse, 1951	*Lutjanus guttatus* (Steindachner)	Guerrero and Michoacán (P)	Villalba-Vasquez et al. (2022)
C. bonito Wilson, 1905	*Cratinus agassizii* Steindachner, *Lutjanus novemfasciatus* Gill, & *Sarda chiliensis* (Cuvier)	Oaxaca and Sinaloa (P)	Ho and Lin (2004), Morales-Serna et al. (2012)
C. callaoensis Durán, 1980	*Cynoscion xanthulus* Jordan & Gilbert	Jalisco (P)	Morales-Serna et al. (2014)
C. chamelensis Morales-Serna, Pinacho-Pinacho, Gómez & Pérez-Ponce de León, 2014	*Kyphosus elegans* (Peters)	Jalisco (P)	Morales-Serna et al. (2014)
C. chelifer Wilson, 1905	Found in plankton	Tamaulipas (A)	Morales-Serna et al. (2012)
C. chorinemi Krøyer, 1863	*Caranx caninus* Günther	Jalisco (P)	Morales-Serna et al. (2014)
C. confusus Pillai, 1961	*Caranx caballus* Günther and *Caranx caninus* Günther	Jalisco (P)	Morales-Serna et al. (2014)
C. constrictus Heller, 1865	*Caranx caninus* Günther	Sinaloa (P)	Morales-Serna et al. (2012)
C. curtus Müller, 1785	*Lutjanus guttatus* (Steindachner)	Guerrero and Michoacán (P)	Villalba-Vasquez et al. (2022)
C. dasyaticus Rangnekar, 1957	*Aetobatus narinari* (Euphrasen) and *Hypanus americanus* (Hildebrand & Schroeder)	Campeche and Tabasco (A)	Rodríguez-Santiago et al. (2016)
C. diaphanus Nordmann, 1832	*Lutjanus peru* (Nichols & Murphy)	Jalisco (P)	Morales-Serna et al. (2014)

Species	Host	Locality	References
C. elongatus Nordmann, 1832	*Sphoeroides annulatus* (Jenyns)	Sonora (P)	Morales-Serna et al. (2012)
C. fajerae Morales-Serna, Oceguera-Figueroa & Tang, 2017	*Scomberomorus sierra* Jordan & Starks	Sinaloa (P)	Morales-Serna et al. (2017)
C. haemulonis Krøyer, 1863	*Bagre marinus* (Mitchill)	Veracruz (A)	Morales-Serna et al. (2012)
C. hoplognathi Yamaguti & Yamasu, 1959	*Caranx caballus* Günther, *Caranx caninus* Günther, and *Tylosurus pacificus* (Steindachner)	Jalisco (P)	Morales-Serna et al. (2014)
C. lalandei Barnard, 1948	*Seriola lalandi* Valenciennes	Baja California (P)	Morales-Serna et al. (2012)
C. latigenitalis Shiino, 1954a	*Caranx caballus* Günther, *Lutjanus argentiventris* (Peters), *Kyphosus elegans* (Peters), *Tylosurus pacificus* (Steindachner), and *Prionurus punctatus* Gill	Jalisco (P)	Morales-Serna et al. (2014)
C. lichiae Brian, 1906	*Caranx caballus* Günther and *Caranx caninus* Günther	Jalisco (P)	Morales-Serna et al. (2014)
C. longipedis Bassett-Smith, 1898a	*Caranx lugubris* and *Caranx caninus* Günther	Colima and Jalisco (P)	Morales-Serna et al. (2012, 2014)
C. macarovi Gusev, 1951	*Cololabis saira* (Brevoort)	Unspecified (P)	Morales-Serna et al. (2012)
C. macrurus Heller, 1865	*Kyphosus sectatrix* (Linnaeus) and *Paralabrax maculatofasciatus* (Steindachner)	Sinaloa (P) and Veracruz (A)	Morales-Serna et al. (2012)
C. mutabilis Wilson, 1905	*Balistes* sp., *Calamus brachysomus* (Lockington), *Chaetodipterus zonatus* (Girard), *Centropomus* sp., *Epinephelus labriformis* (Jenyns), *Hoplopagrus guentherii* Gill, *Katsuwonus pelamis* (Linnaeus), *Kyphosus elegans* (Peters), *Lutjanus guttatus* (Steindachner), *Lutjanus peru* (Nichols & Murphy), *Microlepidotus brevipinnis* (Steindachner), *Menticirrhus undulatus* (Girard), *Mugil cephalus* Linnaeus, *Paralabrax clathratus* (Girard), *Paralabrax maculatofasciatus* (Steindachner), *Paralabrax nebulifer* (Girard), *Paraselene orstedii* (Lütken), *Sarda chiliensis* (Cuvier), and *Scomberomorus sierra* Jordan & Starks	Baja California, Guerrero, Nayarit, Oaxaca, Sinaloa, and Sonora (P)	Morales-Serna et al. (2012, 2014)
C. omissus Cressey & Cressey, 1980	*Scomberomorus sierra* Jordan & Starks and *Scomberomorus concolor* (Lockington)	Jalisco (P)	Morales-Serna et al. (2012, 2014)
C. pelamydis Krøyer, 1863	*Scomberomorus cavalla* (Cuvier)	Veracruz (A)	Morales-Serna et al. (2012)
C. productus Dana, 1849–1852	*Balistes polylepis* Steindachner, *Calamus brachysomus* (Lockington), *Centropomus* sp., *Coryphaena hippurus* Linnaeus, *Katsuwonus pelamis* (Linnaeus), *Lutjanus* sp., *Paralabrax clathratus* (Girard), *Paralabrax maculatofasciatus* (Steindachner), *Scomberomorus sierra* Jordan & Starks, *Seriola lalandi* Valenciennes, and *Sphyraena argentea* Girard	Baja California, Guerrero, Nayarit, Oaxaca, Sinaloa, and Sonora (P)	Ho and Lin (2004), Morales-Serna et al. (2012)
C. robustus Bassett-Smith, 1898b	*Caranx caballus* Günther and *Caranx caninus* Günther	Jalisco (P)	Morales-Serna et al. (2014)
C. rufimaculatus Wilson, 1905	Found in plankton	Yucatán (A)	Morales-Serna et al. (2012)
C. sclerotinosus Roubal, Armitage & Rohde, 1983	*Lutjanus Colorado* Jordan & Gilbert, *Lutjanus guttatus* (Steindachner), and *Lutjanus peru* (Nichols & Murphy)	Jalisco (P)	Morales-Serna et al. (2014)
C. selenecola sp. nov.	*Selene brevoortii* (Gill)	Sinaloa (P)	Present study
C. serratus Shiino, 1965	*Calamus brachysomus* (Lockington), *Caranx caballus* Günther, *Caranx caninus* Günther, *Cynoscion xanthulus* Jordan & Gilbert, *Elops affinis* Regan, *Haemulon steindachneri* (Jordan & Gilbert), *Kyphosus elegans* (Peters), *Lutjanus argentiventris* (Peters), *Microlepidotus brevipinnis* (Steindachner), *Scomberomorus sierra* Jordan & Starks, *Sphoeroides annulatus* (Jenyns), and *Tylosurus pacificus* (Steindachner)	Jalisco and Sinaloa (P)	Morales-Serna et al. (2012, 2013, 2014)
C. tenuifurcatus Wilson, 1937	*Centropomus robalito* Jordan & Gilbert and *Nematistius pectoralis* Gill	Jalisco (P)	Morales-Serna et al. (2012, 2014)
C. trachynoti Heller, 1865	*Trachinotus carolinus* (Linnaeus)	Campeche, Quintana Roo and Yucatán (A)	Morales-Serna et al. (2012)
C. tylosuri (Rangnekar, 1956)	*Tylosurus pacificus* (Steindachner)	Jalisco (P)	Morales-Serna et al. (2014)
C. undulatus Shen & Li, 1959	Found in plankton	Yucatán (A)	Suárez-Morales et al. (2012)
C. xystercus Cressey, 1991	*Lutjanus apodus* (Walbaum)	Quintana Roo (A)	Hernández-Olascoaga et al. (2022)

Acknowledgements

We are grateful to M. Sc. Juan Manuel Osuna Cabanillas for the collection of fish and copepod specimens. We are deeply grateful to Dr Geoffrey A. Boxshall for reviewing the final draft of this manuscript and for his constructive criticism. We are grateful also to Dr Il-Hoi Kim and Dr Balu A. Venmathi Maran for their constructive criticism during the peer review process.

Additional information

Conflict of interest

The authors have declared that no competing interests exist.

Ethical statement

No ethical statement was reported.

Funding

Article processing charges were financed by the Instituto de Ciencias del Mar y Limnología of the Universidad Nacional Autónoma de México.

Author contributions

Conceptualization: FNMS. Funding acquisition: SG. Methodology: FNMS. Writing - original draft: FNMS, SG. Writing - review and editing: BYR, SG, FNMS.

Author ORCIDs

Francisco Neptalí Morales-Serna https://orcid.org/0000-0002-2577-5369
Beatriz Yáñez-Rivera https://orcid.org/0000-0002-3192-2142
Samuel Gómez https://orcid.org/0000-0002-8597-8846

Data availability

All of the data that support the findings of this study are available in the main text.

References

Barnard KH (1948) New records and descriptions of new species of parasitic Copepoda from South Africa. Annals & Magazine of Natural History 12(4): 242–254. https://doi.org/10.1080/00222934808653905

Bassett-Smith PW (1898a) Further new parasitic copepods found on fish in the Indo-tropical region. Annals & Magazine of Natural History 7(8): 77–98. https://doi.org/10.1080/00222939808678020

Bassett-Smith PW (1898b) Some new or rare parasitic copepods found on fish in the Indo-tropic region. Annals & Magazine of Natural History 7(11): 357–372. https://doi.org/10.1080/00222939808678056

Bassett-Smith PW (1898c) Some new parasitic copepods found on fish at Bombay. Annals & Magazine of Natural History 1(1): 1–17. https://doi.org/10.1080/00222939808677915

Beneden PJ van (1852) Note sur un nouveau genre de crustacé parasite de la famille des peltocéphales. Bulletin de l’Académie Royale de Belgique 19: 462–467.

Boxshall GA (1990) The skeletomusculature of siphonostomatoid copepods, with an analysis of adaptive radiation in structure of the oral cone. Philosophical Transactions of the Royal Society of London, Series B, Biological Sciences 328(1246): 167–212. https://doi.org/10.1098/rstb.1990.0113

Boxshall G (2018) The sea lice (Copepoda: Caligidae) of Moreton Bay (Queensland, Australia), with descriptions of thirteen new species. Zootaxa 4398(1): 1–172. https://doi.org/10.11646/zootaxa.4398.1.1

Boxshall G, Barton DP (2023) Caligid sea lice (Copepoda: Caligidae) from golden snapper *Lutjanus johnii* (Bloch) in Australian waters, with the recognition of *Sinocaligus* Shen, 1957 as a junior synonym of *Caligus* Müller, 1785. Systematic Parasitology 100(5): 487–504. https://doi.org/10.1007/s11230-023-10099-z

Boxshall GA, Bernot JP (2023) Resolving taxonomic and nomenclatural problems in the genus *Caligus* O.F. Müller, 1785 (Copepoda: Caligidae). Zootaxa 5360(4): 545–567. https://doi.org/10.11646/zootaxa.5360.4.5

Boxshall GA, Gurney AR (1980) Description of two new and one poorly known species of the genus *Caligus* Müller, 1785 (Copepoda: Siphonostomatoida). Bulletin of the British Museum (Natural History). Zoology : Analysis of Complex Systems, ZACS 39: 161–178. https://doi.org/10.5962/p.13270

Boxshall GA, Halsey SH (2004) An introduction to copepod diversity. Vols. I & II. The Ray Society, London, 966 pp.

Brian A (1906) Copepodi parassiti dei pesci d'Italia. Stab. Tipo-Litografico R. Instituto Sordomuti, Genova, 1–187. https://doi.org/10.5962/bhl.title.58642

Burmeister H (1835) Beschreibung einiger neuen oder weniger bekannten Schmarotzerkrebse, nebst allgemeinen Betrachtungen über die Gruppe, welcher sie angehören. Nova Acta Physico-Medica Academiae Caesareae Leopoldino-Carolinae Naturae Curiosorum (Acta der Kaiserlichen Leopoldinisch-Carolinischen Deutschen Akademie der Naturforscher), Halle 17: 269–336. https://doi.org/10.5962/bhl.title.39131

Byrnes T (1986) A new species of *Parapetalus* (Copepoda: Caligidae) parasitic on the samson fish, *Seriola hippos* from Australia and its similarity with *Caligus spinosus*. Publications of the Seto Marine Biological Laboratory 31(1–2): 55–62. https://doi.org/10.5134/176118

Capart A (1941) Copepoda parasitica. Résultats scientifiques des croisières du Navire-école belge "Mercator", 3(5). Mémoires du Musée Royal d'Histoire Naturelle de Belgique 2: 171–197.

Causey DL (1953) Parasitic Copepoda from Grand Isle, Louisiana. Occasional Papers of the Marine Laboratory of Louisiana State University 7: 1–18.

Cressey RF (1967) *Caritus*, a new genus of caligoid copepod, with a key to the genera of Caliginae. Proceedings of the United States National Museum 123(3623): 1–8. https://doi.org/10.5479/si.00963801.123-3623.1

Cressey RF (1969) *Caligus hobsoni*, a new species of parasitic copepod from California. The Journal of Parasitology 55: 431–434. https://doi.org/10.2307/3277430 [Accessed on 12 January 2024]

Cressey R (1991) Parasitic Copepods from the Gulf of Mexico and Caribbean Sea, III: *Caligus*. Smithsonian Contributions to Zoology 497(497): 1–53. https://doi.org/10.5479/si.00810282.497

Cressey R, Cressey HB (1980) Parasitic copepods of mackerel- and tuna-like fishes (Scombridae) of the world. Smithsonian Contributions to Zoology 311(311): 1–139. https://doi.org/10.5479/si.00810282.311.i

Dana JD (1849–1852) Conspectus crustaceorum, quae in orbis terrarum circumnavigatione, Carolo Wilkes, e classe Reipublicae foederatae duce, lexit et descripsit Jacobus

D. Dana. Pars II. Proceedings of the American Academy of Arts and Sciences 2nd series: 9–61. https://www.biodiversitylibrary.org/page/4481593#page/17/mode/1up

Delamare Deboutteville C, Nunes-Ruivo LP (1958) Copépodes parasites des poissons Méditerranéens. (4e série). Vie et Milieu 9: 215–235.

Dojiri M, Ho J-S (2013) Systematics of the Caligidae, copepods parasitic on marine fishes. Crustaceana Monographs 18: 1–448. https://doi.org/10.1163/9789004204256

Durán LEB (1980) Copépodos parásitos en peces del Perú: Género *Caligus* Müller, 1785, *Caligus callaoensis* n. sp. y tres nuevos registros (Crustacea, Copepoda). Boletín del Museo Nacional de Historia Naturale, Santiago, Chile 37: 309–316. https://doi.org/10.54830/bmnhn.v37.1980.496

Froese R, Pauly D (2023) FishBase. World Wide Web electronic publication. www.fishbase.org [Version 02/2023] [accessed on 12 January 2024]

Gusev AV (1951) Paraziticheskie Copepoda s nekotorykh morskikh ryb. Parasitic Copepoda of some marine fishes. Parazitologica Papers of the Zoological Institute. Academia Nauk, USSR 13: 394–463.

Hayes P, Justine J-L, Boxshall GA (2012) The genus *Caligus* Müller, 1785 (Copepoda: Siphonostomatoida): two new species from reef associated fishes in New Caledonia, and some nomenclatural problems resolved. Zootaxa 3534: 21–39. https://doi.org/10.11646/zootaxa.3534.1.2

Heegaard PE (1945) Some parasitic copepods from fishes in the Uppsala University collections. Arkiv för Zoologi 35: 1–27.

Heegaard PE (1955) Parasitic copepods from tropical west Africa. Atlantide Report 3: 41–56.

Heegaard P (1962) Parasitic Copepoda from Australian waters. Records of the Australian Museum 25(9): 149–233. https://doi.org/10.3853/j.0067-1975.25.1962.661

Heller C (1865) Crustaceen. In: Reise der Österreichischen Fregatte Novarra um die Erdre, in den Jahren 1857, 1858, 1859 unter den Befehlen des Commodore B. von Wüllerstorf-Urbair, Zoologischer Theil. Kaiserlich-Königliche Hof- und Staatsdruckerei, Wein, 1–280.

Hernández-Olascoaga A, González-Solís D, Aznar FJ (2022) Parasites as indicators of habitat use by the schoolmaster (*Lutjanus apodus*) in the Mesoamerican Reef System. Estuarine, Coastal and Shelf Science 278: 108120. https://doi.org/10.1016/j.ecss.2022.108120

Ho J-S, Lin C-L (2004) Sea lice of Taiwan (Copepoda: Siphonostomatoida: Caligidae). The Sueichan Press, Keelung, Taiwan, 388 pp.

Ho J-S, Lin C-L (2010) Three more unrecorded sea lice (Copepoda, Caligidae) parasitic on marine fishes collected off Tai-dong, Taiwan. Crustaceana 83(10): 1261–1277. https://doi.org/10.1163/001121610X521262

Huys R, Boxshall GA (1991) Copepod evolution. The Ray Society, London, 468 pp. https://doi.org/10.4319/lo.1993.38.2.0478

Johnson SC, Treasurer JW, Bravo S, Nagasawa K, Kabata Z (2004) A review of the impact of parasitic copepods on marine aquaculture. Zoological Studies (Taipei, Taiwan) 43: 8–19. https://zoolstud.sinica.edu.tw/Journals/43.2/229.pdf

Kabata Z (1979) Parasitic Copepoda of British fishes. Ray Society, London, 468 pp.

Kabata Z (1992) Copepoda parasitic on Australian fishes. XIV. An assemblage of bathypelagic species. Journal of Natural History 26(1): 9–45. https://doi.org/10.1080/00222939200770021

Krøyer H (1863) Bidrag til Kundskab om Snyltekrebsene. Naturhistorisk Tidsskrift Ser. III 2: 75–320.

Krøyer (1864) Bidrag til Kundskab om Snyltekrebsene. Naturhistorisk Tidsskrift Ser. III 2: 321–426.

Leidy J (1889) A parasitic copepod. Proceedings. Academy of Natural Sciences of Philadelphia 1889: 95.

Lewis AG (1967) Copepod crustaceans parasitic on teleost fishes of the Hawaiian Islands. Proceedings of the United States National Museum 121(3574): 1–204. https://doi.org/10.5479/si.00963801.121-3574.1

Luque JL, Takemoto RM (1996) Parasitic copepods on *Orthopristis ruber* and *Haemulon steindachneri* (Osteichthyes: Haemulidae) from the Brazilian littoral, with the description of a new species of *Caligus* (Siphonostomatoida: Caligidae). Revista Brasileira de Biologia 56: 529–546.

Milne Edwards H (1840) Ordre des copépodes. Histoire naturelle des crustacés, comprenant l'anatomie, la physiologie et la classification de ces animaux. 3: 411–529. https://www.biodiversitylibrary.org/page/16103940

Morales-Serna FN, Gómez S, Gerardo P-P de L (2012) Parasitic copepods reported from Mexico. Zootaxa 3234(1): 43–68. https://doi.org/10.11646/zootaxa.3234.1.2

Morales-Serna FN, Hernández-Inda ZL, Gómez S, Pérez-Ponce de León G (2013) Redescription of *Caligus serratus* Shiino, 1965 (Copepoda: Caligidae) parasitic on eleven fish species from Chamela Bay in the Mexican Pacific. Acta Parasitologica/ Witold Stefański Institute of Parasitology, Warszawa, Poland 58: 367–375. https://doi.org/10.2478/s11686-013-0150-x

Morales-Serna FN, Pinacho-Pinacho CD, Gómez S, Pérez-Ponce de León G (2014) Diversity of sea lice (Copepoda: Caligidae) parasitic on marine fishes with commercial and aquaculture importance in Chamela Bay, Pacific coast of Mexico by using morphology and DNA barcoding, with description of a new species of *Caligus*. Parasitology International 63(1): 69–79. https://doi.org/10.1016/j.parint.2013.09.005

Morales-Serna FN, Medina-Guerrero RM, Fajer-Avila EJ (2016) Sea lice (Copepoda: Caligidae) parasitic on fishes reported from the Neotropical region. Neotropical Biodiversity 2(1): 141–150. https://doi.org/10.1080/23766808.2016.1236313

Morales-Serna FN, Oceguera-Figueroa A, Tang D (2017) *Caligus fajerae* n. sp. (Copepoda: Caligidae) parasitic on the Pacific sierra *Scomberomorus sierra* Jordan & Starks (Actinopterygii: Scombridae) in the Pacific Ocean off Mexico. Systematic Parasitology 94(8): 927–939. https://doi.org/10.1007/s11230-017-9752-2

Müller OF (1785) Entomostraca seu Insecta Testacea, quae in aquis Daniae et Norvegiae reperit, descripsit et iconibus illustravit Otho Fridericus Müller. F. W. Thiele, Lipsiae & Havniae, 1–134. https://doi.org/10.5962/bhl.title.14414

Nordmann A von (1832) Mikrographische Beiträge zur Naturgeschichte der wirbellosen Thiere. In: Zweites Heft. Mit zehn Kupfertafeln, G. Reimer, Berlin, 1–150.

Ohtsuka S, Boxshall GA (2019) Two new species of the genus *Caligus* (Crustacea, Copepoda, Siphonostomatoida) from the Sea of Japan, with a note on the establishment of a new species group. ZooKeys 2019: 91–113. https://doi.org/10.3897/zookeys.893.46923

Ohtsuka S, Nawata M, Nishida Y, Nitta M, Hirano K, Adachi K, Kondo Y, Venmathi Maran BA, Suárez-Morales E (2020) Discovery of the fish host of the "planktonic" caligid *Caligus undulatus* Shen & Li, 1959 (Crustacea: Copepoda: Siphonostomatoida). Biodiversity Data Journal 8: e52271. https://doi.org/10.3897/BDJ.8.e52271

Özak AA, Yanar A, Boxshall GA (2017) The discovery of *Caligus macrurus* Heller, 1865 (Copepoda: Caligidae) in the Mediterranean Sea, and the recognition of *Sciaenophilus* van Beneden, 1852 as a junior synonym of *Caligus* Müller, 1785. Systematic Parasitology 94(1): 97–109. https://doi.org/10.1007/s11230-016-9682-4

Pearse AS (1951) Parasitic Crustacea from Bimini, Bahamas. Proceedings of the United States National Museum 101(3280): 341–372. https://doi.org/10.5479/si.00963801.101-3280.341

Pillai NK (1961) Copepods parasitic on South Indian Fishes. Part I, Caligidae. Bulletin of the Research Institute. University of Kerala 8(C): 87–130.

Rangnekar MP (1957) *Caligus dasyaticus* sp. nov. and *Caligus dussumieri* sp. nov. (Copepoda) parasitic on Bombay fishes. Journal of the University of Bombay (B) 25: 16–22.

Rangnekar MP (1984) Parasitic copepods from marine fishes of Bombay. Vervoort W, Vaupel Klein von JC (Eds). Crustaceana, suppl. Studies on Copepoda II. Proceedings of the First International Conference on Copepoda, Amsterdam, The Netherlands, 24–28 August 1981 7: 344–351. https://doi.org/10.1163/9789004629363_036

Rangnekar (1956) Parasitic copepods from the marine fishes of Bombay. Journal of the University of Bombay (B)24: 42–65.

Rodríguez-Santiago MA, Morales-Serna F, Gómez S, Grano-Maldonado MI (2016) New records of parasitic copepods (Copepoda:Pandaridae, Eudactylinidae, Caligidae) on elasmobranchs (Chondrichthyes) in the Gulf of Mexico. Ciencia Pesquera 24: 15–21.

Roubal FR, Armitage J, Rohde K (1983) Taxonomy of metazoan ectoparasites of snapper, *Chrysophrys auratus* (family Sparidae), from southern Australia, eastern Australia and New Zealand. Australian Journal of Zoology, Supplemental Series 94: 1–68. https://doi.org/10.1071/AJZS094

Shen C-J (1957) Parasitic copepods from fishes of China. Part II. Caligoida, Caligidae (1). Acta Zoologica Sinica 9: 351–378.

Shen C-J, Li H-L (1959) Parasitic copepods from fishes of China. IV. Caligoida, Caligidae (3). Acta Zoologica Sinica 11: 12–20.

Shiino SM (1954a) On *Caligus latigenitalis* n. sp., a copepod parasitic on the fish, *Sparus macrocephalus* (Basilewsky). Nippon Suisan Gakkaishi 20(1): 21–25. https://doi.org/10.2331/suisan.20.21

Shiino SM (1954b) On the new copepod, *Caligus calotomi* n. sp., parasitic on the fish, *Calotomus japonicus* (C. & V.). Bulletin of the Japanese Society of Scientific Fisheries. Nippon Suisan Gakkaishi 20(1): 16–20. https://doi.org/10.2331/suisan.20.16

Shiino SM (1960) Copepods parasitic on the fishes collected on the coast of Province Shima, Japan. Reports of the Faculty of Fisheries. Prefectural University of Mie 3: 471–500.

Shiino SM (1965) Parasitic copepods of the eastern Pacific fishes. 5. *Caligus*. Reports of the Faculty of Fisheries. Prefectural University of Mie 5: 391–420.

Soler-Jiménez LC, Morales-Serna FN, Aguirre-Macedo ML, McLaughlin JP, Jaramillo AG, Shaw JC, James AK, Hechinger RF, Kuris AM, Lafferty KD, Vidal-Martínez VM (2019) Parasitic copepods (Crustacea, Hexanauplia) on fishes from the lagoon flats of Palmyra Atoll, Central Pacific. ZooKeys 833: 85–106. https://doi.org/10.3897/zookeys.833.30835

Stebbing TRR (1900) On Crustacea brought by Dr. Willey from the South Seas. In: Willey A (Ed.) Zoological Results based on material from New Britain, New Guinea, Loyalty Islands and Elsewhere collected during the years 1895, 1896 and 1897. Part V. Cambridge University Press, UK, 605–690.

Steenstrup JJS, Lütken CF (1861) Bidrag til kundskab om det aabne havs snyltekrebs og lernæer samt om nogle andre nye eller hidtil kun ufuldstændigt kjendte parasitiske Copepoder. Kongelige Danske Videnskabernes Selskabs Skrifter, Naturhistorisk og Mathematisk Afdeling. Kjöbenhavn 5: 343–432. https://doi.org/10.5962/bhl.title.59539

Suárez-Morales E, Kim I-H, Escamilla BJ (2012) On some caligids (Copepoda: Caligidae) from plankton of a coastal lagoon in the Gulf of Mexico with a description of a new species of *Metacaligus*. Zoological Studies (Taipei, Taiwan) 51: 804–818.

Thomsen R (1949) Copépodos parásitos de los peces marinos del Uruguay. Comunicaciones Zoologicas del Museo de Historia Natural de Montevideo 3: 1–41.

Thorell T (1859) Till kännedomen om vissa arasitiskt lefvande Entomostraceer. Öfversigt af Konglige Vetenskaps-Akademiens förhandlingar, Stockholm 16: 335–362.

Uma Devi DV, Shyamasundari K (1981) A new species of the genus *Caligus* Müller, 1785 from fish, *Dactyloptena orientalis*, at Waltair. Indian Journal of Parasitology 5: 91–94.

Villalba-Vasquez PJ, Violante-González J, Pulido-Flores G, Monks S, Rojas-Herrera AA, Flores-Rodríguez P, Rosas-Acevedo JL, Cayetano CV, Santos-Bustos NG (2022) Parasite communities of the spotted rose snapper *Lutjanus guttatus* (Perciformes: Lutjanidae) off the Mexican Pacific coasts: Spatial and long-term inter-annual variations. Parasitology International 88: 102551. https://doi.org/10.1016/j.parint.2022.102551

Walter TC, Boxshall G (2024a) World of Copepods Database. Caligidae Burmeister, 1835. [Accessed through: World Register of Marine Species at:] https://www.marinespecies.org/aphia.php?p=taxdetails&id=135513 [accessed on 24 January 2024]

Walter TC, Boxshall G (2024b) World of Copepods Database. *Caligus* Müller O.F., 1785. [Accessed through: World Register of Marine Species at:] https://www.marinespecies.org/aphia.php?p=taxdetails&id=135566 [accessed on 24 January 2024]

Walter TC, Boxshall G (2024c) World of Copepods Database. *Lepeophtheirus* Nordmann, 1832. [Accessed through: World Register of Marine Species at:] https://www.marinespecies.org/aphia.php?p=taxdetails&id=135568 [accessed on 24 January 2024].

Wilson CB (1905) North American parasitic copepods belonging to the family Caligidae. Part 1.- The Caliginae. Proceedings of the United States National Museum 28(1404): 479–672. https://doi.org/10.5479/si.00963801.28-1404.479

Wilson CB (1913) Crustacean parasites of West Indian fishes and land crabs, with descriptions of new genera and species. Proceedings of the United States National Museum 44(1950): 189–227. https://doi.org/10.5479/si.00963801.44-1950.189

Wilson CB (1921) Report on the parasitic Copepoda collected during the survey of the Juan Fernandez Islands, 1916–1917. Natural History of the Juan Fernandez & Easter Islands 3(1): 69–74.

Wilson CB (1937) Some parasitic copepods from Panama Bay. Journal of the Washington Academy of Sciences 27: 423–431. https://doi.org/10.1126/science.86.2236.423.b

Yamaguti S (1936) Parasitic copepods from fishes of Japan. Part 2. Caligoida, I. Kyoto Imperial University, 1–22.

Yamaguti S (1939) Parasitic copepods from fishes of Japan. Part 5. Caligoida, III. Volume Jubilare for Prof. Sadao Yoshida 2: 443–487.

Yamaguti S, Yamasu T (1959) Parasitic copepods from fishes of Japan with description of 26 new species and remarks on two known species. Biological Journal of Okayama University 5: 89–165.

Yü SC (1933) Chinese parasitic copepods collected by H.W. Wu, with descriptions of new genera and species. Bulletin of the Fan Memorial Institute of Biology. Zoology: Analysis of Complex Systems, ZACS 4: 117–139.

ZooKeys 1209: 69–197 (2024)
DOI: 10.3897/zookeys.1209.125897

Research Article

Systematics and biogeography of Appalachian Anillini, and a taxonomic review of the species of South Carolina (Coleoptera, Carabidae, Trechinae, Anillini)

Curt W. Harden[1], Michael S. Caterino[1]

[1] *Department of Plant and Environmental Sciences, Clemson University, 277 Poole Agricultural Center, Clemson, South Carolina, 29634, USA*
Corresponding author: Curt W. Harden (c_har@fastmail.com)

Abstract

In the eastern United States, 74 species of Anillini in two genera have been described, with most belonging to *Anillinus* Casey. Until now, no systematic framework has existed for this large genus, hampering integrative studies. Using DNA sequences from 101 Nearctic species, we present a well-resolved molecular phylogeny supporting a sound systematic framework. Sixteen species groups of Appalachian *Anillinus* are diagnosed, in part using newly recognized variation in the number of modified male protarsi and the state of the spermathecal duct. We present the first descriptions of Nearctic anilline larvae, which possess none of the synapomorphies of previously described anilline larvae. Within *Anillinus*, two major clades are mostly consistent with setation of the right paramere: a "hairy clade" with more than four setae, and a "quadrisetose clade." Throughout the phylogeny, microhabitat use varies within each clade, and several endogean lineages are phylogenetically isolated. Our work increases the South Carolina fauna by nearly five-fold. Nine new species are described, *Serranillus monadnock* **sp. nov.**, *Anillinus castaneus* **sp. nov.**, *Anillinus choestoea* **sp. nov.**, *Anillinus dentatus* **sp. nov.**, *Anillinus jancae* **sp. nov.**, *Anillinus mica* **sp. nov.**, *Anillinus micamicus* **sp. nov.**, *Anillinus seneca* **sp. nov.**, and *Anillinus simplex* **sp. nov.** Several species are newly reported from South Carolina, bringing the total to 20 described species representing seven species groups. Two endemic groups inhabit deep clay soils in the Piedmont and possess unique male sexual characters. The Anillini are a unique component of Nearctic biodiversity, with great potential as a model system for studies of biogeography, secondary male sexual modification, and endogean adaptations.

Key words: Evolution, eyeless, flightless, phylogenetics, predaceous, subterranean biology

Academic editor: Rikjan Vermeulen
Received: 22 April 2024
Accepted: 14 June 2024
Published: 8 August 2024

ZooBank: https://zoobank.org/CEE78803-61EB-40CC-8D63-46142E6383A1

Citation: Harden CW, Caterino MS (2024) Systematics and biogeography of Appalachian Anillini, and a taxonomic review of the species of South Carolina (Coleoptera, Carabidae, Trechinae, Anillini). ZooKeys 1209: 69–197. https://doi.org/10.3897/zookeys.1209.125897

Table of contents

Introduction

Members of the tribe Anillini are small, flightless, predaceous ground beetles, ubiquitous in most temperate and tropical regions of the world, with the notable exception of eastern Asia (Jeannel 1963a; Andújar et al. 2016). More than 620 valid species have been described, all entirely eyeless, with the exceptions of the subtribe Nesamblyopina (Sokolov 2023) and the poorly known African genera *Microdipnodes* Basilewsky and *Cryptorites* Jeannel (Jeannel 1963a). Anillines inhabit a variety of dark, interstitial habitats and typically have very small ranges consistent with their limited dispersal capabilities.

The United States east of the Mississippi River is home to 58 described anilline species in two genera, *Anillinus* Casey and *Serranillus* Barr. A third genus, *Stylulus* Schaufuss, has been reported from the region as well (Barr 1969; Cornell 1972, 1977a; Erwin and Sims 1984), but the identity of these records has not been confirmed. Members of *Anillinus* also occur west of the Mississippi River, in Arkansas (4 spp.), Missouri (1 spp.), Oklahoma (2 spp.), and Texas (9 spp.) (Sokolov 2022; Sokolov et al. 2004, 2014; Sokolov and Watrous 2008). *Serranillus* is restricted to the eastern United States, with a relatively small range (Fig. 1A) that is nested within that of *Anillinus* (Fig. 1B). In eastern North America, anillines have been collected from a wide variety of elevations and microhabitats, varying from deep sand near sea level in Florida (Sokolov and Schnepp 2021) to coniferous litter on the summit of Mount Mitchell in North Carolina, the highest point east of the Mississippi River (Carnegie Museum of Natural History, Pittsburgh data). The collective range of the tribe in the eastern United States has its northern limits in Maryland, southern Ohio, and the southern counties of Indiana (Dury 1902; Sokolov et al. 2004). Known occurrence data (Harden 2024) suggest that anillines may be expected to occur anywhere south of this line. Most records are from montane localities, but this likely is an artifact of collecting bias. At lower elevations, where conditions are warmer and drier, anillines are more difficult to collect by hand, except during exceptionally wet periods following heavy rains (Barr 1995; Carlton et al. 2005). In the “TAG” karst region at the corner of Tennessee, Alabama, and Georgia, *Anillinus* can be found in caves, including a small number of species that appear to be strict cave inhabitants or troglobites (Jeannel 1963b; Sokolov 2012, 2020). *Anillinus* have rarely been found in caves outside this region, and no apparent troglobites are known except in TAG caves. Most *Anillinus* found in caves are collected in very small numbers, and may actually be inhabitants of the smaller interstices in the “Milieu Souterrain Superficiel” or “Mesovoid Shallow Substratum” (MSS; Mammola et al. 2016) that enter caves only occasionally.

Anillines in eastern North America are diverse in body size and structure (Fig. 2). The smallest species known is an undescribed *Anillinus* species from northern Georgia (Fig. 2G) and the largest are some members of the genus *Serranillus* (Fig. 2L). Structural differences in convexity and overall habitus are associated with different microhabitats. For example, species readily collected from leaf litter are usually convex and ovoid in outline (Fig. 2A, F, G, K, O), whereas those inhabiting endogean (= deep soil) habitats are usually dorsoventrally flattened and more parallel-sided (Fig. 2B, C, E, H, P, Q). Species in rock interstices and caves are also typically flattened, but usually have relatively broad elytra with stronger humeral angles (Fig. 2I, N, S). However, the distinction between these three broad categories is often not clear, and some species are intermediate in both body structure and microhabitat use (Fig. 2D, J, L, M, R). While litter, soil and caves are convenient habitat “bins” for sorting species, the range of microhabitats experienced by animals less than 3 mm in length is probably more diverse.

Historically, taxonomic progress on Nearctic Anillini has been slow. One of the earliest descriptions of an anilline was the Appalachian Mountain endemic *Anillinus fortis* (Horn, 1868), but nearly a century would pass before any additional valid Appalachian species would be named (Jeannel 1963a). Barr (1969) published a brief but thorough overview of the anilline fauna of the United States. His point map of eastern anillines (fig. 9) has remained the most complete reference for their collective range in the region to date, including many geographically isolated species known to him in 1969, but that remain

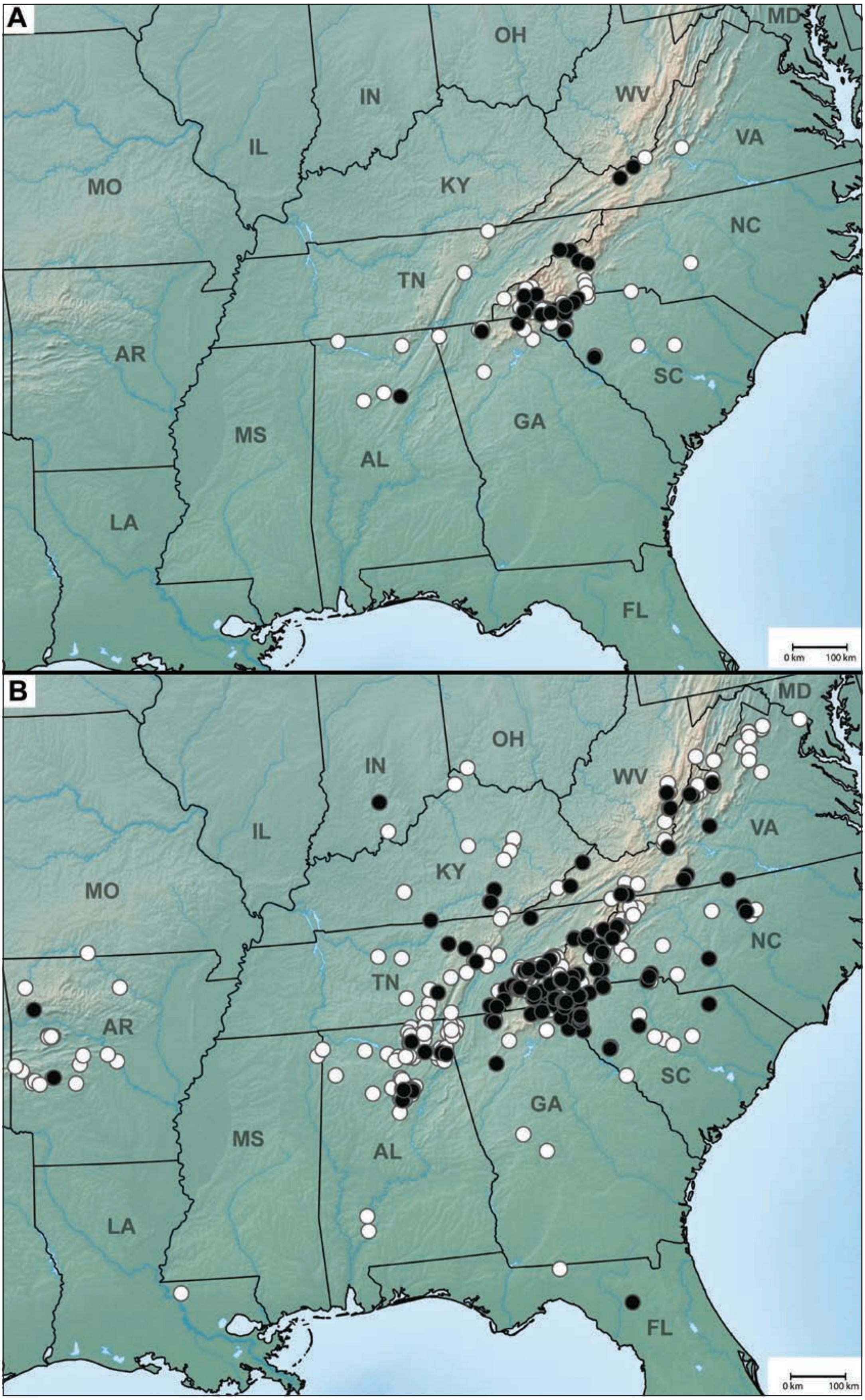

Figure 1. Distribution maps of eastern Nearctic Anillini **A** *Serranillus* **B** *Anillinus*. White dots: all known occurrences. Black dots: locations of new DNA sequence vouchers from this study. Data from Harden (2024).

Figure 2. Habitus of eastern Nearctic Anillini. **A** *Serranillus dunavani* (South Carolina, Oconee Co.) **B** *Anillinus moseleyae* (Tennessee, Sevier Co.) **C** *Anillinus dentatus* (South Carolina, Abbeville Co.) **D** *Serranillus jeanneli* (South Carolina, Oconee Co.) **E** *Anillinus folkertsioides* (Alabama, Blount Co.) **F** *Anillinus pecki* (North Carolina, Avery Co.) **G** *Anillinus* sp. “Georgia, Barnes Creek sp. 1” **H** *Anillinus montrex* (South Carolina, York Co.) **I** *Anillinus* sp. “Tennessee, Kings Saltpeter Cave” **J** *Anillinus virginiae* (Virginia, Bath Co.) **K** *Anillinus erwini* (Virginia, Grayson Co.) **L** *Serranillus* sp. (North Carolina, Graham Co.) **M** *Anillinus* sp. “South Carolina, Waldrop Stone” (South Carolina, Pickens Co.) **N** *Anillinus* sp. “Alabama, Horseshoe Cave sp. 1” **O** *Anillinus loweae* (North Carolina, Haywood Co.) **P** *Anillinus* sp. “Kentucky, Hestand sp. 1” **Q** *Anillinus indianae* (Indiana, Lawrence Co.) **R** *Anillinus* cf. *barberi* (West Virginia, Greenbrier Co.) **S** *Anillinus hirsutus* (Alabama, Madison Co.). Scale bar: 1 mm.

undescribed today. His lone taxonomic contribution to Anillini (Barr 1995) established the genus *Serranillus* and included valuable information about collecting techniques, but most of Barr's extensive knowledge of the group has remained unpublished. The groundbreaking review of *Anillinus* by Sokolov et al. (2004) set in motion a modern period of taxonomic study that has steadily revealed the true diversity of Nearctic Anillini during the past two decades (Sokolov et al. 2007; Sokolov and Carlton 2008, 2010; Giachino 2011; Sokolov 2011, 2021; Sokolov and Schnepp 2021; LaBonte and Maddison 2023; Harden and Caterino 2024), including description of species based on Barr's material, now at the Carnegie Museum of Natural History (Sokolov 2012, 2014, 2020). An early classification scheme of *Anillinus* based on presumed microhabitat use and patterns of dorsal microsculpture (Sokolov et al. 2004) has gradually been abandoned as additional new species and COI sequence data have challenged this classification (Sokolov and Carlton 2010; Sokolov 2020; Sokolov and Schnepp 2021). There is currently no systematic framework for this large genus, which includes at least 70 undescribed species (Harden 2024).

In this paper, we present an updated systematic framework of eastern Anillini based on a molecular phylogeny and newly recognized morphological variation, including novel male secondary modifications. The first larvae of Nearctic Anillini are described. We also present a taxonomic review of the surprisingly diverse and unique South Carolina anilline fauna, describing nine new species, redescribing four species, and designating a neotype for *Serranillus jeanneli* Barr. Combined with a distributional dataset for eastern anillines based upon all published occurrences and the examination of thousands of physical specimens (Harden 2024), our molecular phylogeny reveals the complex biogeographic history of eastern anillines.

Materials and methods

Field collecting

We used litter sifting, litter extraction, soil washing, turning embedded rocks, and soil trapping to collect anillines. Litter sifting involved placing a small amount of deep leaf litter into a ¼" or ½" mesh metal screen and shaking over a white plastic bin, which was then checked for beetles. Litter extraction involved sifting large amounts of litter through a metal screen into a cloth bag, and then placing the sifted material in Berlese funnels (with incandescent light bulbs as a heat source) or Winkler extractors and leaving it for several days. Soil washing involved digging up mineral soil with a large shovel, sifting it through a screen, and then slowly adding it to large buckets filled halfway with water; the mixture was then stirred vigorously and allowed to settle before skimming off the organic material floating on the surface; this material was dried in a cloth bag for one or more days and then processed in a Berlese funnel or placed on metal screens above containers set in direct sunlight (Maquet et al. 2018; Andújar and Grebennikov 2021). In some cases, the sifted soil itself was directly placed in Berlese funnels instead of mixing with water. Turning embedded rocks involved using a metal pry bar to loosen and dislodge rocks deeply embedded in the soil. The underside of the rock and the soil surface beneath it were carefully scanned while wearing a bright headlamp. Soil trapping was conducted using "pipe traps" modified from the design shown in LaBonte and Maddison (2023), with PVC pipes (5.08 cm outer diameter) cut to 20.32 cm lengths and cut with 1 cm wide latitudinal slots spaced along most of the length; a plastic container (Sarstedt #75.9922.421) was attached to one end of the pipe using duct tape. An initial hole was dug to a depth of 15–40 cm and a shaft was created at the bottom of this hole using an auger (Art's Manufacturing and Supply, Inc. SKU: 400.48). A small amount of propylene glycol was added to the plastic container, and the pipe assembly was inserted in the shaft with a plastic sleeve inserted to keep soil out while refilling the soil around the pipe. A plastic lid with a piece of bright flagging tape attached with fishing line was placed on top and reburied, with the flagging marking the trap above ground. Traps were left in place for three months or longer. All of these collecting methods produced anilline specimens. For pipe traps and most hand collecting, geographical coordinates were taken using a Garmin GPSMAP 64 GPS receiver. For some hand collecting events and all literature records for which coordinates were not given, approximate coordinates were obtained retroactively using Google Earth; these have reduced digits to indicate less accuracy.

Morphology

Terminology of most structures follows that of Slipinski and Lawrence (2013). Mandibular tooth terminology follows Maddison (1993). Designations of "dorsal" and "ventral" faces of the median lobe of the aedeagus follow typical convention for carabids, and not their orientation in repose or when everted. Designation of "right" and "left" parameres of the aedeagus also follow typical convention (Sokolov 2022). The sclerotized structures in the internal sac of the median lobe have traditionally been referred to as "dorsal sclerites" and "ventral sclerites" in Nearctic anilline literature (e.g., Sokolov et al. 2004). We consider the "dorsal sclerites" to be equivalent with the flagellum, and refer to it as such; the ejaculatory duct connects to the base of this structure, and we consider it homologous across the taxa treated. Sokolov et al. (2007) used the schematic of the internal sac of *Lionepha* in Erwin and Kavanaugh (1981) to homologize their "dorsal sclerites"; an apparent flagellum is lacking in *Lionepha*, and homology between what we term the flagellum and any of the sclerotized structures shown in Erwin and Kavanaugh (1981) is uncertain. We refer to other sclerotized structures in the internal sac variously based on their shape and position within the sac; these structures are unlikely to be homologous across taxa, and so we avoid the use of a single term for them. Our interpretation of "lateral aspect" differs from that of Sokolov (e.g., 2012). We consider the lateral aspect to be that viewed when the basal lobes of the median lobe are parallel to the plane on which they rest. Most aedeagi of the species are strongly asymmetrical and twisted from this plane, and the aspect illustrated as "left lateral aspect" in previous papers on Appalachian Anillini is an aspect we consider a dorsal or dorsolateral aspect.

Measurements of the length of body regions were taken using calibrated images in Adobe Photoshop and are given using the following abbreviations in the descriptions and key.

ABL	Apparent body length, measured from anterior edge of clypeus to apex of elytra
EL	Elytral length, measured from posterior edge of scutellum to apex of elytra
EW	Maximum elytral width
HW	Maximum head width
PbW	Pronotal basal width, measured at posterior angles and not including external denticles
PL	Pronotal length, measured along midline
PW	Maximum pronotal width
RL	Ring sclerite length

External structures were examined using Amscope (SKU: SM-1BSL-V331), Leica M80, and Olympus SZX7 stereoscopes, at 7–100 × magnifications. Some mouthparts and legs were further examined by placing in glycerin and viewing with a Motic BA300 compound microscope. Dissection of male and female genitalia was performed using Dumont #5 forceps (Item nos. 11251-20 and 11252-20, www.finescience.com/) and bent #000 and minuten insect pins held in short pin vises. For males that had been through the DNA extraction process, removal of the ring sclerite and aedeagus was performed by tearing the tergites with minuten pins and pulling the structures out from the dorsal side. Specimens that were previously dry mounted or stored in ethanol were first relaxed in a warm water bath for 0.5 hr or more, then placed in a drop of weak ethanol or water on a depression slide; fine forceps were used to stabilize the specimen, with the tip of the index finger inserted between the forceps to allow better control and prevent crushing the specimen, and the ring sclerite and aedeagus were removed from the posterior abdominal opening using a bent minuten pin; such genitalia usually required further clearing by placing in 0.5 mL centrifuge vials containing 85% lactic acid or 10% potassium hydroxide and placing in a warm water bath for 15 min or longer to remove hardened musculature. In the case of specimens from vials from which the fluid had evaporated, labels were removed and a small amount of ammonia-based cleaner was sprayed into the vial and left for 0.5 hr or more to relax and clean the specimens; specimens treated in this way were usually pliable enough to be dissected without a warm water bath. To study female genitalia, the entire abdomen was removed and cleared (either by DNA extraction or using short treatments of warm 85% lactic acid or 10% potassium hydroxide) and the genital segment was carefully removed and studied in glycerin. For especially small specimens or single female specimens, the genital segment was left in the abdomen and the spermatheca was studied through the abdominal ventrites. Genitalic structures were studied in glycerin on depression slides using a Motic BA300 compound microscope and photographed using a Canon Powershot A2200 digital camera. Some median lobes were further cleared by placing in clove oil after rinsing in ethanol, and left to sit overnight before viewing. In most cases, genitalia were stored in glycerin in microvials pinned beneath the specimens. Male genitalia of *Anillinus* holotypes and some female genitalia were mounted in Euparal on plastic microslides pinned beneath the specimens. Both the aedeagus and the spermatheca are asymmetrical; mounting them permanently prevents studying their true structure, and for this reason was usually avoided.

Hand line drawings of male genitalia were first made with pen and ink, with proportions traced from printed photographs, and then scanned and digitized in Adobe Illustrator. Habitus photographs were taken with a Visionary Digital Passport II system with a Canon 6D SLR and 65-mm MP-E 1–5X macro lens, with focus stacking performed in Helicon Focus (www.heliconsoft.com). Scanning electron micrographs of uncoated specimens affixed to stubs with double sided tape were taken at 15.0kV in BSE and BSE3D modes using a Hitachi S-3400 Variable Pressure Scanning Electron Microscope (SEM) at the Clemson University Scanning Electron Microscopy Facility in Anderson, SC.

Material examined

Approximately 7,000 specimens of Anillini were examined. The dataset of Harden (2024) provides data for 6,438 of these. All specimens examined are deposited in the following collections.

AMDc	Anthony M. Deczynski personal collection, Central, SC, USA
ADGc	Augusto DeGiovanni personal collection, Bologna, Italy
CMNH	Carnegie Museum of Natural History, Pittsburgh, PA, USA
CMC	Cincinnati Museum Center, Cincinnati, OH, USA
CNC	Canadian National Collection of Insects, Ottawa, Canada
CUAC	Clemson University Arthropod Collection, Clemson, SC, USA
CWHc	Curt Harden personal collection, Central, SC, USA
FSCA	Florida State Collection of Arthropods, Gainesville, FL, USA
GRSM	Great Smoky Mountains National Park collection, Gatlinburg, TN, USA
KESc	Kyle E. Schnepp personal collection, Gainesville, FL, USA
LSAM	Louisiana State Arthropod Museum, Baton Rouge, LA, USA
NCSU	North Carolina State University, Raleigh, NC, USA
NHMUK	The Natural History Museum, London, United Kingdom
OSAC	Oregon State Arthropod Collection, Corvalis, OR, USA
OSUC	Ohio State University Collection, Cleveland, OH, USA
TLc	Todd Lawton personal collection, Winnipeg, MB, Canada
UGCA	University of Georgia Collection of Arthropods, Athens, GA, USA
USNM	United States National Museum of Natural History, Washington, D.C., USA
VMNH	Virginia Museum of Natural History, Martinsville, VA, USA

The holotypes of four eastern Nearctic species, *Anillinus campbelli* Giachino, *Anillinus dohrni* (Ehlers), *Anillinus fortis* (Horn), and *Anillinus pecki* Giachino, were studied only from digital photographs. All other eastern Nearctic anilline holotypes were physically studied, except for six that could not be located. *Anillinus clinei* Sokolov, *Anillinus folkertsioides* Sokolov, *Anillinus hildebrandti* Sokolov, and *Anillinus humicolus* Sokolov were deposited at the CMNH (Sokolov 2020) but could not be found there during a search in August 2023 by CWH and R. Davidson. They have since been located at the CMNH (R. Androw, pers. comm., April 2024) but have not yet been studied by us. The type specimens of *Anillinus steevesi* Barr and *Serranillus jeanneli* Barr were reportedly deposited in the CMNH as well (Barr 1995), but are not present in the type collection, general collection, or the unprocessed Barr material at the CMNH; we believe these types were either lost or were never actually designated by Barr. We designate a neotype for *S. jeanneli* because that species is treated in this paper.

We note that the holotype of *Anillinus relictus* Sokolov, to be deposited at the CMNH, was at the USNM as of August 2023, and the holotype of *Anillinus cornelli* Sokolov & Carlton, to be deposited at the USNM, was at the NCSU as of March 2022.

Distribution maps

All of the coordinates used to create the dot maps in this paper are provided in the dataset of Harden (2024), available at https://doi.org/10.5281/zenodo.10983000. In addition to material examined, this file includes all additional, unique published occurrences of Anillini in the Appalachian, Ozark, and Ouachita regions (Jeannel 1963a; Cornell 1977a, 1977b; Barr 1995; Sokolov et al. 2004, 2007, 2017; Sokolov and Carlton 2008, 2010; Sokolov and Watrous 2008; Giachino 2011; Sokolov 2011, 2012, 2014, 2020, 2021; Sokolov and Schnepp 2021). Coordinates were converted to decimal degrees, and where no coordinates were given in the original citation, approximate coordinates were obtained using Google Earth.

Taxonomy

We follow the modified biological species concept of Coyne and Orr (2004), and therefore consider species to be independently evolving units of individuals that are reproductively isolated from other independently evolving units. Multiple instances of syntopy allowed testing of this concept in several cases. Several species described below are allopatric with respect to other members of their clades. In such cases, there are multiple males known and sufficient morphological differences in the median lobe shape and flagellum shape to provide strong support for their hypothetical species status. DNA sequence data are available from all species described as new except *Serranillus monadnock* sp. nov., which is morphologically distinct from other members of the genus in external structure and male genitalia. All species formally described by us in this paper are monophyletic in our molecular phylogenies, in addition to being morphologically distinctive.

Our species-level taxonomic work in this paper is limited to species occurring in South Carolina. Several additional undescribed species are cited in this paper and in the supplementary checklist of all known eastern anillines (Suppl. material 3), but not described. We use informal placeholder names for these, formed by the state and locality from which specimens were first studied and recognized as new species. These include five species from South Carolina that are either known from insufficient material, or are allopatric to their most similar relatives and cannot be ruled out as one end of a grade.

Two abbreviations are used to indicate uncertainty in identifications: “cf.” stands for the Latin “confer” and is used for specimens that most closely fit our interpretation of the species name that follows, but for which we are not confident of this identification, due to either the sex of the individual or the uncertain identity of the type specimen; “aff.” stands for the Latin “affinis” and is used for a specimen that most closely resembles the species name that follows, but for which we have evidence to indicate the specimen does not belong to that species.

Larvae of *Serranillus dunavani* (Jeannel) and *Anillinus jancae* sp. nov. were associated with adults using DNA sequences.

Molecular phylogenetics

DNA sequences for our analyses came from 125 species, including 101 Nearctic Anillini species, representatives of 16 genera of Anillini from other regions, and seven far outgroups representing the other tribes of Trechitae. The 101 Nearctic Anillini included 42 previously described species, eight species described as new in this paper, and 51 additional undescribed species that will be described in future papers. Twenty-five previously described species have sequences published for the first time. Five previously described eastern Nearctic species are represented only by previously published COI sequences, because we did not collect fresh specimens of them.

DNA was extracted from 488 individuals using ThermoFisher's GeneJet extraction kit (Vilnius, Lithuania) using the standard protocol of the manufacturer, except that in some specimens the elution volume was reduced to increase DNA concentration. For most specimens, DNA was extracted from the abdomen only. Some earlier vouchers were extracted from whole bodies.

We amplified fragments of two nuclear ribosomal genes (18S and 28S), one mitochondrial protein-coding gene (cytochrome oxidase I, 5' [COIbc] and 3' [COIjp] ends), and three nuclear protein-coding genes (carbamoyl phosphate synthetase domain of the rudimentary gene [CAD2 and CAD4], wingless [Wg], muscle-specific protein 300 [MSP]) using primers from Folmer et al. (1994), Simon et al. (1994), Wild and Maddison (2008), Moulton and Wiegmann (2004), Ward and Downie (2005), Maddison and Cooper (2014), Ober (2002), and Shull et al. (2001); primers, PCR programs, and PCR protocols are given in Tables 1–3. Cleaning and Sanger sequencing of PCR products was performed by Psomagen, Inc. (Maryland, USA).

Table 1. List of primers used in amplification ($_a$) and Sanger sequencing ($_b$).

Gene	Location	Primer	Direction	Sequence	Reference
COIbc	mitochondrial	LCO1490$_{a,b}$	forward	GGTCAACAAATCATAAAGATATTGG	Folmer et al. (1994)
COIbc	mitochondrial	HCO2198$_{a,b}$	reverse	TAAACTTCAGGGTGACCAAAAAATCA	Folmer et al. (1994)
COIjp	mitochondrial	Jerry$_{a,b}$	forward	CAACATTTATTTTGATTTTTTGG	Simon et al. (1994)
COIjp	mitochondrial	Pat$_{a,b}$	reverse	TCCAATGCACTAATCTGCCATATTA	Simon et al. (1994)
CAD	nuclear	CD439F$_{a,b}$	forward	TTCAGTGTACARTTYCAYCCHGARCAYAC	Wild and Maddison (2008)
CAD	nuclear	CD806F$_{a,b}$	forward	GTNGTNAARATGCCNMGNTGGGA	Moulton and Wiegmann (2004)
CAD	nuclear	CD688R$_{a,b}$	reverse	TGTATACCTAGAGGATCDACRTTYTCCATRTTRCA	Wild and Maddison (2008)
CAD	nuclear	CD1098R2$_{a,b}$	reverse	GCTATGTTGTTNGGNAGYTGDCCNCCCAT	Wild and Maddison (2008)
CAD	nuclear	CD1231R$_a$	reverse	TCCACGTGTTCNGANACNGCCATRCA	Wild and Maddison (2008)
Wg	nuclear	wg550F$_a$	forward	ATGCGTCAGGARTGYAARTGYCAYGGYATGTC	Wild and Maddison (2008)
Wg	nuclear	wg578F$_{a,b}$	forward	TGCACNGTGAARACYTGCTGGATG	Ward and Downie (2005)
Wg	nuclear	wgAbR$_{a,b}$	reverse	ACYTCGCAGCACCARTGGAA	Wild and Maddison (2008)
Wg	nuclear	wgAbRZ$_a$	reverse	CACTTNACYTCRCARCACCARTG	Wild and Maddison (2008)
MSP	nuclear	MSP1F$_a$	forward	CGAGAYGARGTYGATAARATGATGCA	Maddison and Cooper (2014)
MSP	nuclear	MSP2F$_{a,b}$	forward	GCYGGACAAAAGGARATYAAYCARTGG	Maddison and Cooper (2014)
MSP	nuclear	MSP1R$_{a,b}$	reverse	TCWACCAGATCCATCCACTTGACCAT	Maddison and Cooper (2014)
28S	nuclear	D1F$_{a,b}$	forward	GGGAGGAAAAGAAACTAAC	Ober (2002)
28S	nuclear	D3R$_{a,b}$	reverse	GCATAGTTCACCATCTTTC	Ober (2002)
18S	nuclear	18S5$_{a,b}$	forward	GACAACCTGGTTGATCCTGCCAGT	Shull et al. (2001)
18S	nuclear	18Sb5$_{a,b}$	reverse	TAACCGCAACAACTTTAAT	Shull et al. (2001)

Table 2. PCR programs. All began with an initial denaturing phase of 180 s at 94 °C, with each cycling phase including 30 s of denaturing at 94 °C and 30 s of annealing; from Maddison (2012).

Program	Denaturing temperature	Annealing temperature	Extension temperature	Extension time (s)	Final extension time (s)	Cycles
C1	94	52	72	45	180	35
C1alt	94	48	72	45	180	35
C2	94	50	72	150	150	35
C3	94	52	72	120	120	37
C4	94	54	72	150	150	35
C5	94	55	72	90	90	37
C7	94	60, 55	72	120	120	9, 30
C9	94	57, 52, 45	72	120	120	6, 6, 36

Table 3. PCR protocols for gene fragments. For nested and hemi-nested reactions, programs and primers for inner and outer reactions are indicated by ^{1} and ^{2}, respectively.

Gene	Program	Primer 1	Primer 2
18S	C2	18SF5	18Sb5
28S	C1	D1F	D3R
COIbc	C1alt	LCO1490	HCO2198
COIjp	C1alt	Jerry	Pat
CAD2	C7^{1}, C5^{2}	CD439F^{1,2}	CD688R^{2}, CD1098R2^{1}
CAD4	C7^{1}, C5^{2}	CD806F^{1,2}	CD1098R2^{2}, CD1231R^{1}
Wg	C3^{1}, C4^{2}	wg550F^{1}, wg578F^{2}	wgAbRZ^{1}, wgAbR^{2}
MSP	C9^{1,2}	MSP1F^{1}, MSP2F^{1}	MSP1R^{1,2}

In total, 1,446 new sequences were generated for this study. Chromatogram assembly and base calls were made using Geneious (ver. 8.1.8; Auckland, NZ). Multiple peaks were scored with ambiguity codes. GenBank accession numbers for the new sequences are OR830242, OR837782–OR838296, OR839193–OR839823, and OR853105–OR853407. Names of taxa and molecular voucher codes associated with each are listed in Suppl. material 2.

The new sequences were supplemented by 191 sequences from previous studies (Sokolov et al. 2007; Sokolov and Watrous 2008; Sokolov and Carlton 2010; Hildebrandt and Maddison 2011; Maddison and Ober 2011; Maddison 2012; Andújar et al. 2016, 2017; Maddison et al. 2019; LaBonte and Maddison 2023; Harden et al. 2024).

Six of the eight species described as new have DNA sequences available from the holotypes: *A. dentatus* (OR853208, OR839248), *A. simplex* (OR853342, OR839331, OR839570, OR837888, OR838032, OR838222), *A. choestoea* (OR839239, OR839627, OR838052), *A. mica* (OR853287, OR839293, OR838076), *A. micamicus* (OR853291, OR839296, OR838075), *A. seneca* (OR853323, OR839466). DNA sequences from the holotypes of three previously described species are also newly published: *A. arenicollis* (OR853123, OR839200, OR838072), *A. montrex* (OR853113, OR853294, OR839300, OR839565, OR837884, OR838029, OR838218, OR838127), and *A. uwharrie* (OR853370, OR839348, OR839693, OR838093, OR838261). These holotype sequences are ‘genseq-1’ (sensu Chakrabarty et al. 2013). All eight new *Anillinus* species have DNA sequences from paratypes (‘genseq-2’), which are indicated in the descriptions. The previously described species *A. montrex* and *A. arenicollis* have newly published ‘genseq-2’ sequences (i.e., from secondary types) as well, which are indicated in the species treatments. Three previously described species have new ‘genseq-2’ sequences and are not otherwise treated in the taxonomic section: *Anillinus albrittonorum* Sokolov & Schnepp (OR839194, OR839530, OR837859, OR838193, OR853109, OR853120, OR839195, OR839545, OR837868, OR838014, OR838202, OR838123), *Anillinus pittsylvanicus* (OR853207, OR839245, OR839412, OR837796, OR837957, OR838147), and *Anillinus uwharrie* (OR853371, OR839349, OR839694, OR839346, OR839695, OR853369, OR839347, OR839696). DNA sequences from three species redescribed in this paper are ‘genseq-3’, and are indicated in the redescriptions. Three previously redescribed species that are not otherwise treated in the taxonomic section have ‘genseq-3’ sequences published for the first time: *Anillinus docwatsoni* Sokolov & Carlton (OR839709, OR853213, OR839253, OR839702, OR838096, OR853214, OR839254, OR839701, OR837928, OR838095, OR838263, OR853211, OR839251, OR839703, OR853212, OR839252), *Anillinus pecki* Giachino (OR839313, OR839560, OR837881, OR838214, OR853309, OR839732, OR853307, OR839733, OR853310, OR839314, OR839758, OR837942, OR838103, OR838281, OR839760, OR839762, OR839741, OR839740, OR853308, OR839768, OR837943, OR838104, OR853311, OR839315, OR839562, OR837882, OR838026, OR838215, OR853312, OR839563, OR838027, OR838216, OR853313, OR839316, OR839555, OR837878, OR838023, OR838211, OR838125, OR853314, OR839317, OR838085, OR838254), and *Anillinus elongatus* Jeannel (OR853218, OR839257, OR839688, OR853219, OR839258, OR839689, OR853216, OR839255, OR839690, OR838091, OR838260, OR853217, OR839256, OR839691). Only a photo voucher is available for the larva of *A. seneca* sp. nov., and so the 28S sequence from the specimen (OR853242) is ‘genseq-5’. All of the remaining new sequences are from specimens that are deposited in collections as vouchers, and are therefore ‘genseq-4’.

Alignment of sequences was performed in Mesquite (Maddison and Maddison 2023b). The ribosomal genes 18S and 28S included numerous insertions and deletions, and were aligned using the L-INS-I option in MAFFT version 7.490 (Katoh and Standley 2013). Sequences from the protein coding genes were mostly free of indels, and were aligned manually. However, several amino acid insertions and deletions were apparent among the outgroups in Wg, CAD2, and MSP. These were aligned by first translating the nucleotides to amino acids using Mesquite (Characters>Make New Matrix from>Translate DNA to Protein), aligning the amino acid matrix using the same MAFFT settings as for the ribosomal genes, and finally aligning the nucleotides to the amino acid alignment (Alter>Align DNA to Protein…).

The modified GBLOCKS algorithm in Mesquite (Talavera and Castresana 2007) was used to select and exclude ambiguously aligned regions of 18S and 28S, using the settings specified by Maddison et al (2019): minimum fraction of identical residues for conserved portions = 0.2, minimum fractions of identical residues for highly-conserved positions = 0.4, counting only fraction within taxa with non-gaps at that position, maximum length of non-conserved blocks = 4, minimum length of a block = 4, fraction of gaps allowed in a character = 0.5, and with sites selected in ambiguously aligned regions.

Two matrices were assembled for analyses. For the 6-gene concatenated analyses, a "core matrix" was used, containing individuals for which three or more of the six genes had been sequenced and individuals belonging to unique species for which only COI sequences were available, from a total of 269 individuals. A "complete matrix" was used for the remaining single-gene analyses, containing all of the newly generated sequences and all available Nearctic anilline sequences, from 551 individuals. Both matrices included the same outgroups: 17 anillines and seven far outgroups representing the other tribes of Trechitae.

Maximum likelihood analyses were performed in IQ-TREE using the Zephyr package (Maddison and Maddison 2023a) in Mesquite (Maddison and Maddison 2023b). For the six-gene concatenated analysis and the single-gene analyses of protein-coding genes, the TESTMERGE option was used to select the best model and partitioning scheme, starting with 18 parts, one each for 18S and 28S and one for each codon position of the protein coding genes. For single gene analyses of 18S and 28S, the MFP option was used, with the data unpartitioned. 100 search replicates were performed for the six-gene concatenated matrix and the single gene analyses. For 28S, two analyses were run, with and without site exclusion with GBLOCKS. Node support was calculated using standard bootstrapping in IQ-TREE, with 500 replicates for all analyses and the same options used in the Maximum Likelihood analyses. Node support for and against hypothetical clades was calculated using the "Frequency of clades in trees" feature in Mesquite, and are shown in Fig. 4.

Results

Molecular phylogenetics

The maximum likelihood tree from the 6-gene concatenated core matrix (Fig. 3) found a well-supported Nearctic Anillini clade (standard bootstrap support [SBS] 96%; Fig. 4), in which *Anillinus* and *Serranillus* are well supported as sister to each other, and together as sister to the two western Nearctic genera sampled, *Anillodes* Jeannel and *Medusapyga* LaBonte & Maddison. Monophyly of *Serranillus* is supported by all genes sampled, with SBS values 97% or greater except in 18S (SBS 68%). All *Serranillus* sampled have several shared unique insertions in 28S, the longest of which is 11 (in *S. dunavani*) or 12 bp (in other species) in length. In our 6-gene tree, three strongly supported clades (SBS 97% or greater) within *Serranillus* are present (Fig. 5): *S. jeanneli* and two undescribed species from North Carolina and Alabama (SBS 98%), the northern *Serranillus septentrionis* Sokolov & Carlton and an undescribed species from North Carolina and Tennessee (SBS 100%), and *S. dunavani* (SBS 97%). The lone female of *Serranillus* sp. "South Carolina, Coon Branch" is recovered as sister to the northern *S. septentrionis* clade in the 6-gene (SBS 55%), COIjp (SBS 53%), CAD4 (SBS 96%) and MSP (SBS 72%) trees. In the 6-gene tree, the widespread *S. dunavani* is sister to the clade containing *S.* sp. "South Carolina, Coon Branch" and the *S. septentrionis* clade, but with low support (SBS 44%).

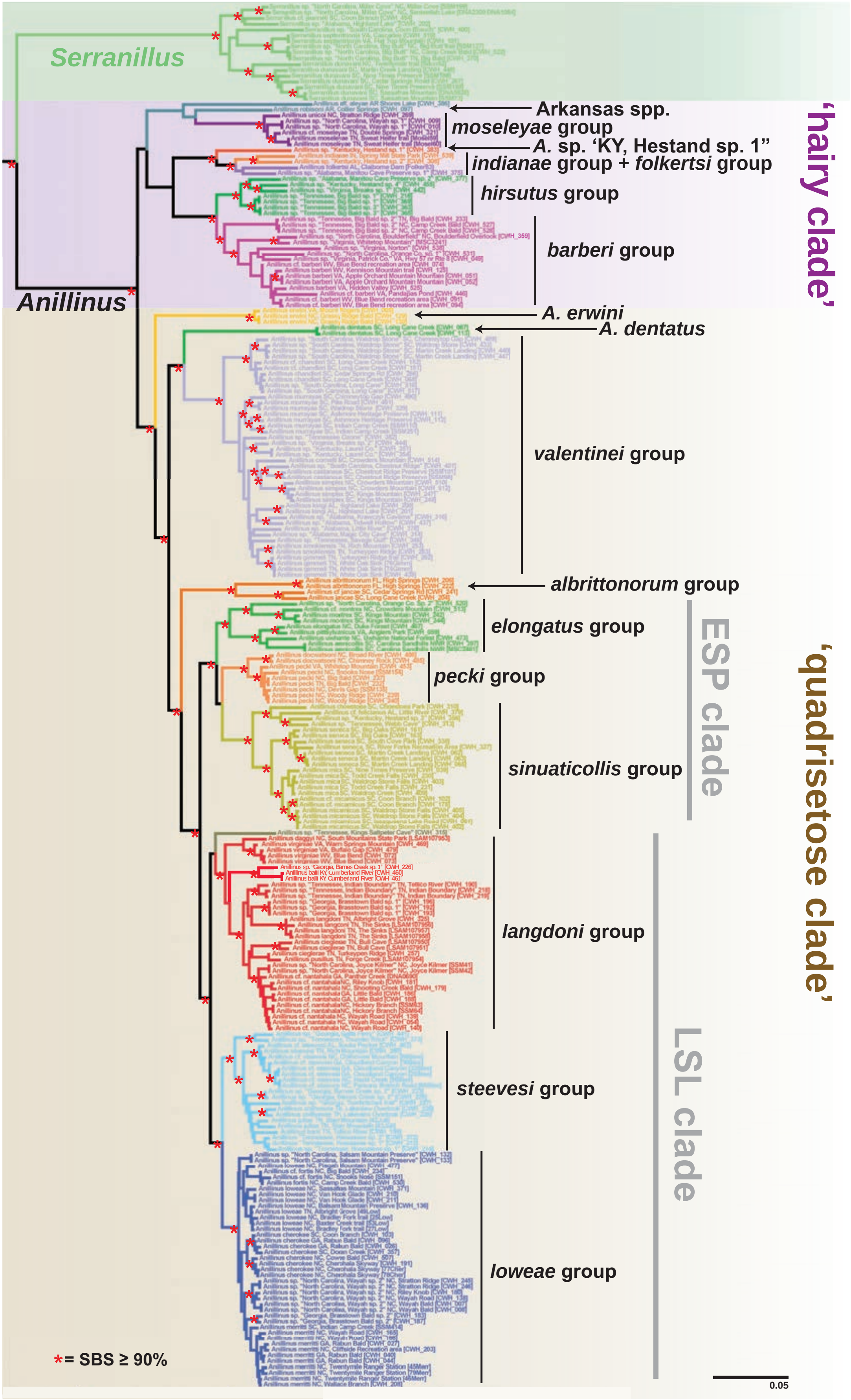

Figure 3. Maximum likelihood tree of 6-gene concatenated matrix. Outgroups cropped. Red asterisks = SBS 90% or greater.

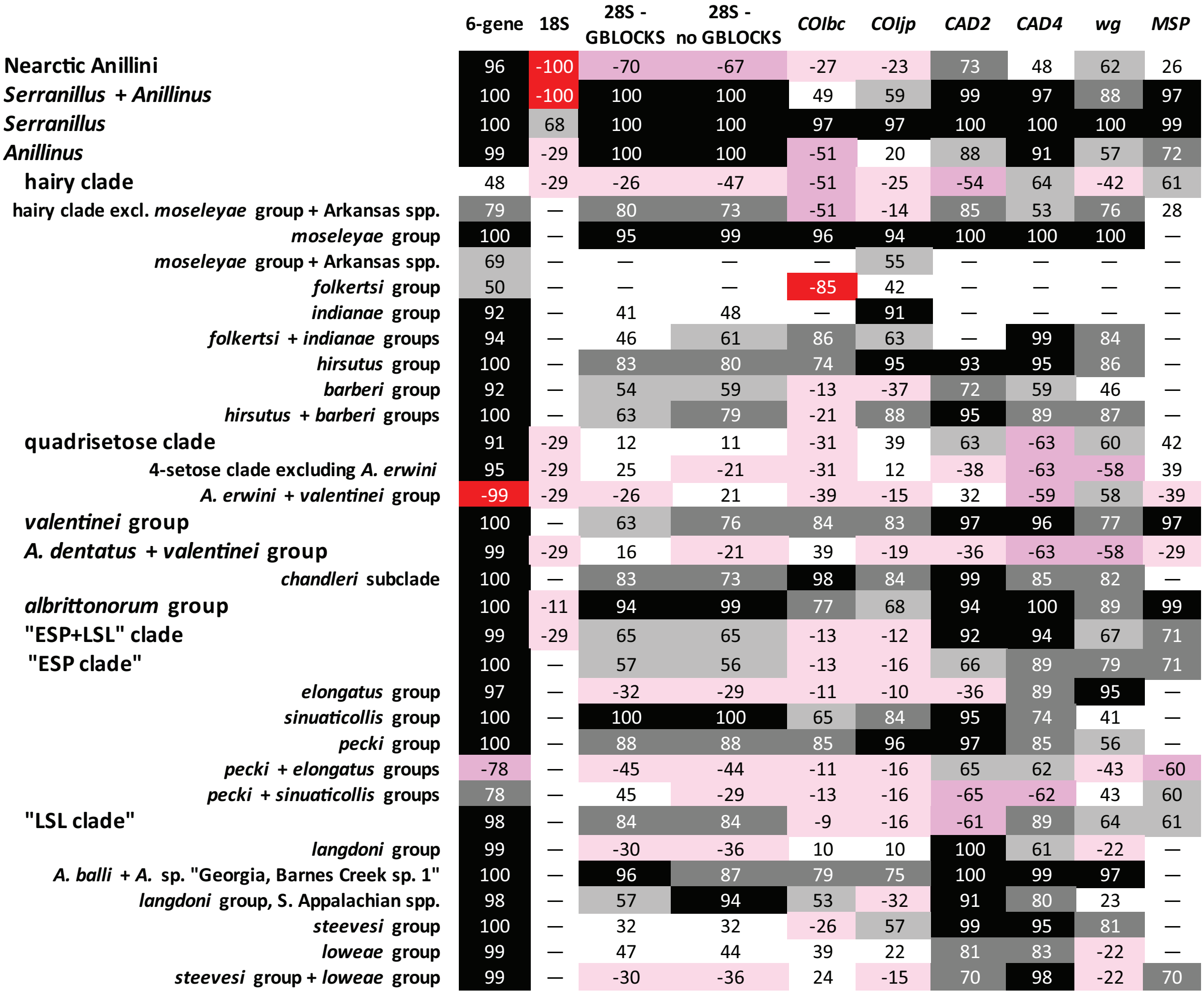

	6-gene	18S	28S - GBLOCKS	28S - no GBLOCKS	*COIbc*	*COIjp*	*CAD2*	*CAD4*	*wg*	*MSP*
Nearctic Anillini	96	-100	-70	-67	-27	-23	73	48	62	26
Serranillus* + *Anillinus	100	-100	100	100	49	59	99	97	88	97
Serranillus	100	68	100	100	97	97	100	100	100	99
Anillinus	99	-29	100	100	-51	20	88	91	57	72
hairy clade	48	-29	-26	-47	-51	-25	-54	64	-42	61
hairy clade excl. *moseleyae* group + Arkansas spp.	79	—	80	73	-51	-14	85	53	76	28
***moseleyae* group**	100	—	95	99	96	94	100	100	100	—
***moseleyae* group + Arkansas spp.**	69	—	—	—	—	55	—	—	—	—
***folkertsi* group**	50	—	—	—	-85	42	—	—	—	—
***indianae* group**	92	—	41	48	—	91	—	—	—	—
***folkertsi* + *indianae* groups**	94	—	46	61	86	63	—	99	84	—
***hirsutus* group**	100	—	83	80	74	95	93	95	86	—
***barberi* group**	92	—	54	59	-13	-37	72	59	46	—
***hirsutus* + *barberi* groups**	100	—	63	79	-21	88	95	89	87	—
quadrisetose clade	91	-29	12	11	-31	39	63	-63	60	42
4-setose clade excluding *A. erwini*	95	-29	25	-21	-31	12	-38	-63	-58	39
***A. erwini* + *valentinei* group**	-99	-29	-26	21	-39	-15	32	-59	58	-39
***valentinei* group**	100	—	63	76	84	83	97	96	77	97
***A. dentatus* + *valentinei* group**	99	-29	16	-21	39	-19	-36	-63	-58	-29
***chandleri* subclade**	100	—	83	73	98	84	99	85	82	—
***albrittonorum* group**	100	-11	94	99	77	68	94	100	89	99
"ESP+LSL" clade	99	-29	65	65	-13	-12	92	94	67	71
"ESP clade"	100	—	57	56	-13	-16	66	89	79	71
***elongatus* group**	97	—	-32	-29	-11	-10	-36	89	95	—
***sinuaticollis* group**	100	—	100	100	65	84	95	74	41	—
***pecki* group**	100	—	88	88	85	96	97	85	56	—
***pecki* + *elongatus* groups**	-78	—	-45	-44	-11	-16	65	62	-43	-60
***pecki* + *sinuaticollis* groups**	78	—	45	-29	-13	-16	-65	-62	43	60
"LSL clade"	98	—	84	84	-9	-16	-61	89	64	61
***langdoni* group**	99	—	-30	-36	10	10	100	61	-22	—
***A. balli* + *A.* sp. "Georgia, Barnes Creek sp. 1"**	100	—	96	87	79	75	100	99	97	—
***langdoni* group, S. Appalachian spp.**	98	—	57	94	53	-32	91	80	23	—
***steevesi* group**	100	—	32	32	-26	57	99	95	81	—
***loweae* group**	99	—	47	44	39	22	81	83	-22	—
***steevesi* group + *loweae* group**	99	—	-30	-36	24	-15	70	98	-22	70

Figure 4. Support for and against clades of Anillini. Black = clade present in ML tree, SBS 90 or greater, Dark grey = clade present in ML tree, SBS between 70 and 89, light grey = clade present in ML tree, SBS between 50 and 69, white = clade present in ML tree, SBS less than 50. Red = clade absent in ML tree, highest SBS of contradictory clade greater than 80, dark pink = clade absent in ML tree, highest SBS of contradictory clade between 50 and 69, light pink = clade absent in ML tree, highest SBS of contradictory clade less than 50. "–" indicates insufficient data.

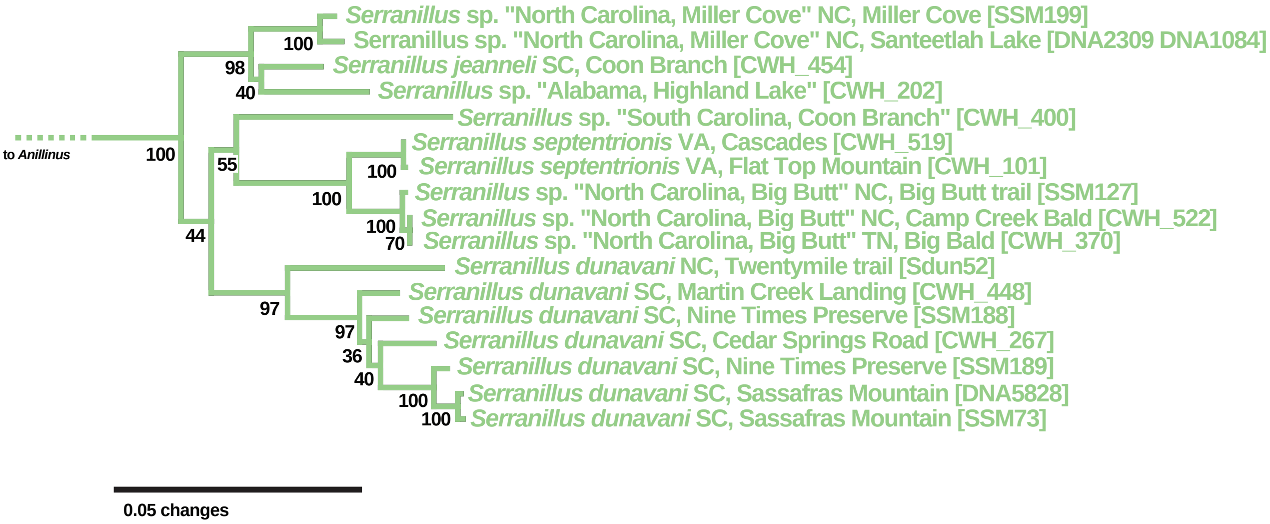

Figure 5. Maximum likelihood tree of *Serranillus*, from 6-gene concatenated core matrix. SBS values shown below nodes.

Anillinus is recovered as sister to *Serranillus* in all genes sampled except 18S, and as monophyletic in all except 18S and COIbc. Support for the monophyly of *Anillinus* is strong in 28S (SBS 100% with and without GBLOCKS) and CAD4 (SBS 91%), moderately strong in CAD2 (SBS 88%), Wg (SBS 57%), and MSP (SBS 72%), with weaker support from COIjp (SBS 20%). In our 6-gene phylogeny, the sampled species of *Anillinus* are divided into two clades that are largely consistent with the setation of the right paramere: a "hairy clade" in which the apical setae form a dense brush and a "quadrisetose clade" in which four apical setae are present. Bootstrap support for the "hairy clade" in the 6-gene tree is low (SBS 48%), and the clade is present in only two single-gene trees, CAD4 (SBS 64%) and MSP (SBS 61%). In our 6-gene tree, the "hairy clade" species are split into two main clades that are better supported (Fig. 6), one with the Appalachian high elevation endemic *moseleyae* group and the Arkansas species (SBS 69%), and the other with the remaining species (SBS 79%). The latter clade contains two well-supported clades: one with the *indianae* group, *folkertsi* group, and the isolated species *Anillinus* sp. "Kentucky, Hestand sp. 1" (SBS 94%) and the other with the *hirsutus* group and *barberi* group (SBS 100%).

The "quadrisetose clade" of *Anillinus* is recovered in the 6-gene tree (SBS 91%), 28S with (SBS 12%) and without GBLOCKS (SBS 11%), COIjp (SBS 39%), CAD2 (SBS 63%), Wg (SBS 60%), and MSP (SBS 42%). The topology of the "quadrisetose clade" in the 6-gene tree (Fig. 3) is well-resolved, with eight strongly supported species groups (SBS 97% or greater) and three isolated individual taxa. The isolated species *Anillinus erwini* is recovered as sister to

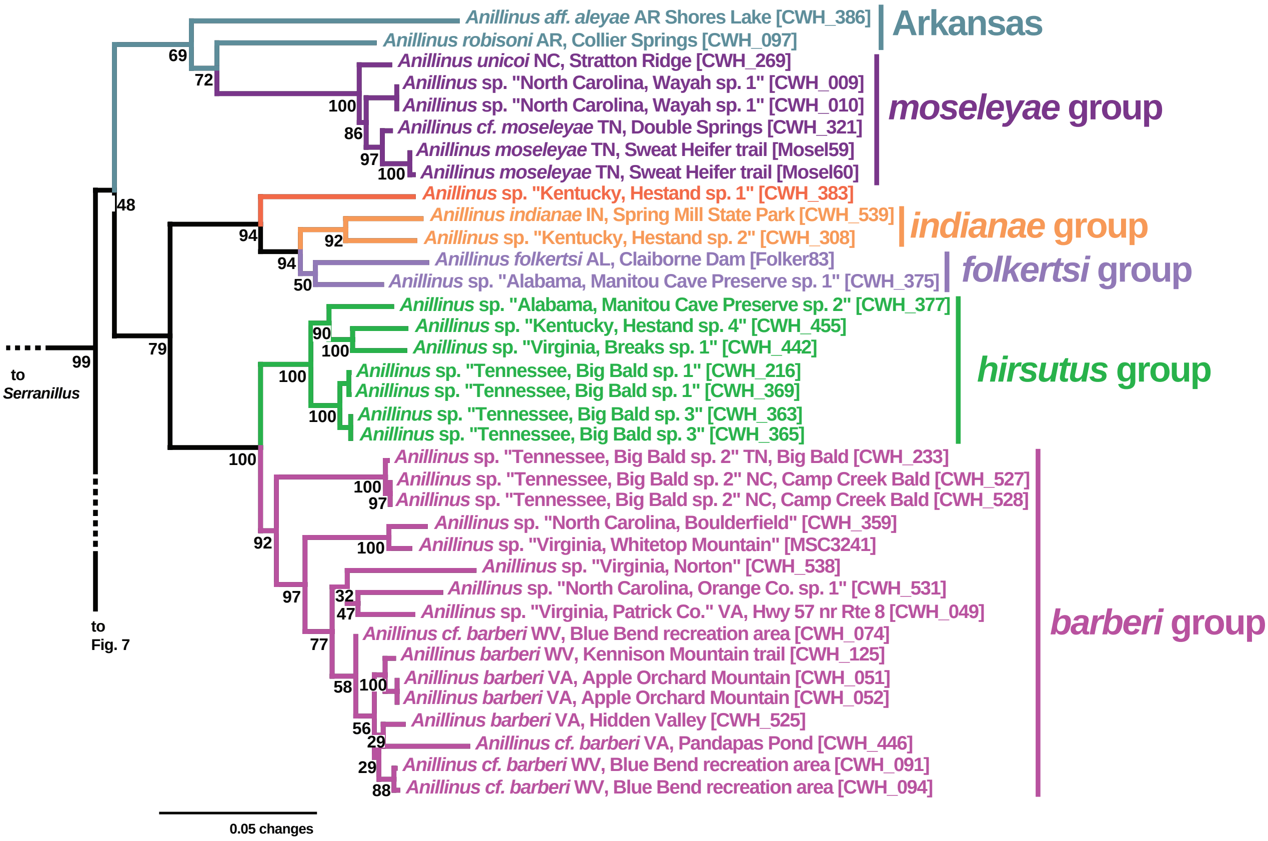

Figure 6. Maximum likelihood tree of the "hairy clade" of *Anillinus*, from 6-gene concatenated core matrix. SBS values shown below nodes.

the remaining species (SBS 95%), a relationship also recovered in 28S with GBLOCKS (SBS 25%) and MSP (SBS 39%) trees. *Anillinus erwini* is sister to the *valentinei* group in 28S without GBLOCKS (SBS 21%), CAD2 (SBS 32%) and Wg (58%) trees. The remaining single gene trees recover unique placements of *A. erwini*: sister to the *A. dentatus*+*valentinei* group clade (COIbc), sister to *A. dentatus* alone (18S and COIjp), and sister to the "hairy clade" (CAD4), all with low support. The "quadrisetose clade" species besides *A. erwini* are divided into two well-supported clades in the 6-gene tree, one containing *A. dentatus* and the *valentinei* group (SBS 99%) and the other containing the *albrittonorum* group and the "ESP+LSL" clade (SBS 95%). The former clade recovers the isolated species *A. dentatus* as sister to the *valentinei* group (SBS 100%) (Fig. 7), a diverse and widespread lineage of mostly low-elevation species. The *valentinei* group is recovered as a clade in all of the genes sampled, with moderate to strong support in all (SBS 63% or greater). In contrast, the sister relationship between *A. dentatus* and the *valentinei* group is present only in 28S with GBLOCKS (SBS 16%) and COIbc trees (SBS 39%). Placement of *A. dentatus* varies between the single gene trees: sister to *A. erwini* (18S and COIjp), sister to the "ESP+LSL" clade (28S without GBLOCKS), sister to *A. erwini*+*valentinei* group (CAD2), sister to all other *Anillinus* species (CAD4), sister to the "quadrisetose

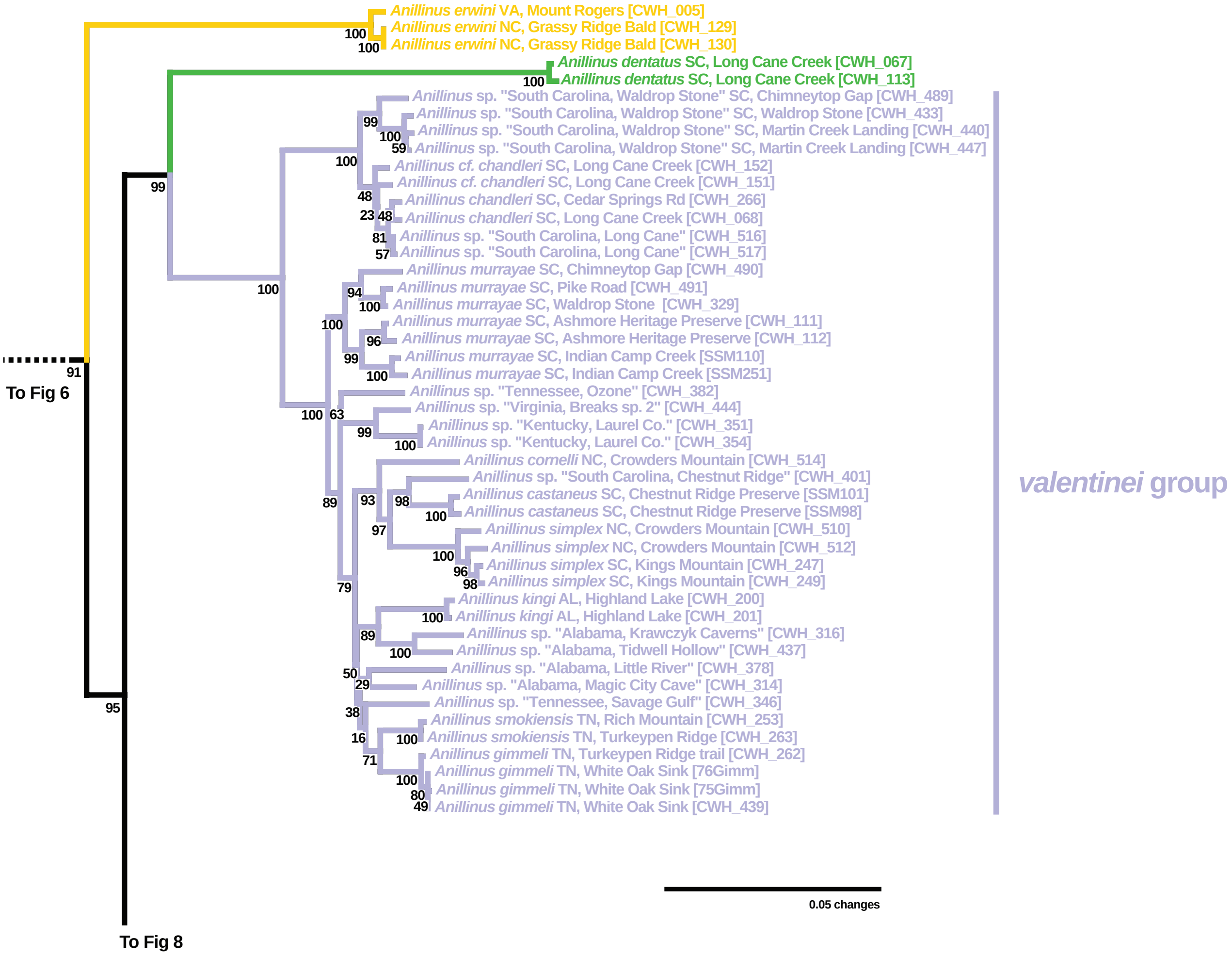

Figure 7. Maximum likelihood tree of portion of "quadrisetose clade" of *Anillinus*, from 6-gene concatenated core matrix. SBS values shown below nodes.

clade” except *A. erwini* (MSP), and sister to the *albrittonorum* group (Wg). The *albrittonorum* group, consisting of two isolated species in South Carolina (*A. jancae*) and Florida (*A. albrittonorum*) is present in all gene trees except 18S, with SBS values of 68 or greater. The *albrittonorum* group is recovered as sister to the “ESP+LSL” clade in the 6-gene (SBS 95%), CAD2 (SBS 65%), CAD4 (SBS 82%), and MSP (SBS 22%) trees. Placement of the *albrittonorum* group varies in the remaining single gene trees: sister to “quadrisetose clade” except *A. erwini* (28S with GBLOCKS), sister to all “quadrisetose clade” *Anillinus* (28S without GBLOCKS), sister to the *moseleyae* group (COIbc), and sister to the *sinuaticollis* group (COIjp), all with low support.

The “ESP” and “LSL” clades are sister to each other in the 6-gene tree (SBS 99%) and all single gene trees except 18S, COIbc, and COIjp, with moderate support in 28S (SBS 65% with and without GBLOCKS), Wg (SBS 67%), and MSP (SBS 71%), and strong support in CAD2 (SBS 92%), CAD4 (SBS 94%). The “ESP” clade (Fig. 8), consisting of the *elongatus* group, *sinuaticollis* group, and *pecki* group is present in all gene trees except COIbc and COIjp, and is strongly supported

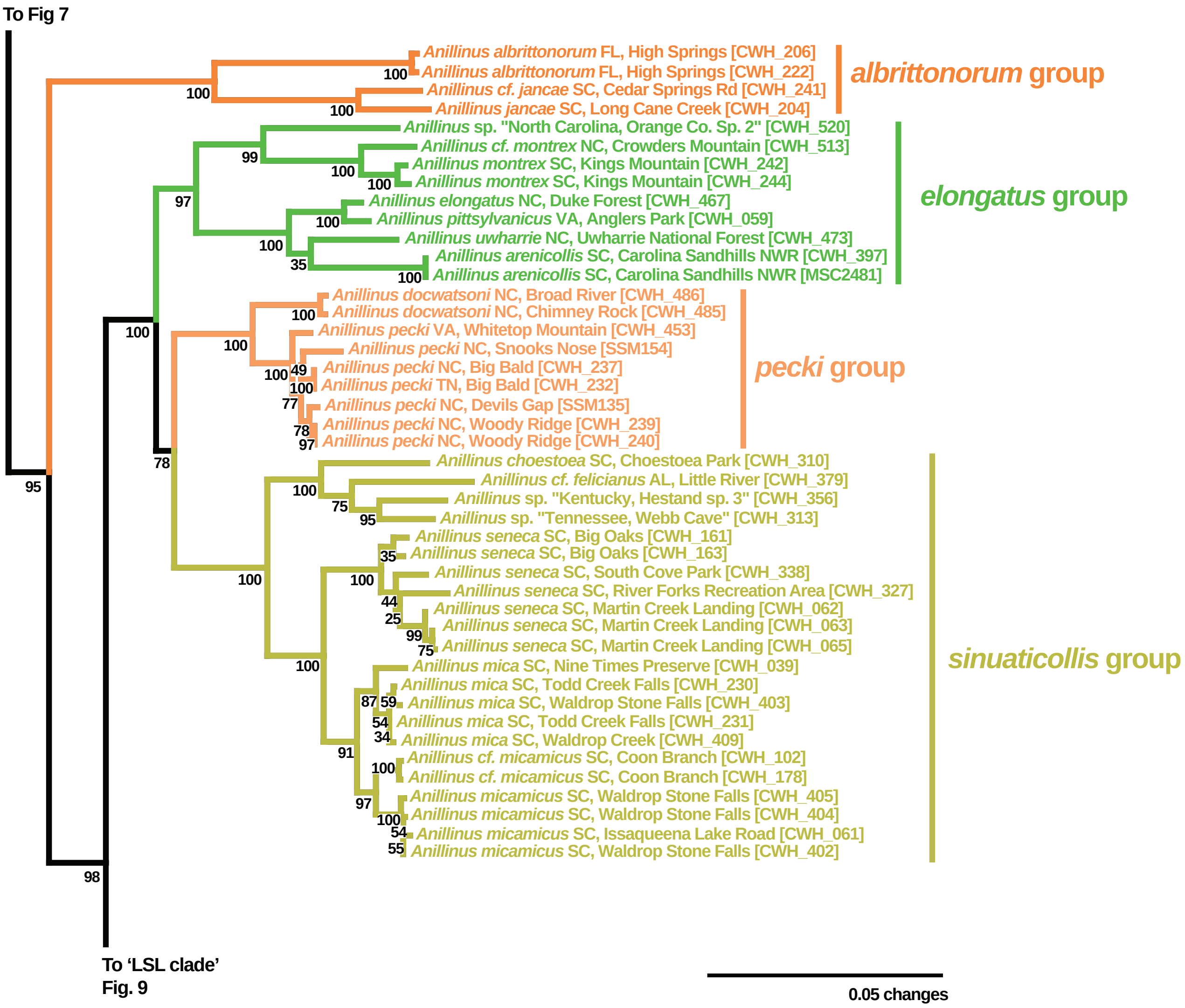

Figure 8. Maximum likelihood tree of *albrittonorum* group and “ESP clade” of *Anillinus*, from 6-gene concatenated core matrix. SBS values shown below nodes.

by the 6-gene tree (SBS 100%), and moderately supported by CAD2 (SBS 66%), CAD4 (SBS 89%), Wg (SBS 79%), and MSP (SBS 71%), with weaker support in 28S with (SBS 57%) and without (SBS 56%) GBLOCKS. The *sinuaticollis* group and *pecki* group are both recovered as clades in all genes sampled, with moderate to strong support from most. The *elongatus* group is strongly supported as a clade in the 6-gene tree (SBS 97%), but is present only in the CAD4 (SBS 89%) and Wg (SBS 95%) individual gene trees. There are two consistently recovered subclades in the *elongatus* group, one containing *A. montrex* and an undescribed North Carolina species, and the other containing the remaining species. These two clades are paraphyletic to each other in 28S (with and without GBLOCKS), COIbc, and CAD2 and polyphyletic to each other in COIjp. Only one individual of the *elongatus* group was sampled for 18S and MSP.

The "LSL" clade (Fig. 9), consisting of the *langdoni* group, *steevesi* group, and *loweae* group, is recovered in all genes except COIbc, COIjp, and CAD2, with strong support in the 6-gene (SBS 98%) and CAD4 (SBS 89%) trees, moderate support in 28S with and without GBLOCKS (SBS 84%), Wg (SBS 64%), and MSP (SBS 61%). The *langdoni* group is recovered in the 6-gene (SBS 99%), COIbc (SBS 10%), COIjp (SBS 10%), CAD2 (SBS 100%), and CAD4 (SBS 61%) trees. Three clades are consistently recovered in the *langdoni* group: the northern *Anillinus virginiae* (and *A. daggyi* in COI trees), the Kentucky endemic *Anillinus balli* and an undescribed Georgia species, and the remaining southern Appalachian endemic species. The latter clade is absent from the COIjp tree, but otherwise the three clades are recovered in all genes, with moderate to strong support from most. The isolated species *Anillinus* sp. "Tennessee, Kings Saltpeter Cave" is recovered as sister to the *langdoni* group in the 6-gene (SBS 51%) and MSP (SBS 98%) trees, but its placement varies within the remaining genes. Its inclusion in the "LSL" clade is supported by the 6-gene (SBS 98%), CAD4 (SBS 89%), Wg (SBS 64%) and MSP (SBS 61%) trees. The *steevesi* group is present in 6-gene (SBS 100%), 28S with and without GBLOCKS (SBS 32%), COIjp (SBS 57%), CAD2 (SBS 99%), CAD4 (SBS 95%), and Wg (SBS 81%) trees. Only a single individual was included in 18S and MSP analyses. The *loweae* group is strongly supported in 6-gene (SBS 99%), CAD2 (SBS 81%) and CAD4 (SBS 83%), and weakly supported in 28S with (SBS 47%) and without GBLOCKS (SBS 44%), COIbc (SBS 39%), and COIjp (SBS 22%). In the Wg tree, the *loweae* group is polyphyletic, with some individuals of *A. merritti* and *A.* sp. "North Carolina Wayah sp. 2" sister to the Southern Appalachian *langdoni*-group species and the remaining individuals paraphyletic at the base of a clade including *A. balli* and its sister species and the *steevesi* group. The *steevesi* group and *loweae* group are strongly supported as sister clades in the 6-gene (SBS 98%) and CAD4 (SBS 98%) trees, moderately supported as sister in the MSP (SBS 70%) and CAD2 (SBS 70%) trees, and weakly supported as sister in the COIbc tree (SBS 24%). The species we include in the *steevesi* group were formerly included in the *loweae* group (Sokolov and Carlton 2010, Sokolov 2011), but we find the *steevesi* group to be monophyletic with respect to the *loweae* group in all genes except COIbc, in which two undescribed *steevesi*-group species from Tennessee and Georgia are recovered as sister to the *loweae* group.

Complete trees from all Maximum Likelihood and Standard Bootstrap analyses are shown in Suppl. material 1.

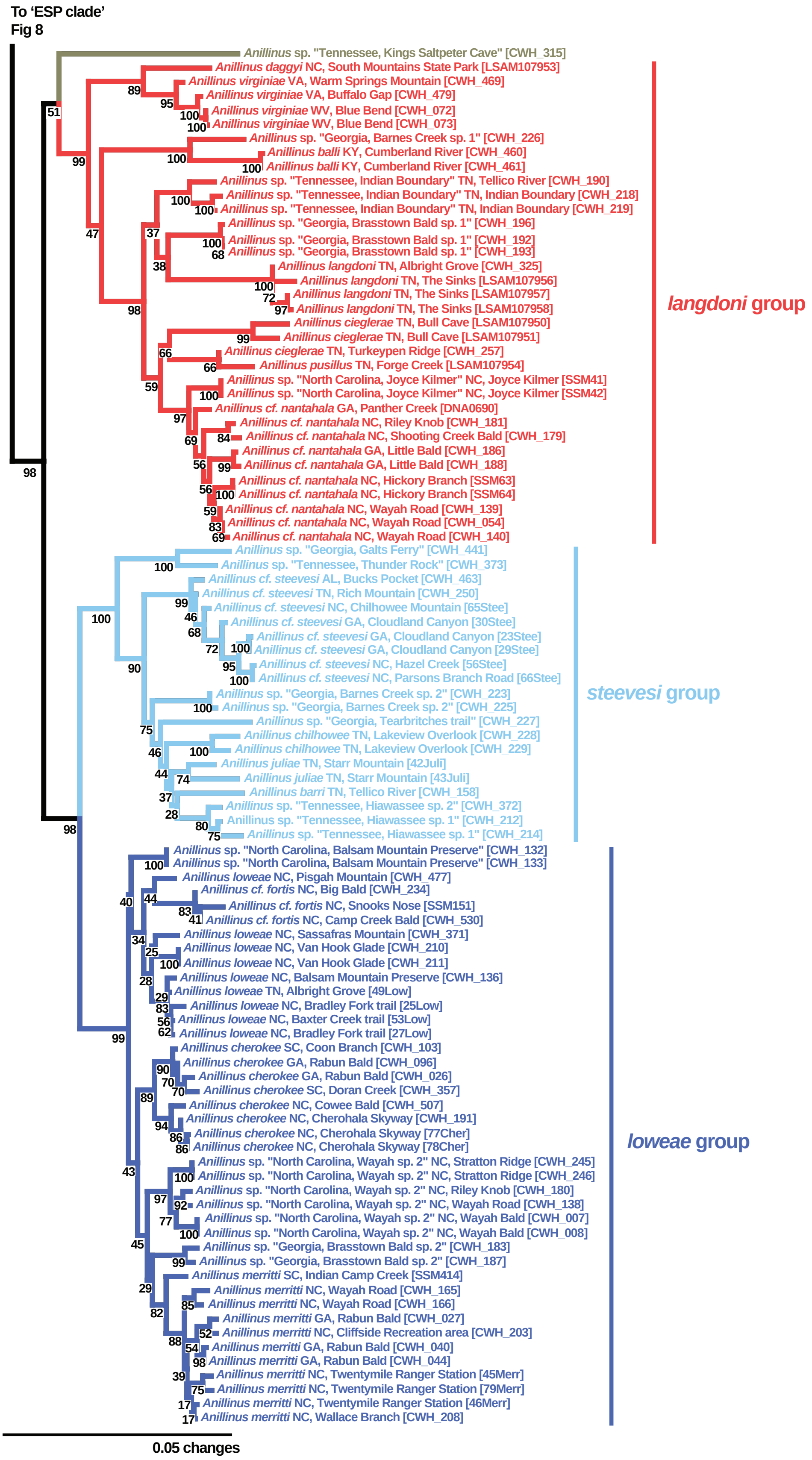

Figure 9. Maximum likelihood tree of "LSL clade" of *Anillinus*, from 6-gene concatenated core matrix. SBS values shown below nodes.

Systematics of Appalachian *Anillinus*

Key to eastern genera of Anillini and most species groups of *Anillinus*

Precise identification of *Anillinus* and *Serranillus* specimens requires examination of the male genitalia, and genitalic characters could not be avoided in the key below. The key below will aid with initial sorting of an unknown specimen, but species-level identifications must be made by comparison of genitalia with descriptions or authoritatively identified specimens.

1 Males; first protarsomere enlarged and with thick adhesive setae ventrally (Fig. 10), last abdominal ventrite with two fixed setae on posterior margin **2**

– Females; first protarsomere not enlarged and without thick adhesive setae ventrally, last abdominal ventrite with four fixed setae on posterior margin **23**

2(1) Last abdominal ventrite “serrate”, with three blunt lobes on posterior margin (Fig. 15B); medial setae of mentum on tooth (Fig. 11A), left mandible with retinacular tooth (Fig. 11C) .... ***Serranillus***

– Last abdominal ventrite not “serrate”, without blunt lobes on posterior margin; medial setae of mentum set basad to tooth (Fig. 11B), left mandible without retinacular tooth (Fig. 11D) (*Anillinus*) **3**

3(2) Metafemur with angulate tooth or blunt spine on posterior margin (Fig. 12A, E, F) **4**

– Metafemur with posterior margin evenly rounded, at most with medial field of coarse microsculpture (Fig. 12B, C, D) **12**

4(3) Only first protarsomere with ventral adhesive setae, second unmodified (Fig. 10D, E, F) **5**

– Both first and second protarsomeres with ventral adhesive setae (Fig. 10G, H, I) **10**

5(4) Right paramere of aedeagus with more than eight apical setae **6**

– Right paramere of aedeagus nearly always with four apical setae, rarely with three or six **7**

6(5) Flagellum of internal sac long, filamentous; median lobe of aedeagus almost entirely membranous dorsally; range: central Tennessee, Kentucky, Indiana .... ***indianae* group**

– Flagellum of internal sac short, thick; median lobe of aedeagus with sclerotized section apically, demarcated by a distinct notch; range: eastern Tennessee, North Carolina, Virginia, West Virginia .... ***barberi* group (in part)**

7(5) Body strongly flattened dorsoventrally, with additional leg modifications, either profemora or mesotrochanters spinose **8**

– Body at least moderately convex, without additional leg modifications **9**

8(7) Profemora with prominent spine on posterior face, mesotrochanters simple; second abdominal ventrite with median keel; large, ABL > 2 mm .... ***albrittonorum* group (in part; *A. jancae* sp. nov.)**

– Profemora simple, mesotrochanters spinose; second abdominal ventrite without median keel; smaller, ABL < 2 mm .... ***dentatus* group**

9(7) Flagellum of aedeagus long and filamentous, often protruding beyond ostium; range: high elevations in mountains north of French Broad River ..... ***erwini* group**

– Flagellum of aedeagus short, not protruding beyond ostium; range: low elevations in Piedmont, south and west of Appalachian Mountains ..... ***sinuaticollis* group (in part)**

10(4) Body strongly flattened dorsoventrally, flagellum of aedeagus long and filamentous; range: Piedmont of Virginia, North Carolina, and South Carolina OR south-central Kentucky **11**

– Body moderately convex and ovoid, flagellum of aedeagus short and thick; range: mountains of northwestern Virginia and northern West Virginia ..... ***langdoni* group (in part; *A. virginiae*)**

11(10) Head with frontoclypeal horn reduced, nearly absent; median lobe of aedeagus with a saddle-like sclerite beneath flagellum; range: south-central Kentucky ..... ***Anillinus* sp. “Kentucky, Hestand Sp. 1”**

– Head with frontoclypeal horn well-developed and conspicuous; median lobe of aedeagus lacking saddle-like sclerite beneath flagellum; range: Piedmont of Virginia, North Carolina, and South Carolina ..... ***elongatus* group**

12(3) Only first protarsomere with ventral adhesive setae, second protarsomere unmodified **13**

– Both first and second protarsomeres with ventral adhesive setae **17**

13(12) Right paramere with more than eight apical setae **14**

– Right paramere with four apical setae (three in rare individuals) **15**

14(13) Dorsal margin of median lobe of aedeagus with prominent notch where membranous ostium meets apical dorsal sclerotized portion; femora not densely setose ..... ***barberi* group (in part)**

– Dorsal margin of median lobe of aedeagus without notch; femora densely setose or not ..... ***hirsutus* group**

15(13) Flagellum of median lobe short, not filamentous apically ..... ***sinuaticollis* group (in part)**

– Flagellum of median lobe long, filamentous apically in most species **16**

16(15) Metafemur swollen posteriorly; body narrower; range: high elevations in mountains northeast of French Broad River ..... ***erwini* group**

– Metafemur simple; body broader; range: low to mid elevations, western edge of Great Smoky and Unicoi mountains, west to northern Mississippi ..... ***steevesi* group (in part)**

17(12) Right paramere with dense brush of apical setae; left paramere with five or more poriferous canals on ventral margin ..... ***folkertsi* group**

– Right paramere with four apical setae; left paramere with four or less poriferous canals on ventral margin **18**

18(17) Walls of median lobe of aedeagus heavily sclerotized, left side with abruptly membranous section ..... ***loweae* group**

– Walls of median lobe less heavily sclerotized, left side without abruptly membranous section **19**

19(18) Internal sac of aedeagus with prominent sclerotized spines or scales ... **20**

– Internal sac of aedeagus without prominent sclerotized spines or scale **21**

20(19) Flagellum of internal sac well-sclerotized and elongate .... **_valentinei_ group (in part)**

– Flagellum of internal sac lightly sclerotized and short .... **_pecki_ group (in part; _A. docwatsoni_)**

21(19) Dorsal surface of head with microsculpture effaced in part, absent at least from sides of vertex **22**

– Dorsal surface of head entirely covered with microsculpture .... **_langdoni_ group (in part)**

22(21) Flagellum weakly sclerotized and short, appearing W-shaped in lateral aspect; range: mountains northeast of French Broad River .... **_pecki_ group (in part; _A. pecki_)**

– Flagellum well-sclerotized, shape various but never W-shaped in lateral aspect; range: lower elevations south and west of southern Appalachian Mountains southwest of French Broad River **23**

23(22) Apex of median lobe small and rounded .... **_valentinei_ group (in part)**

– Apex of median lobe modified, broadly rounded with ventral margin greatly expanded or with dorsal margin deeply excavated .... **_steevesi_ group (in part)**

24(1) Paramedial setae of mentum on mentum tooth (Fig. 11A); spermatheca short and curved, gradually enlarged apically (Fig. 21S, T) .... **_Serranillus_**

– Paramedial setae of mentum basad of tooth (Fig. 11B); spermatheca variable, if short and curved then abruptly enlarged apically (Fig. 21N) (*Anillinus*) **25**

25(24) Spermathecal duct coiled **26**

– Spermathecal duct not coiled **31**

26(25) Spermatheca shorter, not S- or 2-shaped **27**

– Spermatheca longer, with S- or 2 shape **29**

27(26) Spermatheca with smooth stem, abruptly enlarged apically .... **_albrittonorum_ group (in part; _A. jancae_ sp. nov.)**

– Spermatheca with annulated stem, more gradually enlarged apically **28**

28(27) Body robust and broad, head relatively larger; range: southern Tennessee north to southern Indiana .... **_indianae_ group**

– Body narrower, head relatively smaller; range: central Tennessee south to southern Alabama .... **_folkertsi_ group**

29(26) Body strongly dorsoventrally flattened and parallel sided **30**

– Body at least moderately convex and ovoid .... **_steevesi_ group OR _valentinei_ group**

30(29) Stem of spermatheca nearly straight, without basal bend; frontoclypeal horn absent .... **_dentatus_ group**

– Stem of spermatheca more sinuate, with basal bend; frontoclypeal horn present .... **_elongatus_ group**

31(25) Spermathecal duct greatly reduced, not apparent .... **_valentinei_ group (in part)**

– Spermathecal duct variable in length, but long enough to be apparent **32**

32(31) Stem of spermatheca rough, “ribbed” in part **33**

– Stem of spermatheca entirely smooth **36**

33(32) Base of spermatheca swollen at basal bend **34**

– Base of spermatheca not swollen **35**

34(33) Spermatheca long; range: high elevations in Southern Appalachians ....***moseleyae* group**

– Spermatheca short; range: south-central Kentucky............. ***Anillinus* sp. “Kentucky, Hestand Sp. 1”**

35(33) Spermatheca with basal bend smoothly rounded***loweae* group (in part)**

– Spermatheca with basal bend angulate ....***pecki* group**

36(32) Pronotum entirely covered in microsculpture **37**

– Pronotum with microsculpture at least partially effaced on disc........**39**

37(36) Body dorsoventrally flattened..**38**

– Body convex, ovoid ....***loweae* group (in part)**

38(37) Spermathecal duct short, evenly curved; metafemora simple................ ....***barberi* group OR *hirsutus* group**

– Spermathecal duct longer, not curved; metafemora with tooth on posterior margin ....***Anillinus* sp. “South Carolina, Wateree”**

39(36) Stem of spermatheca looped over itself proximally; endogean species south and west of southern Appalachians................***sinuaticollis* group**

– Stem of spermatheca not looped over itself proximally **40**

40(39) Spermatheca short, stem shorter than enlarged apex; endogean species in South Carolina and Florida ....***albrittonorum* group (in part)**

– Spermatheca longer, stem longer than enlarged apex **41**

41(40) Elytra broadest at humeri; range: low elevations west of Appalachian Mountains in northeastern Tennessee .... ***Anillinus* sp. “Tennessee, Kings Saltpeter Cave”**

– Elytra broadest approximately middle; range: high elevations in mountains northeast of French Broad River ....***erwini* group**

Species groups of Appalachian *Anillinus*

Below, we list the species groups supported by both DNA sequence data and morphology, and provide diagnoses for each. We summarize available data on distribution and habitat use for each group.

Suppl. material 3 includes a checklist of all eastern Nearctic Anillini species, including those not sampled for our phylogeny, with their hypothetical placement within this new systematic arrangement. The dataset of Harden (2024) includes full locality and deposition data for all specimens studied, including undescribed species not treated in this work.

‘*moseleyae* group’

“group VII endogean species” Sokolov et al. 2004: 228, in part.

Diagnosis. Dorsal microsculpture largely lacking from head and pronotum. Pronotum strongly constricted posteriorly. Elytra long and narrow (Fig. 2B). Male protarsomeres 1 and 2 both dilated and bearing ventral adhesive vestiture. Median lobe of aedeagus with left side bearing a patch of long setae, right paramere with dense brush of apical setae. Spermatheca long, with ribbed stem and short spermathecal duct. Humeri of females usually strongly sloped (not so in *A. unicoi*).

Diversity. Three described species (Sokolov 2011) and one undescribed ("North Carolina, Wayah sp. 1" in our phylogeny).

Distribution and habitat. All of the *moseleyae*-group species are restricted to elevations above 4,500ft in the mountains southwest of the French Broad River; specimens are known from the Great Smoky, Plott Balsam, Unicoi, Snowbird, and Nantahala Mountains (Fig. 42B). Their apparent absence from the Great Balsam Mountains is notable. In the Great Smoky Mountains, *Anillinus carltoni* Sokolov, *Anillinus moseleyae* Sokolov & Carlton, and *Anillinus unicoi* Sokolov have been collected in series by sifting leaf litter (Sokolov 2011; NCSU data). At lower elevations in the Unicoi, Snowbird, and Nantahala Mountains, specimens have been collected from endogean habitats using pipe traps or by searching under embedded rocks.

Anillinus sp. "Kentucky, Hestand sp. 1"

Diagnosis. Members of this phylogenetically isolated species (Fig. 2P) possess the following unique set of character states: head entirely microsculptured, disc of pronotum lacking microsculpture, male protarsomeres 1 and 2 expanded and with ventral adhesive setae, male metafemora swollen with large triangular tooth on posterior margin, internal sac of aedeagus with large saddle-like sclerite beneath flagellum, flagellum long and filamentous, left side of median lobe channelized near apex, right paramere with four setae and two or three additional pores without setae, left paramere with seven pores on ventral margin, female spermatheca small and S-shaped, base thick, stem ribbed, duct not coiled.

Distribution and habitat. This species is known only from a single stream hollow in Hestand, Kentucky (Fig. 42B). Specimens have been collected using pipe traps, soil extraction, and hand collecting underneath deeply embedded rocks.

Notes. A description of this species is in progress, based on specimens in the CUAC and CWHc collections.

'*indianae* group'

"group I litter species" Sokolov et al. 2004: 228, in part.

Diagnosis. Dorsal microsculpture fully developed on head and pronotum. Body broad and dorsoventrally flattened (Fig. 2Q). Males with one or two protarsomeres with ventral adhesive setae. Male metafemora swollen and angularly produced posteriorly in middle, bearing a sharp tooth or not. Dorsal margin of median lobe membranous except basal 1/4, apex of median lobe large and concave on left side, not channelized. Saddle-like sclerite present in internal sac near sclerotized ostial plate on left side, flagellum long and filamentous. Right paramere with dense brush of apical setae. Left paramere with many pores on ventral margin but without setae. Spermatheca (examined only in *A. indianae*) small and weakly ribbed, gradually enlarged distally, with short proximal bend, spermathecal duct long and loosely coiled.

Diversity. This group includes the described species *Anillinus indianae* Jeannel and *Anillinus longiceps* Jeannel, as well as two undescribed species from Kentucky.

Distribution and habitat. The collective range of the group extends from the vicinity of Sewanee, Tennessee north to Lawrence Co., Indiana (Fig. 42B). These species inhabit deep soils, MSS and caves.

‘*folkertsi* group’

“group I litter species” Sokolov et al. 2004: 228, in part.

Diagnosis. Dorsal microsculpture fully developed on head and pronotum. Body dorsoventrally flattened, head relatively small (Fig. 2E). Males with protarsomeres 1 and 2 with ventral adhesive setae. Male metafemora unmodified. Median lobe with dorsal margin more extensively sclerotized than in *indianae* group, apex broad, left side channelized. Internal sac with long filamentous flagellum that is coiled apically and an ostial saddle-like sclerite on left side. Right paramere with apical setae forming one or two dense brushes. Left paramere with eight or more short setae on ventral margin. Spermatheca short and weakly ribbed, spermathecal duct long and coiled.

Diversity. Two described species, *Anillinus folkertsi* Sokolov & Carlton and *Anillinus folkertsioides* Sokolov, and two undescribed species from Alabama and Tennessee comprise this group.

Distribution and habitat. The range of this group extends from southern Alabama to central Tennessee (Fig. 42B). Specimens have been extracted from leaf litter on the surface and in caves (Sokolov et al. 2004; Sokolov 2021), and collected from underneath embedded rocks.

‘*barberi* group’

“group I litter species” Sokolov et al. 2004: 228, in part.
“*virginiae* group” Sokolov et al. 2007: 4, in part.

Diagnosis. Dorsal microsculpture fully developed on head and pronotum in most species, sculpticels on pronotum relatively small and dense. Body dorsoventrally flattened (Fig. 2R). Males with protarsomere 1 expanded and bearing ventral adhesive setae, male protarsomere 2 unmodified. Male leg modifications variable but metafemora always modified, either greatly swollen and bowed anteriorly with straight posterior margin or evenly swollen with posterior margin slightly angulate medially. Median lobe of aedeagus almost entirely membranous dorsally, only base and apex sclerotized. Apical dorsal sclerotized plate of median lobe variable in form but always abruptly set off posteriorly from dorsal ostium by abrupt notch. Left side of median lobe not channelized in most species. Flagellum heavily sclerotized and short, rotated dorsally and curved, internal sac scaly or spined. Right paramere with dense brush of apical setae. Left paramere with many scattered pores on ventral margin, some bearing short setae. Spermatheca long, with stem smooth except short ribbed region proximally, spermathecal duct short and evenly curved.

Diversity. One described species, *Anillinus barberi* Jeannel, and seven undescribed species comprise this group.

Distribution and habitat. *Anillinus barberi* occurs in Virginia, Maryland, and West Virginia. The undescribed species occur in Virginia, North Carolina, and Tennessee (Fig. 42C). Specimens of the *barberi* group have been primarily collected from endogean habitats using pipe traps or searching under embedded rocks. A small number of specimens have been collected from sifted leaf litter.

'*hirsutus* group'

"*kovariki* group" Sokolov 2012: 65, in part.

Diagnosis. Members of this group are large (Fig. 2S) and share most of the character states of the *barberi* group, differing in the following: male femora and trochanters of all legs densely setose in most species, dorsal margin of aedeagus less irregularly structured, with ostium not separated from apex by sclerotized apical portion, internal sac usually without scales or spines.

Diversity. Three described species (*Anillinus clinei* Sokolov, *Anillinus hildebrandti* Sokolov, and *Anillinus hirsutus* Sokolov) and 10 undescribed species comprise this group.

Distribution and habitat. Members of the *hirsutus* group range from the Cumberland Plateau in extreme southwest Virginia and central Kentucky south to northern Alabama and Georgia (Fig. 42C). The only high elevation occurrence of the group is on Big Bald on the North Carolina-Tennessee border in the Bald Mountains, where two undescribed species have been collected from leaf litter and underneath embedded rocks. All other species are known only from endogean or cave habitats.

Notes. The right paramere of *A. hirsutus* was described and illustrated as having only four setae (Sokolov 2012). Our examination of three male paratypes found that the right paramere actually bears a dense brush of apical setae. *Anillinus cavicola* Sokolov is similar in some characters to members of the *hirsutus* group, especially the thick and dorsally rotated flagellum of the aedeagus, but for now we place *A. cavicola* in its own species group along with a closely similar undescribed species (Suppl. material 3).

'*erwini* group'

"group VI litter species" Sokolov et al. 2004: 228.

Diagnosis. Dorsal microsculpture weakly impressed and difficult to trace on most of head and pronotum. Body relatively narrow and elongate, slightly depressed dorsoventrally (Fig. 2K). Males with protarsomere 1 enlarged and bearing ventral adhesive setae, male protarsomere 2 unmodified and without ventral setae. Male metafemora swollen and slightly angulate medially on posterior margin. Median lobe of aedeagus slightly twisted dorsally. Flagellum elongate and filamentous. Right paramere quadrisetose. Left paramere with three or four ventral setae. Spermatheca long and smooth, spermathecal duct long with a few loose coils medially.

Diversity. This group consists of only *Anillinus erwini* Sokolov & Carlton.

Distribution and habitat. *Anillinus erwini* is a high elevation endemic that ranges from Mount Mitchell in the Black Mountains north to the Mount Rogers vicinity in southwestern Virginia, including Roan Mountain and Grandfather Mountain, but apparently absent from the Great Craggy and Bald Mountains (Fig. 43B). Specimens have been collected from leaf litter and underneath embedded rocks.

‘*dentatus* group’

Diagnosis. Body small (ABL = 1.49–1.69), dorsoventrally flattened (Fig. 2C). Dorsal microsculpture fully developed on head and pronotum. Head with frontoclypeal horn inconspicuous. Males with protarsomere 1 expanded and with adhesive setae ventrally, second protarsomere unmodified and without ventral setae. Male mesotrochanters spinose ventrally. Male metafemora swollen and with a triangular tooth on posterior margin near middle. Median lobe of aedeagus nearly straight, with dorsal margin largely unsclerotized. Flagellum long and coiled over itself in a proximal loop in repose. Right paramere quadrisetose. Left paramere asetose with four ventral pores. Stem of spermatheca straight at proximal end, without abrupt angulation, spermathecal duct long and evenly coiled several times.

Diversity. Only *Anillinus dentatus* sp. nov. belongs to this group.

Distribution and habitat. *Anillinus dentatus* is known only from two localities within a small area near Long Cane Creek in Sumter National Forest, Abbeville Co., SC (Fig. 43B). One specimen was collected by Berlese extraction of sifted dead wood, but all other specimens were collected from endogean habitats using pipe traps, soil washing, and searching under embedded rocks.

‘*valentinei* group’ sensu novo

“group VIII litter species” Sokolov et al. 2004: 228, in part.

“a group of ovoid species with partially microsculptured head” Sokolov and Carlton 2008: 44, in part.

“*valentinei* group” Sokolov 2011: 12; Sokolov 2012: 69, in part.

“*barri* group” Sokolov 2012: 66, in part.

Diagnosis. Dorsal microsculpture effaced from most of head and pronotum in most species, always absent from sides of vertex. Males with protarsomeres 1 and 2 both with adhesive setae ventrally in most species. Median lobe of aedeagus often with a carinate channel on left side near base. Flagellum well-sclerotized, internal sac often with various other well sclerotized structures such as spines or ostial plates. Right paramere quadrisetose. Left paramere with four pores on ventral margin, bearing setae or not. Spermatheca variable, long or short, with smooth or ribbed stem, spermathecal duct long and coiled or short.

Diversity. This is the most speciose group of *Anillinus*, with eight previously described species (*Anillinus chandleri* Sokolov, *Anillinus cornelli* Sokolov & Carlton, *Anillinus gimmeli* Sokolov & Carlton, *Anillinus humicolus* Sokolov, *Anillinus kingi* Sokolov, *Anillinus murrayae* Sokolov & Carlton, *Anillinus smokiensis* Sokolov, and *Anillinus valentinei* (Jeannel)) and two species from South

Carolina described as new below. More than 20 additional species are known and will be described in future papers.

Distribution and habitat. The range of the group extends from western North Carolina to northern Alabama, north to southeastern Kentucky and adjacent southwestern Virginia (Fig. 43B). The group is apparently absent from most of northern Georgia, and with the exception of *A. murrayae*, members of this group do not inhabit montane habitats in the Appalachians, and are restricted to lower elevations. Specimens have been collected from every microhabitat from which Appalachian anillines are known to occur: shallow leaf litter, deep soils, dead wood, and caves. *Anillinus valentinei* (sensu Sokolov 2012) is the only species of *Anillinus* that has been repeatedly collected in large series from caves, and according to Barr (1969) the species "exhibits the ecology and behavior of a troglobite."

Note. Sokolov (2012) placed *Anillinus tombarri* Sokolov in this group, based on its large body size, presumably troglobitic habits (the lone specimen was collected in a cave), and the presence of spines in the internal sac. The type of *A. tombarri* has numerous character states that indicate it is not closely related to this clade: second protarsomere without ventral adhesive setae, right paramere with more than four apical setae, dorsal margin of median lobe almost entirely membranous, metafemora modified. The thick, strongly curved flagellum of *A. tombarri* is similar to that of all members of the *hirsutus* and *barberi* groups, but for now we leave it in its own distinct group (Suppl. material 3).

'*albrittonorum* group'

"group VII endogean species" Sokolov and Schnepp 2021: 40, in part.

Diagnosis. The two species known to belong to this lineage are quite different in external morphology and most male genitalic characters, but share the following: male protarsomere 1 expanded and with ventral adhesive setae, protarsomere 2 unmodified and without ventral setae, flagellum of median lobe of aedeagus lightly sclerotized and filamentous, spermatheca short and abruptly enlarged distally, with long spermathecal duct.

Diversity. This group consists of *Anillinus albrittonorum* Sokolov & Schnepp and *Anillinus jancae* sp. nov., described below.

Distribution and habitat. *Anillinus albrittonorum* inhabits deep sand in northern Florida, where it has only been collected using passive traps (Sokolov and Schnepp 2021). *Anillinus jancae* sp. nov. lives in deep red clay soils in South Carolina, and has been collected using pipe traps and by turning deeply embedded rocks.

'*elongatus* group' sensu Harden and Caterino (2024)

"group V endogean species" Sokolov et al. 2004: 228, in part.
"*sinuaticollis* group" Sokolov 2012: 62, in part.

Diagnosis. This group includes the flattest and narrowest species of *Anillinus* in the eastern U.S., with parallel-sided elytra and relatively large heads (Fig. 2H). Development of dorsal microsculpture varies from fully developed on head and pronotum to lacking on most of pronotum and sides of vertex. Males have protarsomeres 1 and 2 expanded laterally on inner margin and both bear adhesive vestiture ventrally. Metafemora of males are modified, swollen apically with posterior margin tuberculate and in some species bearing a prominent peg-like tooth. The median lobe of the aedeagus is slightly twisted dorsally. Flagellum lightly sclerotized and open laterally, long and filamentous distally. Right paramere quadrisetose. Left paramere with four preapical pores, bearing setae or not. Spermatheca elongate and moderately sinuate or straight, with surface either smooth or ribbed, spermathecal duct long and coiled.

Diversity. This group includes five described species (*Anillinus arenicollis*, *Anillinus elongatus* Jeannel, *Anillinus montrex*, *Anillinus pittsylvanicus*, and *Anillinus uwharrie*), and two undescribed species (Harden and Caterino 2024).

Distribution and habitat. This group is distributed in the Piedmont ecoregion from Virginia, North Carolina, and northeastern South Carolina (Fig. 43D). Members of this group are endogean, and have been collected using pipe traps, soil washing, soil extraction, and underneath embedded rocks. One specimen of *A. arenicollis* was collected in a litter sample taken in February.

'***sinuaticollis*** **group' sensu novo**

"group V endogean species" Sokolov et al. 2004: 228, in part.
"*sinuaticollis*-group" Sokolov 2012: 62, in part.

Diagnosis. Relatively small in size (ABL less than 2 mm). Dorsal microsculpture usually present on entire dorsal surface of head, absent from disc of pronotum in most species. Males with protarsomere 1 expanded and bearing ventral adhesive setae, male protarsomere 2 not expanded and not bearing ventral adhesive setae. Flagellum of median lobe lightly sclerotized, open laterally. Internal sac with or without other sclerotized structures. Stem of spermatheca long and coiled proximally, spermathecal duct short and without coils.

Diversity. This group includes two previously described species (*Anillinus sinuaticollis* Jeannel and *Anillinus felicianus* Sokolov). Four new species from South Carolina are described below. Two undescribed species are known and will be described in future papers.

Distribution and habitat. This group occupies three disjunct regions: the Cumberland Plateau from Kentucky south to northern Alabama, southeastern Louisiana, and the inner Piedmont and Blue Ridge of South Carolina (Fig. 43D). The apparent absence of this group from Georgia is notable. Members of this group are endogean and have been collected using pipe traps, soil washing, searching under embedded rocks, and from caves.

'***pecki*** **group' sensu Harden and Caterino (2024)**

"group II litter species" Sokolov et al. 2004: 228, in part.

Diagnosis. Dorsal microsculpture variable, weakly impressed on head and pronotum in most specimens. Body moderately convex and ovoid (Fig. 2F). Male protarsomeres 1 and 2 expanded and bearing ventral adhesive setae. Male metafemora unmodified except for patch of coarse microsculpture on posterior margin. Median lobe twisted dorsally, flagellum of median lobe short and lightly sclerotized, open laterally. Left side of internal sac with small scales of variable sclerotization. Spermatheca long with stem strongly ribbed medially and angulate at base, spermathecal duct short and not coiled.

Diversity. This group consists of *Anillinus pecki* Giachino and *Anillinus docwatsoni* Sokolov & Carlton.

Distribution and habitat. *Anillinus pecki* is widespread in the southern Appalachians north of the French Broad River, ranging from the Black Mountains in western North Carolina to Whitetop Mountain in southwest Virginia, whereas *Anillinus docwatsoni* is a micro-range endemic known only from the Hickory Nut Gorge in Rutherford and Henderson Counties, North Carolina (Fig. 43D). *Anillinus pecki* has been collected from leaf litter and underneath embedded rocks. Most specimens of *A. docwatsoni* have been collected under embedded rocks (Harden and Caterino 2024), but a small number have been collected from flood debris.

Anillinus sp. "Tennessee, Kings Saltpeter Cave"

Diagnosis. The single specimen of this unique lineage, a female, has an ABL of 2.09 mm. Dorsal microsculpture effaced from most of pronotum and head. Three supraorbital setae present on each side of head. Elytra are widest at the base, where the humeri are strongly produced (Fig. 2I). Spermatheca long and S-shaped, with a short spermathecal duct. Males of the species are unknown.

Distribution and habitat. The specimen was collected in a cave in northeastern Tennessee (Fig. 43E).

'*langdoni* group' sensu novo

"group I litter species" Sokolov et al. 2004: 228, in part.
"group II litter species" Sokolov et al. 2004: 228, in part.
"*virginiae* group" Sokolov et al. 2007: 4, in part.
"*langdoni* group" Sokolov et al. 2007: 4, in part.

Diagnosis. Dorsal microsculpture fully developed on head and pronotum in most specimens, sculpticels relatively large. Male protarsomeres 1 and 2 expanded and with ventral adhesive setae in most species. Male metafemora unmodified in all species except *A. virginiae*, in which they are swollen and bear a blunt angulate projection on posterior margin. Median lobe twisted dorsally. Flagellum thick, variable in length and degree of sclerotization. Both parameres quadrisetose. Spermatheca short, spermathecal duct variable in length, not coiled.

Diversity. In the broad sense that we adopt here, six described species are assigned to this group (*A. balli*, *Anillinus cieglerae* Sokolov & Carlton, *Anillinus langdoni* Sokolov & Carlton, *Anillinus nantahala* Dajoz, *Anillinus pusillus* Sokolov & Carlton, and *Anillinus virginiae* Jeannel). Four undescribed species are known, and will be described in future papers.

Distribution and habitat. Members of this group are found in four disjunct geographic regions: southern Appalachian Mountains (*A. cieglerae*, *A. langdoni*, *A. nantahala*, *A. pusillus*, and the four undescribed species), South Mountains of western North Carolina (*A. daggyi*), northwestern Virginia and adjacent West Virginia (*A. virginiae*), and eastern Cumberland Plateau of Kentucky (*A. balli*) (Fig. 43E). The southern montane species are readily collected from leaf litter, while most specimens of *A. virginiae* have been collected from endogean habitats using pipe traps and searching under embedded rocks.

Notes. Giachino (2011) described *Anillinus campbelli* as a member of the *langdoni* group. An examination of photos of the holotype, including the genitalia, suggests that *A. campbelli* is conspecific with *A. cherokee* of the *loweae* group, which is abundant near the type locality of *A. campbelli* (Van Hook Glade, Macon Co., NC).

'*loweae* group' sensu novo

"group II litter species" Sokolov et al. 2004: 228 in part.

"a group of ovoid species with partially microsculptured head" Sokolov and Carlton 2008: 44, in part.

"*loweae* group" Sokolov and Carlton 2010: 2, in part.

Diagnosis. In most members of this group the dorsal microsculpture is well developed on the forebody, absent only from a small area on either side of the head near the base. Males have adhesive vestiture present ventrally on both protarsomeres 1 and 2. Male profemora often strongly swollen. Median lobe twisted dorsally, with well-defined ostium of variable shape on left side. Internal sac with well-sclerotized flagellum of variable length, never filamentous. Right paramere quadrisetose. Left paramere with four preapical pores, bearing setae or not. Spermatheca long and well-sclerotized, gradually enlarged distally, stem smooth or ribbed, spermathecal duct short and uncoiled.

Diversity. This species group includes four described species (*Anillinus cherokee* Sokolov & Carlton, *Anillinus fortis* (Horn), *Anillinus loweae* Sokolov & Carlton, and *Anillinus merritti* Sokolov & Carlton) and three undescribed species that will be treated in a future paper.

Distribution and habitat. The range of this group encompasses most of the southern Appalachians from the Bald Mountains on the Tennessee-North Carolina border south to northern South Carolina and Georgia (Fig. 43G). Members of this group are strictly montane and most species can be readily collected in leaf litter. *Anillinus merritti* is primarily endogean, and most specimens have been collected under rocks and using pipe traps.

Notes. The type of *A. fortis* has not been critically studied by modern workers (Sokolov et al. 2004), and the concept of the late T.C. Barr encompassed three species (*A. erwini*, *A. fortis* sensu Sokolov and Carlton 2010, and *A. pecki*). Barr's concept informed the concept of later workers (Sokolov et al. 2004, Sokolov and Carlton 2010). To indicate the uncertainty of the identity of the type of *A. fortis*, we refer to the species as "*A.* cf. *fortis*" in our phylogeny.

‘*steevesi* group’

“group II litter species” Sokolov et al. 2004: 228, in part.
“group VIII litter species” Sokolov et al. 2004: 228, in part.
“a group of ovoid species with partially microsculptured head” Sokolov and Carlton 2008: 44, in part.
“*loweae* group” Sokolov and Carlton 2010: 2, in part.
“*barri* group” Sokolov 2012: 66, in part.

Diagnosis. Dorsal microsculpture effaced from most of head and pronotum in most species. Males of most species with only protarsomere 1 expanded and bearing adhesive setae ventrally. Median lobe twisted dorsally, left side without well-defined ostial opening. Flagellum well-sclerotized and variable in length, filamentous in some species. Right paramere quadrisetose. Left paramere with four preapical pores, bearing setae or not. Spermatheca similar to that of the *loweae* group, but differing in having the spermathecal duct long and heavily coiled (the female genitalia of only three species have been examined, however).

Diversity. Five described species belong to this group (*Anillinus barri* Sokolov & Carlton, *Anillinus chilhowee* Sokolov, *Anillinus inexpectatus* Sokolov, *Anillinus juliae* Sokolov & Carlton, and *Anillinus steevesi* Barr), and eight undescribed species are known.

Distribution and habitat. This group is a dominant component of the anilline fauna of northern Georgia and adjacent Tennessee, where numerous short-range undescribed species are known. *Anillinus steevesi* has the largest range of any *Anillinus*, ranging from far western North Carolina across northern Alabama and into northeastern Mississippi (Fig. 43F). *Anillinus steevesi* has been collected from leaf litter, under rocks, and in caves. The other species in the group have been collected in leaf litter and under rocks. Members of this group occur at lower elevations than the *loweae* group.

Notes. The holotype of *A. steevesi* was not found at CMNH, and has probably been lost or was never designated by Barr. To indicate the uncertainty of the type status, we refer to the species as “*A.* cf. *steevesi*” in our phylogeny.

Taxonomic review of Anillini of South Carolina

Tribe Anillini Jeannel, 1937

Adult diagnosis. In the United States, adult specimens of Anillini are the only carabids that are both eyeless and possess subulate palpomeres.

Larval diagnosis. Late-instar larvae of Anillini in South Carolina share the following characters: body pale and soft, largely unsclerotized (Fig. 13A, B); legs with single tarsal claw; stemmata absent; coronal suture absent; retinaculum large; penicillus present and consisting of several setae; urogomphus with seven large setae (Fig. 14A, E). Other known carabid larvae in SC of similar size with a single tarsal claw and potentially lacking stemmata are the genera *Trechus*, *Semiardistomis*, *Clivina*, and the tribe Tachyini. Larvae of *Trechus* are easily recognized by the possession of 4-segmented labial palps and 5-segmented maxillary palps (versus 2- and 4-segmented, respectively, in anillines). *Semiardistomis* and *Clivina* can be readily separated by the small size of the retinaculum and a penicillus consisting of a single, large seta. South Carolina anilline larvae are similar to larvae of the tribe Tachyini, but differ by having seven large setae on the urogomphus (Fig. 14E), versus six in tachyines.

Serranillus Barr, 1995: 246

Adult diagnosis. Males of *Serranillus* are easily distinguished from *Anillinus* by the "serrate" modification of the last abdominal ventrite, which bears three protruding blunt lobes (Figs 15B, 18B, 19B), and by the greatly reduced and inconspicuous right paramere which lacks setae (Figs 15D, 19D). The last abdominal ventrite of male *Serranillus* also has large lateral extensions internally, visible when the abdomen is removed and cleared (Fig. 20C). The dorsal body surfaces of *Serranillus* are typically more setose than members of *Anillinus*, particularly the elytra (Sokolov et al. 2004), but members of some *Anillinus* species are similarly setose (Sokolov 2021). The pair of median setae on the mentum are on the mentum tooth itself in all specimens of *Serranillus* examined by us (Fig. 11A), while in *Anillinus* they are typically basad the tooth (Fig. 11B). Both mandibles in *Serranillus* possess a retinacular tooth near the base (Fig. 11C), while in *Anillinus* only the right mandible has a tooth (Fig. 11D). In addition to the reduced size of the right paramere, the right basal lobe of the median lobe of the aedeagus in *Serranillus* is reduced to a thin strip. The internal sac of the aedeagus in all species also contains a coiled sclerite on the left side, which is absent in *Anillinus*. The female spermathecae of *Serranillus* species are relatively small and have a stem that is nearly straight before the curved apex (Fig. 21S, T). The spermathecae are similar in shape to those of *A. albrittonorum* and *A jancae*, but the stem in those species is more slender and curved outward from the base (Fig. 21N).

Larval diagnosis. Differing from the single known late-instar *Anillinus* larva by mandibles with terebrae lacking serrations (Fig. 14B) and stipes of maxilla with setae of group gMX unevenly placed (Fig. 14D).

Diversity. Four previously described species, one species described as new below, and at least 10 undescribed species (Suppl. material 3).

Distribution. Few occurrence records have been previously published for *Serranillus*. The type locality of *Serranillus dunavani* (Jeannel) is Sassafras Mountain, near Rocky Bottom in Pickens Co, South Carolina, and the species has also been reported from Great Smoky Mountains National Park (Sokolov and Carlton 2008, 2010). Barr (1995) described *Serranillus jeanneli* from Coweeta Hydrologic Laboratory in Macon County, North Carolina, and stated the range extended from the Great Balsam Mountains in western North Carolina to northern Georgia, but gave no further details. He also mentioned in passing the existence of additional species in Cloudland Canyon (Dade County, GA) and the Piedmont of North Carolina and South Carolina. The Cloudland Canyon species is currently interpreted as *Serranillus magnus* (Zaballos & Mateu, 1997), described from material mislabeled as from Brazil (Sokolov and Carlton 2012). Sokolov and Carlton (2008) described *Serranillus septentrionis* from southwestern Virginia and cite a record of *S. jeanneli* from White County, Georgia. Museum records and personal collecting provide a more complete view of the range of the genus (Fig. 1A). Collectively, the genus occupies most of the southern Appalachians from NC to northwest GA, with disjunct occurrences in southwestern VA, the

Black and Bald Mountains of NC and TN, central and western Alabama, and the Cumberland Plateau of northern Tennessee. A pair of female *Serranillus* in the CMNH collection bearing Connecticut locality labels is mislabeled according to the collector (S. Peck, pers. comm., July 2019).

Partial key to the species of *Serranillus* of South Carolina and adjacent parts of North Carolina and Georgia

Note. Females of *Serranillus* are currently impossible to identify to species without associated males. Therefore, females are not separated in the key below. Confirmation of identifications should always be made by examining male genitalia.

1 Posterior margin of last abdominal ventrite modified, with three blunt projections; first and second protarsomeres expanded and bearing ventral adhesive setae (males) **2**

– Posterior margin of last abdominal ventrite unmodified; first and second protarsomeres unmodified (females, not treated further)

2(1) Smaller, ABL = 1.79–2.03 mm; dorsal and ventral margins of median lobe in right dorsolateral aspect straight and parallel-sided for most of length before abruptly enlarged apex (Fig. 15E) .... ***S. dunavani***

– Larger, ABL = 1.99–2.87 mm; margins of median lobe in right dorsolateral aspect not parallel-sided or straight **3**

3(2) Lobes of last abdominal ventrite with outer pair narrower and more prominent than inner lobe (Fig. 18B); body smaller, ABL = 1.99–2.35 mm... **4**

– Lobes of last abdominal ventrite subequal in width and prominence, or with inner lobe slightly more prominent than outer pair; body larger, ABL = 2.48–2.87 mm... **5**

4(3) Ventral surface of median lobe of aedeagus with carinate shelf near apex, causing ventral margin to appear deeply notched by a semicircular channel (Fig. 18D); left side of internal sac with long, dark spine that is bluntly hooked apically where it protrudes beyond ostium ..... ***S. jeanneli***

– Ventral surface of median lobe without carinate shelf, ventral margin without deep semicircular channel; left side of internal sac with short, broad claw-shaped sclerite that is acutely pointed apically and ends well before ostium .... ***S.* sp. “North Carolina, Miller Cove”**

5(3) Hind angles of pronotum strongly projecting posteriorly (Fig. 19A) .... ***S. monadnock* sp. nov.**

– Hind angles of pronotum not strongly projecting posteriorly (as in Fig. 18A)... **6**

6(5) Apex of median lobe produced ventrally, dorsal margin of median lobe channelized .... ***S.* sp. “Georgia, Rabun Bald sp. 1”**

– Apex of median lobe not produced ventrally, dorsal margin of median lobe not channelized.. **7**

7(6) Ventral margin of median lobe with central tuft of long setae; ventral margin not notched..........................***S.* sp. “North Carolina, Riley Knob”**

– Ventral margin of median lobe without central tuft of long setae; ventral margin notched .... ***S.* sp. “Georgia, Rabun Bald sp. 3”**

Serranillus dunavani (Jeannel, 1963)

Figs 2A, 10G, 11A, C, 13A, 14B, D, 15A–E, 16, 17A, 21S, 25A–C

Anillinus dunavani Jeannel, 1963: 76; Barr 1995: 245.
Serranillus dunavani (Jeannel): Sokolov et al. 2004: 188.

Material examined. ***Holotype male*** **(USNM)**: point mounted, not dissected, labeled: “Rocky Bottom, Pickens Co. S.C., 25 Aug. 1932, D. Dunavan Co.” “Sassafras Mtn. 3,500 ft” “In leaf mold” “TYPE [red paper]” “Type No. 69542 USNM [red paper]” “Anillinus dunavani n.sp. R. Jeannel det. 19/”.

Other material (*n* = 177, CMNH, CUAC, CWHc, NCSU, OSUC, USNM). USA • **North Carolina** • 1 ♂; **Clay Co**.; Nantahala National Forest, Shooting Creek Bald; 35.0679, -83.6466; 11 May 2020; C.W. Harden and M.S. Caterino leg.;

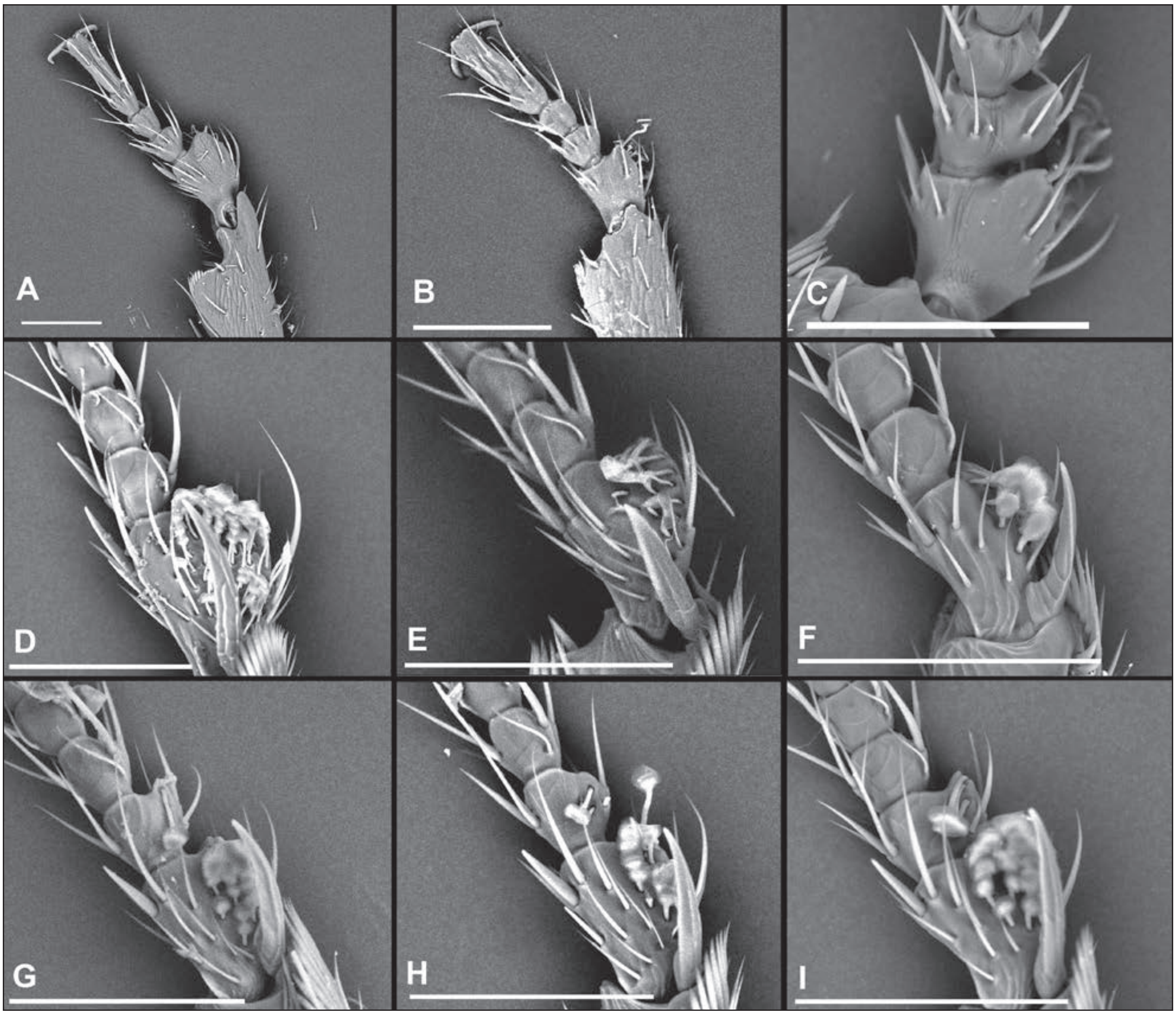

Figure 10. SEM micrographs of male protarsi **A** *Anillinus jancae*, left protarsus, dorsal aspect **B** *Anillinus mica*, left protarsus, dorsal aspect **C** *Anillinus montrex* left protarsus, dorsal aspect **D** *A. jancae*, right protarsus, ventral aspect **E** *Anillinus choestoea*, right protarsus, ventral aspect **F** *Anillinus dentatus*, right protarsus, ventral aspect **G** *Serranillus dunavani* (Jeannel), right protarsus, ventral aspect **H** *Anillinus murrayae* Sokolov & Carlton, right protarsus, ventral aspect **I** *A. montrex*, right protarsus, ventral aspect. Scale bars: 0.1 mm.

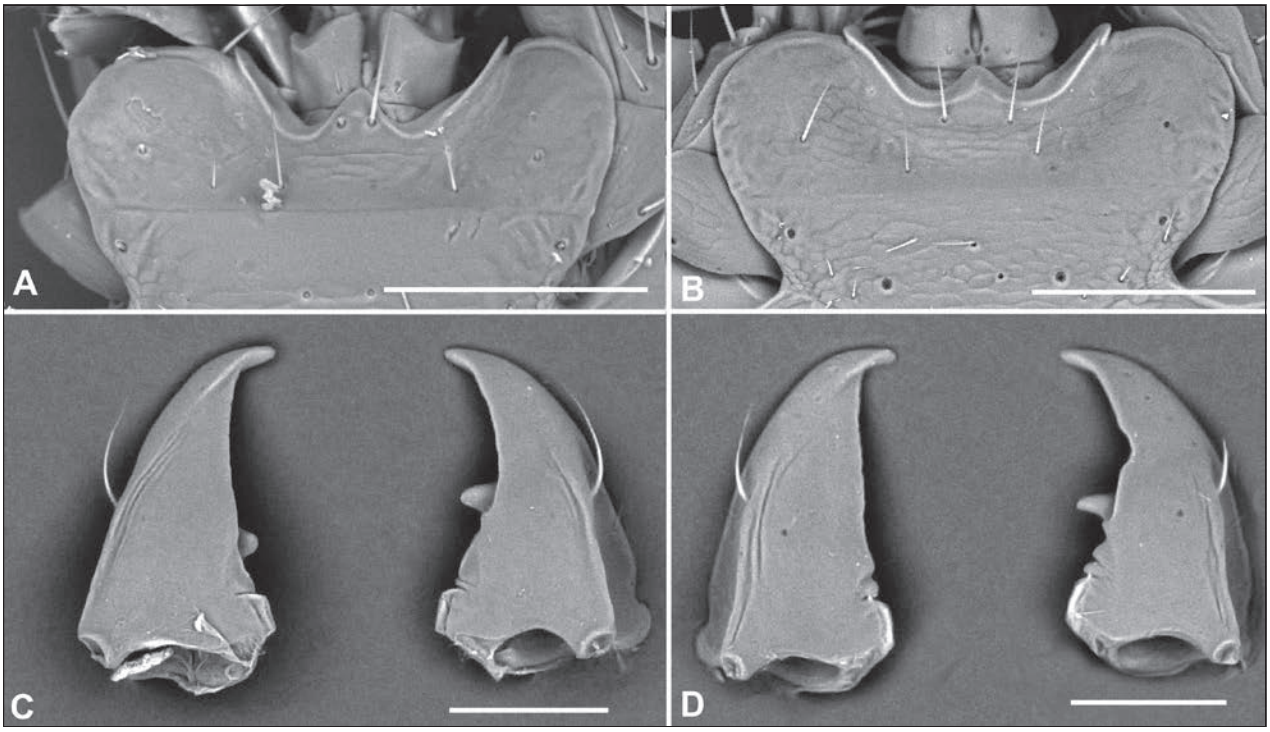

Figure 11. SEM micrographs of mouthparts of Appalachian Anillini genera **A** mentum of *Serranillus dunavani* (Jeannel) **B** mentum of *Anillinus choestoea* **C** mandibles of *S. dunavani*, dorsal aspect **D** mandibles of *A. choestoea*, dorsal aspect. Scale bars: 0.1 mm.

CWH-381, CUAC000066851; • 1 ♂, 4 ♀; same data as previous; CWHc; • 1 ♂, 1 ♀; **Clay Co.**; Nantahala National Forest, Shooting Creek Bald; 35.0681, -83.6464; 11 May 2020; C.W. Harden leg.; CWHc; • 2 ♀; **Henderson Co.**; 0.3 miles southwest of Bat Cave; 35.4470, -82.2910; 22 July 1967; S. Peck and A. Fiske leg.; CMNH; • 2 ♂, 1 ♀; **Macon Co.**; 1 mile northwest of Highlands; 35.061, -83.217; 16 Aug. 1981; Q.D. Wheeler leg.; OSUC; • 1 ♂, 1 ♀; **Macon Co.**; Nantahala National Forest, Cowee Bald; 35.3269, -83.3350; 15 Sep. 2020; • 1 ♂; **Montgomery Co.**; Uwarrie National Forest, 2 miles south of Eldorado, Route 109; 35.4340, -80.0190; 27 Aug. 1990; W. Reeves leg.; LSAM0153884; NCSU; • 2 ♂, 1 ♀; **Polk Co.**; Green River Game Lands; 35.2940, -82.2610; 18 Mar. 2018; M.S. Caterino leg.; CUAC000107846, CUAC000107847, CUAC000107856; • 1 ♀; **Polk Co.**; Lower Bradley Falls Trail; 35.3580, -82.2878; 19 Mar. 2018; M.S. Caterino leg.; CUAC000107772; • 2 ♂, 2 ♀; **Polk Co.**; Melrose Falls; 35.2217, -82.2985; 10 Aug. 2021; M.S. Caterino leg.; • 1 unsexed; **Swain Co.**; Great Smoky Mountains National Park, Deep Creek area, loop trail at Sunkota Ridge trail; 35.4750, -83.4200; 25 Jul. 2002; C.E. Carlton leg.; NCSU_ENT00293747; NCSU; • 1 unsexed; **Swain Co.**; Great Smoky Mountains National Park, Lakeshore Trail; 35.4520, -83.5410; 18 Jul. 2018; A.K. Tishechkin leg.; NCSU_ENT00293744; NCSU; • 1 ♂, 1 ♀; **Transylvania Co.**; Sassafras Mountain; 35.0656, -82.7776; 11 Jun. 2020; CUAC; • 1 ♂, 2 ♀; **Transylvania Co.**; 1 mile south of Rosman, NC 178; 35.1290, -82.8230; [no date]; J.F. and S. Cornell leg.; NCSU; • **South Carolina**; • 1 ♂; **Abbeville Co.**; Sumter National Forest, Long Cane Creek; 34.1345, -82.3230; 4 Feb. 2022; M. Ferro leg.; CWHc; • 1 ♀; **Abbeville Co.**; Sumter National Forest, off Cedar Springs Road; 34.1086, -82.3390; 25 Sep. 2020; C.W. Harden leg.; CWH-267, CUAC000066830; • 1 ♂; **Greenville Co.**; Highway 97, River

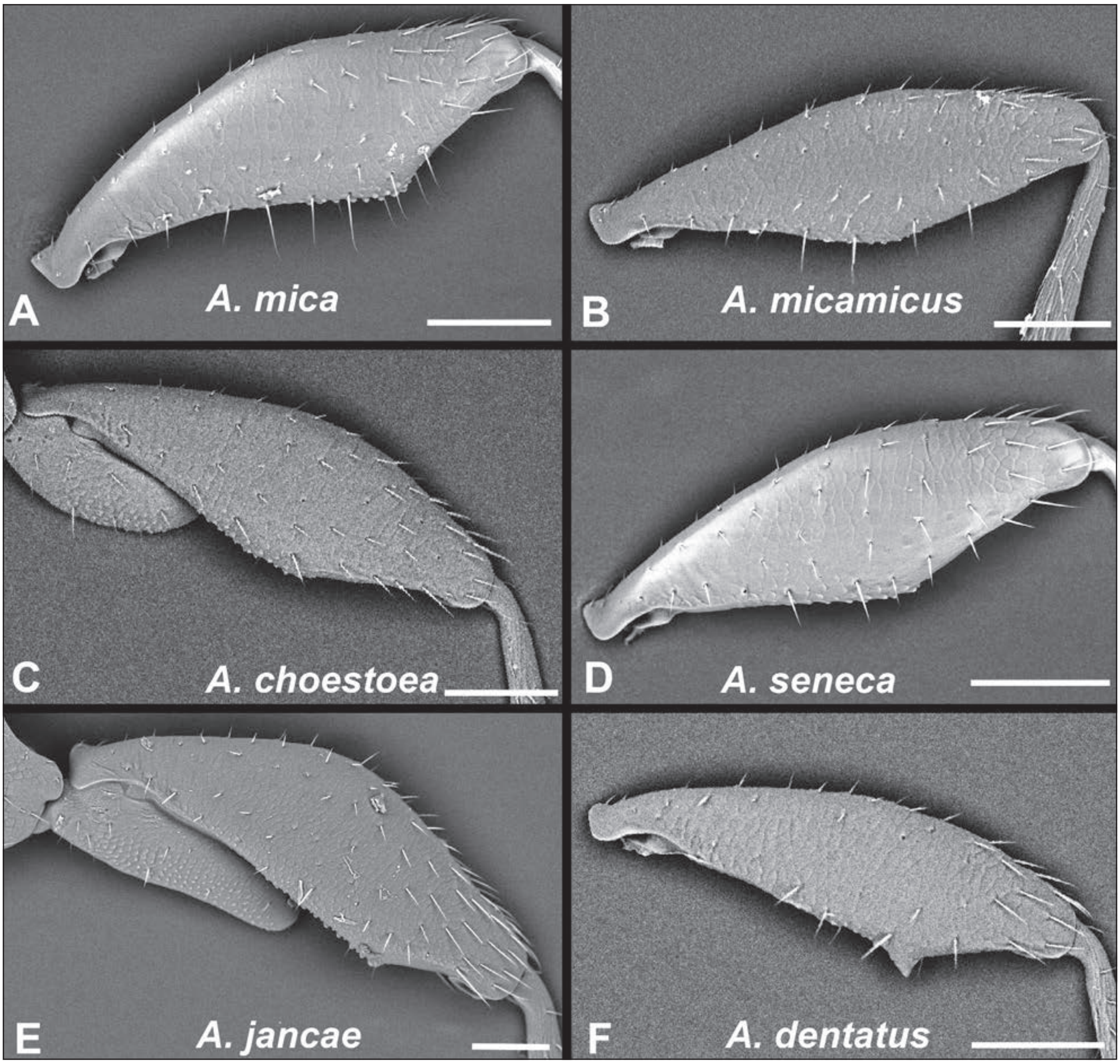

Figure 12. SEM micrographs of male left metafemora of *Anillinus* species. Scale bar: 0.1 mm.

Falls Lodge; 35.1221, -82.5405; 18 Mar. 2017; M. Ferro leg.; CUAC000049982; • 1 ♂, 11 ♀; **Greenville Co.**; Ashmore Heritage Preserve; 35.0867, -82.5788; 14 Mar. 2020; C.W. Harden and L.M. Thompson leg.; CWHc; • 1 ♂; **Greenville Co.**; Ashmore Heritage Preserve; 35.0933, -82.5930; 29 Jun. 2015; S. Myers leg.; MSC-2463, CUAC000185783; • 1 ♂; **Greenville Co.**; Chestnut Ridge Heritage Preserve; 35.1506, -82.2779; 8 Apr. 2018; M. Caterino and L. Vasquez leg.; CUAC000108123; • 1 ♀; **Greenville Co.**; Chestnut Ridge Heritage Preserve; 35.1507, -82.2821; 20 Oct. 2021; C.W. Harden leg.; CWHc; • *n* = 11; **Kershaw Co.**; English Swamp, Wateree Floodland Memorial Forest; 34.0911, -80.6578; 27 Feb. 2010; J.F. Cornell, S. Cornell and B. Gregory leg.; NCSU; • 2 ♀; **Oconee Co.**; Coon Branch Natural Area; 35.0200, -83.0000; 21 Jun. 2018; D. Chandler leg.; CUAC000109930 and CUAC000109964; • 4 ♂, 2 ♀; **Oconee Co.**; Coon Branch Natural Area; 35.0170, -82.9970; 18 Oct. 2020; C.W. Harden leg.; CWHc; • 1 ♂; **Oconee Co.**; Devils Fork State Park; 34.9390, -82.8798; 26 Apr. 2015;

S. Myers leg.; MSC-2454, CUAC000185791; • 1 ♂, 2 ♀; **Oconee Co.**; East Fork [Chattooga River]; 34.9843, -83.0981; 4 May 2015; M.S. Caterino and S. Myers leg.; CUAC000110650, CUAC000110651, CUAC000110653; • 1 ♀; **Oconee Co.**; East Fork trail, Ellicott Rock Wilderness; 34.9913, -83.0980; 29 Jun. 2015; S. Myers leg.; SSM250, CUAC000185792; • 1 unsexed; **Oconee Co.**; East Fork trail; 34.9838, -83.0979; 4 May. 2015; S. Myers leg.; SSM415, CUAC000185793; • 2 ♂, 1 ♀; **Oconee Co.**; Hill above parking lot near Stumphouse Tunnel; 34.8097, -83.1235; 5 Jul. 2019; C.W. Harden leg.; CWHc; • 1 ♂; **Oconee Co.**; Martin Creek Landing; 34.6389, -82.8663; 26 May 2022; C.W. Harden leg.; CWH-448, CUAC000066843; • 1 ♀; **Oconee Co.**; Oconee State Park, 6.7 miles north-northwest of Walhalla; 34.8690, -83.1050; 1 Jul. 1983; J. Pakaluk leg.; NCSU; • 2 ♂, 5 ♀; **Oconee Co.**; Oconee State Park; 34.8690, -83.1050; 21 Jul. 1967; S. Peck and A. Fiske leg.; CMNH; • 1 ♂, 1 ♀; **Oconee Co.**; Sumter National Forest, Yellow Branch Falls; 34.8067, -83.1283; 12 Oct. 2017; M.S. Caterino leg.; CUAC000107624 and CUAC000107625; • 3 ♂, 1 ♀; **Oconee Co.**; Sumter National Forest, Forest service road 725; 34.8395, -83.1677; 13 Sep. 2020; A. Deczynski leg.; CWHc; • 1 ♂; **Oconee Co.**; Sumter National Forest, Indian Camp Branch; 34.9898, -83.0724; 4 May 2015; M.S. Caterino and S. Myers leg.; CUAC000010470; • 2 ♂, 2 ♀; **Oconee Co.**; Sumter National Forest, Tater Hill trail; 34.9612, -83.0116; 24 Feb. 2018; M. Caterino leg.; CUAC; • 1 ♂; **Pickens Co.**; Chimneytop Gap; 35.0620, -82.8008; 10 Jun. 2015; S. Myers leg.; MSC-2457, CUAC000185780; • 1 ♂; **Pickens Co.**; Chimneytop Gap; 35.0632, -82.7964; 23 Mar. 2023; C.W. Harden leg.; CWHc; • 1 ♂, 1 ♀; **Pickens Co.**; Chimneytop Gap; 35.0630, -82.7968; 23 Mar. 2023; C.W. Harden leg.; CWHc; • 1 ♂; **Pickens Co.**; Clemson Experimental Forest; 34.7384, -82.8436; 20 Feb. 2023; E. Recuero leg.; CWHc; • 1 ♀; **Pickens Co.**; Clemson Experimental Forest, Waldrop Stone area; 34.7390, -82.8216; 2 Feb. 2021; C.W. Harden leg.; CWHc; • 1 ♂; **Pickens Co.**; Clemson Experimental Forest, Wildcat Creek; 34.7561, -82.8551; 20 Jun. 2018; C.W. Harden leg.; CWHc; • 3 ♂, 1 ♀; **Pickens Co.**; Clemson; 34.6820, -82.8330; 4 Oct. 1966; J.A. Payne leg.; CMNH; • 1 ♀; **Pickens Co.**; Clemson; 34.6820, -82.8330; 19 May 1962; J.A. Payne leg.; CMNH; • 4 ♂, 2 ♀; **Pickens Co.**; Clemson; 34.6820, -82.8330; 20 Jun. 1962; J.A. Payne leg.; CMNH; • 1 ♂; **Pickens Co.**; Eastatoe Creek Heritage Preserve; 35.1577, -82.4910; 30 Mar. 2015; S. Myers leg.; MSC-2455, CUAC000185778; • 1 ♂; **Pickens Co.**; Eastatoe Creek Heritage Preserve; [incorrect coordinates]; 30 Mar. 2015; S. Myers leg.; MSC-2461, CUAC000185781; • 1 ♀; **Pickens Co.**; Eastatoe Heritage Preserve; 35.0462, -82.8178; 6 Apr. 2014; M. Caterino and K. Caterino leg.; CUAC000002709; • 2 ♂, 1 ♀; **Pickens Co.**; near Chimneytop Gap; 35.0639, -82.7996; 11 Sep. 2019; M.S. Caterino leg.; CUAC; • 4 ♀; **Pickens Co.**; Nine Times Preserve, 34.9460, -82.8023; 31 Sep. 2015; S. Myers leg.; SSM184 to SSM187, CUAC000185770, CUAC000185773 to CUAC000185775; • 2 ♂, 1 ♀; **Pickens Co.**; Nine Times Preserve; 34.9465, -82.7992; 27 Mar. 2015; S. Myers leg.; SSM188 to SSM190; CUAC000185769, CUAC000185776, CUAC000185777; • 3 ♂, 1 ♀; **Pickens Co.**; Nine Times Preserve; 34.9464, -82.8027; 27 Mar. 2015; M.S. Caterino and S. Myers leg.; CUAC000173553, CUAC000173556, CUAC000173557, CUAC000173559; • 1 larva, 1 ♂; **Pickens Co.**; Sassafras Mountain; 35.0640, -82.7767; 20 Oct. 2020; F. Etzler and P. Wooden leg.; CWH-311 and CWH-312, CUAC000185899 and CUAC000066867; • 8 ♂, 9 ♀; same data as previous; CUAC; • 2 ♀; **Pickens Co.**; Sassafras Mountain; 35.0645, -82.7774; 10 Jun. 2015; S. Myers leg.; SSM67 and SSM68, CUAC000185771 and CUAC000185785;

Figure 13. Dorsal habitus of late-instar larvae **A** *Serranillus dunavani* (Jeannel) **B** *Anillinus jancae*. Scale bars: 1 mm.

• 2 ♀; **Pickens Co.**; Sassafras Mountain; 35.0634, -82.7760; 10 Jun. 2015; S. Myers leg.; SSM69 and SSM70, CUAC000185784 and CUAC000185790; • 3 ♂, 1 ♀; **Pickens Co.**; Sassafras Mountain; 35.0579, -82.7705; 10 Jun. 2015; S. Myers leg.; SSM71 to SSM74, CUAC000185786 to CUAC000185789; • 3 ♂, 5 ♀; **Pickens Co.**; Sassafras Mountain; 35.0647, -82.7774; 11 Jun. 2020; F. Etzler leg.; CUAC; • 5 ♂, 4 ♀; **Pickens Co.**; Sassafras Mountain; 35.0650, -82.7750; 21 Jul. 1967; S. Peck and A. Fiske leg.; CMNH.

GenBank accession numbers for specimens from Sassafras Mountain: OR839609, OR839610, OR839814, OR839815, OR839816, OR839817, OR839818, OR838294, OR853396, OR839363, OR839819, OR837946, OR838111, OR838295.

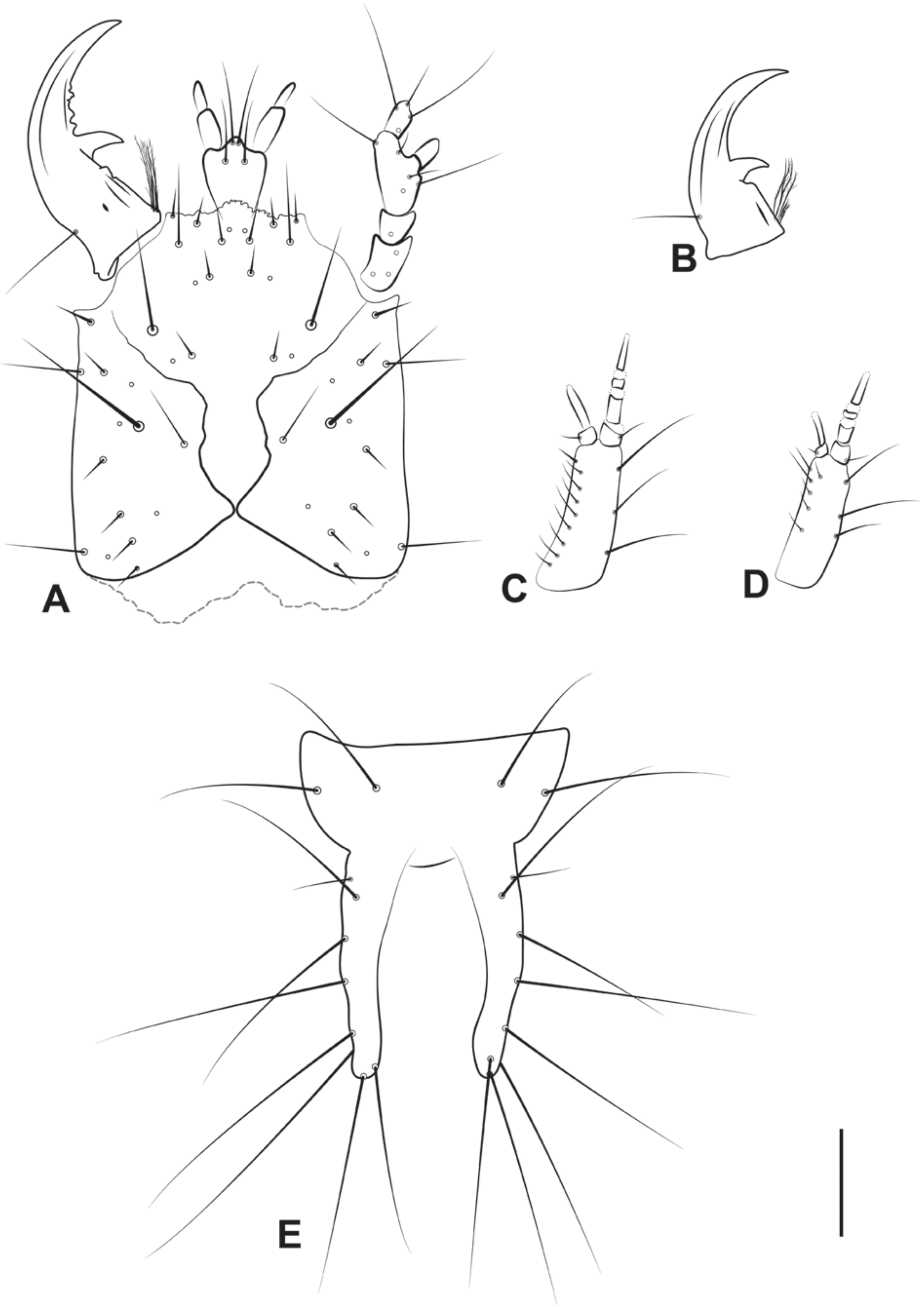

Figure 14. Details of late-instar larvae of Appalachian Anillini **A** head of *Anillinus jancae* sp. nov., dorsal aspect, left antenna and right mandible omitted **B** left mandible of *Serranillus dunavani* (Jeannel), dorsal aspect **C** right maxilla of *A. jancae*, dorsal aspect **D** right maxilla of *S. dunavani*, dorsal aspect **E** urogomphi of *A. jancae*, dorsal aspect. Scale bar: 0.1 mm.

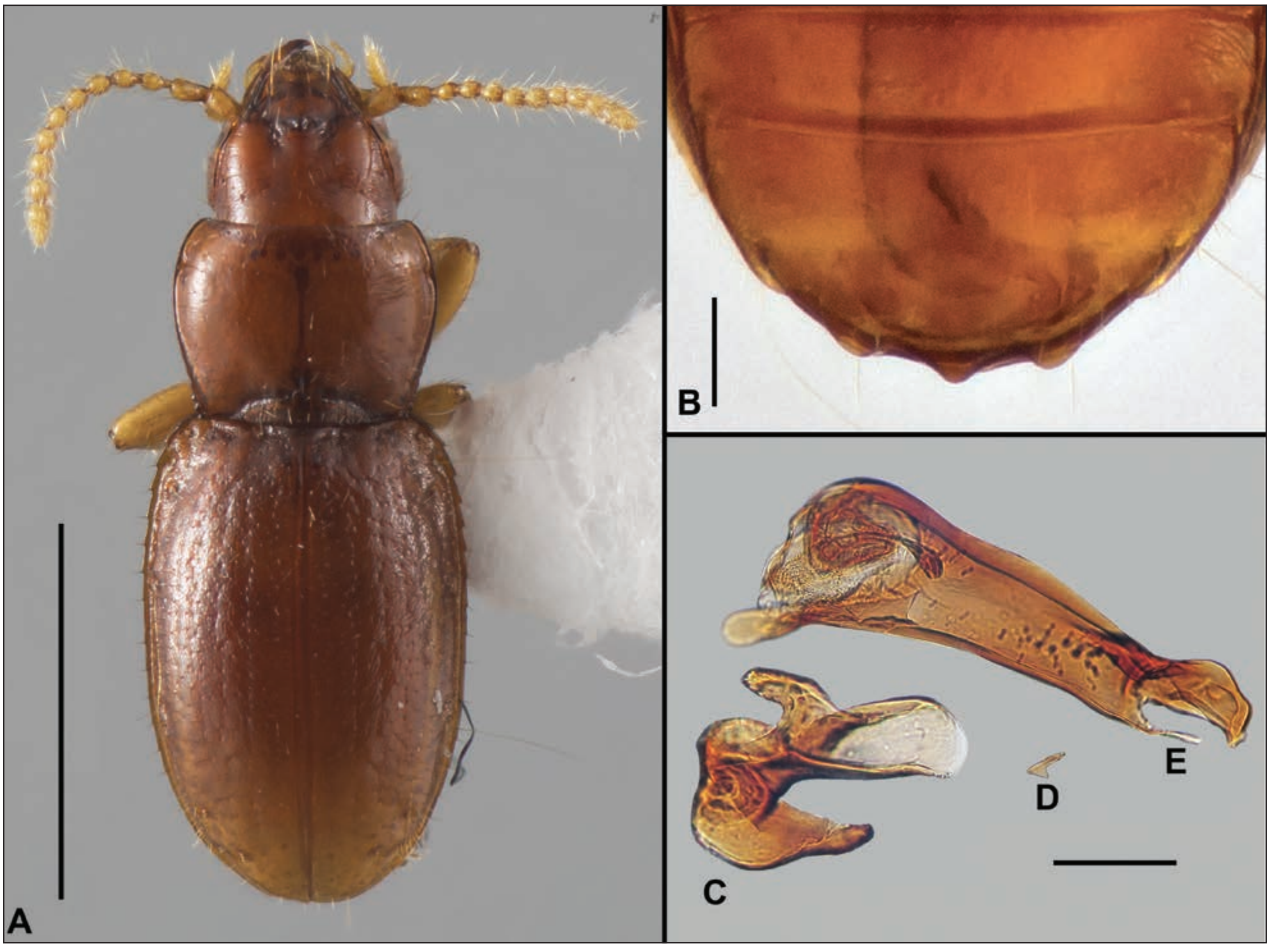

Figure 15. *Serranillus dunavani* (Jeannel) **A** habitus **B** last abdominal ventrite, ventral aspect **C** left paramere, left lateral aspect **D** right paramere, right lateral aspect **E** median lobe, right dorsolateral aspect. Scale bars: 1 mm (**A**); 0.1 mm (**B–E**).

Literature records. Besides the type locality, no specific records have been previously published for *S. dunavani*. Sokolov and Carlton (2010) cite a molecular voucher of *S. dunavani* from "GSMNP, Twentymile Trail." Sokolov and Carlton (2008) state that they studied material of *S. dunavani* only from "GSMNP". Their fig. 7 shows the range of *S. dunavani* covering over 30 counties in Tennessee, North Carolina, and South Carolina, citing "original data" as the source for the figure. However, these data are not apparently available and we have not seen any material of *S. dunavani* from Tennessee nor from most of the North Carolina counties that are shaded in that figure.

Diagnosis. This is the smallest *Serranillus* species, with most specimens having an ABL of 2 mm or less. The median lobe of the aedeagus is distinctive in being elongate with a recurved apex and lacking large, sclerotized spines in the internal sac (Fig. 15E).

Redescription. ***Habitus*** Small for the genus (ABL = 1.79–2.03 mm), convex and ovoid, robust (Fig. 15A). ***Integument*** Microsculpture indistinct on dorsal surfaces of head and pronotum, giving a shiny appearance. ***Head*** Relatively large (HW/PW = 0.73–0.75), antennomeres IV–X moniliform, slightly clavate. Frontoclypeal horn present, conspicuous. Ocular tubercles variable, present at least as a slight bulge, sometimes developed as a conspicuous hornlike projection below lateral carina. In some specimens, dorsad to lateral carina above

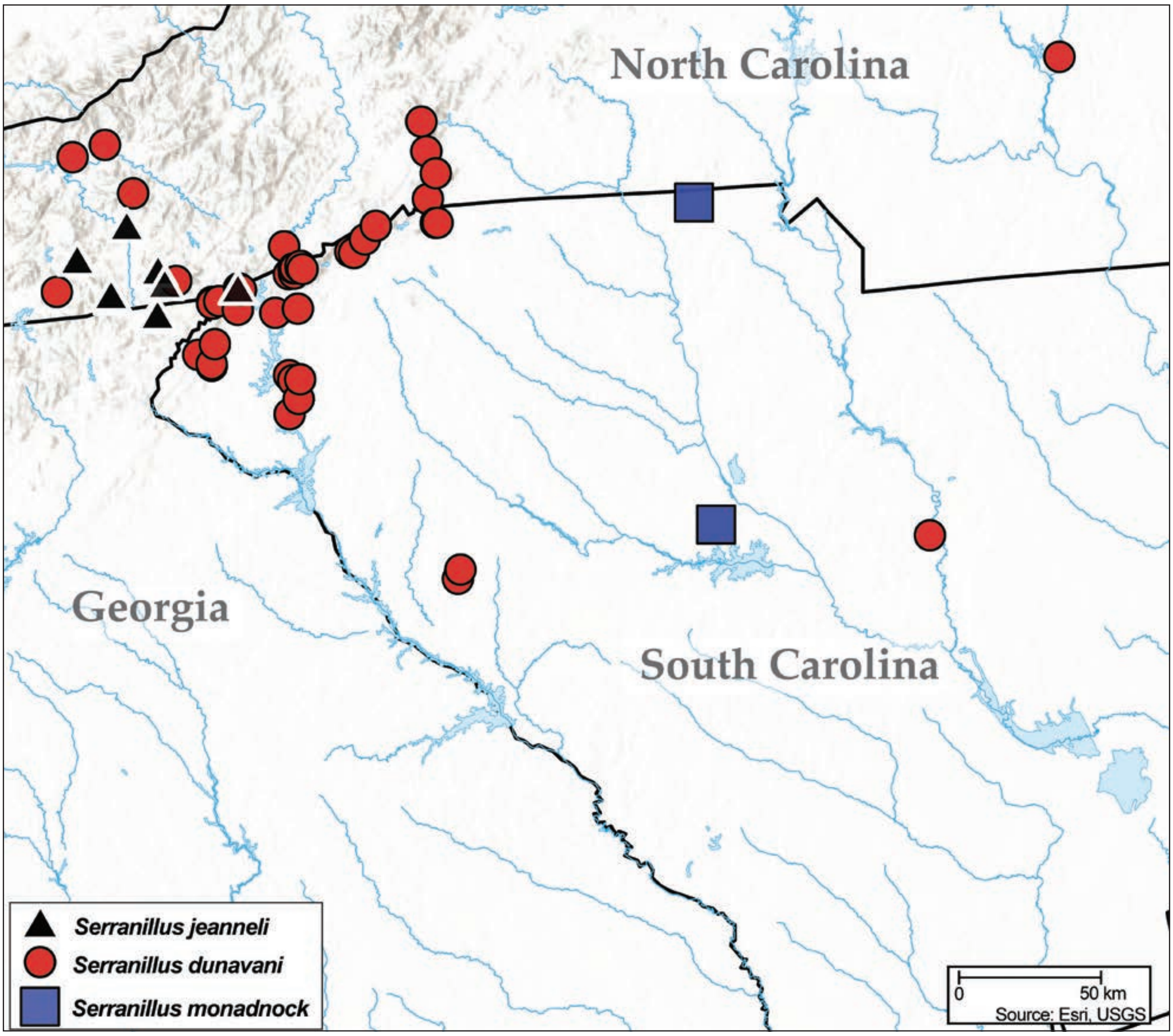

Figure 16. Distribution map of *Serranillus* species that occur in South Carolina. The locality for *Serranillus* sp. "South Carolina, Coon Branch" is the same as the single South Carolina *S. jeanneli* occurrence, and is not shown. Data are from Harden (2024).

tubercle on either side is a pale circular mark, more evident in teneral individuals. Two pairs of supraorbital setae present. Mentum with median pair of setae on tooth. ***Pronotum*** Relatively short (PL/ABL = 0.23–0.24) and broad (PW/EW = 0.83–0.84), moderately constricted posteriorly (PbW/PW = 0.72–0.78), sides evenly convergent to obtuse posterior angles. ***Elytra*** Moderately convex and ovoid, relatively broad (EW/ABL = 0.37–0.39), with weak traces of four striae. ***Legs*** Male protarsomeres 1 and 2 expanded and dentate on inner margin, with thick white adhesive setae ventrally (Fig. 10G). Male metatrochanters and posterior face of metafemora with coarse papillate microsculpture, metafemora slightly swollen. Female legs unmodified. ***Abdominal ventrites*** Last abdominal ventrite in males modified, apex protruding and bearing three blunt lobes, the inner slightly more prominent than the outer two (Fig. 15B). ***Male genitalia.*** Ring sclerite relatively large (RL/ABL = 0.30), narrow and subtriangular, with lightly-sclerotized expansions laterally; apex narrow and bent ventrally. Median lobe (Fig. 15E) complex, strongly asymmetrical (Fig. 17A), twisted dorsally from plane of basal lobes, heavily sclerotized on all faces. In strict right lateral

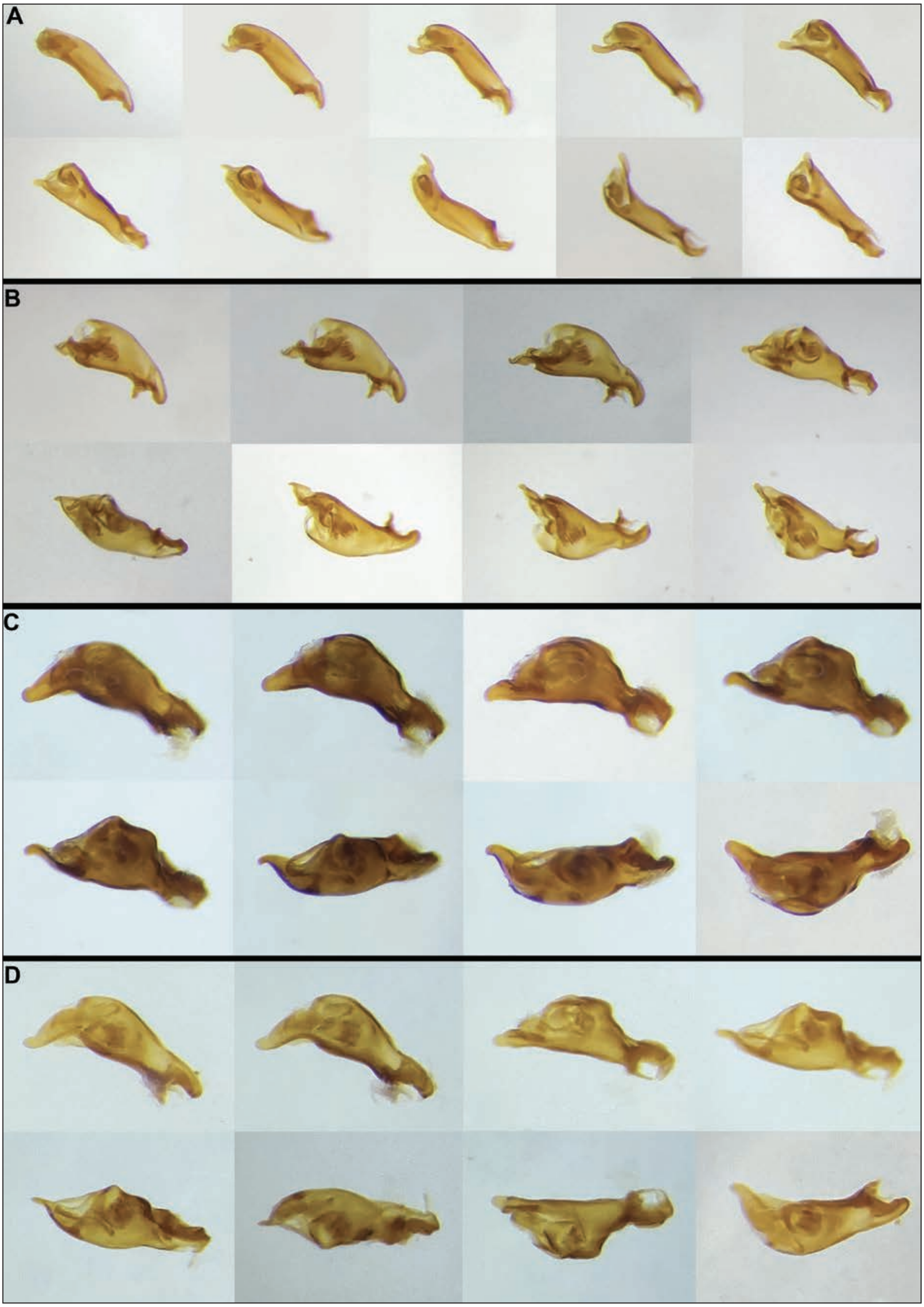

Figure 17. Multiple aspects of median lobes of South Carolina *Serranillus* species, progressively rotated dorsally from right lateral aspect (upper left) to left lateroventral aspect (lower right) **A** *Serranillus dunavani* **B** *Serranillus jeanneli* **C** *Serranillus monadnock*, holotype (Kings Mountain, SC) **D** *Serranillus monadnock*, paratype (Little Mountain, SC). Photographs not to same scale.

Figure 18. *Serranillus jeanneli* Barr. **A** dorsal habitus, abdomen removed for DNA extraction **B** last abdominal ventrite, ventral aspect **C** left paramere, left lateral aspect **D** median lobe (with right paramere attached, black arrow), right dorsolateral aspect. Scale bars: 1 mm (**A**); 0.1 mm (**B–D**).

aspect appearing as a blunt club-shaped organ without discernible apex. In dorsal aspect, nearly straight for basal 2/3, without basal bend, with ventral margin abruptly curved ventrally with apical sinuation. Left side of median lobe with a small, deep channel at base, with associated carina running obliquely for ~ 1/2 the length of median lobe. Apex variable: in topotype specimens, it is small, rounded, and deflected ventrally; in Clay Co., North Carolina, it is larger and more angularly produced ventrally. Small setae present on ventral surface of median lobe in some individuals. Basal lobes strongly asymmetrical, right lobe reduced to a narrow strap, left lobe large and cup-shaped. Flagellum long, thick at base and filamentous for most of its length beyond, evenly curved. Internal sac covered in small scales. Short scroll-like sclerite present at left side of ostium (behind flagellum in right lateral aspect), rolled into a tube; in lateral view appearing as a lightly sclerotized plate, rolled shape apparent in more posterior or anterior aspects. Right paramere minute and asetose, difficult to see in some aspects (Fig. 15D). Left paramere conchoidal, with enlarged base that is subequal in size to the rest of the paramere; ventral margin asetose (Fig. 15C). ***Female genitalia*.** Spermatheca small, curved, gradually enlarged apically, with swollen base (Fig. 21S). Spermathecal gland present, elongate. Spermathecal duct long and heavily coiled.

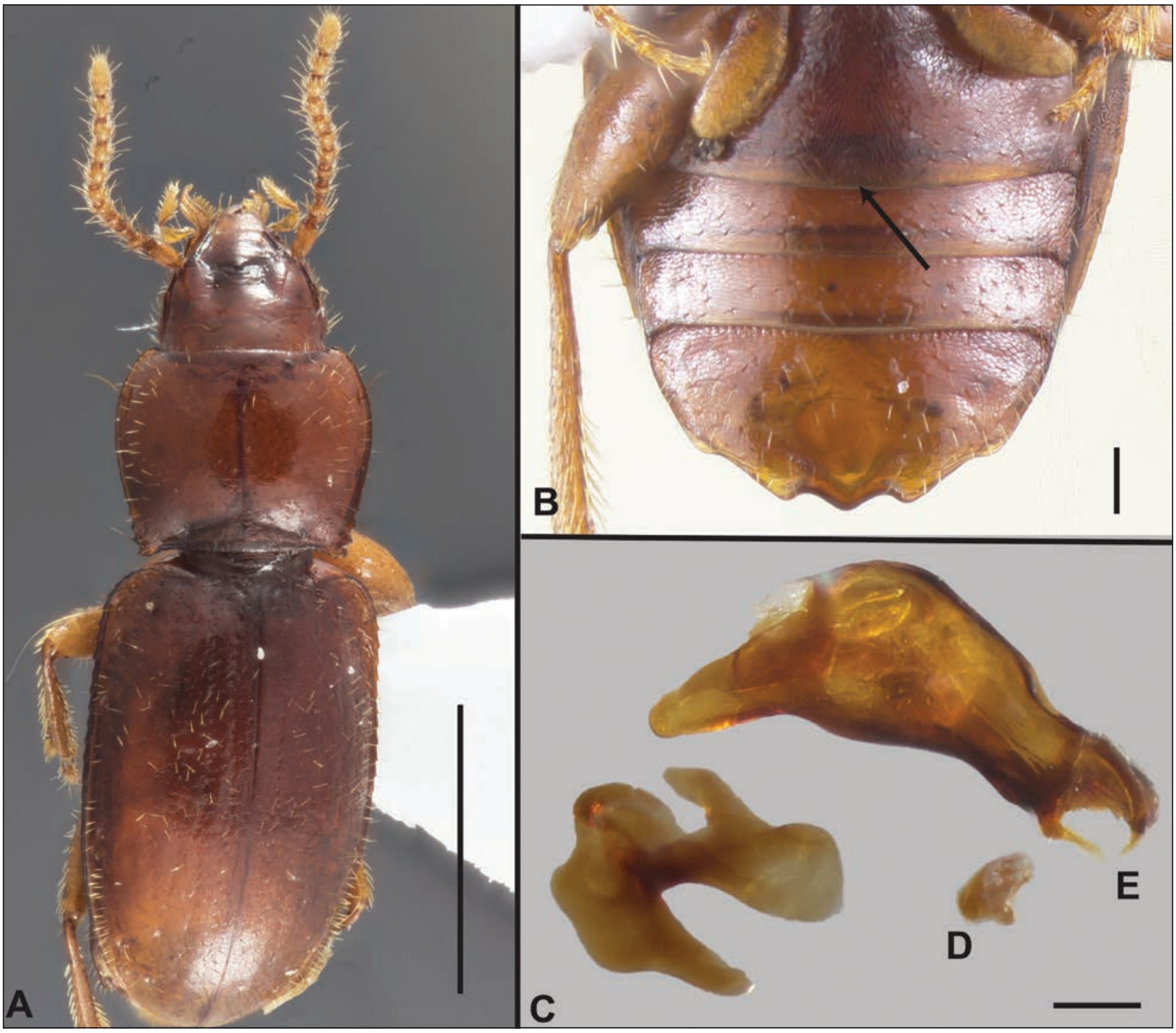

Figure 19. *Serranillus monadnock* holotype **A** dorsal habitus **B** abdominal ventrites, ventral aspect (black arrow = posterior margin of medial area with stretched microsculpture) **C** left paramere **D** right paramere **E** median lobe. Scale bars: 1 mm (**A**); 0.1 mm (**B, C, D, E**).

Distribution. This is the most widely distributed anilline in South Carolina (Fig. 16), with specimens known from Oconee Co. to Greenville Co. along the North Carolina border, south at least to Abbeville Co. and Kershaw Co. in the outer Piedmont and Sandhills physiographic regions, respectively. In North Carolina, the species has been found as far east as Montgomery Co., west to Clay Co., and north to Swain Co.

Sympatry. In South Carolina, this species has been collected in association with the following eight anilline species: *A. castaneus* sp. nov. (Greenville Co.), *A.* sp. “South Carolina, Chestnut Ridge” (Greenville Co.), *A. cherokee* (Oconee Co.), *A. murrayae* (Greenville Co., Pickens Co., Oconee Co.), *A. dentatus* sp. nov. (Abbeville Co.), *Anillinus* sp. “South Carolina, Wateree”, *S. jeanneli*, and *S.* sp. “South Carolina, Coon Branch”.

Natural history. Specimens have been obtained by Berlese extraction of sifted soil, litter, and coarse woody debris, and have been hand collected from under embedded rocks, bear dung, and pig carcasses. Two late instar larvae

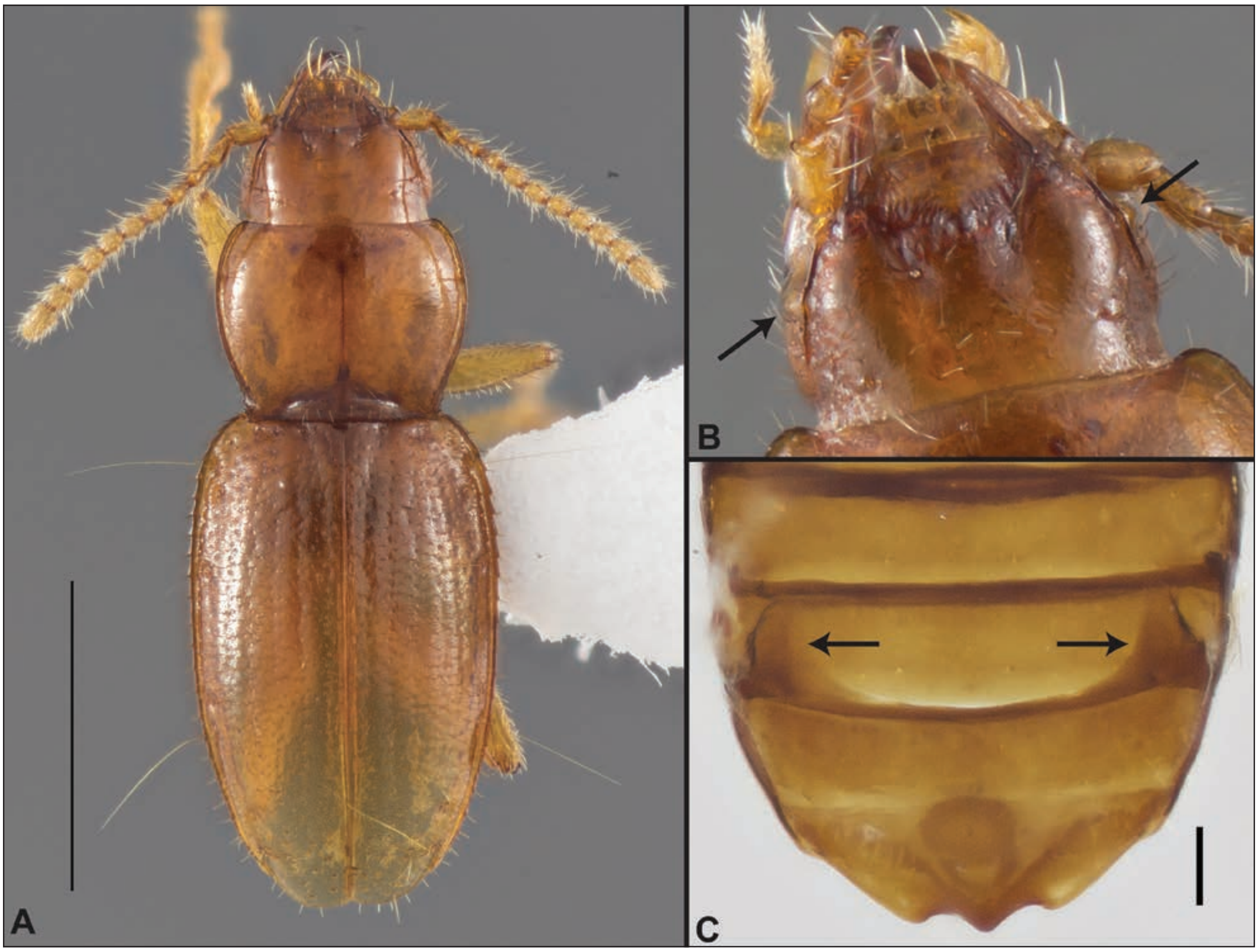

Figure 20. Morphological features of *Serranillus* **A** *Serranillus* sp. "South Carolina, Coon Branch" dorsal habitus **B** head of *Serranillus monadnock*, dorsal aspect (black arrows = ocular tubercles) **C** dorsal aspect of abdominal ventrites of *Serranillus septentrionis* (black arrows = lateral extensions of last abdominal tergite). Scale bars: 1 mm (**A**); 0.1 mm (**C**).

were collected in a sifted litter sample taken near the summit of Sassafras Mountain in October, in a mixed forest of pines and hardwoods. In a study of the soil and litter fauna of several South Carolina Piedmont forests, DuRant and Fox (1966) reported "*Anillus carolinae* (Horn)" as the most abundant species of Coleoptera captured in a single litter sample; these specimens were probably *S. dunavani*.

Serranillus jeanneli Barr, 1995

Figs 2D, 16, 17B, 18A–D, 21T, 25B

Serranillus jeanneli Barr 1995: 247.

Neotype male (CMNH), here designated. Dissected, with abdomen glued to point and genitalia in glycerin in plastic microvial pinned below labels, labeled: "NC: Macon Co. #62 Coweeta Exp. Sta. Ball Creek 3700' 13Aug1969 T. Barr" "THOMAS C. BARR COLLECTION 2011 Acc. No. 38,014" "*Serranillus jeanneli* ♂ det. C.W. Harden 2024" "NEOTYPE *Serranillus jeanneli* Barr, 1995 des. Harden & Caterino 2024 [red cardstock]"

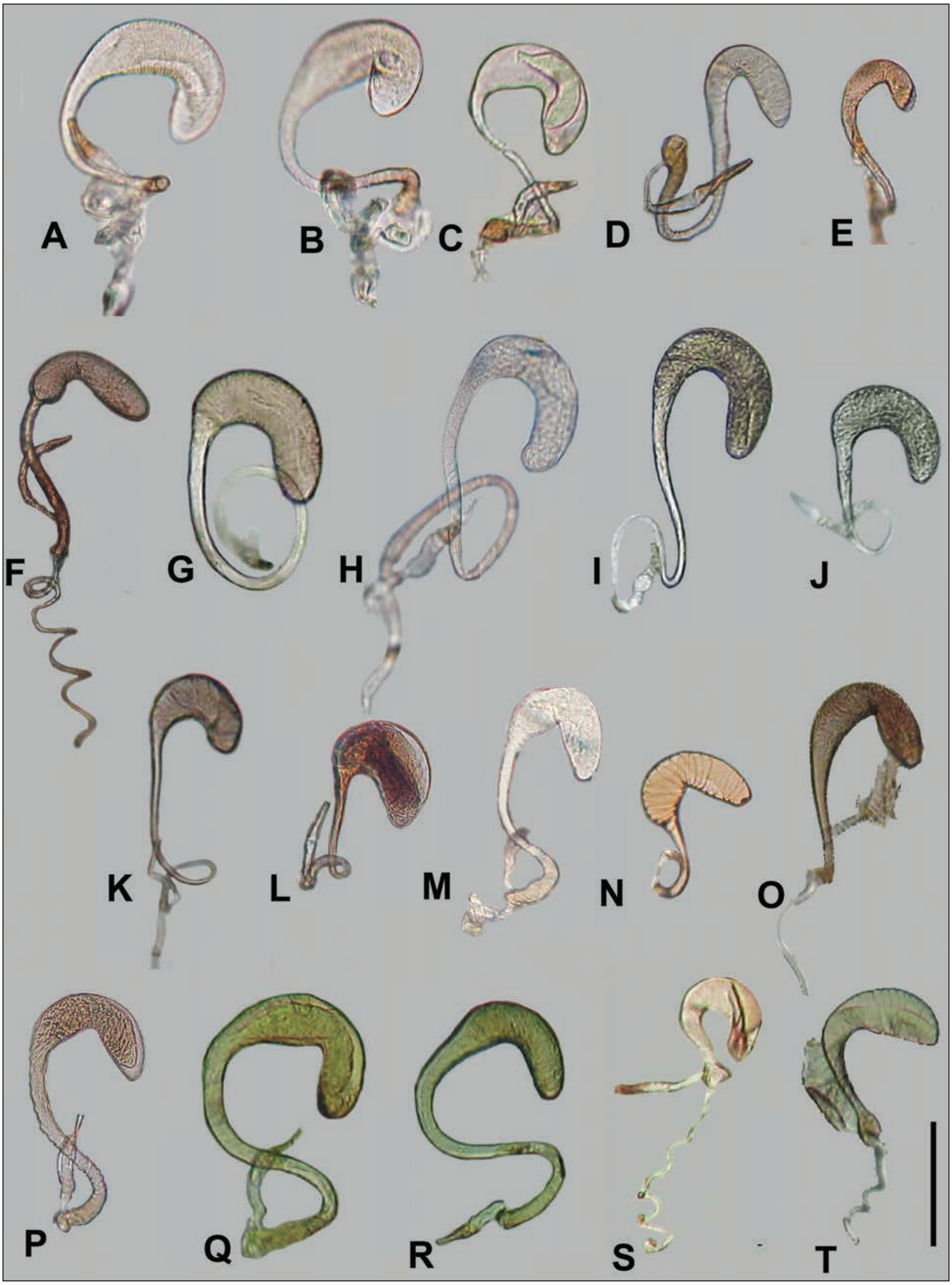

Figure 21. Spermathecae of Anillini species **A, B** *Anillinus chandleri* **C** *Anillinus castaneus* **D** *Anillinus murrayae* **E** *Anillinus simplex* **F** *Anillinus dentatus* **G** *Anillinus* sp. “South Carolina, Coon Branch” **H** *Anillinus micamicus* **I** *Anillinus mica* **J** *Anillinus choestoea* **K** *Anillinus seneca* **L** *Anillinus montrex* **M** *Anillinus arenicollis* **N** *Anillinus jancae* **O** *Anillinus* cf. *nantahala* **P** *Anillinus cherokee* **Q** *Anillinus loweae* **R** *Anillinus merritti* **S** *Serranillus dunavani* **T** *Serranillus jeanneli*. Scale bar: 0.1 mm.

Material examined (*n* = 67). USA • Georgia • 1 ♂; **Rabun Co.**; Chattahoochee National Forest, Rabun Cliffs; 34.913, -83.2978; 11 May 2021; M. Caterino and A. Haberski leg.; MSC-7026, CUAC000135496; • 1 ♂, 1 ♀; same data as previous; CUAC000172330 and CUAC000172322;• 2 ♀; **Rabun Co.**; Rabun Bald; 34.967, -83.299; 9 Jul. 2014; T. Lawton leg.; CWHc; • 1 ♀; **Rabun Co.**; Rabun Bald; 34.967, -83.299; 24 May 2014; T. Lawton leg.; CWHc; • 19 ♂, 15 ♀; **Rabun Co.**; Rabun Bald; 34.9708, -83.3032; 2 Jul. 2020; C.W. Harden leg.; CWHc; • 1 ♂; **Rabun Co.**; Chattahoochee National Forest, south of Beegum Gap; 34.9759, -83.3041; 5 Jun. 2023; C.W. Harden leg.; CWHc; • **North Carolina** • 4 ♂, 2 ♀; **Macon Co.**; Coweeta Hydrological Lab, ca. 13 miles west of Highlands; 35.045, -83.451; 23 May 1965; H.R. Steeves leg.; CMNH; • 1 ♀; **Macon Co.**; Coweeta Experimental Station [sic.], Ball Creek, #62, 3700’; 35.0339, -83.4505; 13 Aug. 1969; T.C. Barr leg.; CMNH; • 2 ♀; **Macon Co.**; Coweeta Experimental Station [sic.], Ball Creek #42, 3100’; 35.0432, -83.4535; 13 Aug. 1969; T.C. Barr leg.; CMNH; • 1 ♂; **Macon Co.**; Turtle Pond Creek, ca. 4 miles west-northwest of Highlands; 35.06, -83.26; 8 Aug. 1970; T.C. Barr leg.; CMNH; • 1 ♂, 1 ♀; **Macon Co.**; 0.6 miles northeast of Goldmine, California Ridge; 35.10, -83.28; 14 May 1971; T.C. Barr leg.; CMNH; • 5 ♂; **Macon Co.**; Nantahala National Forest, off Wayah Road ca. 10 km west from Route 64; 35.1554, -83.5584; 3 Aug. 2020; C.W. Harden leg.; CWHc; • 1 ♀; same data as previous; 4 Jun. 2021; • 1 ♀; **Macon Co.**; Nantahala National Forest, off Wayah Road ca. 10 km west from Route 64; 35.1557, -83.5583; 20 Oct. 2019; C.W. Harden leg.; CWHc; • 6 ♀; same data as previous; 3 Aug. 2020; CWHc; • 2 ♂; **Macon Co.**; four miles north of Franklin; 35.239, -83.374; 18 Mar. 1976; OSUC442503 and OSUC442504; OSUC; • **South Carolina** • 1 ♂; **Oconee Co.**; Coon Branch Natural Area, near Whitewater River; 35.023, -83.004; 23 Aug. 2022; C.W. Harden leg.; CWH-454, CUAC000185794.

GenBank: OR853398, OR839364, OR839681, OR837924, OR838086, OR838255.

Literature records. Barr (1995) stated that the type locality was “along Ball Creek, elevation approximately 950 m, Coweeta Hydrologic Laboratory, U.S. Forest Service, Macon Co., North Carolina.” Field notes for the date of collection (13 August 1969) state that the site was below the first switchback of Ball Creek Road, approximate coordinates 35.0432, -83.4535. Barr also wrote that the species occurred in the Great Balsam Mountains in North Carolina and Towns Co., Georgia. Sokolov and Carlton (2008) state they studied specimens of *S. jeanneli* from “White County, Georgia” without further data. The *Serranillus* that we have studied from Towns Co. and White Co., Georgia are not *S. jeanneli* but two undescribed species.

Diagnosis. From other species of *Serranillus*, *S. jeanneli* is best distinguished by the male median lobe of the aedeagus, which has a distinctive carinate shelf on the ventral surface, causing a preapical notch in the ventral margin in right lateral aspect (Fig. 18D). Externally, members of *S. jeanneli* are moderately sized for *Serranillus*, with male ABL = 2.13–2.35 mm and tentatively assigned females ABL = 2.07–2.51. The denticles on the last abdominal ventrite in males differ from other South Carolina species by having the inner denticle broader and less pronounced than the outer two (Fig. 18B).

Redescription. *Habitus* Robust and convex (Fig. 18A), moderately sized for genus, ABL = 2.07–2.51. ***Integument*** Dorsal microsculpture absent from most of head and pronotum, present at center of vertex. Small, irregular patches of weak microsculpture present on disc of pronotum in some individuals. ***Head*** Relatively narrow (male HW/PW = 0.70–0.71), frontoclypeal horn present and well developed. Ocular area behind antennal insertion with a dorsoventral linear tubercle at midpoint of carina. ***Pronotum*** Cordate, with sides broadly rounded and evenly converging posteriorly to constricted base, PbW/PW = 0.69–0.73. Approximately 1/4 body length (PL/ABL = 0.23–0.26). ***Elytra*** Ovoid and convex, with rounded humeri, weak traces of three striae present. ***Legs*** Male protarsomeres 1 and 2 expanded and bearing ventral adhesive setae. Male metatrochanters with coarse microsculpture, metafemora unmodified in either sex. ***Abdominal ventrites*** Males with last abdominal ventrite bearing three denticles on posterior margin, the outer two narrower and more prominent than the inner one. ***Male genitalia*** Ring sclerite long (RL/ABL = 0.32), similar in form to that of *S. dunavani*. Median lobe strongly asymmetrical (Fig. 17B), abruptly enlarged beyond base, outline a blunt-topped broad triangle in lateral aspects. Ventral face with a carinate shelf projecting below ventral margin; in right lateral aspect causing the ventral margin to appear notched (Fig. 18D). Apex of median lobe abruptly narrowed to a small curved hooklike apex visible in dorsal or ventral aspects. Internal sac of median lobe with two long sclerites. The right sclerite ribbonlike and corkscrewed along right side of internal sac, appearing as a dark curved shape in right lateral aspect (Fig. 18D), narrowing distally, where it protrudes from the ostium as a long evenly curved spine. The left sclerite is stouter, gradually narrowing along its sinuate length until it protrudes from the ostium beside the right sclerite as a bluntly hooked and curved spine. The left side of the ostium is dominated by a large rolled sclerite that curves dorsally from the left face of the median lobe into the internal sac, where it is rolled over itself twice; in right dorsolateral aspect, the scrolled sclerite appears to be a complex sclerotized structure resembling several stacked plates or a group of blunt spines (Fig. 18D); the true rolled shape is visible in posterior or anterior aspects. Flagellum not observed, possibly represented by a narrow, lightly sclerotized structure located in a similar position as the prominent flagellum in *S. dunavani* (cf. Fig. 15E). The parameres are as in *S. dunavani*, thus the right paramere is minute and asetose and the left paramere is large and conchoid, with a large base (Fig. 18C, D). The basal lobes of the median lobe are similarly asymmetrical, with the right lobe reduced to a thin strap and the left lobe larger and cup-shaped. ***Female genitalia*** Spermatheca small, less curved than in *S. dunavani* and with base less swollen (Fig. 21T). Spermathecal duct long and coiled.

Distribution. Notwithstanding the comments of Barr (1995) and Sokolov and Carlton (2008), we have seen specimens only from a small area centered around the North Carolina-South Carolina-Georgia corner (Fig. 16).

Sympatry. At Coon Branch in Oconee Co., South Carolina, this species co-occurs with *S. dunavani*, *S.* sp. “South Carolina, Coon Branch”, *Anillinus murrayae*, *Anillinus cherokee*, and *A.* sp. “South Carolina, Coon Branch”.

Natural history. Specimens have been collected from leaf litter, underneath embedded rocks, and using buried pipe traps.

Notes. Barr’s concept of *S. jeanneli* involved at least three species: the one whose male genitalia he illustrated and which we consider *S. jeanneli*, a larger species whose median lobe has a ventral medial tuft of long curved setae (*Serranillus* sp. “North Carolina, Riley Knob”), and a closely related species that occurs in northern Georgia and the southern edge of the Great Smoky Mountains (*Serranillus* sp. “North Carolina, Miller Cove”). We have studied all of Barr’s anilline genitalia slide mounts, and the ones he identified as *S. jeanneli* were either those matching our concept or those belonging to *S.* sp. “North Carolina, Miller Cove.” The latter species does not occur at the type locality. Apparently, Barr never dissected *S.* sp. “North Carolina, Riley Knob”, the larger species that occurs at Coweeta, although his description implies that he considered it to be the same species whose genitalia he illustrated.

Barr (1995) designated a holotype and four paratypes for *S. jeanneli* and stated they were deposited at CMNH. However, no record exists of these specimens being deposited, and they could not be found in the type collection or the general collection (R. Androw, R. Davidson and A. Seago, pers. comm., January 2024). The specimens were also not found in any of the unprocessed material accessioned to CMNH after Barr’s death. One dried-out vial of undetermined specimens was found with label data matching Barr’s type series. In it were six anillines, including two female and one male *Serranillus*. However, the male was not the species that Barr illustrated as *S. jeanneli*, but the larger species we call *S.* sp. “North Carolina, Riley Knob.” To stabilize the name and clarify the identity of *S. jeanneli*, we have chosen as neotype a male of the correct species that was collected by Barr on the same day, along the same forest road approximately 1 km airline distance from the given type locality.

We noted that the previously published sequences from individuals identified as *S. jeanneli* (DNA1084 and DNA2309) were in a clade with *S.* sp. “North Carolina, Miller Cove” in our phylogeny, and the genitalia were confirmed to match that species rather than our concept of *S. jeanneli* (D. Maddison pers. comm., January 2024).

Serranillus monadnock **sp. nov.**

https://zoobank.org/9968711C-1A42-426E-B295-23D834F53A73
Figs 16, 17C, D, 19A–E, 20B

Type material. ***Holotype male*** **(NCSU):** point mounted, with genitalia in glycerin in plastic microvial pinned beneath labels. Original labels: “SCYorkCoKings MtStPklogslit Oct 28. 1989 JF&TADCornell” “Serranillus new species ♂ det. C.W. Harden 2021” “[QR Code] NCSU_ENT 00327997” “HOLOTYPE *Serranillus monadnock* Harden & Caterino 2024” [red cardstock].

Paratypes (*n* = 2, NCSU). **USA • South Carolina** • 1 ♂, 1 ♀; **Newberry Co.**; Little Mountain; 34.188, -81.408; 8 Dec. 2007; J. and S. Cornell leg.; sift and berlese litter 20”D Pine Stump Hole #5; NCSU_ENT00327998 and NCSU_ENT00327999; NCSU.

Diagnosis. This is the only *Serranillus* species in which males have a flattened medial section of the second abdominal ventrite with longitudinally stretched microsculpture (Fig. 19B). The body is large, ABL = 2.82 mm (holotype), 2.79–2.87 mm (paratypes), the elytra and pronotum are broad, the head is relatively small (HW/PW = 0.65–0.70), the pronotum has the posterior angles produced posteriorly (Fig. 19A), and the median lobe of the aedeagus has a sinuate ventral surface, without ventral carinal shelf, with a large, blunt apex (Fig. 19E).

Description. ***Habitus*** Large (ABL = 2.79–2.87) and robust (PW/EW = 0.84–0.88, EW/ABL = 0.36–0.38), with relatively small head (HW/PW = 0.65–0.70). ***Integument*** Dorsal microsculpture largely absent from surfaces of head, present across entire pronotum. ***Head*** Frontoclypeal horn well-developed and prominent. Ocular tubercle present on each side in the form of a short, rounded ridge running from lateral dorsal carina down a short distance laterally (Fig. 20B). Antennae short, not reaching posterior margin of pronotum when bent backward. ***Pronotum*** Broad (PW/EW = 0.84–0.88), margins not sinuate before posterior angles, which are slightly constricted (PbW/PW = 0.69–0.71) and protrude beyond posterior pronotal margin. ***Elytra*** Broad (EW/ABL = 0.36–0.38), disc flattened, with traces of five striae. ***Legs*** Male protarsomeres 1 and 2 expanded and bearing ventral adhesive setae. Male metatrochanters and posterior face of metafemora with coarse papillate microsculpture, metafemora swollen. Female legs unmodified. ***Abdominal ventrites*** Males with second abdominal ventrite with a flattened medial region where the microsculpture cells are stretched longitudinally (irregularly isodiametric elsewhere on abdomen). Males with last abdominal ventrite bearing three denticles on posterior margin, the inner one slightly more prominent than the outer two. ***Male genitalia*** Median lobe strongly asymmetrical and slightly twisted dorsally from plane of basal lobes (Fig. 17C, D). In right lateral aspect, the ventral margin undulating, with deep subapical sinuation before the blunt, rounded apex which is deflected ventrally. Row of short, stout setae present on ventral margin near and within subapical sinuation, visible at 100× or greater. Left side at base with broad, carinate channel that is interrupted medially by prominent dorsolateral region with two raised lumps; narrowed channel continuing across ventral surface, ending at subapical sinuation. Apex of median lobe in holotype curved to right side, appearing sinuous in dorsal or ventral aspects; apex in paratype straight and bladelike, possibly due to teneral condition of the specimen. Internal sac with thin, curved flagellum visible in right lateral aspect near dorsal margin. Large rolled sclerite present on left side of internal sac, making two coils over itself from left lateral wall of median lobe. Lightly sclerotized, blunt paddle-shaped sclerite extending apically from rolled sclerite, meeting left side before apex. Right paramere minute, bluntly rounded, asetose. Left paramere large, conchoidal, with thickened base. ***Female genitalia*** Spermatheca with enlarged base, otherwise similar to that of *S. jeanneli* (Fig. 21T). Spermathecal duct long and coiled.

Distribution. Known from two localities in York and Newberry Counties (Fig. 16), both isolated monadnocks in the Piedmont ecoregion, Kings Mountain and Little Mountain.

Sympatry. Three species of *Anillinus* occur at Kings Mountain State Park, and may co-occur with this species there. Three female *Anillinus* were collected from the same sample at Little Mountain, and are either unusually small individuals of *Anillinus chandleri* Sokolov or an undescribed species. A male *A. chandleri* was taken from a separate litter sample at the same locality.

Natural history. The Kings Mountain specimen was presumably collected from extraction of sifted litter associated with logs, and the two Little Mountain specimens were collected by extraction of sifted litter from within a pine stump hole.

Species status justification. Members of this species differ from those of the four previously described species in several external characters: pronotum with posterior angles produced posteriorly, males with flattened medial area with stretched microsculpture on second abdominal ventrite. The male genitalia are also unique, especially the relatively large, blunt apex of the median lobe.

Derivation of species name. Noun in apposition, from “monadnock”, a word in the Abenaki language meaning an isolated, abruptly rising mountain or hill, in reference to the two known localities of this species on such features.

Notes. The paratype male from Little Mountain is teneral, paler than both the female from the same collecting event at Little Mountain and the male holotype from Kings Mountain. The shape of the median lobe of the teneral paratype differs slightly from that of the holotype (Fig. 17C, D). In the paratype, the supabical sinuation on the ventral margin is deeper, and the apex of the median lobe is thinner and not curved to the right. Otherwise, the characters of the median lobe agree in both specimens. The unique medial microsculpture of the second abdominal ventrite is also the same in both males. The differences in the median lobe are either due to the teneral condition of the paratype, or may reflect slight geographic variation.

Serranillus **sp. “South Carolina, Coon Branch”**

Figs 16, 20A, 25B

Material examined. USA • South Carolina • 1 ♀; **Oconee Co.**; Coon Branch Natural Area; 35.0251, -83.0053; 2 Oct. 2021; C.W. Harden leg.; On underside of embedded rock, steep north-facing slope; CUAC000169317, CWH-400; CUAC.

GenBank: OR853116, OR853403, OR839367, OR839665, OR837916, OR838073, OR838250, OR838133.

Diagnosis. In addition to being larger (ABL = 2.70 mm), this female specimen differs from the widespread *S. dunavani* by the presence of faint microsculpture on the disc of the pronotum and the less ovoid shape of the elytra (Fig. 20A). The phylogeny based on the genes we sampled places the specimen in a well-supported clade with *S. septentrionis* Sokolov & Carlton and another potentially undescribed species from the Black Mountains in North Carolina.

Distribution. Coon Branch Natural Area, near the Whitewater River in Oconee Co.

Sympatry. The specimen was collected with adults of *Anillinus murrayae* Sokolov & Carlton and two individuals of *Anillinus* that belong to the *sinuaticollis* group, discussed below as *Anillinus* sp. “South Carolina, Coon Branch”.

Natural history. The specimen was collected in October from the underside of a large embedded rock in fine soil on a steep forested slope above the Whitewater River. Litter samples collected in June 2018, October 2020, and August 2022 did not collect this species, nor did a soilwash sample taken in June 2018.

Notes. Without associated males, the identity of this species is uncertain. This female from Coon Branch possibly belongs to one of the undescribed species known from adjacent parts of Georgia and North Carolina that we lack DNA sequence data for. Males of both *S.* sp. “Georgia, Rabun Bald sp. 1” and *S.* sp. “North Carolina, Riley Knob” possess genitalia similar to *S. septentrionis*, suggesting they likely belong to the same clade as this Coon Branch female.

Genus Anillinus Casey, 1918

Anillinus Casey 1918: 167. Type species: *Anillus* (*Anillinus*) *carolinae* Casey, 1918, by original designation.

Micranillodes Jeannel 1963a: 57. Synonymy established by Bousquet (2012: 699). Type species: *Micranillodes depressus* Jeannel, 1963a, by original designation.

Troglanillus Jeannel 1963b: 147. Synonymy established by Barr (1995: 240). Type species: *Troglanillus valentinei* Jeannel, 1963b, by original designation.

Adult diagnosis. From *Serranillus*, members of *Anillinus* can be recognized by the position of the medial setae of the mentum not on the tooth (Fig. 11B), the last abdominal ventrite of males without dentate projections or lateral internal extensions, left mandible without a retinacular tooth (Fig. 11D), and right paramere well developed and bearing at least four setae. Most *Anillinus* also have shorter background pubescence on the elytral disc and a less robust habitus than *Serranillus*.

Larval diagnosis. The single late-instar larval specimen of *Anillinus* that is known (Fig. 13A) differs from that of *S. dunavani* in possessing a serrate terebra (Fig. 14A) and stipes with gMX setae arranged in an even row (Fig. 14C). Early instar *Anillinus* do not seem to differ from early instar *Serranillus*.

Diversity. The eight species described below bring the total number of described species of *Anillinus* to 78, making it the most speciose genus of Anillini. Including undescribed species that we have studied (Suppl. material 3), the total known diversity of *Anillinus* is at least 149 species.

Distribution. West of the Mississippi, *Anillinus* are known from the Ozark Plateau in southern Missouri and Northern Arkansas, the Ouachita Mountains in Oklahoma and Arkansas, and the Balcones Escarpment in central Texas. In the east, *Anillinus* are known from Washington, D.C., Pendleton Co., WV, Cincinnati, OH (Dury 1902) and Lawrence Co., IN south to northern Florida, southern Alabama, and southeastern Louisiana.

‘*dentatus* group’

Anillinus dentatus sp. nov.

https://zoobank.org/250222AD-2A01-4DC5-90C2-58409C909833
Figs 2C, 12F, 21F, 22A–C, 23A–C, 24F, 25C, 43B

Type material. ***Holotype male*** **(USNM):** point mounted, with abdominal ventrites and genitalia in Euparal on microslide pinned beneath specimen. Original labels: “USA: SC, Abbeville Co. Sumter NF Long Cane Crk at end of FS rd 530. 34.1133, -82.3300. 5.ii.2022. CW Harden & K Ivanov. Beneath embedded mossy rock in waterlogged soil.” “[QR Code] CLEMSON-ENT CUAC000163530” “Harden DNA Voucher CWH-420 *Anillinus* ‘dentate’ M Ext. 6-February-2022[green-bordered cardstock]” “HOLOTYPE *Anillinus dentatus* Harden & Caterino [orange cardstock]”

GenBank: OR853208, OR839248.

Paratypes (*n* = 21; CMNH, NCSU, VMNH, OSAC, CUAC). **USA • South Carolina** • 1 ♂; same data as holotype; CUAC000163531, CWH-421; CUAC; • 5 ♀; same data as holotype; CUAC000163539 to CUAC000163541, CWH-422 to CWH-428; CUAC; • 1 ♀; **Abbeville Co.**; Sumter National Forest, near Secession St bridge; 34.134, -82.324; 25 Jan. 2020; C.W. Harden leg.; Underside of embedded rock;

CUAC000163526, CWH-113; CUAC; • 1 ♂; **Abbeville Co.**; Sumter National Forest; 34.1345, -82.3230; 5 Feb. 2022; M. Ferro leg.; Sift subcort CWD; CUAC000168286; • 2 ♂; **Abbeville Co.**; Sumter National Forest, near Secession Street bridge; 34.1366, -82.3252; 5.February.2022; CW Harden leg.; beneath embedded mossy rock CUAC000163524 and CUAC000163529, CWH-417 and CWH-418; CUAC; • 1 ♀; same data as previous; CUAC000163542, CWH-419; CUAC; • 1 ♂; **Abbeville Co.**; Sumter National Forest, Long Cane Creek; 34.13519, -82.32503; 12 Jan. 2020; C.W. Harden & L.M. Thompson leg.; Soilwash flotation Berlese, clay-rich soil from ferny hill above floodplain; CUAC000163525, CWH-067; CUAC; • 2 ♂; **Abbeville Co.**; Sumter National Forest, Long Cane Creek; 34.1350, -82.3239; 15 Mar.–16 Jul. 2020; C.W. Harden leg.; Buried pipe trap baited with cheese, deep clay soil, LCC-05-0716; CUAC000163527, CUAC000163528; • 7 ♀; same data as for proceeding; CUAC000163532 to CUAC000163536; • 3 ♂, 3 ♀; **Abbeville Co.**; Sumter National Forest, Long Cane Creek area; 34.1370, -82.3226; 5 May 2023; C.W. Harden leg.; Under small rocks in ditch.; OSAC, VMNH, ADGc.

GenBank accession numbers for paratypes: OR853105, OR853210, OR839250, OR839420, OR837801, OR837962, OR838150, OR838114, OR853209, OR839249, OR839458, OR839458, OR837972, OR839247, OR839246.

Other material (*n* = 5). USA • South Carolina • 2 ♂, 1 ♀; **Abbeville Co.**; Sumter National Forest, Long Cane Creek area; 34.1370, -82.3226; 5 May 2023;

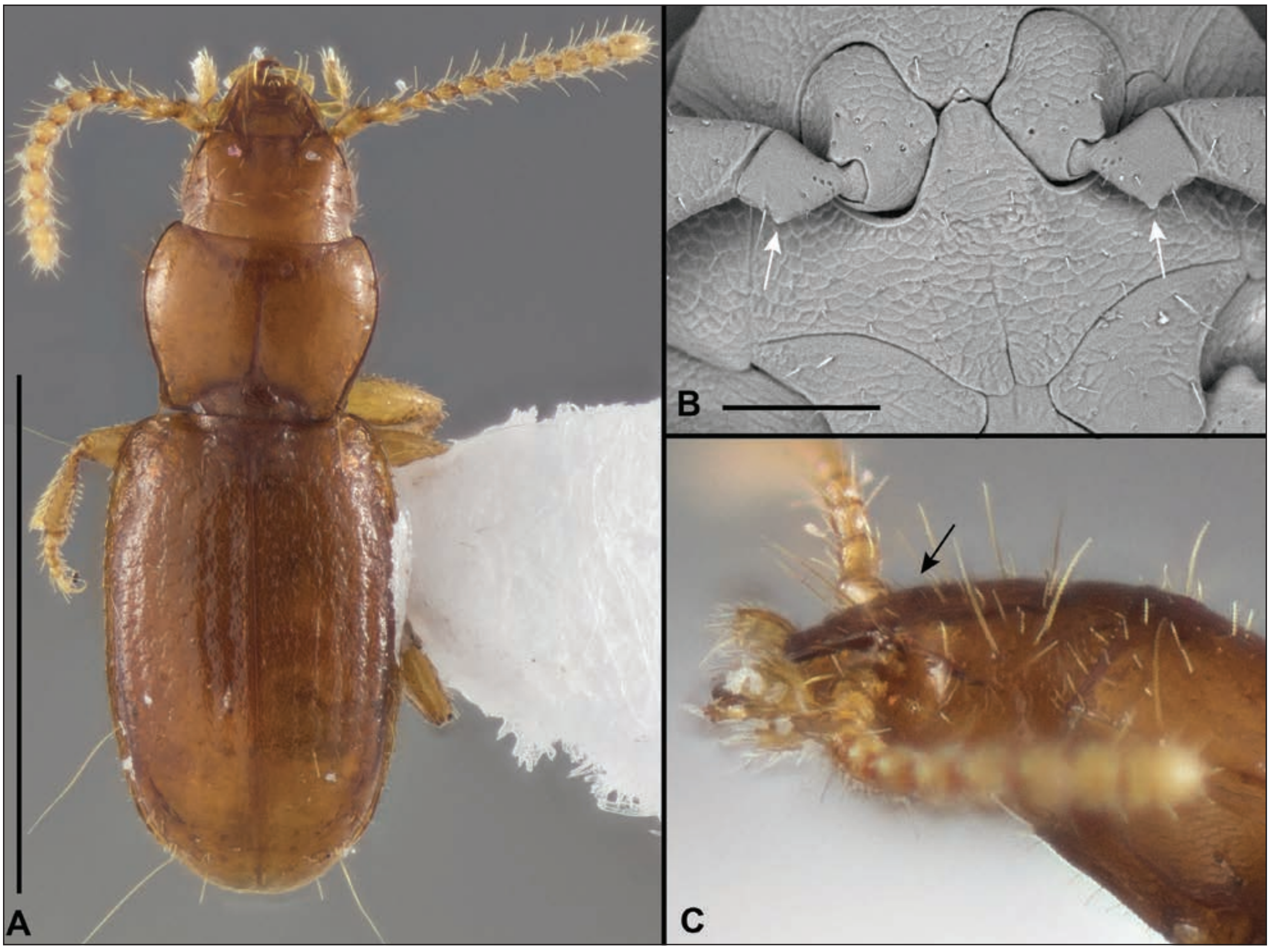

Figure 22. *Anillinus dentatus* **A** dorsal habitus **B** SEM micrograph of metaventrite, ventral aspect (white arrows = mesotrochanter spines) **C** head, left lateral aspect (black arrow = absence of frontoclypeal horn). Scale bars: 1 mm (**A**); 0.1 mm (**B**).

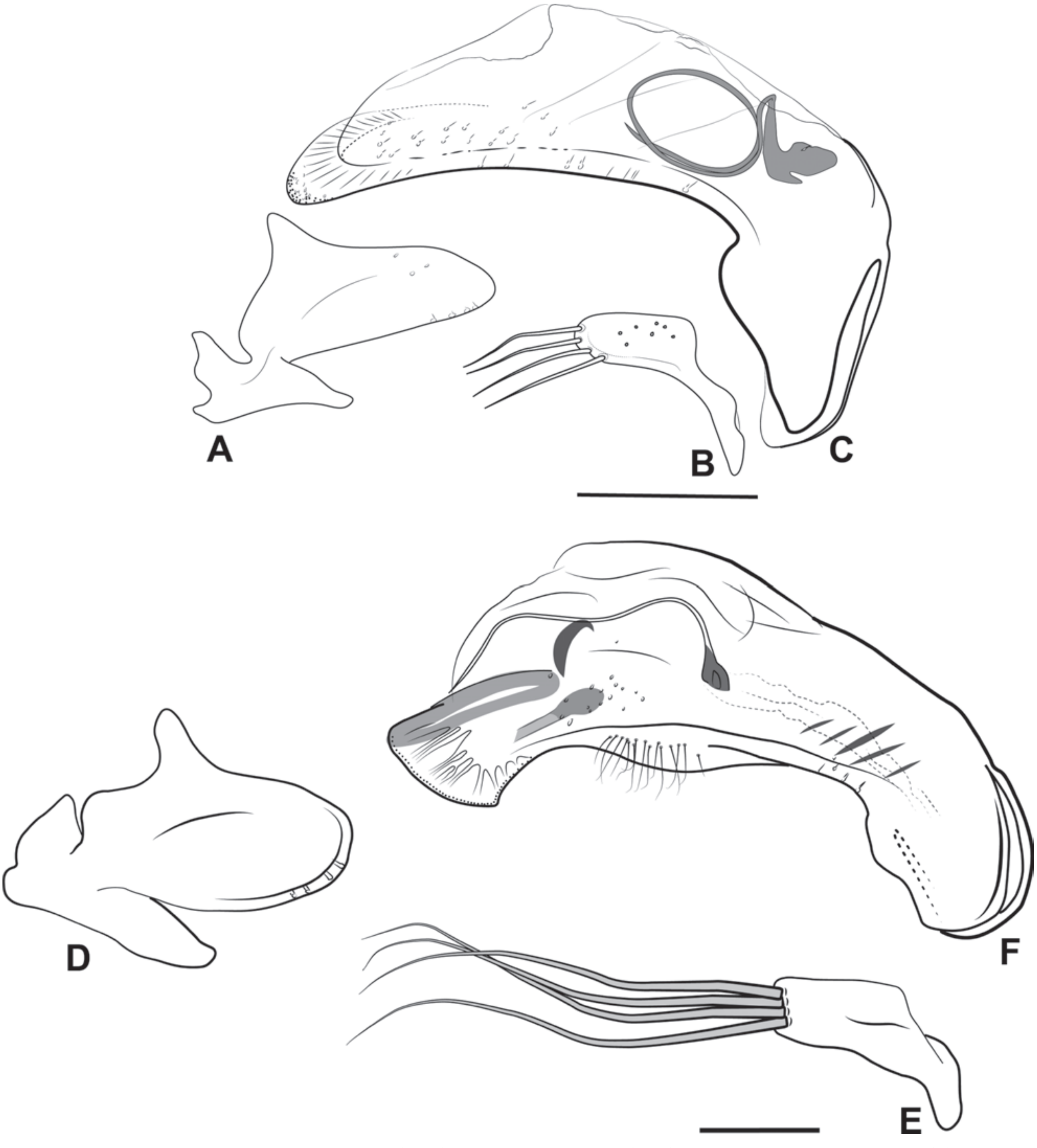

Figure 23. Male genitalia of *Anillinus dentatus* (**A–C**) and *Anillinus jancae* (**D–F**). Median lobes in right lateral (**C**) and right dorsolateral (**F**) aspects. Left parameres (**A, D**) and right parameres (**B, E**) in left and right lateral aspects, respectively. Scale bars: 0.1 mm.

C.W. Harden leg.; Under small rocks in ditch.; CWHc; • 1 ♂; **Abbeville Co.**; Sumter National Forest, Long Cane Cr near Secession St bridge; 34.134, -82.324; 25 Jan. 2020; C.W. Harden leg.; Underside of embedded rock; CWHc; • 1 ♀; **Abbeville Co.**; Sumter National Forest, Long Cane Creek; 34.1349, -82.3241; 21 Mar. 2021; C.W. Harden and L.M. Thompson leg.; On underside of rock; CWHc.

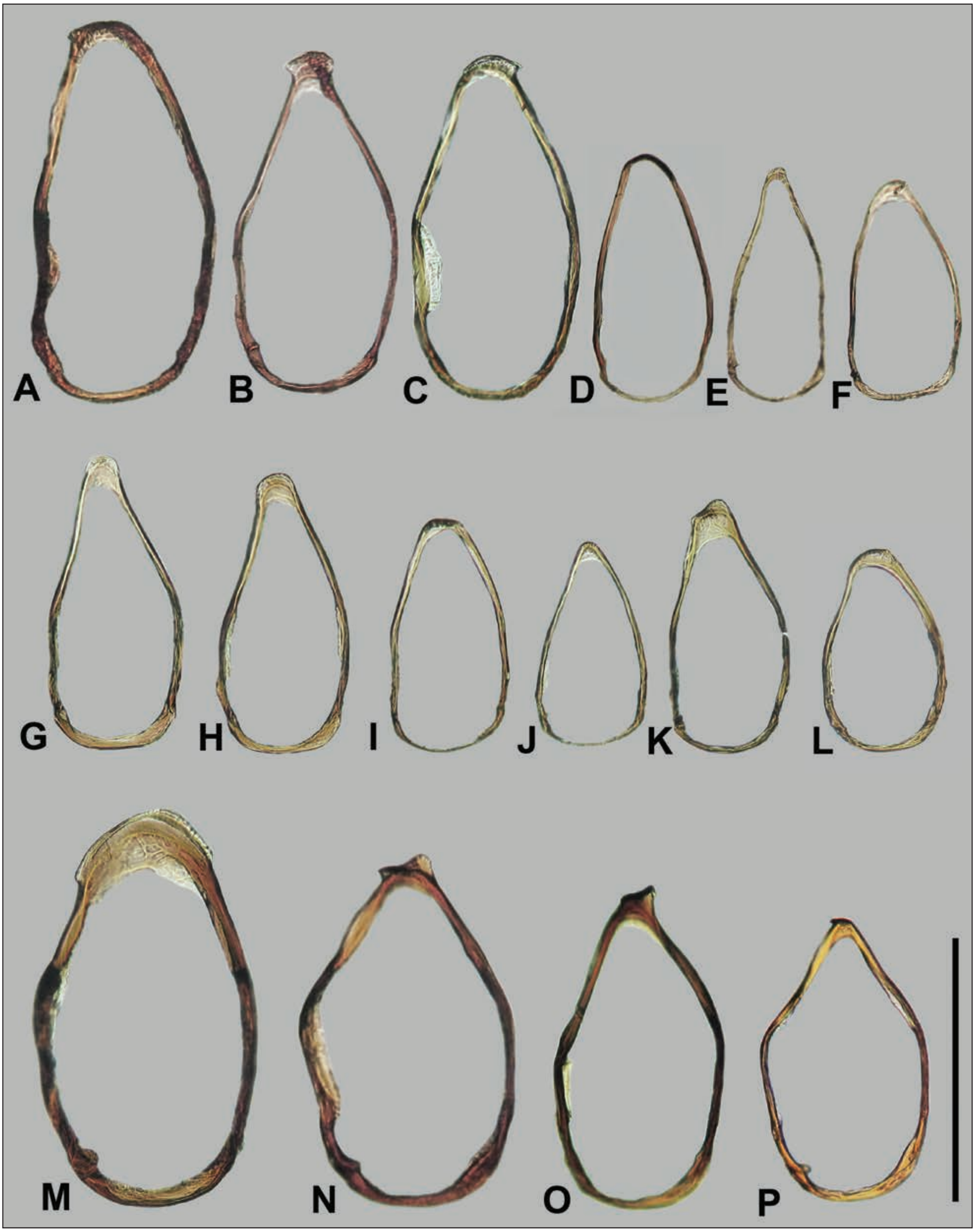

Figure 24. Male ring sclerite, ventral aspect. **A** *Anillinus chandleri* **B** *Anillinus castaneus* **C** *Anillinus* sp. "South Carolina, Chestnut Ridge" **D** *Anillinus murrayae* **E** *Anillinus simplex* **F** *Anillinus dentatus* **G** *Anillinus mica* **H** *Anillinus micamicus* **I** *Anillinus choestoea* **J** *Anillinus seneca* **K** *Anillinus arenicollis* **L** *Anillinus montrex* **M** *Anillinus jancae* **N** *Anillinus loweae* **O** *Anillinus cherokee* **P** *Anillinus merritti*. Scale bar: 0.5 mm.

Figure 25. Anillini habitat in South Carolina **A** Waldrop Stone Falls, Pickens Co. (*Anillinus mica*, *Anillinus micamicus*, *Anillinus murrayae*, *Serranillus dunavani*) **B** Lower Whitewater River gorge, Oconee Co. (*Anillinus cherokee*, *A. murrayae*, *Anillinus* sp. "South Carolina, Coon Branch", *S. dunavani*, *Serranillus jeanneli*, *Serranillus* sp. "South Carolina, Coon Branch" **C** Long Cane Creek, Abbeville Co. (*Anillinus chandleri*, *Anillinus dentatus*, *Anillinus jancae*, *S. dunavani*). The holotypes of *A. mica* and *A. micamicus* were collected under embedded rocks uphill of the wooden staircase in **A**. The holotype of *A. jancae* was collected in a pipe trap set on a hill just out of view in **C**.

Diagnosis. Males of this species are easily recognized by the dentate mesotrochanters, a unique character in the genus. Females are most likely to be confused with *A. jancae* sp. nov., described below. Females of *A. jancae* are larger (ABL = 1.88 mm or greater), and the spermatheca is smaller (Fig. 21N).

Description. ***Habitus*** Body small (ABL = 1.49–1.69 mm, average = 1.59 ± 0.05 mm), flattened dorsoventrally and relatively narrow (avg. EW/ABL = 0.35) (Fig. 22A). Average ABL of males (1.63 mm, *n* = 5) greater than females (1.57 mm, *n* = 11). ***Integument*** Dorsal surfaces of forebody completely microsculptured with coarse mesh of irregular isodiametric cells. ***Head*** HW/PW = 0.73–0.83. Antennomeres IV–X moniliform, slightly clavate. Frontoclypeal horn absent or barely suggested, inconspicuous in lateral view (Fig. 22C). Three pairs of supraorbital setae present. Mentum with median pair of setae posterior to the bead of the subtriangular mentum tooth, which is relatively large and blunt. ***Pronotum*** Relatively short (PL/ABL = 0.22–0.23), width variable (PW/EW 0.78–0.85); subcordate, strongly to moderately narrowed basally (bPW/PW = 0.70–0.80), anterior angles slightly prominent; sides typically slightly sinuate or evenly convergent towards obtuse hind angles; rarely, the sides are abruptly parallel sided just anterior to nearly right hind angles; pronotal sides with 3 or 4 basal serrulations. ***Elytra*** Parallel sided and flat, relative length variable (EL/ABL = 0.53–0.58); margins strongly serrulate; traces of five striae evident on disc of each elytron (Fig. 22A); without prominent subapical plica; fused inner margins slightly carinate at apex. ***Legs*** Profemora of males unmodified; protarsomere 1 of males moderately expanded, with inner margin spinose, bearing adhesive setae ventrally; protarsomere 2 not expanded, without adhesive setae ventrally (Fig. 10F). Mesotrochanters of males with spinose projection ventrally (Fig. 22B); mesotrochanters of females either evenly rounded or with blunt projection ventrally. Metafemora of males with prominent triangular toothlike projection on posterior margin (Fig. 12F). Tarsomeres of middle and hind legs of both sexes short and broad. ***Abdominal ventrites*** Unmodified in either sex. ***Male genitalia*** Ring sclerite (Fig. 24F) ~ 1/4 the total body length (RL/ABL = 0.25), sides asymmetric, margin of narrowed end slightly thickened but not deflexed in lateral view; sides without flattened lateral expansions medially. Median lobe of aedeagus (Fig. 23C) narrow and moderately curved, not twisted from plane of basal lobes; dorsal margin largely unsclerotized; ventral margin bladelike toward apex; apex rounded and slightly bent ventrally. Internal sac with flagellum elongate and filamentous distally, in repose coiled around itself in a circle and situated in basal 1/3 of median lobe. Right paramere (Fig. 23B) small and narrow, bearing four long setae on apex. Left paramere (Fig. 23A) with three or four small pores on ventral margin near apex, without setae. ***Female genitalia*** Spermatheca elongate, abruptly expanded distally; stem slightly sinuate, straight at proximal juncture with duct; duct long, tightly coiled in corkscrew pattern *in situ* (shown partially distended in Fig. 21F).

Distribution. Known from two localities within a small area of Sumter National Forest in Abbeville Co., SC along Long Cane Creek (Figs 25C, 43B)

Sympatry. Members of this species have been collected under rocks in association with adults of *A. chandleri* and a larva of *A. jancae* sp. nov., and with *S. dunavani* in a sample of sifted coarse woody debris. Adults of *A. jancae* sp. nov. have been collected nearby.

Natural history. Members of this species are endogean, inhabiting deep clay soils in mesic deciduous woods. Specimens have been found on the underside of embedded rocks in January, February, March, and May, and were collected in buried pipe traps operating from March to July but not January to March. One male specimen was collected in early February from Berlese extraction of sifted coarse woody debris. The sifted material was primarily subcortical, but some may have possibly come from the underside of logs that were on the soil surface (M. Ferro, pers. comm., February 2022). This material was collected near Long Cane Creek following a period of heavy rainfall, when the water level was above normal. Most of the specimens examined have had Laboulbeniales fungi present on the dorsum of the elytra, usually near the apex.

Species status justification. The combination of morphological characters is unique within the genus, and DNA sequence data indicate that *A. dentatus* is distantly related to all other *Anillinus*. No known species of *Anillinus* possess characters suggesting a close relationship to *A. dentatus*.

Derivation of species name. A male adjective referring to the triangular projections on the male metafemora, from the Latin for “toothed.”

Notes. The long, coiled form of the flagellum in *A. dentatus* is also seen in *Anillinus barri* Sokolov & Carlton, *Anillinus erwini* Sokolov & Carlton, *Anillinus folkertsioides* Sokolov, and *Anillinus inexpectatus* Sokolov. However, with the exception of *A. folkertsioides*, all of these species differ from *A. dentatus* in most external characters. Members of *A. folkertsioides* and a possibly undescribed sister species from Fort Payne, Alabama are similar to *A. dentatus* in having fully developed microsculpture on the forebody and a depressed habitus, but differ from *A. dentatus* in having numerous long hairlike setae on the right paramere and male legs without modifications. Two character-states seen in members of *A. dentatus* are unique among known members of the genus: the nearly straight stem of the spermatheca and the spinose mesotrochanters of males.

'*albrittonorum* group'

Anillinus jancae sp. nov.

https://zoobank.org/0538E4CD-4117-4820-914F-399A48F0BFE2
Figs 10A, D, 12E, 13B, 14A, C, E, 21N, 23D–F, 24M, 25C, 26A–C, 27A, 43C

Type material. ***Holotype male* (USNM):** point mounted, with genitalia in Euparal on microslide pinned beneath specimen. Original label: "USA: SC, Abbeville Co. Sumter NF Long Cane Creek. 34.1350, -82.3239. 15.March-16.July.2020. C.W Harden. Buried pipe trap baited with cheese. Deep clay soil. Oak, hickory, beech. LCC-01-0716." "CLEMSON-ENT CUAC000168362" "HOLOTYPE *Anillinus jancae* Harden & Caterino [orange cardstock]"

Paratypes (*n* = 7, CUAC). **USA • South Carolina • Abbeville Co.** • Sumter National Forest, Long Cane Creek; • 1 ♂; same data as holotype; CUAC000168363, CWH-204; • 1 ♀; same data as holotype; CUAC000168364, CWH-205; • 5 ♀; same data as holotype; CUAC000168365 to CUAC000168369.

GenBank accession numbers for paratypes: OR853233, OR839266, OR838005.

Other material (*n* = 2). USA • South Carolina • Abbeville Co. • Sumter National Forest, Long Cane Creek • 1 ♀; 34.1362, -82.3235; 21 March 2021; C.W. Harden leg.; Underside of rock. CWHc; • 1 ♀; Near Cedar springs Rd.; 34.10914, -82.33948; 25 September 2020; C. W. Harden leg.; Underside of large rock; CUAC, CUAC000168370, CWH-241.

Diagnosis. Largest species of *Anillinus* in SC, with distinctive habitus (Fig. 26A), dorsoventrally flattened and not as compact as typical *Anillinus*; head relatively small (HW/PW 0.71–0.74); pronotum cordate, with sides subparallel at base, hind angles of pronotum prominent and rectangular or acute and extending posteriorly past hind margin. Protibiae of both sexes with a deep semicircular outer notch apically (Fig. 10A). Males with unique combination of secondary sexual characters: profemora with ventral spine (Fig. 27A), hind femora swollen and tuberculate, hind tibiae bowed inward and with inner surface scalloped, first abdominal ventrite bearing a short fin-like carina medially on posterior margin (Fig. 26B, C). Females with short spermatheca (Fig. 21N).

Description. ***Habitus*** Body dorsoventrally flattened and large (ABL = 2.32–2.64 mm). Males (2.63–2.64 mm) larger than females (2.32–2.36 mm). Less compact than most *Anillinus*, with relatively narrow forebody

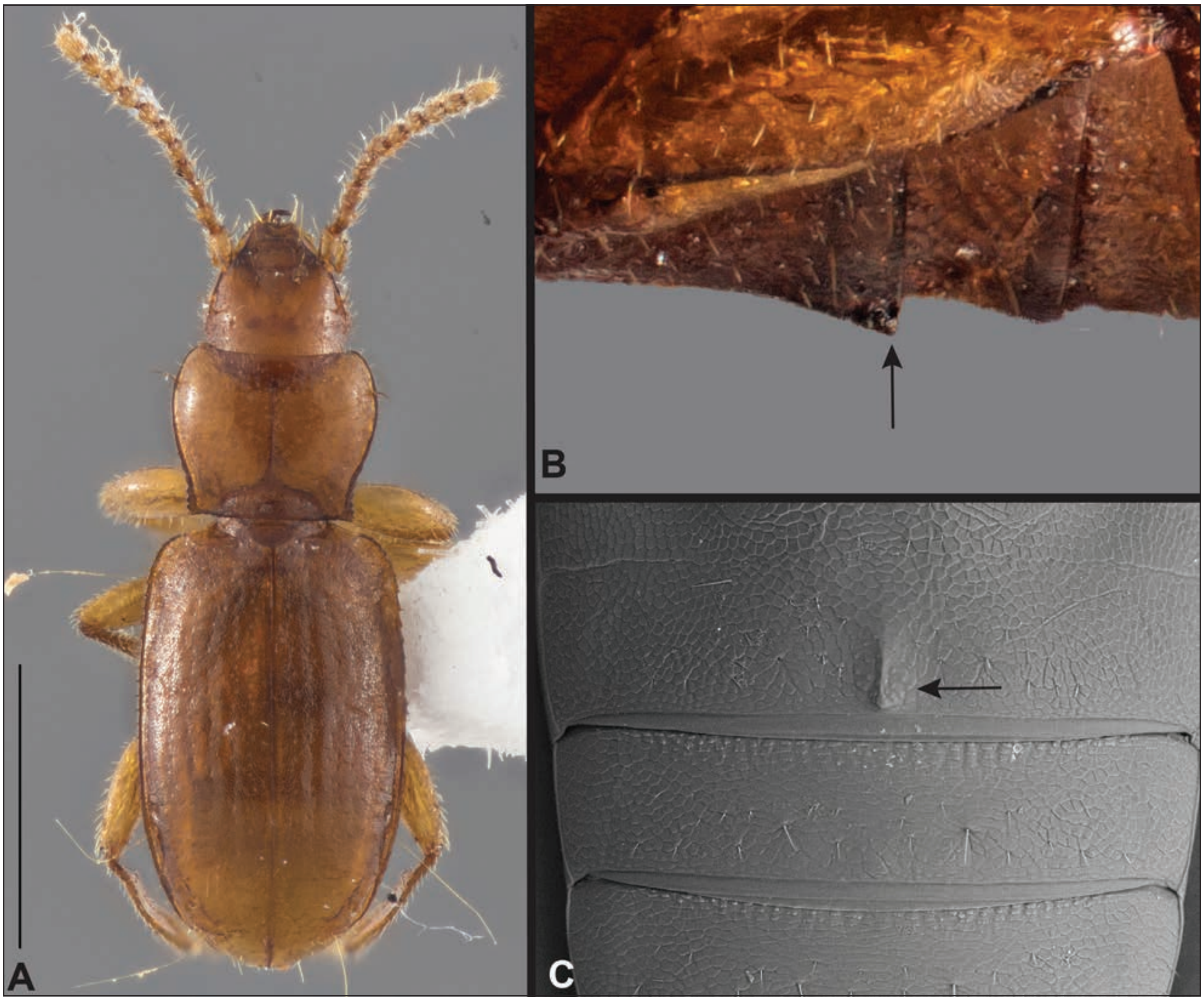

Figure 26. *Anillinus jancae* **A** habitus **B** abdominal ventrites, left lateral aspect **C** SEM micrograph of abdominal ventrites, ventral aspect. Black arrows point to abdominal keel. Scale bar: 1 mm.

(HW/PW 0.71–0.74, PW/ EW = 0.76–0.83]). Pronotum with sinuate sides and long, parallel-sided posterior angles. ***Integument*** Dorsal surfaces of forebody mostly covered with irregularly isodiametric mesh of microsculpture, microsculpture absent from at least a small area on pronotal disc on each side of midline and from center of vertex, females more extensively microsculptured than males. Elytra with coarse mesh of isodiametric microsculpture, sculpticels small. ***Head*** HW/PW = 0.71–0.74. Antennomeres I–IV[♂] or I–III[♀] longer than wide, V–X[♂] or VI–X[♀] moniliform. Frontoclypeal horn small, nearly absent in some specimens. Two pairs of supraorbital setae present. Mentum with median pair of setae posterior to bead of mentum tooth, which is relatively small and obtusely triangular, blunt. ***Pronotum*** Cordate, base strongly constricted in females (average Pbw/PW = 0.71, *n* = 3), moderately so in males (average Pbw/PW = 0.75, *n* = 2). Average PW/EW 0.81 (females), 0.77 (males). Relatively short (PL/ABL = 0.22 in all specimens measured, *n* = 5). Sides sinuate before long hind angles which are parallel sided and rectangular or slightly acute and projected posteriorly. ***Elytra*** Parallel sided and flat, relatively long (EL/ABL = 0.54–0.57); each with five striae, inner two or three more strongly impressed

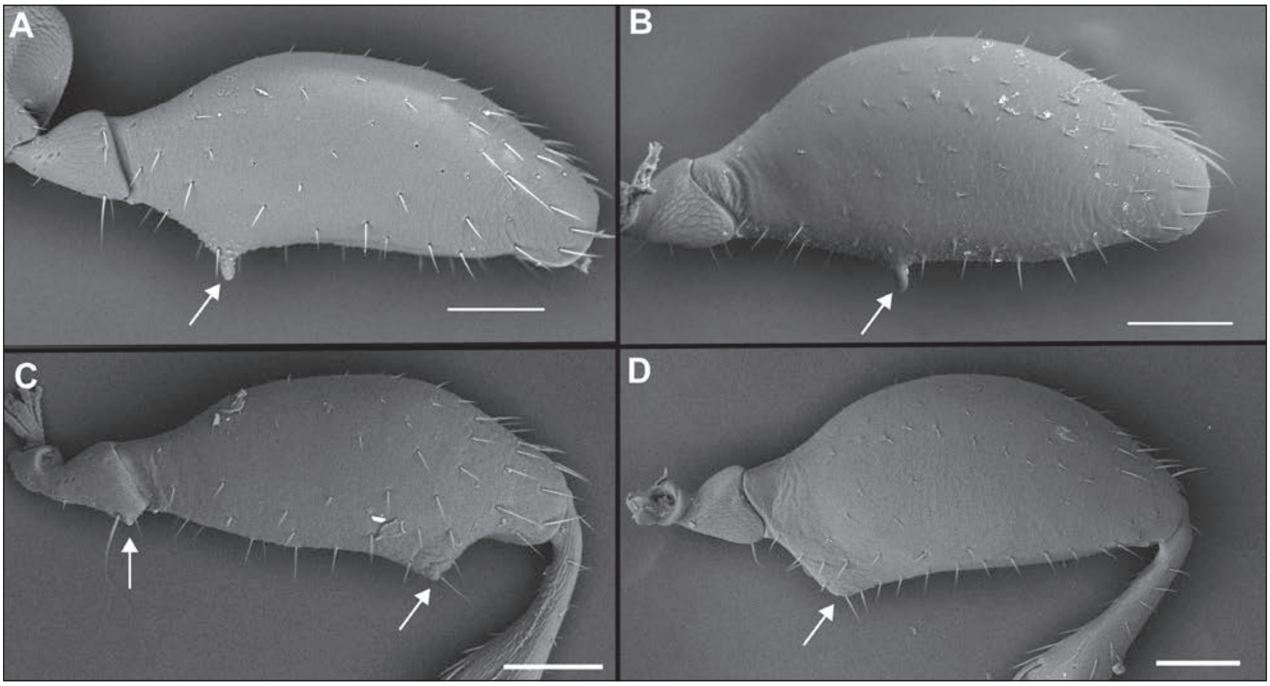

Figure 27. Modified profemora of *Anillinus* species. **A** *Anillinus jancae* **B** *Anillinus* sp. "North Carolina, Orange Co. sp. 2" **C** *Anillinus lescheni* **D** *Anillinus sp*. "Alabama, Aladdin Cave sp. 1". White arrows point to protrusions on profemur and/or protrochanter. Scale bars: 0.1 mm.

than outer two; small subapical plica evident; fused inner margins carinate at apex. ***Legs*** Profemora of males modified, swollen, and bearing a peg-like spine on posterior margin at proximal 1/3 (Fig. 27A). Protibiae of both sexes with deep semicircular notch on outer edge of apex; males with inner margin of protibiae extended as a bifid spine (Fig. 10A). Protarsi of males with first protarsomere greatly enlarged and produced on inner surface as a blunt lobe, with adhesive setae ventrally, second protarsomere unmodified and without ventral adhesive setae (Fig. 10D). Mesotrochanters of males unmodified. Male metatrochanters flattened, elongate, and covered in small tubercles; metafemora of males swollen and bearing several tubercles along posterior margin and a blunt angulate protrusion in distal 1/3 (Fig. 12E). Metatibiae of males concave along inner margin. Tarsomeres of middle and hind legs relatively short in both sexes. ***Abdominal ventrites*** Males with keel-like median carina at posterior margin of second visible ventrite (Fig. 26C); females without modifications. ***Male genitalia*** Ring sclerite large (RL/ABL = 0.28), oval; margins thickened; narrowed end with margin slightly deflexed; sides with small flattened lateral expansions medially. Median lobe (Fig. 23F) heavily sclerotized, with several parallel, diagonal sulci across surface in proximal 1/3 on left side, appearing as dark lines; strongly bicarinate ventrally, carinae forming a channel along most of ventral surface; band of many hairlike setae present across ventral surface and left side medially; apex expanded, with sides strongly curved ventrally, appearing bill-like in head-on view; in right lateral view, apex appears hatchet shaped, and thickened portions of curved cuticle appear as dark linear structures. Internal sac with long flagellum abruptly narrowed and filamentous past bulb-like base; small sclerotized straplike structure present ventrally at ostial opening. Right paramere (Fig. 23E) relatively short, with blunt apical margin bearing four or six long, thick setae that surpass the apex of the median lobe when paramere is attached. Left paramere (Fig. 23D) bluntly rounded at apex, with four poriferous canals and no setae on apical margin. ***Female genitalia*** Spermatheca short and small, abruptly enlarged distally, with short curved stem (Fig. 21N). Spermathecal duct longer than spermatheca, with a few loose coils.

Distribution. Known for sure only from a single hillside on the southeast side of Long Cane Creek in Abbeville Co, within Sumter National Forest (Figs 25C, 43C).

Sympatry. *Anillinus chandleri* and *A. dentatus* have been collected with this species. *Serranillus dunavani* is known from nearby.

Natural history. Members of this species are endogean in habit. Most of the type series was collected from a buried pipe trap operated from March to July. The trap was set deeply in a layer of pure red clay, well below the shallow organic soil horizon. A late-instar larva was found underneath a deeply embedded rock in early February, indicating either overwintering of the egg or larval stage, or winter breeding and oviposition. A female adult was collected underneath a large, embedded stone. This female was kept alive for several months in a container with soil from the same locality packed into the bottom. The female quickly found a way around and underneath the packed clay soil on the bottom of the container, and apparently spent the remainder of its life in an inverted position on the underside of the clay. Given this behavior, and the microhabitat in which the trap that collected most of the type series was set, the habitat of this species is probably the series of crevices formed naturally in clay soils. Although clay is typically thought to be impervious, it forms naturally into aggregates called “peds” (Sherwood and Garst 2016), creating a series of crevices through which air and water (and small invertebrates) can pass. This habitat is widely distributed in the southeastern U.S., and further targeted sampling of it using buried traps is likely to discover many more species of anillines and other subterranean arthropods.

Species status justification. The overall habitus, male secondary sexual characters, great length of setae on the apex of the right paramere, and characters of the median lobe are all unique within the genus. The consistent placement of this species in a clade with the geographically distant *A. albrittonorum* support its distinction from other *Anillinus* species.

Derivation of species name. This remarkable species is named in honor of Janet C. Ciegler, in recognition of her contributions to the study of Coleoptera in South Carolina and the southeastern United States. Her many identification guides have made the study of beetles more accessible to amateur and professional entomologists alike. The specific name is a genitive noun derived from the shortened first name (“Jan”) and first letter of the surname.

Notes. The female from the Cedar Springs Road site (CUAC000168370) is from the opposite side of Long Cane Creek, and differs from the type series in several respects. The specimen is smaller (ABL = 1.88 mm) and more compact, resembling *A. dentatus* in habitus. The head also has three supraorbital setae on each side, versus two in the type series. The spermatheca agrees with the females of the type series. DNA sequence data indicate that this female could represent a different species. The uncorrected p-distance of the barcoding region of COI of this specimen is 3.7% and 3.8% divergent from the two paratypes with sequenced barcodes. Its 28S sequence differs from that of the paratype male at only two sites – one substitution and a 2-bp insertion.

CAD4 sequences of these same two specimens differ in 15 nucleotides. Male specimens from the Cedar Springs Road site would help resolve the situation. We note that members of *A. dentatus* have been collected from the same two sites, and show no differences in COI or 28S, so Long Cane Creek is likely not a barrier to dispersal in that species.

The male holotype of *A. jancae* is the only specimen in the "quadrisetose clade" to have more than four apical setae on the right paramere. Considering that the right paramere of the other known male of *A. jancae* is quadrisetose, we interpret the extra setae on the right paramere of the holotype to represent an unusual variant.

Our description of *Anillinus jancae* represents the first documented example of modified profemora in the genus. However, we found that the male profemora of the previously described *Anillinus lescheni* are also modified, though quite different in form, having a large, triangular tooth distally (Fig. 27C). Two undescribed species with modified male profemora are known, from North Carolina (Fig. 27B) and Alabama (Fig. 27D). The profemora of these two undescribed species are similar in form to *A. jancae* and *A. lescheni*, respectively. In the case of the North Carolina species, from which we have DNA sequence data, the similarities are the result of convergence.

'*valentinei* group'

Anillinus chandleri **Sokolov, 2011**

Figs 21A, B, 24A, 25C, 28B, E, 29

Anillinus chandleri Sokolov, 2011: 11.

Material examined. ***Holotype male*** **(USNM)**, glued to card, genitalia mounted on clear plastic slide pinned beneath specimen, labeled: "USA: SC: Edge. Co. Ft. Sumter Nat. For. Jct. Rds. 235 & 199" "VII-8-1987 RMReeves, sift forest litter" "Anillinus sp. det Bell" "HOLOTYPE *Anillinus chandleri* sp. n. Sokolov des. 2009"

Other material (*n* = 20, CUAC, CWHc, NCSU, UGCA). USA • South Carolina • 1 ♂; **Abbeville Co.**; Sumter National Forest, Long Cane Creek; 34.1352, -82.3250; 12 Jan. 2020; C.W. Harden leg.; CWH-068, CUAC000168267; • 2 ♀; **Abbeville Co.**; Sumter National Forest, Long Cane Creek; 34.1356, -82.3238; 15 Mar. 2020; C.W. Harden leg.; CWH-151 and CWH-152, CUAC000153578 and CUAC000153579; • 1 ♂; same data as previous; CWHc; • 4 ♂, 4 ♀; **Abbeville Co.**; Sumter National Forest, Long Cane Creek; 34.1350, -82.3239; 15 Mar. to 16 Jul. 2020; C.W. Harden leg.; CWHc; • 1 ♂; **Abbeville Co.**; Sumter National Forest, off Cedar Springs Road; 34.1086, -82.3390; 25 Sep. 2020; C.W. Harden leg.; CWH-266, CUAC000168266; • 2 ♀; **Lexington Co.**; West Columbia; 34.001, -81.064; 10 Mar. 1991; J.C. Ciegler leg.; CUAC000153575 and CUAC000153576; • 1 ♂, 2 ♀; **Newberry Co.**; Little Mountain; 34.188, -81.408; 8 Dec. 2007; J.F. and S. Cornell leg.; NCSU; • 1 ♀; **Richland Co.**; Ballentine; 34.120, -81.236; 5 Nov. 2006; J.C. Ciegler leg.; CUAC000153574; • 1 ♂; **Union Co.**; Calhoun Critical Zone Observatory; 34.5866, -81.6472; 26 Sep. 2016; R. Carrera-Martinez leg.; UGCA.

Literature records. The species was described from the male holotype only and has not been subsequently reported.

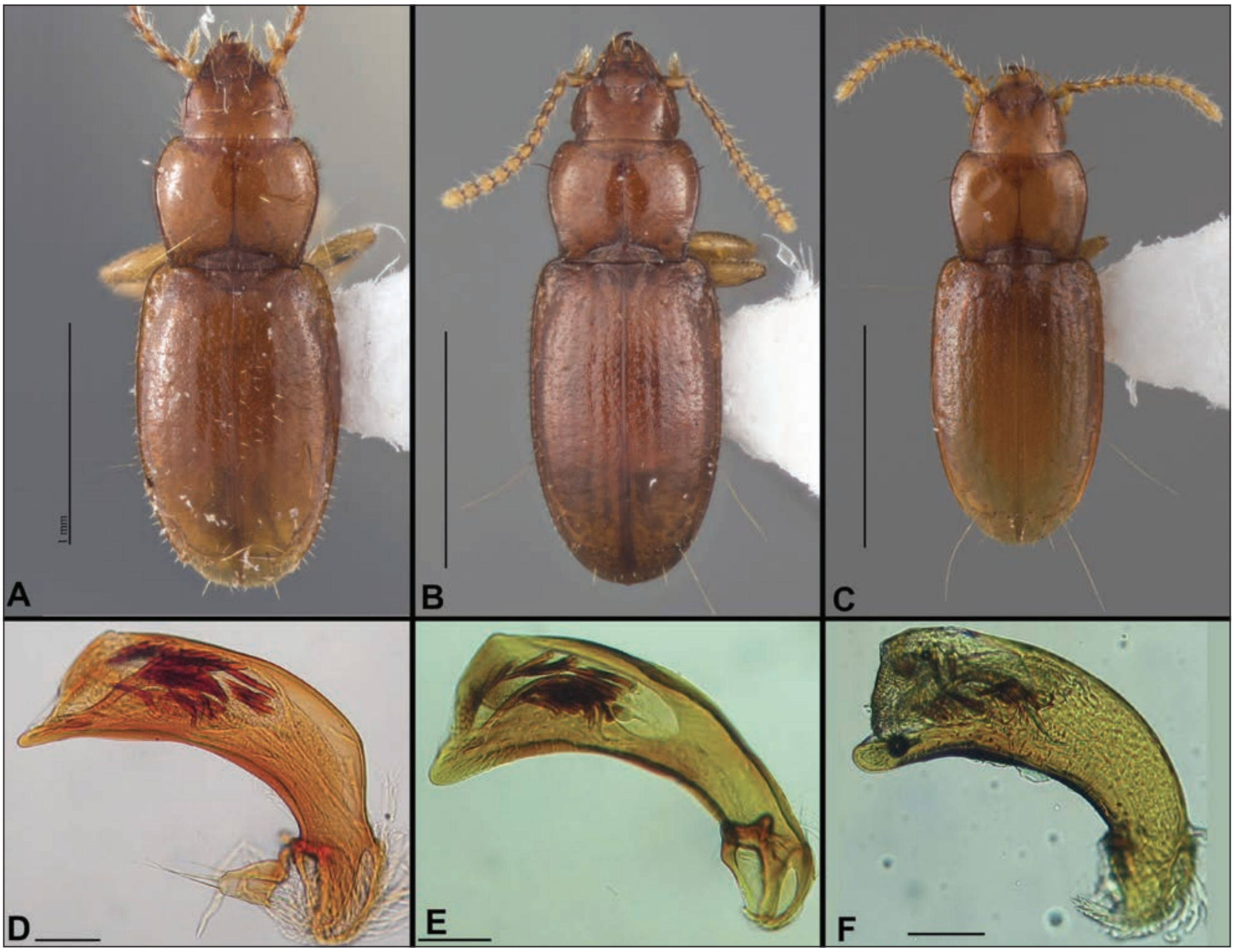

Figure 28. Dorsal habitus and dorsolateral aspect of median lobe of aedeagus of *Anillinus chandleri* and related species **A, D** *Anillinus* sp. "South Carolina, Waldrop Stone" **B, E** *Anillinus chandleri* Sokolov **C, F** *Anillinus* sp. "South Carolina, Long Cane". Scale bars: 1 mm (**A, B, C**); 0.1 mm (**D, E, F**).

Diagnosis. This is one of the largest species of *Anillinus* in South Carolina (Fig. 28B), and that combined with the effaced microsculpture from the forebody distinguishes it from nearly all other known species in the state. There are two undescribed *valentinei*-group species that approach the size of *A. chandleri*, but both differ in the form of male genitalia. The median lobe of *A. chandleri* is distinctive: long and strongly twisted dorsally from the plane of basal lobes, strongly constricted proximally, and expanded distally, internal sac with a dense group of large dark spines surrounding the long flagellum in repose (Fig. 28E).

Variation noted. ABL = 1.89–2.26 mm, average = 2.11 ± 0.11 mm. Males (2.11–2.26 mm) larger than females (1.89–2.17 mm). The shape of the pronotum is variable, especially the relative width (PW/EW = 0.78–0.84). The proximal constriction of the median lobe is wider in the specimen from Union Co. than in other specimens studied. The number of spines in the internal sac is also variable, but the size and shape of the flagellum is constant. The ring sclerite (Fig. 24A), not described previously, is relatively large (RL/ABL = 0.34) and oval, asymmetrically narrowed anteriorly.

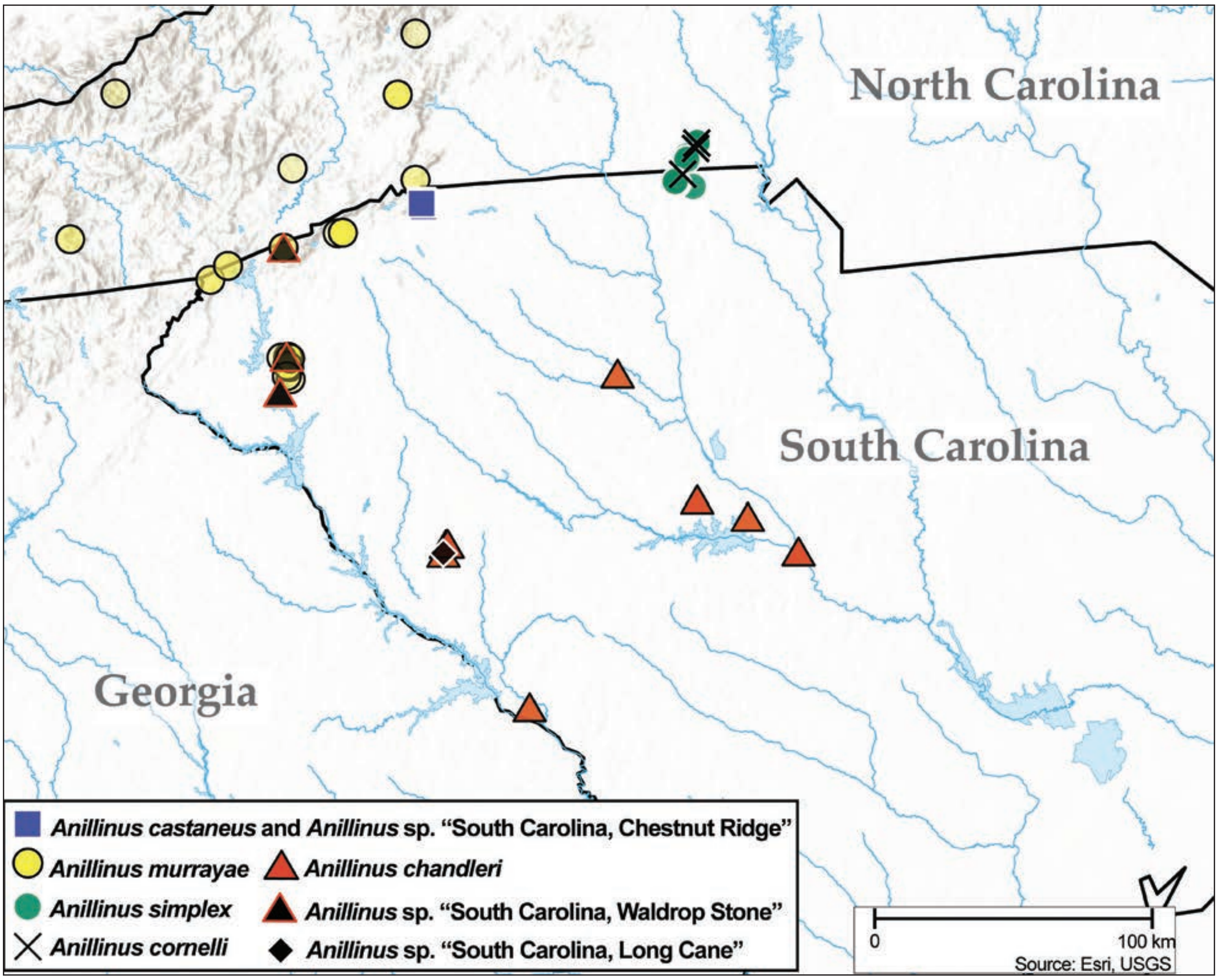

Figure 29. Distribution map of *valentinei*-group species in South Carolina and adjacent states. Data are from Harden (2024).

Description of female genitalia. Spermatheca (Fig. 21A, B) broadly curved, gradually enlarged distally, proximally with abrupt perpendicular angulation. Spermathecal duct long and tightly coiled. Bursa with conspicuously sclerotized folds.

Distribution. Although known only from South Carolina, this species has a larger range than most members of the *valentinei* group, from Abbeville and Edgefield Cos. east to Columbia and north to Union Co. (Fig. 29).

Sympatry. At Long Cane Creek in Abbeville Co., SC, *A. chandleri* has been collected with *A. dentatus*, *A. jancae* and *S. dunavani*. *Anillinus* sp. "South Carolina, Long Cane", an undescribed and apparently recently diverged member of the *valentinei* group, also occurs at Long Cane Creek. At Little Mountain, *A. chandleri* has been collected with *S. monadnock*.

Natural history. Most of the material we have seen was collected from deep soil habitats. Several large litter samples collected from Long Cane Creek at various seasons (January, February, March, July, September) failed to produce specimens. Several specimens collected by J. Ciegler were sifted from litter, as were the holotype and the specimen from Union Co. The Union Co. site, the Calhoun Critical Zone Observatory, contains habitats that are an extreme example of highly eroded Piedmont forests, due to poor historical agricultural practices.

The apparent persistence of a blind, flightless beetle such as *A. chandleri* at such a site is notable.

Notes. Two undescribed species related to *A. chandleri* are discussed below.

Anillinus **sp. "South Carolina, Long Cane"**

Figs 28C, F, 29

Material examined (*n* = 2, CUAC). USA • South Carolina • 1 ♂, 1 ♀; **Abbeville Co.**; Sumter National Forest, Long Cane Creek; 34.1095, -82.3397; 5 May 2023; C.W. Harden leg.; CWH-516 and CWH-517, CUAC000182318 and CUAC000182319.

GenBank: OR853246, OR839276, OR839722, OR837938, OR838268, OR853245, OR839275, OR839723, OR837939.

Diagnosis. Large (ABL of male = 2.13 mm), dorsoventrally flattened and parallel-sided (Fig. 28C). The median lobe of the aedeagus is similar to *A. chandleri* except it is not constricted basally, the ventral margin is less curved, the flagellum is shorter, and the spines in the internal sac are fewer and smaller (Fig. 28F).

Notes. The two specimens were collected together underneath the same large rock. Several previous collecting visits to the same locality had produced specimens of *A. chandleri*, *S. dunavani*, and *A.* cf. *jancae*. The DNA sequences from the two specimens of *A.* "South Carolina, Long Cane" are nearly identical to those of *A. chandleri*, despite the apparent sympatry (Fig. 29) and morphological distinctiveness of the male genitalia.

Anillinus **sp. "South Carolina, Waldrop Stone"**

Figs 2M, 28A, D, 29

Material examined (*n* = 4, CUAC). **USA • South Carolina** • 1 ♀; **Oconee Co.**; Martin Creek landing; 34.638, -82.866; 12 Apr. 2022; C.W. Harden leg.; Under large rock; CUAC000170070, CWH-440; • 1 ♀; **Oconee Co.**; Martin Creek landing; 34.6389, -82.8663; 26 May 2022; C.W. Harden leg.; Underside of large rock after heavy rain; CUAC000170071, CWH-447; • 1 ♂; **Pickens Co.;** Clemson Forest, Waldrop Stone Falls. 34.7385, -82.8252; 4 Aug. 2018; M. Caterino leg.; CUAC000109295, CWH-433; • 1 ♀; **Pickens Co.**; Chimneytop Gap; 35.0630, -82.7969; 21 Mar. 2023; C.W. Harden leg.; CUAC000066900, CWH-489.

GenBank: OR853159, OR839217, OR839704, OR837929, OR838097, OR838264, OR853160, OR839218, OR839673, OR837920, OR838081, OR839219, OR839353.

Diagnosis. A large (ABL = 2.10–2.53 mm) and unusually setose member of the *valentinei* group (Fig. 28A). The armature of the internal sac as well as the shape of the flagellum are similar to those of *A. chandleri*, but the median lobe lacks the pronounced proximal constriction characteristic of that species (Fig. 28D).

Notes. Repeated attempts to collect additional specimens of this species at Waldrop Stone Falls have been unsuccessful. The individuals from Martin Creek Landing and Chimneytop Gap are all female, so their association is tentative and mostly based on DNA sequence data. The individual from Chimneytop Gap (Fig. 2M) is smaller (2.10 mm) than the specimens collected near Clemson (2.47

and 2.53 mm), is divergent in DNA sequences from those specimens, and could represent a different species. With scattered material, only one male, and the allopatric distribution with respect to *A. chandleri* (Fig. 29), the support for our hypothetical distinctiveness of this species is not strong. Further sampling and collection of additional males, and perhaps more extensive molecular data, are required to clarify the status of this species and *A.* sp. "South Carolina, Long Cane."

Anillinus murrayae **Sokolov & Carlton, 2004**

Figs 10H, 21D, 24D, 25A, B, 29, 30J–N, 31A–O

Anillinus murrayae Sokolov & Carlton, 2004: 222.

Material examined. ***Holotype male*** (**USNM**), point-mounted backwards (on left side), dissected with genitalia in dried-out glycerin cup pinned beneath specimen, labeled: "USA: NC, Swain Co., GSMNP Collins Picnic Area, Quiet walk UTM 287857 E 3938299 N, C. Carlton 20 July 2002"

Other material (*n* = 64, CMNH, CUAC, CWHc, NCSU, OSUC, USNM). USA • **North Carolina** • 1 ♂; **Buncombe Co.**; Round Knob; 35.6510, -82.2430; [no date]; OSUC442492; OSUC; • 1 ♂; **Henderson Co.**; Florence Nature Preserve; 35.4750, -82.3310; 13 Sep. 2020; C.W. Harden leg.; CWH-393, CUAC000168278; • 4 ♂, 4 ♀; same data as previous; CWHc; • 2 ♂, 4 ♀; **Jackson Co.**; Tennessee Mt [*sic*], Tom Beautell's land; 18 May 1972; J. Hunter leg.; NCSU_ENT00293709 to NCSU_ENT00293714; NCSU; • 2 ♂; **Macon Co.**; Nantahala National Forest, west of Franklin; 35.1554, -83.5584; 4 June 2021; C.W. Harden leg.; CWHc; • 2 ♀; **Polk Co.**; Melrose Falls; 35.2217, -82.2985; 10 Aug. 2021; M.S. Caterino leg.; CWH-394 and CWH-395; CUAC000168276 and CUAC000168277; • 2 ♀; **Transylvania Co.**; White Pines group campground on Avery Creek; 35.2909, -82.7371; 24 Jul. 2009; J.F. and S. Cornell leg.; NCSU; • **South Carolina (new state record)** • 1 ♂, 1 ♀; **Greenville Co.**; Ashmore Heritage Preserve; 35.0878, -82.5800; 14 Apr. 2018; M. Caterino, M. Ferro, G. Powell leg.; CWH-111 and CWH-112, CUAC000168273 and CUAC000168274; • 1 ♀; **Greenville Co.**; Ashmore Heritage Preserve; 35.0888, -82.5979; 29 Jun. 2015; S. and C. Myers leg.; • 1 ♂, 2 ♀; **Greenville Co.**; Ashmore Heritage Preserve; 35.0867, -82.5788; 14 Mar. 2020; C.W. Harden and L.M. Thompson leg.; CWH-143 to CWH-145, CUAC000168263, CUAC000168265, CUAC000168268; • 2 ♂, 3 ♀; **Greenville Co.**; Ashmore Heritage Preserve; 35.0874, -82.5790; 14 Mar. 2020; C.W. Harden and L.M. Thompson leg.; CWH-146 to CWH-150, CUAC000168264, CUAC0001689269, CUAC000168270 to CUAC000168272; • 2 ♂; same data as previous; CWHc; • 1 ♀; **Oconee Co.**; Indian Camp Creek; 34.9899, -83.0724; 4 May 2015; M.S. Caterino and S. Myers leg.; SSM110, CUAC000169288; • 1 ♂, 1 ♀; **Oconee Co.**; Indian Camp Creek; 34.9903, -83.0723; 4 May 2015; M.S. Caterino and S. Myers leg.; SSM251 and SSM252, CUAC000169289 and CUAC000169290; • 1 ♂, 2 ♀; **Oconee Co.**; Coon Branch Natural Area; 35.0256, -83.0050; 2 Oct. 2021; C.W. Harden leg.; CWHc; • 1 ♂, 1 ♀; **Pickens Co.**; South Carolina Botanical Garden; 34.6718, -82.8234; 23 Apr. 2023; P. Rodrigues Flores and E. Recuero leg.; CWH-497 and CWH-498, CUAC000182300 and CUAC000182301; • 1 ♀; **Pickens Co.;** Clemson; 34.6820, -82.8330; 4 Oct. 1966; J.A. Payne leg.; CMNH; • 1 ♂; **Pickens Co.**; Clemson Experimental Forest, Pike

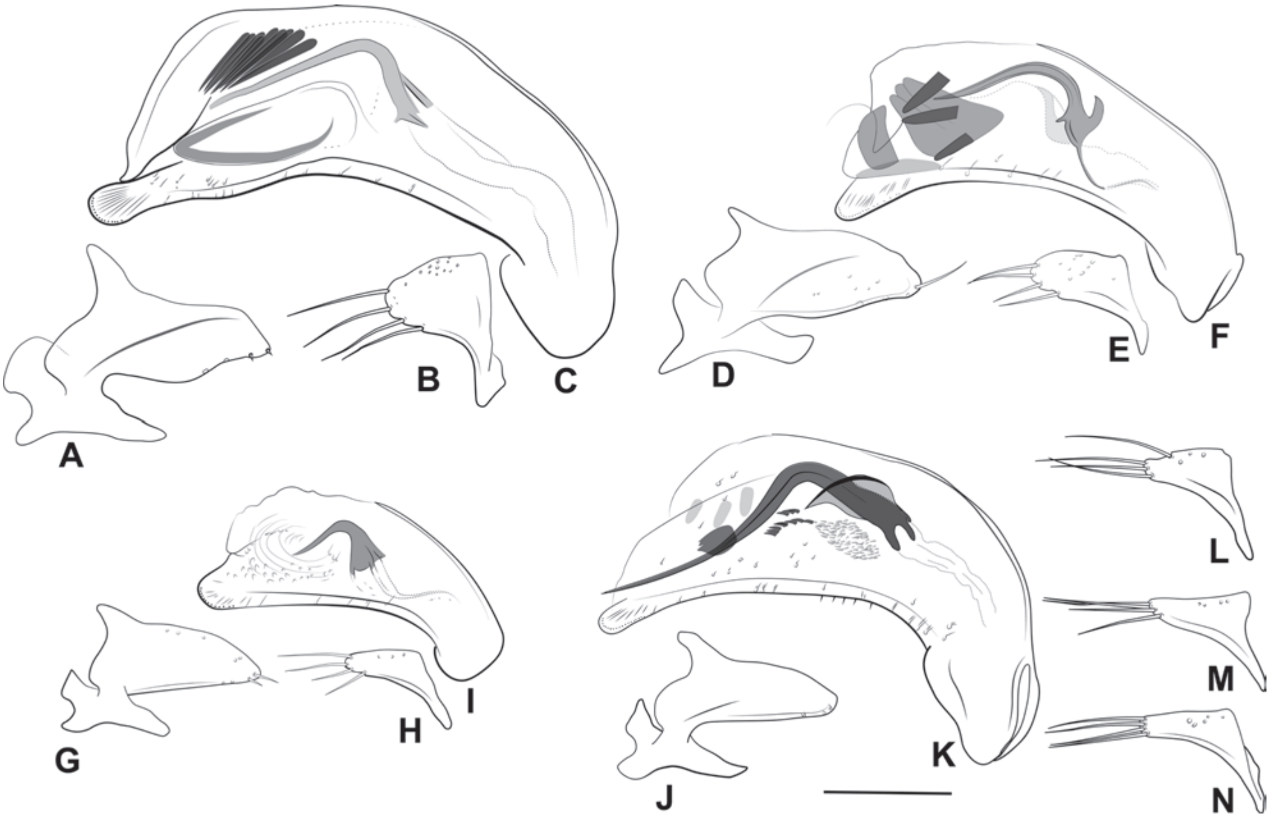

Figure 30. Aedeagi of *valentinei* group *Anillinus* species **A–C** *Anillinus castaneus* sp. nov. **D–F** *Anillinus cornelli* **G–I** *Anillinus simplex* sp. nov. **J–N** *Anillinus murrayae*. Median lobes **C, F, I** in right dorsolateral aspect, median lobe **K** in right lateral aspect. Left **A, D, G, J** and right **B, E, H, L–N** parameres in left and right lateral aspects, respectively. Scale bar: 0.1 mm.

Road inlet; 34.7109, -82.8238; 11 Mar. 2023; C.W. Harden and L.M. Thompson leg.; CWH-491, CUAC000066916; • 1 ♂; same data as previous; CWHc; • 1 ♀; **Pickens Co.**; Clemson Experimental Forest, Pike Road inlet; 34.7116, -82.8280; 26 Apr. 2023; C.W. Harden leg.; CWH-509, CUAC000182311; • 3 ♂, 2 ♀; same data as previous; CWHc; • 2 ♂, 2 ♀; **Pickens Co.**; Clemson Experimental Forest, Waldrop Stone area; 34.7358, -82.8187; 12 Nov. 2020; C.W. Harden leg.; CWH-329 to CWH-332, CUAC000168279 to CUAC000168282; • 1 ♂; same data as previous; CWHc; • 1 ♂, 2 ♀; **Pickens Co.**; Clemson Experimental Forest, Waldrop Stone Falls; 34.7393, -82.8205; 8 Oct. 2021; C.W. Harden leg.; CWH-406 to CWH-408, CUAC000168283 to CUAC000168285; • 1 ♀; **Pickens Co.**; Clemson Experimental Forest; 34.7396, -82.8479; 20 Feb. 2023; E. Recuero leg.; CWHc; • 1 ♀; **Pickens Co.**; Chimneytop Gap; 35.0628, -82.7977; 21 Mar. 2023; C.W. Harden leg.; CWH-508, CUAC000182310; • 1 ♂; **Pickens Co.**; Chimneytop Gap; 35.0631, -82.7960; 23 Mar. 2023; C.W. Harden leg.; CWH-490, CUAC000066882; • 1 ♂; **Pickens Co.**; Chimneytop Gap; 35.0632, -82.7964; 1 Jun. 2023; C.W. Harden leg.; CWHc.

Literature records. There are no additional previously reported localities.

Diagnosis. Medium to large typical members of the *valentinei* group (ABL = 1.63–1.98 mm), with distinctive male and female genitalia, described below.

Redescription of male genitalia. The median lobe (Figs 30K, 31A–O) has a narrow ventral margin and a small, rounded apex. In some individuals, there are several short setae present on the ventral margin. The flagellum is large and heavily sclerotized, rotated dorsally so that in right lateral aspect it is viewed

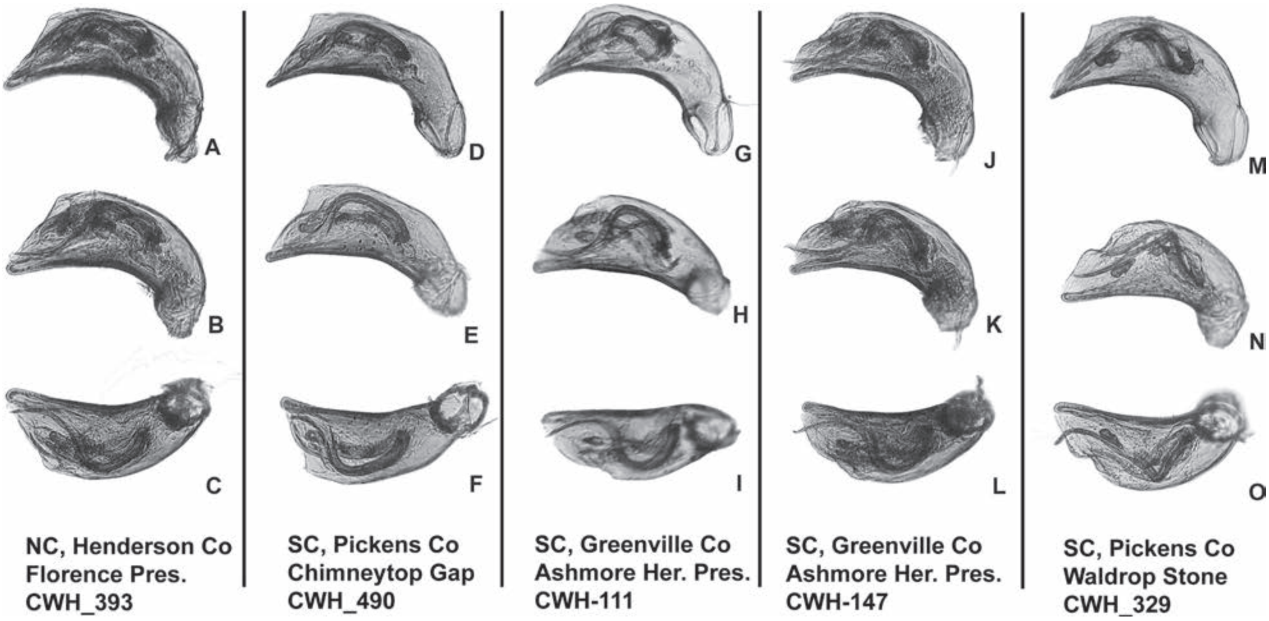

Figure 31. Median lobe of the aedeagus of *Anillinus murrayae* **A, D, G, J, M** right lateral aspect **B, E, H, K, N** right dorsolateral aspect **C, F, I, L, O** ventral aspect.

through its base, falsely appearing to be evenly curved basally and straight beyond sinuation (Figs 30K, 31A, D, G, J, M). In dorsolateral aspect, the flagellum appears as illustrated in Sokolov et al. (2004), with a large basal piece and a long bisinuate shape that slightly surpasses the ostium (Fig. 31E, H, K, N). Several small blunt sclerites are present in the internal sac, as well as a small field of acute spines. Right paramere small and narrow, with four long apical setae that vary in their placement (Fig. 30L, M). The left paramere is narrowly conchoid and asetose (Fig. 30J).

Description of female genitalia. Spermatheca long, deeply bisinuate, gradually enlarged distally (Fig. 21D). Spermathecal duct apparently absent. Bursa without sclerotization.

Variation noted. In specimens from the vicinity of Sassafras Mountain in northern Pickens Co, SC, the flagellum of the internal sac of the aedeagus has a longer and broader basal curve and shorter apical curve (Fig. 31D–F). In specimens from southern localities in Pickens Co., SC, the internal sac of the median lobe lacks the blunt teeth present in other populations, the apical sclerite is saddle-shaped and lacks sharp projections, and the flagellum appears quite different from other populations in right lateral aspect (Fig. 31M) and dorsal aspect (Fig. 31N), because it is rotated differently within the median lobe in repose. Similarly, the spermatheca is the same size, but is oriented in a C-shape rather than an S. Further studies might support splitting *A. murrayae* into two or more species, but our sampling is too limited to support such an action.

Distribution. This species is widely distributed, from Macon Co., NC east to Henderson Co., NC, north to the type locality in GSMNP and Round Knob in Buncombe Co. (Fig. 29). The population at the South Carolina Botanical Garden is the southernmost known locality.

Sympatry. Specimens of *A. murrayae* have been collected in association with *A. mica* and *A. micamicus* at Waldrop Stone Falls, SC; with *A. merritti* at Indian Camp Creek, SC; with *A. cherokee* and *A.* sp. “South Carolina, Coon Branch” at

Coon Branch, SC; with *A. merritti* and *A. langdoni*-group sp. near Wayah Bald, NC; and the paratype series from Jackson Co., NC is a mixture of *A. murrayae* and *A. loweae* (see Notes below). *Serranillus dunavani* co-occurs with *A. murrayae* at most of the known localities.

Natural history. A mating pair was observed on the underside of a rock on 14 March 2020 at Ashmore Heritage Preserve in Greenville Co., SC. Specimens have been collected from sifted leaf litter, under embedded rocks, and using modified buried pitfall traps.

Notes. Three of the male paratypes of *A. murrayae* in the NCSU collection are actually members of *A. loweae*, and have been labeled as such.

Anillinus cornelli **Sokolov & Carlton, 2004**

Figs 29, 30D–F, 32C, F

Anillinus cornelli Sokolov & Carlton, 2004: 209.

Material examined. ***Holotype male*** **(NCSU):** USA. North Carolina: Gaston Co., Crowder's Mt. State Park, Pine Log litter, J.F. Cornell leg., 23 June 1982. Specimen intact; aedeagus in microvial pinned beneath specimen, both parameres missing. (Sokolov et al. [2004] list USNM as the type depository).

Other material (*n* = 2, CUAC). USA • North Carolina • 1 ♂, 1 ♀; **Gaston Co.**; Crowder's Mountain State Park, near Linwood Access; 35.2417, -81.2717; 29 Apr. 2023; C.W. Harden leg.; under embedded rock; CWH-514 and CWH-515, CUAC000182316 and CUAC000182317.

GenBank accession numbers for topotype specimens: OR853205, OR839243, OR839720, OR837937, OR838267, OR853204, OR839242, OR839721.

Literature records. The species has been reported from Kings Mountain State Park in South Carolina, without more specific locality information (Sokolov et al. 2004).

Notes on the type. The median lobe of the aedeagus is damaged: the basal lobes appear to be partially torn off, and the organ is laterally flattened and distorted, as if it were previously crushed beneath a cover slip. The illustration of the median lobe in Sokolov et al. (2004) reflects this condition, and is not an accurate depiction of its shape and structure.

Diagnosis. Members of *A. cornelli* are relatively large (ABL = 1.75–1.81 mm) and broad (PW/EW = 0.83–0.85, EW/ABL = 0.36–0.38) (Fig. 32C). As is typical of the *valentinei* group, microsculpture is effaced from most of the dorsal surfaces of the forebody, three large supraorbital setae are present and both the first and second protarsomeres of males have thick white adhesive setae ventrally. The metafemora of males are slightly swollen, larger than in females, but without teeth or coarse microsculpture patches. The male genitalia are distinctive, and are redescribed based on a recently collected specimen below.

Redescription of male genitalia. Ring sclerite average sized for genus (RL/ABL = 0.27), oval and asymmetrically narrowed anteriorly, with anterior margin deflected ventrally. Median lobe (Fig. 30F) strongly asymmetrical, with apex abruptly and conspicuously curved to right side. In right lateral aspect, appearing obtusely angulate proximately, nearly straight medially and abruptly curved ventrally at apex. In right dorsolateral aspect, slightly curved and enlarged

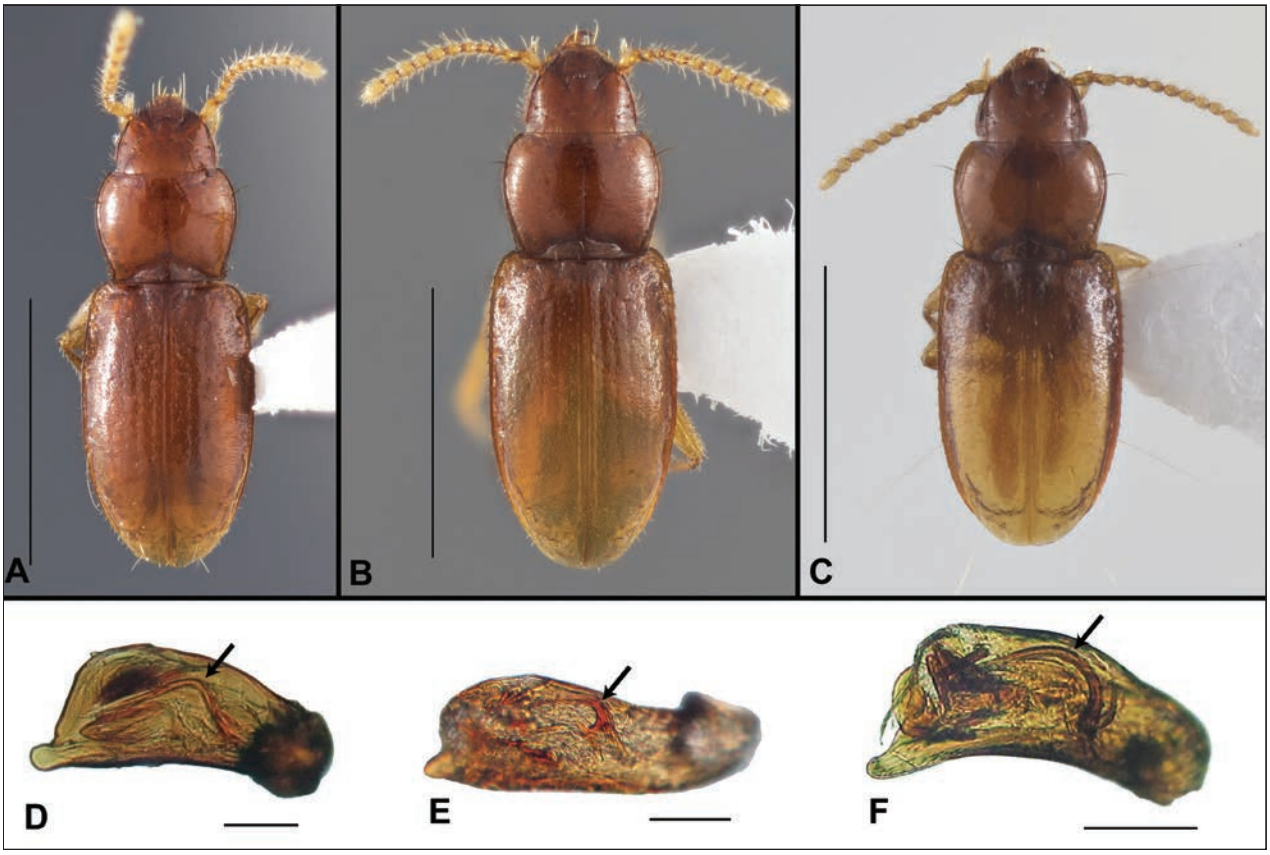

Figure 32. Dorsal habitus and median lobes of *Anillinus* species **A** *Anillinus castaneus* sp. nov. Holotype **B** *Anillinus* sp. "South Carolina, Chestnut Ridge" **C** *Anillinus cornelli*, abdomen removed for DNA extraction. **D** *A. castaneus* sp. nov. Holotype, dorsal aspect **E** *A.* sp. "South Carolina, Chestnut Ridge", dorsal aspect **F** *A. cornelli*, dorsal aspect. Black arrows point to proximal curve of flagellum. Scale bars: 1 mm (**A–C**); 0.1 mm (**D–F**).

distally. Left side with small excavation proximally and long carina extending along nearly entire length. Internal sac with long, well-sclerotized flagellum that in dorsolateral aspect is strongly curved proximately (Fig. 32F), with long basal extension, becoming filamentous distally, where it coils and extends beyond ostium on right side. Three large, blunt spines are present on right side of internal sac near ostium; a fourth spine appears to be present ventral to the others, just before the apex of the median lobe, but this is an artifact caused by the thick, curved sclerotized wall of the aedeagus seen through its curve in right lateral aspect. Behind the three spines, against the ostial opening, a sclerite with three blunt spines fused at the base is present, appearing comb-like. Distal to this comb-like structure is a smaller semicircular ostial sclerite. Right paramere short, bearing four short apical setae (Fig. 30E). Left paramere conchoidal, with four preapical pores on ventral margin, the apical one bearing a long seta (Fig. 30D).

Description of female genitalia. Spermatheca long, bisinuate, gradually enlarged distally. Spermathecal duct long and heavily coiled. Bursa with lightly sclerotized folds.

Distribution. Endemic to Kings Mountain, a monadnock that spans the North Carolina-South Carolina border. (Fig. 29).

Sympatry. At Crowders Mountain State Park, *A. cornelli* co-occurs with *A. simplex* sp. nov. and a species belonging to the *elongatus* group, possibly conspecific with *A. montrex*. Both *A. simplex* and *A. montrex* also occur at Kings Mountain, along with an undescribed species of *Serranillus*.

Natural history. The type material was reportedly collected by litter extraction. On 29 April 2023, CWH collected a pair of *A. cornelli* from the underside of a large embedded rock on a gently sloping wooded hillside. Several large samples of sifted litter and soil taken from the same locality and another locality within Crowders Mountain State Park on the same date failed to produce specimens of *A. cornelli.* Two days of intensive hand collecting and litter extraction at Kings Mountain State Park also failed to produce specimens of *A. cornelli*.

Notes. We have not seen material of this species from South Carolina. No paratypes were found in collections, including those from Kings Mountain State Park reported by Sokolov et al. (2004) to be deposited in the NCSU collection (Bob Blinn pers. comm., March 2022).

Anillinus castaneus **sp. nov.**

https://zoobank.org/4CFF8F11-E1CE-422A-B68E-F3EA28B831EA

Figs 21C, 24B, 29, 30A–C, 32A, D

Type material. ***Holotype male*** **(USNM):** point mounted, with genitalia in Euparal on microslide pinned beneath specimen. Original label: "USA: S. Carolina: Greenville Co. Chestnut Ridge Heritage Pres. N 35.1471, W -82.2841. 8 April 2018 (373) Sift/Berl CWD5 M. Ferro" "CLEMSON-ENT CUAC000080962" "HOLOTYPE *Anillinus castaneus* Harden & Caterino [orange cardstock]"

Paratypes (*n* = 9, CUAC). **USA • South Carolina • Greenville Co.**; Chestnut Ridge Heritage Preserve; • 2 ♀; same data as holotype; CUAC000080963 and CUAC000080964; • 1 ♀; **Greenville Co.**; Chestnut Ridge Heritage Preserve; 35.1506, -82.2779; 8 Apr. 2018; M. Caterino & L. Vasquez leg.; sifted litter; CUAC000108120; • 2 ♂; **Greenville Co.**; Chestnut Ridge Heritage Preserve; 35.1523, -82.2814; 5 Jun. 2015; S. Myers leg.; Hardwood litter; CUAC000170064 and CUAC000170065, SSM098 and SSM099 [these two specimens do not have molecular voucher labels, but have been extracted and bear identical locality data to that entered for these voucher numbers by S. Myers]; • 1 ♀; **Greenville Co.**; Chestnut Ridge Heritage Preserve; 35.1501, -82.2820; 5 Jun. 2015; S. Myers leg.; Hardwood litter; CUAC000170066, SSM-101; • 1 ♀; **Greenville Co.**; Chestnut Ridge Heritage Preserve; 35.14970, -82.28207; 20 Oct. 2021; C.W. Harden leg.; On underside of large rock beside rivulet; CUAC000170067, CWH-415; • 1 ♀; **Greenville Co.**; Chestnut Ridge Heritage Preserve; 35.1507, -82.2821; 15 Mar. 2022; C.W. Harden leg.; Berlese, deep duff/soil; CUAC000170068;• 1 ♀; **Greenville Co.**; Chestnut Ridge Heritage Preserve; 35.1406, -82.2790; 5 Jun. 2015; S. Myers leg.; Secondary litter; CUAC000025521.

GenBank accession numbers for paratypes: OR839224, OR853178, OR839223, OR839749, OR837941, OR838100, OR838278, OR853179, OR839821, OR838112, OR838296.

Diagnosis. A moderately large typical member of the *valentinei* group, externally similar to *A. murrayae* and *A. cornelli* (Fig. 32A). The male genitalia are distinctive, particularly the tripartite apex of the median lobe formed by the ventral margin, dorsal margin, and ostial plate (Fig. 30C), which is unique among *Anillinus* species east of the Appalachians.

Description. ***Habitus*** ABL = 1.81–1.85 mm. ***Integument*** Dorsal microsculpture effaced from most of forebody, present only medially on vertex and weakly impressed on frons and extreme margins of pronotum. ***Head*** HW/PW = 0.73–0.74. Frontoclypeal horn well-developed. Three pairs of supraorbital setae present, posterior outer pair smaller than other two. ***Pronotum*** Form variable, either convex and smoothly polished, or subdepressed and with microsculpture along margins. Relatively short (PL/ABL = 0.22–0.23) and broad (PW/EW = 0.82–0.85), sides evenly convergent behind middle, moderately constricted basally (PbW/PW = 0.74–0.77). ***Elytra*** Slightly ovoid, convex, broad (EW/ABL = 0.35–0.36), with large umbilicate punctures. ***Legs*** Male protarsi with protarsomeres 1 and 2 expanded and dentate on inner margin, both bearing adhesive setae ventrally. Male profemora unmodified. Male mesotrochanters unmodified. Male metafemora slightly swollen, with patch of coarse papillate microsculpture medially on posterior face. ***Abdominal ventrites*** Unmodified in either sex. ***Male genitalia*** Ring sclerite large (RL/ABL = 0.35), oval, strongly constricted anteriorly where it forms a curved shelf projecting ventrally. Median lobe (Fig. 30C) strongly asymmetrical, twisted dorsally from plane of basal lobes and curved to the right side. In right lateral aspect, appearing strongly curved, with the ventral margin somewhat angular and sinuate before apex, with several short setae present in proximal bend. In right dorsolateral view, appearing slightly curved and slightly enlarged distally, dorsal margin well sclerotized and forming a sharp beak apically, ventral margin narrowly expanded, apex small and produced, buttonlike. Left side of median lobe at base with large semicircular excavation that occupies the entire basal section before bend, associated carina distal to excavation short, ending at ostium that is large, occupying most of the left face of the median lobe. Internal sac with complex armature: the flagellum is long, well sclerotized, with long basal projections, obtusely bent medially or evenly curved depending on angle at which it is viewed, apex ending at ostium; a group of large, dark sharp spines is present dorsally at ostium; a large, spade-like ostial plate is present on left ventrolateral face of apex; in dorsal or ventral views, the apex appears tripartite, with the dorsal and ventral margins meeting and the pointed ostial plate projecting between them. Shape of flagellum and other internal sclerites appearing as an indecipherable dark mass in right lateral aspect. Right paramere short and broad, with four apical setae (Fig. 30B). Left paramere conchoid, with fore preapical pores on ventral face, apical two bearing short setae (Fig. 30A). ***Female genitalia*** Spermatheca long, abruptly enlarged distally, stem bent at a slightly acute angle proximally or evenly curved (Fig. 21C). Spermathecal duct not apparent in the two specimens examined. Bursa copulatrix with conspicuous sclerotized folds.

Distribution. Known only from a small area of Chestnut Ridge Heritage Preserve in Greenville Co., SC (Fig. 29).

Sympatry. Members of this species have been collected with *A.* sp. “South Carolina, Chestnut Ridge” and *S. dunavani*.

Natural history. Most specimens have been collected through Berlese extraction of sifted leaf litter and dead wood. Two specimens were collected from the undersides of rocks.

Species status justification. The male genitalia are unique within the genus, particularly the complex tripartite apex of the median lobe. DNA sequence data indicate the species is most closely related to *A. simplex*, *A. cornelli* and the undescribed species *A.* sp. “South Carolina, Chestnut Ridge”, which all differ from *A. castaneus* in external structure and male genitalic characters. *Anillinus castaneus* and “South Carolina, Chestnut Ridge” occur in syntopy, providing strong evidence that the two are reproductively isolated.

Derivation of species name. A male adjective, from the Latin for Chestnut, in reference to the color of the mature specimens and the name of the type locality, which itself is presumably named for the American Chestnut tree, once an abundant component of Appalachian forests.

Anillinus sp. “South Carolina, Chestnut Ridge”

Figs 24C, 29, 32B, E

Material examined. USA • **South Carolina** • 1 ♂; **Greenville Co.**; Chestnut Ridge Heritage Preserve; 35.15071, -82.28211; 20 Oct. 2021; C.W. Harden leg.; on underside of embedded rock, alluvial forest near Little Pacolet River; CWH-401, CUAC000170069.

GenBank: OR853206, OR839244, OR839666, OR837917, OR838074, OR838251.

Diagnosis. The single specimen, a male (Fig. 32B), is large (ABL = 1.98 mm) and unusual in having the dorsal microsculpture of the forebody strongly developed in the pattern of the *loweae* group (present on entire surface except for paramedian patches on vertex) while being an otherwise typical member of the *valentinei* group, whose members typically have dorsal microsculpture largely absent. The median lobe is typical of the *valentinei* group, with a long, well-sclerotized flagellum and several well-sclerotized spines lining the internal sac. The proximal curve of the flagellum (Fig. 32E) is shorter than in *A. castaneus* (Fig. 32D).

Notes. The data from morphology and DNA sequences both support recognition of this individual as a species distinct from any other in the genus, but we feel more specimens are needed to allow an adequate description. A return trip in March 2022 to search for more specimens was unsuccessful, but the site is readily accessible and the habitat is protected, so it is likely that more individuals can be obtained in the future.

Anillinus simplex sp. nov.

https://zoobank.org/CA863666-9208-48EC-8AB0-B2E006B1F0E9

Figs 21E, 24E, 29, 30G–I, 33A–C

Type material. ***Holotype male*****:** (**USNM**), point mounted, with abdominal ventrites glued to point and genitalia in Euparal on microslide pinned beneath specimen. Original label: “USA: SC, York Co. Kings Mountain S.P. 35.1307, -81.3649. 26.September.2020. C.W. Harden. Under rock near stream.” “[QR Code] CLEMSON-ENT CUAC000185896” “Harden DNA Voucher CWH-247 Anill. ‘kingsmtnsp1’ M Ext. 30/September/2020 [green-bordered label].” “HOLOTYPE *Anillinus simplex* Harden & Caterino [orange cardstock]”

GenBank: OR853342, OR839331, OR839570, OR837888, OR838032, OR838222.

Figure 33. *Anillinus simplex* sp. nov. **A** dorsal habitus, abdomen removed for DNA extraction **B** last abdominal ventrite, ventral aspect **C** head, left lateral aspect (black arrow = frontoclypeal horn). Scale bars: 1 mm (**A**); 0.1 mm (**B**).

Paratypes (*n* = 46, ADGc, CMNH, CNC, CUAC, FSCA, LSAM, NCSU, NHMUK, OSAC, USNM, VMNH). **USA** • **South Carolina** • **York Co.** • Kings Mountain State Park; • 1 ♂; same data as holotype; CUAC000170024, CWH-248; CUAC; • 1 ♀; same data as holotype; CUAC000170025, CWH-249; CUAC; • 8 ♂, 2 ♀; same data as holotype; CUAC000170026 to CUAC000170035; CNC, CUAC; • 3 ♂; same data as holotype; ADGc; • 12 ♂, 12 ♀; 35.13198, -81.36608; 26 Sep. 2020; C.W. Harden leg.; Berlese, deep litter and topsoil, oak, maple, sourwood, pine; CUAC000170036 to CUAC000170059; CMNH, CNC, FSCA, LSAM, OSAC, USNM, VMNH; • 1 ♀; 35.13062, -81.36439; 26 Sep. 2020; C.W. Harden leg.; Berlese, litter near stream, mesic hardwoods; CUAC00017060; VMNH; • 2 ♂, 1 ♀; 35.13018, -81.36205; 23 Dec. 2021; C.W. Harden leg.; under embedded rock; CUAC000167147 to CUAC000167149; NCSU; • 1 ♂, 2 ♀; 35.1301, -81.3637; 23 Dec. 2021; C.W. Harden leg.; Berlese, soil near seepage; CUAC000170061 to CUAC000170063; NHMUK.

GenBank accession numbers for paratypes: OR839571, OR853339, OR839328, OR839572, OR837889, OR838033, OR838223.

Other material (*n* = 30, CUAC, CWHc, NCSU). USA • **North Carolina** • 3 ♂, 5 ♀; **Gaston Co.**; Crowders Mountain State Park, near Linwood parking; 35.2417, -81.2717; 29 Apr. 2023; C.W. Harden leg.; Berlese, sifted duff/litter; NCSU; • 2 ♂; same data as previous; under embedded rock; CUAC000182312 and CUAC000182313, CWH-510 and CWH-511; CUAC; • 1 ♂; **Gaston Co.**; Crowders Mountain State Park; Ridgeline Trail at Road 1104; 35.1977, -81.3152; 29 Apr. 2023; C.W. Harden leg.; under embedded rock; CUAC000182314, CWH-512; CUAC; • 3 ♂; **Gaston Co.**; Crowders Mountain State Park; Ridgeline Trail at Road 1104; 35.1977, -81.3152; 29 Apr. 2023; C.W. Harden leg.; under embedded rock; CWHc; • 1 ♀; **Gaston Co.**; Crowders Mountain State Park, near Pinnacle, open piney ridge; 35.2011, -81.3148; 29 Apr. 2023; C.W. Harden leg.; under rock; CWHc; • 1 ♂; **Gaston Co.**; Crowders Mountain State Park, near Pinnacle, recently washed gully; 35.1993, -81.3152; 29 Apr. 2023; C.W. Harden leg.; under rock; CWHc; • 3 ♂; **Gaston Co.**; Crowders Mountain State Park, near Pinnacle, recently washed gully; 35.2031, -81.3144; 29 Apr. 2023; C.W. Harden leg.; under rock; CWHc; • **South Carolina** • **York Co.** • 7 ♂, 3 ♀; Kings Mountain State Park; 35.13198, -81.36608; 26 Sep. 2020; C.W. Harden leg.; Berlese, deep litter and topsoil, oak, maple, sourwood, pine; CWHc; • 1 ♀; Bethany; 35.116, -81.305; 9 Feb. 1998; J.C. Ciegler leg.; in leaf litter; CUAC.

Diagnosis. Males of *A. simplex* are the only members of the *valentinei* group known to lack ventral adhesive setae on protarsomere 2, but this character is difficult to confirm without strong magnification. From most anillines occurring in South Carolina, members of *A. simplex* can be recognized by their small size (ABL < 1.65 mm) and effaced microsculpture on the sides of the vertex. The median lobe of *A. simplex* is distinctive, with a short, thick well-sclerotized curved flagellum in the internal sac and the absence of other well-sclerotized structures (Fig. 30I). Some individuals of *A. murrayae* from southern Pickens Co. overlap in size with members of *A. simplex* but are easily distinguished by the different male and female genitalia (Figs 21D, 30J–N).

Description. ***Habitus*** Body small (ABL = 1.45–1.64 mm), moderately convex, slightly ovoid, robust (EW/ABL = 0.35–0.38) (Fig. 33A). ***Integument*** Dorsal microsculpture of forebody variable. In specimens from the type locality, microsculpture is effaced from most of the pronotum, present only along extreme outer margins, and weakly impressed there, and absent from large portions on both sides of the vertex posteriorly. In specimens from Crowders Mountain, the pronotum is entirely covered in strong, easily visible isodiametric microsculpture, and the smooth patches on the vertex are smaller. ***Head*** HW/PW = 0.71–0.77. Three pairs of supraorbital setae present, outer posterior pair shorter than other two. Frontoclypeal horn well-developed (Fig. 33C). ***Pronotum*** Relatively short (PL/ABL = 0.22–0.24) and broad (PW/EW = 0.80–0.85), sides evenly convergent or slightly sinuate before slightly narrowed posterior angles (PbW/PW = 0.73–0.78). ***Elytra*** Slightly ovoid, widest approximately middle, length variable (EL/ABL = 0.51–0.57). Umbilicate punctures relatively large and conspicuous. Striae weakly impressed, difficult to trace. ***Legs*** Profemora of males unmodified; protarsomere 1 of males expanded and with inner margin spinose, protarsomere 2 unmodified and apparently lacking ventral adhesive setae in most specimens (a single adhesive seta observed in one male). Mesofemora of males unmodified. Metafemora of males with patch of coarse papillate microsculpture medially on posterior face. ***Abdominal ventrites*** Unmodified in either sex (Fig. 33B). ***Male genitalia*** Ring sclerite (Fig. 24E) moderately small (RL/ABL = 0.28) and asymmetrical, strongly narrowed anteriorly. Median lobe (Fig. 30I) evenly curved, slightly twisted dorsally from level of basal lobes, gradually expanded in width from base to apex. Ventral margin slightly expanded, asetose. Apex small and evenly rounded. Left side of base with semicircular excavation visible in left posterolateral aspect, with carina extending distally from the excavation to approximately middle. Internal sac with well-sclerotized flagellum short and stout, evenly curved, with one short basal extension. Ventral surface of internal sac with field of weakly sclerotized teeth. Sides of internal sac near ostium appearing grooved with curved parallel lines. Ostial plate on left side, small and weakly sclerotized. Right paramere narrow, with four long apical setae (Fig. 30H). Left paramere conchoidal, with four ventral subapical pores, the apical two bearing short setae (Fig. 30G). ***Female genitalia*** Spermatheca long, gradually and slightly enlarged distally, stem slightly sinuate before basal curve, which is rotated perpendicular from rest of stem (Fig. 21E). Spermathecal duct short and not coiled.

Distribution. Known only from Kings Mountain, a short linear monadnock spanning from York County, South Carolina to Gaston County, North Carolina (Fig. 29).

Sympatry. This species has been collected with *A. montrex* and *A. cornelli* underneath embedded rocks. *Serranillus monadnock* sp. nov. also occurs at Kings Mountain State Park.

Natural history. Specimens have been collected in February, April, September, and December, from underneath embedded rocks on sandy clay rich soil near an ephemeral stream and through Berlese extraction of sifted litter and soil.

Species status justification. The male and female genitalic characters are unique within the genus, and the DNA sequence data indicate *A. simplex* is most closely related to *A. cornelli*, *A. castaneus*, and “South Carolina, Chestnut Ridge”, all of which differ markedly in male genitalic characters, especially by possessing several sclerotized spines in the internal sac.

Derivation of species name. A noun in apposition, from the Latin, meaning “simple”, in reference to the structure of the median lobe of the aedeagus, which lacks the complex sclerotized structures in the internal sac that are present in the other South Carolina species in the *valentinei* group, and the lack of modifications to male protarsomere 2.

‘*elongatus* group’

The five described species of the *elongatus* group were revised by Harden and Caterino (2024) and are discussed and illustrated in more detail in that paper.

Anillinus arenicollis **Harden & Caterino, 2024**

Figs 21M, 24K, 34B

Anillinus arenicollis Harden & Caterino, 2024: 18.

GenBank. OR853123, OR839200, OR838072, OR839197, OR839198, OR853122, OR839199, OR839746, OR837940, OR838098, OR838277.

Diagnosis. Robust, dorsoventrally flattened, and parallel-sided (Fig. 34B). Dorsal surfaces of head and pronotum entirely covered in microsculpture. Males with both protarsomeres 1 and 2 expanded and dentate on inner margin with ventral adhesive setae. Male metafemora swollen with prominent tooth on

Figure 34. Dorsal habitus of *Anillinus* species in the *elongatus* group and *sinuaticollis* group **A** *Anillinus montrex* **B** *Anillinus arenicollis* **C** *Anillinus choestoea* sp. nov. **D** *Anillinus seneca* sp. nov. **E** *Anillinus mica* sp. nov. **F** *Anillinus micamicus* sp. nov. Abdomens removed in **B–F** for DNA extraction. Scale bars: 1 mm.

posterior margin, median lobe of male aedeagus narrow and long with blocky apex that is deflexed ventrally. Female spermatheca (Fig. 21M) long, stem ribbed, not coiled proximally. Spermathecal duct long and coiled.

Distribution. Known from a small area within the boundaries of the Carolina Sandhills National Wildlife Refuge in Chesterfield Co., SC.

Sympatry. Members of this species have not been collected with other species of anillines.

Natural history. The first specimen collected was in a sample of sifted litter collected in February. All other known specimens were collected in buried pipe traps set in sandy soil. Further litter sampling at the only known locality failed to produce further specimens, and members of this species are presumably endogean in habit.

Anillinus montrex Harden & Caterino, 2024

Figs 2H, 10C, I, 21L, 24L, 34A

Anillinus montrex Harden & Caterino, 2024: 25.

GenBank. OR853113, OR853294, OR839300, OR839565, OR837884, OR838029, OR838218, OR838127, OR839566, OR839299, OR839567, OR837885, OR838030, OR838219.

Diagnosis. Members of this species are strongly flattened dorsoventrally, narrow, and parallel sided (Fig. 34A). Males have the first and second protarsomeres expanded and spinose on inner margin with ventral adhesive setae; the male second protarsomeres of this species are more enlarged than any other known *Anillinus* species (Fig. 10C, I). The male genitalia are also distinctive, with a small apex that is abruptly bisected by the membranous dorsal margin. Female spermatheca (Fig. 21L) with stem coiled proximally, abruptly enlarged distally.

Distribution. Known for certain only from a single hillside above a small stream in Kings Mountain State Park, York Co., SC.

Sympatry. Members of this species have been collected under rocks with *A. simplex* sp. nov.

Natural history. Members of this species are endogean in habit, occurring under deeply embedded rocks at cold times of year. Specimens have been collected in December.

'*sinuaticollis* group'

Anillinus choestoea sp. nov.

https://zoobank.org/E62B04B0-C153-4513-B053-69648A96E3BA

Figs 10E, 11B, D, 12C, 21J, 24I, 34C, 35A–C, 36

Type material. ***Holotype male* (USNM):** point mounted, with abdominal ventrites glued to point and genitalia in Euparal on microslide pinned beneath specimen. Original label: "USA: SOUTH CAROLINA, Oconee Co. Choestoea Park. 34.54616, -83.10479. 21.December.2020. CW Harden. Under small rocks, pine/oak hill. Soft, moist sandy soil." "[QR code] CLEMSON-ENT CUAC000163546" "Harden DNA Voucher CWH-335 A. 'choestoea' M Ext. 1/May/2021 [green-bordered cardstock]" "HOLOTYPE *Anillinus choestoea* Harden & Caterino [orange cardstock]"

GenBank: OR839239, OR839627, OR838052.

Paratypes (*n* = 4, CUAC). **USA • South Carolina** • 2 ♀; same data as holotype; CUAC000163544 and CUAC000163545, CWH-336 and CWH-337; • 1 ♂; **Oconee Co.**; Choestoea Park; 34.54318, -83.09894; 21 Dec. 2020; C.W. Harden leg.; Under rock in *Camponotus* nest; CUAC000163543, CWH-310; • 1 ♀; **Oconee Co.**; Choestoea Park; 34.5477, -83.1052; 19 Feb. 2022; C.W. Harden leg.; Under rock; CUAC000163547.

GenBank accession numbers for paratypes: OR853202, OR839240, OR839608, OR837897, OR838043, OR838232, OR839628, OR839629.

Diagnosis. Compared to other members of the *sinuaticollis* group, the habitus of this species is broader (EW/ABL 0.37 or 0.38) and more convex (Fig. 34C). The microsculpture on the pronotum is more extensive, present anteriorly

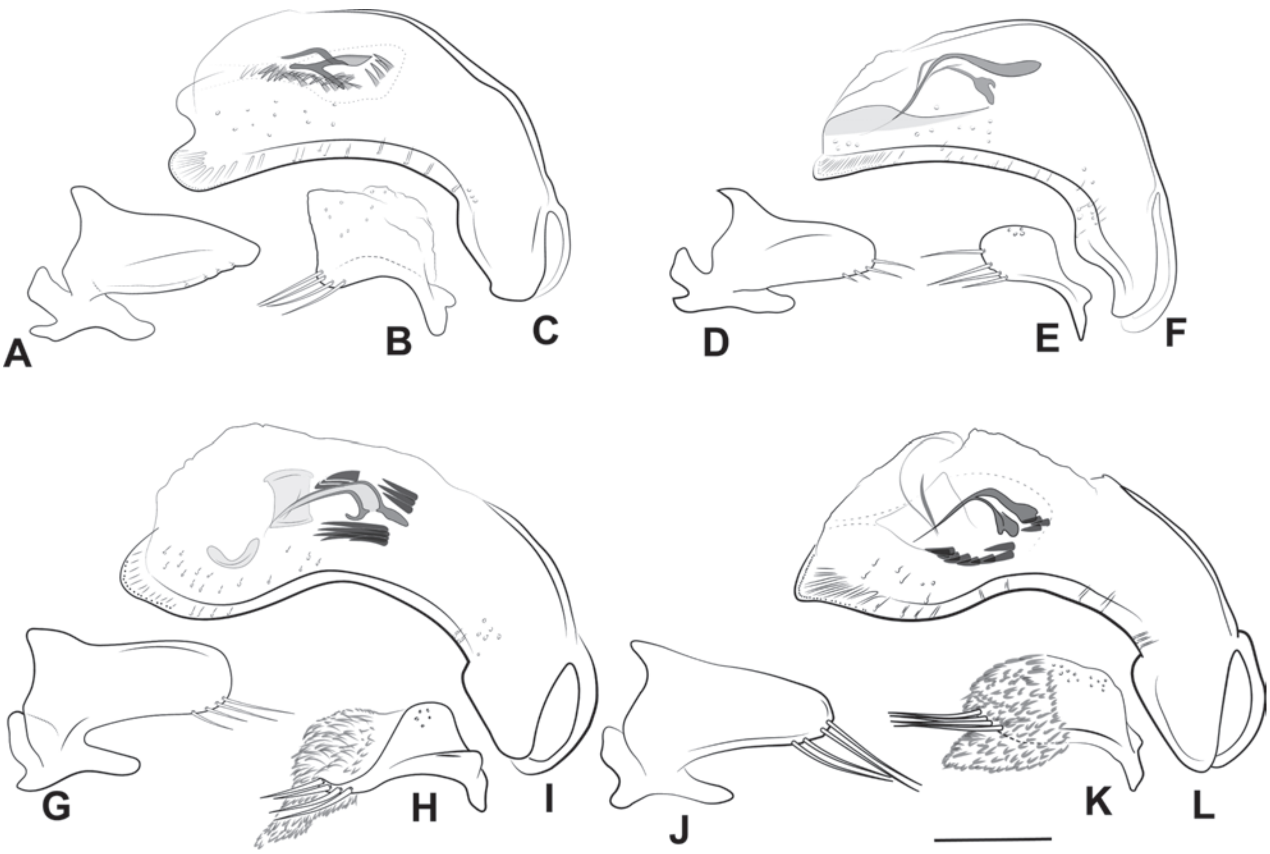

Figure 35. Male genitalia of *Anillinus* species in the *sinuaticollis* group **A–C** *Anillinus choestoea* sp. nov. **D–F** *Anillinus seneca* sp. nov. **G–I** *Anillinus mica* sp. nov. **J–L** *Anillinus micamicus* sp. nov. Median lobe of aedeagus in right dorsolateral (**C, I, L**) or right lateral (**F**) aspect. Left parameres (**A, D, G, J**) and right parameres (**B, E, H, K**) in left and right lateral aspects, respectively. Scale bar: 0.1 mm.

and extending onto the disc in some specimens. The aedeagus is also unique (Fig. 35C), most notably the dorsally expanded apex of the median lobe and the short, dorsally rotated flagellum of the internal sac.

Description. ***Habitus*** (Fig. 34C) ABL = 1.61–1.81 mm, males (1.81 mm) larger than females (1.61–1.65 mm), slightly convex and ovoid (EW/ABL = 0.37–0.38). ***Integument*** Irregular isodiametric microsculpture present anteriorly on pronotum, becoming effaced posteriorly and indistinguishable from surface rugosity, which is strong; microsculpture present across entire dorsal surface of head. Dorsal microsculpture is stronger in males than in females. ***Head*** HW/PW = 0.74–0.78. Antennomeres IV–X moniliform. Labrum shallowly emarginate anteriorly. Frontoclypeal horn present, well developed. Three pairs of supraorbital setae present, outer posterior pair shorter than other two. Mentum with median pair of setae posterior to bead of mentum tooth, which is small and subtriangular. ***Pronotum*** Strongly constricted basally in females (Pbw/PW = 0.73–0.74), less so in males (Pbw/PW = 0.78); short in both sexes (PL/ABL = 0.22–0.24). Moderately broad (average PW/EW = 0.81). Sides straight or slightly sinuate before obtuse hind angles; 2–4 basal serrulations. ***Elytra*** Moderately to markedly ovoid, more so in females than in males; moderately convex; relatively long (EL/ABL = 0.55–0.57); humeri not sloped; inner two striae well impressed, traces of two or three additional striae visible. ***Legs*** Protarsi of males with protarsomere 1 expanded and spinose on inner margin, with adhesive setae ventrally,

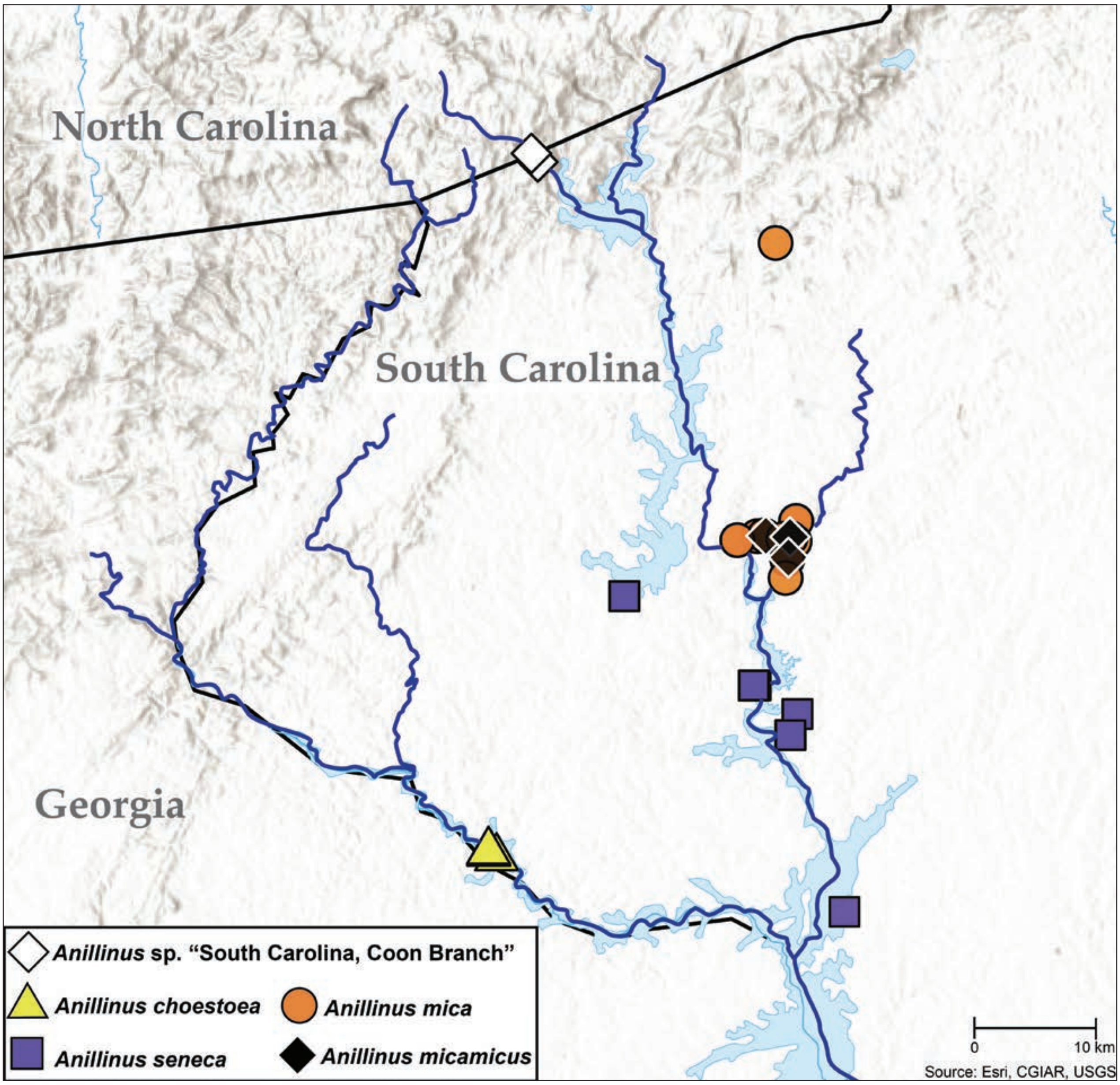

Figure 36. Distribution map of *sinuaticollis*-group species of *Anillinus* in South Carolina. Data are from Harden (2024). Blue lines show modern and pre-inundation courses of the Tugaloo River and Seneca River and their major tributaries. The confluence of the two rivers becomes the Savannah River.

protarsomere 2 unmodified and without adhesive setae (Fig. 10E). Metafemora of males (Fig. 12C) not strongly swollen, without prominent tubercle or tooth on posterior margin. ***Abdominal ventrites*** Unmodified in either sex. ***Male genitalia*** Aedeagus relatively small (RL/ABL = 0.24). Median lobe (Fig. 35C) not twisted, evenly curved; dorsal margin sclerotized for ~1/2 its length; ventral margin without setae; apex large and broadly rounded, produced dorsally into lightly sclerotized lobe subequal to apex in size and shape; internal sac with flagellum rotated dorsally so that it is viewed through base in right lateral view and appears as a complex sclerotized structure; in dorsal view, flagellum is short and evenly curved, broadly "open" laterally, not closed at apex, with elongate basal extension; rows of lightly sclerotized teeth present along left side of internal sac beside flagellum and ostium; texture of internal sac slightly scaly at ostial opening. Right paramere (Fig. 35B) lightly sclerotized and quadrate, apical margin blunt and enlarged, with four moderately long setae basally. Left paramere (Fig. 35A) subtriangular, with four pores along lower margin near apex, without setae. ***Female genitalia*** Spermatheca long, gradually enlarged distally, stem coiled proximally (Fig. 21J); duct damaged in all specimens examined.

Distribution. Known from a small area of Choestoea Park in Oconee Co., SC, located along the former course of the Tugaloo River, currently inundated by Lake Hartwell (Fig. 36).

Sympatry. This species has not been collected in association with other anilline species.

Species status justification. The genitalic morphology of males and females of this species is unique within the genus. DNA sequence data indicate that *A. choestoea* is most closely related to geographically distant members of the *sinuaticollis* group, all of which differ from *A. choestoea* in external structure and male genitalic characters.

Natural history. Known from endogean microhabitats. One specimen was collected in the galleries of *Camponotus* ants under a large rock. The remaining specimens were collected underneath smaller rocks embedded in sandy clay rich soil without evidence of *Camponotus* galleries. It is unlikely that the species is closely associated with ant hosts. Specimens were collected in December and February.

Derivation of species name. From the type locality, Choestoea Park, to be treated as a noun in apposition.

Notes. *Anillinus choestoea* belongs to a subclade that is otherwise comprised of western species. All share a similar flagellum shape that is short and rotated dorsally so that in lateral aspect it is viewed through the base.

Anillinus mica **sp. nov.**

https://zoobank.org/10A909F3-814E-4576-9F93-14B8EB0173C3
Figs 10B, 12A, 21I, 24G, 25A, 34E, 35G–I, 36

Type material. *Holotype male* (USNM): point mounted, with abdominal ventrites glued to point and genitalia in Euparal on microslide pinned beneath specimen. Original labels: “USA: SC, Pickens Co. Clemson Experimental Forest Waldrop Stone Falls. 34.7393, -82.8205. 8.x.2021. CW Harden. Under rock on steep slope near falls.” “[QR code] CLEMSON-ENT CUAC000163558” “Harden DNA Voucher CWH-403 *Anillinus* ‘caterino’ M Ext. 19-December-2021 [green-bordered cardstock]” “HOLOTYPE *Anillinus mica* Harden & Caterino [orange cardstock]”

GenBank: OR853287, OR839293, OR838076.

Paratypes (*n* = 18, CUAC, USNM). **USA • South Carolina** • 2 ♂; **Pickens Co.**; Keowee WMA, near Todd Creek Falls; 34.74986, -82.81467; 6 Sep. 2020; C.W. Harden leg.; Under embedded rock on dry soil, mixed woods; CUAC000163551 and CUAC000163552, CWH-230 and CWH-231; • 1 ♂; **Pickens Co.**; Central, ~3 mi N Clemson; 34.7251, -82.8248; 2 Oct. 2020; C.W. Harden leg.; Buried pipe trap, sandy clay mica-rich soil; CUAC000134435; USNM; • 1 ♂; same locality as previous; 14 Aug. to 24 Oct. 2021; C.W. Harden leg.; Buried pipe trap, clay soil, trap 07; CUAC000170072; USNM; • 1 ♂; same locality as previous; 24 Oct. 2021 to 10 Apr. 2022; C.W. Harden leg.; Buried pipe trap, mica-rich sand/clay.

Trap 05; CUAC000170073; • 1 ♂, 1 ♀; **Pickens Co.**; 5 mi N Clemson; 34.7252, -82.8245; 8 Nov. 2016; M & P Caterino leg.; floated from soil; CUAC000163553 and CUAC000163554, MSC-2458 and MSC-2466; • 1 ♂, 1 ♀; **Pickens Co.**; Clemson Experimental Forest, Issaqueena Lake Rd., West side; 34.74136, -82.86541; 12 Nov. 2020; C.W. Harden leg.; Underside of rock, clay soil; CUAC000163555 and CUAC000163556, CWH-333 and CWH-334; • 1 ♂; **Pickens Co.**; Clemson Experimental Forest, Waldrop Stone area; 34.73603, -82.81725; 12 Nov 2020; C.W. Harden leg.; Under large rock at lake edge; CUAC000163557, CWH-328; • 3 ♂, 3 ♀; **Pickens Co.**; Clemson Experimental Forest, Waldrop Stone Creek; 34.7395, -82.8270; 11 Sep. 2021; C.W. Harden leg.; Under embedded rock on stream bank; CUAC000163559 to CUAC000163564, CWH-409 to CWH-414; • 1 ♀; **Pickens Co.**; Clemson Experimental Forest; 34.7431, -82.8481; 14 Oct. 2019; C.W. Harden leg.; Soilwash-flotation berlese, mesic oak-pine woods, dark sandy soil near stream; CWH-057, CUAC000168224; • 1 ♀; **Pickens Co.**; Clemson Experimental Forest; 34.74265, -82.84167; 23 Nov. 2019; C.W. Harden leg.; On underside of large embedded rock during rain, oak-hickory woods, clay soil; CUAC000168225, CWH-060.

GenBank accession numbers for paratypes: OR839739, OR839745, OR839626, OR853280, OR839410, OR853281, OR839413, OR853283, OR838130, OR853110, OR853285, OR839292, OR839553, OR837876, OR838021, OR838209, OR838124, OR853286, OR839554, OR837877, OR838022, OR838210, OR853288, OR839294, OR838079, OR853289, OR839288, OR839289, OR839290.

Other material (*n* = 5, CWHc, CUAC). USA • South Carolina • 1 ♂; **Pickens Co.**; Nine Times Preserve; 34.946, -82.806; 10 Nov. 2019; C.W. Harden leg.; On underside of embedded rock, steep rocky ditch, oak-hickory woods; CUAC000168226, CWH-039; CUAC • 2 ♂; **Pickens Co.**; 3 miles N Clemson; 34.7252, -82.8247; 4 July to 19 December 2022; C.W. Harden leg; buried pipe trap, trap 07; CWHc; • 1 ♀; **Pickens Co.**; Clemson Experimental Forest.; 34.7431, -82.8481; 14 Oct. 2019; C.W. Harden leg.; Soilwash-flotation berlese, mesic oak-pine woods, dark sandy soil near stream; CWH-056, CUAC000163565; CUAC; • 1 ♂; **Pickens Co.**; Clemson Experimental Forest, Pike Road, south of inlet; 34.7116, -82.828; 1 Jun 2023; C.W. Harden and J.R. LaBonte; under rock; CWHc.

Diagnosis. Among members of the *sinuaticollis* group, males are recognized by the modified hind femora (Fig. 12A) bowed anteriorly and triangularly produced posteriorly, with a blunt tuberculate projection in the distal 1/3. The male genitalia (Fig. 35G–I) are similar to those of *A. micamicus*, but differ in the more rounded shape of the apex of the median lobe and the presence of two well-sclerotized strips along the ostium of the internal sac.

Description. ***Habitus*** (Fig. 34E) ABL 1.60–1.89 mm, avg. 1.82 mm, *n* = 7), males larger than females (male mean ABL = 1.85 *n* = 5; female mean ABL = 1.74, *n* = 2). Body moderately depressed dorsoventrally and parallel-sided, relatively elongate (EW/ABL = 0.35–0.37). ***Integument*** Irregular isodiametric microsculpture weakly impressed at anterior angles of pronotum, absent from disk, which is slightly rugose; microsculpture distinct on dorsal surface of head except for sides at base of vertex, where it is stretched and weak or entirely absent. ***Head*** HW/PW = 0.74–0.80, wider in females than in males. Antennomeres IV–X moniliform, slightly clavate. Labrum slightly emarginate. Frontoclypeal horn present, well developed. Three pairs of supraorbital setae present.

Pronotum Variable in length (PL/ABL = 0.23–0.29), broader in males (PW/EW = 0.82) than females (0.78–0.79). Moderately constricted basally (Pbw/PW = 0.75–0.80). Sides slightly sinuate before obtuse hind angles; 3 or 4 basal serrulations present. ***Elytra*** Moderately depressed and parallel sided, not markedly elongate (average EL/ABL = 0.55); humeri not sloped; 3 or 4 weakly impressed striae present; without prominent subapical plica. ***Legs*** Profemora of males not modified; protarsi of males with first tarsomere enlarged and spinose on inner margin (Fig. 10B), with adhesive setae ventrally, second tarsomere unmodified and without adhesive setae. Mesotrochanters of males unmodified. Metafemora of males modified: anterior margin arcuately swollen, posterior margin arcuate proximally towards broad, triangular tuberculate projection in distal 1/2; with several long setae along posterior margin (Fig. 12A). Female legs unmodified. ***Abdominal ventrites*** Unmodified in either sex. ***Male genitalia*** Ring sclerite relatively large (RL/ABL = 0.30), subtriangular and slightly asymmetrical in anterior 1/2. Median lobe (Fig. 35I) arcuate, not strongly twisted from plane of basal lobes; dorsal margin lightly sclerotized for ~ 1/2 of its length; ventral margin without setae, deeply arcuate medially, with shallow sinuation just before apex, which is broadly rounded. Internal sac with flagellum not rotated dorsally, relatively small, and abruptly curved past enlarged basal area; sides lightly sclerotized, "open" laterally; three groups of long, dark spines present near flagellum on left side of internal sac, variable in number; two sclerotized straps present at ostium, one on left side appearing as a broad, vertical strip and the other ventrally, appearing as a U-shape just beyond apex of flagellum in repose. Right paramere (Fig. 35H) partially membranous and enclosed in a feathery sheath, with four setae on apical margin. Left paramere (Fig. 35G) slightly quadrate, with apical margin relatively broad; four long setae present ventrally near apex. The male from the Nine Times Preserve has the dorsal margin of the median lobe nearly straight proximally, giving the organ a more triangular shape overall; the shape of the flagellum and additional sclerites are identical to those in males of other populations. ***Female genitalia*.** Bursa copulatrix with sclerotized folds. Spermatheca long, gradually enlarged distally, forming a loose coil proximally (Fig. 21I). Spermathecal duct short and slightly curved, not coiled.

Distribution. Known only from Pickens Co., SC, from Nine Times Forest south to the historic course of the Twelve Mile River north of Clemson (Fig. 36).

Sympatry. Collected under rocks in association with *A. murrayae* and *Anillinus micamicus* sp. nov. The ranges of *Serranillus dunavani* and *Anillinus* sp. "South Carolina, Waldrop Stone" overlap with this species, but have so far not been collected in association.

Natural history. Members of this species are endogean in habit. Specimens examined were collected from beneath rocks, buried pipe traps and soil washing. Hand collected specimens were found in May, September, October, and November. Teneral specimens were hand collected in September, indicating that immature stages occur in the Spring and Summer.

Species status justification. The combination of external characters is unique within the genus, and the male genitalia are distinct from those of any other described species. The closely related and morphologically similar species *A. micamicus* sp. nov. shows consistent morphological differences in the characters of the male hind legs and genitalia, and sampled individuals of the two species are reciprocally monophyletic in our molecular phylogeny despite occurring together in syntopy under the same rocks. This provides strong support for the hypothesis that the two species are reproductively isolated.

Derivation of species name. A noun in apposition, named for the mineral mica, which is conspicuous in the soils at most localities where this species has been collected.

Anillinus micamicus **sp. nov.**

https://zoobank.org/8230753F-5ECB-4A81-A70B-254DAA91B2FE
Figs 12B, 21H, 24H, 25A, 34F, 35J–L, 36

Type material. *Holotype male* (USNM): point mounted, with abdominal ventrites glued to point and genitalia in Euparal on microslide pinned beneath specimen. Original labels: "USA: SC, Pickens Co. Clemson Experimental Forest Waldrop Stone Falls. 34.7393, -82.8205. 8.x.2021. CW Harden. Under rock on steep slope near falls." "[QR code] CLEMSON-ENT CUAC000168229" "Harden DNA Voucher CWH-402 *Anillinus* "wildcat" M Ext. 19-December-2021 [green-bordered cardstock]" "HOLOTYPE *Anillinus micamicus* Harden & Caterino [orange cardstock]"

GenBank: OR853291, OR839296, OR838075.

Paratypes (*n* = 4; CUAC). **USA • South Carolina • Pickens Co.** • 1 ♂, 1 ♀; same data as Holotype; CUAC000168228 and CUAC000168230, CWH-404 and CWH-405; • 1 ♂; Clemson Experimental Forest; 34.74265, -82.84167; 23 Nov. 2019; CW Harden leg.; On underside of large embedded rock during rain, oak-hickory woods, clay soil; CUAC000168227, CWH-061; • 1 ♂; 3 mi N Clemson; 34.7252, -82.8247; 24 Oct. 2021 to 10 Apr. 2022; CW Harden leg.; Buried pipe trap. Mica-rich sand/clay. Trap 07; CUAC000170085.

GenBank accession numbers for paratypes: OR853293, OR839298, OR839414, OR837797, OR837958, OR838148, OR853292, OR839297, OR838077, OR853290, OR839295, OR838078, OR838252.

Diagnosis. Closely similar to *A. mica*, differing in: metafemora of males not strongly modified (Fig. 12B); the shape of the median lobe (Fig. 35L), especially the sinuate ventral margin near the apex and the armature of the internal sac, which lacks the two distinct saddle-like sclerites present in *A. mica*. The single known female of *A. micamicus* has a spermatheca with a larger proximal coil and slightly shorter stem beyond the coil, and lacks sclerotized folds in the bursa.

Description. *Habitus* ABL = 1.77–1.93 mm, average = 1.87 ± 0.07 mm. Moderately flattened dorsoventrally, body relatively narrow (average EW/ABL = 0.35) (Fig. 34F). ***Integument*** Isodiametric microsculpture present on most of dorsal surface of head, stretched and weakly impressed on center of vertex and sides at base in some specimens; absent from disc of pronotum, but present along all outer margins. ***Head*** HW/PW = 0.75–0.80; antennomeres IV–X moniliform; frontoclypeal horn small, inconspicuous in lateral view; labrum shallowly emarginate; three pairs of supraorbital setae present. ***Pronotum*** PL/ABL = 0.24, PW/EW = 0.81–0.84; Moderately constricted posteriorly (Pbw/PW = 0.76–0.80); sides slightly sinuate before the slightly obtuse hind angles; 3 or 4 basal serrulations present. ***Elytra*** Dorsoventrally flattened, parallel-sided; relatively long (EL/ABL = 0.56–0.57); humeri not sloped; with traces of 3–5 weakly impressed striae; without prominent subapical plica. ***Legs*** Profemora of males unmodified; protarsi of males with first protarsomere moderately expanded and spinose in inner margin, with ventral adhesive setae; second protarsomere of males not expanded and without ventral setae; metafemora of males not swollen, posterior surface weakly tuberculate medially, without prominent projection (Fig. 12B). ***Abdominal ventrites*** Unmodified in either sex. ***Male genitalia*** Ring sclerite large (RL/ABL = 0.29), subtriangular and slightly asymmetrical in anterior 1/2. Median lobe (Fig. 35L) of aedeagus arcuate, enlarged distally, slightly twisted from plane of basal lobes; dorsal margin weakly sclerotized for ~ 1/2 its length; ventral margin asetose, bisinuate before apex, which is abruptly narrowed to a slightly obtuse point. Internal sac with flagellum small and curved, not rotated dorsally, "open" laterally; two groups of small, elongate spines present on left side of sac in repose, in right lateral view appearing as a long U-shaped row below flagellum and a separate small, dark shape behind base of flagellum; left side of ostium with a lightly sclerotized fold, situated above apex of flagellum in right lateral view. Right paramere (Fig. 35K) partially membranous and enclosed in a feathery membranous sheath, with four setae apically. Left paramere (Fig. 35J) subtriangular, with four long subequal setae on ventral margin near apex. ***Female genitalia*** Spermatheca long, gradually enlarged distally, stem coiled proximally (Fig. 21H). Spermathecal duct present, short, slightly curved, without coils. Bursa without sclerotized folds.

Distribution. Known from three nearby localities in southern Pickens Co., SC (Fig. 36).

Sympatry. All of the hand collected specimens were found with *A. mica* under the same rocks. At Waldrop Stone Falls (Fig. 25A), *A. murrayae* was also collected with both species.

Natural history. Specimens have been collected beneath embedded rocks in clay-rich soils and in buried pipe traps. They are presumably endogean in habit. Hand collected specimens were found in October and November.

Species status justification. The combined male genitalic and secondary sexual modifications are unique within the genus, and the DNA sequence data indicate reproductive isolation from other *sinuaticollis*-group species. See justification under *A. mica* above.

Derivation of species name. A noun in apposition created by combining *mica* and *amicus*, meaning friend or companion in Latin, in reference to the repeated cooccurrence of this species and the closely related *A. mica*.

Notes. The following female specimens belong to either *A. mica* or *A. micamicus* (*n* = 5, CUAC): **USA • South Carolina • Pickens Co.**; • 4 ♀; Central, 3 mi N Clemson; 34.7252, -82.8247; 26 Apr. to 12 Jul. 2020; C.W. Harden & M.S. Caterino leg.; Buried pipe trap baited w/ cheese. Mica-rich clay soil, beech, oak; CUAC00017074 to CUAC000170077; • 1 ♀; same locality as previous; 11 Apr. to 14 Aug. 2021; C.W. Harden leg.; Buried pipe trap. Mica-rich sand/clay. Trap-01; CUAC000170078.

Anillinus seneca **sp. nov.**

https://zoobank.org/3ECB8AD7-7F13-46A2-8500-F72D6A9C2B32
Figs 12D, 21K, 24J, 34D, 35D–F, 36

Type material. *Holotype male* (USNM): point mounted, with abdominal ventrites glued to point and genitalia in Euparal on microslide pinned beneath specimen. Original labels: "USA: SOUTH CAROLINA, Oconee Co. Lake Hartwell, Martins Creek Landing, SW of Clemson. 34.6389, -82.8656. 11-January-2020. C.W. Harden. Under embedded rocks in oak-hickory woods near lake.” “[QR Code] CLEMSON-ENT CUAC000168244” “Harden DNA Voucher CWH-121 Anill. sp n ‘martincrk’ Ext. 13/May/2020 [green-bordered cardstock]” “HOLOTYPE *Anillinus seneca* Harden & Caterino [orange cardstock]”

GenBank: OR853323, OR839466.

Paratypes (*n* = 27; CMNH, CUAC, LSAM, USNM, VMNH). **USA • South Carolina** • 2 ♂, 2 ♀; same data as holotype; CUAC000168247, CUAC000168248, CUAC000168250, CUAC000168242; CWH-118, CWH-120, CWH-122, CWH-124; CUAC;• 1 ♂, 2 ♀; same locality as holotype; 4 Jan. 2020; C.W. Harden & L.M. Thompson leg.; soilwash flotation Berlese; CWH-115 to CWH-117, CUAC000168239 to CUAC000169241; CUAC; • 2 ♂, 5 ♀; **Oconee Co**.; Martin Creek Landing; 34.6388, -82.8655; 15 May 2022; C.W. Harden and L.M. Thompson leg.; soilwashing; CMNH, USNM; • 3 ♂, 2 ♀; **Oconee Co.**; Martin Creek Landing; 34.6390, -82.8638; 22 Oct. 2021; C.W. Harden leg.; under rock; LSAM, VMNH; • 4 ♂, 4 ♀; **Oconee Co.**; South Cove Park; 34.71165, -82.96594; 30 Jan. 2020; C.W. Harden & L.M. Thompson leg.; Berlese, sifted soil/wood, pine stump near fishing pier; CWH-338 to CWH-345, CUAC000168255 to CUAC000168262; CUAC.

GenBank accession numbers for paratypes: OR839463, OR839465, OR839467, OR853324, OR839469, OR839460, OR839461, OR839462, OR853327, OR839630, OR838053, OR853328, OR839631, OR839632, OR839633, OR853326, OR839621, OR838050.

Other material (*n* = 40 CUAC, CWHc). USA • South Carolina • 2 ♂; **Anderson Co.**; Clemson Experimental Forest, Big Oaks area near Lake Hartwell; 34.60262, -82.83858; 21 May 2020; C.W. Harden; Under embedded rock in clay soil; CWH-161 and CWH-162, CUAC000168245 and CUAC000168251; CUAC; • 1 ♂, 1 ♀; **Anderson Co.**; Clemson Experimental Forest, Big Oaks area; 34.60225, -82.83893; 21 May 2020; C.W. Harden & L.M. Thompson; Berlese, deep soil by large stump near lake, after flood; CWH-163 and CWH-164, CUAC000168252 and CUAC000168253; CUAC; • 1 ♂; **Anderson Co.**; River Forks Recreation Area; 34.47497, -82.80914; 19 Mar. 2021; C.W. Harden & L.M. Thompson; Berlese, sifted pine stump soil, near lake; CWH-327, CUAC000168254; CUAC; • 2 ♂, 1 ♀; **Anderson Co.**; Clemson Experimental Forest, Big Oaks Area near Lake Hartwell; 34.60225, -82.83893; 21 May 2020; C.W. Harden and L.M. Thompson leg.; deep soil Berlese; CWHc; • 1 ♂, 2 ♀; **Anderson Co.**; Clemson Experimental Forest, Big Oaks; 34.61559, -82.83061; 25 Mar 2020; C.W. Harden leg.; deep soil and litter Berlese; CWHc; • 2 ♂; **Oconee Co.**; Lake Hartwell, Martin Creek Landing, SW of Clemson; 34.6389, -82.8656; 4 Jan. 2020; C.W. Harden & L.M. Thompson leg.; soilwash flotation Berlese; CUAC000168237 and CUAC000168238; CWH-070 and CWH-114; CUAC; • 1 ♂, 2 ♀; same data as previous; CWHc; • 2 ♂; **Oconee Co.**; Lake Hartwell, Martin Creek Landing, SW of Clemson; 34.6389, -82.8656; 4 Jan. 2020; C.W. Harden leg.; On underside of deeply embedded rocks; CUAC000168243 and CUAC000168233; CWH-062 and CWH-063; CUAC; • 3 ♂; **Oconee Co.**; Lake Hartwell, Martin Creek Landing, SW of Clemson; 34.6389, -82.8656; 31 Dec. 2019; C.W. Harden & L.M. Thompson leg.; On underside of deeply embedded rocks; CUAC000168234 to CUAC000168236; CWH-064 to CWH-066; CUAC; • 1 ♂, 1 ♀; **Oconee Co.**; Lake Hartwell, Martin Creek Landing, SW of Clemson; 34.6389, -82.8656; 11 Jan. 2020; C.W. Harden leg.; Under embedded rocks; CUAC000168246 and CUAC000168249; CWH-119 and CWH-

123; CUAC; • 1 larva; **Oconee Co.**; Martin Creek Landing; 34.6388, -82.8655; 15 May 2022; C.W. Harden and L.M. Thompson leg.; soilwashing; CWHc; • 2 ♂, 6 ♀; **Oconee Co.**; Martin Creek Landing; 34.6388, -82.8644; 22 Oct 2021; C.W. Harden leg.; under rock; CWHc; • 1 ♂, 2 ♀; **Oconee Co.**; Martin Creek Landing; 34.6390, -82.8638; 22 Oct 2021; C.W. Harden leg.; under rock; CWHc; • 1 ♀; **Oconee Co.**; Martin Creek Landing; 34.6391, -82.8636; 22 Oct 2021; C.W. Harden leg.; under rock; CWHc; • 1 ♀; **Oconee Co.**; Martin Creek Landing; 34.6393, -82.8633; 22 Oct 2021; C.W. Harden leg.; under rock; CWHc; • 2 ♀; **Oconee Co.**; Lake Hartwell, Martin Creek Landing, southwest of Clemson; 34.6389, -82.8656; 4 Jan 2020; C.W. Harden and L.M. Thompson leg.; CWHc; • 1 ♂; **Oconee Co.**; Martin Creek Landing, southwest of Clemson; 34.6389, -82.8656; 13 Feb. 2023; C.W. Harden leg.; under rock; CWHc.

Diagnosis. Males with metafemora not heavily modified, with a median tuberculate area on posterior margin (Fig. 12D), sometimes with a small blunt tooth. Male genitalia distinctive (Fig. 35D–F): median lobe of aedeagus with straight and narrow ventral margin, internal sac without groups of spines, flagellum relatively large and evenly curved.

Description. ***Habitus*** Widely variable in body size (ABL = 1.46–1.78 mm, average = 1.63 ± 0.08) and shape, with smaller specimens being more convex and ovoid (Fig. 34D) and larger specimens being flatter and more parallel sided (similar to Fig. 34E). Males and females similarly variable in size (ABL = 1.51–1.78 mm and 1.46–1.78 mm, respectively). Not markedly narrow (average EW/ABL = 0.36). ***Integument*** Dorsal surface of head fully microsculptured; microsculpture coverage of pronotum varying: usually lacking from disc and present across entire anterior margin and along sides, sometimes absent anteriorly except for anterior angles; sometimes distinct across entire anterior 1/4, including part of disc. ***Head*** HW/PW = 0.74–79, antennomeres IV–X moniliform; frontoclypeal horn small, but distinct in lateral view; three pairs of supraorbital setae present, outer posterior pair smaller than other two. ***Pronotum*** Size and shape variable: PL/ABL = 0.22–0.24, PW/EW = 0.78–0.87, PbW/PW = 0.73–0.79. Sides either convergent or distinctly sinuate before posterior angles, which are either obtuse or nearly right. ***Elytra*** Variable in shape, either parallel sided and flat or slightly ovoid and convex. EL/ABL = 0.52–0.56. ***Legs*** Profemora of males unmodified. First protarsomere of males dilated and spinose on inner margin, bearing adhesive setae ventrally; second protarsomere of males unmodified. Mesotrochanters of males unmodified. Metafemora of males variable, either slightly enlarged medially with patch of coarse microsculpture (Fig. 12D) or swollen and bearing a blunt tooth on posterior margin. Females without leg modifications. ***Abdominal ventrites*** Unmodified in either sex. ***Male genitalia*** Aedeagus small (RL/ABL = 0.23). Median lobe (Fig. 35F) slightly rotated dorsally from plane of basal lobes, also curved towards left side in apical 1/2; slightly narrowed apically; ventral margin evenly curved, not expanded, without setae; dorsal margin sclerotized for ~ 2/3 its length; apex small, rounded. Internal sac covered in small scales, without spines; flagellum relatively long, not rotated dorsally, sinuate, abruptly narrowed apically, lightly sclerotized, and “open” laterally. Right paramere (Fig. 35E) small, broadly rounded, with four apical setae. Left paramere (Fig. 35D) subtriangular, ventral margin with four apical setae of variable length. ***Female genitalia*** Spermatheca long, abruptly expanded distally, stem with loose proximal coil, nearly straight before enlarged apex which is strongly curved (Fig. 21K). Spermathecal duct short, not coiled.

Distribution. Endemic to South Carolina, known from Oconee and Anderson Counties on both sides of the former Seneca River (currently Lake Hartwell) from Seneca south to River Forks recreation area (Fig. 36).

Sympatry. At the type locality, *S. dunavani* and a large *Anillinus* species belonging to the *valentinei* group (*Anillinus* sp. "South Carolina, Waldrop Stone") also occur. The other South Carolina members of the *sinuaticollis* group are apparently allopatric with respect to *A. seneca*.

Natural history. Members of this species are endogean, inhabiting mineral soil layers in sandy clay rich soils. They have been collected beneath embedded rocks and through Berlese extraction of soil and washed soil. In samples from the type locality, Laboulbeniales fungi were observed on the dorsal surface of pronotum and elytra of several females and on the abdominal apex in a male. Specimens were collected in January, February, March, May, October, and December.

Species status justification. The male genitalia are unique within the genus. DNA sequence data indicate that *A. seneca* is sister to the pair of *A. mica* and *A. micamicus*, both of which differ markedly in male genitalic characters.

Derivation of species name. A noun in apposition, named for the former Seneca River. The known localities for this species are all near the former course of this river, which was lost due to the construction of Lake Hartwell in the 1950s.

Notes. DNA sequences of individuals from the opposite side of the historic course of the Seneca River in Anderson Co. are divergent from Oconee Co. individuals. There are no differences in genitalic morphology, and the divergence is interpreted as recent intraspecific variation. Still, those Anderson Co. individuals are not made part of the type series, in case future study concludes they are specifically distinct.

Anillinus **sp. "South Carolina, Coon Branch"**

Figs 21G, 25B, 36

Material examined (*n* = 3). USA • South Carolina • Oconee Co.; Coon Branch Natural Area; • 1 ♂, 1 ♀; 35.020, -83.000; 21 Jun. 2018; B. Owens and C. Carlton leg.; soil flotation; CUAC000168231 and CUAC000168232, CWH-102 and CWH-178; CUAC • 1 ♂; 35.0256, -83.0050; 2 Oct. 2021; C.W. Harden leg.; on soil under large rock.; CWHc.

GenBank: OR853183, OR839228, OR839449, OR837811, OR837968, OR838156, OR839507, OR837843, OR837990, OR838176.

Diagnosis. The male genitalia are similar to those of *A. mica* and *A. micamicus*, but differ in several characters: the shape of the median lobe is more elongate, with the ventral margin less curved and abruptly straightened at apex, which is obtusely angulate; the internal sac has a flagellum that is similar to *A. micamicus*, and has a single group of approximately 12 elongate, well-sclerotized spines on the left side; there is a sclerotized saddle like structure near the ostium, as in *A. mica*, but it is situated dorsal to the level of the flagellum; a pair of parallel rows of small sclerotized teeth run along the left side of the ostium, appearing as a pair of dark curved lines below the saddle like structure. The right paramere is encased in a membranous sheath as in *A. mica* and *A. micamicus*. The left paramere is shaped similar to that of *A. micamicus*, but the inner two setae on the apical margin are much shorter than the outer two, which are elongate but not as much as in *A. mica* and *A. micamicus*. The spermatheca (Fig. 21G) has a stem that is coiled evenly in a spiral; it is evenly enlarged distally. The duct has a single sharp bend just behind the junction with the spermatheca, and is otherwise straight and relatively wide, without coils. The bursa has a few lightly sclerotized regions.

Notes. The data from morphology and DNA sequences indicate that these individuals might represent a species distinct from *A. micamicus*. However, more sampling in the intervening area between Coon Branch and the localities of *A. micamicus* will be necessary to test this hypothesis.

'*langdoni* group'

***Anillinus* cf. *nantahala* Dajoz, 2005**

Figs 21O, 37A,B, 38

Anillinus nantahala Dajoz: 2005: 210.

Notes on type material. Dajoz (2005) designated a holotype and an unspecified number of paratypes, all deposited in his personal collection. Upon Dajoz's death in 2019, his collection was deposited in the Muséum National d'Histoire Naturelle in Paris (Kippenhan 2023). On 11 December 2023, CWH submitted a request for a digital loan of the holotype of *A. nantahala* (request #181113), but as of March 2024 this has not been processed. We have not studied the type material of this species, and our interpretation of the name is explained in the notes section below.

Material examined (*n* = 148). USA • **Georgia** • 1 ♂; **Habersham Co.**; Big Panther Creek Trail; 34.68, -83.40; 12 Sep. 1999; W. Reeves leg.; CWHc; • 3 ♂, 1 ♀; **Towns Co.**; Chattahoochee National Forest, Little Bald Mountain, north of Brasstown Bald; 34.8829, -83.8094; 2 Jul. 2020; M. Caterino leg.; CWH-186, CWH-188, CWH-194, CWH-195, CUAC000182284 to CUAC000182287; CUAC; • **North Carolina** • 3 ♂, 2 unsexed; **Cherokee Co.**; Hickory Branch trail; 35.2165, -83.7047; 26 Jul. 2015; S. Myers leg.; SSM59, SSM62 to SSM66, CUAC000182289, CUAC000182290, CUAC000185551, CUAC000182293, CUAC000182294; CUAC; • 32 ♂, 16 ♀; **Clay Co.**; Nantahala National Forest, Tusquitee Bald; 35.1425, -83.7260; 6 Jul. 2021; • 1 ♂; **Clay Co.**; Nantahala National Forest, Shooting Creek Bald trail; 35.0674, -83.6452; 11 May 2020; C.W. Harden and M.S. Caterino leg.; CWH-179, CUAC000182280; • 1 ♀; **Clay Co.**; Nantahala National Forest, Riley Knob, off Highway 64 ca. 8 km northeast of Shooting Creek; 35.0678, -83.6193; 11 May 2020; C.W. Harden and M.S. Caterino leg.; CWH-181, CUAC000182279; • 1 ♂; **Graham Co.**; Nantahala National Forest, Huckleberry Knob; 35.3216, -83.9929; 4 May 2020; M. Caterino and F. Etzler leg.; CWH-283, CUAC000182281; • 1 ♂; **Graham Co.**; Joyce Kilmer Memorial Forest; 35.3467, -83.9688; 20 Jul. 2015; S. Myers leg.; SSM22, CUAC00182288; • 1 ♀; **Graham Co.**; Joyce Kilmer Memorial Forest; 35.3448, -83.9649; 24 Jun. 2015; S. Myers and M. Caterino leg.; SSM37, CUAC000182292; • 2 unsexed; **Graham Co.**; Joyce Kilmer Memorial Forest; 35.3426, -83.9660; 24 Jun. 2015; S. Myers and M. Caterino; SSM38 and SSM61, CUAC000185877 and CUAC000182291;

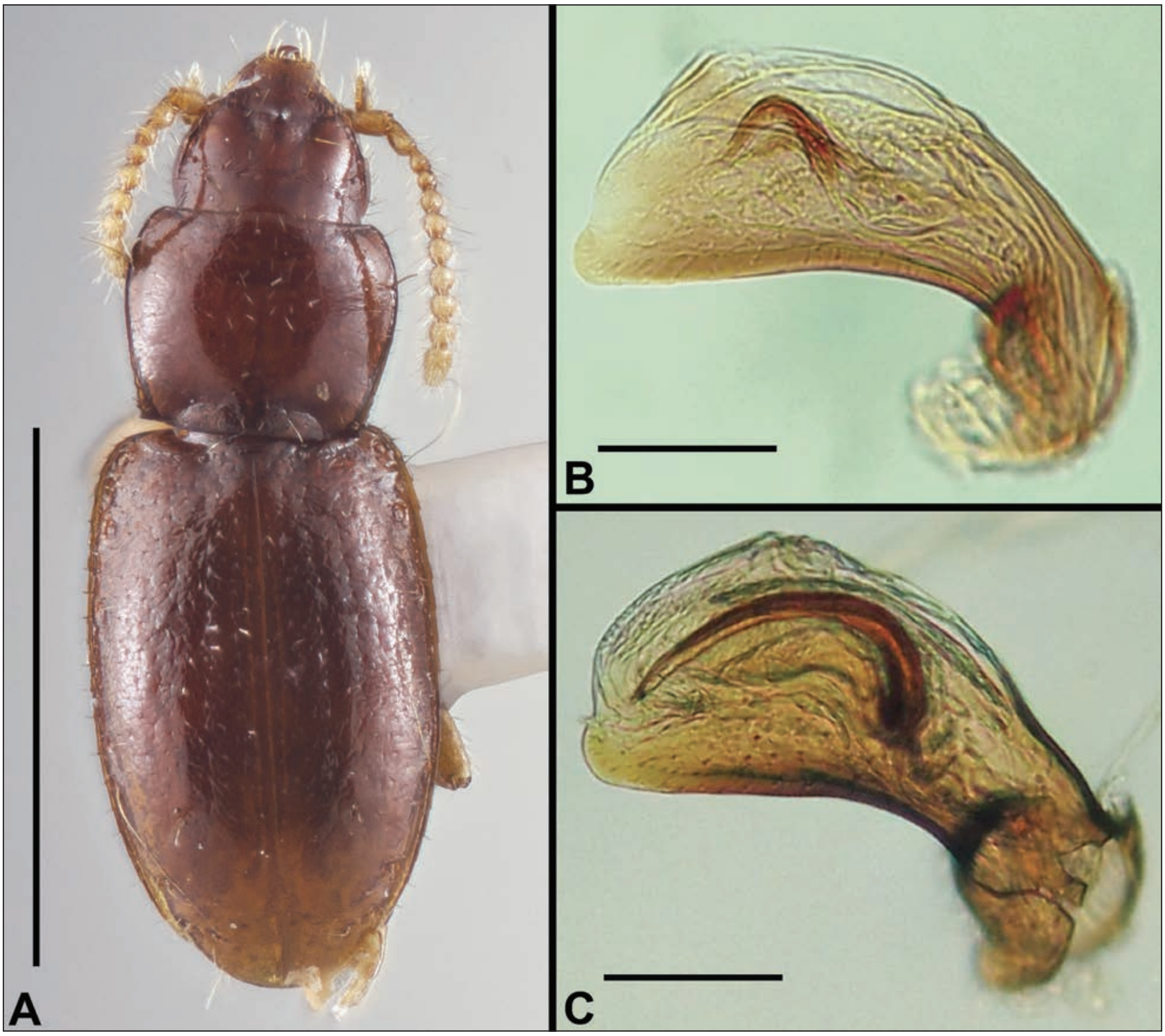

Figure 37. *Anillinus* species in the *langdoni* group **A** *Anillinus* cf. *nantahala*, dorsal habitus **B** median lobe, right dorsolateral aspect of *A. nantahala* **C** median lobe right dorsolateral aspect of *Anillinus* sp. "Georgia, Brasstown Bald sp. 1". Scale bars: 1 mm (**A**); 0.1 mm (**B, C**).

• 1 ♂, 1 ♀; **Graham Co.**; Nantahala National Forest, Teyahalee Bald; 35.2559, -83.8043; 12 Apr. 2022; • 1 ♂, 2 ♀; **Graham Co.**; Nantahala National Forest, Teyahalee Bald; 35.2585, -83.7959; 19 Jul. 2019; • 5 ♂, 3 ♀; **Graham Co.**; Nantahala National Forest, Teyahalee Bald; 35.2598, -83.7970; 12 Apr. 2022; • 1 ♂; **Graham Co.**; Nantahala National Forest, Cherohala Skyway, Stratton Ridge; 35.3382, -84.0249; 4 May 2020; C.W. Harden leg.; • 1 ♀; **Macon Co.**; Nantahala National Forest, off Wayah Road ca. 10 km east of Rte 64; 35.1554, -83.5581; 20 Oct. 2019; C.W. Harden leg.; CWH-054, CUAC000182274; • 3 ♂, 2 ♀; **Macon Co.**; Nantahala National Forest, Wayah Bald Road; 35.1700, -83.5811; 18 Apr. 2020; C.W. Harden leg.; CWH-139 to CWH-142, CWH-167, CUAC000182275 to CUAC000182278, CUAC000185892; • 4 ♂; same data as previous; • 1 ♂; **Macon Co.**; Eight miles west of Franklin; 35.1550, -83.5220; 19 Mar. 1976; Q.D. Wheeler leg.; OSUC441957; OSUC; • 5 ♂, 9 ♀; **Macon Co.**; Wayah Bald; 35.1790, -83.5620; 29 Jun. 2013; T. Lawton leg.; TLc; • **South Carolina** • 1 ♂; **Oconee Co.**; Sumter

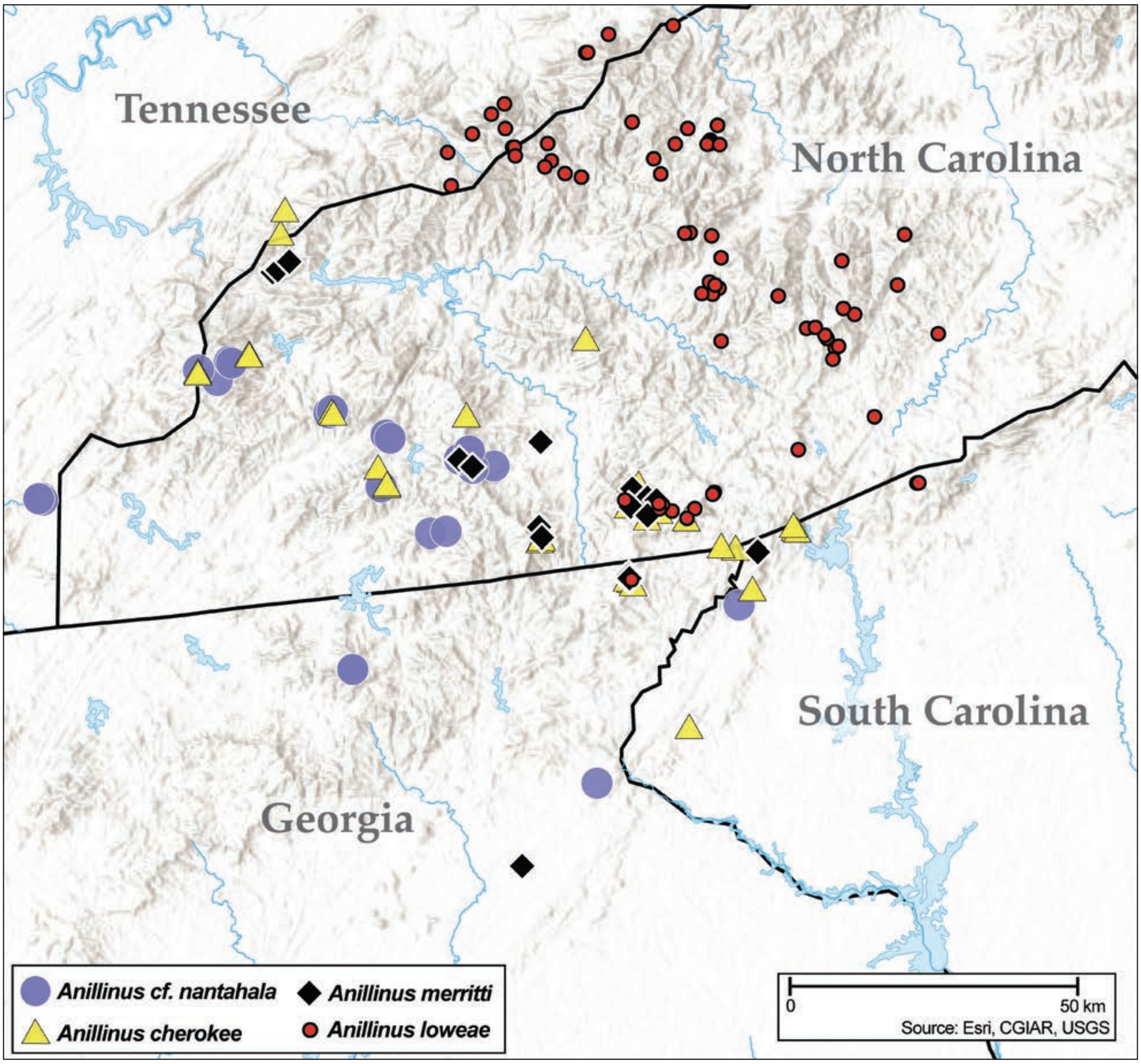

Figure 38. Distribution map of *langdoni*-group and *loweae*-group species that occur in South Carolina. Data are from Harden (2024).

N.F., near Chattooga River; 34.9170, -83.1166; 5 Sep. 2015; M. and K. Caterino leg.; CWH-494, CUAC000110284; • TENNESSEE • 1 ♂; **Polk Co.**; Cherokee National Forest, Miller Cove; 35.1766, -84.3241; 28 May 2020; C.W. Harden leg.; CWH-349, CUAC000182282; • 1 ♀; **Polk Co.**; Cherokee National Forest, Miller Cove; 35.1758, -84.3246; 28 May 2020; C.W. Harden leg.; CWH-350, CUAC000182283; • 8 ♂, 5 ♀; **Polk Co.**; Cherokee National Forest, John Muir trail, Highway 68 ca. 3 km north of Farner; 35.1771, -84.3298; 23 May 2021; C.W. Harden and K. Ivanov leg.; • 12 ♂, 16 ♀; **Polk Co.**; Cherokee National Forest, John Muir trail, Highway 68 ca. 3 km north of Farner; 35.1771, -84.3298; 7 Nov. 2022; C.W. Harden leg.

GenBank: GU556025, GU556075, MK112078, MK118201, OR830242, OR837795, OR837826, OR837827, OR837844, OR837846, OR837849, OR837956, OR837980, OR837981, OR837991, OR837993, OR837995, OR838110, OR838120, OR838146, OR838167, OR838168, OR838177,

OR838179, OR838181, OR838183, OR838292, OR838293, OR839324–OR839327, OR839407, OR839483– OR839486, OR839506, OR839508, OR839510, OR839514, OR839516, OR839522, OR839523, OR839604, OR839637, OR839748, OR839812, OR839813, OR853329–OR853338.

Literature records. This species has previously been reported only from the type locality, Wayah Bald, Macon Co., North Carolina (Dajoz 2005).

Diagnosis. Externally typical of the *langdoni* group (Fig. 37A), with fully developed dorsal microsculpture on the head and pronotum and a moderately convex habitus. The male genitalia (Fig. 37B) are most similar to *A. pusillus*, with the ventral margin narrow and the flagellum short, but unlike *A. pusillus*, the flagellum in *A. nantahala* is sinuate at its apex. Spermatheca with short basal bend, gradually enlarged apically (Fig. 21O). Spermathecal duct long and not coiled. The single individual of this species known from South Carolina has an ABL of 1.73 mm.

Distribution. Relatively widespread in the southern Appalachians from the flank of the Unicoi Mountains in Tennessee to South Carolina, where it is known only from Oconee Co. near the Chattooga River (Fig. 38).

Sympatry. Other species of anillines known from the Chattooga River gorge include *Serranillus dunavani*, *A. cherokee*, *A. merritti*, and *A. murrayae*.

Natural history. The single South Carolina specimen was collected in a sample of sifted litter, as were most of the other specimens examined.

Notes. The description and illustrations of *A. nantahala* are terse, and it is impossible to confidently determine the identity of the species that the name refers to. Four species of *Anillinus* have been collected at the type locality (Wayah Bald, Macon Co., NC), and so the name could apply to any of these. However, the description did specify that members of *A. nantahala* have the dorsal microsculpture on the forebody fully developed, and the species we have chosen to apply the name to is the most abundant and readily collected species at Wayah Bald, and therefore most likely to be encountered by a traveling collector with limited time (as Dajoz was).

***Anillinus* sp. “Georgia, Brasstown Bald sp. 1”**

Fig. 37C

Material examined (*n* = 5). **USA** • **Georgia** • 2 ♂; **Towns Co.**; Chattahoochee National Forest, Little Bald Mountain north of Brasstown Bald; 34.8829, -83.8094; 2 Jul. 2020; M.S. Caterino leg.; CWH-192 and CWH-193, CUAC000182295 and CUAC0001822296; • 2 ♂; **Towns Co.**; Chattahoochee National Forest, Brasstown Bald; 34.8766, -83.8109; 2 Jul. 2020; M.S. Caterino leg.; CWH-196 and CWH-197; CUAC000182297 and CUAC000182298; • **South Carolina** • 1 ♂; **Pickens Co.**; Sassafras Mtn; 21 July 1967; S. Peck and A. Fiske leg.; B-1377A; CMNH.

GenBank: OR837853– OR837855, OR837999, OR838000, OR838186–OR838188, OR839277, OR839520, OR839521, OR839524, OR839525, OR853248, OR853249.

Diagnosis. The only specimen of this species seen from South Carolina is slide mounted and distorted beneath a cover slip. The genitalia are identical to specimens from the vicinity of Brasstown Bald in northern Georgia (Fig. 37C). Individuals from Georgia are externally typical members of the *langdoni* group, measuring 1.63–1.77 mm. The median lobe is simple, with the ventral margin moderately expanded and the apex not deflected, simply rounded. The flagellum is enormous, well-sclerotized and strongly curved, without an apical sinuation; a lightly sclerotized basal piece is apparent ventral to the flagellum.

Notes. Considering the disjunct locality and the absence of this species in any other samples taken from Sassafras Mountain, or anywhere other than the vicinity of Brasstown Bald, the South Carolina record is doubtful.

‘*loweae* group’

Anillinus cherokee Sokolov & Carlton, 2008

Figs 21P, 24O, 25B, 38, 39C

Anillinus cherokee Sokolov & Carlton, 2008: 40.

Material examined. ***Holotype male*** (**USNM**), point mounted, not dissected, labeled: “USA: NC: Graham Co. Nantahala NF, Joyce Kilmer Memorial, 83°56'03" W 35°21'20" N leaf/log Berlese C. Carlton 05 Apr 2004” “♂” “HOLOTYPE *Anillinus cherokee* sp. n. Sokolov and Carlton des. 2008”

Other material (*n* = 323). USA • Georgia (new state record) • 1 ♂; **Rabun Co.**; Chattahoochee National Forest, Rabun Bald trail; 34.9724, -83.3020; 29 Sep. 2019; C.W. Harden leg.; CWH-026, CUAC000169308; • 1 ♀; **Rabun Co.**; Chattahoochee National Forest, Rabun Bald trail; 34.9716, -83.3013; 29 Sep. 2019; C.W. Harden leg.; CWH-028, CUAC000169307; • 1 ♀; **Rabun Co.**; Chattahoochee National Forest, 0.6 km south of Rabun Bald trailhead; 34.9748, -83.3059; 26 Oct. 2019; C.W. Harden leg.; CWH-096, CUAC000169306; • 4 ♂, 1 ♀; **Rabun Co.**; Rabun Bald, rotten wood debris; 34.967, -83.299; 30 May 1964; H.R. Steeves and J.D. Patrick, Jr. leg.; CMNH; • 1 ♀; **Rabun Co.**; Rabun Bald, rotten wood debris; 34.967, -83.299; 9 Jul. 2014; T. Lawton leg.; TLc; • **North Carolina** • 1 ♂; **Clay Co.**; Nantahala National Forest, Chunky Gal trail; 35.1467, -83.7146; 1 Sep. 2020; P. Wooden and F. Etzler leg.; CWH-506, CUAC000182308; • 2 ♂; **Clay Co.**; Nantahala National Forest, Chunky Gal trail; 35.1471, -83.7144; 6 Jul. 2021; M.S. Caterino leg.; • 1 ♂, 1 ♀; **Graham Co.**; Nantahala National Forest, Teyahalee Bald; 35.2585, -83.7959; 19 Jul. 2019; • 1 ♂; **Graham Co.**; Nantahala National Forest, Teyahalee Bald; 35.2598, -83.7970; 12 Apr. 2022; • 2 ♂; **Graham Co.**; Nantahala National Forest, Stratton Ridge, Cherohala Skyway; 35.3382, -84.0249; 27 Sep. 2020; C.W. Harden leg.; • 1 ♂; **Graham Co.**; Nantahala National Forest, below Stratton Ridge parking; 35.3390, -84.0250; 28 May 2020; C.W. Harden leg.; CWH-191, CUAC000169309; • 1 ♂, 2 ♀; **Graham Co.**; Joyce Kilmer Memorial Forest, 25 mi southwest of Tapoco; 35.357, -83.933; 24 Aug. 1974; J.L. Bengston; CMNH; • 1 ♂; **Graham Co.**; Cherokee National Forest, Wright Creek Trail [*sic*]; 19 Oct. 2007; I. Sokolov leg.; NCSU_ENT00293740; • 1 ♀; **Macon Co.**; Ellicott Rock; 35.0029, -83.1094; 29 Jun. 2015; S. Myers leg.; SSM249, CUAC000170595; • 1 ♂, 1 ♀; **Macon Co.**; Ellicott Rock; 35.0075, -83.1358; 18 Jul. 2015; S. Myers leg.; SSM97 and SSM248, CUAC000169311 and CUAC000170594; • 5 ♂, 7 ♀; **Macon Co.**; Coweeta Hydrological Lab, ca. 13 mi west of Highlands; 35.045, -83.451; 8 Aug. 1965; H.R. Steeves leg.; CMNH; • 8 ♂, 30 ♀; **Macon Co.**; Coweeta Hydrological Lab, ca. 13 mi west of Highlands; 35.045, -83.451; 22 May 1965; H.R. Steeves leg.; • 47 ♂, 63 ♀; **Macon Co.**; Coweeta Hydrological Lab, ca. 13 mi west of Highlands; 35.045, -83.451;

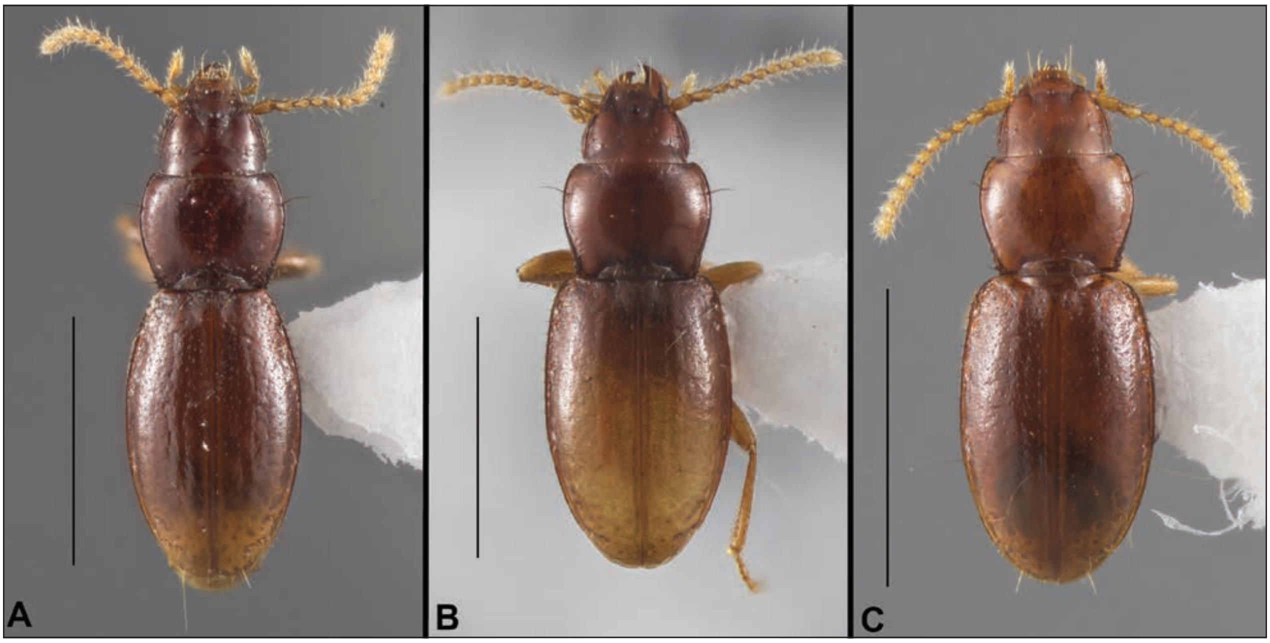

Figure 39. Dorsal habitus of female *Anillinus* in the *loweae* group **A** *Anillinus merritti*, sloped-humeri form (Georgia, Rabun Bald) **B** *Anillinus loweae* (Georgia, Rabun Cliffs) **C** *Anillinus cherokee* (South Carolina, Coon Branch). Scale bars: 1 mm.

23 May 1965; H.R. Steeves leg.; • 11 ♂; **Macon Co.**; Coweeta Hydrological Lab, ca. 13 mi west of Highlands; 35.045, -83.451; no date; H.R. Steeves leg.; • 2 ♂, 1 ♀; **Macon Co.**; Coweeta Hydrological Lab; 35.045, -85.451; 8 Jun. 1973; W. Suter leg.; • 1 ♂, 7 ♀; **Macon Co.**; Highlands vicinity; 35.05, -83.19; 7 Jul. 1981; J. Pakaluk leg.; • 1 ♂; **Macon Co.**; Turtle Pond Creek, ca. 4 mi west northwest of Highlands; 35.06, -83.26; 8 Aug. 1970; T.C. Barr leg.; • 1 ♂, 1 ♀; **Macon Co.**; Dry Fall, Cullasaja River; 35.067, -83.238; 27 Jun. 1949; J.M. Valentine leg.; • 1 ♂; **Macon Co.**; Jones Gap; 35.0785, -83.2923; 22 Jul. 2015; S. Myers leg.; SSM173, CUAC000169310; • 26 ♂, 31 ♀; **Macon Co.**; 4 mi northwest of Highlands near Buckhorn Gap; 35.0850, -83.2600; 22 Aug. 1982; J. Pakaluk leg.; • 3 ♂, 4 ♀, 2 unsexed; **Macon Co.**; 0.6 mi northeast of Goldmine, California Ridge; 35.110, -83.2710; 14 May 1971; T.C. Barr leg.; • 8 ♂, 2 ♀; **Macon Co.**; 0.2 mi southeast of Old Road Gap; 35.173, -83.726; 15 May 1971; T.C. Barr leg.; • 2 ♂; **Macon Co.**; Nantahala National Forest, Copper Ridge Bald; 35.2348, -83.5596; 15 Sep. 2020; F. Etzler leg.; CWH-504 and CWH-505, CUAC000182306 and CUAC000182307; • 1 ♂; **Macon Co.**; Nantahala National Forest, Cowee Bald; 35.3269, -83.3350; 15 Sep. 2020; F. Etzler leg.; CWH-507, CUAC000182309; • **South Carolina** • 1 ♀; **Oconee Co.**; Sumter National Forest, Doran Creek, off Spy Rock Road; 34.7512, -83.2244; 30 Mar. 2021; C.W. Harden and L.M. Thompson leg.; CWH-357, CUAC000169305; • 3 ♂, 1 ♀; **Oconee Co.**; 7 mi south of NC state line on Highway 107; 34.942, -83.089; 29 May 1983; D.S. Chandler leg.; LSAM0295327 to LSAM0295330; • 8 ♀; **Oconee Co.**; Coon Branch Natural Area; 35.017, -82.997; 18 Oct. 2020; C.W. Harden leg.; • 8 ♂; **Oconee Co.**; Coon Branch Natural Area; 35.0200, -83.0000; 21 Jun. 2018; B. Owens and C. Carlton leg.; CWH-103 to CWH-110, CUAC000169292 to CUAC000169299; • 10 ♀; **Oconee Co.**; Coon Branch Natural Area; 35.0200, -83.0000; 21 Jun. 2018; B. Owens and C. Carlton leg.; CUAC000169300 to CUAC000169316; • 1 ♂, 1 ♀; **Oconee Co.**; Coon Branch Natural Area; 35.0256, -83.0050; 2 Oct. 2021; C.W. Harden leg.

Literature records. USA • Tennessee • Blount Co.; Great Smoky Mountains National Park, upper Gregory Ridge Trail; 35.5268, -83.8530; 12 Apr. 2006; A.K. Tishechkin leg.; • **Blount Co.**; Great Smoky Mountains National Park, upper Gregory Ridge Trail; 35.5583, -83.8416; 28 Jul. 2004; A.K. Tishechkin leg.

Diagnosis. The male genitalia are unique: the median lobe is strongly curved and twisted dorsally, lacking a prominent dorsal projection apically; the flagellum is short and rotated dorsally so that in right dorsolateral view it is seen through the base. The female spermatheca is S-shaped (Fig. 21P), with the basal bend shallower than that in *A. loweae* and *A. merritti*. The spermathecal duct is short and not coiled. In SC, females are smaller than those of other *loweae*-group species (Fig. 39C).

Distribution. Western Smokies (Blount Co., TN) south to Graham Co, NC and east to Rabun Co, GA and Oconee Co, SC (Fig. 38).

Sympatry. In SC, specimens of *A. cherokee* have been collected with *A. murrayae*, *A.* sp. "South Carolina, Coon Branch", and *S. dunavani* at Coon Branch, Oconee Co. At Rabun Bald, GA, *A. cherokee* co-occurs with the closely-related species *A. merritti*.

Natural history. Specimens examined were collected from sifted litter, sifted woody debris, underneath rocks, soil washing, and buried pipe traps. Ferro et al. (2012) found *A. cherokee* to be significantly associated with primary forest.

Notes. Jeannel's illustration of the aedeagus of *Anillinus dohrni* (Ehlers) (1963a, fig. 64) is identical to the appearance of that of *A. cherokee* in left lateral aspect. The specimen figured was collected in Clayton, GA, within the known range of *A. cherokee*. The specimen Jeannel had before him was most likely a member of *A. cherokee*. The identity of *A. dohrni* remains unknown; the female type (Academy of Natural Sciences, Philadelphia) is labeled "Florida" without further information. Images of the type sent to us by J. Weintraub show the specimen to be in good condition, with an ABL of 1.60 mm and a moderately convex habitus similar to females of several species groups of *Anillinus*.

Anillinus loweae **Sokolov & Carlton, 2004**

Figs 2O, 21Q, 24N, 38, 39B

Anillinus dunavani Jeannel 1963: 76; Barr 1995: 245.
Anillinus loweae Sokolov & Carlton, 2004: 218.

Material examined. ***Holotype male*** (**USNM**), point mounted, not dissected, labeled "USA: NC: Haywood Co., GSMNP, Cataloochee Divide Trail near Purchase, UTM311819 E 3940339 N C. Carlton 17 July 2002" "HOLOTYPE *Anillinus loweae* sp. n. Sokolov and Carlton des 2003"

Other material (*n* = 244). USA • Georgia (new state record) • 2 ♂, 1 ♀; **Rabun Co.**; Chattahoochee National Forest, Rabun Cliffs; 34.9707, -83.3008; 25 Nov. 2019; M.S. Caterino leg.; CWH-280 to CWH-282, CUAC000168354 to CUAC000168356; • **North Carolina** • 1 ♀; **Canton Co.**; Art Loeb Trail; 35.3957, -82.8690; 15 Jul. 2015; S. Myers leg.; MSC-2462, CUAC000185782; • 1 ♂; **Haywood Co.**; Pisgah National Forest, Mount Hardy summit; 35.3036, -82.9274; 8 Sep. 2020; C.W. Harden leg.; • 1 ♂, 1 ♀; **Haywood Co.**; Pisgah National Forest, Black Balsam Knob; 35.327, -82.874; 20 Oct. 2020; M.S. Caterino leg.; • 14 ♂, 15 ♀; **Haywood Co.**; Mount Pisgah; 35.4250, -82.7529; 10 Aug. 2021; M. Caterino and A. Haberski leg.; • 1 ♂; same data as previous; CWH-477, CUAC000066797; • 6 ♂, 9 ♀; **Haywood Co.**; Great Smoky Mountains National Park, Cataloochee Divide; 35.5859, -83.0815; 8 Jun. 2020; B. Camper leg.; • 6 ♂, 9 ♀; **Haywood Co.**; Great Smoky Mountains National Park, Cataloochee Divide; 35.5865, -83.0811; 8 Jun. 2020; B. Camper leg.; • 1 ♂; **Haywood Co.**; Great Smoky Mountains National Park, Cataloochee area, Rough Fork Trail; 35.610, -83.117; 29 Jul. 2002; C. Carlton leg.; NCSU_ENT00293718; • 1 ♂; **Haywood/Jackson Cos.**; Waterrock Knob; 35.46, -83.13; 30 May 2001; R. Davidson leg.; •2 ♂, 3 ♀; **Jackson Co.**; Whiteside Mountain, near Highlands; 35.083, -83.138; 25 May 2014; T. Lawton leg.; TLc; • 2 ♂; **Jackson Co.**; Toxaway Mountain; 35.132, -82.982; 5 Aug. 2020; • 13 ♂, 10 ♀; same data as previous; 13 Oct. 2020; • 1 ♂; **Jackson Co.**; Balsam Mountain Preserve; 35.3008, -83.0971; 20 Jul. 2016; M. Caterino and L. Vasquez leg.; CUAC000055510; • 1 ♂; **Jackson Co.**; Blue Ridge Parkway, Rough Butt Overlook; 35.3039, -82.9429; 27 Jun. 2018; K.E. Schnepp leg.; KESc; • 1 ♂; **Jackson Co.**; Blue Ridge Parkway, Cowee Mountain Overlook; 35.3556, -82.9888; 27 Jun. 2018; K.E. Schnepp leg.; KESc; • 2 ♂; **Jackson Co.**; Balsam Mountain Preserve; 35.3681, -83.1036; 17 Jun. 2015; S. Myers leg.; SSM 236 and SSM237, CUAC000185547 and CUAC185548; • 1 ♀; **Jackson Co.**; Balsam Mountain Preserve; 35.3703, -83.1216; 17 Jun. 2015; S. Myers leg.; SSM412, CUAC000185549; • 2 ♂; **Jackson Co.**; Balsam Mountain Preserve; 35.3772, -83.0921; 17 Jun. 2015; S. Myers leg.; SSM229 and SSM231, CUAC000185545 and CUAC000185546; • 1 ♀; **Jackson Co.**; Balsam Mountain Preserve; 35.3808, -83.0971; 17 Jun. 2015; S. Myers leg.; SSM413, CUAC000185550; • 2 ♂, 1 ♀; **Jackson Co.**; Balsam Mountain Preserve; 35.3869, -83.1507; 16 Jun. 2015; S. Myers leg.; CWH-135 to CWH-137, CUAC000168348 to CUAC000168350; • 3 ♂, 4 ♀; **Jackson Co.**; Balsam; 35.42, -83.08; 17 Jul. [no year]; OSUC442495 to OSUC442501; OSUC; • 3 ♂; **Jackson Co.**; Tennessee Mt [*sic*]; 18 May 1972; J. Hunter leg; NCSU_ENT00293720 to NCSU_ENT00293722; • 1 ♀; **Macon Co.**; Highlands; 35.05, -83.19; 24 Jul. 1962; R.C. and A. Graves leg.; NCSU; • 3 ♂, 3 ♀; **Macon Co.**; 1 mi northwest of Highlands; 35.061, -83.217; 24 Aug. 1981; J. Pakaluk leg.; NCSU; • 1 ♀; **Macon Co.**; 1.5 mi northwest of Highlands; 35.063, -83.174; 2 Jul. 1983; J. Pakaluk leg.; NCSU; • 6 ♂, 4 ♀; **Macon Co.**; 2.5 mi northwest of Highlands; 35.072, -83.230; 30 Jun. 1983; NCSU; • 1 ♂, 1 ♀; **Macon Co.**; Nantahala National Forest, trail to Cliffside Lake near Highway 28; 35.0745, -83.2390; 2 Jul. 2020; C.W. Harden and L.M. Thompson leg.; CWH-210 and CWH-211, CUAC000168351 and CUAC000168352; • 4 ♀; **Macon Co.**; Jones Gap; 35.0841, -83.29786; 28 Jul. 2015; S. Myers leg.; SSM163 to SSM166, CUAC000185542 to CUAC000185544 and CUAC000185903; • 1 ♂, 1 ♀; **Swain Co.**; Great Smoky Mountains National Park, Double Springs Gap; 35.5646, -83.5447; 3 Jun. 2020; S. Bewick leg.; CUAC; • 3 ♂; **Swain Co.**; Great Smoky Mountains National Park, Double Springs Gap; 35.5649, -83.5447; 3 Jun. 2020; B. Camper leg.; CUAC; • 1 ♂; **Swain Co.**; Great Smoky Mountains National Park, Newfound Gap; 35.6103, -83.4285; 29 Sep. 2020; C.W. Harden; CUAC; • 10 ♀; **Transylvania Co.**; Sassafras Mountain; 35.0656, -82.7776; 11 Jun. 2020; CUAC; • 8 ♂, 19 ♀; **Transylvania Co.**; Sassafras Mountain; 35.0657, -82.7757; 20 Oct. 2020; F. Etzler and P. Wooden leg.; CUAC; • 1 ♂; **Transylvania Co.**; Sassafras Mountain; 35.0658, -82.7763; 20 Oct. 2020; F. Etzler and P. Wooden leg.; CWH-371, CUAC000168357; • 2 ♂, 11 ♀; same data as previous; • 1 ♂, 3 ♀; **Transylvania Co.**; Balsam Grove; 35.2530, -82.9032; 11 Sep.

2019; M.S. Caterino leg.; CUAC; • 1 ♀; **Transylvania Co.**; Courthouse Falls Trail; 35.2716, -82.8964; 23 Jul. 2015; S. Myers leg.; SSM263, CUAC000170596; • 1 ♂, 1 ♀; **Transylvania Co.**; Courthouse Falls Trail; 35.2747, -82.8902; 23 Jul. 2015; S. Myers leg.; SSM264 and SSM265, CUAC000170597 and CUAC000170598; • 1 ♂; **Transylvania Co.**; Pisgah National Forest, Sycamore Flats; 35.2760, -82.7120; 15 Jun. 1965; J.F. Cornell leg.; ex slime mold; NCSU; • 1 ♂; **Transylvania Co.**; Blue Ridge Parkway; 35.2871, -82.9080; 29 May 2015; S. Myers leg.; MSC-2456, CUAC000185779; • 1 ♀; **Transylvania Co.**; Pisgah National Forest, Highway 215 1 mi south of Blue Ridge Parkway; 35.2910, -82.9133; 8 May 2018; M.S. Caterino, R. Kucuk, L. Cushman leg.; • 1 ♂; **Transylvania Co.**; Near Brevard, Pisgah National Forest, Pink Bed Area, Forest Road 1206, in deer dung; 4 Aug. 2009; J.F. and T.A.D. Cornell leg.; NCSU; • 9 ♂, 2 ♀; • same data as previous, but ex flood debris; • **Tennessee** • 1 ♂; **Cocke Co.**; Great Smoky Mountains National Park, Albright Grove; 35.7340, -83.2807; 6 Aug. 2006; J.F. Cornell and S. Ranger leg.; NCSU; • 3 ♂, 1 ♀; **Sevier Co.**; Great Smoky Mountains National Park, Newfound Gap; 35.6110, -83.4250; 17 Jul. 2003; S. O'Keefe leg.; NCSU; • 1 ♂; **Sevier Co.**; Great Smoky Mountains National Park, Newfound Gap; 35.6110, -83.4250; 16 Jul. 2003; J.S. Ashe leg.; NCSU; • 1 ♂; **Sevier Co.**; Great Smoky Mountains National Park; 35.6125, -83.5425; 6 Jun. 2020; B. Camper leg.; CUAC; • 2 ♂, 1 ♀; **Sevier Co.**; Great Smoky Mountains National Park; 35.6130, -83.5427; B. Camper leg.; 6 Jun. 2020; B. Camper leg.; CUAC; • 3 ♂; **Sevier Co.**; Great Smoky Mountains National Park, Mount LeConte; 35.6382, -83.4387; 28 Sep. 2021; M. Caterino and E. Recuero leg.; MSC-9549, CUAC000160000, CUAC000173086 and CUAC000173087; CUAC & GRSM; • 2 ♂, 2 ♀; **Sevier Co.**; Great Smoky Mountains National Park, Trillium Gap; 35.6734, -83.4338; 7 Jun. 2020; B. Camper leg.; CUAC; • 1 ♀; **Sevier Co.**; Great Smoky Mountains National Park, Trillium Gap; 35.6738, -83.4336; 7 Jun. 2020; S. Bewick Leg.; CUAC; • 1 ♀; **Sevier Co.**; Great Smoky Mountains National Park, Albright Grove; 35.7340, -83.2807; 4 Jun. 2020; B. Camper leg.; CUAC.

Literature records. USA • **North Carolina** • **Haywood Co.**; Blue Ridge Parkway, Woodfin Cascade; 35.4526, -83.0634; 28 May 1986; A. Smetana leg.; CNC; • **Haywood Co.**; Great Smoky Mountains National Park, Purchase Knob; 35.5828, -83.0625; 20 Jul. 2002; C.E. Carlton leg.; GRSM; • **Haywood Co.**; Great Smoky Mountains National Park, McKee Branch Trail; 35.5850, -83.0833; 14 Jul. 2002; C.E. Carlton leg.; LSAM; • **Haywood Co.**; Great Smoky Mountains National Park, Rough Fork Trail upper; 35.5893, -83.1415; 29 Jul. 2002; C.E. Carlton; LSAM; • **Haywood Co.**; Great Smoky Mountains National Park, Cataloochee Divide Trail north; 35.6113, -83.0630; 23 Jul. 2002; C.E. Carlton leg.; GRSM; • **Haywood Co.**; Great Smoky Mountains National Park, Chestnut Branch Trail; 35.760, -83.123; 1 Aug. 2001; A.K. Tishechkin leg.; LSAM; • **Jackson Co.**; Whiteside Mountain near Highlands; 35.0797, -83.1412; 21 May 1986; A. Smetana leg.; CNC; • **Jackson Co.**; Blue Ridge Parkway, Waterrock Overlook, Mile 452; 35.4607, -83.1406; 1 Nov. 1967; J.M. and B.A. Campbell leg.; CNC; • **Macon Co.**; Highway 64 near Dry Falls; 35.0673, -83.2385; 16 May 1986; A. Smetana leg.; CNC; • **Swain Co.**; Great Smoky Mountains National Park, Flat Creek Trail; 35.5502, -83.1725; 31 Jul. 2001; A.K. Tishechkin leg.; LSAM; • **Swain Co.**; Great Smoky Mountains National Park, Collins Picnic area, Quiet Walk; 35.5656, -83.3408; 20 Jul. 2002; C.E. Carlton leg.; LSAM; • **Swain Co.**; Great Smoky Mountains National Park, Heintooga overlook; 35.5727, 83.1807; 29 Jun. 1994; J.F. Cornell leg.; LSAM; • **Swain Co.**; Great Smoky

Mountains National Park, Kanati Fork Trail; 35.5765, -83.3745; 20 Jul. 2002; C.E. Carlton leg.; LSAM; • **Swain Co.**; Great Smoky Mountains National Park, Quiet Walk, across from Kanati Fork Trail; 35.5859, -83.3628; 20 Jul. 2002; C.E. Carlton leg.; LSAM; • **Swain Co.**; Great Smoky Mountains National Park, Deep Creek trail upper; 35.5977, -83.4245; 22 Jul. 2002; C.E. Carlton leg.; LSAM; • **Swain Co.**; Great Smoky Mountains National Park, Kephart Prong trail; 35.6100, -83.3655; 20 Jul. 2003; A.K. Tishechkin; LSAM; • **Swain Co.**; Great Smoky Mountains National Park, Beech Gap trail; 35.6275, -83.2116; 20 Oct. 2001; C.E. Carlton and A. Cline leg.; LSAM; • **Swain Co.**; Great Smoky Mountains National Park, Smokemont Campground; 35.5573, -83.3116; 10 Jun. 1982; Y. Bousquet leg.; CNC; • **Transylvania Co.**; Pisgah National Forest, along Forest Road 215; 35.166, -82.840; 4 Mar. 1997; C.E. Carlton leg.; LSAM; • **South Carolina** • **Pickens Co.**; Sassafras Mountain; • **Tennessee** • **Cocke Co.**; Great Smoky Mountains National Park, Albright Grove Trail; 35.7361, -83.2791; 19 Oct. 2001; C.E. Carlton, A. Cline, A. Tishechkin leg.; LSAM; • **Cocke Co.**; Great Smoky Mountains National Park, Gabes Mountain Trail at Hen Wallow Falls; 35.7586, -83.2381; 19 Jul. 2002; C.E. Carlton leg.; LSAM; • **Sevier Co.**; Great Smoky Mountains National Park; Chimneys Picnic Area nature trail; 35.6350, -83.4958; 30 Jun. 2001; C.E. Carlton, A. Tishechkin, V. Moseley leg.; LSAM; • **Sevier Co.**; Great Smoky Mountains National Park, Roaring Fork area, Rainbow Falls Trail; 35.6614, -83.4608; 1 Aug. 2002; C.E. Carlton leg.; LSAM.

Diagnosis. The male genitalia are unique within the *loweae* group in having a group of dark, sclerotized spines in the endophallus. The apex of the median lobe has a more prominent dorsal projection. The flagellum is slightly rotated dorsally, and is slightly sinuate, with the distal 1/2 nearly straight. Females (Fig. 39B) are similar in habitus to males, though smaller. The spermatheca is S-shaped (Fig. 21Q), with a deep basal bend, similar that of *A. merritti*. The spermathecal duct is short and not coiled.

Distribution. The species has a relatively wide range that includes the Great Balsams, Plott Balsams, Eastern Smokies, and portions of the Southern Blue Ridge escarpment as far west as Rabun Bald in Georgia. Sassafras Mountain is the only known South Carolina occurrence (Fig. 38).

Sympatry. In South Carolina, specimens have been collected in association with *Serranillus dunavani*. Elsewhere, the species has also been collected with *A. murrayae*, *A. langdoni*, and *A.* sp. “North Carolina, Balsam Mountain.”

Natural history. Specimens examined were collected from sifted litter, sifted flood debris, deer dung, slime mold (*Stemonitis* sp.), and underneath rocks.

Notes. Jeannel (1963a) and Barr (1995) illustrated this species as *Anillinus dunavani* Jeannel, but the holotype of that species was found to be a *Serranillus*. See Sokolov et al (2004) for discussion. We have not seen specimens collected in South Carolina.

Anillinus merritti Sokolov & Carlton, 2010

Figs 21R, 24P, 38, 39A

Anillinus merritti Sokolov & Carlton, 2010: 9.

Material examined. Holotype male (**USNM**), point mounted and dissected with genitalia in dried-out glycerin cup pinned beneath specimen.

Other material (*n* = 77). USA • Georgia (new state record) • 1 ♂, 1 ♀; **Habersham Co.**; 34.5726, -83.5477; Jun. 1946; J.M. Valentine leg.; CMNH; • 2 ♂, 4 ♀; **Rabun Co.**; Chattahoochee National Forest, ca. 1 km south of Rabun bald trailhead; 34.9708, -83.3032; 2 Jul. 2020; C.W. Harden leg.; buried pipe trap; CWHc; • 1 ♀; **Rabun Co.**; Chattahoochee National Forest, ca. 1 km south of Rabun bald trailhead; 34.9709, -83.3031; 2 Jul. 2020; C.W. Harden leg.; buried pipe trap; CWHc; • 1 ♂, 4 ♀; **Rabun Co.**; Chattahoochee National Forest, ca. 1 km south of Rabun bald trailhead; 34.9711, -83.3032; 2 Jul. 2020; C.W. Harden leg.; buried pipe trap; CWHc; • 1 ♂; **Rabun Co.**; Chattahoochee National Forest, ca. 1 km south of Rabun bald trailhead; 34.9712, -83.3030; 2 Jul. 2020; C.W. Harden leg.; CWHc; • 1 ♀; **Rabun Co.**; Chattahoochee National Forest, Rabun Bald trail; 34.9724, -83.3020; 29 Sep. 2019; C.W. Harden leg.; under rock; CWH-027, CUAC000169281; • 1 ♂, 4 ♀; **Rabun Co.**; Chattahoochee National Forest, 0.6 km south of Rabun Bald trailhead, east of Sky Valley; 34.9736, -83.3085; 26 Oct. 2019; C.W. Harden leg.; under rock; CWH-041, CWH-043 to CWH-046, CUAC000168372, CUAC000169274 to CUAC000169277; • 2 ♂, 3 ♀; **Rabun Co.**; Chattahoochee National Forest, 0.6 km south of Rabun Bald trailhead, east of Sky Valley; 34.9748, -83.3059; 26 Oct. 2019; C.W. Harden leg.; under rock; CWH-040, CWH-042, CWH-047, CWH-048, CWH-095, CUAC000168371, CUAC000168373, CUAC000169278 to CUAC000169280; • **Rabun Co.**; Beegum Gap; 34.9786, -83.3032; 11 Aug. 1970; T.C. Barr leg.; CMNH; • **North Carolina** • 1 ♂; **Macon Co.**; Coweeta Hydrological Lab, ca. 13 mi west of Highlands; 35.0450, -83.4510; 22 May 1965; H.R. Steeves leg.; CMNH; • 3 ♂, 4 ♀; **Macon Co.**; Turtle Pond Creek, ca 4 mi west-northwest of Highlands; 35.06, -83.26; 8 Aug. 1970; T.C. Barr leg.; CMNH; • 1 ♂, 1 ♀; **Macon Co.**; Jones Gap; 35.0752, -83.2883; 16 Jul. 2015; S. Myers leg.; SSM245 and SSM246, CUAC000170592 and CUAC000170593; • 1 ♀; **Macon Co.**; Jones Gap; 35.0785, -83.2923; 22 Jul. 2015; S. Myers leg.; SSM174, CUAC000169286; • 1 ♀; **Macon Co.**; Nantahala National Forest, Cliffside Vista trail; 35.0795, -83.2416; 2 Jul. 2020; C.W. Harden and L.M. Thompson leg.; under rock; CWH-203, CUAC000169284; • 1 ♀; **Macon Co.**; 4 mi northwest of Highlands; 35.0840, -83.2570; 19 Mar. 1976; Q.D. Wheeler leg.; litter extraction; OSUC; • 1 ♂, 1 ♀; **Macon Co.**; 0.6 mi northeast of Goldmine, California Ridge; 35.10, -83.28; 14 May 1971; T.C. Barr leg.; CMNH; • 1 ♀; **Macon Co.**; Nantahala National Forest, off Wayah Road ca. 10 km from Route 64; 35.1554, -83.5584; 3 Aug. 2020; C.W. Harden leg.; buried pipe trap; CWHc; • 1 ♀; **Macon Co.**; Nantahala National Forest, off Wayah Road ca. 10 km from Route 64; 35.1556, -83.5583; 20 Oct. 2019; C.W. Harden leg.; under rock; CWH-055; CUAC000169291; • 3 ♂, 14 ♀; **Macon Co.**; Nantahala National Forest, off Wayah Road ca. 10 km from Route 64; 35.1557, -83.5583; 3 Aug. 2020; buried pipe trap or under rock; C.W. Harden leg.; CWHc; • 2 ♂, 9 ♀; **Macon Co.**; Nantahala National Forest, off Wayah Road ca. 10 km from Route 64; 35.1557, -83.5583; 4 Jun. 2021; C.W. Harden leg.; buried pipe trap; • 1 ♂, 1 ♀; **Macon Co.**; Nantahala National Forest, Forest Service road 1.25 mi south of Wayah Bald; 35.1700, -83.5810; 18 Apr. 2020; C.W. Harden leg.; under rock; CWH-165 and CWH-166, CUAC000169282 and CUAC000169283; • 1 ♀; **Macon Co.**; Nantahala National Forest, Bartram Trail, Wallace Branch, end of Ray Cove Road; 35.1809, -83.4336; 3 Aug. 2020; C.W. Harden leg.; under rock; CWH-208, CUAC000169285; **Swain Co.**; Twentymile Trail near Twentymile Creek; 35.4800, -83.8450; 19 Oct. 2007; I.M. Sokolov leg.; litter sifting; NCSU_ENT00293734; NCSU; • **South Carolina**

(**new state record**) • 1 ♀; **Oconee Co.**; Indian Camp Creek; 34.9899, -83.0724; 4 May 2015; S. Myers leg.; litter extraction; SSM414, CUAC000169287.

Literature records. USA • North Carolina • Macon Co.; Coweeta Hydrobiological Station, Shope Fork; 35.0597, -83.4532; 29 May 1983; D.S. Chandler leg.; litter extraction; LSAM.

Diagnosis. The male genitalia are diagnostic: the median lobe is straighter than in other *loweae*-group species, and the apex is more elongate. The flagellum is slightly rotated dorsally; in right lateral view it is similar to that of *A. loweae*, but shorter; in dorsal view it is evenly curved. Female spermatheca (Fig. 21R) is similar in form to that of *A. loweae*, S-shaped with deep basal bend, and a short uncoiled spermathecal duct.

Females of this species have two distinct phenotypes: west of the Little Tennessee River, most females resemble those of *A. cherokee* (cf. Fig. 39C), whereas east of the Little Tennessee River, females have greatly narrowed humeri without angles, giving the body a striking hourglass shape (Fig. 39A). The two forms seem to intergrade in the vicinity of Wayah Bald in Macon Co., NC, and the DNA sequence data associate both forms with typical males of *A. merritti.*

Distribution. The range of this species is similar to that of *A. cherokee*, but it has not yet been found in Tennessee (Fig. 38).

Sympatry. At the single known SC locality, this species was collected with *A. murrayae* and *S. dunavani*.

Natural history. This species inhabits deeper strata than the other described members of the *loweae* group, and should be considered endogean in habit. Evidence for this comes from seven years of extensive litter sampling within the range of *A. merritti* producing only four specimens, while a single year of endogean collecting (turning rocks during rain and using buried pitfall traps) yielded more than 50 specimens. The morphology of the sloped-humeri females is also considered to be associated with increased mobility through deeper soil strata (Sokolov 2013).

Note. The single specimen known from South Carolina is a female.

Species group incertae sedis

Anillinus sp. "South Carolina, Wateree"

Fig. 40A–C

Material examined. USA • South Carolina • 2 ♀; **Kershaw Co.**; English Swamp, Wateree Floodland Memorial Forest; 34.0911, -80.6578; 27 Feb. 2010; J.F. Cornell, S. Cornell, and B. Gregory leg.; litter ex *Pinus* stumps; NCSU.

Diagnosis. The two female specimens of this species are unique among known eastern *Anillinus* females in having a sharp tooth on the posterior margin of the metafemur in the distal 1/3 (Fig. 40B). The specimens are large, ABL = 2.25 mm, dorsoventrally flattened and parallel-sided (Fig. 40A). Dorsal microsculpture is fully developed on the head and pronotum. The spermatheca is long, 2-shaped in ventral aspect (Fig. 40C), stem narrow with an acute bend basally, abruptly enlarged at curved apex. Spermathecal duct long and not coiled. The gonocoxites are longer and narrower than in most *Anillinus* species.

Notes. The proper systematic placement of this species is unclear. Externally, the species is similar to members of the *elongatus* group, but all species

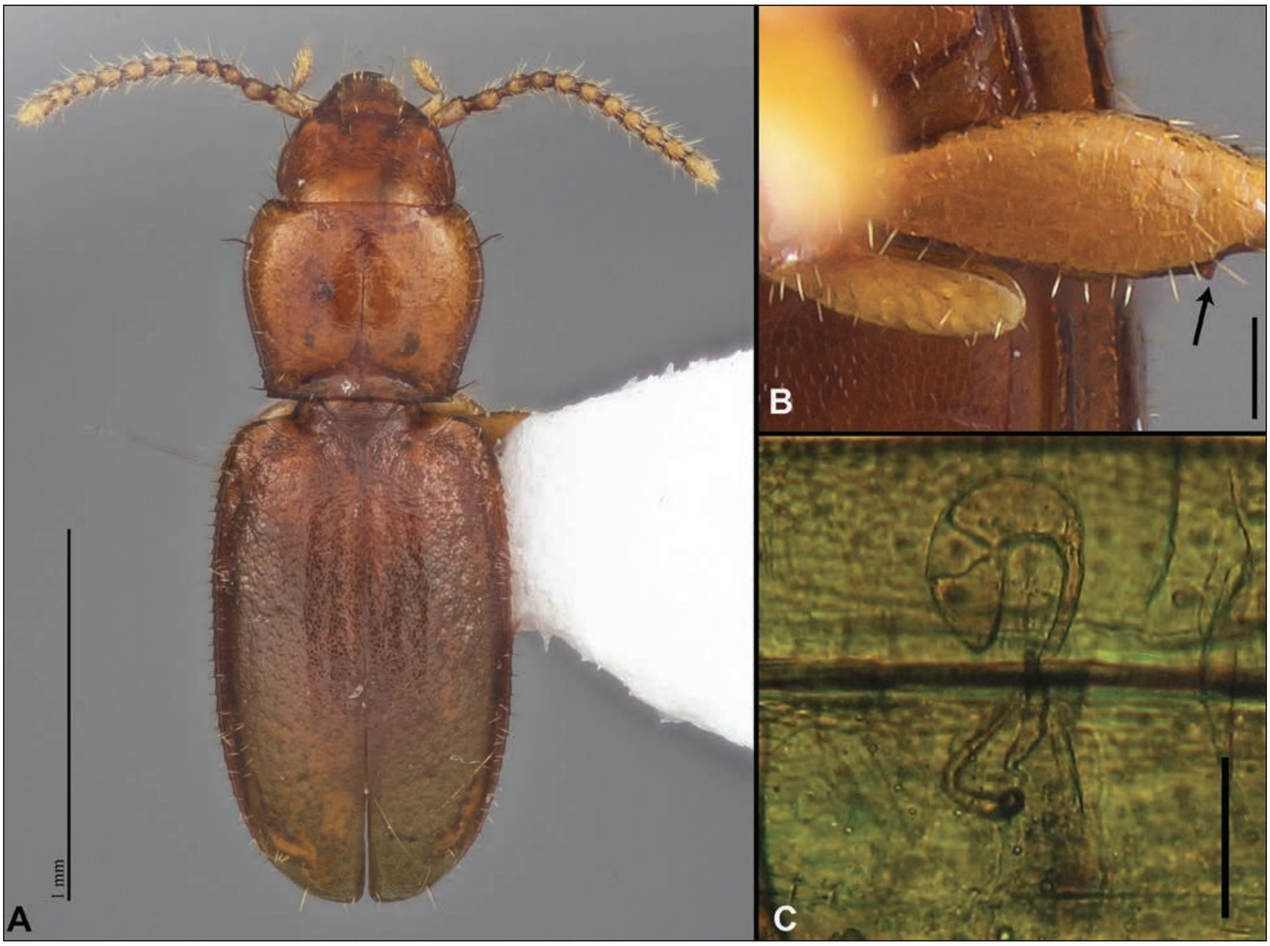

Figure 40. *Anillinus* sp. "South Carolina, Wateree." **A** dorsal habitus **B** left metafemora, ventral aspect (black arrow = metafemoral spine) **C** spermatheca within cleared abdomen. Scale bars: 1 mm (**A**) and 0.1 mm (**B, C**).

in that group have a long and heavily coiled spermathecal duct, and modified metafemora are unknown in females. Several large samples of sifted wood and soil taken from large pine stumps at the known locality in April 2021 failed to produce specimens.

Discussion

Phylogenetics and systematics of eastern Nearctic Anillini

The Nearctic Anillini, and the Appalachian species in particular, have long been recognized as distinct from other anillines, beginning with Jeannel's monograph (Jeannel 1963a, 1963b) in which *Anillinus* is placed in its own phyletic series based on the relatively small right paramere. Most genera of anillines have not yet been sampled for molecular phylogenetics, but several studies have consistently recovered an Anillini topology in which the New Zealand endemic genus *Nesamblyops* Jeannel is sister to all other anillines, and the Nearctic taxa are sister to all anillines sampled except for *Nesamblyops* (Maddison and Ober 2011; Andújar et al. 2016; Maddison et al. 2019; LaBonte and Maddison 2023), as in our 6-gene phylogeny (Suppl. material 1: fig. S10). Sokolov (2023) formally erected the subtribe Nesamblyopina for the species of *Nesamblyops*, and pointed out that the Nearctic anillines share with the species of *Nesamblyops* an asetose posterior pronotal margin, an apparently plesiomorphic state within Trechitae. In other anillines that have been studied, the posterior pronotal margin is setose.

The newly discovered larvae of *Anillinus* and *Serranillus* add further support for the exclusion of Nearctic Anillini from the large clade of other Anillina, Scotodipnina, and Typhlocharina (Andújar et al. 2016; Maddison et al. 2019; Sokolov 2023). Larvae of three anilline genera have been previously described, *Zapotecanillus* Sokolov from Mexico (as *Geocharidius* Jeannel) (Grebennikov 2002), *Typhlocharis* Dieck, and *Microcharidius* Coiffait from Spain (Arndt et al. 1999; Andújar et al. 2010; Pérez-González et al. 2018). Grebennikov (2002) listed ten possible synapomorphies of the two known anilline larvae, five of which were found to strongly support monophyly of Anillini (Grebennikov and Maddison 2005): presence of only two pores on antennomere 1, reduction or absence of antennomere 2, antennal fossa separated from pleurostoma by a strip of cuticle, mandible with two large terebral teeth, and mandible with greatly reduced retinaculum. None of these character states are found in larvae of *Anillinus* and *Serranillus*; in both genera, antennomere 1 has three pores, antennomere 2 is typical in length for Trechitae, the antennal fossa is not separated from the pleurostoma, the mandible lacks large terebral teeth, and the retinaculum is well-developed (Fig. 14).

Another character, the ocular tubercles in adults of *Serranillus*, has not been previously noted, although it has bearing on the matter. The position of the tubercles on the head in *Serranillus* is the same as the ommatidia in *Nesamblyops* (cf. Sokolov 2023: fig. 1a–c); the tubercles could represent 'scars' left from the fusion of integument at the site of former ommatidia. Similar ocular tubercles are found in other eyeless beetles, including several clivinine carabid species (Barr 1967; Bousquet and Skelley 2012; Huang et al. 2021) and most pselaphine rove beetles of the tribe Amauropini (Carlton 2008; Hlaváč et al. 2021). We have noted ocular tubercles in a small number of *Anillinus* species, but none are as prominent as in *Serranillus* except in *A. indianae* and in an undescribed species from Washington Co., Arkansas. The character requires more study, but it could represent another plesiomorphy of Nearctic Anillini.

Likely morphological apomorphies of *Serranillus* are the greatly reduced right paramere that lacks pores or setae, the large internal rolled sclerite on the left side of the median lobe, and the modified last male abdominal ventrite. The presence of a retinacular tooth on the left mandible is rare within Anillini, and is another possible apomorphy, but mandibular teeth are not described for most anillines, and not all *Serranillus* species have been checked. There are at least ten additional known species of *Serranillus*, some of which are quite divergent in male genitalic morphology, which were not sampled by us. Including these species in future molecular phylogenetic studies will help clarify the higher classification of the genus.

While morphological support for monophyly of *Anillinus* is lacking, each of the species groups identified by us is morphologically diagnosable. Furthermore, we have identified characters that show promise to be phylogenetically informative, given their consistency within clades in the 6-gene phylogeny (Fig. 41). Among male genitalic characters that vary across species of *Anillinus*, for example, is setation of the right paramere. Some species have numerous setae forming a

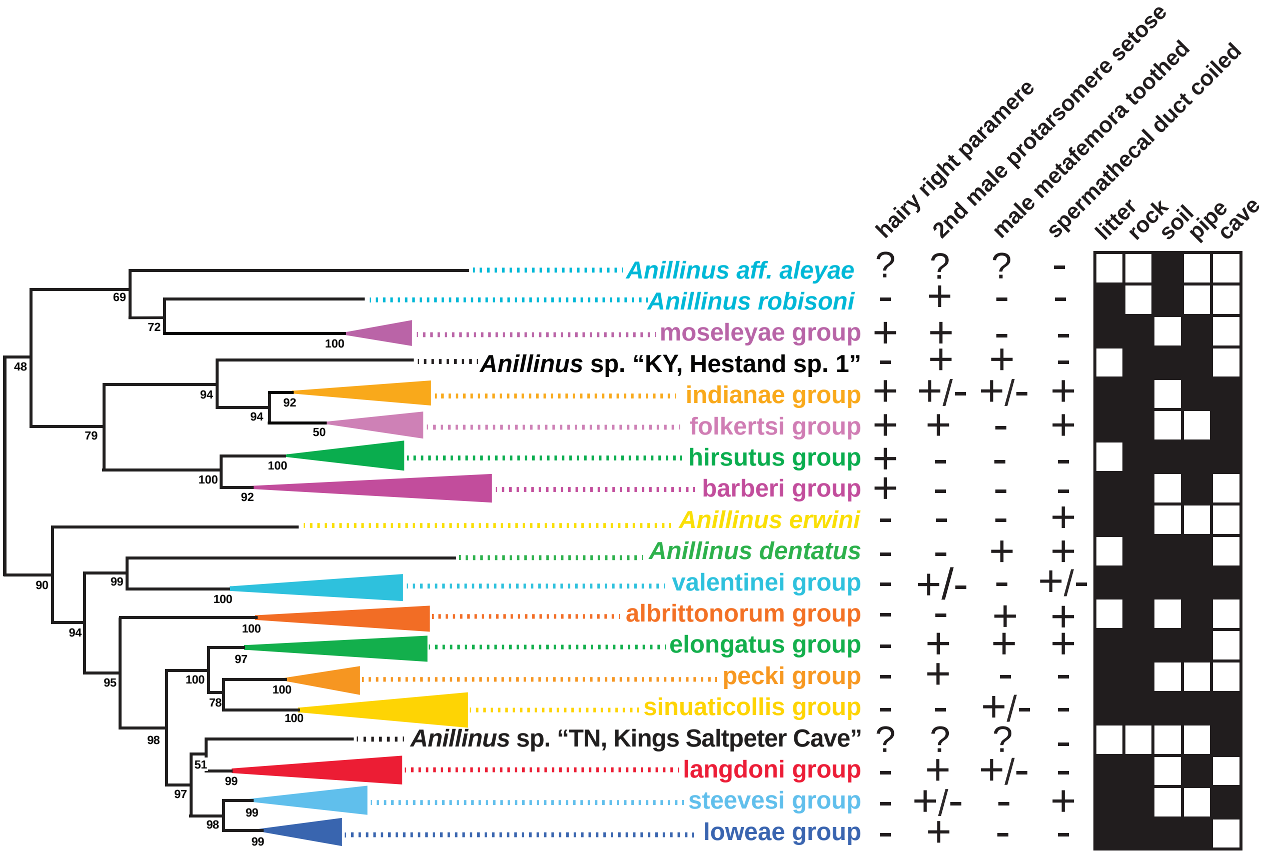

Figure 41. 6-gene maximum likelihood tree of *Anillinus*, with select character states and microhabitats shown. Numbers below nodes are SBS values. '+' denotes presence of character and '-' denotes absence; these do not correspond to presumed derived and plesiomorphic states in all characters. Black squares indicate records of collections from litter (hand sifting, Berlese or Winkler extraction), rock (hand collecting under rocks), soil (Berlese extraction of washed or unwashed soil), pipe (buried pipe trap), and cave (hand collected in cave).

dense brush on the apex of the paramere, whereas in other species only a few stout setae are present, typically four in number (Sokolov 2011, 2012, 2020). The presence of more than four setae on the right paramere is a unique state within Anillini; in all other anilline genera, the right paramere has four setae or fewer, with most species having only two (e.g., Jeannel 1963a; Giachino and Vailati 2011; Sokolov 2013, 2023; Giachino 2015; Pérez-González and Zaballos 2019; Giachino et al. 2021). Thus, a right paramere with more than four apical setae is likely a derived condition within the tribe. However, two of the sampled species recovered in the "hairy clade" have only four setae on the right paramere: *Anillinus robisoni* has a stout, semicircular right paramere with four apical setae, and *Anillinus* sp. "Kentucky, Hestand sp. 1" has a small, narrow right paramere with numerous apical pores but only four apical setae. The additional pores present on the right paramere of "Kentucky, Hestand sp. 1" suggest that the reduced number of setae is a secondary loss in that species. We also note that within the "quadrisetose clade" one of the two males of *A. jancae* (the holotype) has six apical setae on the right paramere, while the other has four. Most known *Anillinus* species with more than four setae on their right parameres were not sampled for our phylogeny, so further studies will be necessary to test the reality of the "hairy clade" and the number of times a hairy right paramere has evolved.

One valuable character that has been overlooked in previous work is the number of male protarsomeres that are dilated and bear ventral adhesive setae; all *Serranillus* have the first and second protarsomeres modified, while the number varies within *Anillinus*. The typical number of dilated protarsomeres in Trechitae is two, although examples of reduction are found throughout the supertribe. The number of modified male protarsomeres has been considered a phylogenetically useful character in other trechite genera, such as *Paratachys* (Lindroth 1966), *Trechus* (Barr 1979), and the closely similar pair of anilline genera, *Binaghites* Jeannel and *Scotodipnus* Schaum (Magrini 2008). If two modified male protarsomeres is considered the plesiomorphic state, given its occurrence in most trechites, then reduction to one has likely evolved multiple times within *Anillinus*. Of the sixteen distinct lineages of *Anillinus* in eastern North America, the number of modified male protarsomeres varies in only three, the *indianae*, *steevesi*, and *valentinei* groups, in which only a single species is an exception (Fig. 41). The number of modified male protarsomeres has proven to be one of the most useful diagnostic characters for classifying newly discovered *Anillinus* species. For example, the species *Anillinus* sp. "North Carolina, Orange Co. sp. 2" shares some characters with *A. jancae*, including an almost identical profemoral spine (Fig. 27B), a unique character within the genus. However, unlike *A. jancae*, the single known male of "North Carolina, Orange Co. sp. 2" has a modified second protarsomere, and our initial prediction that it was related to the *elongatus* group was supported by its placement in the molecular phylogeny.

A more common male secondary sexual leg modification is the presence of a spine or tooth on the posterior face of the metafemur. Such toothed metafemora are known in seven of the eastern *Anillinus* lineages (Fig. 41). In all instances, species with toothed metafemora in males are primarily endogean in habit. The most likely function of these toothed male femora is to allow the male to securely grip the female during courtship, mating, and/or post-mating. We have observed mating pairs of *Anillinus* on two occasions on the undersides of embedded rocks, and the beetles were coupled in typical carabid fashion, with the male on top of the female, moving as a single unit when disturbed by exposure. If such in-copula pairs move throughout the interstices of deep soil habitats, males with a stronger grip would be less likely to be dislodged. Not all endogean *Anillinus* species have modified male legs, however. The *folkertsi* group and *valentinei* group are notable in being largely endogean in habit and having no species with modified male metafemora. Other endogean groups have male metafemora that are not toothed but are greatly swollen (some *barberi*-group species) or densely setose (most *hirsutus*-group species). Modified female metafemora are known only in *Anillinus alleni*, in which the males have enormous metafemoral spines and females have the posterior margin angularly produced apically (Sokolov et al. 2017) and in *Anillinus* sp. "South Carolina, Wateree", in which females have a small, sharp tooth on the posterior face near the apex; males of "South Carolina, Wateree" are unknown.

A female character useful for diagnosing groups of *Anillinus* is the presence or absence of many coils in the spermathecal duct. Although the coiled shape is doubtfully homologous across all species, it is consistent within all species groups studied except the *valentinei* group (Fig. 41). Most species studied in this group have a long, coiled spermathecal duct, but *A. murrayae* and *A. castaneus* seem to lack a duct entirely, and *A. simplex* has a short, simple duct. The length of the spermathecal duct has been found to correspond to the length of the flagellum of the aedeagus in some groups of carabids (Schuler 1971; Liebherr 2008). We have not attempted to measure these structures in *Anillinus*, but note that the apparent lack of a spermathecal duct in *A. murrayae*, a species in which the flagellum is quite long, is a clear exception to such a pattern.

Patterns of dorsal microsculpture on the head and pronotum are variable within *Anillinus* and have been previously used to group species (Sokolov et al. 2004; Sokolov 2012). While consistent within most lineages, intraspecific variation has been documented (Sokolov and Carlton 2010; Harden and Caterino 2024), including for *A. simplex* described in this paper. In each species group, we have observed exceptions to the typical microsculpture pattern. Dorsal microsculpture, while frequently valuable for species recognition and diagnosis of species groups, is too variable to be a reliable indicator of relationships.

Patterns of observed microhabitat use have been used to classify species of *Anillinus* (Sokolov et al. 2004). Microhabitat use is consistent in many species and in some species groups, such as the largely endogean *elongatus* group and largely litter-dwelling *langdoni* group. However, the distinction between use of litter and soil habitats is not always a clear, and presumed microhabitat associations are not always consistent with collecting data. For example, the *moseleyae* group has been considered endogean, despite all of the previously reported specimens being collected from leaf litter (Sokolov et al. 2004; Sokolov 2011). In Fig. 41, we demonstrate the consistency (and lack thereof) between collecting method and phylogenetic placement of members of the species groups in our 6-gene tree. One pattern that is repeated throughout the tree is a sister relationship between a phylogenetically and geographically isolated endogean lineage and a more diverse and widespread lineage: the micro-range endemics *A.* sp. "Kentucky, Hestand sp. 1" and *A. dentatus* are sister to the *indianae* group+*folkertsi* group clade and the *valentinei* group, respectively; the *albrittonorum* group is sister to the 'ESP+LSL' clade, and the Piedmont endemic *elongatus* group is sister to the montane *pecki* group and widespread *sinuaticollis* group.

Biogeography of eastern Nearctic Anillini and the unique South Carolina assemblage

The anilline fauna of South Carolina was previously considered to be among the least diverse of the states from which anillines have been reported. Tallies of the state's fauna in Bousquet (2012) and Sokolov (2021) overlooked the South Carolina record of *A. cherokee* in Sokolov and Carlton (2010), and listed only three *Anillinus* and one *Serranillus* species from South Carolina. Our work has increased the number of described anilline species in South Carolina nearly five-fold, with three described *Serranillus* and 17 described *Anillinus* now known, making South Carolina one of the most diverse states along with North Carolina and Tennessee, which previously had the highest number (19) of *Anillinus* species known among eastern states. We report nine endemic species from South Carolina (53%) as well as two unique lineages not found elsewhere in the Appalachian region, the *dentatus* group and the *albrittonorum* group. The diverse assemblage of anillines present in South Carolina doubtlessly reflects the unique combination of ecoregions and dispersal barriers present in the state.

The *Serranillus* species found in South Carolina belong to all three of the main clades in our 6-gene phylogeny. *Serranillus dunavani* is the most commonly collected anilline in South Carolina, and also the most widespread (Fig. 16). The range of the species is concentrated along the Blue Ridge escarpment, a region of high relief where many narrow streams cascade through rich cove forests, and drier oak-pine forests dominate the exposed south-facing slopes; *S. dunavani* has been collected in large numbers from both habitat extremes. Its unusually large geographic range is likely a reflection of this broad ecological tolerance. This tolerance likely also explains the occurrence of *S. dunavani* on both sides of the French Broad River basin (FBR). The FBR is an important biogeographic barrier for many groups of flightless animals, as distinctly different montane faunas and/or genotypes exist of opposite sides (Barr 1979; Donabauer 2009; Hedin and Thomas 2010; Keith and Hedin 2012; Garrick et al. 2018; Hennen et al. 2022; Caterino and Recuero 2023). The range of *S. dunavani* skirts south of the headwaters of the FBR and extends on the northeast side to the Hickory Nut Gorge in western North Carolina. Three disjunct occurrences of *S. dunavani* are known in the outer Piedmont of South Carolina and the Uwharrie Mountains of North Carolina. Little dedicated collecting has been done in the intervening areas, so this disjunction could be an artifact, but it is another illustration of both the surprising dispersal capabilities of *S. dunavani* and its wide habitat tolerances.

Two species of *Serranillus*, *S. jeanneli* and *S.* sp. “South Carolina, Coon Branch” occur in South Carolina only in the extreme northwest corner, where both are known from the mesic north-facing slopes in the lower Whitewater River gorge. Given that *S.* sp. “South Carolina, Coon Branch” has been collected at only a single locality, its full range is unknown, but *S. jeanneli* is limited to higher elevations in a small area in the North Carolina-South Carolina-Georgia corner. Other flightless carabids endemic to the Southern Appalachians that are rare or absent elsewhere in South Carolina are found in the Whitewater River Gorge, including *Scaphinotus* (*Maronetus*) *unistriatus* Darlington, *Scaphinotus* (*Steniridia*) *violaceus* (LeConte), *Trechus* (*Microtrechus*) *barberi* (Jeannel), and *Pterostichus* (*Monoferonia*) *carolinus* Darlington (CUAC data).

The last *Serranillus* occurring in South Carolina, *S. monadnock*, is known from two disjunct monadnocks, Kings Mountain in York Co. and Little Mountain in Newberry Co. The median lobe of the aedeagus, with a relatively broad apex, distinct flagellum, and lack of large spines, is similar in form to that of *S. septentrionis* and its undescribed sister species, as well as several undescribed species known from Georgia and Alabama. Without DNA sequence data the affinities of *S. monadnock* are uncertain, but it could be part of the clade that includes *S. septentrionis*, *S.* sp. “South Carolina, Coon Branch” and the other undescribed species with similar genitalia. Both collections of *S. monadnock* were made at colder times of year, and the apparent restriction of the species to isolated monadnocks suggests it is a cold-adapted lineage that has been extirpated elsewhere in South Carolina.

In *Anillinus*, the absence of any “hairy clade” species in South Carolina is notable, because representatives of the clade are present in every other Appalachian state in which anillines occur (Fig. 42). In terms of airline distance, the only “hairy clade” group found close enough to South Carolina to be expected to occur is the *moseleyae* group; the southernmost known occurrence of the group is at Coweeta Hydrological Lab (CMNH data), less than 30 km airline distance from the

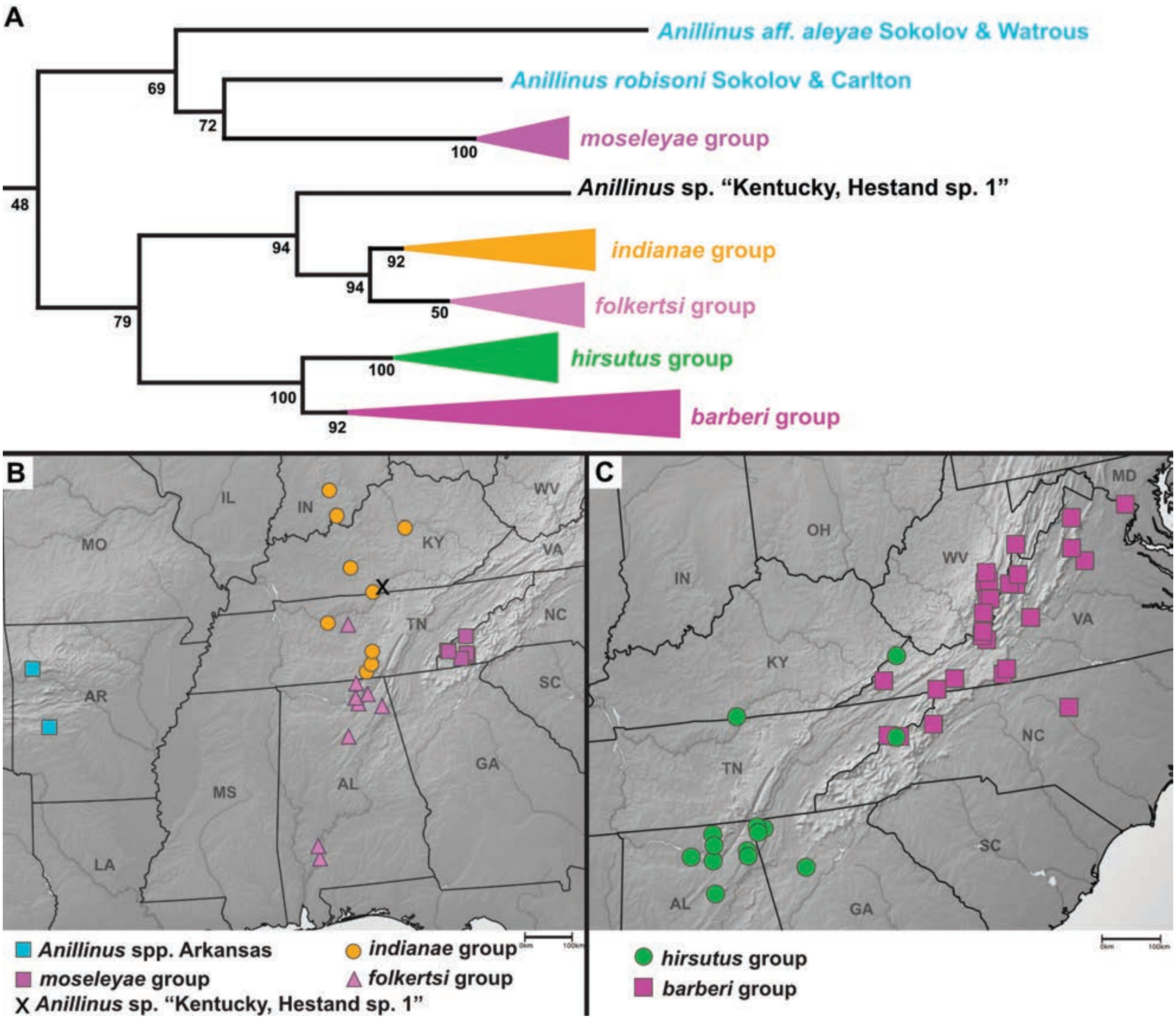

Figure 42. Topology and distribution of "hairy clade" species groups of *Anillinus* **A** collapsed maximum likelihood tree of "hairy clade" of *Anillinus*, from 6-gene concatenated core matrix, SBS values shown below nodes **B** distribution map of Arkansas *Anillinus* specimens sampled, *Anillinus* sp. "Kentucky, Hestand sp. 1", and all occurrences of the *moseleyae* group, *indianae* group and *folkertsi* groups **C** distribution map of all occurrences of the *hirsutus* group and *barberi* group. Data for distribution maps come from Harden (2024).

northwestern corner of South Carolina (Fig. 42B). The *moseleyae*-group species are all strictly high-elevation endemics, with no known occurrences below 1370 m. Such elevations do not occur in South Carolina, and it is unlikely that species of the group are present in the state. The factors that limit *moseleyae*-group species to higher elevations are unknown, but they seem to include more than simple microclimatic requirements, since no specimens have been found at lower elevations in endogean habitats in mesic North-facing slopes adjacent to mountains on which they occur. Two *moseleyae*-group species have surprisingly large geographic ranges, considering the apparent elevation restriction: *A. unicoi* occurs on both sides of the Little Tennessee River in the Unicoi and Great Smoky Mountains, where it has been collected on Thunderhead Mountain approximately 0.8 km west of the type locality of *A. carltoni* (NCSU data); an undescribed species has been collected in the Snowbird and Nantahala Mountains.

Other "hairy clade" groups are also unlikely to be found in South Carolina. The *indianae* group+*folkertsi* group clade is found only West of the Appalachian Mountains. Members of the *folkertsi* group are the least strictly endogean of eastern "hairy clade" species, having been collected several times in series from sifted litter, so ecological factors are unlikely to limit their occurrence in South Carolina. Rather, the distribution of the group suggests that the Alabama River drainage is a barrier to eastward dispersal (Fig. 42B). The *indianae* group is known only west of the Tennessee River, and these species seem to be ecologically restricted to cooler subterranean habitats; in Kentucky and Indiana, specimens have been collected from deep soil and MSS, while at lower and hotter elevations in southern Tennessee the group is known only from caves. A similar pattern is shown in the *hirsutus* group, which ranges from the Cumberland Mountains on the Virginia—Kentucky border and the Interior Plateau of southern Kentucky south to northern Alabama and Georgia. A notably disjunct site for the group is Big Bald, in the Bald Mountains, a short chain northeast of the FBR on the North Carolina-Tennessee border. In northern hardwood forests on the northwestern-facing slope below the treeless summit of Big Bald, at approximately 1660 m elevation, two *hirsutus*-group species co-occur under rather small rocks; one individual was even collected in a sample of sifted litter. This is in contrast to all other known localities for the group, where specimens are rarely encountered without laborious deep soil extraction methods or – as with several species in Alabama and Georgia, including *A. hirsutus* itself – known only from caves. The ecological requirements of the *hirsutus* group have apparently prevented their dispersal into South Carolina. The absence of the group from suitable habitats in the mountains southwest of the FBR (Fig. 42C) suggests that ancestors of the group never occurred in these mountains, and dispersed to Alabama and Georgia from more northern areas. The sister group to the *hirsutus* group is the *barberi* group, which ranges from Big Bald (where an undescribed species co-occurs syntopically with the two *hirsutus*-group species) north to Plummers Island in the Potomac River west of Washington D.C (Fig. 42C). Most records of the *barberi* group are from higher elevations in the Ridge and Valley and Blue Ridge ecoregions, but an undescribed species has been collected in Duke Forest near Chapel Hill, North Carolina, in an endogean Piedmont habitat similar to those that can be found in South Carolina. An undescribed *elongatus*-group species that is sister to *A. montrex* is found at the same Duke Forest site, so a biogeographic connection between the Duke Forest and South Carolina is known to exist. Further trapping in deep soils in the Piedmont of northeastern South Carolina could lead to discovery of the *barberi* group in the state, but this 200-km range extension for a predominately northern/high elevation clade would be surprising. One last biogeographical pattern we have noted in the "hairy clade" is that with the exception of *A. robisoni*, all *Anillinus* species known from West of the Mississippi river have right parameres with more than four setae (Sokolov and Watrous 2008; Sokolov et al. 2014, 2017; Sokolov 2022). We found the right paramere to have more than four setae in the western species *Anillinus lescheni* Sokolov & Carlton, *Anillinus magazinensis* Sokolov & Carlton, *Anillinus stephani* Sokolov & Carlton, and *Anillinus tishechkini* Sokolov & Carlton, which were all described without mention of the parameres (Sokolov et al. 2004). Inclusion of more western *Anillinus* species in future molecular phylogenetic studies will be key to uncovering the broader biogeographic history of the genus.

All but three lineages of the “quadrisetose clade” of *Anillinus* are present in South Carolina (Fig. 43). The exceptions are the isolated species *A. erwini*, the *pecki* group, and the *steevesi* group. *Anillinus erwini* is endemic to higher

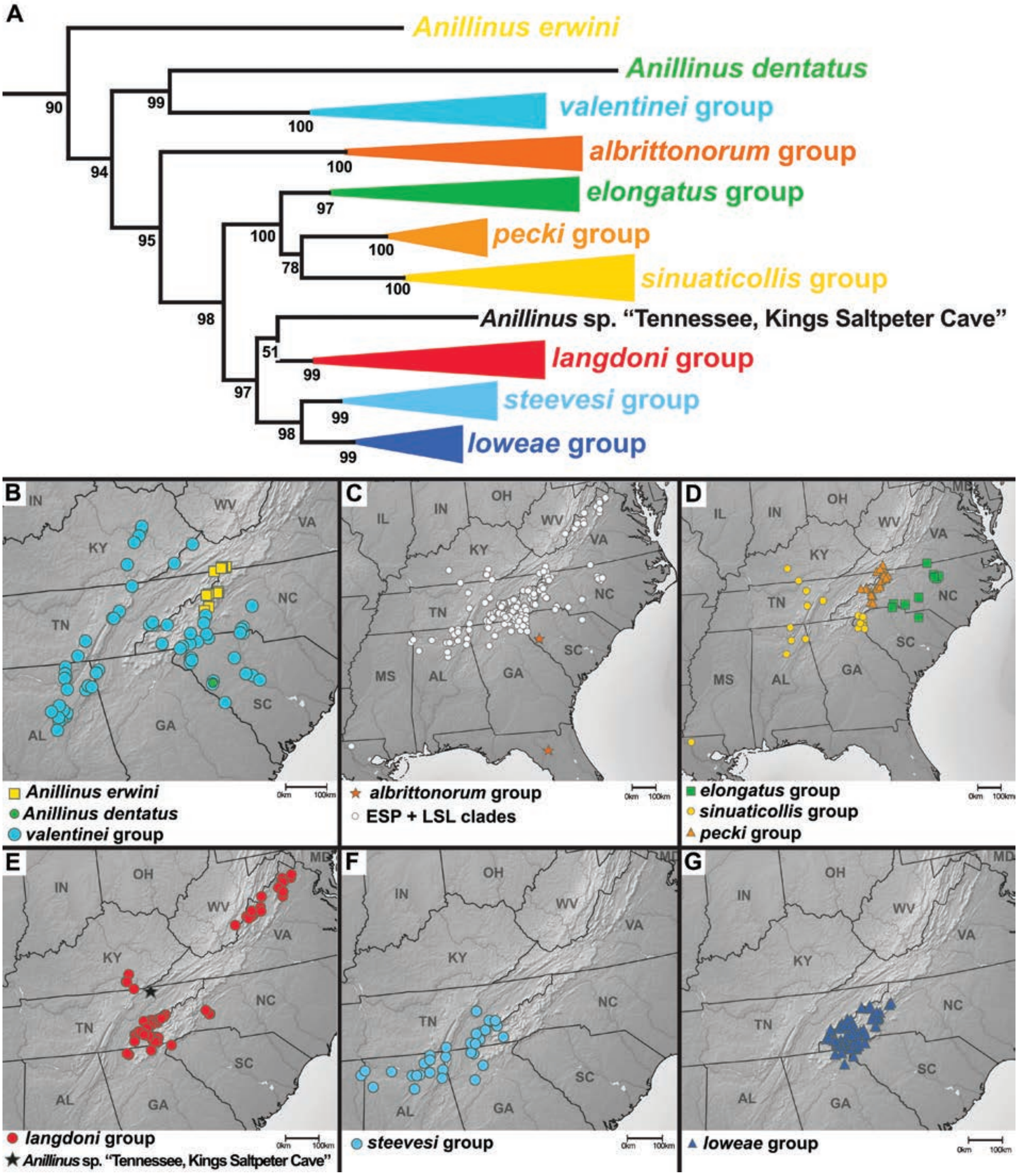

Figure 43. Topology and distribution maps of “quadrisetose clade” species groups of *Anillinus* **A** collapsed maximum likelihood tree of “quadrisetose clade” *Anillinus* species, from 6-gene concatenated core matrix, SBS values shown below nodes **B** distribution map of all known occurrences of *Anillinus erwini* and the *valentinei* group **C** distribution map of all known occurrences of the “ESP+LSL” clade and *albrittonorum* group **D** distribution map of all known occurrences of the “ESP clade” **E** distribution map of all known occurrences of the *langdoni* group and *Anillinus* sp. “Tennessee, Kings Saltpeter Cave” **F** distribution map of all known occurrences of the *steevesi* group **G** distribution map of all known occurrences of the *loweae* group. Data for distribution maps come from Harden (2024).

elevations in the mountains northeast of the FBR; the FBR apparently has prevented this species from dispersing to the southern mountains (Fig. 43B). As discussed above, the phylogenetic placement of *A. erwini* is enigmatic, which limits hypothesizing about its biogeographic history. The *pecki* group is also endemic to montane habitats northeast of the French Broad River, with the southernmost limit being the Hickory Nut Gorge in western North Carolina. The known occurrences of the *pecki* group in the Hickory Nut Gorge are all from the south side of the gorge, where steep Northeast-facing slopes create a cool, mesic habitat despite the relatively low elevation. Ecological factors limiting the *pecki* group to colder microhabitats probably have prevented the southward dispersal of the group into South Carolina. The likely sister lineage of the *pecki* group, the *sinuaticollis* group, occurs in northwestern South Carolina, and the common ancestor of the two groups might have historically had a distribution similar to that of *S. dunavani*, with subsequent extinction during warm, dry periods along most of the southern Blue Ridge escarpment. The third quadrisetose *Anillinus* lineage lacking in South Carolina, the *steevesi* group is distributed mostly west of the southern Appalachians, with no known occurrences east of the Little Tennessee River (Fig. 43F). Members of the *steevesi* group are found mostly at lower elevations, and the absence of the group of South Carolina is probably due to physical barriers such as the Little Tennessee River or the high mountains that flank the northwestern corner of the state.

The dominant clade of *Anillinus* found at lower elevations in South Carolina is the *valentinei* group (Fig. 43B). This group is the most species-rich lineage in the genus, and also the most widespread, ranging from the Cumberland Mountains in eastern Kentucky south to northern Alabama and across the Blue Ridge escarpment to western North Carolina. Except for *A. murrayae*, members of the *valentinei* group are largely restricted to lower elevations, and are absent from most of the southern Appalachian Mountains in the strict sense. Three clades are recovered in our 6-gene phylogeny, and all are represented in South Carolina: a clade consisting of *A. chandleri* and two closely related undescribed species, a clade consisting of all sampled individuals of *A. murrayae*, and a widespread clade containing all remaining *valentinei*-group species sampled. The *chandleri* subclade is strongly supported as sister to the remaining *valentinei* group, and is endemic to South Carolina. *Anillinus chandleri* is known from scattered localities in the Piedmont between the Savannah and Broad Rivers, while the two undescribed species are known from Long Cane Creek in Abbeville Co. and a few localities in the Piedmont and Blue Ridge ecoregions in Pickens County, respectively (Fig. 29). Other than the single specimen of *A.* sp. "South Carolina, Waldrop Stone" collected at Chimneytop Gap in the Blue Ridge, all members of the *chandleri* subclade are restricted to lower elevations.

Anillinus murrayae is the most widespread member of the *valentinei* group, with a range similar to that of *S. dunavani*, with which it frequently co-occurs (Fig. 29). *Anillinus murrayae* seems to be less tolerant of hot, dry microhabitats than *S. dunavani*, and occurrences are limited to mesic habitats, usually at colder seasons. Like *S. dunavani*, *A. murrayae* spans the FBR along the Blue Ridge escarpment, and reaches a slightly more northern limit at the southern end of the Black Mountains in North Carolina. The large amount of intraspecific COI variation in *A. murrayae* (uncorrected p-distance 0.00–5.47% in COIbc, 0.00–4.61% in COIjp) suggests that more than one cryptic species may be involved.

Morphological variation is also apparent (Fig. 31), but not always consistent with the molecular data. All 28S sequences sampled for *A. murrayae* are identical, and the uncorrected p-distances in CAD and Wg are less than 1.50%.

The remaining *valentinei*-group species sampled, from Virginia, Kentucky, Tennessee, Alabama, and South Carolina form the third clade in our 6-gene phylogeny. Four species in this clade occur in South Carolina, and themselves form a well-supported clade: *A. castaneus*, *A. cornelli*, *A. simplex*, and *A.* sp. "South Carolina, Chestnut Ridge". *Anillinus cornelli* and *A. simplex* are endemic to Kings Mountain, an isolated monadnock that spans the South Carolina-North Carolina border, and *A. castaneus* and *A.* sp. "South Carolina, Chestnut Ridge" are endemic to a small area in the gorge of the upper South Pacolet River, separated from Kings Mountain by an airline distance of ~ 80 km. These Kings Mountain and South Pacolet species are widely disjunct from the remaining species in the clade, which are all known from the opposite side of the Appalachian Mountains. Dismissing a possible relationship between *A. chandleri* and the troglobitic *A. valentinei* Sokolov (2011) suggested, "As a rule *Anillinus* spp. from the same lineage are allopatric and occupy the same types of habitats", the habitats in this case being leaf litter, soil, and caves. Our results disagree with this hypothesis. This is best exemplified in the widespread subclade of the *valentinei* group. Specimens in this clade were sampled from leaf litter, deep soil, and caves, and three cases of syntopy were documented: *A. simplex* and *A. cornelli* at Crowders Mountain, Gaston Co., NC; *A. castaneus* and *A.* sp. "South Carolina, Chestnut Ridge" at Chestnut Ridge Heritage Preserve, Greenville Co., SC; and *A. gimmeli* and *A. smokiensis* at Turkeypen Ridge, Blount Co, TN. Syntopy of two or more species belonging to the same lineage was also documented in other species groups: *A. merritti* and *A.* sp. "North Carolina, Wayah sp. 2" (Wayah Road, NC), *A. merritti* and *A. cherokee* (Rabun Bald, GA), *A. mica* and *A. micamicus* (Waldrop Stone Falls, SC), *A. castaneus* and *A.* sp. "South Carolina, Chestnut Ridge" (Chestnut Ridge Heritage Preserve, SC), *A.* cf. *nantahala* and *A.* sp. "Georgia, Brasstown Bald sp. 1" (Little Bald, GA), and *A.* sp. "Tennessee, Hiawassee sp. 1" and *A.* sp. "Tennessee, Hiawassee sp. 2" (John Muir Trail, TN).

The lack of consistency between microhabitat and the phylogeny is not surprising, considering the ecological similarities shared by deep litter, soil, and caves. Use of "cave" microhabitats is also difficult to distinguish from accidental occurrence of endogean or surface species. The only eastern *Anillinus* that has been repeatedly collected from any cave in large series is the species that lives near Clay, Alabama in the cave known as Crystal Caverns or McCluney Cave. The species was illustrated and interpreted as *Anillinus valentinei* (Jeannel) by Sokolov (2012). In addition to *A. valentinei* (sensu Sokolov (2012)), three other *Anillinus* were considered troglobitic by Sokolov et al. (2014): *A. tombarri*, *A. longiceps*, and *A. smokiensis*. The type series of *A. smokiensis* was collected from leaf litter in a cave entrance, which is not a troglobitic habitat. We collected specimens of *A. smokiensis* from beneath rocks at two localities in deciduous forest in the Cades Cove area of Great Smoky Mountains National Park, and the species should not be considered troglobitic.

Two of the most biogeographically important anillines in South Carolina are *A. dentatus* and *A. jancae*. Both are phylogenetically isolated, possess a unique combination of male secondary sexual modifications, and are known only from the vicinity of Long Cane Creek in Abbeville Co. *Anillinus dentatus* is recovered as sister to the widespread *valentinei* group in our 6-gene phylogeny, but there is no obvious morphological support for this relationship. Nor are there other known *Anillinus* species that are likely relatives. Thus, *A. dentatus* represents a unique, relict lineage that has apparently been extirpated elsewhere (Fig. 43B). Males possess dentate mesotrochanters, a unique character in *Anillinus* but shared with males of the Oregon endemic *Medusapyga alsea* LaBonte (LaBonte and Maddison 2023). Most specimens of *A. dentatus* have been collected in cooler seasons in the months of January and March, but that is also when most collecting has taken place. Members of the species are endogean in habit, often being found beneath deeply embedded rocks in pure, red clay. The beetles move slowly when exposed, and their small distribution perhaps reflects both a strictly endogean lifestyle and greatly limited dispersal capabilities. The other notable Long Cane Creek species, *A. jancae*, is strongly supported as sister to the Florida endemic *A. albrittonorum* (Fig. 43C). Females of both species possess a unique form of spermatheca not found elsewhere in the genus, and males lack adhesive setae on the second protarsomere. Aside from these characters, there are no obvious morphological synapomorphies, but every gene sampled recovers the two species as a clade with strong support.

In the 6-gene phylogeny, the sister to the *albrittonorum* group is the large “ESP+LSL” clade, containing the bulk of quadrisetose Appalachian *Anillinus* species. A history of ancient hydrochory – transport from higher elevations by intense floods – is a tempting explanation for this pattern, but if that were the case one would expect *A. jancae* and *A. albrittonorum* to be polyphyletic within the “ESP+LSL” clade rather than each other’s closest relative. The *albrittonorum* group likely represents an even older relict lineage that was formerly more widespread across the southeastern United States. As in *A. dentatus*, the endogean habits and limited dispersal capabilities of *A. jancae* explain its very small range. In a case of remarkable convergence, male *A. jancae* possess an abdominal keel and dentate profemora, as in the Washington endemic *Medusapyga chehalis* LaBonte (LaBonte and Maddison 2023). The selective pressures that have resulted in convergence between two distantly related but co-occurring *Anillinus* in the Piedmont of South Carolina and a pair of anillines in the Pacific Northwest are difficult to fathom, but it is noteworthy that all four of the species inhabit mineral soil layers and have greatly limited dispersal capabilities.

The “ESP clade”, consisting of the *elongatus*, *sinuaticollis*, and *pecki* groups, is represented in South Carolina by members of the *elongatus* and *sinuaticollis* groups. South Carolina is the only state known to have representatives of both groups, and both groups reach their southwestern and eastern-most limits, respectively, within South Carolina. The *elongatus* group contains endogean species endemic to a small area of the Piedmont ecoregion, ranging from southern Virginia to northeastern South Carolina (Fig. 43D). Most of the species are known from a single locality, and their endogean habits and slow, sluggish behavior when exposed are similar to those of *A. dentatus*; their limited ranges probably reflect poor dispersal capabilities. Sampling within the range of the group has not been dense enough to precisely identify the biogeographic barriers separating most species, but the closely related and geographically proximate *Anillinus elongatus* Jeannel and *Anillinus pittsylvanicus* occur on opposite sides of the divide between two watersheds, and the ranges of the other species suggest that passive movement by hydrochory has been an important mode of dispersal in the group (Harden and Caterino 2024), as has been suggested for other anillines (Ortuño and Gilgado 2011; Andújar et al. 2017).

The two South Carolina *elongatus*-group species are known from quite different habitats. *Anillinus montrex* is endemic to Kings Mountain, where it has been found under rocks in a small, mesic stream hollow, whereas *A. arenicollis* lives in deep sand in longleaf pine (*Pinus palustris* Mill.) savannah. The two species also belong to two different subclades within the *elongatus* group, with *A. montrex* sister to an undescribed species from Orange Co., North Carolina and *A. arenicollis* in a clade with the remaining species. Both clades co-occur at the Orange Co. site, where *A. elongatus* is relatively common and the undescribed species has been collected only once, from a pipe trap set in deep rocky soil. The non-sister relationship between the two Orange Co. species indicates that allopatric speciation with subsequent dispersal has occurred, rather than sympatric speciation.

Anillinus montrex and its undescribed Orange Co. sister species show more pronounced morphological adaptations to endogean existence than other *elongatus*-group species, with a flatter and more parallel sided body. These two species also have larger metafemoral spines, with the Orange Co. species having two spines, a unique state in the genus. As seen also in *A. dentatus* and *A. albrittonorum*, accumulation of male secondary sexual modifications is a common pattern in endogean *Anillinus* in the southeastern United States. Endogean habit and male secondary leg modifications are found also in the *sinuaticollis* group, which is known in South Carolina only from the upper Savannah River drainage (Fig. 36). Three closely related species occur along the tributaries and historic course of the Seneca River, with *A. mica* and *A. micamicus* found north of the confluence of the Keowee and Twelvemile Rivers, and *A. seneca* found west and south of this point. *Anillinus mica* and *A. micamicus* are syntopic at all three sites from which *A. micamicus* is known. The sister to *A. micamicus* is *A.* sp. “South Carolina, Coon Branch” which is morphologically similar to *A. micamicus* and might be one end of a grade of variation. *Anillinus* sp. “South Carolina, Coon Branch” occurs in the Whitewater River Gorge, at a higher elevation than any other *sinuaticollis* group occurrences. As in the two clades of the *elongatus* group, the syntopy of *A. mica* and *A. micamicus* is the result of dispersal; the two species may have evolved allopatrically in isolated stream gorges in the Blue Ridge Escarpment and subsequently been brought together by hydrochory.

The fourth *sinuaticollis*-group species known from South Carolina, *A. choestoea*, is phylogenetically distant from the clade of *A. mica*, *A. micamicus*, and *A. seneca*, and in the 6-gene phylogeny *A. choestoea* is in a clade with species from Alabama, Tennessee, and Kentucky. Hydrochory also provides a compelling explanation for the occurrence of this western lineage in South Carolina. The Tugaloo River, along which *A. choestoea* occurs, captured the Tallulah and Chattooga Rivers during the Pleistocene (Voss et al. 1993), rerouting their waters to the Atlantic Ocean via the Savannah River watershed. Prior to this, both the Tallulah and Chattooga Rivers entered the ancestral Chattahoochee River, which eventually flowed to the Gulf of Mexico. The ancestral Chattahoochee River may have been a barrier separating the eastern and western *sinuaticollis* group lineages, and capture by the Tugaloo River could have transported *A. choe-*

stoea (or its ancestor) into the Savannah River drainage. As Fig. 35 shows, most of the land along the Tugaloo River drainage remains to be explored for members of the *sinuaticollis* group, and the clade is entirely unknown from Georgia. Discovery of *sinuaticollis* group specimens along the Chattooga River and Chattahoochee Rivers would allow testing of this biogeographical hypothesis.

The remaining *Anillinus* species found in South Carolina belong to the *langdoni* group and *loweae* group, which make up part of the well-supported "LSL clade". This large clade includes the *Anillinus* species most commonly collected in litter samples in the Southern Appalachians. The *langdoni* group has been found in four disjunct regions (Fig. 43E): northwestern Virginia and adjacent West Virginia (*A. virginiae*), the South Mountains in western North Carolina, the Cumberland Plateau in southeastern Kentucky, and the Southern Appalachians southwest of the FBR. The gap between *A. virginiae* and the Southern Appalachian *langdoni*-group species does not correspond to any obvious biogeographic barriers, but a somewhat similar gap is seen in the distribution of *Serranillus* (Fig. 1A). The sister lineage to the Southern Appalachian species is not *A. virginiae* but a surprising clade that spans the Tennessee River Valley, consisting of the Kentucky endemic *A. balli* and an undescribed species from northern Georgia. The single *langdoni*-group species known from South Carolina, *A.* cf. *nantahala*, belongs to the Southern Appalachian lineage. *Anillinus* cf. *nantahala* is the most widespread species in the clade, ranging from the western flank of the Unicoi Mountains in eastern Tennessee to northwestern South Carolina and eastern Georgia (Fig. 38). The South Carolina specimen was collected from a litter sample taken from a mesic stream hollow near the Chattooga River gorge.

The *loweae* group has a smaller range, limited to the Southern Appalachians (Fig. 43G). Collectively, the range of the *loweae* group skirts the FBR above its headwaters, as in *S. dunavani* and *A. murrayae*, with *A. fortis* occurring in several mountain ranges to the northeast, including elevations above 1650 m on Big Bald in the Bald Mountains. The two most commonly collected species of the *loweae* group, *A. loweae* and *A. cherokee*, can be readily collected from rather shallow leaf litter where they occur. Specimens of *A. loweae* have been captured in traditional pitfall traps in Great Smoky Mountains National Park (National Ecological Observatory Network data), which attests to their active movement above-ground, as does their extensive geographic range and wide elevational distribution (Sokolov and Carlton 2010). In South Carolina, *A. loweae* is known only from Sassafras Mountain, the highest mountain in the state, while *A. cherokee* is known from several localities further west. The third described species, *A. merritti*, is primarily endogean in habit and is only rarely collected in leaf litter. Its range is similar to that of *A. cherokee* (Fig. 38).

Females of *A. merritti* are unusually variable in external structure; in some populations east of the Little Tennessee River, the humeri are strongly sloped and constricted, giving the body an hourglass-shaped appearance (Fig. 39A). Such a body form, otherwise known in *Anillinus* only in females of some *moseleyae*-group species, has been hypothesized to be an adaptation to endogean existence, allowing greater flexibility to move through tighter interstices (Sokolov 2013). Only females of these *A. merritti* populations have the hourglass-shaped body, so either females have adapted to reach deeper strata, possibly for oviposition, or the shape is involved in sexual recognition. The area occupied by hourglass-shaped *A. merritti* is also where the greatest local diversity of *loweae*-group species is found; at Rabun Bald, all three described species occur. Competition and/or detrimental interbreeding between these closely related species could have also been selective factors. Like several other more montane anillines, *A. merritti* is known in South Carolina only from the extreme northwest corner of the state.

Habitats used by members of the *langdoni* and *loweae* groups may explain aspects of their distributions. For example, members of the *langdoni* group are typically collected in leaf litter, and seem to be strongly associated with primary-growth forest (Ferro et al. 2012). Strong association with such habitats would limit their occurrence in South Carolina to the few relatively undisturbed steep hollows at higher elevations in the northwest corner of the state.

Conservation of Appalachian Anillini

While all anillines are short range (or micro-range) endemics with apparently limited dispersal capabilities, there are currently none officially listed as of conservation concern, although it has been suggested that they deserve such ranking (Cornell 1979). Anillines are difficult to collect and therefore are rarely detected in non-specialist survey efforts, which can skew perceptions about rarity. For example, in the first symposium of endangered species of South Carolina (Brooks et al. 1979), *Anillinus dunavani* Jeannel (now placed in the genus *Serranillus*) was described as rare and "only known from type specimen"; in fact, *Serranillus dunavani* is the most abundant and commonly collected anilline in South Carolina. On the other hand, our study has shown that many more species of anillines exist in the eastern United States than are formally recognized, and most of them occur at lower elevations that receive less conservation attention than montane habitats (Timpe et al. 2009). It is important to note that almost all of the forested habitats in which anillines currently occur have been heavily impacted by humans throughout recent history by logging and agriculture. At Long Cane Creek in Abbeville Co., SC, for example, one of the most diverse and important anilline sites in the state, the woods are scarred by deep gullies formed by erosion from poor farming practices when the area would have been a barren cotton field (Fig. 25C). The persistence of anillines through such periods of habitat destruction and alteration is incredible, and offers some hope that at least the endogean species are resilient to these disturbances.

However, it is unlikely that anillines could survive "development" of a site, which necessarily requires heavy compaction of the soil to support man-made structures. The Piedmont ecoregion of the southeastern United States is rapidly undergoing such habitat destruction, and anilline species are likely being lost before being even being discovered. The damage that such losses could cause to our understanding of biodiversity are best illustrated by *A. dentatus* and *A. jancae*, the most phylogenetically important species of anillines in South Carolina, both known only from a small area in the vicinity of Long Cane Creek, Abbeville County. The discovery of such unusual anillines in the outer Piedmont of the southeastern United States reflects the fact that the soil and litter arthropod fauna in the region has been generally overlooked. In reference to millipedes, Richard Hoffman (1963) wrote that the species inhabiting this area "are as poorly known as those of any comparable area in the world." Examples of phylogenetically and morphologically isolated taxa found in the vicinity of Long Cane Creek include the millipede *Parvulodesmus prolixogonus* (Shelley 1983) and the spider *Epiceraticelus mandyae* (Draney et al. 2019). Disjunct occurrences of Appalachian endemics are also known, including beetles such as the stayphylinid *Dasycerus carolinensis* (Caterino and Harden 2024), otherwise known only from mountains northeast of the French Broad River, and the carabid *Pterostichus acutipes* Barr, otherwise known in South Carolina only on the Blue Ridge Escarpment (CUAC data).

These concerns are not restricted to small and cryptic speices. For example, unusual populations of the carabid subgenera *Pterostichus* (*Gastrosticta*) and *Dicaelus* (*Paradicaelus*) have been discovered in the outer Piedmont of South Carolina in the past two decades, and likely represent new species (CUAC and AMDc data). The latter are relatively large, more than 20 mm in length, with distinctive external and genitalic characters. That such conspicuous taxa can still be discovered in the eastern United States emphasizes the desperate need for baseline bioinventory work in the Piedmont of the southeastern United States. The situation for anillines must be even more desperate.

Conclusions

The Anillini of the Eastern United States comprise a unique component of the region's rich biodiversity. Conservatively, 148 species of anillines are now known from east of the Mississippi River. The majority of these remain undescribed (Suppl. material 3). The systematic framework that we present here will facilitate description and classification of these species and others that will doubtlessly be discovered in the future. While our sampling has been relatively thorough, large swaths of the region are entirely unexplored for endogean anillines, and additional unique lineages such as those represented by *A. dentatus* and *A. jancae* may remain to be discovered. We hope that our contributions will influence more biologists to focus on this surprising and diverse tribe of beetles.

Acknowledgements

Collecting permits were granted by Blue Ridge Parkway (BLRI-2018-SCI-0022), Carolina Sandhills National Wildlife Refuge (21-019), Duke Forest (R2223-531), Great Smoky Mountains National Park (GRSM-2019-SCI-2045), North Carolina Division of Parks and Recreation (2023_0697), South Carolina State Park Service (N-1-15), and Virginia Department of Conservation and Recreation (ZZ-RCP-010522). For permission to sample on their private land, we thank Terry and Sandra Thompson (Hestand, KY), Annette Reynolds (Manitou Cave Preserve, AL), Benjamin Williams (Patrick Co., VA), Phil Lucas (Water Sinks, VA), and Jamie Guy (Wateree Floodlands Memorial Forest, SC).

For facilitating collections access and/or specimen loans, we thank Ainsley Seago, Robert L. Davidson, and Robert Androw (Carnegie Museum of Natural History), Torsten Dikow and Charyn Micheli (United States National Museum of Natural History), Kal Ivanov and Liberty Hightower (Virginia Museum of Natural History), E. Richard Hoebeke (University of Georgia Collection of Arthropods), Gareth Powell and Kyle Schnepp (Florida State Collection of Arthropods), Luciana Musetti (Ohio State University), Tommy McElrath (Illinois Natural History Survey) and Robert Blinn and Gareth Powell (North Carolina State University).

Several individuals contributed specimens to this project. Shelley Langton-Myers collected, extracted, and amplified COI sequences from several vouchers used in this study as part of a preliminary exploration of Appalachian litter biodiversity. Valuable specimens came from Tim King, Kyle Schnepp, Michael Ferro, Ernesto Recuero, Patricia Wooden, Adam Haberski, Frank Etzler, Anthony Deczynski, Daniel Malagon, Sharon Bewick, Benjamin Camper, Julian J. Lewis, Christopher Carlton, Matthew Niemiller, Derek Hennen, Kal Ivanov, Jackson Means, Liberty Hightower, Benjamin Williams, and Todd Lawton. Additional assistance in the field came from Lily Thompson, James LaBonte, and Thomas Malabad. CWH extends special thanks to Lily M. Thompson for her support and encouragement both in the field and during the preparation of this manuscript.

For stimulating conversations and correspondence about Anillini, CWH is grateful to Rolf Aalbu, Peter Adler, Robert Anderson, Christopher Carlton, Augusto Degiovanni, Drew Hildebrandt, Kenneth Karns, Dave Kavanaugh, Tim King, James LaBonte, Todd Lawton, Julian J. Lewis, David Maddison, R. Wyatt Mendez, Stewart Peck, Kyle Schnepp, Igor Sokolov, Alexey Tishechkin, Larry Watrous, and Kipling Will.

We thank Peter Adler and David Maddison for their critical reviews of an earlier draft of this manuscript, and John Spence for a thorough peer review, which improved the quality of this work.

This paper is technical contribution No. 7315 of the Clemson University Experiment Station.

Additional information

Conflict of interest

The authors have declared that no competing interests exist.

Ethical statement

No ethical statement was reported.

Funding

Funding for this project was provided in part by the U.S. National Science Foundation (Award DEB-1916263 to MSC), the Clemson University Experiment Station (SC-1700596 to MSC) and the John and Suzanne Morse Endowment for Arthropod Biodiversity at Clemson University. Additional funding for DNA sequencing, SEM micrography and museum work came from a Coleopterists Society Graduate Student Research Enhancement Award to CWH in 2020, two E.W. King Memorial Grant Fund awards to CWH in 2020 and 2022, and a Clemson University Graduate Student Travel Grant to CWH in 2023.

Author contributions

Conceptualization: CWH. Data curation: CWH. Formal analysis: CWH. Funding acquisition: MSC, CWH. Investigation: CWH. Methodology: CWH. Resources: MSC. Visualization: CWH. Writing - original draft: CWH. Writing - review and editing: MSC, CWH.

Author ORCIDs

Curt W. Harden https://orcid.org/0000-0002-5226-8725
Michael S. Caterino https://orcid.org/0000-0002-2597-5707

Data availability

The data underpinning the analyses reported in this paper are deposited in the Dryad Data Repository at https://doi.org/10.5061/dryad.g79cnp5z3.

References

Andújar C, Grebennikov VV (2021) Endogean beetles (Coleoptera) of Madagascar: Deep soil sampling and illustrated overview. Zootaxa 4963(2): 317–334. https://doi.org/10.11646/zootaxa.4963.2.4

Andújar C, Grebennikov VV, Lencina JL, Serrano J (2010) A new *Typhlocharis* (Coleoptera: Carabidae: Anillina) from Spain: combining adult and larval morphological data with DNA information. Zootaxa 2485(1): 47. https://doi.org/10.11646/zootaxa.2485.1.4

Andújar C, Faille A, Pérez-González S, Zaballos JP, Vogler AP, Ribera I (2016) Gondwanian relicts and oceanic dispersal in a cosmopolitan radiation of euedaphic ground beetles. Molecular Phylogenetics and Evolution 99: 235–246. https://doi.org/10.1016/j.ympev.2016.03.013

Andújar C, Pérez-González S, Arribas P, Zaballos JP, Vogler AP, Ribera I (2017) Speciation below ground: Tempo and mode of diversification in a radiation of endogean ground beetles. Molecular Ecology 26(21): 6053–6070. https://doi.org/10.1111/mec.14358

Arndt E, Grebennikov VV, Zaballos JMP (1999) Description of the larvae of a representative of Anillina with a key to the Palearctic genera of Bembidiini. Koleopterologische Rundschau 69: 11–19.

Barr Jr TC (1967) *Antroforceps*, an eyeless cave scaritine from Mexico. Coleopterists Bulletin 21(3): 65–70. https://doi.org/10.5962/p.372482

Barr Jr TC (1969) Evolution of the (Coleoptera) Carabidae in the Southern Appalachians. In: Holt, PC, Roane, MK, Parker, BC (Eds) The distributional history of the biota of the Southern Appalachians. Part I: Invertebrates. Research Monograph. Virginia Polytechnic Institute and State University, 67–92.

Barr Jr TC (1979) Revision of Appalachian *Trechus* (Coleoptera: Carabidae). Brimleyana 2: 29–75.

Barr Jr TC (1995) Notes on some anillines (Coleoptera, Carabidae, Bembidiinae) from Southeastern United States, with descriptions of a new genus and two new species. Special Bulletin of the Japanese Society of Coleopterology 4: 239–248.

Bousquet Y (2012) Catalogue of Geadephaga (Coleoptera: Adephaga) of America, north of Mexico. ZooKeys 245: 1–1722. https://doi.org/10.3897/zookeys.245.3416

Bousquet Y, Skelley P (2012) Description of two new species of *Clivina* Latreille (Coleoptera, Carabidae, Clivinini) from southeastern United States. ZooKeys 178: 43–50. https://doi.org/10.3897/zookeys.178.2817

Brooks DW, Carlson PH, Cornell JF, Douglass HB, King EW, McCaskill VH, Morse JC, Skelton TE, Spooner J (1979) Status report: Arthropoda other than Crustacea. In: Proceedings of the first South Carolina endangered species symposium. Charleston, S.C., 46–51.

Carlton CE (2008) Eight New Species of *Arianops* Brendel from the Southeastern United States with an Updated Key and Notes on Additional Species (Coleoptera: Staphylinidae: Pselaphinae). Coleopterists Bulletin 62(2): 297–323. https://doi.org/10.1649/1082.1

Carlton CE, Chandler DS, Leschen RAB, Riley EG, Skelley PE (2005) Obituary and dedication: Karl Heinz Stephan 1931–2005. Coleopterists Bulletin 59(3): 277–283. https://doi.org/10.1649/0010-065X(2005)059[0277:KHS]2.0.CO;2

Caterino MS, Harden CW (2024) A review of Appalachian *Dasycerus* Brongniart and the recognition of cryptic diversity within *Dasycerus carolinensis* (Coleoptera: Staphylinidae: Dasycerinae). Insect Systematics and Diversity 8(2)[ixae009]: 1–22. https://doi.org/10.1093/isd/ixae009

Caterino MS, Recuero E (2023) Shedding light on dark taxa in sky-island Appalachian leaf litter: Assessing patterns of endemicity using large-scale, voucher-based barcoding. Insect Conservation and Diversity 17(1): 1–15. https://doi.org/10.1111/icad.12697

Chakrabarty P, Warren M, Page L, Baldwin C (2013) GenSeq: An updated nomenclature and ranking for genetic sequences from type and non-type sources. ZooKeys 346: 29–41. https://doi.org/10.3897/zookeys.346.5753

Cornell JF (1972) The eyeless beetles of North Carolina with notes on their ecology and evolution (Insecta: Coleoptera). Journal of the Elisha Mitchell Scientific Society 88: 260–264.

Cornell JF (1977a) Freshwater and terrestrial arthropods: Species of special concern: Insecta; Coleoptera; Carabidae (Ground Beetles). In: Cooper JE, Robinson SS, Funderburg JB (Eds) Endangered and threatened plants and animals of North Carolina: proceedings of the Symposium on Endangered and Threatened Biota of North Carolina, 1, biological concerns, Meredith College, Raleigh, November 7–8, 1975. North Carolina State Museum of Natural History, 221–222.

Cornell JF (1977b) Freshwater and terrestrial arthropods: Threatened species: Insecta; Coleoptera; Carabidae (Ground Beetles). In: Cooper JE, Robinson SS, Funderburg JB (Eds) Endangered and threatened plants and animals of North Carolina: proceedings of the Symposium on Endangered and Threatened Biota of North Carolina, 1, biological concerns, Meredith College, Raleigh, November 7–8, 1975. North Carolina State Museum of Natural History, 207–208.

Cornell JF (1979) Endangered Coleoptera. In: Proceedings of the first South Carolina endangered species symposium. Charleston, S.C., 107–110.

Coyne JA, Orr HA (2004) Speciation. Sinauer Associates, Inc., Sunderland, Massachusetts, U.S.A., 545 pp.

Dajoz R (2005) Les Coléoptères terricoles de trois stations du sud des Appalaches (États-Unis): Structure des peuplements et description de trois espèces nouvelles. Bulletin de la Société Entomologique de France 110(2): 201–212. https://doi.org/10.3406/bsef.2005.16223

Donabauer M (2009) New species of the *Trechus* (*Microtrechus*) *vandykei* group from the southern Appalachians. Zeitschrift der Arbeitsgemeinschaft Österreichischer Entomologen 61: 129–141.

Draney ML, Milne MA, Ulyshen M, Madriz G (2019) Revision of the spider genus *Epiceraticelus* (Araneae, Linyphiidae) with a description of a new species. Zootaxa 4646(1): 189–200. https://doi.org/10.11646/zootaxa.4646.1.11

DuRant JA, Fox RC (1966) Some arthropods of the forest floor in pine and hardwood forests in the South Carolina Piedmont region. Annals of the Entomological Society of America 59(1): 202–207. https://doi.org/10.1093/aesa/59.1.202

Dury C (1902) A revised list of the Coleoptera observed near Cincinnati, Ohio, with notes on localities, bibliographical references and description of six new species. The Journal of the Cincinnati Society of Natural History 20: 107–196.

Erwin TL, Kavanaugh D (1981) Systematics and zoogeography of *Bembidion* Latreille: I. The *carlhi* and *erasum* groups of western North America (Coleoptera: Carabidae, Bembidiini). Entomologica Scandinavica (Supplement 15): 33–72.

Erwin TL, Sims LL (1984) Carabid beetles of the West Indies (Insects: Coleoptera): A synopsis of the genera and checklists of tribes of Caraboidea, and of the West Indian species. Quaestiones Entomologicae 20: 351–466.

Ferro ML, Gimmel ML, Harms KE, Carlton CE (2012) Comparison of the Coleoptera communities in leaf litter and rotten wood in Great Smoky Mountains National Park, USA. Insecta Mundi 0259: 1–58.

Folmer O, Black M, Hoeh W, Lutz R, Vrijenhoek R (1994) DNA primers for amplification of mitochondrial cytochrome c oxidase subunit I from diverse metazoan invertebrates. Molecular Marine Biology and Biotechnology 3(5): 294–299.

Garrick RC, Newton KE, Worthington RJ (2018) Cryptic diversity in the southern Appalachian Mountains: Genetic data reveal that the red centipede, *Scolopocryptops sexspinosus*, is a species complex. Journal of Insect Conservation 22(5–6): 799–805. https://doi.org/10.1007/s10841-018-0107-3

Giachino PM (2011) A description of two new species of Anillina from North Carolina with notes about the geographical distribution of the genus *Anillinus* Casey, 1918 (Coleoptera: Carabidae: Bembidiini). Studies and Reports. Taxonomical Series 7: 109–116.

Giachino PM (2015) New Anillina from South Africa, Tanzania, Madagascar and Seychelles Islands (Coleoptera: Carabidae, Bembidiini). Fragmenta Entomologica 47(1): 15–31. https://doi.org/10.4081/fe.2015.130

Giachino PM, Vailati D (2011) Review of the Anillina of Greece (Coleoptera, Carabidae, Bembidiini). Biodiversity Journal Monograph 1: 1–112.

Giachino PM, Eberhard S, Perina G (2021) A rich fauna of subterranean short-range endemic Anillini (Coleoptera, Carabidae, Trechinae) from semi-arid regions of Western Australia. ZooKeys 1044: 269–337. https://doi.org/10.3897/zookeys.1044.58844

Grebennikov VV (2002) Description of the first-instar larva of *Geocharidius* (Coleoptera: Carabidae: Trechitae) with a discussion of the phylogeny of the subtribe Anillina. European Journal of Entomology 99(4): 523–527. https://doi.org/10.14411/eje.2002.068

Grebennikov VV, Maddison DR (2005) Phylogenetic analysis of Trechitae (Coleoptera: Carabidae) based on larval morphology, with a description of first-instar *Phrypeus* and a key to genera. Systematic Entomology 30(1): 38–59. https://doi.org/10.1111/j.1365-3113.2004.00259.x

Harden CW (2024) Distribution of Nearctic Anillini (Coleoptera, Carabidae, Trechinae) (Version 01) [Data set]. Zenodo. https://doi.org/10.5281/zenodo.10983000

Harden CW, Caterino MS (2024) Revision of the elongatus and pecki species groups of *Anillinus* Casey, 1918 (Coleoptera, Carabidae, Trechinae, Anillini), with four new species and notes on *Anillinus turneri* Jeannel, 1963. Insecta Mundi 1057: 1–31.

Harden CW, Davidson RL, Malabad TE, Caterino MS, Maddison DR (2024) Phylogenetic systematics of the enigmatic genus *Horologion* Valentine, with description of a new species from Bath County, Virginia (Coleoptera, Carabidae, Trechinae, Horologionini). Subterranean Biology 48: 1–49. https://doi.org/10.3897/subtbiol.48.114404

Hedin M, Thomas SM (2010) Molecular systematics of eastern North American Phalangodidae (Arachnida: Opiliones: Laniatores), demonstrating convergent morphological evolution in caves. Molecular Phylogenetics and Evolution 54(1): 107–121. https://doi.org/10.1016/j.ympev.2009.08.020

Hennen DA, Means JC, Marek PE (2022) A revision of the *wilsoni* species group in the millipede genus *Nannaria* Chamberlin, 1918 (Diplopoda, Polydesmida, Xystodesmidae). ZooKeys 1096: 17118. https://doi.org/10.3897/zookeys.1096.73485

Hildebrandt D, Maddison D (2011) A new species of *Bembidion* Latrielle 1802 from the Ozarks, with a review of the North American species of subgenus *Trichoplataphus* Netolitzky 1914 (Coleoptera, Carabidae, Bembidiini). ZooKeys 147: 261–275. https://doi.org/10.3897/zookeys.147.1872

Hlaváč P, Baňař P, Davranoglou L-R, Kempton J (2021) Endogean and Cavernicolous Coleoptera of the Balkans. XXIII. A new species of *Paramaurops* J. Müller (Coleoptera: Staphylinidae: Pselaphinae) from Greece. Zootaxa 4970(1). https://doi.org/10.11646/zootaxa.4970.1.12

Hoffman RL (1963) A new diplopod genus and species from Georgia (Polydesmida: Xystodesmidae). Proceedings of the Biological Society of Washington 76: 113–120.

Huang S, Zhou J, Tian M, Faille A (2021) Three new species of the subterranean genus *Guiodytes* from Guangxi, China (Coleoptera: Carabidae: Clivinini). European Journal of Taxonomy 774: 135–154. https://doi.org/10.5852/ejt.2021.774.1537

Jeannel R (1963a) Monographie des "'Anillini'", Bembidiides endogés [Coleoptera Trechidae]. Mémoires du Muséum National d'Histoire Naturelle Série A. Zoologie 28: 33–204.

Jeannel R (1963b) Supplément à la monographie des Anillini. Sur quelques espèces nouvelles de l'Amérique du Nord. Revue Française d'Entomologie 30: 145–152.

Katoh K, Standley DM (2013) MAFFT Multiple Sequence Alignment Software Version 7: Improvements in performance and usability. Molecular Biology and Evolution 30(4): 772–780. https://doi.org/10.1093/molbev/mst010

Keith R, Hedin M (2012) Extreme mitochondrial population subdivision in southern Appalachian paleoendemic spiders (Araneae: Hypochilidae: *Hypochilus*), with implications for species delimitation. The Journal of Arachnology 40(2): 167–181. https://doi.org/10.1636/A11-49.1

Kippenhan MG (2023) The taxonomic status of two species of North American Trogossitidae (Coleoptera: Cleroidea) described by Roger Dajoz. Coleopterists Bulletin 77(2): 278–282. https://doi.org/10.1649/0010-065X-77.2.278

LaBonte JR, Maddison DR (2023) *Medusapyga* LaBonte and Maddison, a new genus of Anillini (Coleoptera: Carabidae: Trechinae) from the Pacific Northwest of the United States. Proceedings of the California Academy of Sciences 67: 401–432.

Liebherr JK (2008) Taxonomic revision of Hawaiian *Bembidion* Latreille (Coleoptera: Carabidae: Bembidiini) with a discussion of their reductive and derivative evolutionary specializations. Annals of the Carnegie Museum 77(1): 31–78. https://doi.org/10.2992/0097-4463-77.1.31

Lindroth CH (1966) The ground-beetles (Carabidae, excl. Cicindelinae) of Canada and Alaska. Part 4. Opuscula Entomologica (Supplementum XXXIII): 409–648.

Maddison DR (1993) Systematics of the Holarctic beetle subgenus *Bracteon* and related *Bembidion* (Coleoptera: Carabidae). Bulletin of the Museum of Comparative Zoology 153: 143–299.

Maddison DR (2012) Phylogeny of *Bembidion* and related ground beetles (Coleoptera: Carabidae: Trechinae: Bembidiini: Bembidiina). Molecular Phylogenetics and Evolution 63(3): 533–576. https://doi.org/10.1016/j.ympev.2012.01.015

Maddison DR, Cooper KW (2014) Species delimitation in the ground beetle subgenus *Liocosmius* (Coleoptera: Carabidae: *Bembidion*), including standard and next-generation sequencing of museum specimens. Zoological Journal of the Linnean Society 172(4): 741–770. https://doi.org/10.1111/zoj.12188

Maddison DR, Maddison WP (2023a) Zephyr: a Mesquite package for interacting with external phylogeny inference programs. http://zephyr.mesquiteproject.org

Maddison WP, Maddison DR (2023b) Mesquite: a modular system for evolutionary analysis. Available from: http://www.mesquiteproject.org

Maddison DR, Ober KA (2011) Phylogeny of minute carabid beetles and their relatives based upon DNA sequence data (Coleoptera, Carabidae, Trechitae). ZooKeys 147: 229–260. https://doi.org/10.3897/zookeys.147.1871

Maddison DR, Kanda K, Boyd OF, Faille A, Porch N, Erwin TL, Roig-Juñent S (2019) Phylogeny of the beetle supertribe Trechitae (Coleoptera: Carabidae): Unexpected clades, isolated lineages, and morphological convergence. Molecular Phylogenetics and Evolution 132: 151–176. https://doi.org/10.1016/j.ympev.2018.11.006

Magrini P (2008) Note sul genere *Binaghites* con descrizione di una nuova specie e considerazioni sugli *Scotodipnus* delle Alpi Occidentali (Coleoptera Carabidae). Bollettino della Società Entomologica Italiana 140: 139–150.

Mammola S, Giachino PM, Piano E, Jones A, Barberis M, Badino G, Isaia M (2016) Ecology and sampling techniques of an understudied subterranean habitat: The *Milieu Souterrain Superficiel* (MSS). Naturwissenschaften 103(11–12): 88. https://doi.org/10.1007/s00114-016-1413-9

Maquet D, Dahan L, Raemdonck H, Dekoninck W, Drumont A (2018) Redécouverte en région de Bruxelles-Capitale du rare carabidé endogé *Anillus caecus* Jacquelin du Val 1851 au Jardin botanique Jean Massart grâce à la technique du lavage de terre (Coleoptera, Carabidae, Trechinae, Bembidiini, Anillina). Lambillionea 118: 201–210.

Moulton JK, Wiegmann BM (2004) Evolution and phylogenetic utility of CAD (rudimentary) among Mesozoic-aged Eremoneuran Diptera (Insecta). Molecular Phylogenetics and Evolution 31(1): 363–378. https://doi.org/10.1016/S1055-7903(03)00284-7

Ober KA (2002) Phylogenetic relationships of the carabid subfamily Harpalinae (Coleoptera) based on molecular sequence data. Molecular Phylogenetics and Evolution 24(2): 228–248. https://doi.org/10.1016/S1055-7903(02)00251-8

Ortuño VM, Gilgado JD (2011) Historical perspective, new contributions and an enlightening dispersal mechanism for the endogean genus *Typhlocharis* Dieck 1869 (Coleoptera: Carabidae: Trechinae). Journal of Natural History 45(19–20): 1233–1256. https://doi.org/10.1080/00222933.2011.566944

Pérez-González S, Zaballos JP (2019) Structure of male genitalia in a lineage of minute endogean ground beetles: how four new species of *Microcharidius* Coiffait, 1969 (Coleoptera: Carabidae: Anillini) reveal gradual change and convergent evolution. Arthropod Systematics & Phylogeny 77: 57–86. https://doi.org/10.26049/ASP77-1-2019-04

Pérez-González S, Andújar C, Zaballos JP (2018) Hidden biodiversity: Total evidence phylogenetics and evolution of morphological traits in a highly diverse lineage of endogean ground beetles, *Typhlocharis* Dieck, 1869 (Carabidae, Trechinae, Anillini). Cladistics 34(4): 359–383. https://doi.org/10.1111/cla.12208

Schuler L (1971) Les trechinae de France. L'inversion de la valeur systematique des organes genitaux males et femelles. Nouvelle Revue d'Entomologie I: 265–273.

Shelley RM (1983) *Parvulodesmus prolixogonus*, a new genus and species of xystodesmid milliped from South Carolina (Polydesmida). Proceedings of the Biological Society of Washington 96: 121–126.

Sherwood WC, Garst FM (2016) Soils of Virginia. In: Bailey CM, Sherwood WC, Eaton LS, Powars DS (Eds) The Geology of Virginia. Special Publication. Virginia Museum of Natural History, 291–313.

Shull VL, Vogler AP, Baker MD, Maddison DR, Hammond PM (2001) Sequence alignment of 18S ribosomal RNA and the basal relationships of Adephagan Beetles: Evidence for monophyly of aquatic families and the placement of Trachypachidae. Systematic Biology 50(6): 945–969. https://doi.org/10.1080/106351501753462894

Simon C, Frati F, Beckenback A, Crespi B, Liu H, Flook P (1994) Evolution, weighting and phylogenetic utility of mitochondrial gene sequences and a compilation of conserved polymerase chain reaction primers. Annals of the Entomological Society of America 87: 651–701.

Slipinski A, Lawrence JF (2013) 1. Introduction. In: Australian Beetles Vol. 1: Morphology, Classification and Keys. CSIRO publishing, Collingwood, Victoria, Australia, 94 pp. https://doi.org/10.1071/9780643097292

Sokolov IM (2011) Five new species of *Anillinus* Casey from the Southern Appalachian Mountains and the Piedmont Plateau of eastern U.S.A. (Coleoptera: Carabidae: Trechinae: Bembidiini). Insecta Mundi 0164: 1–14.

Sokolov IM (2012) Five new species of *Anillinus* Casey from Alabama with a key to the Alabama species (Carabidae: Trechinae: Bembidiini). Annals of the Carnegie Museum 81(1): 61–71. https://doi.org/10.2992/007.081.0104

Sokolov IM (2013) A new genus and eight new species of the subtribe Anillina (Carabidae, Trechinae, Bembidiini) from Mexico, with a cladistic analysis and some notes on the evolution of the genus. ZooKeys 352: 51–92. https://doi.org/10.3897/zookeys.352.6052

Sokolov IM (2014) A new species of *Anillinus* Casey from the Oak Ridge area west of the Appalachian mountains in Tennessee (Coleoptera: Carabidae: Trechinae: Bembidiini). Annals of the Carnegie Museum 82(3): 225–229. https://doi.org/10.2992/007.082.0302

Sokolov IM (2020) Four new species of the genus *Anillinus* Casey (Coleoptera, Carabidae, Anillini) from Alabama, U.S.A., with a revised key to the Alabama species. Zootaxa 4808(3): 547–559. https://doi.org/10.11646/zootaxa.4808.3.9

Sokolov IM (2021) Two new species of the genus *Anillinus* Casey (Coleoptera, Carabidae, Anillini) from the southern United States. ZooKeys 1016: 63–76. https://doi.org/10.3897/zookeys.1016.61397

Sokolov IM (2022) Two new cavernicolous species of *Anillinus* Casey (Carabidae, Trechinae, Anillini) from Texas with a revised key to Texas species. Subterranean Biology 44: 153–166. https://doi.org/10.3897/subtbiol.44.91002

Sokolov IM (2023) Fourteen new species of the genus *Nesamblyops* Jeannel (Coleoptera: Carabidae: Anillini) from the South Island of New Zealand with redescription of the genus and description of a new subtribe. Zootaxa 5375(2): 151–192. https://doi.org/10.11646/zootaxa.5375.2.1

Sokolov IM, Carlton CE (2008) Two new species of blind, forest litter-inhabiting ground beetles from the subtribe Anillina (Carabidae: Trechinae: Bembidiini) from eastern U.S.A. Zootaxa 1740(1): 37. https://doi.org/10.11646/zootaxa.1740.1.4

Sokolov IM, Carlton CE (2010) New species of *Anillinus* Casey (Carabidae: Trechinae: Bembidiini) from the Southern Appalachians and phylogeography of the *A. loweae* species group. Zootaxa 2502(1): 1. https://doi.org/10.11646/zootaxa.2502.1.1

Sokolov IM, Carlton CE (2012) Species of *Anillinus* Casey (Coleoptera: Carabidae: Trechinae) described from Brazil and their relation to North American representatives of the genus. Coleopterists Bulletin 66(3): 245–249. https://doi.org/10.1649/072.066.0310

Sokolov IM, Schnepp KE (2021) A new subterranean species of *Anillinus* Casey (Carabidae, Trechinae, Anillini) from Florida. Subterranean Biology 39: 33–44. https://doi.org/10.3897/subtbiol.39.65769

Sokolov IM, Watrous LE (2008) A new species and the first record of the genus *Anillinus* (Carabidae: Trechinae: Bembidiini) from the Ozark region. Coleopterists Bulletin 62(4): 537–543. https://doi.org/10.1649/1114.1

Sokolov IM, Carlton C, Cornell JF (2004) Review of *Anillinus*, with descriptions of 17 new species and a key to soil and litter species (Coleoptera: Carabidae: Trechinae: Bembidiini). Coleopterists Bulletin 58(2): 185–233. https://doi.org/10.1649/611

Sokolov IM, Sokolova YY, Carlton CE (2007) New species of *Anillinus* Casey (Carabidae: Trechinae: Bembidiini) from Great Smoky Mountains National Park, U.S.A. and phylogeography of the *A. langdoni* species group. Zootaxa 1542(1): 1–20. https://doi.org/10.11646/zootaxa.1542.1.1

Sokolov IM, Reddell J, Kavanaugh D (2014) Life beneath the surface of the central Texan Balcones Escarpment: genus *Anillinus* Casey, 1918 (Coleoptera, Carabidae, Bembidiini): new species, a key to the Texas species, and notes about their way of life and evolution. ZooKeys 417: 71–101. https://doi.org/10.3897/zookeys.417.7733

Sokolov IM, Carlton CE, Watrous LE, Robison HW (2017) *Anillinus alleni* Sokolov and Carlton (Coleoptera: Carabidae: Trechinae: Bembidiini), a new species from the Ozark Interior Highlands of Arkansas, USA. Coleopterists Bulletin 71(2): 289. https://doi.org/10.1649/0010-065X-71.2.289

Talavera G, Castresana J (2007) Improvement of phylogenies after removing divergent and ambiguously aligned blocks from protein sequence alignments. Systematic Biology 56(4): 564–577. https://doi.org/10.1080/10635150701472164

Timpe EK, Graham SP, Bonett RM (2009) Phylogeography of the brownback salamander reveals patterns of local endemism in southern Appalachian springs. Molecular Phylogenetics and Evolution 52(2): 368–376. https://doi.org/10.1016/j.ympev.2009.03.023

Voss SR, Smith DG, Beachy CK, Heckel DG (1993) Allozyme variation in neighboring isolated populations of the plethodontid salamander *Leurognathus marmoratus*. Journal of Herpetology 29(3): 493–497. https://doi.org/10.2307/1565011

Ward PS, Downie DA (2005) The ant subfamily Pseudomyrmecinae (Hymenoptera: Formicidae): phylogeny and evolution of big-eyed arboreal ants: Phylogeny and evolution of big-eyed arboreal ants. Systematic Entomology 30(2): 310–335. https://doi.org/10.1111/j.1365-3113.2004.00281.x

Wild AL, Maddison DR (2008) Evaluating nuclear protein-coding genes for phylogenetic utility in beetles. Molecular Phylogenetics and Evolution 48(3): 877–891. https://doi.org/10.1016/j.ympev.2008.05.023

Supplementary material 1

Trees from maximum likelihood analyses of single gene and 6-gene matrices

Authors: Curt W. Harden, Michael S. Caterino

Data type: pdf

Link: https://doi.org/10.3897/zookeys.1209.125897.suppl1

Supplementary material 2

Taxa sampled for molecular phylogenetics and associated GenBank accession numbers

Authors: Curt W. Harden, Michael S. Caterino

Data type: docx

Link: https://doi.org/10.3897/zookeys.1209.125897.suppl2

Supplementary material 3

Systematic checklist of eastern Nearctic Anillini

Authors: Curt W. Harden, Michael S. Caterino

Data type: docx

Link: https://doi.org/10.3897/zookeys.1209.125897.suppl3

ZooKeys 1209: 199–230 (2024)
DOI: 10.3897/zookeys.1209.117368

Checklist

The jumping plant-lice (Hemiptera, Psylloidea) in Urban Green Spaces of Bogotá (Colombia), with descriptions of two new species and redescription of *Mastigimas colombianus* Burckhardt, Queiroz and Drohojowska

Diana Isabel Rendón-Mera[1,2,3], Daniel Burckhardt[1], Juliana Durán[4], Valentina Ocampo[4], Sergio Andrés Vargas-Fonseca[4,5]

1 *Naturhistorisches Museum, Augustinergasse 2, 4001 Basel, Switzerland*
2 *University of Basel, Petersplatz 1, 4001 Basel, Switzerland*
3 *Natural History Museum, Cromwell Road, London, UK*
4 *Jardín Botánico de Bogotá José Celestino Mutis, Av. Calle 63 No. 68-95, Bogotá, D.C., Colombia*
5 *Laboratorio de Entomología, Departamento de Biología, Pontificia Universidad Javeriana, Carrera 7, No. 43-82, Bogotá, D.C., Colombia*
Corresponding author: Diana Isabel Rendón-Mera (diana.rendonmera@nhm.ac.uk)

Abstract

In a survey of the arthropod fauna of 33 Urban Green Spaces (UGS) in Bogotá, Colombia, between 2017 and 2019, 21 species (3,825 specimens) of Psylloidea were collected. These represent all seven recognised families of jumping plant-lice and include seven species identified only to genus. The specimens, all adults, were collected on 30 plant species used for arborization in the UGS. Two species are described as new (*Mastigimas longicaudatus* Rendón-Mera, Burckhardt & Vargas-Fonseca, **sp. nov.** and *Leuronota albilinea* Rendón-Mera, Burckhardt & Vargas-Fonseca, **sp. nov.**), one species is redescribed (*Mastigimas colombianus* Burckhardt, Queiroz & Drohojowska) and one species is recorded for the first time from Colombia (*Calinda trinervis* Olivares & Burckhardt). Among the seven species identified only to genus is an undescribed species of *Melanastera*, representing a genus not previously known from Colombia. Fourteen species found during the survey are probably native (66%) and seven (33%) adventive. Our findings highlight the significance of UGS for preservation of biological diversity and stress the importance of using native plants in urban landscape planning for the conservation of the native entomofauna.

Key words: Biodiversity, city parks, insect–plant interactions, Neotropical region, psyllids, Sternorrhyncha, taxonomy, urbanisation

Academic editor: Igor Malenovský
Received: 14 December 2023
Accepted: 20 June 2024
Published: 8 August 2024

ZooBank: https://zoobank.org/4BEF4E4E-CCCC-49A0-A4F4-07DBA5CF2261

Citation: Rendón-Mera DI, Burckhardt D, Durán J, Ocampo V, Vargas-Fonseca SA (2024) The jumping plant-lice (Hemiptera, Psylloidea) in Urban Green Spaces of Bogotá (Colombia), with descriptions of two new species and redescription of *Mastigimas colombianus* Burckhardt, Queiroz and Drohojowska. ZooKeys 1209: 199–230. https://doi.org/10.3897/zookeys.1209.117368

Introduction

Urbanisation, the most irreversible form of land-use by the ever increasing human population, is one of the main drivers of the current extinction crisis (McKinney 2002; Seto et al. 2012; Díaz et al. 2019; Kong et al. 2021; Jaureguiberry et al. 2022). Accompanied by the degradation, fragmentation and loss of natural habitats (Foley et al. 2005; Elmqvist et al. 2013; Kong et al. 2021), urbanisation usually favours the presence of exotic species, leads to biotic homogeneity, and ultimately results in the loss of native species (McKinney 2002, 2008; Elmqvist et al. 2013; McDonald et al. 2018). Cities have dramatically expanded during the last decades and, as of today, more than half of the world's population resides in urban areas with an expected increase to 70% by 2050 (Elmqvist et al. 2013; United Nations 2019).

As cities grow, Urban Green Spaces (UGS) become increasingly critical for supporting native organisms (Goddard et al. 2010; Aronson et al. 2014; Ives et al. 2016). These spaces comprise natural, semi-natural and artificial habitats, including remnants of native vegetation, parks, gardens, urban wastelands and green infrastructure (Tzoulas et al. 2007; Aronson et al. 2017; Lepczyk et al. 2017). However, not all UGS have equal conservation value, as the degree to which they can support biodiversity depends on several factors such as quality, size, connectivity, biotic interactions, land-use history and human population density (Aronson et al. 2017). Consequently, it is necessary to integrate ecological and biodiversity aspects into urban planning, to develop strategies for the design and management of these spaces to serve biodiversity conservation (McKinney 2002; Elmqvist et al. 2013; Aronson et al. 2017; McDonald et al. 2018).

Colombia is located in the north-west of South America and is one of the world's megadiverse countries, home to approximately 10% of the world's species and two of the world's biodiversity hotspots: Tropical Andes and Tumbes–Chocó–Magdalena (Myers et al. 2000; Baptiste et al. 2017). At the same time, it is a highly urbanised country, with ~ 80% of its 50 million human inhabitants residing in urban areas (OECD 2022). This contrast is particularly evident in the Andean region, which exhibits both the highest levels of biological diversity and endemism, and of urbanisation and population density (Anselm et al. 2018; Carvajal-Castro et al. 2019). The Colombian capital Bogotá, the largest city in the country, is located in the middle of the Andes mountains, in the Eastern Ranges. Like other Latin American cities, much of Bogotá's urban growth during the last two centuries has been unplanned and informal (Andrade et al. 2013), driven by an accelerated increase of rural-to-urban migration (Dufour and Piperata 2004). As a result, UGS only began to appear by the end of the 19th century and, as late as the end of the 20th century, became relevant under the concept of "Ecological Main Structure" (Andrade et al. 2013, 2014). Today, the concept has been decreed as one of the environmental determinants of land use-planning (Andrade et al. 2013, 2014). Bogotá has around 7,000 UGS of different scale and function, and ~ 1.4 million urban trees (Alcaldía Mayor de Bogotá 2009; Jardín Botánico de Bogotá 2023). However, despite the need for information on ecology and biodiversity to develop these strategies (McKinney 2002; Elmqvist et al. 2013; Aronson et al. 2017; McDonald et al. 2018), there are only a few studies that explore urban biodiversity in Colombia (e.g. Marín-Gómez et al. 2016; Ocampo Flórez et al. 2018; Durán-Prieto and Ocampo 2019; Durán-Prieto et al. 2020, 2023; Martínez and Morales 2020; Garizábal-Carmona and Mancera-Rodríguez 2021; Olaya-Arenas et al. 2022; Roncallo et al. 2022).

Psylloidea (jumping plant-lice or psyllids) constitute one of the superfamilies of Sternorrhyncha with more than 4,000 described and probably just as many undescribed species (Burckhardt et al. 2021; Ouvrard 2023). Psyllids are generally monophagous or narrowly oligophagous on one or a few closely related host plant species (Hodkinson 1974; Burckhardt et al. 2014; Ouvrard et al. 2015). A host plant is defined as that plant "on which a psyllid species completes its immature-to-adult life cycle" (Burckhardt et al. 2014). In practice, a host plant can be recognised by the presence of fifth instar immatures. Unlike the relatively immobile immatures, the winged adults disperse through flight or by air currents and are often found also on non-host plants (Burckhardt et al. 2014).

Psyllids are found in all biogeographic realms but are probably most species-rich in the tropics and the south temperate regions though these faunas are only poorly known, particularly those of the Afrotropical and Neotropical realms (Hollis 2004; Hodkinson 2009; Burckhardt and Queiroz 2020; Mauck et al. 2024). Little is known about the psyllid fauna of Colombia. Rendón-Mera et al. (2017) published a generic overview on the Colombian psyllids with a list of species known at the time. Additional information on psyllids from Bogotá is provided by Pinzón et al. (2002).

Here, the psyllids collected during a survey of the arthropod fauna of 33 UGS in Bogotá by the Botanical Garden "José Celestino Mutis" of Bogotá are discussed. The survey was conducted between 2017 and 2019, focussing on 30 species of native and exotic plants.

Material and methods

Material

Collections were conducted between 2017 and 2019 in 33 Urban Green Spaces (UGS) of nine of the 19 urban districts ("localidades") of Bogotá (Figs 1, 2, Table 1, Appendix 1). Specimens were collected using sweep nets and entomological aspirators on the tree/shrub canopy cover of 30 plant species used for arborization in the city (Table 2). Unless stated otherwise, material is preserved pinned.

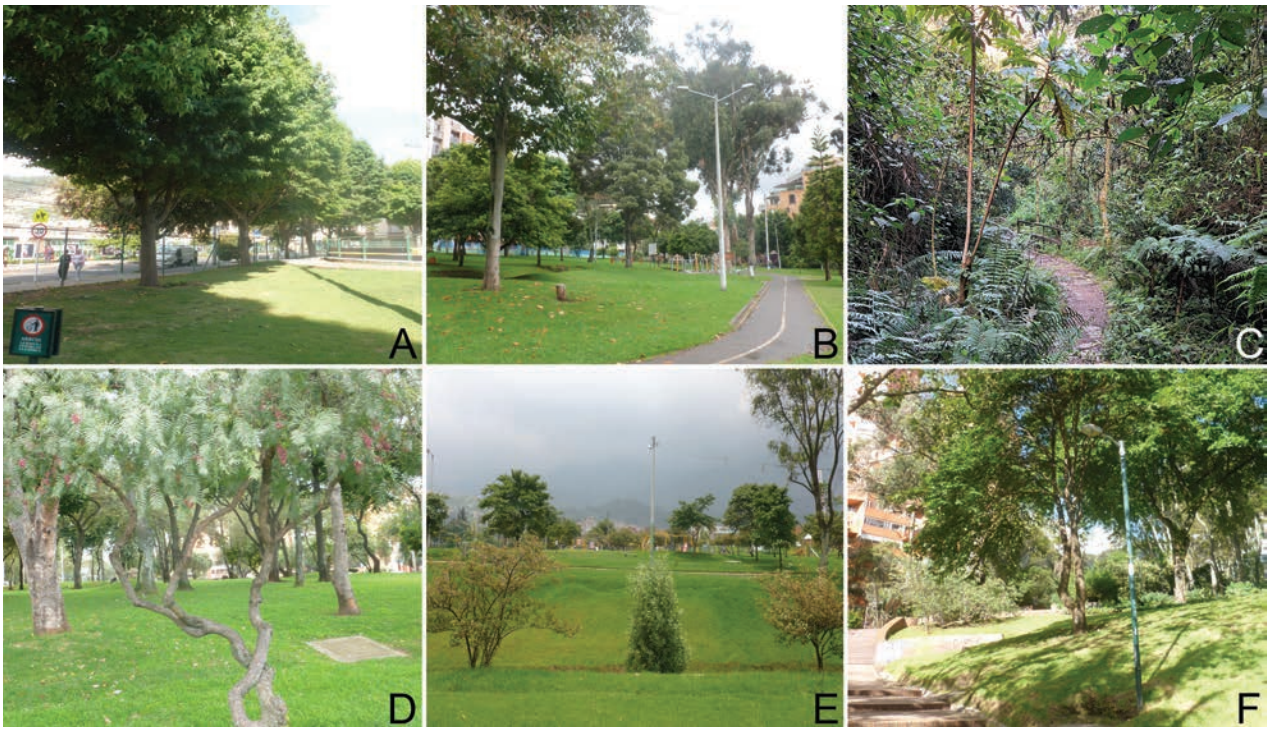

Figure 1. Some urban green spaces of Bogotá **A** Parque Altablanca **B** Parque Ginebra-Bella Suiza **C** Sendero Quebrada la Vieja **D** Parque La Francia **E** Parque San Cristóbal **F** Parque La Independencia.

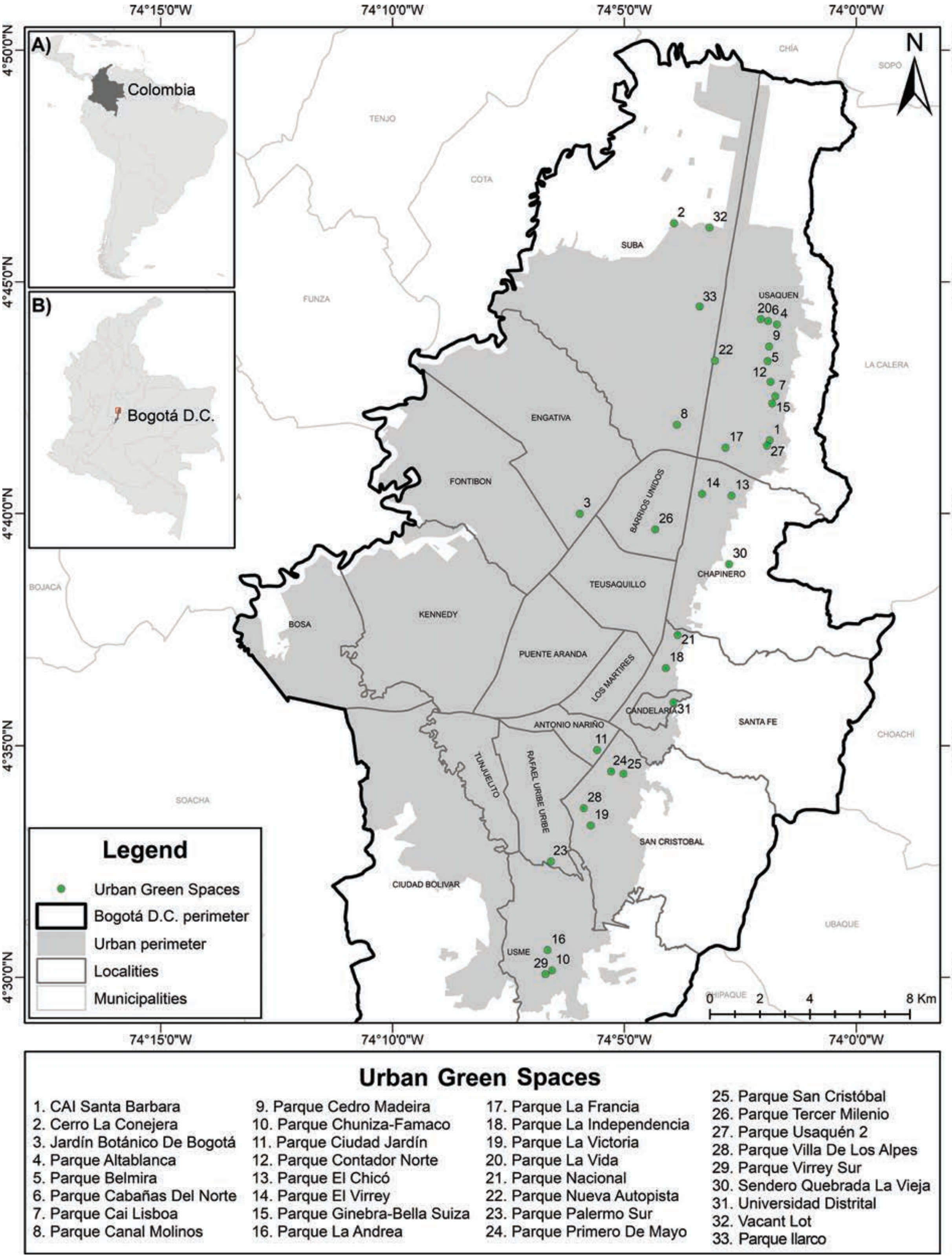

Figure 2. Map of Bogotá indicating localities and sampled urban green spaces.

Holotypes are deposited in the entomological collection of the Museo Javeriano de Historia Natural of the Pontificia Universidad Javeriana, Bogotá, Colombia (**MPUJ_ENT**). Paratypes and non-type material are deposited in MPUJ_ENT and the Naturhistorisches Museum, Basel, Switzerland (**NHMB**).

Table 1. Urban Green Spaces (UGS) with examined plants and psyllid species with number of collected adults. Plants confirmed in the literature as hosts or likely hosts are marked with § (see also text).

UGS	Plant species	Psyllid species	Number of adults
CAI Santa Barbara	*Quercus humboldtii* (Fagaceae)	*Calophya schini*	1
Cerro La Conejera	§ *Acacia dealbata* (Fabaceae)	*Acizzia acaciaebaileyanae*	4
Cerro La Conejera	§ *Acacia melanoxylon* (Fabaceae)	*Acizzia uncatoides*	2
Cerro La Conejera	§ *Baccharis* sp. (Asteraceae)	*Calinda gibbosa*	1
Cerro La Conejera	*Myrcianthes leucoxyla* (Myrtaceae)	*Tuthillia latipennis*	1
Jardín Botánico de Bogotá	*Myrcianthes* sp. (Myrtaceae)	*Trioza* sp. 1	1
Jardín Botánico de Bogotá	*Myrcianthes* sp. (Myrtaceae)	*Tuthillia latipennis*	1
Parque Altablanca	*Lafoensia acuminata* (Lythraceae)	*Synoza cornutiventris*	2
Parque Belmira	*Schinus areira* (Anacardiaceae)	*Acizzia acaciaebaileyanae*	1
Parque Belmira	§ *Schinus areira* (Anacardiaceae)	*Calophya schini*	8
Parque Cabañas del Norte	*Lafoensia acuminata* (Lythraceae)	*Acizzia acaciaebaileyanae*	5
Parque Cabañas del Norte	*Lafoensia acuminata* (Lythraceae)	*Calophya schini*	1
Parque Cabañas del Norte	*Lafoensia acuminata* (Lythraceae)	*Ctenarytaina spatulata*	1
Parque Cabañas del Norte	*Lafoensia acuminata* (Lythraceae)	*Mastigimas colombianus*	1
Parque Cabañas del Norte	*Pittosporum undulatum* (Pittosporaceae)	*Mastigimas longicaudatus* Rendón-Mera, Burckhardt & Vargas-Fonseca, sp. nov.	1
Parque Cabañas del Norte	§ *Schinus areira* (Anacardiaceae)	*Calophya schini*	419
Parque CAI Lisboa	*Pittosporum undulatum* (Pittosporaceae)	*Acizzia uncatoides*	2
Parque CAI Lisboa	*Pittosporum undulatum* (Pittosporaceae)	*Synoza cornutiventris*	6
Parque Canal Molinos	*Bocconia frutescens* (Papaveraceae)	*Acizzia acaciaebaileyanae*	2
Parque Canal Molinos	§ *Cedrela montana* (Meliaceae)	*Mastigimas colombianus*	17
Parque Canal Molinos	§ *Cedrela montana* (Meliaceae)	*Mastigimas longicaudatus* Rendón-Mera, Burckhardt & Vargas-Fonseca, sp. nov.	38
Parque Canal Molinos	§ *Ficus* americana subsp. andicola (Moraceae)	*Synoza cornutiventris*	9
Parque Cedro Madeira	§ *Ficus* sp. (Moraceae)	*Synoza cornutiventris*	17
Parque Chuniza-Famaco	*Quercus humboldtii* (Fagaceae)	*Calophya schini*	2
Parque Chuniza-Famaco	§ *Schinus areira* (Anacardiaceae)	*Calophya schini*	558
Parque Ciudad Jardín	§ *Ficus* sp. (Moraceae)	*Synoza cornutiventris*	9
Parque Ciudad Jardín	*Lafoensia acuminata* (Lythraceae)	*Calophya schini*	2
Parque Ciudad Jardín	*Lafoensia acuminata* (Lythraceae)	*Syncoptozus mexicanus*	1
Parque Ciudad Jardín	§ *Schinus areira* (Anacardiaceae)	*Calophya schini*	726
Parque Contador Norte	§ *Ficus* sp. (Moraceae)	*Synoza cornutiventris*	117
Parque Contador Norte	*Lafoensia acuminata* (Lythraceae)	*Acizzia acaciaebaileyanae*	2
Parque Contador Norte	*Liquidambar styraciflua* (Altingiaceae)	*Acizzia acaciaebaileyanae*	2
Parque Contador Norte	*Liquidambar styraciflua* (Altingiaceae)	*Calophya schini*	1
Parque Contador Norte	*Liquidambar styraciflua* (Altingiaceae)	*Ctenarytaina spatulata*	1
Parque Contador Norte	*Liquidambar styraciflua* (Altingiaceae)	*Synoza cornutiventris*	2
Parque Contador Norte	*Pittosporum undulatum* (Pittosporaceae)	*Synoza cornutiventris*	1
Parque El Chicó	§ *Ficus* sp. (Moraceae)	*Synoza cornutiventris*	10
Parque El Chicó	§ *Schinus areira* (Anacardiaceae)	*Calophya schini*	7
Parque El Virrey	§ *Acacia melanoxylon* (Fabaceae)	*Acizzia uncatoides*	19
Parque El Virrey	§ *Cedrela montana* (Meliaceae)	*Mastigimas colombianus*	38
Parque El Virrey	§ *Cedrela montana* (Meliaceae)	*Mastigimas longicaudatus* Rendón-Mera, Burckhardt & Vargas-Fonseca, sp. nov.	13
Parque El Virrey	*Croton coriaceus* (Euphorbiaceae)	*Calophya schini*	14
Parque El Virrey	*Delostoma integrifolium* (Bignoniaceae)	*Synoza cornutiventris*	1
Parque El Virrey	*Feijoa sellowiana* (Myrtaceae)	*Glycaspis brimblecombei*	1
Parque El Virrey	*Fraxinus chinensis* (Oleaceae)	*Syncoptozus mexicanus*	1

UGS	Plant species	Psyllid species	Number of adults
Parque El Virrey	*Ligustrum* sp. (Oleaceae)	*Syncoptozus mexicanus*	2
Parque El Virrey	*Magnolia grandiflora* (Magnoliaceae)	*Acizzia uncatoides*	28
Parque El Virrey	§ *Magnolia grandiflora* (Magnoliaceae)	*Syncoptozus mexicanus*	37
Parque El Virrey	*Pittosporum undulatum* (Pittosporaceae)	*Acizzia uncatoides*	1
Parque El Virrey	*Salix humboldtiana* (Salicaceae)	*Calophya schini*	4
Parque Ginebra-Bella Suiza	*Ficus* sp. (Moraceae)	Triozidae gen. sp. 3	1
Parque Ginebra-Bella Suiza	*Liquidambar styraciflua* (Altingiaceae)	*Mastigimas longicaudatus* Rendón-Mera, Burckhardt & Vargas-Fonseca, sp. nov.	1
Parque Ginebra-Bella Suiza	§ *Schinus areira* (Anacardiaceae)	*Calophya schini*	148
Parque Ginebra-Bella Suiza	*Schinus areira* (Anacardiaceae)	*Mastigimas longicaudatus* Rendón-Mera, Burckhardt & Vargas-Fonseca, sp. nov.	2
Parque Ginebra-Bella Suiza	*Schinus areira* (Anacardiaceae)	*Synoza cornutiventris*	1
Parque Tercer Ilarco	*Bocconia frutescens* (Papaveraceae)	*Acizzia acaciaebaileyanae*	2
Parque Tercer Ilarco	*Clusia* sp. (Clusiaceae)	*Glycaspis brimblecombei*	1
Parque Tercer Ilarco	*Croton coriaceus* (Euphorbiaceae)	*Calinda* sp.	1
Parque Tercer Ilarco	*Croton coriaceus* (Euphorbiaceae)	*Mastigimas colombianus*	1
Parque Tercer Ilarco	*Croton coriaceus* (Euphorbiaceae)	*Platycorypha* sp.	1
Parque Tercer Ilarco	*Croton coriaceus* (Euphorbiaceae)	*Synoza cornutiventris*	1
Parque Tercer Ilarco	*Prunus serotina* (Rosaceae)	*Leuronota albilinea* Rendón-Mera, Burckhardt & Vargas-Fonseca, sp. nov.	1
Parque Tercer Ilarco	§ *Schinus areira* (Anacardiaceae)	*Calophya schini*	8
Parque La Andrea	§ *Ficus* sp. (Moraceae)	*Synoza cornutiventris*	99
Parque La Francia	*Lafoensia acuminata* (Lythraceae)	*Synoza cornutiventris*	2
Parque La Francia	§ *Schinus areira* (Anacardiaceae)	*Calophya schini*	7
Parque La Independencia	§ *Ficus* sp. (Moraceae)	*Synoza cornutiventris*	30
Parque La Independencia	*Liquidambar styraciflua* (Altingiaceae)	*Synoza cornutiventris*	1
Parque La Independencia	*Quercus humboldtii* (Fagaceae)	*Synoza cornutiventris*	1
Parque La Victoria	*Pittosporum undulatum* (Pittosporaceae)	*Calophya schini*	1
Parque La Victoria	*Quercus humboldtii* (Fagaceae)	*Calophya schini*	5
Parque La Victoria	§ *Schinus areira* (Anacardiaceae)	*Calophya schini*	250
Parque La Vida	§ *Ficus* sp. (Moraceae)	*Synoza cornutiventris*	244
Parque La Vida	*Ficus* sp. (Moraceae)	Triozidae gen. sp. 3	1
Parque La Vida	*Pittosporum undulatum* (Pittosporaceae)	*Synoza cornutiventris*	6
Parque Nacional	§ *Ficus* sp. (Moraceae)	*Synoza cornutiventris*	4
Parque Nueva Autopista	*Ficus* sp. (Moraceae)	*Calophya schini*	1
Parque Nueva Autopista	§ *Ficus* sp. (Moraceae)	*Synoza cornutiventris*	3
Parque Palermo Sur	§ *Ficus* sp. (Moraceae)	*Synoza cornutiventris*	2
Parque Palermo Sur	*Pittosporum undulatum* (Pittosporaceae)	*Acizzia uncatoides*	1
Parque Palermo Sur	*Pittosporum undulatum* (Pittosporaceae)	*Calophya schini*	1
Parque Palermo Sur	*Pittosporum undulatum* (Pittosporaceae)	Triozidae gen. sp. 2	1
Parque Palermo Sur	§ *Schinus areira* (Anacardiaceae)	*Calophya schini*	26
Parque Primero de Mayo	§ *Ficus* sp. (Moraceae)	*Synoza cornutiventris*	106
Parque Primero de Mayo	*Quercus humboldtii* (Fagaceae)	*Synoza cornutiventris*	1
Parque San Cristóbal	*Lafoensia acuminata* (Lythraceae)	*Synoza cornutiventris*	1
Parque San Cristóbal	*Pittosporum undulatum* (Pittosporaceae)	*Synoza cornutiventris*	1
Parque San Cristóbal	§ *Schinus areira* (Anacardiaceae)	*Calophya schini*	89
Parque Tercer Milenio	§ *Clusia* sp. (Clusiaceae)	*Leuronota albilinea* Rendón-Mera, Burckhardt & Vargas-Fonseca, sp. nov.	85
Parque Tercer Milenio	*Magnolia grandiflora* (Magnoliaceae)	*Calophya schini*	6
Parque Tercer Milenio	§ *Magnolia grandiflora* (Magnoliaceae)	*Syncoptozus mexicanus*	33
Parque Tercer Milenio	*Sambucus nigra* (Viburnaceae)	*Mastigimas longicaudatus* Rendón-Mera, Burckhardt & Vargas-Fonseca, sp. nov.	2
Parque Usaquén 2	*Ficus* sp. (Moraceae)	*Calophya schini*	1
Parque Usaquén 2	§ *Ficus* sp. (Moraceae)	*Synoza cornutiventris*	4

UGS	Plant species	Psyllid species	Number of adults
Parque Usaquén 2	*Liquidambar styraciflua* (Altingiaceae)	*Calophya schini*	1
Parque Usaquén 2	*Pittosporum undulatum* (Pittosporaceae)	*Calophya schini*	1
Parque Usaquén 2	*Pittosporum undulatum* (Pittosporaceae)	*Synoza cornutiventris*	1
Parque Villa de los Alpes	§ *Ficus* sp. (Moraceae)	*Synoza cornutiventris*	120
Parque Villa de los Alpes	§ *Schinus areira* (Anacardiaceae)	*Calophya schini*	81
Parque Virrey Sur	§ *Ficus* sp. (Moraceae)	*Synoza cornutiventris*	29
Parque Virrey Sur	§ *Schinus areira* (Anacardiaceae)	*Calophya schini*	51
Sendero Quebrada La Vieja	*Miconia elaeoides* (Melastomataceae)	*Ctenarytaina spatulata*	1
Sendero Quebrada La Vieja	*Miconia elaeoides* (Melastomataceae)	*Melanastera* sp.	1
Sendero Quebrada La Vieja	*Piper bogotense* (Piperaceae)	*Acizzia uncatoides*	1
Sendero Quebrada La Vieja	*Piper bogotense* (Piperaceae)	*Ctenarytaina eucalypti*	5
Universidad Distrital	*Acacia decurrens* (Fabaceae)	*Acizzia uncatoides*	15
Universidad Distrital	§ *Acacia melanoxylon* (Fabaceae)	*Acizzia uncatoides*	125
Universidad Distrital	§ *Baccharis latifolia* (Asteraceae)	*Calinda gibbosa*	3
Universidad Distrital	*Baccharis latifolia* (Asteraceae)	*Calinda* trinervis	1
Universidad Distrital	*Croton coriaceus* (Euphorbiaceae)	*Acizzia uncatoides*	2
Universidad Distrital	Lycianthes lycioides (Solanaceae)	*Acizzia uncatoides*	24
Universidad Distrital	*Oreopanax incisus* (Araliaceae)	*Acizzia uncatoides*	1
Universidad Distrital	*Oreopanax incisus* (Araliaceae)	*Ctenarytaina spatulata*	7
Universidad Distrital	*Quercus humboldtii* (Fagaceae)	*Acizzia uncatoides*	1
Universidad Distrital	*Quercus humboldtii* (Fagaceae)	*Calinda gibbosa*	1
Universidad Distrital	*Quercus humboldtii* (Fagaceae)	*Ctenarytaina spatulata*	1
Universidad Distrital	*Quercus humboldtii* (Fagaceae)	Triozidae gen. sp. 3	1
vacant lot	*Quercus humboldtii* (Fagaceae)	*Acizzia uncatoides*	1
vacant lot	*Quercus humboldtii* (Fagaceae)	Triozidae gen. sp. 1	1

Table 2. Psyllid species, hosts (cf. text) and numbers of adult psyllid specimens collected on hosts and non-hosts.

Psyllid species	Host taxon	Adults on host	Adults on non-host
Calophya schini	*Schinus areira*	2378	42 (= 1.8%)
Synoza cornutiventris	*Ficus* spp.	803	28 (= 3.5%)
Acizzia uncatoides	mimosoid Fabaceae	161	62 (= 38.5%)
Leuronota albilinea Rendón-Mera, Burckhardt & Vargas-Fonseca, sp. nov.	*Clusia* sp.	85	1 (= 1.2%)
Mastigimas colombianus	*Cedrela montana*	55	2 (= 3.6%)
Mastigimas longicaudatus Rendón-Mera, Burckhardt & Vargas-Fonseca, sp. nov.	*Cedrela montana*	51	6 (= 11.8%)
Syncoptozus mexicanus	*Magnolia grandiflora*	30	4 (= 13.3%)
Acizzia acaciaebaileyanae	mimosoid Fabaceae	4	12
Calinda gibbosa	*Baccharis* spp.	4	1
Ctenarytaina spatulata	*Eucalyptus* spp.		11
Ctenarytaina eucalypti	*Eucalyptus* spp.		5
Triozidae gen. sp. 3	unknown		3
Glycaspis brimblecombei	*Eucalyptus* spp.		2
Tuthillia latipennis	*Myrcianthes* spp.		2
Calinda trinervis	unknown		1
Calinda sp.	unknown		1
Melanastera sp.	unknown		1
Platycorypha sp.	unknown		1
Trioza sp. 1	unknown		1
Triozidae gen. sp. 1	unknown		1
Triozidae gen. sp. 2	unknown		1

Species description

Morphological terminology follows Bastin et al. (2023). Body length was taken from ethanol-preserved specimens in lateral view, measuring the distance from the tip of genal process to the tip of wings when folded over the body. All other measurements were taken from slide mounted specimens as indicated in Bastin et al. (2023). In *Leuronota*, vein length is measured as a linear distance. Measurements are given in mm and expressed as range (mean ± standard deviation). Slide preparation protocol follows Queiroz et al. (2017).

Conventions

Taxa are arranged alphabetically (families and genera) following the classification of Burckhardt et al. (2021). Plant names and information of their origin correspond to POWO (2023). The following markings are used: (*) for new species records for Colombia and (‡) for adventive species. Material examined is presented per urban district, written in bold and arranged alphabetically. Plants mentioned in this section are those from which specimens were collected and not necessarily host plants as defined by Burckhardt et al. (2014). Distribution in Colombia is presented by department.

Host plants

No immature psyllids were collected during the survey and none of the sampled plant species could, therefore, be confirmed as host in the sense of Burckhardt et al. (2014). Under "Host plant" we cite reliable literature records with the respective reference, or we discuss reasons for assuming that a particular plant constitutes a host. In Table 1 we use this information to classify plants into hosts (marked with §) and non-hosts.

Abbreviations

AL—Antenna length; **AP**—Apical portion of female proctiger length; **BL**—Body length; **CRL**—Circumanal ring length; **DL**—Distal segment of aedeagus length; **FL**—Forewing length; **FP**—Female proctiger length; **FW**—Forewing width; **GL**—Genal processes length; **HW**—Head width; **MP**—Male proctiger length; **PL**—Paramere length; **SP**—Female subgenital plate length; **TL**—Metatibia length; **UGS**—Urban Green Space; **VL**—Vertex length.

Taxonomy

Psylloidea Latreille, 1807
Aphalaridae Löw, 1879

‡ *Ctenarytaina eucalypti* (Maskell, 1890)

Material examined. Chapinero: • 1 ♂, 4 ♀; Quebrada La Vieja; 4.6495, −74.0466; 2764 m; 06.iv.2017; J. Duran leg.; *Piper bogotense* (Piperaceae); MPUJ_ENT.

Distribution. Colombia: Boyacá and Bogotá (Pinzón et al. 2002; Rendón-Mera et al. 2017).—Native to Australia, introduced into Africa, the Americas, Asia, Europe, and New Zealand (Makunde et al. 2020).

Host plant. *Eucalyptus* L'Hér. spp. (Myrtaceae) (Makunde et al. 2020).

‡ *Ctenarytaina spatulata* Taylor, 1997

Material examined. Chapinero: • 1 ♀; Quebrada La Vieja; 4.6474, –74.0447; 2785 m; 20.vi.2017; J. Duran leg.; *Miconia elaeoides* (Melastomataceae); MPUJ_ENT. **Santa Fe:** • 4 ♂, 3 ♀; Universidad Distrital; 4.5989, –74.0656; 2701 m; 05.v.2017; J. Duran leg.; *Oreopanax incisus* (Araliaceae); MPUJ_ENT• 1 ♀; same but 4.5987, –74.0653; 2713 m; *Quercus humboldtii* (Fagaceae); MPUJ_ENT. **Usaquén:** • 1 ♀; Parque Cabañas del Norte; 4.7359, –74.0318; 2575 m; 16.iii.2018; V. Ocampo leg.; *Lafoensia acuminata* (Lythraceae); MPUJ_ENT • 1 ♀; Parque Contador Norte; 4.715, –74.0302; 2595 m; 02.iv.2018; V. Ocampo leg.; *Liquidambar styraciflua* (Altingiaceae); MPUJ_ENT.

Distribution. Colombia: Bogotá (Rendón-Mera et al. 2017).—Native to Australia, introduced into the Americas, Europe, and New Zealand (Makunde et al. 2020).

Host plant. *Eucalyptus* L'Hér. spp. (Myrtaceae) (Makunde et al. 2020).

‡ *Glycaspis brimblecombei* Moore, 1964

Material examined. Chapinero: • 1 ♀; Parque El Virrey; 4.6736, –74.0548; 2590 m; 28.iii.2017; J. Duran leg.; *Feijoa sellowiana* (Myrtaceae); MPUJ_ENT. **Santa Fe:** • 1 ♀; Parque Ilarco; 4.7003, –74.0655; 2569 m; 19.ix.2017; J. Duran leg.; *Clusia* sp. (Clusiaceae); MPUJ_ENT.

Distribution. Colombia: Antioquia, Bogotá, Casanare, Risaralda, and Valle del Cauca (Rodas et al. 2014; Rendón-Mera et al. 2017).—Native to Australia, introduced into Africa, the Americas, Asia, Europe, and New Zealand (Pugh et al. 2017; Makunde et al. 2020).

Host plant. *Corymbia* K.D.Hill and L.A.S.Johnson, and *Eucalyptus* L'Hér. spp. (Myrtaceae) (Makunde et al. 2020).

‡ *Syncoptozus mexicanus* Hodkinson, 1990

Material examined. Antonio Nariño: • 1 ♂; Parque Ciudad Jardín; 4.5819, –74.0937; 2601 m; 13.iv.2018; V. Ocampo leg.; *Lafoensia acuminata* (Lythraceae); MPUJ_ENT. **Chapinero:** • 1 ♂; Parque El Virrey; 4.6744, –74.0571; 2580 m; 20.vi.2017; J. Duran leg.; *Fraxinus chinensis* (Oleaceae); MPUJ_ENT • 1 ♂, 1 ♀; same but 4.674, –74.0565; 2581 m; *Ligustrum* sp. (Oleaceae); MPUJ_ENT • 3 ♂, 6 ♀; same but 4.6712, –74.0497; 2583 m; *Magnolia grandiflora* (Magnoliaceae); MPUJ_ENT • 12 ♂, 16 ♀; same but 4.6753, –74.0581; 2579 m; 28.iii.2017; MPUJ_ENT. **Santa Fe:** • 14 ♂, 17 ♀; Parque Tercer Milenio; 4.5971, –74.0830; 2607 m; 23.iii.2017; J. Duran leg.; *Magnolia grandiflora* (Magnoliaceae); MPUJ_ENT • 1 ♂, 1 ♀; same but 4.5971, –74.0829; 2606 m; 19.ix.2017; MPUJ_ENT.

Distribution. Colombia: Bogotá (Rendón-Mera et al. 2017), Mexico (Hodkinson 1990).

Host plant. *Magnolia grandiflora* L. (Magnoliaceae) (unpublished NHMB data from Mexico).

Calophyidae Vondráček, 1957

‡ *Calophya schini* Tuthill, 1959

Material examined. Antonio Nariño: • 1 ♀; Parque Ciudad Jardín; 4.5818, –74.0933; 2601 m; 13.iv.2018; V. Ocampo leg.; *Lafoensia acuminata* (Lythraceae); MPUJ_ENT • 1 ♀; same but 4.5819, –74.0937; 2601 m; MPUJ_ENT • 58 ♂, 73 ♀; same but 4.5814, –74.0932; 2601 m; *Schinus areira* (Anacardiaceae); MPUJ_ENT • 116 ♂, 104 ♀; same but 4.5816, –74.0931; 2600 m; MPUJ_ENT • 114 ♂, 159 ♀; same but 4.5817, –74.0931; 2602 m; MPUJ_ENT • 1 ♀; same but 4.5821, –74.0914; 2599 m; MPUJ_ENT • 45 ♂, 56 ♀; same but 4.5822, –74.0932; 2597 m; MPUJ_ENT. **Chapinero:** • 1 ♂, 6 ♀; Parque El Chicó; 4.673, –74.0452; 2599 m; 27.iv.2018; V. Ocampo leg.; *Schinus areira* (Anacardiaceae); MPUJ_ENT • 1 ♂, 2 ♀; Parque El Virrey; 4.6754, –74.0581; 2579 m; 25.ix.2017; J. Duran leg.; *Croton coriaceus* (Euphorbiaceae); MPUJ_ENT • 6 ♂, 5 ♀; same but 28.iii.2017; MPUJ_ENT • 2 ♂, 2 ♀; same but 4.6739, –74.0557; 2580 m; *Salix humboldtiana* (Salicaceae); MPUJ_ENT. **Rafael Uribe Uribe:** • 1 ♀; Parque Palermo Sur; 4.5412, –74.1100; 2698 m; 09.iv.2018; V. Ocampo leg.; *Pittosporum undulatum* (Pittosporaceae); MPUJ_ENT • 10 ♂, 16 ♀; same but 4.5417, –74.1097; 2689 m; *Schinus areira* (Anacardiaceae); MPUJ_ENT. **San Cristóbal:** • 1 ♀; Parque La Victoria; 4.5546, –74.0954; 2757 m; 09.iv.2018; V. Ocampo leg.; *Pittosporum undulatum* (Pittosporaceae); MPUJ_ENT • 4 ♂, 1 ♀; same but 4.5548, –74.0955; 2764 m; *Quercus humboldtii* (Fagaceae); MPUJ_ENT • 79 ♂, 92 ♀; same but 4.5546, –74.0953; 2759 m; *Schinus areira* (Anacardiaceae); MPUJ_ENT • 31 ♂, 48 ♀; same but 4.5547, –74.0953; 2760 m; MPUJ_ENT • 3 ♂, 4 ♀; Parque San Cristóbal: 4.5735, –74.0832; 2639 m; 13.iv.2018; V. Ocampo leg.; *Schinus areira* (Anacardiaceae); MPUJ_ENT • 2 ♂, 3 ♀; same but 4.5736, –74.0834; 2638 m; MPUJ_ENT • 60 ♂, 17 ♀; same but 4.5736, –74.0827; 2642 m; MPUJ_ENT • 44 ♂, 37 ♀; Parque Villa de los Alpes; 4.5593, –74.0977; 2692 m; 13.iv.2018; V. Ocampo leg.; *Schinus areira* (Anacardiaceae); MPUJ_ENT. **Santa Fe:** • 4 ♂, 2 ♀; Parque Tercer Milenio; 4.5971, –74.0829; 2606 m; 19.ix.2017; J. Duran leg.; *Magnolia grandiflora* (Magnoliaceae); MPUJ_ENT • 1 ♂, 7 ♀; same but 4.7011, –74.0655; 2570 m; 23.iii.2017; *Schinus areira* (Anacardiaceae); MPUJ_ENT. **Usaquén:** • 1 ♀; CAI Santa Barbara; 4.693, –74.0311; 2601 m; 06.iv.2018; V. Ocampo leg.; *Quercus humboldtii* (Fagaceae); MPUJ_ENT • 4 ♂, 4 ♀; Parque Belmira; 4.7215, –74.0318; 2576 m; 02.iv.2018; V. Ocampo leg.; *Schinus areira* (Anacardiaceae); MPUJ_ENT • 1 ♂; Parque Cabañas del Norte; 4.7359, –74.0318; 2575 m; 16.iii.2018; V. Ocampo leg.; *Lafoensia acuminata* (Lythraceae); MPUJ_ENT • 33 ♂, 27 ♀; same but 4.7359, –74.0317; 2574 m; *Schinus areira* (Anacardiaceae); MPUJ_ENT • 102 ♂, 116 ♀; same but 4.7359, –74.0315; 2576 m; MPUJ_ENT • 19 ♂, 18 ♀; same but 4.7359, –74.0316; 2575 m; MPUJ_ENT • 48 ♂, 56 ♀; same but 4.736, –74.0317; 2571 m; MPUJ_ENT • 1 ♀; Parque Contador Norte; 4.7152, –74.0297; 2599 m; 02.iv.2018; V. Ocampo leg.; *Liquidambar styraciflua* (Altingiaceae); MPUJ_ENT • 19 ♂, 21 ♀; Parque Ginebra-Bella Suiza; 4.7061, –74.0300; 2595 m; 06.iv.2018; V. Ocampo leg.; *Schinus areira* (Anacardiaceae); MPUJ_ENT • 13 ♂, 6 ♀; same but 4.7062, –74.0305;

2596 m; MPUJ_ENT • 55 ♂, 34 ♀; same but 4.7067, –74.0299; 2601 m; MPUJ_ENT • 2 ♂, 1 ♀; Parque La Francia; 4.6896, –74.0470; 2577 m; 05.iii.2018; V. Ocampo leg.; *Schinus areira* (Anacardiaceae); MPUJ_ENT • 1 ♀; same but 4.6902, –74.0464; 2577 m; MPUJ_ENT • 1 ♀; same but 4.6906, –74.0464; 2575 m; MPUJ_ENT • 1 ♂, 1 ♀; same but 4.6908, –74.0466; 2577 m; MPUJ_ENT • 1 ♀; Parque Nueva Autopista; 4.7217, –74.0507; 2579 m; 05.iii.2018; V. Ocampo leg.; *Ficus* sp. (Moraceae); MPUJ_ENT • 1 ♀; Parque Usaquén 2; 4.691, –74.0323; 2586 m; 05.iii.2018; V. Ocampo leg.; *Ficus* sp. (Moraceae); MPUJ_ENT • 1 ♂; same but 4.691, –74.0320; 2591 m; 27.iv.2018; *Liquidambar styraciflua* (Altingiaceae); MPUJ_ENT • 1 ♀; same but 4.6912, –74.0317; 2571 m; 05.iii.2018; *Pittosporum undulatum* (Pittosporaceae); MPUJ_ENT. **Usme:** • 1 ♂, 1 ♀; Parque Chuniza-Famaco; 4.5018, –74.1086; 2775 m; 09.iv.2018; V. Ocampo leg.; *Quercus humboldtii* (Fagaceae); MPUJ_ENT • 158 ♂, 173 ♀; same but 4.5015, –74.1088; 2686 m; *Schinus areira* (Anacardiaceae); MPUJ_ENT • 28 ♂, 31 ♀; same but 4.5018, –74.1087; 2774 m; MPUJ_ENT • 55 ♂, 44 ♀; same but 4.5031, –74.1100; 2759 m; MPUJ_ENT • 16 ♂, 15 ♀; same but 4.5032, –74.1097; 2761 m; MPUJ_ENT • 20 ♂, 18 ♀; same but 4.5036, –74.1101; 2754 m; MPUJ_ENT • 22 ♂, 29 ♀; Parque Virrey Sur; 4.5009, –74.1125; 2768 m; 23.iv.2018; V. Ocampo leg.; *Schinus areira* (Anacardiaceae); MPUJ_ENT.

Distribution. Colombia: Bogotá (Pinzón and González 2002).—Probably originating from Bolivia or Peru, adventive elsewhere in the Americas, Africa, Europe, and New Zealand (Burckhardt et al. 2018).

Host plant. *Schinus areira* L. (Anacardiaceae) (Burckhardt et al. 2018).

Carsidaridae Crawford, 1911

Synoza cornutiventris Enderlein, 1918

Material examined. Antonio Nariño: • 4 ♂, 5 ♀; Parque Ciudad Jardín; 4.5818, –74.0932; 2601 m; 23.iv.2018; V. Ocampo leg.; *Ficus* sp. (Moraceae); MPUJ_ENT. **Chapinero:** • 2 ♀; Parque El Chicó; 4.6731, –74.0447; 2605 m; 27.iv.2018; V. Ocampo leg.; *Ficus* sp. (Moraceae); MPUJ_ENT • 6 ♂, 2 ♀; same but 4.6732, –74.0445; MPUJ_ENT • 1 ♂; Parque El Virrey; 4.6733, –74.0554; 2591 m; 28.iii.2017; J. Duran leg.; *Delostoma integrifolium* (Bignoniaceae); MPUJ_ENT. **Rafael Uribe Uribe:** • 2 ♂; Parque Palermo Sur; 4.5423, –74.1102; 2676 m; 09.iv.2018; V. Ocampo leg.; *Ficus* sp. (Moraceae); MPUJ_ENT. **San Cristóbal:** • 8 ♂, 7 ♀; Parque Primero de Mayo; 4.5734, –74.0882; 2625 m; 23.iv.2018; V. Ocampo leg.; *Ficus* sp. (Moraceae); MPUJ_ENT • 28 ♂, 24 ♀; same but 4.5738, –74.0879; 2622 m; 13.iv.2018; MPUJ_ENT • 25 ♂, 14 ♀; same but 4.5745, –74.0881; 2621 m; MPUJ_ENT • 1 ♀; same but 4.5746, –74.0880; 2621 m; *Quercus humboldtii* (Fagaceae); MPUJ_ENT • 1 ♂; Parque San Cristóbal: 4.5728, –74.0848; 2638 m; 13.iv.2018; V. Ocampo leg.; *Lafoensia acuminata* (Lythraceae); MPUJ_ENT • 1 ♂; same but 4.5728, –74.0838; *Pittosporum undulatum* (Pittosporaceae); MPUJ_ENT • 36 ♂, 24 ♀; Parque Villa de los Alpes; 4.5591, –74.0974; 2698 m; 23.iv.2018; V. Ocampo leg.; *Ficus* sp. (Moraceae); MPUJ_ENT • 11 ♂, 4 ♀; same but 4.5593, –74.0972; 2695 m; MPUJ_ENT • 11 ♂, 16 ♀; same but 4.5595, –74.0978; 2686 m; MPUJ_ENT • 1 ♀; same but 4.5621, –74.0982; 2676 m; 13.iv.2018; MPUJ_ENT • 4 ♂, 6 ♀; same but 4.5624, –74.0983; 2667 m; MPUJ_ENT • 4 ♂, 1 ♀; same but 4.5625, –74.0983; 2665 m; 13.iv.2018; MPUJ_ENT • 2 ♀; same but 4.5628, –74.0982; 2658 m; 23.iv.2018; MPUJ_ENT. **Santa Fe**: • 5 ♂, 1 ♀; Parque La Independencia; 4.6108, –74.0678; 2645 m;

27.iv.2018; V. Ocampo leg.; *Ficus* sp. (Moraceae); MPUJ_ENT • 12 ♂, 11 ♀; same but 4.6114, –74.0682; 2639 m; MPUJ_ENT • 1 ♂; same but 4.6116, –74.0687; 2631 m; MPUJ_ENT • 1 ♂; same but 4.6108, –74.0678; 2644 m; *Liquidambar styraciflua* (Altingiaceae); MPUJ_ENT • 1 ♂; same but 4.6119, –74.0694; 2583 m; *Quercus humboldtii* (Fagaceae); MPUJ_ENT • 1 ♂; Parque Nacional; 4.6217, –74.0643; 2576 m; 27.iv.2018; V. Ocampo leg.; *Ficus* sp. (Moraceae); MPUJ_ENT • 3 ♀; same but 4.6242, –74.0640; 2624 m; MPUJ_ENT • 1 ♂; Parque Ilarco; 4.7008, –74.0657; 2569 m; 23.iii.2017; J. Duran leg.; *Croton coriaceus* (Euphorbiaceae); MPUJ_ENT. **Suba:** • 4 ♂, 5 ♀; Parque Canal Molinos; 4.6981, –74.0634; 2575 m; 23.iii.2017; J. Duran leg.; *Ficus americana* subsp. *andicola* (Moraceae); MPUJ_ENT. **Usaquén:** • 1 ♂, 1 ♀; Parque Altablanca; 4.7347, –74.0285; 2581 m; 16.iii.2018; V. Ocampo leg.; *Lafoensia acuminata* (Lythraceae); MPUJ_ENT • 3 ♂, 2 ♀; Parque CAI Lisboa; 4.7085, –74.0290; 2604 m; 06.iv.2018; V. Ocampo leg.; *Pittosporum undulatum* (Pittosporaceae); MPUJ_ENT • 1 ♀; same but 4.7088, –74.0292; 2599 m; MPUJ_ENT • 12 ♂, 5 ♀; Parque Cedro Madeira; 4.7268, –74.0313; 2574 m; 23.iii.2018; V. Ocampo leg.; *Ficus* sp. (Moraceae); MPUJ_ENT • 40 ♂, 24 ♀; Parque Contador Norte; 4.7127, –74.0312; 2594 m; 06.iv.2018; V. Ocampo leg.; *Ficus* sp. (Moraceae); MPUJ_ENT • 13 ♂, 13 ♀; same but 4.7129, –74.0312; 2601 m; MPUJ_ENT • 14 ♂, 13 ♀; same but 4.713, –74.0312; 2598 m; MPUJ_ENT • 1 ♂, 1 ♀; same but 4.7132, –74.0314; 2593 m; *Liquidambar styraciflua* (Altingiaceae); MPUJ_ENT • 1 ♂; same but 4.7128, –74.0311; 2603 m; *Pittosporum undulatum* (Pittosporaceae); MPUJ_ENT • 1 ♀; Parque Ginebra-Bella Suiza; 4.7067, –74.0298; 2601 m; 06.iv.2018; V. Ocampo leg.; *Schinus areira* (Anacardiaceae); MPUJ_ENT • 2 ♂, 2 ♀; Parque La Francia; 4.6899, –74.0466; 2579 m; 05.iii.2018; V. Ocampo leg.; *Ficus* sp. (Moraceae); MPUJ_ENT • 2 ♀; same but 4.6908, –74.0480; 2580 m; MPUJ_ENT • 2 ♂; same but 4.6905, –74.0475; 2581 m; *Lafoensia acuminata* (Lythraceae); MPUJ_ENT • 21 ♂, 13 ♀; Parque La Vida; 4.7361, –74.0339; 2585 m; 16.iii.2018; V. Ocampo leg.; *Ficus* sp. (Moraceae); MPUJ_ENT • 39 ♂, 22 ♀; same but 4.7362, –74.0339; 2586 m; MPUJ_ENT • 32 ♂, 32 ♀; same but 4.7365, –74.0341; 2577 m; MPUJ_ENT • 12 ♂, 6 ♀; same but 4.7367, –74.0342; 2579 m; MPUJ_ENT • 17 ♂, 17 ♀; same but 4.7369, –74.0350; 2576 m; MPUJ_ENT • 23 ♂, 10 ♀; same but 4.737, –74.0344; 2573 m; MPUJ_ENT • 1 ♂, 5 ♀; same but 4.7371, –74.0352; 2572 m; *Pittosporum undulatum* (Pittosporaceae); MPUJ_ENT • 1 ♂, 1 ♀; Parque Nueva Autopista; 4.7216, –74.0507; 2571 m; 05.iii.2018; V. Ocampo leg.; *Ficus* sp. (Moraceae); MPUJ_ENT • 1 ♂; same but 4.7217, –74.0507; 2579 m; MPUJ_ENT • 2 ♂, 2 ♀; Parque Usaquén 2; 4.691, –74.0323; 2586 m; 05.iii.2018; V. Ocampo leg.; *Ficus* sp. (Moraceae); MPUJ_ENT • 1 ♂; same but 4.6912, –74.0323; 2587 m; *Pittosporum undulatum* (Pittosporaceae); MPUJ_ENT. **Usme:** • 7 ♂, 12 ♀; Parque Diana Turbay; 4.5478, –74.1015; 2672 m; 23.iv.2018; V. Ocampo leg.; *Ficus* sp. (Moraceae); MPUJ_ENT • 5 ♂, 10 ♀; same but 4.5483, –74.1013; MPUJ_ENT • 14 ♂, 8 ♀; Parque La Andrea; 4.5098, –74.1109; 2741 m; 09.iv.2018; V. Ocampo leg.; *Ficus* sp. (Moraceae); MPUJ_ENT • 39 ♂, 32 ♀; same but 4.5098, –74.1109; 2701 m; MPUJ_ENT • 6 ♂, 7 ♀; Parque Virrey Sur; 4.5009, –74.1115; 2779 m; 23.iv.2018; V. Ocampo leg.; *Ficus* sp. (Moraceae); MPUJ_ENT • 4 ♀; same but 4.5012, –74.1113; 2780 m; MPUJ_ENT • 4 ♂, 1 ♀; same but 4.5013, –74.1114; 2781 m; MPUJ_ENT • 4 ♂, 3 ♀; same but 4.5014, –74.1116; 2778 m; MPUJ_ENT.

Distribution. Colombia: Bogotá, Cundinamarca, Meta (Brown and Hodkinson 1988; Rendón-Mera et al. 2017), Costa Rica, Panama, and Peru (Brown and Hodkinson 1988; Hollis 2000).

Host plant. *Ficus hartwegii* Miq. (Moraceae) (Hollis 2000). Several adults were collected in the present study on *Ficus americana* subsp. *andicola* (Standl.) C.C.Berg. This species has to be confirmed as host. Many adults were collected on unidentified *Ficus* trees. It is possible that these also constitute hosts, but they should be identified to species and examined for psyllid immatures for further conclusions.

Liviidae Löw, 1879

* *Melanastera* sp.

Material examined. Chapinero: • 1 ♀; Quebrada La Vieja; 4.6474, –74.0447; 2785 m; 20.vi.2017; J. Duran leg.; *Miconia elaeoides* (Melastomatacea); MPUJ_ENT.

Distribution. Colombia: Bogotá.

Host plant. Unknown.

Comments. The single female appears to belong to an undescribed species of *Melanastera*, a predominantly Neotropical genus associated with Melastomataceae, Annonaceae, and other plant families (Burckhardt et al. 2024). This is the first record of the genus from Colombia.

Mastigimatidae Bekker-Migdisova, 1973

Mastigimas colombianus Burckhardt, Queiroz & Drohojowska, 2013

Fig. 3A–G

Material examined. Chapinero: • 17 ♂, 17 ♀; Parque El Virrey; 4.6728, –74.0533; 2581 m; 28.iii.2017; J. Duran leg.; *Cedrela montana* (Meliaceae); MPUJ_ENT • 2 ♂, 2 ♀; same but NMHB • 2 ♂, 2 ♀; same but slide mounted; NMHB. **Santa Fe:** • 1 ♂; Parque Ilarco; 4.7008, –74.0657; 2569 m; 23.iii.2017; J. Duran leg.; *Croton coriaceus* (Euphorbiaceae); MPUJ_ENT. **Suba:** • 9 ♂, 6 ♀; Parque Canal Molinos; 4.6976, –74.0637; 2575 m; 10.vii.2017; J. Duran leg.; *Cedrela montana* (Meliaceae); MPUJ_ENT • 1 ♂, 1 ♀; same but 03.x.2017; MPUJ_ENT. **Usaquén:** • 1 ♀; Parque Cabañas del Norte; 4.7358, –74.0315; 2578 m; 16.iii.2018; V. Ocampo leg.; *Lafoensia acuminata* (Lythraceae); MPUJ_ENT.

Redescription. ***Colouration*.** Male (Fig. 3A) dark yellow with dark brown markings. Vertex with pale brown longitudinal stripe along lateral and anterior margins on either side; discal foveae with dark brown spot; margin of toruli brown. Genal processes and clypeus whitish. Antennal segments 1 and 2 yellow, segment 3 yellow basally, gradually darkening to dark brown apex, segments 4–10 dark brown. Pronotum whitish with lateral sutures brown. Mesopraescutum pale yellow along posterior margins. Mesoscutum with two dark yellow longitudinal stripes on either side, the outer one black posteriorly. Mesoscutellum and metascutellum whitish. Metapostnotum with dark brown spots medially and laterally. Pleura whitish, propleurites black dorsally. Mesosternum brown. Forewing colourless, with black spot at base of C+Sc and basally on anal cell; veins and pterostigma brown. Fore and mid legs with femur dark yellow, tibia and tarsi brown; hind leg with femur dark brown, tibia and tarsi pale yellow. Abdomen brown with yellow spot medially, narrowing to apex; intersegmental membrane straw-coloured. Terminalia dark brown, parameres black, subgenital plate pale yellow dorsally.—Female (Fig. 3B) yellow with only a few black markings. Discal

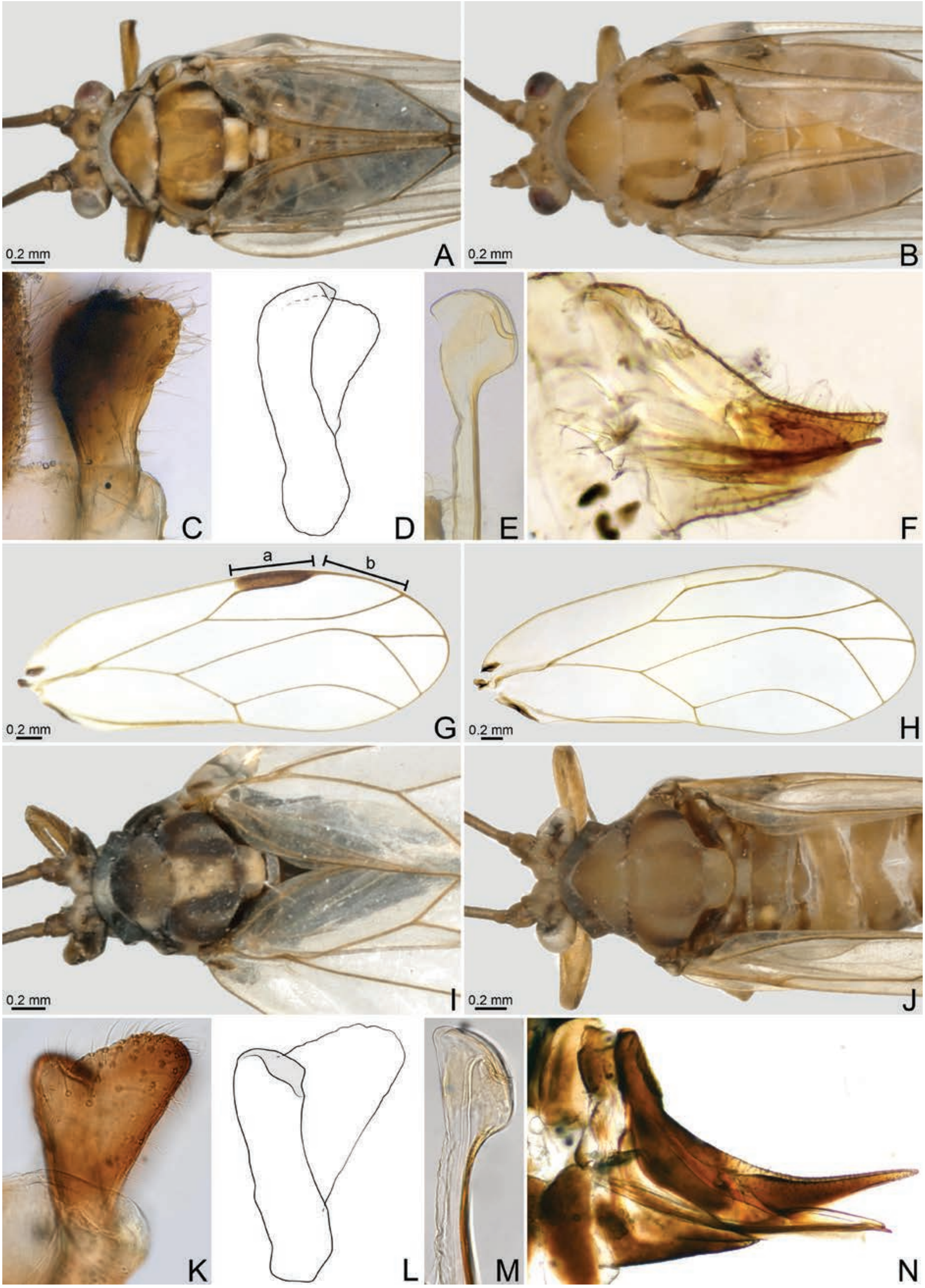

Figure 3. A–G *Mastigimas colombianus* Burckhardt, Queiroz & Drohojowska, 2013 **H–N** *Mastigimas longicaudatus* Rendón-Mera, Burckhardt & Vargas-Fonseca, sp. nov. **A, I** male, dorsal view **B, J** female, dorsal view **C, K** paramere, outer surface, lateral view **D, L** paramere, inner surface, lateral view **E, M** distal segment of aedeagus, lateral view **F, N** female terminalia, lateral view **G, H** forewing.

foveae dark yellow. Pronotum with lateral indentations dark yellow. Meso- and metanotum as in male but markings dark yellow, with outermost stripes on mesoscutum black posteriorly. Forewing as in male but pterostigma colourless. Pleura as in male. Fore and mid legs with femora pale yellow, tibiae dark yellow, and tarsi brown, hind leg pale yellow. Terminalia yellow, apex of proctiger black.

***Structure*.** Antenna 4.0–4.1× as long as head width; segment 3 1.3–1.4× as long as segment 4. Forewing (Fig. 3G) 4.5–5.3× as long as head width, and 2.6× as long as wide, pterostigma long and narrow, ratio a/b 0.9–1.0, cell cu_1 long and flat, length/height ratio 3.3.

***Terminalia*.** Male. Paramere (Fig. 3C, D) bifid, clavate, outer lobe rounded anteriorly and angular posteriorly. Apical dilatation of aedeagus with small blunt apico-ventral hook (Fig. 3E), 1.2× as long as paramere.—Female (Fig. 3F). Terminalia short and cuneate, dorsal outline of proctiger slightly concave; proctiger as long as head width, and 2.4× as long as subgenital plate.

Measurements (in mm). BL 2 ♂ 3.6–5.0 (4.36±0.74), 2 ♀ 5.3–5.4 (5.31±0.08); HW ♂ 0.85, ♀ 0.82; AL ♂ 3.44, ♀ 3.39; FL ♂ 3.8, ♀ 4.36; FW ♂ 1.47, ♀ 1.67; PL ♂ 0.24; DL ♂ 0.28; FP ♀ 0.8; FS ♀ 0.34.

Distribution. Colombia: Bogotá (Burckhardt et al. 2013).

Host plant. Most adults (types and material at hand) were collected on *Cedrela montana* Turcz. (Meliaceae). *Mastigimas* species develop, as far as known, on *Cedrela*, suggesting that *C. montana* is a host.

Comments. *Mastigimas colombianus* was described from two males and two females collected in Bogotá (Burckhardt et al. 2013). As more material is available from this study, a redescription of the species is provided here. The females in the material at hand fit the original description perfectly but the male paramere is slightly variable with respect to the shape of the outer lobe. As in the two type specimens, the paramere in the material at hand is strongly sclerotised which seems characteristic for the species.

* ***Mastigimas longicaudatus*** **Rendón-Mera, Burckhardt & Vargas-Fonseca, sp. nov.**

https://zoobank.org/7AED528B-ED19-4544-96D1-15488A4D5A2F
Fig. 3H–N

Type locality. Colombia, Bogotá: Suba, Parque Canal Molinos, 4.6976389, –74.063694, 2575 m.

Type material. ***Holotype*:** Colombia • ♂, pinned; Bogotá, Suba, Parque Canal Molinos; 4.6976389, –74.063694; 2575 m; 03.x.2017; J. Duran leg; on *Cedrela montana* (Meliaceae); MPUJ_ENT0074272. ***Paratypes*: Chapinero:** • 6 ♂, 7 ♀; Parque El Virrey; 4.6728, –74.0533; 2581 m; 28.iii.2017; J. Duran leg.; *Cedrela montana* (Meliaceae); MPUJ_ENT. **Santa Fe:** • 2 ♀; Parque Tercer Milenio; 4.5974, –74.0835; 2605 m; 23.iii.2017; J. Duran leg.; *Sambucus nigra* (Viburnaceae); MPUJ_ENT. **Suba:** • 8 ♂, 3 ♀; Parque Canal Molinos; 4.6976, –74.0637; 2575 m; 10.vii.2017; J. Duran leg.; *Cedrela montana* (Meliaceae); MPUJ_ENT • 11 ♂, 13 ♀; same data as for holotype • 1 ♂, 1 ♀; same data as for holotype but NHMB • 1 ♂, 1 ♀; same data as for holotype but slide mounted; NHMB. **Usaquén:** • 1 ♀; Parque Cabañas del Norte; 4.7363, –74.0317; 2575 m; 16.iii.2018; V. Ocampo leg.; *Pittosporum undulatum* (Pittosporaceae); MPUJ_ENT • 1 ♂; Parque Ginebra-Bella Suiza; 4.7061, –74.0304; 2596 m; 06.iv.2018; V. Ocampo leg.; *Liquidambar styraciflua* (Altingiaceae); MPUJ_ENT • 2 ♂; same but 4.7062, –74.0305; *Schinus areira* (Anacardiaceae); MPUJ_ENT.

Diagnosis. Forewing (Fig. 3H) with pterostigma long and narrow, ratio a/b 1.2 Antennal segment 3 approx. as long as segment 4. Paramere (Fig. 3K, L) bifid, irregularly triangular, strongly widening to apex. Aedeagal head lacking apico-ventral hook. Female terminalia (Fig. 3N) elongate, falcate; proctiger 1.0–1.2× as long as head width.

Description. ***Colouration*.** Male (Fig. 3I) dark brown. Head pale yellow; vertex with pale brown longitudinal stripe along lateral and anterior margins on either side; discal foveae with dark brown spot, sometimes much expanded; margin of toruli brown. Genal processes and clypeus whitish. Antennae yellowish brown. Pronotum whitish with lateral quarter dark brown. Mesopraescutum with dark brown polygon-shaped spot anteriorly. Mesoscutum with two dark brown longitudinal stripes on either side. Mesoscutellum and metascutellum whitish. Metapostnotum dark brown. Pleura whitish, with dark brown markings dorsally. Mesosternum dark brown. Forewing colourless, with brown spot at base of C+Sc and base of anal cell; veins yellow; pterostigma dark brown or yellowish brown. Fore and mid legs brown and yellowish brown, metafemur and base of metatibia dark brown, rest of hind leg pale yellow. Abdomen dark brown; intersegmental membrane straw-coloured. Terminalia dark brown, parameres sometimes dark yellow.—Female (Fig. 3J) yellow. Discal foveae dark brown; margin of toruli brown. Pronotum with lateral indentations brown. Tergum as in male but markings dark yellow on mesopraescutum and brownish on mesoscutum, with outermost stripe dark brown posteriorly. Forewing as in male but pterostigma colourless. Pleura and legs as in male. Abdominal sclerites usually brown laterally. Terminalia yellow, brown apically, proctiger sometimes completely brown.

***Structure*.** Conforms to the generic description of Brown and Hodkinson (1988). Antenna 4.3–4.5× as long as head width; segment 3 1.1–1.3× as long as segment 4. Forewing (Fig. 3H) 4.8–5.2× as long as head width, and 2.6–2.7× as long as wide, pterostigma long and narrow, ratio a/b 1.1–1.2, cell cu_1 long and flat, length/height ratio 3.5–3.8.

***Terminalia*.** Paramere (Fig. 3K, L), bifid, in lateral view irregularly triangular, strongly widening to apex. Apical dilatation of aedeagus lenticular (Fig. 3M), 1.5× as long as paramere.—Female terminalia (Fig. 3N) elongate, falcate; proctiger 1.5× as long as head width, and 1.9× as long as subgenital plate.

Measurements (in mm). BL ♂ 4.8, 2 ♀ 5.8–5.9 (5.85±0.1); HW ♂ 0.88, ♀ 0.92; AL ♂ 3.95, ♀ 3.93; FL ♂ 4.23, ♀ 4.78; FW ♂ 1.57, ♀ 1.85; PL ♂ 0.24; DL ♂ 0.36; FP ♀ 1.26; FS ♀ 0.65.

Etymology. From Latin *longus* = long, and *caudatus* = bearing a tail, referring to the long female terminalia. Adjective.

Distribution. Colombia: Bogotá.

Host plant. Most of the examined adults were collected on *Cedrela montana* Turcz. (Meliaceae). *Mastigimas* species develop, as far as known, on *Cedrela*, suggesting that *C. montana* is a host.

Comments. *Mastigimas longicaudatus* Rendón-Mera, Burckhardt & Vargas-Fonseca, sp. nov. resembles *M. anjosi* Burckhardt et al., 2011 (known from Brazil, Trinidad, and Venezuela) in the irregularly triangular paramere and the elongate, falcate female terminalia; it differs in the antennal segment 3 approx.

as long as segment 4 (instead of twice as long), and the aedeagal head lacking an apico-ventral hook (Burckhardt et al. 2011, 2013). The falcate female terminalia are shared also with *M. drepanodis* Burckhardt, Queiroz & Drohojowska, 2013 (Brazil) which differs in the slenderer paramere (Burckhardt et al. 2013). In the key by Burckhardt et al. (2013), the new species keys out with *M. colombianus* from which it differs in details of the male and female terminalia.

Psyllidae Latreille, 1807

‡ *Acizzia acaciaebaileyanae* (Froggatt, 1901)

Material examined. Suba: • 1 ♂, 3 ♀; Cerro La Conejera; 4.7705, –74.0656; 2620 m; 28.iii.2017; J. Duran leg.; *Acacia dealbata* (Fabaceae); MPUJ_ENT • 1 ♀; Parque Ilarco; 4.701, –74.0663; 2567 m; 23.iii.2017; J. Duran leg.; *Bocconia frutescens* (Papaveraceae); MPUJ_ENT • 1 ♂; same but 10.vii.2017; MPUJ_ENT. **Usaquén:** • 1 ♂; Parque Belmira; 4.7215, –74.0318; 2576 m; 02.iv.2018; V. Ocampo leg.; *Schinus areira* (Anacardiaceae); MPUJ_ENT • 5 ♂; Parque Cabañas del Norte; 4.7358, –74.0315; 2578 m; 16.iii.2018; V. Ocampo leg.; *Lafoensia acuminata* (Lythraceae); MPUJ_ENT • 1 ♂, 1 ♀; Parque Contador Norte; 4.7158, –74.0322; 2581 m; 06.iv.2018; V. Ocampo leg.; *Lafoensia acuminata* (Lythraceae); MPUJ_ENT • 1 ♂; same but 4.715, –74.0301; 2597 m; 02.iv.2018; *Liquidambar styraciflua* (Altingiaceae); MPUJ_ENT • 1 ♀; same but 4.7151, –74.0299; 2600 m; MPUJ_ENT.

Distribution. Colombia: Bogotá (Rendón-Mera et al. 2017).—Native to Australia, adventive in Africa, North America, Asia, Europe, and New Zealand (Ouvrard 2023).

Host plant. *Acacia* Mill. and *Samanea* (Benth.) Merr. spp. (Fabaceae) (Ouvrard 2023).

‡ *Acizzia uncatoides* (Ferris & Klyver, 1932)

Material examined. Chapinero: • 9 ♂, 10 ♀; Parque El Virrey; 4.6713, –74.0504; 2591 m; 28.iii.2017; J. Duran leg.; *Acacia melanoxylon* (Fabaceae); MPUJ_ENT • 18 ♂, 10 ♀; same but 4.6753, –74.0581; 2579 m; *Magnolia grandiflora* (Magnoliaceae); MPUJ_ENT • 1 ♀; same but 4.6738, –74.0563; 2581 m; *Pittosporum undulatum* (Pittosporaceae); MPUJ_ENT • 1 ♂; Quebrada La Vieja; 4.6495, –74.0466; 2764 m; 06.iv.2017; J. Duran leg.; *Piper bogotense* (Piperaceae); MPUJ_ENT. **Rafael Uribe Uribe:** • 1 ♂; Parque Palermo Sur; 4.542, –74.1089; 2692 m; 09.iv.2018; V. Ocampo leg.; *Pittosporum undulatum* (Pittosporaceae); MPUJ_ENT. **Santa Fe:** • 9 ♂, 6 ♀; Universidad Distrital; 4.5991, –74.0656; 2695 m; 19.ix.2017; J. Duran leg.; *Acacia decurrens* (Fabaceae); MPUJ_ENT • 1 ♂, 1 ♀; same but 4.5986, –74.0656; 2702 m; 05.v.2017; *Acacia melanoxylon* (Fabaceae); MPUJ_ENT • 71 ♂, 52 ♀; same but 4.5987, –74.0667; 2667 m; 19.ix.2017; MPUJ_ENT • 1 ♂, 1 ♀; same but 4.5983, –74.0654; 2712 m; 05.v.2017; *Croton coriaceus* (Euphorbiaceae); MPUJ_ENT • 10 ♂, 14 ♀; same but 4.5985, –74.0655; 2704 m; *Lycianthes lycioides* (Solanaceae); MPUJ_ENT • 1 ♂; same but 4.5989, –74.0656; 2701 m; *Oreopanax incisus* (Araliaceae); MPUJ_ENT • 1 ♂; same but 4.5987, –74.0653; 2713 m; *Quercus humboldtii* (Fagaceae); MPUJ_ENT. **Suba:** • 2 ♀; Cerro La Conejera; 4.7718, –74.0648; 2622 m; 10.vii.2017; J. Duran leg.; *Acacia melanoxylon* (Fabaceae); MPUJ_ENT • 1 ♂; same but 4.7695, –74.0527; 2674 m; 03.x.2017; *Quercus humboldtii* (Fagaceae); MPUJ_ENT. **Us-**

aquén: • 1 ♂; Parque CAI Lisboa; 4.7088, –74.0292; 2599 m; 06.iv.2018; V. Ocampo leg.; *Pittosporum undulatum* (Pittosporaceae); MPUJ_ENT • 1 ♂; same but 4.7094, –74.0291; 2590 m; MPUJ_ENT.

Distribution. Colombia: Bogotá, Cundinamarca, Huila (Rendón-Mera et al. 2017).—Native to Australia, adventive in Africa, the Americas, Asia, Europe, North Africa, and New Zealand (Ouvrard 2023).

Host plant. *Acacia* Mill. and *Albizia* A. ex Benth. (Fabaceae) (Halbert and Burckhardt 2020); in this survey several adults were collected on *Acacia decurrens* (J.C.Wendl.) Willd. and *A. melanoxylon* R.Br. While the latter is confirmed in the literature as host, the former is not. Further studies will be necessary to find out whether *A. decurrens* serves as host to *A. uncatoides*.

***Platycorypha* sp.**

Material examined. Santa Fe: • 1 ♀; Parque Ilarco; 4.7008, –74.0657; 2569 m; 23.iii.2017; J. Duran leg.; *Croton coriaceus* (Euphorbiaceae); MPUJ_ENT.

Distribution. Colombia: Bogotá, Magdalena (Rendón-Mera et al. 2017).

Host plant. Unknown. The single female at hand was collected on *Croton*, an unlikely host as all *Platycorypha* species, for which hosts are known, develop on Fabaceae (Burckhardt and Queiroz 2020).

Comments. The single female at hand resembles specimens reported as *Platycorypha erythrinae* (Lizer) from Panama (Brown and Hodkinson 1988) and Peru (Burckhardt 1987). These specimens are probably not conspecific with *P. erythrinae* from Argentina, Brazil, Paraguay, and Uruguay, but represent an undescribed species. The specimens from Colombia, Panama and Peru differ from the latter in the presence of distinct brown dots on the radular areas of the forewing and the small hook on the apex of the female proctiger. More material is required for solving this issue.

***Tuthillia latipennis* Hodkinson, Brown & Burckhardt, 1986**

Material examined. Suba: • 1 ♀; Cerro La Conejera; 4.7718, –74.0651; 2631 m; 03.x.2017; J. Duran leg.; *Myrcianthes leucoxyla* (Myrtaceae); MPUJ_ENT. **Engativá:** • 1 ♂; Jardín Botánico de Bogotá; 4.6666, –74.0993; 2553 m; 16.x.2019; S. Vargas leg.; *Myrcianthes* sp. (Myrtaceae); MPUJ_ENT.

Distribution. Colombia: Bogotá (Rendón-Mera et al. 2017), Costa Rica, Panama (Brown and Hodkinson 1988; Hollis 2000).

Host plant. *Myrcianthes fragrans* (Sw.) McVaugh (Myrtaceae) (Hollis 2000). If *Myrcianthes leucoxyla* (Ortega) McVaugh, on which one female was collected, also constitutes a host, needs further observations.

Triozidae Löw, 1879

***Calinda gibbosa* (Tuthill, 1959)**

Material examined. Santa Fe: • 1 ♂, 2 ♀; Universidad Distrital; 4.5995, –74.0664; 2673 m; 19.ix.2017; J. Duran leg.; *Baccharis latifolia* (Asteraceae); MPUJ_ENT

• 1 ♀; same but 4.5997, –74.0653; 2692 m; *Quercus humboldtii* (Fagaceae); MPUJ_ENT. **Suba:** • 1 ♀; Cerro La Conejera; 4.7702, –74.0664; 2634 m; 10.vii.2017; J. Duran leg.; *Baccharis* sp. (Asteraceae); MPUJ_ENT.

Distribution. Colombia: Antioquia, Bogotá, Boyacá, Cundinamarca, Nariño (Olivares and Burckhardt 1997; Rendón-Mera et al. 2017), Cuba, Ecuador, Peru, Venezuela (Olivares and Burckhardt 1997).

Host plant. *Baccharis latifolia* Pers. (Asteraceae) (Olivares and Burckhardt 1997).

* *Calinda trinervis* Olivares & Burckhardt, 1997

Material examined. Santa Fe: • 1 ♀; Universidad Distrital; 4.5995, –74.0664; 2673 m; 19.ix.2017; J. Duran leg.; *Baccharis latifolia* (Asteraceae); MPUJ_ENT.

Distribution. Colombia: Bogotá, Costa Rica, Panama (Olivares and Burckhardt 1997).

Host plant. Unknown. Adults from Colombia were collected on *Baccharis latifolia* Pers. and adults from Costa Rica on *B. trinervis* Pers. (Asteraceae). Both should be checked to determine whether they are hosts.

Comments. *Calinda trinervis* is reported here for the first time from Colombia.

Calinda sp.

Material examined. Santa Fe: • 1 ♀; Parque Ilarco; 4.7008, –74.0657; 2569 m; 23.iii.2017; J. Duran leg.; *Croton coriaceus* (Euphorbiaceae); MPUJ_ENT.

Distribution. Colombia: Bogotá.

Host plant. Unknown.

Comments. The single female at hand represents probably an undescribed species. It shares the following characters with *Calinda albonigra* Olivares & Burckhardt, 1997 and *C. gladiformis* Olivares & Burckhardt, 1997: antenna shorter than 1.2 mm; forewing lacking surface spinules in distal 1/2; apical projection of proctiger well delimited from base, not inflated, straight, pointed apically, with well-defined teeth along dorsal margin; subgenital plate long; valvula dorsalis long; ventral saw of valvula ventralis not well delimited at base. From the former it differs in the relatively longer processes on the proctiger and subgenital plate. From the latter it differs in the relatively shorter apical process of the proctiger and the presence of a small ventral hump in the basal 1/3 of the subgenital plate.

* *Leuronota albilinea* Rendón-Mera, Burckhardt & Vargas-Fonseca, sp. nov.

https://zoobank.org/B778B877-DF95-4CAD-9A27-D325DE459AF0
Fig. 4

Type locality. Colombia, Bogotá: Santa Fe, Parque Tercer Milenio, 4.70025, –74.0654667, 2569 m.

Type material. ***Holotype***: Colombia • ♂, pinned; Bogotá, Santa Fe, Parque Tercer Milenio; 4.70025, –74.0654667; 2569 m; 19.ix.2017; J. Duran leg.; on *Clusia* sp. (Clusiaceae); MPUJ_ENT0074271. ***Paratypes*****: Santa Fe**: • 28 ♂, 23 ♀; same data as for holotype but 4.7003, –74.0655; MPUJ_ENT • 1 ♂, 1 ♀; same data as for preceding but NHMB • 1 ♂, 1 ♀; same data as for preceding but slide mounted; NHMB • 4 ♂, 4 ♀; same data as for preceding but in ethanol 70%; NHMB • 19 ♂, 11 ♀; same data as for preceding but 27.vi.2017; MPUJ_ENT • 1 ♂; same data as for preceding but 4.5989, –74.0814; 2607 m; *Prunus serotina* (Rosaceae); MPUJ_ENT.

Diagnosis. Mesonotum with white longitudinal stripe (Fig. 4B). Forewing (Fig. 4C) with three brown transverse bands as follows: one along vein R_1, base of cells r_2 and m_2, vein Cu_1 and apex of cell cu_2 adjacent to vein Cu_{1b}, one from subapex of cell r_1, through approx. middle of r_2 and m_2, to radular spinules of cu_1, and one from subapex of r_2, through base of m_1 to radular spinules of m_2; clavus brown along A_1 distal to apex of Cu_2. Paramere (Fig. 4E, F) with apical process short and posterior margin with apical 1/2 sinuous. Female proctiger (Fig. 4H) with apical portion relatively slender.

Description. ***Colouration*****.** Head, pronotum and pleura white, rest of notum and abdomen dark brown (Fig. 4A, B). Vertex with dark brown longitudinal stripes adjacent to eyes, curving inwards distal to torulus; anterior margin usually brownish; discal foveae dark brown; margin of toruli brown. Genal process sometimes slightly darker apically. Antennal segments 1–8 pale-yellow, 9–10 black. Clypeus white, slightly brown posteriorly. Pronotum with two brown longitudinal stripes medially; sublateral and lateral indentations dark brown. Mesopraescutum and mesoscutum with white longitudinal stripe medially. Forewing membrane (Fig. 4C) colourless, with three brown transverse bands as follows: one along vein R_1, base of cells r_2 and m_2, vein Cu_1 and apex of cell cu_2 adjacent to vein Cu_{1b}, one from near apex of cell r_1, through approx. middle of r_2 and m_2, to radular spinules of cu_1, and one from near apex of r_2, through base of m_1 to radular spinules of m_2; clavus brown along A_1 distal to apex of Cu_2; veins yellow, brown within the colour pattern; radular spinules brown. Fore, mid legs and metafemur brown, rest of hind leg yellow with apicotarsus brown. Abdominal basal sternites white or yellow medially; intersegmental membrane straw-coloured. Male terminalia dark brown. Female terminalia brown dorsally and ventrally, yellow apically.

Structure**.** Genal processes (Fig. 4A) 1.1–1.3× as long as vertex along midline, subcylindrical, slightly narrowing apically, sometimes slightly curved outwards, divergent; apex rounded. Antenna 3.1–3.6× as long as head width; longest terminal seta 3.5–4.0× as long as short seta, and 0.6–0.8× as long as segment 10. Labium with apical segment 0.3–0.4× as long as medial segment. Forewing (Fig. 4C) 5.2–5.6× as long as head width, and 2.5–2.6× as long as wide, obovate with angular apex; vein C+Sc evenly curved; vein Rs straight; vein M 2.1–2.3× as long as M_{1+2}, bifurcating after imaginary line between apices of veins Rs and Cu_{1a}; vein M_{1+2} reaching wing margin approximately at imaginary line through trifurcation of vein R+M+Cu and bifurcation of vein M; vein Cu 1.3–1.4× as long as R, and 1.6–1.8× as long as Cu_{1b}; cell r_1 approx. as wide as the narrowest section of r_2. Surface spinules widely spaced (Fig. 4D), covering m_1, cu_1, and cu_2, and colour pattern on r_2 and m_2. Radular spinules forming triangular fields. Metafemur with six or seven apical bristles; metatibia 1.2–1.4× as long as head width.

Terminalia**.** Male proctiger, in lateral view, subconical; apex constricted at anterior margin; anus large, occupying most part of apex, obliquely blunt. Paramere, in lateral view (Fig. 4E, F), 0.9× as long as proctiger; apical process short; bearing posterior lobe; anterior margin sinuous, concave submedially; posterior margin strong-

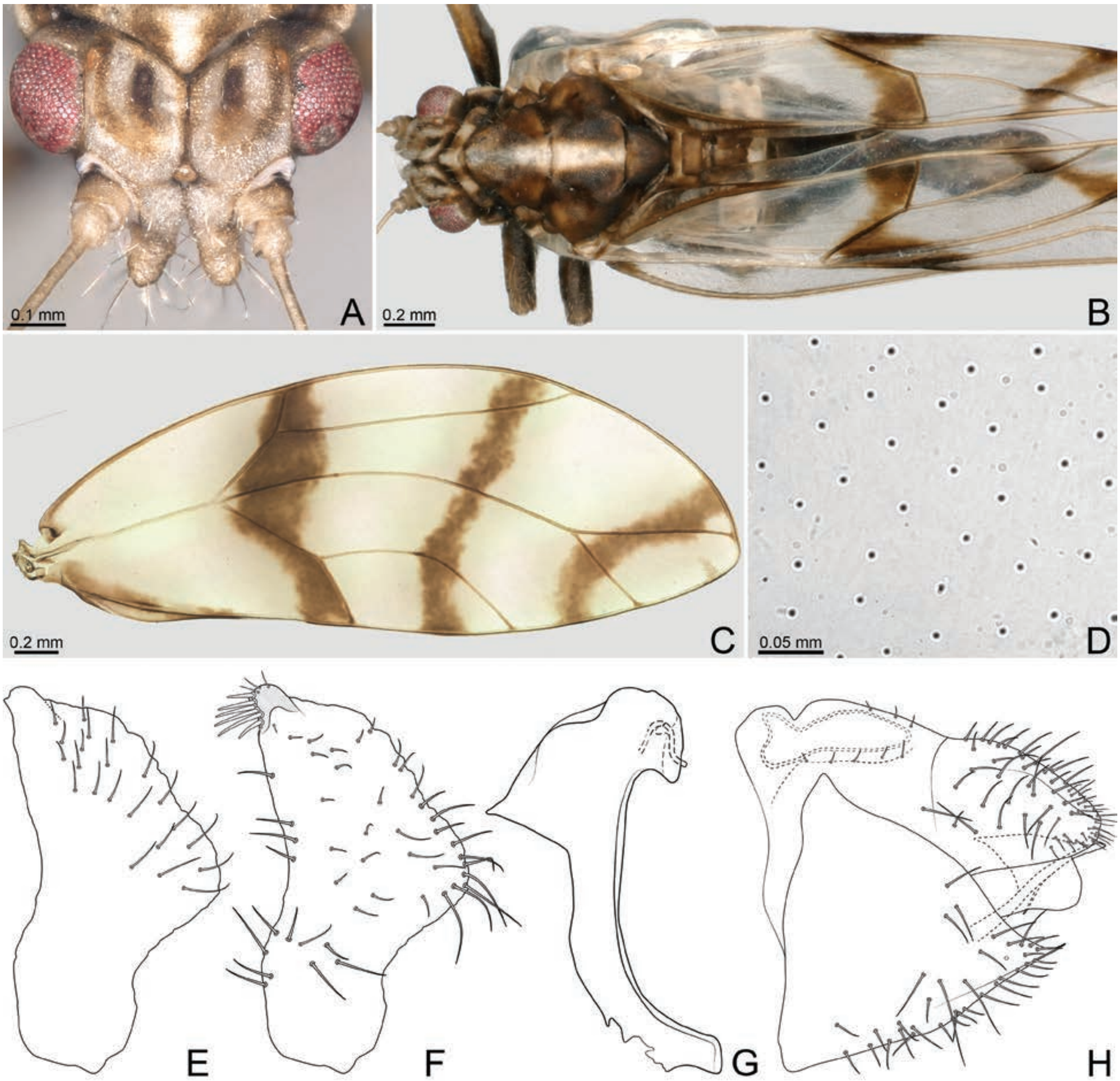

Figure 4. *Leuronota albilinea* Rendón-Mera, Burckhardt & Vargas-Fonseca, sp. nov. **A** head, dorsal view **B** habitus, dorsal view **C** forewing **D** surface spinules **E–G** male terminalia, lateral view **E** paramere, outer surface **F** paramere, inner surface **G** distal segment of aedeagus **H** female terminalia, lateral view.

ly irregular, concave in basal 1/3, strongly convex in median 1/3, sinuous in apical 1/3; outer surface (Fig. 4E) covered in medium long setae along posterior apical 1/2; inner surface (Fig. 4F) covered in short setae medially, long setae along anterior and posterior margins, and thick bristles anteriorly on apical tooth. Apical dilatation of aedeagus (Fig. 4G) with ventral extension beak-like, short; apically slightly convex, with small subapical hump; sclerotised end tube of ductus ejaculatorius short, weakly sinuate.—Female proctiger (Fig. 4H), in lateral view, 0.9× as long as head width; apical portion ~ 1/2 proctiger length; dorsal outline weakly incised at transverse groove, apical portion relatively slender, apex blunt; covered in long setae laterally, medium long setae dorsally, and short setae apically. Circumanal ring 0.4× as long as proctiger. Subgenital plate (Fig. 4H), in lateral view, 0.8× as long as proctiger; ventral outline straight in basal 1/2, weakly angular in the middle, straight in apical 1/2; sparsely covered in long setae, mostly ventrally and apically.

Measurements (in mm). BL 2 ♂ 3.7–4.1 (3.8±0.31), 2 ♀ 4.4–4.7 (4.79±0.37); HW ♂ 0.63, ♀ 0.67; VL ♂ 0.19, ♀ 0.18; GL ♂ 0.21, ♀ 0.23; AL ♂ 2.2, ♀ 1.78; LAB2 ♂ 0.22, ♀ 0.27; LAB3 ♂ 0.09, ♀ 0.09; FL ♂ 3.36, ♀ 3.46; TL ♂ 0.85, ♀ 0.78; MP 0.29; PL 0.26; FP 0.57; CRL 0.21; AP 0.25; SP 0.47.

Etymology. From Latin *albus* = white, and *linea* = line, referring to the contrasting longitudinal white stripe on the mesonotum. Noun in the ablative case.

Distribution. Colombia: Bogotá.

Host plant. Unknown. Many adults were collected on *Clusia* sp. (Clusiaceae) in the same area suggesting it is a host rather than just a casual plant. Further studies are necessary to to check this assumption.

Comments. *Leuronota albilinea* Rendón-Mera, Burckhardt & Vargas-Fonseca, sp. nov. resembles *L. inusitata* (Tuthill, 1944) (known from Costa Rica, Mexico, and Panama) in the brown body colour with white head and pleura, and white longitudinal stripe on mesonotum. It differs in the forewing pattern, the obovate forewing (vs ovate), the paramere with short (vs long) apical process and sinuous (vs concave) apical 1/2 of posterior margin, the aedeagal head with a weakly sinuous apical margin (vs evenly convex), and the female proctiger with a relatively slender apical portion (vs massive). In the key of Brown and Hodkinson (1988), *L. albilinea* Rendón-Mera, Burckhardt & Vargas-Fonseca, sp. nov. keys out with *L. inusitata*. In the key of Burckhardt (1988), the species keys out in couplet 4 with *L. digitulata* Burckhardt, 1988 (Paraguay) and *L. fagarae* Burckhardt, 1988 (Brazil, Ecuador, Mexico, Paraguay, USA), from which it differs in the forewing pattern with three brown transverse bands (vs restricted to anal margin or completely or almost completely covering the entire membrane).

* Triozidae gen. sp. 1

Material examined. Engativá: • 1 ♂; Jardín Botánico de Bogotá; 4.6666, –74.0993; 2553 m; 16.x.2019; S. Vargas leg.; *Myrcianthes* sp. (Myrtaceae); MPUJ_ENT. **Suba:** • 1 ♂; Cerro La Conejera; 4.7695, –74.0527; 2674 m; 03.x.2017; J. Duran leg.; *Quercus humboldtii* (Fagaceae); MPUJ_ENT.

Distribution. Colombia: Bogotá.

Host plant. Unknown.

Comments. The two males at hand probably represent an undescribed species. More material is required for a proper identification.

* Triozidae gen. sp. 2

Material examined. Rafael Uribe Uribe: • 1 ♀; Parque Palermo Sur; 4.5413, –74.1097; 2692 m; 09.iv.2018; V. Ocampo leg.; *Pittosporum undulatum* (Pittosporaceae); MPUJ_ENT.

Distribution. Colombia: Bogotá.

Host plant. Unknown.

Comments. The single female at hand fits in the *Trioza psyllihabitus* species group of Brown and Hodkinson (1988). More material is required for a species identification.

* Triozidae gen. sp. 3

Material examined. Santa Fe: • 1 ♂; Universidad Distrital; 4.5987, –74.0653; 2713 m; 27.vi.2017; J. Duran leg.; *Quercus humboldtii* (Fagaceae); MPUJ_ENT. **Usaquén:** • 1 ♀; Parque Ginebra-Bella Suiza; 4.706, –74.0302; 2591 m; 06.iv.2018; V. Ocampo leg.; *Ficus* sp. (Moraceae); MPUJ_ENT • 1 ♀; Parque La Vida; 4.7362, –74.0339; 2586 m; 16.iii.2018; V. Ocampo leg.; *Ficus* sp. (Moraceae); MPUJ_ENT.

Distribution. Colombia: Bogotá.

Host plant. Unknown.

Comments. The three specimens share the conspicuous dark longitudinal stripe on the forewing with species of *Triozoida* Crawford, 1911, a feature also found in other unrelated species of Triozidae (unpublished NHMB data). More material is required for a species identification.

Discussion and conclusions

During the survey of the arthropod fauna of 33 UGS in Bogotá between 2017 and 2019, 3,825 adult specimens of 21 psyllid species of seven families were found, seven species of which could be identified only to genus. Psyllids were found in all UGS ranging from 1–8 species per UGS. The UGS with the highest number (8 spp.) is Parque Ilarco, followed by Parque El Virrey (7 spp.), Parque Cabañas del Norte (5 spp.) and Universidad Distrital (Pueblo Viejo) (5 spp.) (Table 1). Parque El Virrey serves as a "contemplative" park while the other three UGS are designed for different purposes, primarily recreational use, and two of them, viz. Parque Ilarco and Parque Cabañas del Norte, are small parks with an area of less than 1 hectare each (Alcaldía Mayor de Bogotá 2021, 2022). At first sight this may be surprising, and one would expect that larger UGS specifically designed for conservation purposes would support the largest number of psyllid species. As psyllids are host specific, the presence of the host is the most important factor allowing the occurrence of psyllid species at a particular place. Local psyllid diversity usually reflects local host diversity.

The number of 21 species found during the survey is high in comparison to the number of taxa previously reported from Colombia: 34 identified species plus ten species identified only to genus (Pinzón et al. 2002; Rendón-Mera et al. 2017). This high percentage is, however, an artefact of the poor knowledge of the psyllid fauna of Colombia. From Brazil, whose psyllid diversity is slightly better known than that of Colombia, 163 species have been recorded (Burckhardt and Queiroz 2023). However, the actual number of species is likely to be in excess of 1000 (Burckhardt and Queiroz 2020). Comparing the number of plant species of the two countries with 44,000 species in Brazil and 37,000 species in Colombia (Flora e Funga do Brasil 2023; SiB Colombia 2023), it is reasonable to expect several hundreds of psyllid species in Colombia. The presence of previously undescribed species and the high percentage (38%) of species identified only to genus is a further indication of the hazy state of taxonomic knowledge.

Most specimens (3,800) were taken on plants which we consider hosts (vs 184 on non-hosts) (Table 2). Among the seven species with more than 20 collected specimens, less than 10% of the specimens were collected on non-hosts for four of them, while two species had between 10 and 15% of specimens on non-hosts. In only one species, *Acizzia uncatoides*, almost 40% of specimens were collected on non-hosts, reflecting the high mobility of this invasive species.

Of these seven species, two, viz. *Calophya schini* and *Syncoptozus mexicanus*, are known to be monophagous, while the others are oligophagous. The suspected hosts of *Leuronota albilinea* Rendón-Mera, Burckhardt & Vargas-Fonseca, sp. nov. (*Clusia* sp.), *Mastigimas colombianus* (*Cedrela montana*), *M. longicaudatus* Rendón-Mera, Burckhardt & Vargas-Fonseca, sp. nov. (*Cedrela montana*) and *Synoza cornutiventris* (*Ficus americana* subsp. *andicola*, *Ficus* sp.) are native, probably including those not identified to species.

A third of the psyllid species and more than 70% of the specimens found during the survey are exotic: the Australian *Acizzia acaciaebaileyanae*, *A. uncatoides*, *Ctenarytaina eucalypti*, *C. spatulata* and *Glycaspis brimblecombei*, the North American *Syncoptozus mexicanus*, and the Peruvian *Calophya schini*. The high abundance of these species is promoted by urban landscaping practices using exotic tree species (Molina-Prieto and Acosta-Hernández 2018; Bernal et al. 2022; Molina 2022), such as *Acacia decurrens*, *A. melanoxylon*, *Schinus areira*, and *Magnolia grandiflora*. Incidently, species like *A. decurrens*, *A. melanoxylon*, *Eucalyptus globulus*, and *S. areira* were among the earliest species used for urban arborisation in Bogotá (Molina-Prieto and Acosta-Hernández 2018). *Schinus areira*, the host of *C. schini*, the most abundant psyllid species of the survey (63% of all specimens), constitutes one of the most characteristic trees of Bogotá (Jardín Botánico de Bogotá 2022). Native to Bolivia, northern Chile, and Peru (Bernal et al. 2016; POWO 2023), *S. areira* was introduced into Bogotá around 1850 (Molina-Prieto and Acosta-Hernández 2018) and now numbers approximately 24,000 trees (Jardín Botánico de Bogotá 2023). Immatures of *C. schini* induce pit-galls on the leaflets of their host (Pinzón and González 2002; Rendón-Mera et al. 2017), and it is not uncommon to find the heavily galled foliage of *S. areira* throughout the city (pers. observation of the authors).

There are twice as many native as exotic psyllid species (66%) but only four of these (*Leuronota albilinea* Rendón-Mera, Burckhardt & Vargas-Fonseca, sp. nov., *Mastigimas colombianus*, *M. longicaudatus* Rendón-Mera, Burckhardt & Vargas-Fonseca, sp. nov., and *Synoza cornutiventris*) are represented by more than five individuals. Of the other ten species, three are identified to species and the other seven may be undescribed, but more material is needed to confirm this.

The psyllid data from our arthropod survey show that the UGS in Bogotá support a diverse psyllid fauna. The dominance of exotic tree species (Jardín Botánico de Bogotá 2023), however, promotes adventive, potentially invasive psyllids at the expense of the native fauna. For conservation of the native insect fauna, the use of native trees and shrubs should be considered a priority when new UGS are planned.

Acknowledgements

We are grateful to Giovanny Fagua, Dimitri Forero, Alejandra Rodríguez (MPUJ), and Francisco Serna (UNAB) for granting access to the collections; Kristian Rubiano for designing the map figure; Jowita Drohojowska, Diana Percy, Igor Malenovský, Alexandra Viertler, and Armando Rosario-Lebrón for useful comments on previous manuscript drafts. DIR-M and SAV-F would like to thank Sara for her assistance at the MPUJ. This study forms part of the work of DIR-M towards a Ph.D. degree at the University of Basel, funded by a Swiss Government Excellence Scholarship for Foreign Students from the Federal Commission (ESKAS), the Freiwillige Akademische Gesellschaft (FAG) and the Maria Parmigiani-Fonds, Basel.

Additional information

Conflict of interest

The authors have declared that no competing interests exist.

Ethical statement

No ethical statement was reported.

Funding

DIR-M was funded by the Swiss Government Excellence Scholarship for Foreign Students from the Federal Commission (ESKAS), the Freiwillige Akademische Gesellschaft (FAG) and the Maria Parmigiani-Fonds, Basel.

Author contributions

Conceptualization: VO, DB, JD, SAVF, DIRM. Data curation: DIRM, SAVF, VO, JD. Formal analysis: DIRM, DB. Investigation: DB, DIRM. Methodology: VO, JD. Project administration: VO, JD, SAVF. Resources: SAVF, DB, DIRM, VO, JD. Supervision: SAVF, JD, DB, VO. Validation: DB, DIRM. Visualization: DIRM. Writing - original draft: DIRM. Writing - review and editing: DIRM, VO, SAVF, DB, JD.

Author ORCIDs

Diana Isabel Rendón-Mera https://orcid.org/0000-0003-2553-9486
Daniel Burckhardt https://orcid.org/0000-0001-8368-5268
Sergio Andrés Vargas-Fonseca https://orcid.org/0000-0002-6716-905X

Data availability

All of the data that support the findings of this study are available in the main text.

References

Alcaldía Mayor de Bogotá (2009) Bogotá. Ciudad de estadísticas. No. 4. Ciudad Verde. Alcaldía Mayor de Bogotá, Secretaría Distrital de Planeación, Bogotá, 31 pp. https://observatorio.dadep.gov.co/documento/bogota-ciudad-de-estadisticas-no-4-ciudad-verde [accessed 24 Nov 2023]

Alcaldía Mayor de Bogotá (2021) Anexo 03. Inventario de espacio público peatonal y para el encuentro. In: Plan de Ordenamiento Territorial: Bogotá Reverdece 2022–2035. Alcaldía Mayor de Bogotá, Secretaría Distrital de Planeación, Bogotá, 200. https://www.sdp.gov.co/sites/default/files/anexo_03_inventario_espacio_publico_0.pdf [accessed 24 Nov 2023]

Alcaldía Mayor de Bogotá (2022) Manual de espacio público. Alcaldía Mayor de Bogotá, Secretaría Distrital de Planeación, Bogotá, 476 pp. https://www.sdp.gov.co/sites/default/files/generales/mep_p1-mon.pdf [accessed 24 Nov 2023]

Andrade GI, Remolina F, Wiesner D (2013) Assembling the pieces: A framework for the integration of multi-functional ecological main structure in the emerging urban region of Bogotá, Colombia. Urban Ecosystems 16(4): 723–739. https://doi.org/10.1007/s11252-013-0292-5

Andrade GI, Montenegro F, Remolina F, Wiesner D (2014) La Estructura Ecológica Principal en lo local. Propuesta de aplicación en la renovación urbana de Fenicia, Las Aguas, Bogotá. Revista Nodo 8: 42–54. https://revistas.uan.edu.co/index.php/nodo/article/view/100/81 [accessed 24 Nov 2023]

Anselm N, Brokamp G, Schütt B (2018) Assessment of land cover change in peri-urban high Andean environments south of Bogotá, Colombia. Land (Basel) 7(2): 1–28. https://doi.org/10.3390/land7020075

Aronson MFJ, La Sorte FA, Nilon CH, Katti M, Goddard MA, Lepczyk CA, Warren PS, Williams NSG, Cilliers S, Clarkson B, Dobbs C, Dolan R, Hedblom M, Klotz S, Kooijmans JL, Kühn I, Macgregor-Fors I, Mcdonnell M, Mörtberg U, Pyšek P, Siebert S, Sushinsky J, Werner P, Winter M (2014) A global analysis of the impacts of urbanization on bird and plant diversity reveals key anthropogenic drivers. Proceedings of the Royal Society B: Biological Sciences 281. https://doi.org/10.1098/rspb.2013.3330

Aronson MFJ, Lepczyk CA, Evans KL, Goddard MA, Lerman SB, MacIvor JS, Nilon CH, Vargo T (2017) Biodiversity in the city: Key challenges for urban green space management. Frontiers in Ecology and the Environment 15(4): 189–196. https://doi.org/10.1002/fee.1480

Baptiste B, Pinedo-Vasquez M, Gutierrez-Velez VH, Andrade GI, Vieira P, Estupiñán-Suárez LM, Londoño MC, Laurance W, Lee TM (2017) Greening peace in Colombia. Nature Ecology & Evolution 1(4): 0102. https://doi.org/10.1038/s41559-017-0102

Bastin S, Burckhardt D, Reyes-Betancort JA, Hernández-Suárez E, Ouvrard D (2023) A review of the jumping plant-lice (Hemiptera: Psylloidea) of the Canary Islands, with descriptions of two new genera and sixteen new species. Zootaxa 5313(1): 1–98. https://doi.org/10.11646/zootaxa.5313.1.1

Bernal R, Gradstein SR, Celis M (2016) Catálogo de plantas y liquenes de Colombia. Instituto de Ciencias Naturales, Universidad Nacional de Colombia, Bogotá. http://catalogoplantasdecolombia.unal.edu.co [accessed 24 Nov 2023]

Bernal FA, Matulevich JA, Corredor JA, Coy-Barrera E (2022) GC/MS-based fingerprinting reveals two chemotypes in the leaf essential oils from *Magnolia grandiflora* trees within the urban forestry of a Colombian Andean plateau. Chemistry & Biodiversity 19(9): e202200448. https://doi.org/10.1002/cbdv.202200448

Brown RG, Hodkinson ID (1988) Taxonomy and ecology of the jumping plant-lice of Panama (Homoptera: Psylloidea). Lyneborg L (Ed.). E. J. Brill/Scandinavian Science Press Ltd., Leiden, 304 pp. https://doi.org/10.1163/9789004631304

Burckhardt D (1987) Jumping plant lice (Homoptera: Psylloidea) of the temperate neotropical region. Part 2: Psyllidae (subfamilies Diaphorininae, Acizziinae, Ciriacreminae and Psyllinae). Zoological Journal of the Linnean Society 90(2): 145–205. https://doi.org/10.1111/j.1096-3642.1987.tb01353.x

Burckhardt D (1988) Jumping plant lice (Homoptera: Psylloidea) of the temperate neotropical region. Part 3: Calophyidae and Triozidae. Zoological Journal of the Linnean Society 92(2): 115–191. https://doi.org/10.1111/j.1096-3642.1988.tb00101.x

Burckhardt D, Queiroz DL (2020) Neotropical jumping plant-lice (Hemiptera, Psylloidea) associated with plants of the tribe Detarieae (Leguminosae, Detarioideae). Zootaxa 4733(1): 1–73. https://doi.org/10.11646/zootaxa.4733.1.1

Burckhardt D, Queiroz DL (2023) Psylloidea. Catálogo Taxonômico da Fauna do Brasil. PNUD. http://fauna.jbrj.gov.br/fauna/faunadobrasil/97523 [accessed 24 Nov 2023]

Burckhardt D, Queiroz DL, Queiroz EC, Andrade DP, Zanol K, Rezende MQ, Kotrba M (2011) The jumping plant-louse *Mastigimas anjosi* spec. nov., a new pest of *Toona ciliata* (Meliaceae) in Brazil. Spixiana 34: 109–120.

Burckhardt D, Queiroz DL, Drohojowska J (2013) Revision of the neotropical jumping plant-louse genus *Mastigimas* (Hemiptera, Psylloidea) attacking *Cedrela* and *Toona* species (Meliaceae). Zootaxa 3745(1): 1–18. https://doi.org/10.11646/zootaxa.3745.1.1

Burckhardt D, Ouvrard D, Queiroz D, Percy D (2014) Psyllid Host-plants (Hemiptera: Psylloidea): resolving a semantic problem. The Florida Entomologist 97(1): 242–246. https://doi.org/10.1653/024.097.0132

Burckhardt D, Cuda JP, Diaz R, Overholt W, Prade P, de Queiroz DL, Vitorino MD, Wheeler GS (2018) Taxonomy of *Calophya* (Hemiptera: Calophyidae) Species Associated with *Schinus terebinthifolia* (Anacardiaceae). The Florida Entomologist 101(2): 178–188. https://doi.org/10.1653/024.101.0205

Burckhardt D, Ouvrard D, Percy DM (2021) An updated classification of the jumping plant-lice (Hemiptera: Psylloidea) integrating molecular and morphological evidence. European Journal of Taxonomy 736: 137–182. https://doi.org/10.5852/ejt.2021.736.1257

Burckhardt D, Serbina LŠ, Malenovský I, Queiroz DL, Aléné DC, Cho G, Percy DM (2024) Phylogeny and classification of jumping plant lice of the subfamily Liviinae (Hemiptera: Psylloidea: Liviidae) based on molecular and morphological data. Zoological Journal of the Linnean Society 201(2): 387–421. https://doi.org/10.1093/zoolinnean/zlad128

Carvajal-Castro JD, Ana María Ospina L, Toro-López Y, Anny Pulido G, Cabrera-Casas LX, Guerrero-Peláez S, García-Merchán VH, Vargas-Salinas F (2019) Birds vs bricks: Patterns of species diversity in response to urbanization in a Neotropical Andean city. PLoS ONE 14(6): 1–20. https://doi.org/10.1371/journal.pone.0218775

Díaz S, Settele J, Brondízio ES, Ngo HT, Agard J, Arneth A, Balvanera P, Brauman KA, Butchart SHM, Chan KMA, Lucas AG, Ichii K, Liu J, Subramanian SM, Midgley GF, Miloslavich P, Molnár Z, Obura D, Pfaff A, Polasky S, Purvis A, Razzaque J, Reyers B, Chowdhury RR, Shin YJ, Visseren-Hamakers I, Willis KJ, Zayas CN (2019) Pervasive human-driven decline of life on Earth points to the need for transformative change. Science 366(6471): eaax3100. https://doi.org/10.1126/science.aax3100

Dufour DL, Piperata BA (2004) Rural-to-urban migration in Latin America: An update and thoughts on the model. American Journal of Human Biology 16(4): 395–404. https://doi.org/10.1002/ajhb.20043

Durán-Prieto J, Ocampo V (2019) Registro de *Diversinervus elegans* Silvestri (Hymenoptera: Encyrtidae) para la ciudad de Bogotá, Colombia. Dugesiana 26(1): 51–52. https://doi.org/10.32870/dugesiana.v26i1.7057

Durán-Prieto J, Tulande-Marín E, Ocampo-Flóres V (2020) Avispas (Insecta: Hymenoptera) asociadas a árboles urbanos de la ciudad de Bogotá, Colombia. Revista Chilena de Entomologia 46(4): 681–698. https://doi.org/10.35249/rche.46.4.20.14

Durán-Prieto J, Olmi M, Tulande-Marín E (2023) New records of pincer wasps in urban parks of Bogotá city (Colombia) (Hymenoptera: Dryinidae). Osmia 11: 23–26. https://doi.org/10.47446/OSMIA11.5

Elmqvist T, Fragkias M, Goodness J, Güneralp B, Marcotullio PJ, McDonald RI, Parnell S, Schewenius M, Sendstad M, Seto KC, Wilkinson C (Eds.) (2013) Urbanization, biodiversity and ecosystem services: challenges and opportunities. Springer Netherlands, Dordrecht, 453–459. https://doi.org/10.1007/978-94-007-7088-1

Flora e Funga do Brasil (2023) Flora e Funga do Brasil. Jardim Botânico do Rio de Janeiro. http://floradobrasil.jbrj.gov.br [accessed 24 Nov 2023]

Foley JA, DeFries R, Asner GP, Barford C, Bonan G, Carpenter SR, Chapin FS, Coe MT, Daily GC, Gibbs HK, Helkowski JH, Holloway T, Howard EA, Kucharik CJ, Monfreda C, Patz JA, Prentice IC, Ramankutty N, Snyder PK (2005) Global consequences of land use. Science 309(5734): 570–574. https://doi.org/10.1126/science.1111772

Garizábal-Carmona JA, Mancera-Rodríguez NJ (2021) Bird species richness across a Northern Andean city: Effects of size, shape, land cover, and vegetation of urban green spaces. Urban Forestry & Urban Greening 64: 127243. https://doi.org/10.1016/j.ufug.2021.127243

Goddard MA, Dougill AJ, Benton TG (2010) Scaling up from gardens: Biodiversity conservation in urban environments. Trends in Ecology & Evolution 25(2): 90–98. https://doi.org/10.1016/j.tree.2009.07.016

Halbert SE, Burckhardt D (2020) The psyllids (Hemiptera: Psylloidea) of Florida: newly established and rarely collected taxa and checklist. Insecta Mundi, 1–88. https://digitalcommons.unl.edu/insectamundi [accessed 24 Nov 2023]

Hodkinson ID (1974) The biology of the Psylloidea (Homoptera): A review. Bulletin of Entomological Research 64(2): 325–338. https://doi.org/10.1017/S0007485300031217

Hodkinson ID (1990) A new species of *Syncoptozus* Enderlein from Mexico with a redefinition of the subfamily Togepsyllinae Bekker-Migdisova (Insecta: Homoptera: Psylloidea). Journal of Natural History 24(3): 711–717. https://doi.org/10.1080/00222939000770491

Hodkinson ID (2009) Life cycle variation and adaptation in jumping plant lice (Insecta: Hemiptera: Psylloidea): a global synthesis. Journal of Natural History 43(1–2): 65–179. https://doi.org/10.1080/00222930802354167

Hollis D (2000) Preliminary list of Psylloidea known from Costa Rican cloud forests (1200–2000 m). In: Nadkarni NM, Wheelwright NT (Eds) Monteverde: ecology and conservation of a tropical cloud forest. Oxford University Press, New York, 573 pp.

Hollis D (2004) Australian Psylloidea: jumping plantlice and lerp insects. Australian Biological Resorces Study, Canberra, 216 pp.

Ives CD, Lentini PE, Threlfall CG, Ikin K, Shanahan DF, Garrard GE, Bekessy SA, Fuller RA, Mumaw L, Rayner L, Rowe R, Valentine LE, Kendal D (2016) Cities are hotspots for threatened species. Global Ecology and Biogeography 25(1): 117–126. https://doi.org/10.1111/geb.12404

Jardín Botánico de Bogotá (2022) Crónica – Falso pimiento: un árbol apetecido por un insecto foráneo. https://jbb.gov.co/cronica-falso-pimiento-un-arbol-apetecido-por-un-insecto-foraneo/ [accessed 24 Nov 2023]

Jardín Botánico de Bogotá (2023) Geoportal Datos Abiertos JBB. https://jardinbotanico-bogota-jbb.hub.arcgis.com/ [accessed 24 Nov 2023]

Jaureguiberry P, Titeux N, Wiemers M, Bowler DE, Coscieme L, Golden AS, Guerra CA, Jacob U, Takahashi Y, Settele J, Díaz S, Molnár Z, Purvis A (2022) The direct drivers of recent global anthropogenic biodiversity loss. Science Advances 8(45): 1–12. https://doi.org/10.1126/sciadv.abm9982

Kong X, Zhou Z, Jiao L (2021) Hotspots of land-use change in global biodiversity hotspots. Resources, Conservation and Recycling 174: 105770. https://doi.org/10.1016/j.resconrec.2021.105770

Lepczyk CA, Aronson MFJ, Evans KL, Goddard MA, Lerman SB, Macivor JS (2017) Biodiversity in the city: Fundamental questions for understanding the ecology of urban green spaces for biodiversity conservation. Bioscience 67(9): 799–807. https://doi.org/10.1093/biosci/bix079

Makunde PT, Slippers B, Burckhardt D, de Queiroz DL, Lawson SA, Hurley BP (2020) Current and potential threat of psyllids (Hemiptera: Psylloidea) on eucalypts. Southern Forests 82(3): 233–242. https://doi.org/10.2989/20702620.2020.1813650

Marín-Gómez OH, Garzón Zuluaga JI, Santa-Aristizabal DM, López JH, López-Garcia MM (2016) Use of urban areas by two emblematic and threatened birds in the central Andes of Colombia. Revista Brasileira de Ornitologia 24(3): 260–266. https://doi.org/10.1007/BF03544353

Martínez DC, Morales I (2020) Annotated list of beetles (Insecta, Coleoptera) in an urban area of the Eastern Andes of Colombia. Check List 16(6): 1679–1693. https://doi.org/10.15560/16.6.1679

Mauck KE, Gebiola M, Percy DM (2024) The Hidden Secrets of Psylloidea: Biology, Behavior, Symbionts, and Ecology. Annual Review of Entomology 69(1): 277–302. https://doi.org/10.1146/annurev-ento-120120-114738

McDonald RI, Colbert M, Hamann M, Simkin R, Walsh B (2018) Nature in the Urban Century: A global assessment of where and how to conserve nature for biodiversity and human wellbeing. The Nature Conservancy, 78 pp. https://www.nature.org/en-us/what-we-do/our-insights/perspectives/nature-in-the-urban-century/

McKinney ML (2002) Urbanization, biodiversity, and conservation. Bioscience 52(10): 883–890. https://doi.org/10.1641/0006-3568(2002)052[0883:UBAC]2.0.CO;2

McKinney ML (2008) Effects of urbanization on species richness: A review of plants and animals. Urban Ecosystems 11(2): 161–176. https://doi.org/10.1007/s11252-007-0045-4

Molina D (2022) The forced retirement of a hard worker: The rise and fall of Eucalyptus in Bogotá. Environmental History 27(1): 58–85. https://doi.org/10.1086/717611

Molina-Prieto LF, Acosta-Hernández CF (2018) Orígenes y evolución de las arborizaciones urbanas en América Latina con énfasis en Bogotá y Medellín. Formas urbanas colonial, republicana y protomoderna. Gestion y Ambiente 21(2): 276–290. https://doi.org/10.15446/ga.v21n2.74906

Myers N, Mittermeler RA, Mittermeler CG, Da Fonseca GAB, Kent J (2000) Biodiversity hotspots for conservation priorities. Nature 2000 403: 853–858. https://doi.org/10.1038/35002501

Ocampo Flórez V, Durán Prieto J, Albornoz M, Forero D (2018) New plant associations for *Monalonion velezangeli* (Hemiptera: Miridae) in green urban areas of Bogotá (Colombia). Acta Biologica Colombiana 23(2). https://doi.org/10.15446/abc.v23n2.69374

OECD (2022) National urban policy review of Colombia. OECD Publishing, Paris, 316 pp. https://doi.org/10.1787/9ca1caae-en

Olaya-Arenas P, Durán-Prieto J, Pinzón-Florían OP, Becerra-Guerrero NS (2022) Insectos del arbolado urbano de Bogotá (Colombia): explorando su diversidad y función. Jardín Botánico de Bogotá José Celestino Mutis, Instituto de Investigación de Recursos Biológicos Alexander von Humboldt., Bogotá, 99 pp.

Olivares TS, Burckhardt D (1997) Jumping plant-lice of the New World genus *Calinda* (Hemiptera: Psylloidea: Triozidae). Revue Suisse de Zoologie 104: 231–344. https://doi.org/10.5962/bhl.part.79999

Ouvrard D (2023) Planthoppers: Psylles Website. http://dbtnt.hemiptest.infosyslab.fr/psyllist/?db=psylles&page=explorer&card=genera&lang=en [accessed 24 Nov 2023]

Ouvrard D, Chalise P, Percy DM (2015) Host-plant leaps versus host-plant shuffle: A global survey reveals contrasting patterns in an oligophagous insect group (Hemiptera, Psylloidea). Systematics and Biodiversity 13(5): 434–454. https://doi.org/10.1080/14772000.2015.1046969

Pinzón FOP, Guzmán CM, Navas NF (2002) Contribución al conocimiento de la biología, enemigos naturales y daños del pulgón del eucalipto *Ctenarytaina eucalypti* (Homoptera: Psyllidae). Revista Colombiana de Entomologia 28(2): 123–128. https://doi.org/10.25100/socolen.v28i2.9636

Pinzón OP, González RH (2002) Caracterización biológica, hábitos, enemigos naturales y fluctuación poblacional de *Calophya schini* Tuthill, en la especie forestal *ornamental Schinus molle* L. en Bogotá. Revista Científica, 2002, 137–154.

POWO (2023) Plants of the World Online. Facilitated by the Royal Botanic Gardens, Kew. https://powo.science.kew.org/ [accessed 24 Nov 2023]

Pugh A, Withers T, Sopow S (2017) New eucalypt feeding insect established in New Zealand. NZ Farm Forestry. https://www.nzffa.org.nz/farm-forestry-model/the-essentials/forest-health-pests-and-diseases/Pests/glycaspis-brimblecombei-red-gum-lerp-psyllid/new-eucalypt-feeding-insect-established-in-new-zealand/ [accessed 24 Nov 2023]

Queiroz DL, Burckhardt D, Garrastazu MC (2017) Protocolo de coleta e montagem de psilídeos. Comunicado Técnico Embrapa 393: 1–11.

Rendón-Mera DI, Serna F, Burckhardt D (2017) Generic synopsis of the jumping plant-lice (Hemiptera: Sternorrhyncha: Psylloidea) from Colombia. Zootaxa 4350(3): 436–468. https://doi.org/10.11646/zootaxa.4350.3.2

Rodas CA, Serna R, Hurley BP, Bolaños MD, Granados GM, Wingfield MJ (2014) Three new and important insect pests recorded for the first time in Colombian plantations. Southern Forests 76(4): 245–252. https://doi.org/10.2989/20702620.2014.965983

Roncallo J, Ramos Ortega LM, Guerrero RJ, Sierra H (2022) Las hormigas exóticas en ambientes urbanos de Santa Marta, Colombia. Intropica: 202–217. https://doi.org/10.21676/23897864.4758

Seto KC, Güneralp B, Hutyra LR (2012) Global forecasts of urban expansion to 2030 and direct impacts on biodiversity and carbon pools. Proceedings of the National Academy of Sciences of the United States of America 109(40): 16083–16088. https://doi.org/10.1073/pnas.1211658109

SiB Colombia (2023) Biodiversidad en cifras. Sistema de Información sobre Biodiversidad de Colombia. https://cifras.biodiversidad.co/colombia (November 24, 2023).

Tzoulas K, Korpela K, Venn S, Yli-Pelkonen V, Kaźmierczak A, Niemela J, James P (2007) Promoting ecosystem and human health in urban areas using Green Infrastructure: A literature review. Landscape and Urban Planning 81(3): 167–178. https://doi.org/10.1016/j.landurbplan.2007.02.001

United Nations (2019) World urbanization prospects 2018: highlights. United Nations, Department of Economic and Social Affairs, Population Division, New York, 30 pp. https://population.un.org/wup/

Appendix 1

Table A1. Green Spaces (UGS) per district ("localidades"). In some instances, the park names as indicated on the collection labels differ from the official names, which are here provided in parentheses. See glossary of terms below, compilated from: Alcaldía Mayor de Bogotá 2021, 2022, IDRD 2023a, 2023b.

Neighbourhood / UGS	Identifier	Park level and typology	Park classification
Antonio Nariño			
Parque Ciudad Jardín	15-027	Structuring (sport)	Zonal
Chapinero			
Parque El Chicó	02-097	Proximity	Pocket
Parque El Virrey	02-014	Structuring (contemplative)	Zonal
Sendero Quebrada La Vieja	–	Protected area	–
Engativá			
Jardín Botánico de Bogotá	10-291	Structuring (contemplative)	Metropolitan
Rafael Uribe Uribe			
Parque Palermo Sur	18-035	Proximity	Neighbourhood
San Cristóbal			
Parque La Victoria	04-122	Structuring (sport)	Zonal

Neighbourhood / UGS	Identifier	Park level and typology	Park classification
Parque Primero de Mayo (Deportivo Primero de Mayo)	04-196	Structuring (sport)	Metropolitan
Parque San Cristóbal	04-127	Structuring (cultural)	Metropolitan
Parque Villa de los Alpes	04-075	Structuring (sport)	Zonal
Santa Fe			
Parque La Independencia (Independencia-Bicentenario)	03-039	Structuring (cultural)	Metropolitan
Parque Nacional	03-035	Structuring (cultural)	Metropolitan
Parque Ilarco	11-007	Proximity	Neighbourhood
Parque Tercer Milenio	03-085	Structuring (cultural)	Metropolitan
Universidad Distrital (Pueblo Viejo)	–	Structuring (NIA)	Zonal
Suba			
Cerro La Conejera	–	Protected area	Ecological
Parque Canal Molinos (Parque La Alhambra Sector Sur)	11-097	Proximity	Neighbourhood
Vacant lot	–		
Usaquén			
CAI Santa Barbara (Urbanización Santa Bárbara Primer Sector)	01-198	Proximity	Neighbourhood
Parque Altablanca	01-075	Structuring (sport)	Zonal
Parque Belmira	01-187	Proximity	Neighbourhood
Parque Cabañas del Norte	01-244	Proximity	Neighbourhood
Parque CAI Lisboa (Urbanización Ginebra Norte)	01-120	Proximity	Neighbourhood
Parque Cedro Madeira (El Cedro Maderia)	01-250	Proximity	Neighbourhood
Parque Contador Norte	01-083	Proximity	Neighbourhood
Parque Ginebra-Bella Suiza	01-106	Proximity	Neighbourhood
Parque La Francia (Urbanización Los Molinos)	01-118	Proximity	Neighbourhood
Parque La Vida	01-012	Structuring (recreational)	Zonal
Parque Nueva Autopista	01-064	Structuring (contemplative)	Zonal
Parque Usaquén 2 (Santa Barbara Primer Sector)	01-087	Proximity	Neighbourhood
Usme			
Parque Chuniza-Famaco (Famaco)	05-086	Structuring (cultural)	Zonal
Parque La Andrea	05-004	Structuring (sport)	Zonal
Parque Virrey Sur	05-016	Structuring (sport)	Zonal

Glossary

Contemplative: Spaces designed to promote the richness and diversity of vegetation cover for environmental enjoyment and low-impact human activities. They focus on a contemplative and educational relationship achieved through both permanence and travel. Their main spatial design component is ecological.

Cultural: Spaces designed to serve as meeting places, promoting permanence for the development of civic or cultural activities and outdoor events that highlight cultural values, traditions, and collective memory. The design can incorporate various care and social services, with permanence as the main spatial design component.

Ecological park: Parks that due to their high scenic and/or biological value, as well as their location and accessibility, are intended for the preservation, restoration, and sustainable ecological use of their biophysical elements for environmental education and passive recreation.

Metropolitan park: Parks covering an area of more than 10 hectares, designated for the development of both active and passive recreational uses, aiming to generate landscape and environmental values. The influence of these spaces extends across the entire territory of the city.

Neighbourhood park: Parks with an area of less than one hectare, designed for the recreation, meeting, and integration of the community, addressing the specific needs of the neighbourhoods.

Pocket park: Neighbourhood-type parks but with an area of less than 0.1 hectares, intended primarily for the recreation of children and senior citizens.

Protected area: Spaces with unique value for the natural heritage of the Capital District, ecosystems, biodiversity conservation, and the evolution of culture in the area.

Proximity space: Spaces mostly smaller than one hectare that offer a diverse range of leisure activities at a local scale.

Recreational: Spaces designed to provide facilities for the development of recreational activities, promoting relationships between individuals, the development of skills, and engagement in both free and structured activities. Their main spatial design component is play.

Sport: Spaces designed to accommodate physical activities and sports practice at different levels, including recreational, training, and competitive levels. The activities focus on the physical conditioning of different age groups, either individually or collectively. The main spatial design component of these spaces is sports.

Structuring space: Spaces larger than one hectare that provide a diverse range of leisure activities, supporting both regional and district scales. These spaces contribute not only to human interactions but also to environmental and ecosystemic connectivity.

Zonal park: Parks ranging from 1 to 10 hectares designed to fulfil the active recreational needs of a group of neighbourhoods and can accommodate specialized sport facilities.

References

Alcaldía Mayor de Bogotá (2021) Anexo 03. Inventario de espacio público peatonal y para el encuentro. In: Plan de Ordenamiento Territorial: Bogotá Reverdece 2022–2035. Alcaldía Mayor de Bogotá, Secretaría Distrital de Planeación, Bogotá, 200. https://www.sdp.gov.co/sites/default/files/anexo_03_inventario_espacio_publico_0.pdf [Accessed 24 Nov 2023]

Alcaldía Mayor de Bogotá (2022) Manual de espacio público. Alcaldía Mayor de Bogotá, Secretaría Distrital de Planeación, Bogotá, 476 pp. https://www.sdp.gov.co/sites/default/files/generales/mep_p1-mon.pdf [Accessed 24 Nov 2023]

IDRD (2023a) Buscador de parques. https://portalciudadano.idrd.gov.co/parques/buscar [Accessed 24 Nov 2023]

IDRD (2023b) Parques. Instituto Distrital de Recreación y Deporte. https://sim1.idrd.gov.co/parques-0 [Accessed 24 Nov 2023]

ZooKeys 1209: 231–244 (2024)
DOI: 10.3897/zookeys.1209.124692

Research Article

Discovery and lectotype designation of *Longitarsus californicus* (Motschulsky) (Coleoptera, Chrysomelidae, Galerucinae, Alticini)

Alexander S. Konstantinov[1], Vladimir Yu. Savitsky[2], Il'ya A. Zabaluev[2]

1 *Systematic Entomology Laboratory, USDA, ARS, c/o Smithsonian Institution, National Museum of Natural History, Washington DC, USA*
2 *Zoological Museum of Lomonosov Moscow State University, Moscow, 125009, Russia*
Corresponding author: Alexander S. Konstantinov (alex.konstantinov@usda.gov)

Abstract

The lectotype of *Longitarsus californicus* (Motschulsky, 1845) is designated, described, and illustrated. An illustrated key to eight light-colored *Longitarsus* species known to occur in the western United States is presented. A brief history of Russian entomological collecting in North America during the first half of 19th century, with specimens preserved in Zoological Museum of Moscow University, Moscow and Zoological Institute, St. Petersburg, is provided.

Key words: America north of Mexico, Il'ya Gavrilovich Voznesensky, Johann Friedrich Gustav von Eschscholtz, key for identification, leaf beetles

Academic editor: Ron Beenen
Received: 4 April 2024
Accepted: 17 May 2024
Published: 9 August 2024

ZooBank: https://zoobank.org/191301E5-7C11-4CE1-A296-8A0E90A88C18

Citation: Konstantinov AS, Savitsky VYu, Zabaluev IA (2024) Discovery and lectotype designation of *Longitarsus californicus* (Motschulsky) (Coleoptera, Chrysomelidae, Galerucinae, Alticini). ZooKeys 1209: 231–244. https://doi.org/10.3897/zookeys.1209.124692

Introduction

Longitarsus Latreille, 1829 is the most species-rich genus among flea beetles, with more than 700 species worldwide (Konstantinov unpublished compilation). Fifty-one valid species of *Longitarsus* are known to occur in America north of Mexico (Riley et al. 2003; Konstantinov unpublished compilation). Thirty-nine of them are native, and 12 are introduced, either as biological control agents of invasive weeds or unintentionally (LeSage 1988; Pentinsaari et al. 2019). North American *Longitarsus* has never been reviewed or revised. The most recent available key for species identification is that of Horn (1889). A few regional keys were later published, which included *Longitarsus* (e.g. Beller and Hatch 1932; Wilcox 1954; Balsbaugh and Hays 1972). Most North American *Longitarsus* species were described by Blatchley (1923), Horn (1889), and LeConte (1859), and their type specimens are available for study at major Canadian and United States entomological collections (Canadian National Collection, Ottawa, Ontario; Museum of Comparative Zoology, Cambridge, Massachusetts; Purdue Entomological Research Collection, West Lafayette, Indiana; and National Museum of Natural History, Washington DC). However, the whereabouts of the type specimen and, therefore, the certain identity of one species, *Longitarsus californicus* (Motschulsky, 1845), has remained a mystery until recently, when a single female specimen was discovered by VYS in one of the drawers of the Motschulsky collection in the Zoological Museum of Moscow University, Moscow, Russia (ZMUM). The Motschulsky beetle collection contains approximately 60,000 specimens, of which about 4,000 are types (Lyubarsky 2009). Most of the types have been recognized as such and transferred from the main holdings to special drawers. However, beetle types previously considered missing are still being discovered in the main holdings of Motschulsky collection (Savitsky 2018). The *Longitarsus californicus* specimen was pinned on a short pin with a small label in such a way that the specimen was close to the bottom of the drawer and was not recognized as the type by previous ZMUM curators.

The origin of the specimen and its exact collecting locality remain unknown. It could not have come from Motschulsky's own collecting in the United States, which he visited in 1853–1854, nearly 10 years after the description of *L. californicus* was published. In a letter to Édouard Ménétries dated July 15, 1854, Motschulsky mentioned a visit to the LeConte collection which contained "very different things than what Dr. Voznesensky brought" from California (Motschulsky 2013). Indeed, there is a slight possibility that the specimen of *L. californicus* came from Il'ya Gavrilovich Voznesensky (1816–1871), who travelled to western North America in 1839–1849 (Gnucheva 1940), where he visited Fort Ross, Drake's Cape, San Francisco Bay, Fort Ross at Bodega Bay, Mount St. Helens, and Khlebnikov Valley. Each location originally had its own color-coded label (Feklova 2014). However, Motschulsky often replaced original labels with his own (Koponen and Niemelä 2020), so the color of the *L. californicus* label cannot help in identifying its type locality. The bulk of the Voznesensky zoological collection was transferred to the Zoological Institute (St. Petersburg, Russia) most likely around 1849 (Feklova 2014).

The other likely source of California specimens described by Motschulsky in 1845 is collection of Johann Friedrich Gustav von Eschscholtz (1793–1831), an early pioneer in the western North American coleopterology. He was the naturalist in two expeditions in 1815–1817 and 1823–1826 to the western United States (Koponen and Niemelä 2020). Beetles are well represented among large biological collections that he made. New beetle genera and species were described by Eschscholtz (1829–1833) and Mannerheim (1843) based on North American specimens collected by Eschscholtz. Eschscholtz's collection was transferred to the Zoological Museum of Moscow University in the summer of 1837 (Lyubarsky 2009) at a time of Motschulsky's affiliation with the museum and well before 1845 (Koponen and Niemelä 2020).

Materials and methods

The source of the flea beetle diversity is an unpublished compilation of flea beetle genera and species of the world, which is a FileMakerPro database maintained by ASK since 2006. It is cited as "Konstantinov unpublished compilation". The lectotype of *L. californicus* was processed as follows. The abdomen, genitalia and terminalia were studied at magnifications up to ×400 (spermatheca) and documented from glycerol preparations, using a Micromed-3 microscope equipped with a ToupCam 9.0 MP digital eyepiece camera. The other photographs were taken using a Canon EOS 5D Mark IV camera with a Canon MP-E 65 mm objective lens. The USNM specimen of *L. californicus* was photographed with Macropod Pro photomacrography system (Macroscopic Solutions, LLC, Tolland, CT, USA) and processed with Zerene Stacker v. 1.04 and edited with

Adobe Photoshop Elements 2020. Dissecting techniques and morphological terminology follow Konstantinov (1998). Numbering only visible tarsomeres and abdominal segmentation justified previously (Konstantinov et al. 2022). The type locality is cited verbatim as it appears in the original description.

Specimens studied in this paper are deposited in the following collections:

USMN	National Museum of Natural History, Washington DC, USA.
ZMUM	Zoological Museum of Moscow University, Moscow, Russia.

Results

***Longitarsus californicus* (Motschulsky)**
Figs 1–23

Teinodactyla californica Motschulsky, 1845: 382 (type locality: Californie; lectotype, ♀, designated here, ZMUM).

Type material examined. *Lectotype*: ♀, labels (Figs 7, 8) (ZMUM).

(1) “Teinodact californica m California” in V.I. Motschulsky’s handwriting on white paper;

(2) “Zoomuseum of MSU (Moscow, RUSSIA) [in Russian] Nº ZMUM Col 02777 Zool. Mus. Mosq. Univ. (Mosquae, ROSSIA) ex coll. V. I. Motschulsky” printed on pink paper;

(3) “ Lectotypus *Teinodactyla californica* Motschulsky, 1845 A. Konstantinov, V. Savitsky et I. Zabaluev des. 2024” printed on red paper;

(4) “ *Longitarsus californicus* (Motschulsky, 1845) A. Konstantinov det. 2024” printed on white paper.

Lectotype is missing hind right leg, left protarsomeres 2–4, and 11 antennomere of right antenna. Antennomeres 3–11 of left antenna, left protarsomere 1, right mesotibia and mesotarsi are glued to a white card below the specimen mount. Abdomen and genitalia are placed in genitalia vial with glycerin.

Material examined. (2 ♀, 1 ♂, USNM).

(1) “Amedee, Cal, July 21–28, 4200 ft, Wickham”;

(2) “Wickham Collection, 1933”;

(3) “*Longitarsus californicus* Horn” handwritten on yellowed paper with a red border;

(4) “*Longitarsus californicus* (Motschulsky), det A. Konstantinov 2024”.

Diagnosis. Head with vertex covered by reticulation. Supracallinal sulci thin, antennal calli separated from vertex by thin line. Frontal ridge elongate, wider between antennal sockets, narrower towards clypeus. Antennomere 2 longer than 3. Antennomere 3 as long as 4. Pronotal surface with coarse reticulation. Elytra posteriorly about as long as abdomen, covering nearly all abdominal tergites. Receptacle of spermatheca elongate. Receptacle and pump distinctly to abruptly separated from each other. Spermathecal canal with coils. Vaginal palpus slender, with apex subdeltoid. Anterior sclerotization of vaginal palpus much narrower than posterior sclerotization.

Description. *Body* (Figs 1, 5) length 2.21–2.40 mm, width 1.08–1.15 mm (the lectotype 2.4 mm long and 1.15 mm wide). Pronotum and elytra light yellowish; 5 apical antennomeres, head and metafemur slightly darker.

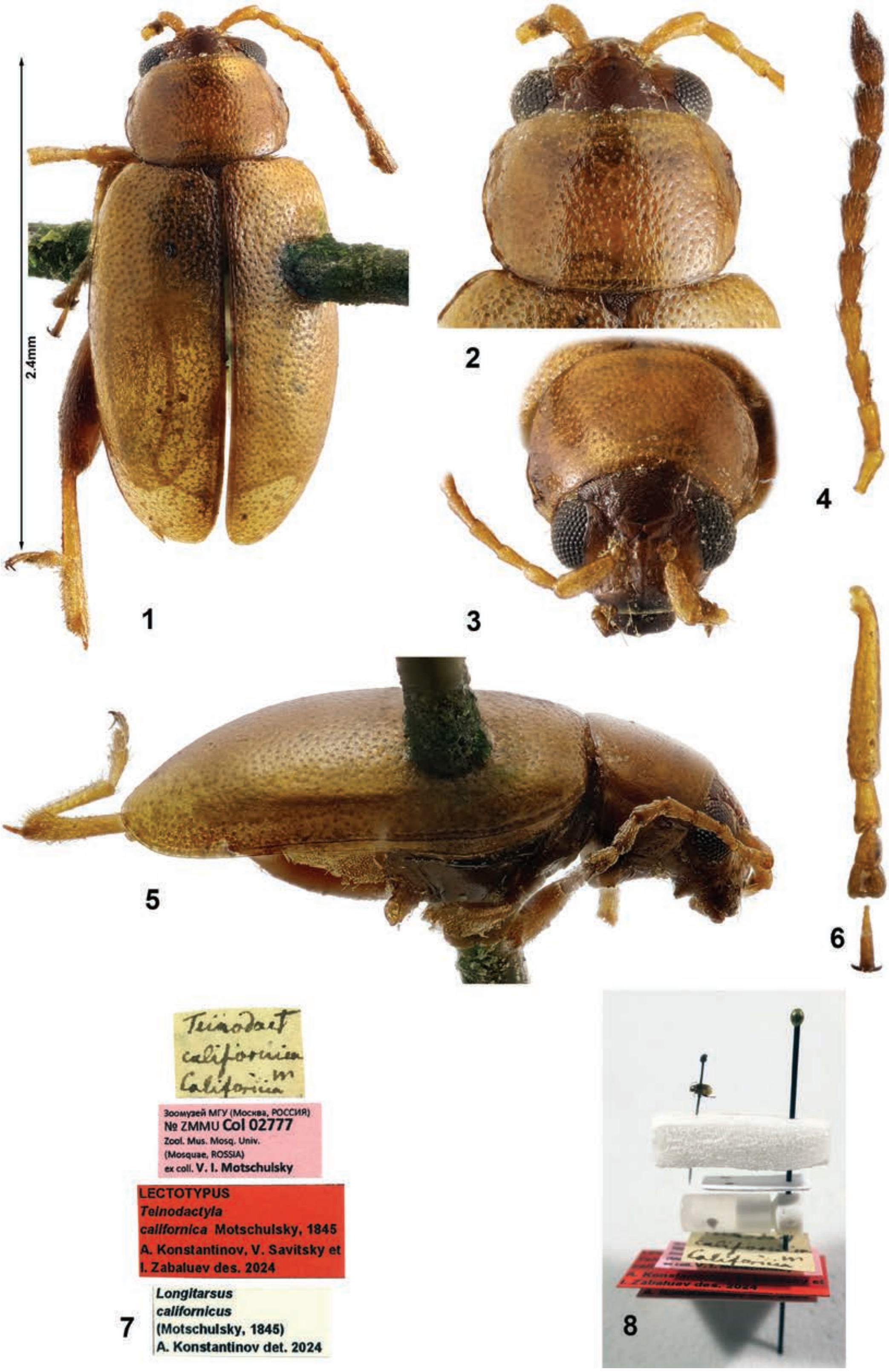

Teinodact
californica
California m

Зоомузей МГУ (Москва, РОССИЯ)
№ ZMMU **Col 02777**
Zool. Mus. Mosq. Univ.
(Mosquae, ROSSIA)
ex coll. **V. I. Motschulsky**

LECTOTYPUS
Teinodactyla
***californica* Motschulsky, 1845**
A. Konstantinov, V. Savitsky et
I. Zabaluev des. 2024

Longitarsus
californicus
(Motschulsky, 1845)
A. Konstantinov det. 2024

Figures 1–8. *Longitarsus californicus* (Motschulsky), Lectotype **1** habitus, dorsal view **2** pronotum **3** head, frontal view **4** left antennae with antennomeres 1 and 2 missing **5** habitus lateral view **6** right mesotibia and mesotarsi **7** labels **8** lectotype as currently mounted with labels and genitalia vial.

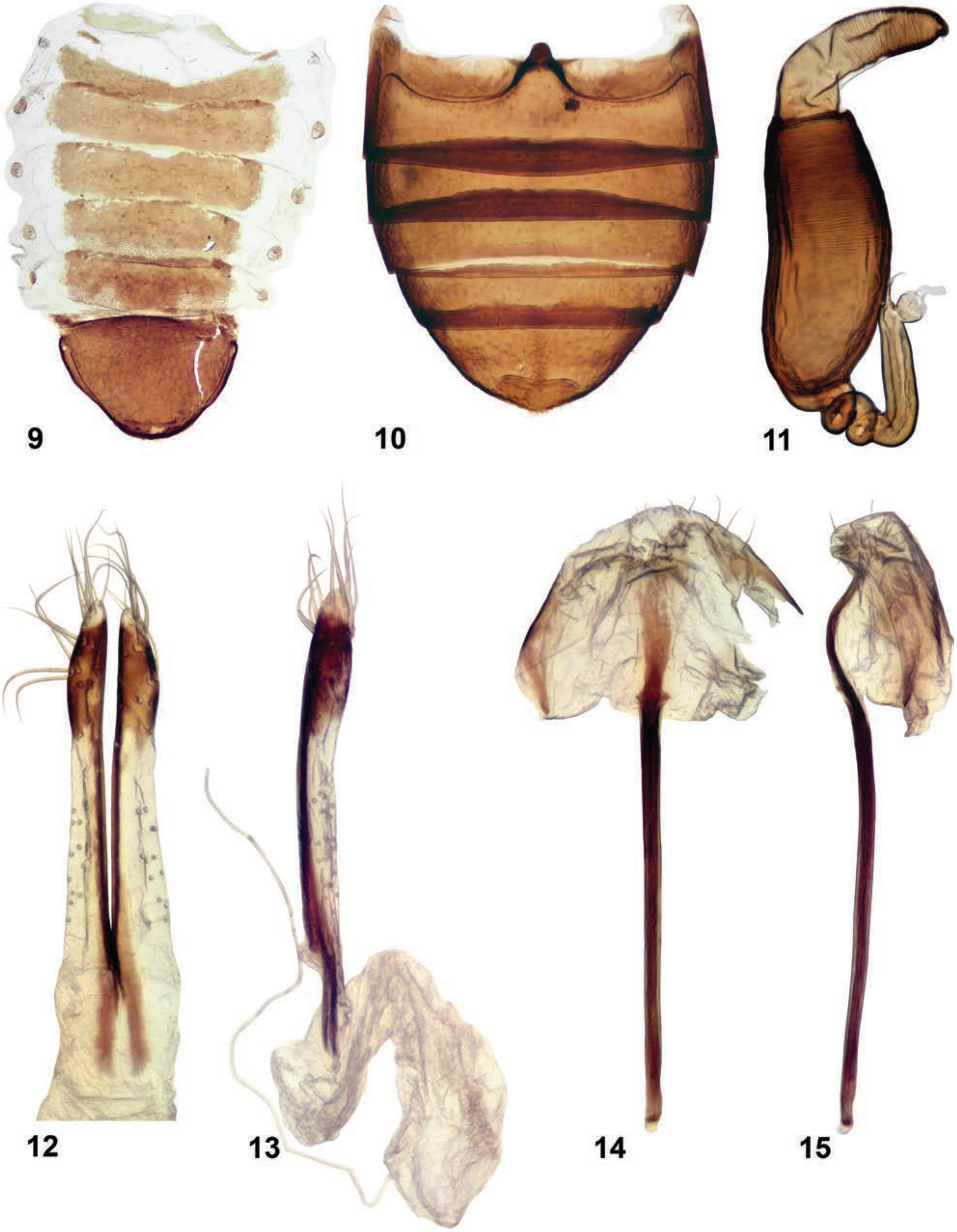

Figures 9–15. *Longitarsus californicus* (Motschulsky), Lectotype **9** abdominal tergites **10** abdominal ventrites **11** spermatheca **12, 13** vaginal palpi, ventral and lateral views **14, 15** tignum, ventral and lateral views.

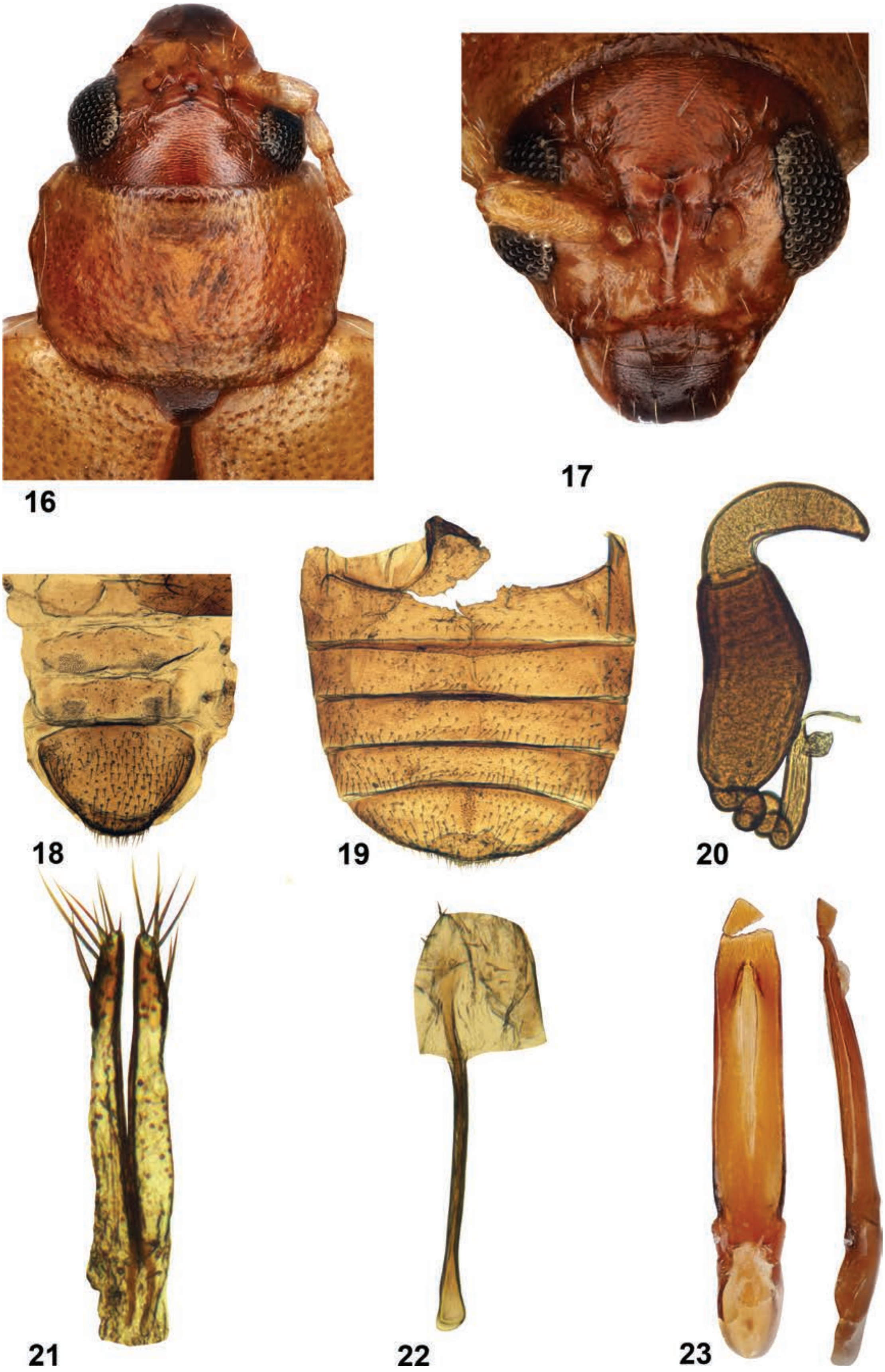

Figures 16–23. *Longitarsus californicus* (Motschulsky), California specimens (USNM) **16** pronotum and head dorsal view **17** head, frontal view **18** abdominal tergites **19** abdominal ventrites **20** spermatheca **21** vaginal palpi, ventral view **22** tignum, ventral view **23** median lobe of aedeagus, ventral and lateral views.

Head (Figs 2, 3, 16, 17). Vertex covered with relatively coarse reticulation. Supracallinal sulci thin, antennal calli separated from vertex by thin line. Surface of antennal calli moderately shiny, lacking reticulation, but with few minute punctures. Frontal ridge elongate, wider between antennal sockets, narrower towards clypeus. Anterofrontal ridge relatively narrow (Figs 3, 17), posteriorly gradually merging with frons, forming inverted T-shaped structure with frontal ridge. Antennomere 2 longer than 3. Antennomere 3 about as long as 4.

Thorax. Pronotal punctures relatively large (Figs 2, 16), slightly smaller than elytral punctures, as densely placed as elytral punctures. Surface between punctures coarsely reticulated. Elytra with humeral calli well developed. Elytral punctures do not form longitudinal rows. Surface between punctures reticulated. Female pro- and mesotarsomere 1 as wide as pro- and mesotarsomere 2. In males protarsomere 1 about twice as wide as protarsomere 2; mesotarsomere 1 wider at the base narrowing towards apex.

Abdomen (Figs 9, 10, 18, 19). In female, abdominal tergites 5 and 6 with two symmetrically placed patches of short setae. Pygidium with evenly spaced long setae. Abdominal ventrite 2 with marginal setae interrupted on both sides of the middle (Fig. 19). Complete rows of marginal setae situated on ventrites 3 and 4. Ventrite 5 with middle strip lacking long setae.

Genitalia (Figs 11–15, 20–23). Receptacle of spermatheca elongate, distinctly separated from pump, much longer than it. Internal side convex, external side concave. Pump with short curved denticle on top. Spermathecal canal with multiple coils, at base directed along the side of receptacle. Vaginal palpus slender with apex subdeltoid. Anterior sclerotization of vaginal palpus much narrower than posterior sclerotization. Tignum with posterior sclerotization about as wide as middle. Anterior sclerotization variable; in lectotype narrow, not wider than middle; in USNM specimen wider than middle, spoon-shaped. Median lobe of aedeagus nearly straight in lateral view, apex slightly S-shaped. In ventral view nearly parallel-sided. Apex gradually narrowing, without denticle. Membranous window narrow, constricting towards base and not reaching it.

Discussion

In addition to the female lectotype, we studied three other specimens, two females and one male, identified as *L. californicus* (USNM). The identification label for these does not have the name of the identifier, and we could not recognize the handwriting, so we do not know who made that identification. The identification label lists Horn as the author of the species; however, we could not find any *Longitarsus* named *californicus* by Horn. Dissection of one female revealed that the genitalia, especially the spermatheca and vaginal palpi, are very similar to those of the lectotype of *L. californicus*. The tignum of the lectotype (Fig. 14) is slightly different from that of the USNM specimen (Fig. 22) in having a narrower anterior part. In other features, the lectotype and female USNM specimens are very similar. Therefore, we confirm the identification of the three USNM specimens, including the male, as *L. californicus*.

Eight yellow *Longitarsus* species are known to occur in the western United States, as delimited by Lingafelter (2007) and Yanega (1996). Two species, *L. jacobaeae* Waterhouse and *L. flavicornis* Stephens, were introduced into North America (LeSage 1988). As shown in previous studies, *Longitarsus* species may be sorted into species groups based on the general shape of their median lobe of aedeagi (Konstantinov and Dorr 2023; Liang et al. 2023). *Longitarsus californicus* is clearly close to *L. livens* LeConte and *L. vanus* Horn in having the median lobe nearly straight in lateral view and with only a slightly S-shaped apex. In ventral view, the lobe is nearly parallel-sided but slightly narrower in the middle. The apex is gradually narrowing and without a well-differentiated denticle. The membranous window is narrow and constricted towards base but not reaching it (Fig. 23). *Longitarsus californicus* can be separated from these and other light-colored *Longitarsus* species known to occur in western United States using the following key.

Preliminary illustrated key to yellow *Longitarsus* species occurring in the western United States

Some species in this sample are represented by only a single male or female, and, therefore, in it is impossible to use characters of genitalia in some parts of the key.

1 Antennomere 2 longer than 3 .... **2**
– Antennomere 2 as long as or shorter than 3 .... **4**
2 Spermatheca with canal not extending away from receptacle and runs parallel to it at base. Spermathecal pump much shorter and narrower than receptacle. Median lobe of aedeagus nearly parallel-sided in ventral view .... ***L. californicus* (Motschulsky)**

– Spermatheca with canal extending away from receptacle and runs away from it at base. Spermathecal pump about as long as receptacle. Median lobe of aedeagus more or less constricted in ventral view **3**

3 Horizontal part of spermathecal pump merging with vertical part. Median lobe of aedeagus less constricted more or less parallel sided in ventral view. Apex more elongate. .... ***L. jacobaeae*** **Waterhouse**

– Horizontal and vertical parts of spermathecal pump with distinct border. Median lobe of aedeagus more constricted in ventral view. Apex rounder. ....***L. flavicornis*** **(Stephens)**

4 Supracallinal sulci absent, antennal calli at times make fold with vertex **5**

– Supracallinal sulci thin, but present, antennal calli separated from vertex by thin line... **7**

5 Lateral sides of aedeagus in ventral view constricted before apical one-third .... ***L. flavicornis* (Stephens)**

– Lateral sides of aedeagus in ventral view converging from base to apex, nearly straight **6**

6 Median lobe of aedeagus in lateral view nearly straight before apical one-quarter, in ventral view apex less acute .... ***L. livens* LeConte**

– Median lobe of aedeagus in lateral view bends dorsally and then ventrally before apical one-quarter, in ventral view apex more acute..... ***L. vanus* Horn**

7 Pronotal punctures small, sharply impressed ...... ***L. flavicornis*** **(Stephens)**

– Pronotal punctures comparatively larger, less sharply impressed **8**

8 Head nearly same color as pronotum .... ***L. subrufus*** **LeConte**

– Head darker in color than pronotum **9**

9 Vertex covered with coarse, deeply impressed reticulation .... ***L. repandus*** **LeConte**

– Vertex covered with fine, shallowly impressed reticulation......................... .... ***L. occidentalis*** **Horn**

Acknowledgements

We are grateful to Maurizio Biondi (University of L'Aquila, L'Aquila, Italy) and Michael Schmitt (Universität Greifswald, Greifswald, Germany), who kindly provided valuable comments on an earlier version of the manuscript.

Mention of trade names or commercial products in this publication is solely for the purpose of providing specific information and does not imply recommendation or endorsement by the USDA; the USDA is an equal opportunity provider and employer.

Additional information

Conflict of interest

The authors have declared that no competing interests exist.

Ethical statement

No ethical statement was reported.

Funding

The work of VYS and IAZ was carried out within the framework of State research project 121032300105-0 at Lomonosov Moscow State University.

Author contributions

All authors have contributed equally.

Author ORCIDs

Alexander S. Konstantinov https://orcid.org/0000-0001-6578-6735
Vladimir Yu. Savitsky https://orcid.org/0000-0002-6680-754X
Il'ya A. Zabaluev https://orcid.org/0000-0002-1558-5502

Data availability

All of the data that support the findings of this study are available in the main text.

References

Balsbaugh EU, Hays KL (1972) The leaf beetles of Alabama (Coleoptera: Chrysomelidae). Agricultural Experimental Station, Auburn University. Bulletin 441: 1–223.

Beller S, Hatch MH (1932) Coleoptera of Washington: Chrysomelidae. University of Washington Publications in Biology 1(2): 65–114.

Blatchley WS (1923) Notes on the Coleoptera of southern Florida with descriptions of new species. Canadian Entomologist 52(2): 30–36. https://doi.org/10.4039/Ent5530-2

Eschscholtz F (1829–1833) Zoologischer Atlas 1–5, enthaltend Abbildungen und Beschreibungen neuer Thierarten, während des Flottcapitains v. Kotzebue zweiter Reise um die Welt, auf der russisch-kaiserlichen Kriegsschlupp Predpriaetië in den Jahren 1823–1826. Reimer, Berlin, 120 pp. [+ 25 pls. G.] https://doi.org/10.5962/bhl.title.38055

Feklova TY, Petersburg Academic Museums (2014) The Expedition of Ilya G. Voznesensky to Russian America in 1839–1849 and the Formation of the American Collections in St. Petersburg Academic Museums. Acta Baltica Historiae et Philosophiae Scientiarum 2(2): 55–69. https://doi.org/10.11590/abhps.2014.2.04

Gnucheva VF (1940) (compiled by) Materials for the history of expeditions of Academy of Sciences in XVIII and XIX centuries. Izdatelstvo Academii Nauk SSSR, Moscow–Leningrad, 310 pp.

Horn GH (1889) A synopsis of the Halticinae of boreal America. Transactions of the American Entomological Society 16: 163–320. https://doi.org/10.2307/25076525

Konstantinov AS (1998) Revision of the Palearctic species of *Aphthona* Chevrolat and cladistic classification of the Aphthonini (Coleoptera: Chrysomelidae: Alticinae). Memoirs on Entomology. International 11: 1–429.

Konstantinov AS, Dorr MF (2023) *Longitarsus leonardicarloi* (Coleoptera: Chrysomelidae: Galerucinae: Alticini), new species from Turkmenistan. Natural History Sciences. Atti della Società Italiana di Scienze Naturali e del Museo Civico di Storia Naturale 10(Supplement 1): 45–48. https://doi.org/10.4081/nhs.2023.694

Konstantinov AS, Van Roie M, Furth D, Clark SM, Riley EG (2022) Flea beetles of the West Indies: Subtribe Oedionychina Chapuıs 1875, key to genera, new combinations, synonymy, checklist, and description of new genera and species (Coleoptera: Chrysomelidae: Galerucinae: Alticini). Journal of Insect Biodiversity 33(1): 1–56. https://doi.org/10.12976/jib/2022.33.1.1

Koponen S, Niemelä P (2020) Johann Friedrich Gustav von Eschscholtz—A pioneer naturalist and explorer of the Pacific islands and western North America. Memoranda Societatis Pro Fauna et Flora Fennica 96: 57–64.

LeConte JL (1859) The Coleoptera of Kansas and eastern New Mexico. Smithsonian Contributions to Knowledge 11: 1–58. https://doi.org/10.5962/bhl.title.18986

LeSage L (1988) Notes on European *Longitarsus* species introduced in North America 326 (Coleoptera: Chrysomelidae: Alticinae). Canadian Entomologist 120(12): 1133–1145. https://doi.org/10.4039/Ent1201133-12

Liang Z, Konstantinov AS, Ruan Y, Li Z, Huang Z, Ge S (2023) Two new species of the *Longitarsus violentus* group from China (Coleoptera, Chrysomelidae, Galerucinae, Alticini). ZooKeys 1181: 111–123. https://doi.org/10.3897/zookeys.1181.110538

Lingafelter SW (2007) Illustrated key to the longhorned woodboring beetles of the eastern United States. The Coleopterists Society, Special Publication No 3: 1–206.

Lyubarsky GYu (2009) History of Zoological Museum of MGU: ideas, people, structures. Tovarischestvo nauchnyh izdanii KMK, Moscow, 744 pp.

Mannerheim CG (1843) Beitrag zur Käfer-Fauna der Aleutischen Inseln, der Insel Sitkha und Neu-Kaliforniens. Bulletin de la Société Impériale des Naturalistes de Moscou 16: 3–142. https://doi.org/10.5962/bhl.title.37833

Motschulsky VI (1845) Observations sur le Musée Entomologiqué de l'Université Impériale de Moscow. Bulletin de la Société Impériale des Naturalistes de Moscou 18(3): 332–388.

Motschulsky VI (2013) in Krivokhatsky VA (compiled by) Life adventures of Victor Ivanovich Motschulsky described by himself. Tovarischestvo Nauchnyh Izdanii KMK, Moscow–St. Petersburg, 259 pp.

Pentinsaari M, Anderson R, Borowiec L, Bouchard P, Brunke A, Douglas H, Smith ABT, Hebert PDN (2019) DNA barcodes reveal 63 overlooked species of Canadian beetles (Insecta, Coleoptera). ZooKeys 894: 53–150. https://doi.org/10.3897/zookeys.894.37862

Riley EG, Clark SM, Seeno TN (2003) Catalog of the Leaf Beetles of America North of Mexico (Coleoptera: Megalopodidae, Orsodacnidae and Chrysomelidae, excluding Bruchinae). The Coleopterists Society Special Publication No. 1. The Coleopterists Society, Sacramento, 290 pp.

Savitsky VY (2018) Little known weevil taxa (Coleoptera, Curculionidae) described by V. I. Motschulsky from the Caucasus. Entomological Review 98(1): 43–48. https://doi.org/10.1134/S0013873818010062

Wilcox JA (1954) Leaf Beetles of Ohio (Chrysomelidae: Coleoptera). Ohio State University Studies. Ohio Biological Survey, Bulletin 43, 8(3): 353–506.

Yanega D (1996) Northeastern longhorned beetles (Coleoptera: Cerambycidae). Illinois Natural History Survey. Manual 6: 1–174.

ZooKeys 1209: 245–294 (2024)
DOI: 10.3897/zookeys.1209.124766

Research Article

Delimitation of the widely distributed Palearctic *Stenodema* species (Hemiptera, Heteroptera, Miridae): insights from molecular and morphological data

Anna A. Namyatova[1,2], Polina A. Dzhelali[1], Fedor V. Konstantinov[1,3]

1 *Zoological Institute, Russian Academy of Sciences, Universitetskaya nab. 1, St. Petersburg 199034, Russia*
2 *All-Russian Institute of Plant Protection, Podbelskogo sh. 3, Pushkin, St. Petersburg, 196608, Russia*
3 *National Museum of Natural History, Bulgarian Academy of Sciences, 1 Tsar Osvoboditel Blvd, 1000 Sofia, Bulgaria*
Corresponding author: Anna A. Namyatova (anna.namyatova@gmail.com)

Academic editor: Nikolay Simov
Received: 5 April 2024
Accepted: 25 June 2024
Published: 13 August 2024

ZooBank: https://zoobank.org/069B4575-16D4-4EC4-804D-AB4618C9AB43

Citation: Namyatova AA, Dzhelali PA, Konstantinov FV (2024) Delimitation of the widely distributed Palearctic *Stenodema* species (Hemiptera, Heteroptera, Miridae): insights from molecular and morphological data. ZooKeys 1209: 245–294. https://doi.org/10.3897/zookeys.1209.124766

Abstract

Species delimitation presents a significant challenge in biology, particularly in systematics. Here, an integrative approach is employed to assess the species boundaries of widely distributed Palearctic *Stenodema* species. Due to their diversity, wide distribution, and the absence of comprehensive morphological and molecular data for most species, revising *Stenodema* is both daunting and time-consuming. Our study focuses on detailed examinations of male and female genitalia, coupled with phylogenetic analyses based on two mitochondrial markers (cytochrome c oxidase subunit I and 16S rRNA) and species delimitation analyses. Eight species with wide distributions are reviewed, *Stenodema trispinosa* Reuter, 1904 is synonymized with *S. pilosa* (Jakovlev, 1889), and a lectotype for *Stenodema turanica* Reuter, 1904 is designated. Morphological and molecular data effectively distinguish all species, revealing distinct clades and relationships. Notably, *S. calcarata* and *S. pilosa* form a well-supported clade, while *S. virens* and *S. turanica* share a lineage with Nearctic species. *Stenodema rubrinervis* and *S. sibirica* are morphologically similar and form a distinct clade in all phylogenies. Species delimitation analyses confirm the separation of all studied species, and genetic distances suggest the potential existence of cryptic species within *S. calcarata* and *S. pilosa*. This study highlights the advantages of integrative taxonomy in delimiting species with intricate and relatively recent phylogeographic histories.

Key words: Holarctic, phylogeny, plant bugs, species delimitation, taxonomy

Introduction

Taxonomy and biodiversity of different organisms, including insects, is well studied in the Palearctic. However, the boundaries of many groups and their interrelationships are solely addressed using morphological characters. Although the number of taxonomic works based on molecular data is increasing, studies on species inhabiting both Europe and Asia are scarce. Asian taxa, and those having trans-Holarctic distribution, also remain understudied (e.g., Hortal et al. 2015; Pante et al. 2015; Satler et al. 2021). Such works require relatively fresh material collected from different localities in areas spanning thousands of kilometers. The task of obtaining such specimens is difficult, expensive, and time-consuming, and may not always be feasible. Nevertheless, molecular studies of widespread species are important, because this helps to understand the population structure of such groups, reveal the presence of cryptic species and possible synonymy of other species. The poor knowledge of the widely distributed species might negatively affect further studies in other fundamental and applied fields, such as biodiversity, phylogeography, ecology, evolution, and conservation (e.g., Angulo and Icochea 2010; Taberlet et al. 2012; Namyatova et al. 2023).

Miridae or plant bugs are among the largest insect families and their representatives are abundant and play important roles in many ecosystems. This group is considered well studied in the Palearctic and Nearctic especially in comparison with subtropical and tropical regions (Cassis and Schuh 2012). There are several keys to species published in the 20th century focusing on Europe or Asia (e.g., Kerzhner and Jaczewski 1964; Wagner and Weber 1964; Wagner 1974; Kerzhner 1988; Vinokurov and Kanyukova 1995), and numerous genera have been lately revised (e.g., Namyatova and Konstantinov 2009; Namyatova 2010; Matocq and Pluot-Sigwalt 2012; Knyshov and Konstantinov 2013a, 2013b; Konstantinov 2008, 2019; Konstantinov et al. 2016; Davletshin and Konstantinov 2024). However, these works are solely based on morphology, and to date, only two studies have been performed addressing species delimitation in plant bugs using combined morphological and molecular data (Sanchez and Cassis 2018; Namyatova et al. 2023). There is only a single work attempting to separate trans-Palearctic species with molecular markers, which showed that the morphological and molecular data did not correspond to each other (Namyatova et al. 2023). Miridae also include several trans-Holarctic species (Kerzhner and Josifov 1999), and the species with such distribution was addressed in the previous study (Namyatova et al. 2023).

Stenodema Laporte, 1832 is a large genus, distributed in the Palearctic, South Asia, South and North America, and South Africa. It is included into the tribe Stenodemini within the largest plant bug subfamily Mirinae and is distinguished from other members of its tribe by several morphological characters (Schwartz 1987, 2008). The representatives of this genus are elongate with green, yellow, or brown coloration, generally associated with graminoid monocots, and some of its species are considered pests (Wheeler 2001; Yasunaga 2019). *Stenodema* currently includes 57 species and 37 of them have been described from the Holarctic region, 31 of them inhabit the Palearctic (Schuh 2013; Yasunaga 2019). Some of those taxa are known only from short original descriptions. There are also a number of widespread species: *Stenodema calcarata* (Fallén, 1807), *S. holsata* (Fabricius, 1787), *S. laevigata* (Linnaeus, 1758), *S. pilosa* (Jakovlev, 1889), *S. sibirica* Bergroth, 1914, *S. trispinosa* Reuter, 1904, *S. turanica* Reuter, 1904, and *S. virens* (Linnaeus, 1767), which might potentially represent a complex of cryptic species. Among them, *S. calcarata* and *S. holsata* are trans-Palearctic and *S. trispinosa* has trans-Holarctic distribution. *Stenodema laevigata* and *S. virens* are mostly known from the Western Palearctic, *S. turanica* inhabits Balkans, Caucasus, Middle East, Central Asia, and China, *S. pilosa* was recorded from the south of European Russia, Ukraine, Caucasus, Turkey, Central Asia, and China, while *S. sibirica* inhabits Siberia and East Asia. The identification keys for those species were mostly based on the external morphological characters, and their genitalia were poorly studied. The barcoding region of cytochrome c oxidase subunit I (COI) has been provided for some species, but as a part of the regional barcoding projects (Jung et al. 2011; Raupach et al. 2014; Kim and Jung 2018; Roslin et al. 2022). The intraspecific genetic variation within *Stenodema* species has not been studied and, therefore, it remains uncertain whether the barcoding region can be used for species delimitation.

The diversity and wide distribution of widespread *Stenodema* species, coupled with the limited morphological details and absence of molecular data for most representatives of this genus, make the revisionary work on *Stenodema* difficult and time-consuming. The first step towards the revision of this genus is a detailed study of the widely distributed species and providing the morphological and molecular data for them, which can be a background for further comparisons. In this study we evaluated the species boundaries of the widely distributed Palearctic species of *Stenodema*. We studied their male and female genitalia, provided the phylogeny based on the two mitochondrial markers (COI and 16S rRNA), and performed species delimitation analyses.

Materials and methods

Specimens

The specimens from the historical collection of the Zoological Institute of the Russian Academy of Sciences, St Petersburg, Russia (**ZISP**) and recently collected material were examined. Type specimens of *Stenodema* spp. retained in the Finnish Museum of Natural History (**MZH**) were also studied. The specimens were initially identified using the keys published in Kerzhner and Jaczewski (1964), Wagner (1974), Vinokurov and Kanyukova (1995), and Yasunaga (2019). The following number of specimens were examined for this study: *Stenodema calcarata* (71), *S. holsata* (46), *S. laevigata* (52), *S. rubrinervis* (12), *S. pilosa* (13), *S. sibirica* (50), *S. trispinosa* (64), *S. turanica* (41) and *S. virens* (39). The collection event data for all of them were entered to the Arthropod Easy Capture Database (https://research.amnh.org/pbi/locality/index.php) and available through the Heteroptera Species Pages (https://research.amnh.org/pbi/heteropteraspeciespage/speciesdetails.php). All specimens were examined externally, and at least 10 males and 10 females from different series for each species were dissected for examination of the genitalia. The list of non-type specimens examined for this study is provided in Suppl. material 1.

For the molecular studies, the specimens from the following species were used: *S. calcarata* (13 specimens). *S. holsata* (4 specimens), *S. laevigata* (11 specimens), *S. trispinosa* (3 specimens), *S. turanica* (3 specimens), *S. virens* (3 specimens), *Leptopterna dolobrata* (Linneaus, 1758) (1 specimen) and *Trigonotylus* sp. (1 specimen). The genitalia structures were examined for all *Stenodema* vouchers.

Dissections, drawings, and terminology

To examine the male and female genitalia structures, abdomens were removed and boiled in 10% KOH for up to five minutes and dissected in water. Afterward, the abdomens were stored in glycerol. In some cases, aedeagi were inflated after this procedure. Aedeagi were also inflated using 40% lactic acid, following the detailed procedure described in Namyatova et al. (2021). The drawings were completed using Leica DM2500 microscope with the drawing device attached. The terminology of genitalia follows Konstantinov (2000, 2003) for males and Schwartz (2008) for females.

The digital images were taken in stacks using the Canon EOS 5D Mark IV camera equipped with a Canon MP-E 65 mm f/2.8 1–5× Macro lens and a Twin-Lite MT-26EX-RT flash. Partially focused images were combined using the Helicon Focus software. The SEM images were taken from uncoated specimens using the Hitachi TM1000 tabletop microscope.

Measurements

Measurements were completed using Micromed MS-5 microscope using a graticule and ×10 eyepiece. Measurements statistics is provided in Table 1. Scale bars for habitus images equal 1 mm, the scale bars for genitalia structures equal 0.1 mm. Measurements provided in the diagnoses and descriptions are in mm.

DNA protocols and sequencing

The DNA was extracted from abdomens of ethanol-stored and dry specimens using the Evrogen Extract DNA Blood and Cells kit. The standard protocol was used with two modifications. First, the abdomens were kept overnight in the lysis solution with proteinase K in the water bath. Second, 50 or 25 μl of elution buffer was added at the final stage to increase the DNA concentration. After lysis, the abdomens were kept in glycerol for further examination. To obtain the barcoding region of cytochrome c oxidase subunit I (COI) the primers from Vishnevskaya et al (2016) were used with the annealing temperature equaling 45 °C or 42 °C. To obtain 16S rRNA region, the primers from Menard et al. (2014) were used with the annealing temperature 48 °C. For both markers, temperature of the initial denaturation and denaturation was 94 °C (3 mins and 30 secs, respectively), and extension and final extension temperature was 68 °C (1 min and 10 mins, respectively). The PCR products were cleaned using Evrogen Clean-up S-Cap kits or with Exonuclease I Thermofisher and sequenced in Evrogen (https://evrogen.ru/). The products were between 647 to 847 for COI and between 361 to 403 for 16s rRNA. The base pairs were trimmed at both ends if they were absent in more than half of the sequences in the alignment. The sequences were uploaded to GenBank, the accession numbers are listed in the Suppl. material 2.

The sequence diversity was calculated using P-distance and Kimura-2-parameter (K2P) in MEGA-X (Tamura et al. 2021) within each species, between species and between the clades within species.

Alignments were completed using Geneious algorithm in Geneious v. 11 software for each marker separately. Alignments included 36 original COI and 16S rRNA each. The COI alignment also included 84 sequences downloaded from Genbank: *S. calcarata* (15), *S. holsata* (17), *S. laevigata* (17), *S. pilosipes* (2), *S. rubrinervis* (5), *S. sericans* (3), *S. sibirica* (4), *S. trispinosa* (15), *S. vicina* (5),

Table 1. Measurements for *Stenodema* species.

Species		Length					Width		
		Body	**Cun-Clyp**	**Pronotum**	**AntSeg1**	**AntSeg2**	**Head**	**Pronotum**	**InterOcDi**
S. calcarata	Mean	6.13	4.48	0.92	0.82	2.15	0.77	1.22	0.38
♂ (*n* = 7)	SD	0.23	0.15	0.02	0.03	0.20	0.03	0.04	0.02
	Range	0.58	0.42	0.04	0.08	0.52	0.10	0.10	0.04
	Min	5.92	4.33	0.90	0.79	1.90	0.71	1.15	0.35
	Max	6.50	4.75	0.94	0.88	2.42	0.81	1.25	0.40
♀ (*n* = 7)	Mean	6.26	4.68	0.98	0.85	1.89	0.80	1.32	0.43
	SD	0.28	0.09	0.05	0.03	0.14	0.02	0.06	0.02
	Range	0.92	0.25	0.10	0.06	0.38	0.04	0.15	0.06
	Min	5.75	4.58	0.94	0.83	1.75	0.79	1.25	0.40
	Max	6.67	4.83	1.04	0.90	2.13	0.83	1.40	0.46
S. holsata									
♂ (*n* = 7)	Mean	5.18	3.95	0.85	0.75	1.68	0.79	1.20	0.40
	SD	0.51	0.28	0.07	0.06	0.11	0.04	0.10	0.03
	Range	1.25	0.83	0.23	0.17	0.33	0.13	0.27	0.06
	Min	4.67	3.58	0.75	0.71	1.54	0.75	1.08	0.38
	Max	5.92	4.42	0.98	0.88	1.88	0.88	1.35	0.44
♀ (*n* = 7)	Mean	5.88	4.52	1.01	0.79	1.66	0.87	1.43	0.47
	SD	0.37	0.27	0.05	0.05	0.14	0.04	0.09	0.02
	Range	0.92	0.83	0.10	0.15	0.31	0.13	0.25	0.04
	Min	5.50	4.17	0.96	0.75	1.56	0.81	1.31	0.46
	Max	6.42	5.00	1.06	0.90	1.88	0.94	1.56	0.50
S. laevigata									
♂ (*n* = 7)	Mean	6.45	5.00	1.03	1.04	2.19	0.77	1.21	0.41
	SD	0.32	0.20	0.06	0.02	0.07	0.03	0.05	0.01
	Range	0.83	0.58	0.17	0.06	0.17	0.06	0.13	0.02
	Min	5.92	4.58	0.94	1.02	2.13	0.75	1.13	0.40
	Max	6.75	5.17	1.10	1.08	2.29	0.81	1.25	0.42
♀ (*n* = 7)	Mean	7.10	5.40	1.17	1.07	2.20	0.83	1.37	0.45
	SD	0.26	0.20	0.04	0.05	0.09	0.03	0.05	0.02
	Range	0.67	0.58	0.10	0.13	0.21	0.10	0.13	0.06
	Min	6.83	5.00	1.13	1.00	2.08	0.77	1.31	0.42
	Max	7.50	5.58	1.23	1.13	2.29	0.88	1.44	0.48
S. sibirica									
♂ (*n* = 7)	Mean	6.08	4.38	0.96	0.80	1.86	0.79	1.28	0.41
	SD	0.28	0.17	0.04	0.03	0.11	0.02	0.04	0.01
	Range	0.67	0.50	0.13	0.08	0.31	0.04	0.13	0.02
	Min	5.83	4.17	0.92	0.75	1.77	0.77	1.21	0.40
	Max	6.50	4.67	1.04	0.83	2.08	0.81	1.33	0.42
♀ (*n* = 7)	Mean	6.50	4.80	1.08	0.83	1.94	0.87	1.51	0.49
	SD	0.20	0.26	0.03	0.02	0.12	0.03	0.08	0.03
	Range	0.58	0.83	0.08	0.06	0.33	0.08	0.23	0.06
	Min	6.25	4.50	1.04	0.81	1.81	0.83	1.35	0.46
	Max	6.83	5.33	1.13	0.88	2.15	0.92	1.58	0.52
S. trispinosa									
♂ (*n* = 7)	Mean	5.81	4.24	0.88	0.74	1.95	0.78	1.24	0.40
	SD	0.44	0.31	0.07	0.03	0.20	0.06	0.03	0.03
	Range	1.33	0.92	0.21	0.10	0.54	0.15	0.08	0.08
	Min	5.08	3.75	0.77	0.69	1.73	0.71	1.21	0.35
	Max	6.42	4.67	0.98	0.79	2.27	0.85	1.29	0.44

Species		Length					Width		
		Body	Cun-Clyp	Pronotum	AntSeg1	AntSeg2	Head	Pronotum	InterOcDi
♀ (*n* = 7)	Mean	6.23	4.70	1.01	0.74	1.67	0.81	1.38	0.43
	SD	0.14	0.36	0.05	0.04	0.08	0.03	0.05	0.01
	Range	0.42	1.00	0.13	0.10	0.23	0.06	0.13	0.04
	Min	6.00	4.33	0.94	0.69	1.52	0.77	1.29	0.42
	Max	6.42	5.33	1.06	0.79	1.75	0.83	1.42	0.46
S. turanica									
♂ (*n* = 7)	Mean	6.33	4.95	1.00	0.82	2.73	0.83	1.38	0.36
	SD	0.25	0.23	0.10	0.02	0.16	0.03	0.08	0.01
	Range	0.75	0.75	0.23	0.04	0.48	0.08	0.21	0.02
	Min	6.08	4.58	0.90	0.79	2.60	0.79	1.31	0.35
	Max	6.83	5.33	1.13	0.83	3.08	0.88	1.52	0.38
♀ (*n* = 7)	Mean	7.07	5.61	1.15	0.82	2.19	0.86	1.53	0.43
	SD	0.27	0.49	0.07	0.01	0.16	0.04	0.07	0.03
	Range	0.75	1.33	0.21	0.02	0.46	0.13	0.17	0.08
	Min	6.58	4.92	1.04	0.81	1.92	0.79	1.44	0.40
	Max	7.33	6.25	1.25	0.83	2.38	0.92	1.60	0.48
S. virens									
♂ (*n* = 7)	Mean	6.36	4.74	1.11	0.74	2.07	0.82	1.39	0.40
	SD	0.20	0.21	0.04	0.03	0.09	0.02	0.04	0.02
	Range	0.58	0.50	0.10	0.06	0.23	0.04	0.10	0.04
	Min	6.00	4.50	1.04	0.71	1.96	0.79	1.33	0.38
	Max	6.58	5.00	1.15	0.77	2.19	0.83	1.44	0.42
♀ (*n* = 7)	Mean	6.80	5.06	1.13	0.73	1.92	0.82	1.45	0.44
	SD	0.39	0.22	0.11	0.04	0.15	0.05	0.12	0.03
	Range	1.00	0.67	0.31	0.13	0.40	0.13	0.29	0.10
	Min	6.08	4.58	0.94	0.67	1.69	0.75	1.27	0.38
	Max	7.08	5.25	1.25	0.79	2.08	0.88	1.56	0.48
S. rubrinervis									
♂ (*n* = 7)	Mean	6.93	5.42	0.99	1.04	2.69	0.85	1.40	0.40
	SD	0.45	0.60	0.07	0.05	0.16	0.02	0.11	0.01
	Range	1.25	1.58	0.19	0.15	0.52	0.06	0.33	0.02
	Min	6.25	4.58	0.92	0.98	2.46	0.83	1.27	0.40
	Max	7.50	6.17	1.10	1.13	2.98	0.90	1.60	0.42
♀ (*n* = 7)	Mean	7.49	6.05	1.15	1.14	2.57	0.92	1.48	0.50
	SD	0.10	0.38	0.07	0.05	0.13	0.04	0.07	0.03
	Range	0.33	1.00	0.21	0.13	0.35	0.10	0.21	0.06
	Min	7.33	5.50	1.04	1.10	2.35	0.88	1.38	0.46
	Max	7.67	6.50	1.25	1.23	2.71	0.98	1.58	0.52

S. virens (1). Alignment for 16s rRNA additionally included four sequences of *S. rubrinervis* (2) and *S. sibirica* (2) from GenBank. Both alignments included original sequences of two outgroup taxa, *Leptopterna dolobrata* and *Trigonotylus* sp. All GenBank accession numbers are listed in the Suppl. material 1. Two alignments were concatenated using Geneious. The alignment lengths for COI and 16s rRNA were 787 bp and 399 bp, respectively. Phylogenetic analyses were run on each marker separately and for the combined datasets. Both combined datasets were 1186 bp length. First of them included all sequences available and included 124 terminals (full dataset). The second dataset included 34 specimens for which both markers were obtained (reduced dataset). In all the cases, *Trigonotylus* sp. was chosen as a root.

Maximum Likelihood approach implemented in RAxML v. 8.2.12 (Stamatakis 2014) with 10000 bootstrap replicates (BS) was performed. The phylogenetic trees were also calculated using Bayesian inference with MrBayes v. 3.2.7 (Ronquist et al. 2012). The main settings for MrBayes included 20 million generations, four chains, and the burn-in was set at 25%. Posterior probabilities were used for the node support (PP). Log files were checked to ensure that the standard deviation of split frequencies reached 0.01. All analyses were run using the server Dell PowerEdge R7525 (Dell Inc., USA).

Automatic barcode gap discovery approach (ABGD) was used via the online tool (https://bioinfo.mnhn.fr/abi/public/abgd/abgdweb.html) on the alignment of each marker separately. This algorithm searches for a gap, which can be observed whenever the divergence among organisms belonging to the same species is smaller than the divergence among organisms from different species (Puillandre et al. 2012). The P range was set at 0.001–0.01, and Kimura (K80) model was used to estimate the matrix of pairwise distances.

Poisson tree process model (PTP and bPTP) and Generalized Mixed Yule Coalescent approach (bGMYC) were applied to the phylogenies built on a single marker and on combined datasets. Both approaches model the transition in branch length between species in contrast to within species (e.g., Blair and Bryson 2017) as another indication of speciation events. GMYC is a model-based likelihood approach that combines phylogenetics and coalescence theory, was proposed to estimate species boundaries from DNA sequence data. This algorithm identifies the transition points between inter- and intra-species branching rates on a time-calibrated ultrametric tree by maximizing the likelihood score of the model (Pons et al. 2006; Reid and Carstens 2012; Fujisawa and Barraclough 2013). PTP approach does not need an ultrametric tree and model speciation rate by directly using the number of substitutions (Zhang et al. 2013).

For all analyses, bGMYC, PTP, and bPTP, only unique sequences were left in the datasets, because zero-length branches can affect the results (Reid and Carstens 2012). The duplicates were removed using the online tool sRNAtoolbox (Aparicio-Puerta et al. 2022) (https://arn.ugr.es/srnatoolbox/helper/removedup/). It is recommended to run the species delimitation analysis based on several trees, which helps to overcome the problems with the phylogenetic uncertainty, occurring when the species delimitation is applied for the single tree (Reid and Carstens 2012; da Silva et al. 2018). The trees were calculated using BEAST2 v. 2.6.3 software (Bouckaert et al. 2014) using GTR+G+I nucleotide substitution model with 50 mln chain length. The results were checked in Tracer v. 1.7.1.(Rambaut et al. 2018) to make sure that all parameters had effective sampling size exceeded 200, which is considered adequate for convergence (https://beast.community/analysing_beast_output). The LogCombiner application from the BEAST package was used to obtain the .tre file with ~ 100 trees for each case.

Species delimitation using GMYC was run in R with the bGMYC package with the parameters recommended in the instructions (http://nreid.github.io/assets/bGMYC_instructions_14.03.12.txt), the multiple thresholds was used, MCMC equaled 50000, and thinning equaled 40000. This analysis provides the list of all possible species, and we have chosen the set of species with the highest mean supports.

Bayesian and Maximum Likelihood implementations of the Poisson tree process model (PTP and bPTP) (Zhang et al. 2013) using the scripts in Python (https://github.com/zhangjiajie/PTP accessed in 31/10/2021) were used. The number of iterations equaled 100000. All analyses were run using the server Dell PowerEdge R7525 (Dell Inc., USA).

Bayesian Phylogenetics and Phylogeography (BPP) method tests species using the multispecies coalescent model (Yang 2015), and it was applied to the combined datasets, which includes both, COI and 16s rRNA. It tests whether the separated species has higher supports than the clade comprising combination of species. The specimens should be preliminary assigned to a putative species for this analysis. For each dataset, the specimens were assigned to species based on the phylogenetic results and the bGMYC, PTP, and bPTP analyses ran on the corresponding dataset. The root was removed from the datasets. The analysis was run through the interface version for Windows (https://abacus.gene.ucl.ac.uk/software.html). The A11 (species delimitation and species tree) analysis with nsamples = 50000, sampfreq = 2, burnin = 25000 was applied. All other settings were default.

Results

Morpho-taxonomic account

Our study showed that most of the widely distributed Palearctic species can be separated from each other using external characters, as well as male and female genitalia. The diagnoses for those species are provided in this section.

Below we provide the key to species, where we included all widely distributed Palearctic species. We also added *S. algoviensis* Schmidt, 1934 (Central Europe), *S. alpestris* Reuter, 1904 (China), *S. chinensis* Reuter, 1904 (China), *S. crassipes* Kiritshenko, 1931 (Central Asia), *S. khentaica* Muminov, 1989 (Mongolia), *S. plebeja* Reuter, 1904 (China), *S. rubrinervis* Horváth, 1905 (China, Korea, and Japan), and *S. sericans* (Fieber, 1861) (Europe) to this key, because we had an opportunity to examine them. *Stenodema nippon* Yasunaga, 2019 was included, as Yasunaga (2019) provided a detailed illustrated description for this species. Thus, the key is designed to discriminate all *Stenodema* spp. of the Western Palearctic, Siberia, and the Far East. However, it does not include 16 of the 19 species originally described and currently known only from China. For a taxonomic account of Chinese species of *Stenodema*, refer to Zheng et al. (2004). Species comparisons are provided following the diagnoses.

Key to species

1 Frons not protruding above clypeus (Fig. 1H, I) **2**
– Frons protruding above clypeus (Fig. 1C)... **9**
2 Spines on hind femur present (Fig. 2A, D); swelling above propleural apodeme straight (Fig. 1I).. **3**
– Spines on hind femur absent (Fig. 2B, C, E, F, H); swelling above propleural apodeme curved (Fig. 1H) **4**

3 Hind femur with three spines ventroapically (Fig. 2D); right paramere L-shaped, not bifurcate apically (Fig. 6N); vesica lobes without large spinulate outgrowth (Fig. 3G–I); sclerotized rings on dorsal labiate plate ~ 2–2.5× as wide as long (Fig. 4H) .... ***S. pilosa***

– Hind femur with two spines and small, barely recognizable tubercle ventroapically (Fig. 2A); right paramere bifurcate apically (Fig. 5I); left vesica lobe with large spinulate outgrowth (Fig. 3B); sclerotized rings on dorsal labiate plate ~ 3× as wide as long (Fig. 4A) .... ***S. calcarata***

4 Hind femur distinctly tapering apically (Fig. 2E) .... ***S. laevigata***

– Hind femur straight or slightly tapering apically (Fig. 2H) **5**

5 Hemelytron yellow, without contrasting marking along inner margin; pronotum with calli brown to dark brown, but without longitudinal paired dark brown stripes; hind femora without rows of dark markings .... ***S. sericans***

– Hemelytron often with contrasting marking along inner margin; pronotum with paired longitudinal markings; hind femur often with rows of dark markings **6**

6 Flattened silver setae on hemelytron present .... ***S. chinensis***

– Only simple setae on hemelytron present **7**

7 Antennal segment II/head width ratio in female > 2.7; body length/pronotum width ratio 4.9–5.0; left paramere only slightly inclined basally (Fig. 5N, Wagner 1974: fig. 90E, F) .... ***S. plebeja***

– Antennal segment I/head width ratio in female 1.7–2.2; body length/pronotum width ratio 3.9–4.3; left paramere distinctly curved basally (Wagner 1974: figs 5N, 90E, F) **8**

8 Antennal segment II/vertex width in male 4.0–4.4; left paramere with additional elongate swelling near apical process (Fig. 4N) .... ***S. holsata***

– Antennal segment II/vertex width in male 5.0; left paramere with small swelling near apical process (Tamanini 1982: fig. 2A) .... ***S. algoviensise***

9 Hind femur straight apically with rare setae on posterior side (as in Fig. 2H) **10**

– Hind femur tapering apically with dense setae on posterior side (Fig. 2B, C) **13**

10 Antennal segment I longer than mesal length of pronotum .... ***S. nippon***

– Antennal segment I shorter or as long as mesal length of pronotum **11**

11 Antennal segment I narrower than eye diameter, and as wide as hind femur .... ***S. khenteica***

– Antennal segment I as wide as eye diameter, and narrower than hind femur **12**

12 Antennal segment II/pronotum width ratio in male 1.4–1.6, in female 1.2–1.4, antennal segment II/head width ratio in male 2.2–2.6, in female 2.2–2.5; vertex width/eye ratio in male 2.1–2.4, antennal segment I/head width ratio in female 0.9–1; body length 5.8–6.5 in male, 6.3–6.8 in female .... ***S. sibirica***

– Antennal segment II/pronotum width ratio in male 1.7–2.2, in female 1.6–1.9, antennal segment I/head width ratio in male 3.0–3.3, in female 2.7–2.9; vertex width/eye ratio in male 1.7–2.0; antennal segment I/head width ratio in female 1.2–1.3; body length 6.2–7.5 in male, 7.3–7.7 in female .... ***S. rubrinervis*, *S. alpestris***

13 Hind femur distinctly enlarged, 4–5× as long as wide, antennal segment II in female widened basally with long and dense setae; antennal segment III shorter than vertex ....***S. crassipes***

– Hind femur not enlarged, 6–8× as long as wide; antennal segment II not widened basally with short setae; antennal segment III as long as or longer than vertex...**14**

14 Antennal segment II in male 2.4–2.6× as long as head width; vesica with four lobes (Fig. 7G–I); membranous swelling on dorsal labiate plate large, partly covering sclerotized rings (Fig. 10C) .... ***S. virens***

– Antennal segment II in males 3.1–3.5× as long as head width; vesica with five lobes (Figs 7D–F; 8A); membranous swelling on dorsal labiate plate not covering sclerotized rings (Fig. 10A) ....***S. turanica***

Stenodema calcarata **(Fallén, 1807)**

Figs 1E, I, L, N, 2A, G, J, 3A–C, 4A, C, T, 5I–L, T, 9E, F

Miris calcaratus Fallén, 1807: 110 (original description).

Stenodema calcaratum: Reuter 1904: 3 (comb. nov., key to species); Carvalho 1959: 300 (catalogue); Kerzhner and Jaczewski 1964: 958 (key to species); Wagner and Weber 1964: 92 (key to species); Wagner 1974: 110 (key to species).

Stenodema calcarata: Kerzhner 1988: 99 (key to species); Muminov 1989: 126 (key to species); Vinokurov and Kanyukova 1995: 98 (key to species); Kerzhner and Josifov 1999: 191 (catalogue); Yasunaga 2019: 301 (key to species).[1]

Diagnosis. Body length in male 5.9–6.5, in female 5.8–6.7; frons not protruding above clypeus base (Fig. 1I); labium reaching mesosternum but not surpassing it; hind femur with two distinct spines and small tubercle ventroapically, only slightly tapering toward apex (Fig. 2A); hind tibia straight basally (Fig. 2J); swelling above propleura suture straight (Fig. 1I); groove on posterior part of mesopleuron present and distinct (Fig. 1L); paired pits on pronotum between calli present, rounded (Fig. 1E); setae on posterior margin of hind femur as dense as on other parts of femur, distinctly shorter than hind femur width (Fig. 2A); genital capsule only slightly longer than wide, acute apically, with outgrowth near left paramere socket (Fig. 5T); apical half of right paramere as wide as or slightly wider than basal half, bifurcate apically (Fig. 5I, K); left paramere with apical process acute and somewhat elongate in posterior view (Fig. 5L); sensory lobe of left paramere not swollen (Fig. 5J); vesica with three membranous lobes (Fig. 3A–C); dorsal labiate plate ~ 1.5× as long as wide; sclerotized ring ~ 3× as wide as long; distance between sclerotized rings ~ 0.3–0.5× of sclerotized ring width (Fig. 4A); membranous swelling at the middle of dorsal labiate plate absent; posterior wall without dorsal structure between interramal lobes (Fig. 4C).

---

[1] For more references and a list of synonyms see Carvalho (1959), Schuh (1995), and Kerzhner and Josifov (1999).

Figure 1. SEM images. *S. pilosa* **A** head, anterior view. ZISP_ENT 00009372 **G** head and pronotum, dorsal view, ZISP_ENT 00009372 **Q** hind tarsus, ZISP_ENT 00009386. *S. turanica* **B** head, anterior view, ZISP_ENT 00004934 **C** head, lateral view, ZISP_ENT 00004934. *S. holsata* **D** pretarsus, dorsal view, ZISP_ENT 00013676 **F** head and pronotum, dorsal view, ZISP_ENT 00007905. *S. calcarata* **E** head and pronotum, dorsal view, ZISP_ENT 00007331 **I** head and pronotum, lateral view, ZISP_ENT 00013671 **L** thoracic pleura, ZISP_ENT 00007386 **N** labium, ZISP_ENT 00007382. *S. laevigata* **H** head and pronotum, lateral view, ZISP_ENT 00005650 **K** thoracic pleura, ZISP_ENT 00007921 **O** labium, ZISP_ENT 00013673. *S. virens* **J** scutellum, clavus. and corium, ZISP_ENT 00003645 **P** cuneus and membrane, ZISP_ENT 00003645. *S. sibirica* **M** thoracic pleura, ZISP_ENT 00004930.

Distribution. *Stenodema calcarata* has a trans-Palearctic distribution, ranging from southern and western Europe to the Russian Far East, and extending to Central Asia (Kerzhner and Josifov 1999).

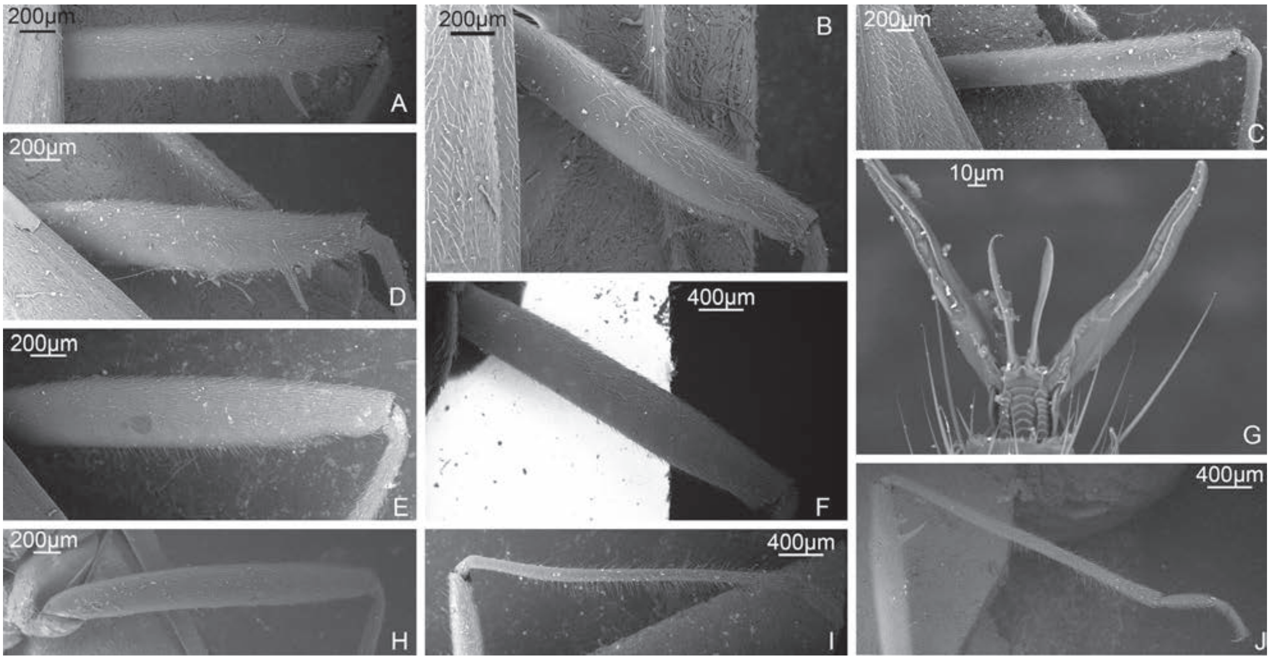

Figure 2. SEM images. *S. calcarata* **A** hind femur, ZISP_ENT 00007331 **G** pretarsus ventrally, ZISP_ENT 00013668 **J** hind tibia, ZISP_ENT 00007331. *S. virens* **B** hind femur, ZISP_ENT 00003645. *S. turanica* **C** hind femur, ZISP_ENT 00004938 **I** hind tibia, ZISP_ENT 00004938. *S. pilosa* **D** hind femur, ZISP_ENT 00009371. *S. laevigata* **E** hind femur, ZISP_ENT 00006444. *S. sibirica* **F** hind femur, ZISP_ENT 00003705. *S. holsata* **H** hind femur, ZISP_ENT 00013674.

Stenodema holsata **(Fabricius, 1787)**

Figs 1D, F, 2H, 3D–F, 4B, D, 5I–L, S, T, 11H, I

Cimex holsatus Fabricius, 1787: 306 (original description).

Stenodema holsatum: Reuter 1904: 6 (comb. nov., key to species); Carvalho 1959: 303 (catalogue); Kerzhner and Jaczewski 1964: 958 (key to species); Wagner and Weber 1964: 97 (key to species); Wagner 1974: 114 (key to species).

Stenodema holsata: Kerzhner 1988: 99 (key to species); Muminov 1989: 128 (key to species); Vinokurov and Kanyukova 1995: 99 (key to species); Kerzhner and Josifov 1999: 194 (catalogue).[2]

Diagnosis. Body length in male 4.7–5.7, in female 5.5–6.4; hemelytron often with brown to dark brown stripe along inner margin; frons not protruding above clypeus base (as in Fig. 1H, I); body length/pronotum width in female 3.9–4.3; antennal segment I in male and female 0.9–1.0× as long as head width; antennal segment I narrower than forefemur; antennal segment II narrower than hind tibia, 4.0–4.4× as long as vertex width; setae on antennal segment I shorter than half of antennal segment I width; labium reaching hind coxa, but not surpassing it; hind femur only slightly tapering toward apex, without spines (Fig. 2H); hind tibia straight basally (as in Fig. 2J); swelling above propleural suture curved (as in Fig. 1H); groove on posterior part of mesopleuron absent (as in Fig. 1M); paired pits on pronotum between calli present, slit-like (Fig. 1F); setae on posterior margin of hind femur as dense as on other parts

---

[2] For more references and a list of synonyms see Carvalho (1959), Schuh (1995), and Kerzhner and Josifov (1999).

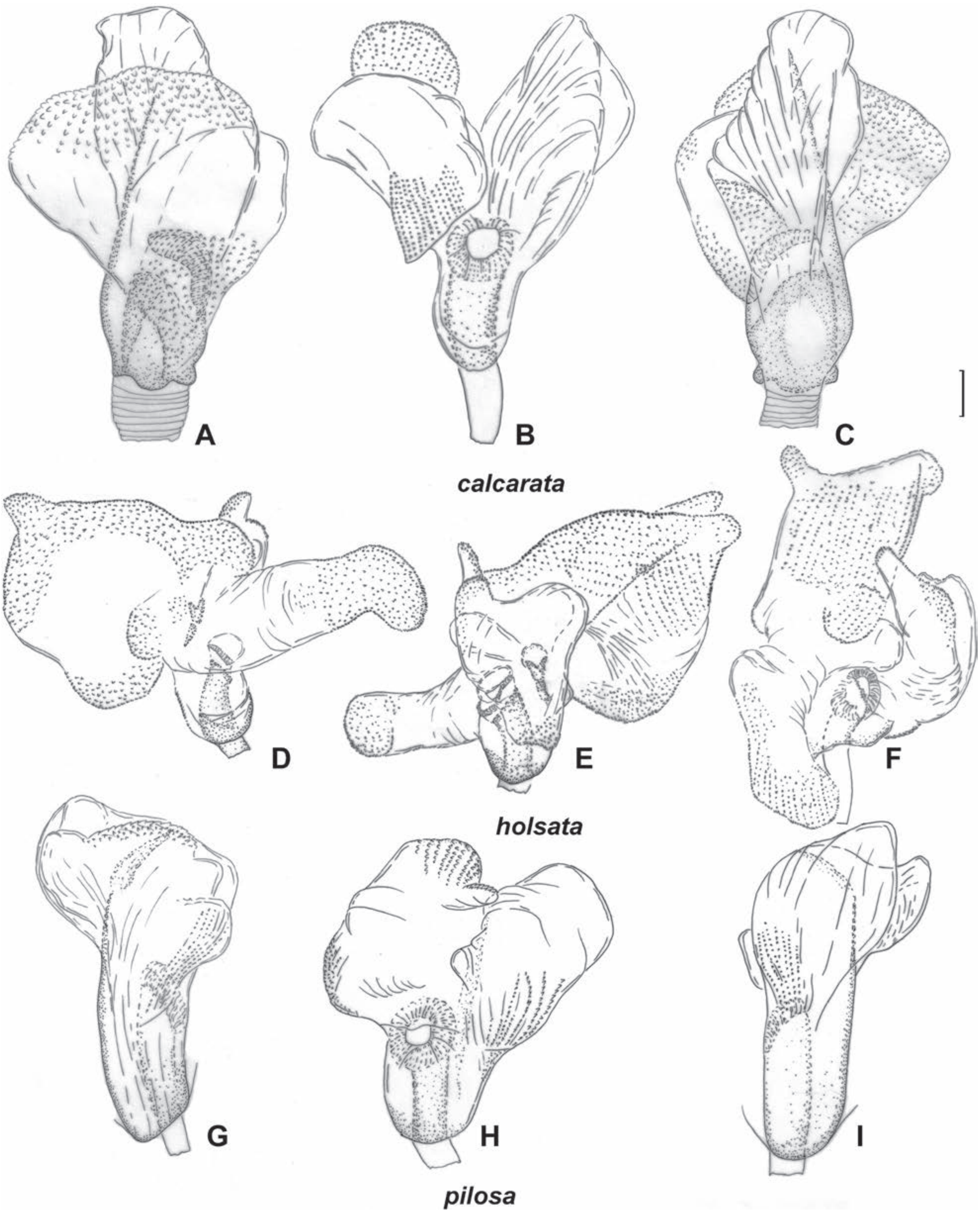

Figure 3. Inflated vesica. *S. calcarata*. ZISP_ENT 00002712 **A** dorsal view **B** left lateral view **C** ventral lateral view. *S. holsata*. ZISP_ENT 00003625 **D** dorsal view **E** ventral **F** left lateral view. *S. pilosa*. ZISP_ENT 00003626 **G** dorsal view **H** left lateral view **I** ventral view.

of femur, distinctly shorter than hind femur width (Fig. 2H); hind femur with distinct markings; genital capsule as wide as long, rounded apically and with swelling near apex, without outgrowths near paramere sockets (Fig. 5U);

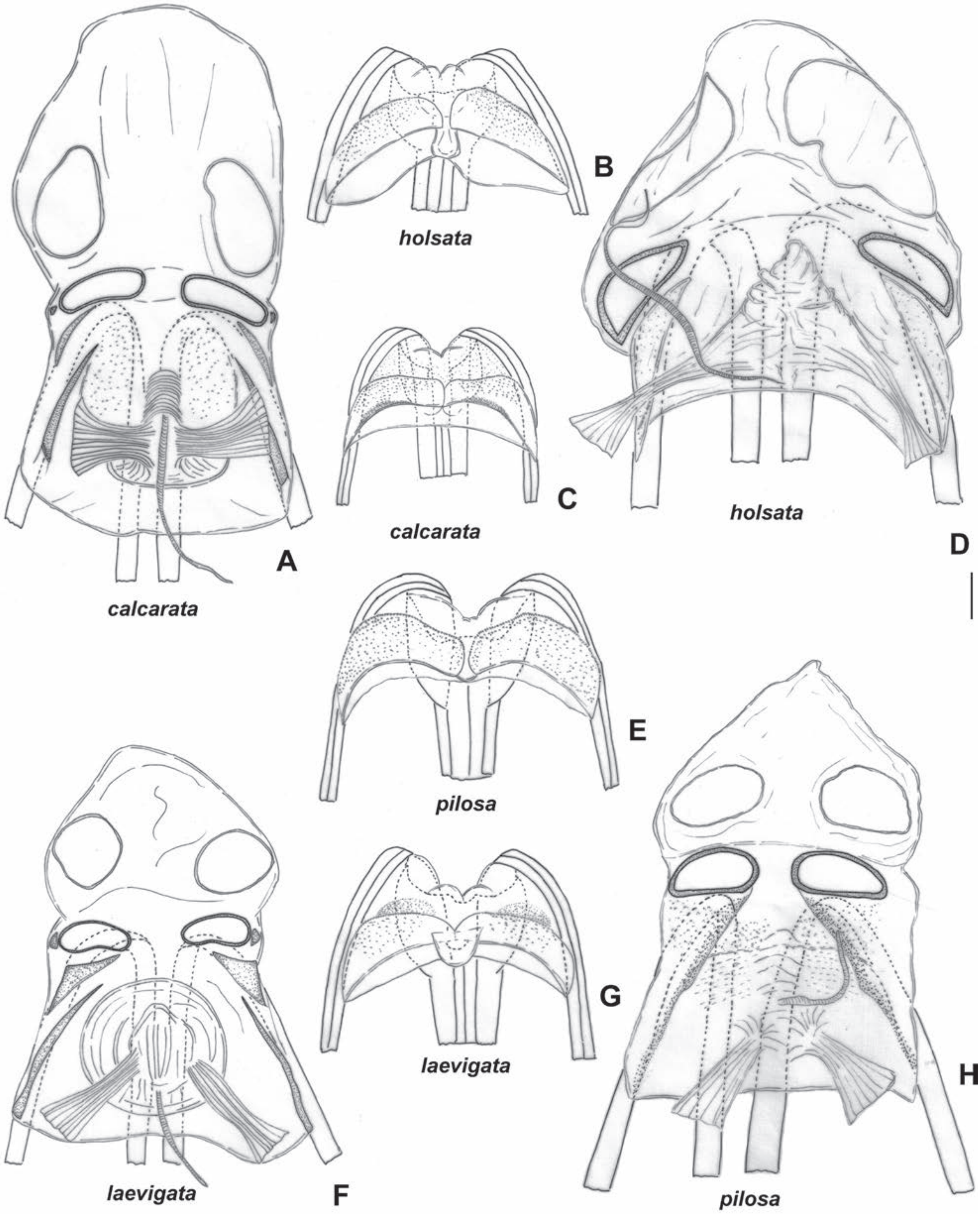

Figure 4. Female genitalia. *S. calcarata*. ZISP_ENT 00002737 **A** dorsal labiate plate **C** posterior wall of bursa copulatrix. *S. holsata*. ZISP_ENT 00003679 **B** posterior wall of bursa copulatrix **D** dorsal labiate plate. *S. pilosa*. ZISP_ENT 00002732 **E** posterior wall of bursa copulatrix **H** dorsal labiate plate. *S. laevigata*. ZISP_ENT 00002738 **F** dorsal labiate plate **G** posterior wall of bursa copulatrix.

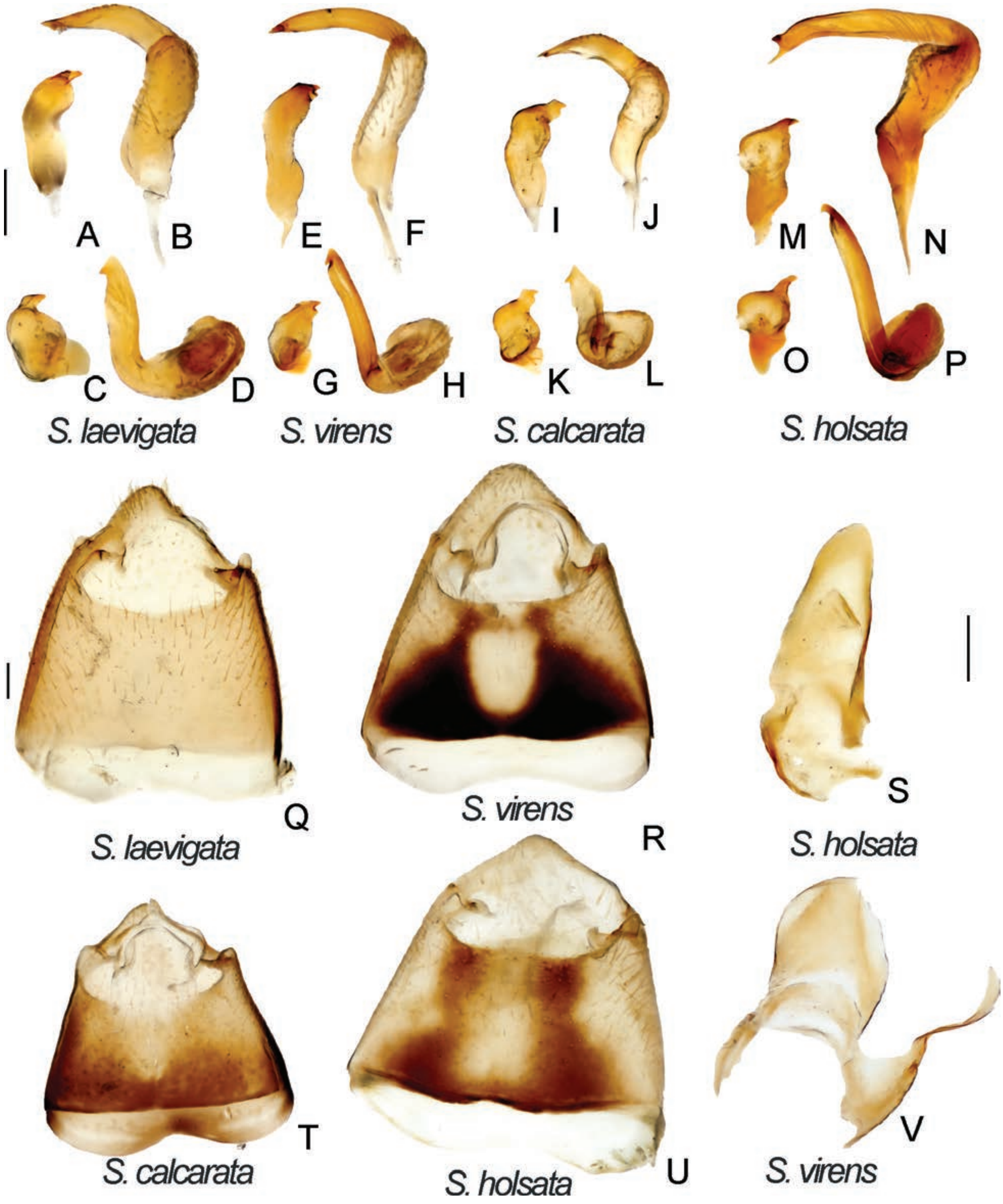

Figure 5. Male genitalia. *S. laevigata*. ZISP_ENT 00002699 **A** right paramere, dorsal view **B** left paramere, dorsal view **C** right paramere, posterior view **D** left paramere. posterior view **Q** genital capsule, dorsal view. *S. virens*. ZISP_ENT 00003616 **E** right paramere, dorsal view **F** left paramere, dorsal view **G** right paramere, posterior view **H** left paramere, posterior view **R** genital capsule **V** theca. *S. calcarata*. ZISP_ENT 00002712 **I** right paramere, dorsal view **J** left paramere, dorsal view **K** right paramere, posterior view **L** left paramere, posterior view **T** genital capsule. *S. holsata*. ZISP_ENT 00003625 **I** right paramere, dorsal view **J** left paramere, dorsal view **K** right paramere, posterior view **L** left paramere, posterior view **S** theca; ZISP_ENT 00002803 **T** genital capsule.

apical half of right paramere wider than basal part (Fig. 5M); left paramere with elongate thin apical process and with additional outgrowth apically, with sensory lobe swollen (Fig. 5N), apical process rounded apically in posterior view (Fig. 5P); vesica with four membranous lobes (Fig. 3D–F); dorsal labiate plate wider than long; sclerotized ring 2.5–3× as wide as long; distance between sclerotized rings ~ 1.5× longer than sclerotized ring width; membranous swelling at middle of dorsal labiate plate present, triangular (Fig. 4D); posterior wall with dorsal structure between interramal lobes (Fig. 4B).

Distribution. *Stenodema holsata* has a trans-Palearctic distribution, spanning from southern and western Europe to the Russian Far East, and also known from Central Asia (Kerzhner and Josifov 1999).

Notes. *Stenodema algoviensis* and *S. holsata* are two similar species. Wagner (1974) in the key to *Stenodema* species separated those two taxa by the antennal segment I length/head width ratio. However, we found that this ratio is only different in males (1.1 in *S. algoviensis*, 0.9–1.0 in *S. holsata*), which was also previously found by Tamanini (1982). Additionally, males are different in the antennal segment II/vertex width ratio (5.0 in *S. algoviensis*, 4.0–4.4 in *S. holsata*). In terms of genital structure, these two species differ in the shape of the left paramere i.e., *S. holsata* has an additional outgrowth near the apical process, whereas in *S. algoviensis* only a small swelling is present (Wagner 1974: figs 5N, 90E, F; Tamanini 1982: fig. 2A, B, F, G). Vesica and female genitalia of *S. algoviensis*, as well as molecular data, were not studied.

Stenodema laevigata **(Linnaeus, 1758)**

Figs 1H, K, O, 2E, 4F, G, 5A–D, Q, 7A–C, 9G, H

Cimex leavigatus Linnaeus, 1758: 449 (original description).
Stenodema laevigatum: Reuter 1904: 6 (comb. nov., key to species); Carvalho 1959: 304 (catalogue); Kerzhner and Jaczewski 1964: 958 (key to species); Wagner and Weber 1964: 95 (key to species); Wagner 1974: 113 (key to species).
Stenodema laevigata: Muminov 1989: 128 (key to species); Kerzhner and Josifov 1999: 195 (catalogue).[3]

Diagnosis. Body length in male 5.9–6.7, in female 6.8–7.5. Frons not protruding above clypeus base (Fig. 1H); labium reaching metasternum, but not surpassing it (Fig. 1O); hind femur distinctly tapering towards apex, without spines (Fig. 2E); hind tibia curved basally (as in Fig. 2E); swelling above propleural suture curved (Fig. 1H); groove on posterior part of mesopleuron present, shallow (Fig. 1K); paired pits on pronotum between calli absent (as in Fig. 1G); setae on posterior margin of hind femur denser than on other parts of femur, distinctly shorter than hind femur width (Fig. 2E); genital capsule slightly longer than wide, acute apically, with outgrowth near each paramere socket (Fig. 5Q); apical half of right paramere as wide as basal half (Fig. 5A); apical process of right paramere more or less acute apically in posterior view but not elongate (Fig. 5D); sensory lobe of left paramere swollen (Fig. 5B); vesica with two mem-

---

[3] For more references and a list of synonyms see Carvalho (1959), Schuh (1995), and Kerzhner and Josifov (1999).

branous lobes (Fig. 7A–C); dorsal labiate plate as long as wide, sclerotized ring 2–2.5× as long as wide; distance between sclerotized rings ~ 0.5–0.75× as long as sclerotized ring width; membranous swelling on dorsal labiate plate present, rounded, not reaching sclerotized ring (Fig. 4F); posterior wall with dorsal structure between interramal lobes (Fig. 5G).

Distribution. *Stenodema laevigata* is mostly known from Western Palearctic, and there are no records from Siberia. However, the species was recorded from Kyrgyzstan and China (Kerzhner and Josifov 1999).

Stenodema pilosa (Jakovlev, 1889)

Figs 1A, G, Q, 2D, 3G–I, 4E, H, 6N–P, R, S, 9A–D

Brachytropis pilosa Jakovlev, 1889: 243 (original description).
Stenodema pilosum: Reuter 1904: 3 (comb. nov., key to species).
Stenodema pilosa: Muminov 1989: 127 (key to species).
Stenodema trispinosum Reuter, 1904: 8 (original description); Carvalho 1959: 301 (catalogue); Wagner and Weber 1964: 93 (key to species); Kerzhner and Jaczewski 1964: 958 (key to species); Wagner 1974: 110 (key to species). New synonym.
Stenodema trispinosa: Kerzhner 1988: 99 (key to species); Muminov 1989: 126 (key to species); Vinokurov and Kanyukova 1995: 98 (key to species); Kerzhner and Josifov 1999: 191 (catalogue); Yasunaga 2019: 301 (key to species).[4]

Type material examined. *Lectotype* of *Brachytropis pilosa* Jakovlev, 1889: China • ♀; Xinjang: Quiemo [oasis Tschertschen]; 38.14°N, 85.53°E; 11 Jun 1885; NM Przhevalsky; (ZISP_ENT 00015588); (ZISP).

Lectotype of *Stenodema trispinosum* Reuter, 1904: Russia: • ♀; Yakutia Rep., Batylim, Lena River; 62.02°N, 129.73°E; 18–19 Jul 1901; B. Poppius; (http://id.luomus.fi/GZ.56520); (MZH).

Paralectotypes of *Stenodema trispinosum* Reuter, 1904: Russia • ♀; Arkhangelsk Prov.: Solovetsky Islands; 65.08°N, 35.88°E; no date provided; Levander; (http://id.luomus.fi/GZ.25545); (MZH) • 3♀; Buryatia Rep.: Dauria; 53°N, 115°E; 1842; R.F. Sahlberg; (http://id.luomus.fi/GZ.56517, http://id.luomus.fi/GZ.56518, http://id.luomus.fi/GZ.56519); (MZH) • ♀; Khakassia Rep.: Sayanogorsk [Osnatjennaja]; 53.09°N, 91.40°E; 1885; R.E. Hammarström; (http://id.luomus.fi/GZ.56523); (MZH) • ♀; Khanty-Mansi Autonomous Okrug: Leushi [Leusch]; 56.62°N, 65.72°E; no date provided; N. Sundman; (http://id.luomus.fi/GZ.56516); (MZH) • ♀; Yakutia Rep.: Olekminsk; 60.37°N, 120.43°E; 1901; B. Poppius; (http://id.luomus.fi/GZ.56521); (MZH) • ♀; Ust-Aldan 63.52°N, 129.41°E; 13 Jul 1901; B. Poppius; (http://id.luomus.fi/GZ.56524); (MZH) • ♀; Yakutsk, 62.03°N, 129.73°E; 1901; B. Poppius; (http://id.luomus.fi/GZ.56522); (MZH).

Diagnosis. Body length in male 5.4–6.4, in female 6.0–6.3; frons not protruding above clypeus base (as in Fig. I); labium reaching middle coxa but not surpassing it; hind femur only slightly tapering toward apex, with three spines ventroapically; setae on posterior margin of hind femur as dense as

---

[4] For more references and list of synonyms see Carvalho 1959, Schuh 1995, and Kerzhner and Josifov 1999.

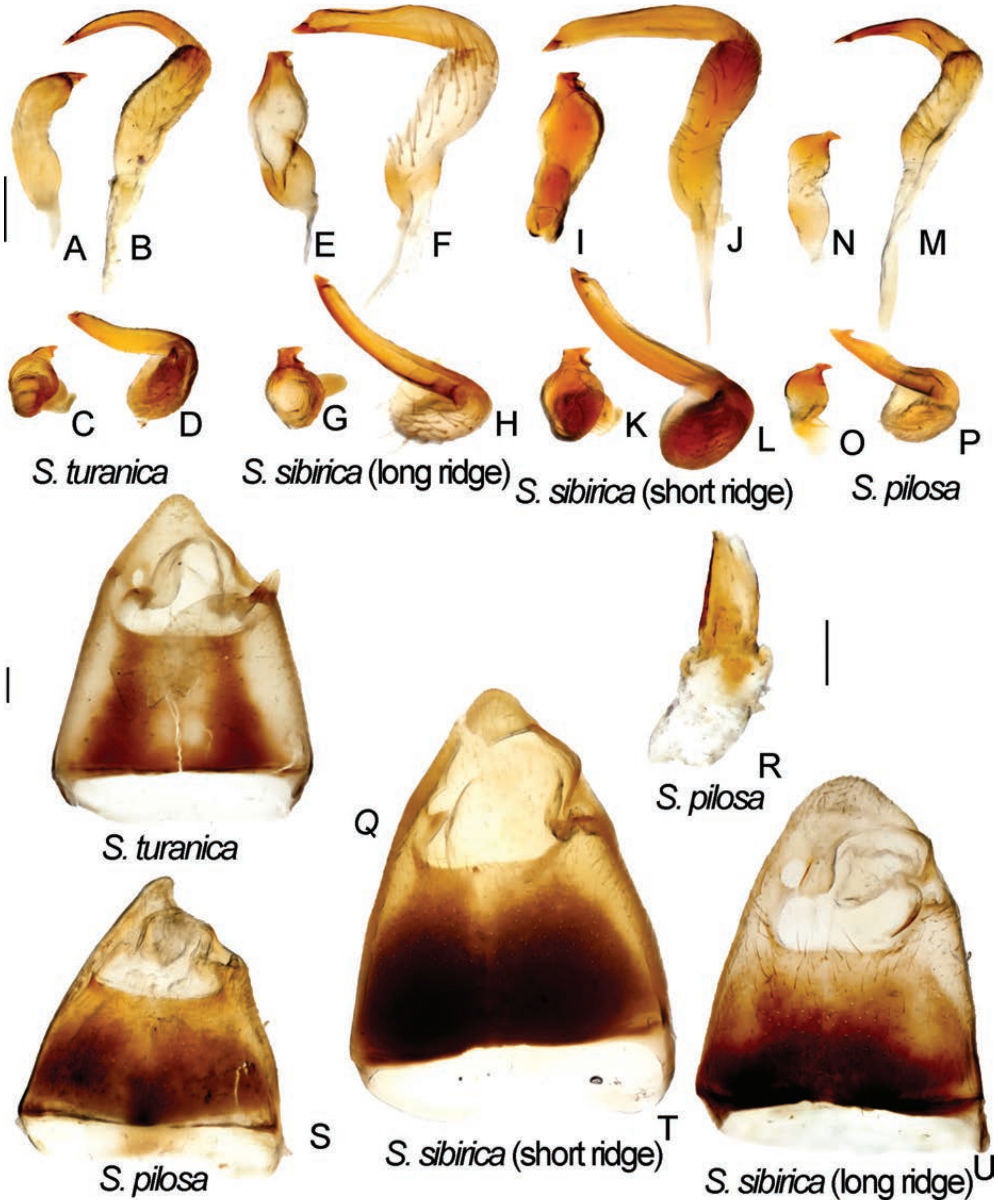

Figure 6. Male genitalia. *S. turanica*. ZISP_ENT 00003654 **A** right paramere, dorsal view **C** right paramere, posterior view **Q** genital capsule, dorsal view; ZISP_ENT 00003618 **B** left paramere, dorsal view **D** left paramere, posterior view. *S. sibirica*. ZISP_ENT 00003617 (vesica with long ridge) **E** right paramere, dorsal view **F** left paramere, dorsal view **G** right paramere, posterior view **H** left paramere, posterior view **U** genital capsule, dorsal view; ZISP_ENT 00003620 (vesica with short ridge) **I** right paramere, dorsal view **J** left paramere, dorsal view **K** right paramere, posterior view **L** left paramere, posterior view **T** genital capsule, dorsal view. *S. pilosa*. ZISP_ENT 00003626 **N** right paramere, dorsal view **M** left paramere, dorsal view **O** right paramere, posterior view **P** left paramere, posterior view **R** theca **S** genital capsule, dorsal view.

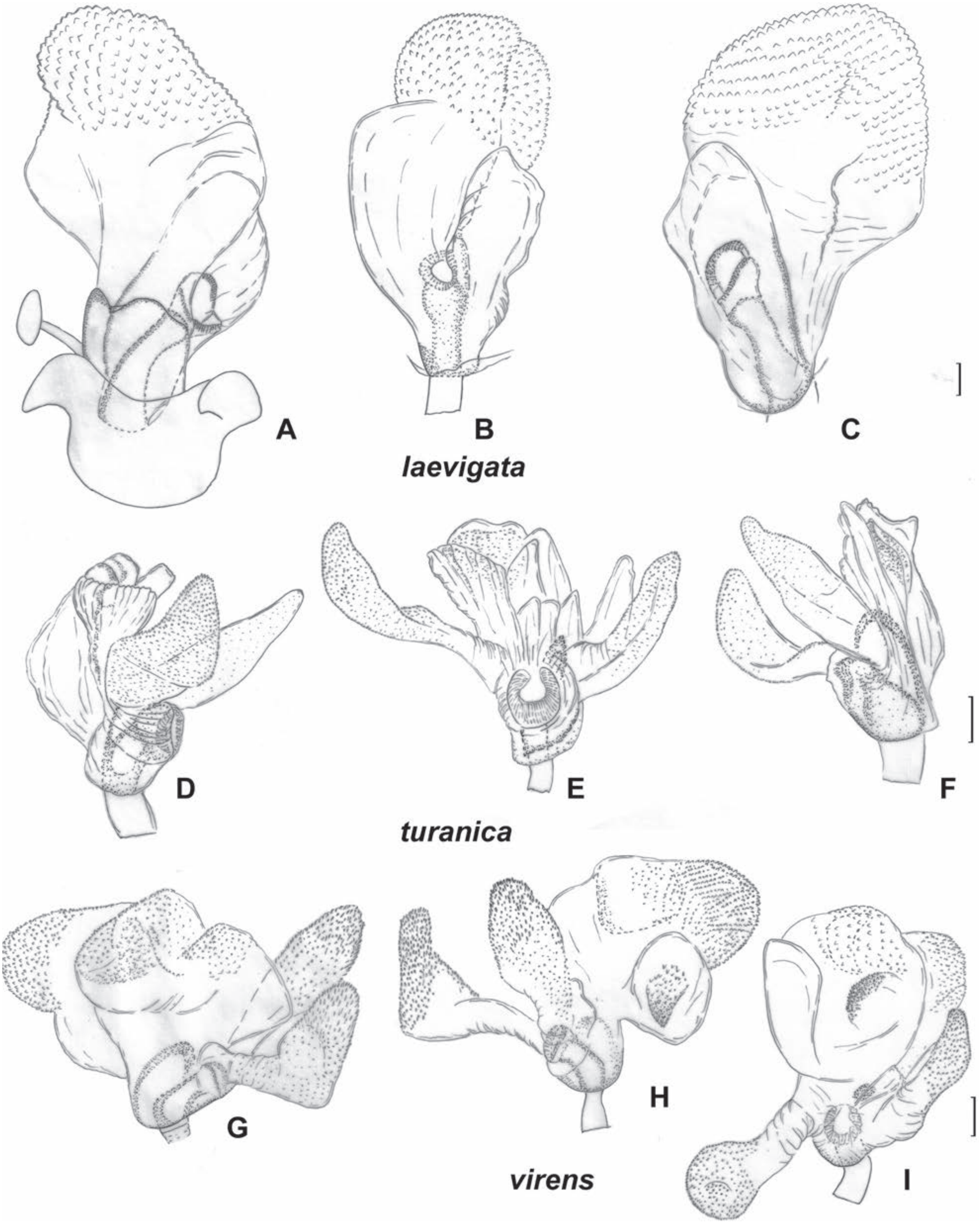

Figure 7. Inflated vesica, *S. laevigata*, ZISP_ENT 00002699 **A** dorsal view **B** left lateral view **C** ventral lateral view. *S. turanica*, ZISP_ENT 00003618 **D** dorsal view **E** left lateral view **F** ventral lateral view. *S. virens*, ZISP_ENT 00003616 **G** dorsal view **H** ventral view **I** left lateral view.

on other parts of femur, distinctly shorter than hind femur width (Fig. 2D); hind tibia straight basally (as in Fig. 2G); swelling above propleura suture straight (as in Fig. 1I); groove on posterior part of mesopleuron absent (as in Fig. 1M); paired pits between calli small, not discernible from punctures or absent (Fig. 1G); genital capsule slightly longer than wide; apex of genital capsule acute and curved left; left paramere socket with outgrowth (Fig. 6S); apical half of right paramere as wide as basal half, not bifurcate apically (Fig. 6N, O); left paramere with apical process acute and elongate in posterior view (Fig. 6P) and with swollen sensory lobe (Fig. 6M); vesica with two membranous lobes (Fig. 3G–I); dorsal labiate plate ~ 1.5× as long as wide; sclerotized ring ~ 1.5× as wide as long; distance between sclerotized rings ~ 0.3–0.4× as long as sclerotized ring width; membranous swelling on dorsal labiate plate absent (Fig. 4H); posterior wall without dorsal structure between interramal lobes (Fig. 4E).

Distribution. In its currently accepted concept, *S. pilosa* is a Holarctic species with a wide circumpolar distribution. It extends south to California, New Mexico, Texas, and Georgia in the Nearctic, and to France, Romania, Turkey, Transcaucasia, Central Asia, Central China, and Korea in the Palearctic (Wheeler and Henry 1992; Kerzhner and Josifov 1999). Based on the distribution pattern, *S. trispinosa*, here synonymized with *S. pilosa*, is considered a true Holarctic species, with possible post-Pleistocene expansion from the Beringia refugium (Lattin and Oman 1983; Wheeler and Henry 1992).

Notes. *Stenodema pilosa* was initially described within the genus *Brachytropis* Fieber, 1858 (Jakovlev 1889), an unnecessary new name for *Brachystira* Fieber, 1858, currently recognized as a subgenus of *Stenodema* (Reuter 1904). In the original description Jakovlev (1889) mentioned that this species had two spines on the hind femur. Reuter (1904) described *Stenodema trispinosa* as a distinctive species with three spines on the hind femur. He included *S. pilosa* in his key to species based solely on the original description, noting that he had not personally examined specimens of this species. Muminov (1989) designated the lectotype of *B. pilosa* and mentioned that it had three spines on the hind femur, and that *S. pilosa* and *S. trispinosa* did not have any differences in the male genitalia structures. He hypothesized that Jakovlev (1889) indicated the presence of two spines on the hind femur in *B. pilosa* due to the relatively small size of the basal one. However, he followed Reuter's key in other respects and differentiated these two species by the length of antennal segment I, although exact measurements or ratios were not provided, and by the length of setae on this segment and hind tibiae.

We examined the lectotypes of both species as well as other specimens authentically identified as *S. pilosa*, and did not find any characters separating this species from *S. trispinosa*. Most probably, *S. trispinosa* was treated as a separate new species by Reuter (1904), because of the mistake in the description of *S. pilosa*. According to our measurements, *S. pilosa* and *S. trispinosa* do not differ in the antennal segment II length and we could not find any differences in the setae on the hind tibia. We fully concur with Muminov (1989) regarding the lack of differences in the male genitalia structure, and we were unable to identify any distinctions in the female genitalia either. Therefore, we synonymize *S. trispinosa* Reuter, 1904 with *S. pilosa* (Jakovlev, 1889).

Stenodema sibirica **Bergroth, 1914**

Figs 1M, 2F, 6E–H, I, U, 10B, F, 12E–G, 13

Miris virens lateralis Sahlberg, 1873: 23 (original description).
Stenodema lateralis: Reuter 1891: 187 (comb. nov.).
Stenodema sibiricum Bergroth, 1914: 183 (new name for junior secondary homonym of *Stenodema lateralis* (Geoffroy, 1785)); Carvalho 1959: 306 (catalogue).
Stenodema sibirica; Kerzhner 1988: 99 (key to species); Muminov 1989: 127 (key to species); Vinokurov and Kanyukova 1995: 98 (key to species); Kerzhner and Josifov 1999: 196 (catalogue); Yasunaga 2019: 301 (key to species).[5]

Type material examined. ***Lectotype*** of *Miris virens lateralis* Sahlberg, 1873: Russia • ♀; Krasnoyarsk Terr., Yeniseysk [Jeniseisk]; 58.45°N, 92.18°E; no date provided; J. Sahlberg; (http://id.luomus.fi/GZ.56515); (MZH).

Diagnosis. Body length in male 5.8–6.5, in female 6.2–6.8; frons protruding above clypeus base (as in Fig. 1H, I); setae on hemelytron simple; hemelytron brown to dark brown medially and yellow to pale brown along outer margin (Fig. 12E–G); male vertex width/eye ratio 2.1–2.4; labium reaching mesocoxa but not surpassing it (as in Fig. 1N); hind femur only slightly tapering towards apex, without spines; setae on posterior margin of hind femur as dense as on other parts of femur, shorter than half of hind femur (Fig. 2F); hind tibia not curved basally (as in Fig. 2J); swelling on propleura curved (Fig. 1H); antennal segment I length/head width ratio in male 1.0, in female 0.9–1.0; antennal segment I / pronotum lengths ratio 0.8–0.9 in male, 0.8 in female; antennal segment I as wide as or slightly narrower than eye diameter; groove on posterior part of mesopleuron absent (Fig. 1M); paired pits between calli absent (as in Fig. 1G), setae on antennal segment I shorter than antennal segment I width; genital capsule ~ 1.5× as long as wide, more or less acute apically, with outgrowth near left paramere socket (Fig. 6T, U); right paramere ca 3× as long as wide, its apical part slightly wider than basal part, its apical process bifurcate, ca 0.1× as long as rest of paramere (Fig. 6E, I); left paramere with apical process acute at posterior view (Fig. 6K, P), its sensory lobe swollen (Fig. 6J, M); vesica with one large and two small membranous lobes (Fig. 13); dorsal labiate plate slightly longer than wide; sclerotized ring ~ 3× as wide as long; distance between sclerotized rings ~ 0.3–0.5× as long as sclerotized ring width (Fig. 10B); posterior wall with sigmoid process between interramal lobes (Fig. 10F).

Distribution. *Stenodema sibirica* is known from Siberia, northern China, Mongolia, the Russian Far East, and Korea (Kerzhner and Josifov 1999).

Notes. Among the material preserved at ZISP, we found specimens with two types of vesica. They differ in the shape of the membranous lobes and the length of the ridge with sclerotized teeth (cf. Fig. 13A–C and Fig. 13D–F). The genital capsule and parameres of specimens with these two types of vesica were very similar (cf. Fig. 6E–H, U and Fig. 6I–L, T). We found only two males with the short, sclerotized ridge, and there were no females from the same series. There were no differences in the habitus between the specimens with two types of male genitalia. The lectotype preserved at the Finnish Museum of Natural His-

---

[5] For more references and a list of synonyms see Carvalho (1959), Schuh (1995), and Kerzhner and Josifov (1999).

tory is a female, and we refrained from dissecting its genitalia, as it will not provide us with additional information on the issue. Therefore, we treat widespread form as *S. sibirica* and refrain from making any taxonomic decisions on the two specimens with another type of vesica, as the corresponding species may have been already described from China (see below for comparisons).

Stenodema sibirica is very similar to *S. rubrinervis* Horváth, 1905. They have minor differences in the measurements i.e., vertex width/eye diameter ratio in male (2.1–2.4 in *S. sibirica* and 1.7–2.0 in *S. rubrinervis*) and length of antennal segment I (1.8–2.1 in *S. sibirica* and 2.5–3.0 in *S. rubrinervis*) (Table 1). The genitalia of those two species are very similar, and vesica of *S. rubrinervis* also has a long ridge of sclerotized teeth (Yasunaga 2019: fig. 8C).

Stenodema turanica **Reuter, 1904**

Figs 1B, C, 2C, I, 6A–D, Q, 7D–F, 8, 10A, E, 11A–D

Stenodema turanicum Reuter, 1904: 23 (original description); Carvalho 1959: 307 (catalogue); Wagner 1974: 112 (key to species).

Stenodema turanica: Muminov 1989: 127 (key to species); Kerzhner and Josifov 1999: 196 (catalogue).[6]

Type material examined. ***Lectotype*** of *Stenodema turanicum* Reuter, 1904 (designated here): Turkmenistan • ♂; Kopet Dagh; 38.06°N, 57.37°E; no date provided; K.O. Ahnger; (http://id.luomus.fi/GZ.56573); (MZH).

Paralectotypes of *Stenodema turanicum* Reuter, 1904: Kyrgyzstan • 2♀; Chiburgan [Tschiburgan] valley; 39.60°N, 70.65°E; no date provided; A.P. Fedchenko; (http://id.luomus.fi/GZ.56577, http://id.luomus.fi/GZ.56580); (MZH) • ♀; Gulcha [Gulscha]; 40.31°N, 73.44°E; no date provided; A.P. Fedchenko; (http://id.luomus.fi/GZ.56575); (MZH) Tajikistan: • ♂ Panjakent [Pendzhikent], valley of Zeravshan River; 39.48°N, 67.60°E; no date provided; A.P. Fedchenko; (AMNH_PBI 00345037, http://id.luomus.fi/GZ.56652); • 2♀; (AMNH_PBI 00345035, http://id.luomus.fi/GZ.56650; AMNH_PBI 00345036, http://id.luomus.fi/GZ.56651); (MZH). Turkmenistan: • ♂; Kopet Dagh; 38.06°N, 57.37°E; no date provided; K.O. Ahnger; (http://id.luomus.fi/GZ.56579); • 2♀ (http://id.luomus.fi/GZ.56578, http://id.luomus.fi/GZ.56572); (MZH) • ♀ Gokdepe [Geok-tepe]; 38.15°N, 57.95°E; K.O. Ahnger; (http://id.luomus.fi/GZ.56574); (MZH). Uzbekistan: • ♀; Shohimardon [Schagimardan]; 39.99°N, 71.81°E; no date provided; A.P. Fedchenko; (http://id.luomus.fi/GZ.56576); (MZH).

Diagnosis. Body length in male 6.1–6.8, in female 6.6–7.3; frons protruding above clypeus base (Fig. 1H, I); labium reaching middle coxa (as in Fig. 1N); hind femur distinctly tapering towards apex, without spines, not enlarged, 6–8× as long as wide (Fig. 2C); hind tibia curved basally (Fig. 2I); swelling on propleura curved (Fig. 1H); antennal segment I length/head width ratio in male 1.0, in female 0.9–1.0; antennal segment I length/pronotum length ratio 0.7–0.9 in male, 0.7 in female; antennal segment I not widened basally, its setae at base as dense as on other parts of this segment; setae of antennal segment I simple; antennal

---

[6] For more references and a list of synonyms see Carvalho (1959), Schuh (1995), and Kerzhner and Josifov (1999).

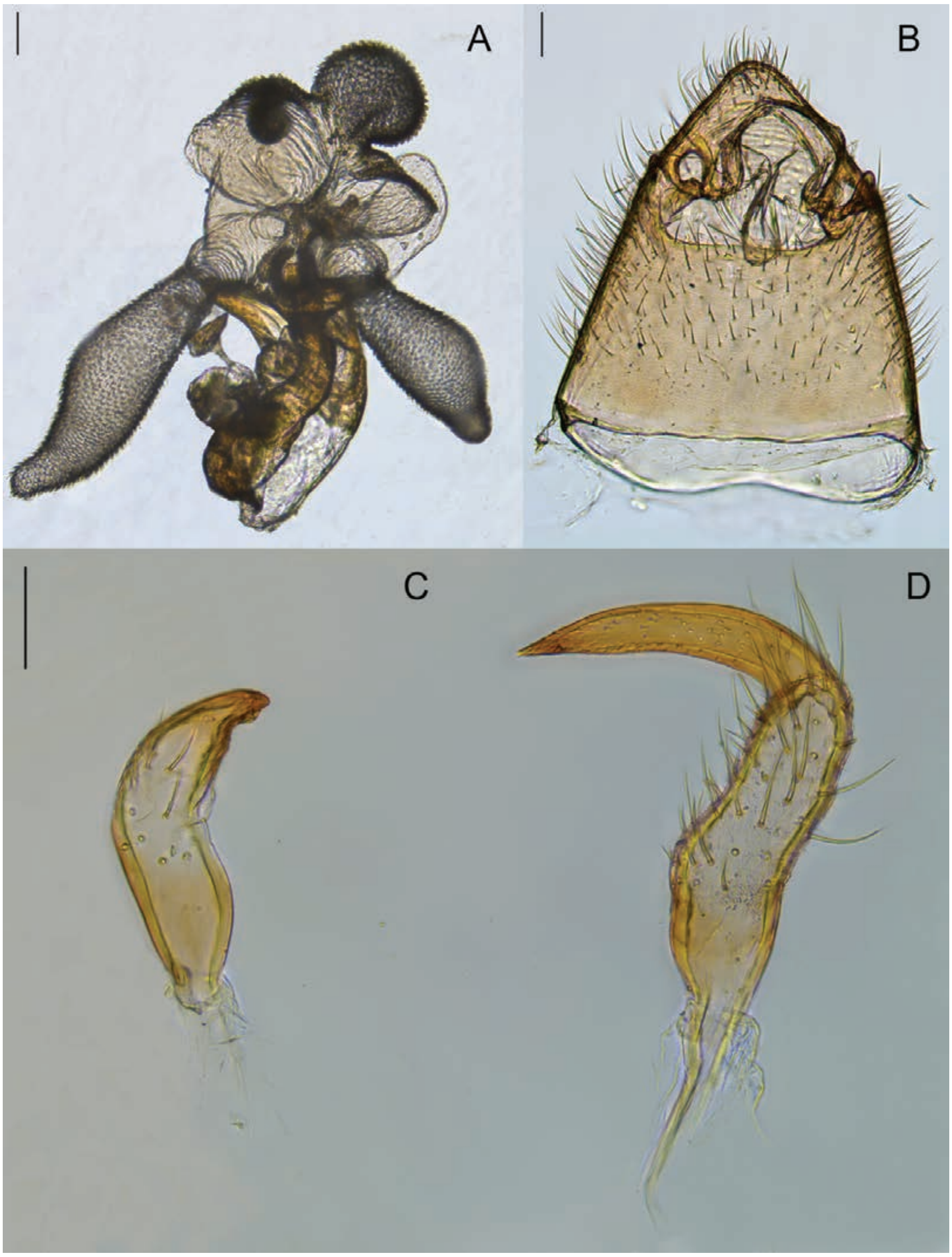

Figure 8. Male genitalia of *Brachytropis turanica*. lectotype **A** inflated aedeagus. left lateral view **B** genital capsule **C** right paramere. dorsal view **D** left paramere. dorsal view.

segment II length/head width ratio in male 3.1–3.5; groove on posterior part of mesopleuron absent (as in Fig. 1M); paired pits between calli absent (as in Fig. 1G); setae on posterior margin of hind femur denser than on other parts of femur, shorter than half of hind femur width (Fig. 2C); genital capsule only slightly longer than wide, acute apically, with outgrowth near left paramere socket (Fig. 6Q); right paramere ca 3× as long as wide, its apical part as wide as basal part, apical process not bifurcate (Fig. 6A); left paramere with apical process acute in posterior view (Fig. 6D), its sensory lobe swollen (Fig. 6B); vesica with four membranous lobes (Figs 7E, F, 8A); dorsal labiate plate as long as wide, sclerotized

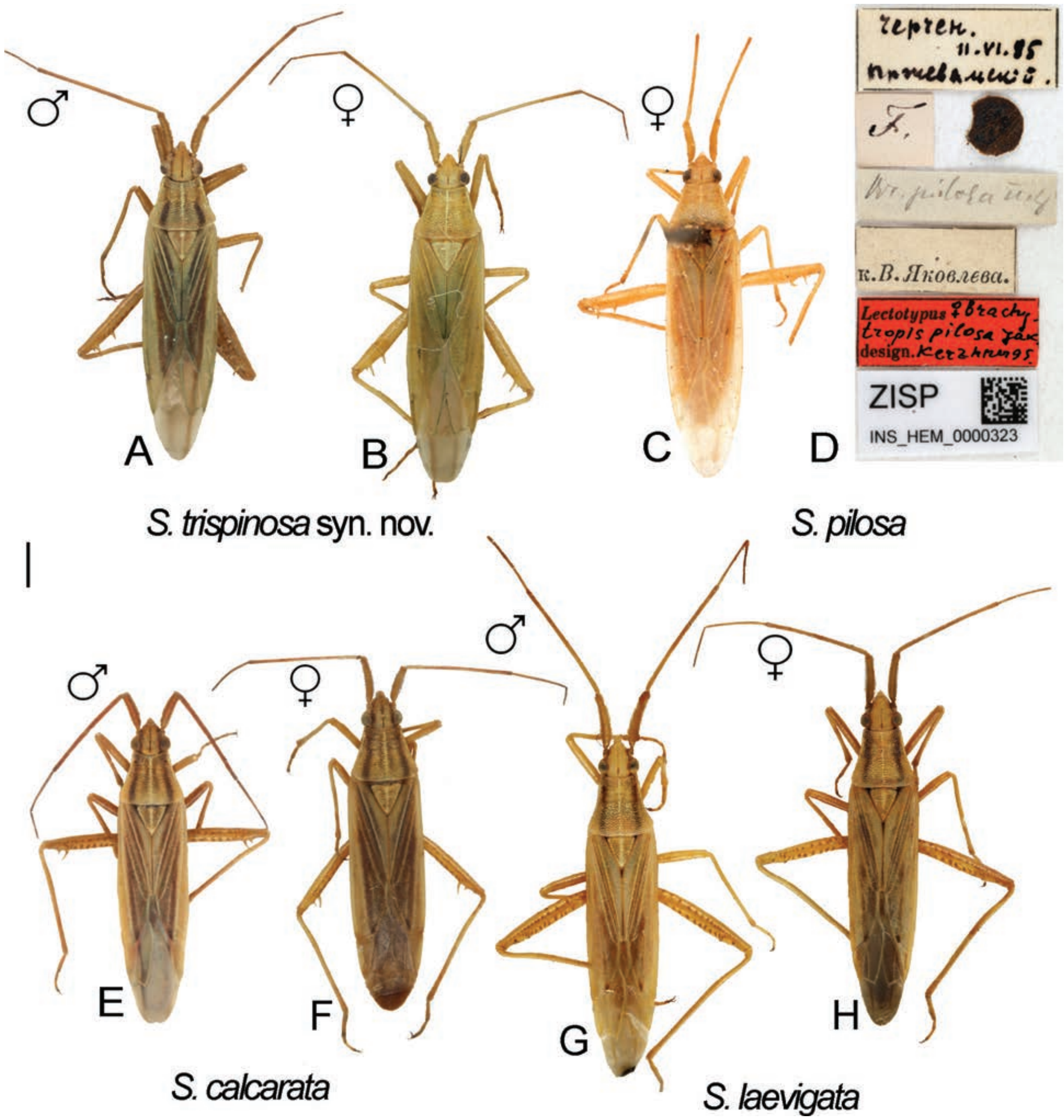

Figure 9. Digital images of habitus. *S. pilosa*. specimens previously identified as *S. trispinosa* **A** ♂ ZISP_ENT 00004882 **B** ♀ ZISP_ENT 00004886 **C** Lectotype of *Brachytropis pilosa* **D** labels attached to the lectotype. *S. calcarata* **E** ♂ ZISP_ENT 00004876 **F** ♀ ZISP_ENT 00004864. *S. laevigata* **G** ♂ ZISP_ENT 00004921 **H** ♀ ZISP_ENT 00004923.

ring 2–3× as long as wide; distance between sclerotized rings 4× as long as sclerotized ring width; membranous swelling on dorsal labiate plate not covering sclerotized rings (Fig. 10A); posterior wall with dorsal structure and sigmoid process between interramal lobes, dorsal structure oval (Fig. 10E).

Distribution. *Stenodema turanica* is known from the Balkans, Caucasus, Turkey, Iraq, Iran, Central Asia, Mongolia, and northwestern China (Kerzhner and Josifov 1999).

Notes. *Stenodema turanica* was originally described (Reuter 1904) from the type series collected by K.O. Ahnger and A.P. Fedchenko in Central Asia and retained at the Finnish Museum of Natural History (MZH). Due to the observed

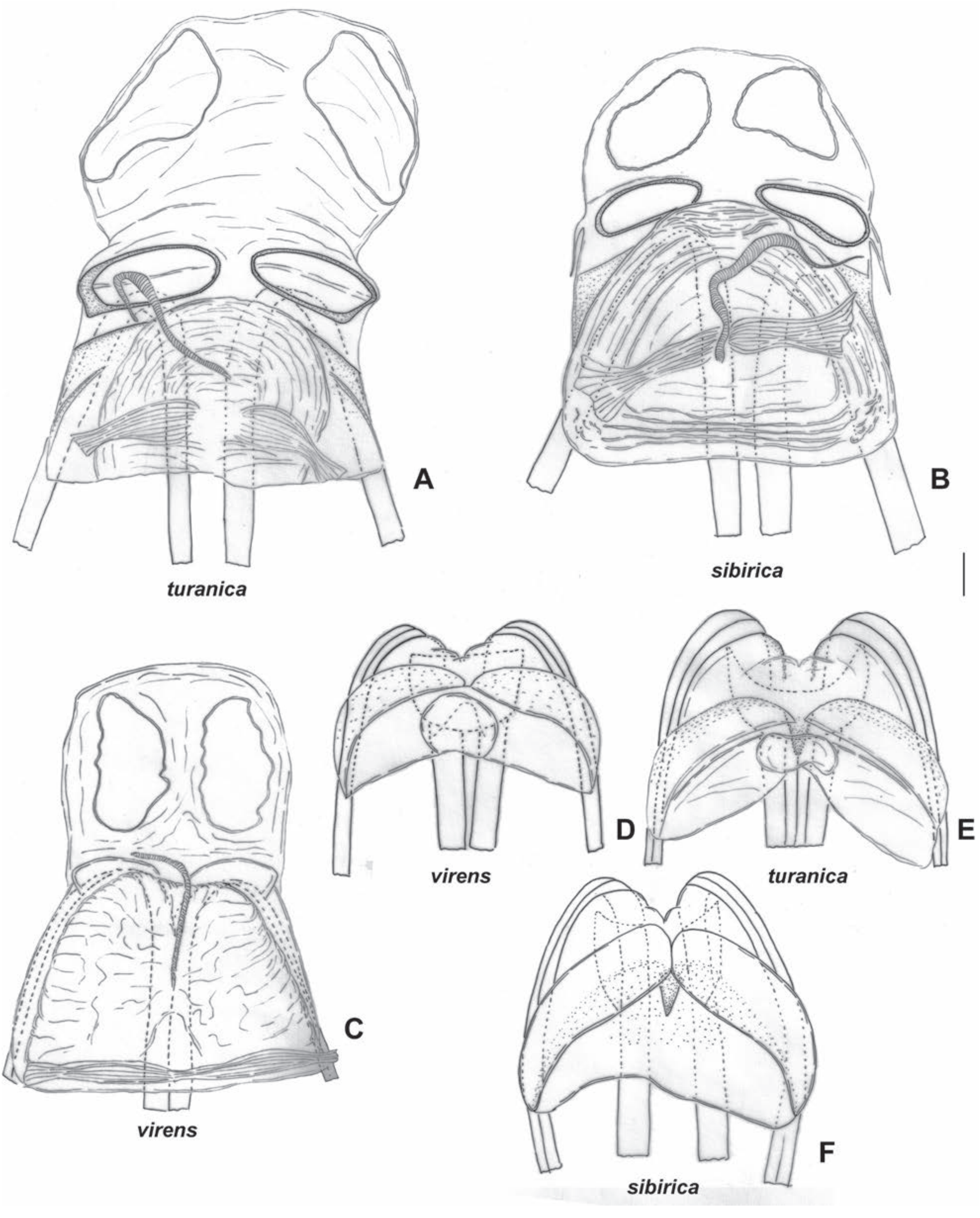

Figure 10. Female genitalia. *S. turanica*. ZISP_ENT 00002735 **A** dorsal labiate plate **E** posterior wall of bursa copulatrix. *S. sibirica*. ZISP_ENT 00003679 **B** posterior wall of bursa copulatrix **F** dorsal labiate plate. *S. virens* ZISP_ENT 00002732 **C** posterior wall of bursa copulatrix **D** dorsal labiate plate.

similarity of *S. turanica* with *S. virens*, here we designated the lectotype for *Stenodema turanicum* Reuter, 1904, the male from Kopet Dagh mountains in Turkmenistan (Fig. 8, http://id.luomus.fi/GZ.56573).

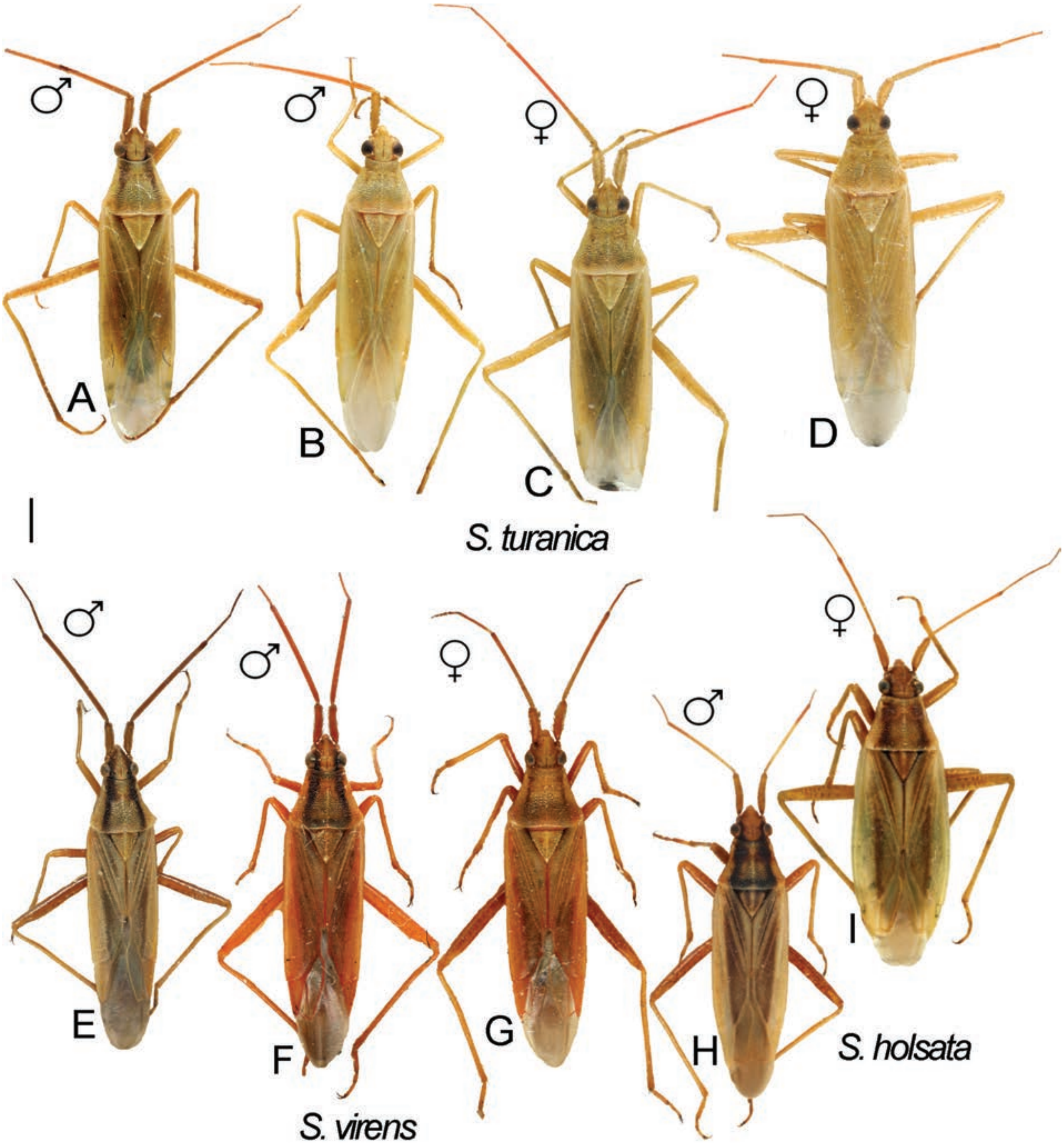

Figure 11. Digital images of habitus. *S. turanica* **A** ♂ ZISP_ENT 00004938 **B** ♂ ZISP_ENT 00004937 **C** ♀. ZISP_ENT 00004935 **D** ♀. ZISP_ENT 00004953. *S. virens* **E** ♂ ZISP_ENT 00004898 **F** ♂ ZISP_ENT 00004897 **G** ♀. ZISP_ENT 00004894. *S. holsata* **H** ♂ ZISP_ENT 00004903 **I** ♀ ZISP_ENT 00004907.

Stenodema turanica and *S. virens* are very similar externally. According to Wagner (1974), in *S. turanica* antennal segment II is twice as long as segments III and IV combined, whereas in *S. virens* this segment is only 1.5× times as long as segments III and IV combined. Additionally, the setae on the inner margin of hind femur are inclined in *S. virens*, whereas they are straight in *S. turanica*. The setae on the hind femur are more or less the same in both species (Fig. 2B, C). We confirm that the antennal segment II is longer in males of *S. turanica* rather than in males of *S. virens*, in particular, antennal segment II/head width ratio is 3.1–3.5 in *S. turanica* and 2.4–2.6 in *S. virens*. However, we were unable

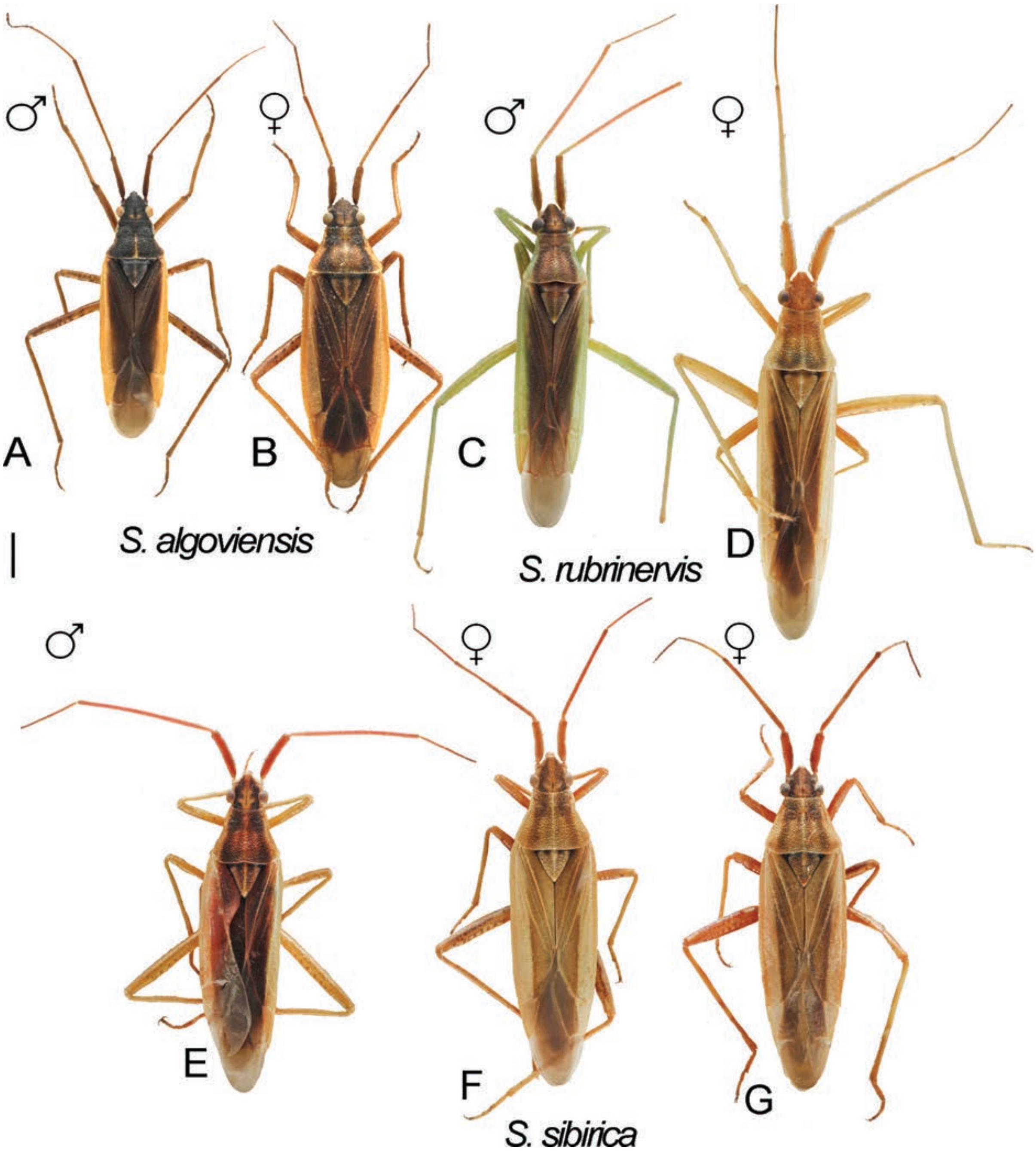

Figure 12. Digital images of habitus. *S. algoviensis* **A** ♂ ZISP_ENT 00004951 **B** ♀ ZISP_ENT 00004950. *S. rubrinervis* **C** ♂ ZISP_ENT 00004941 **D** ♀ ZISP_ENT 00004960. *S. sibirica* **E** ♂ ZISP_ENT 00004919 **F** ♀ ZISP_ENT 00004928 **G** ♀ ZISP_ENT 00004929.

to find reliable differences in female measurements. These two species differ from each other in both, male (compare Fig. 7D–F and Fig. 7G–I) and female (compare Fig. 10A, E and Fig. 10C, D) genitalia.

Stenodema virens **(Linnaeus, 1767)**

Figs 1J, P, 2B, 5E–H, R, V, 7G–I, 10C, D, 11E–G

Cimex virens Linnaeus, 1767: 730 (original description).

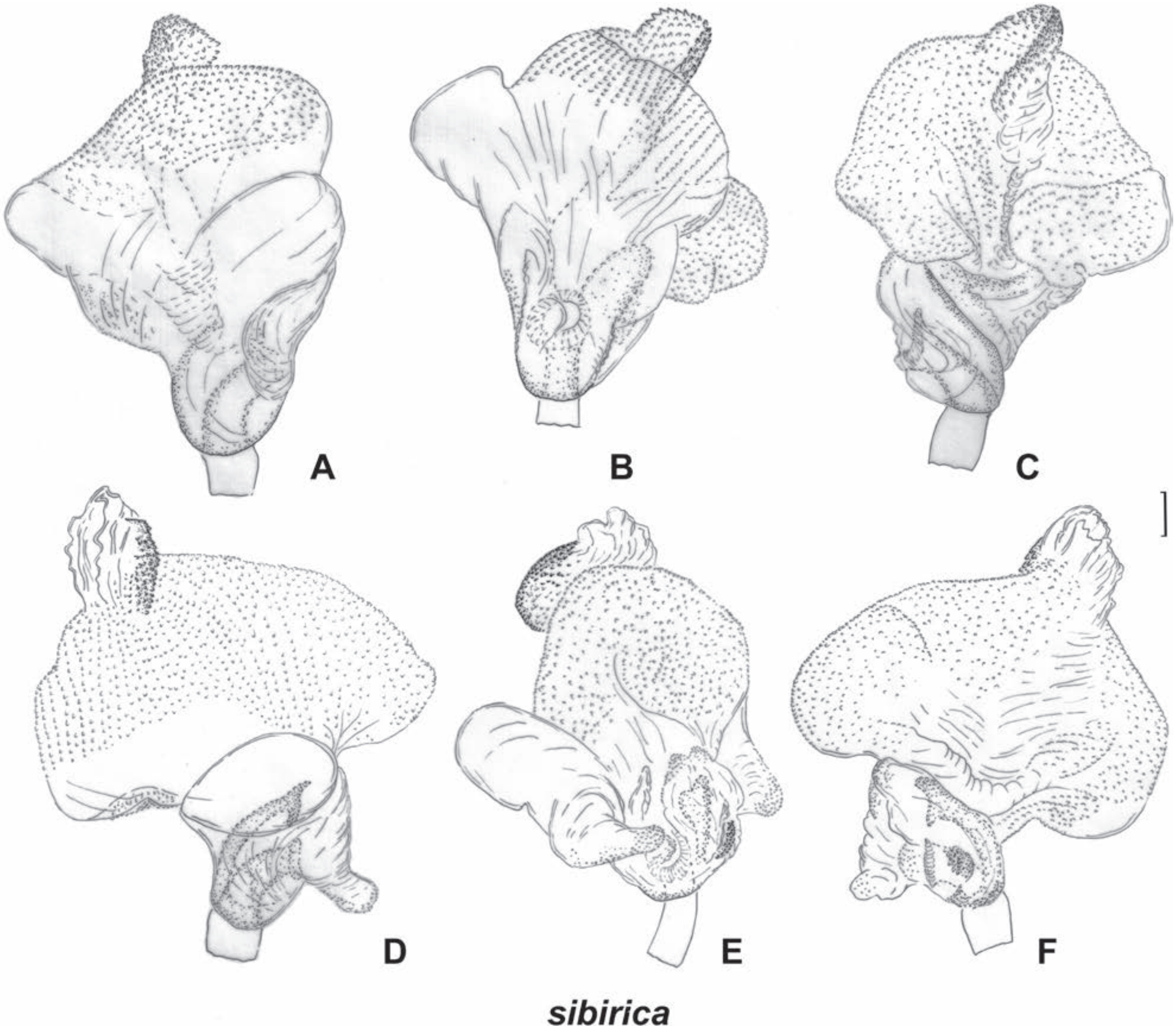

Figure 13. Inflated vesica. *S. sibirica* vesica with long ridge ZISP_ENT 00003617 **A** dorsal view **B** left lateral view **C** ventral lateral view; vesica with short ridge ZISP_ENT 00003620 **D** dorsal view **E** left lateral view **F** ventral lateral view.

Stenodema virens Reuter, 1904: 4 (comb. nov., key to species); Carvalho 1959: 307 (catalogue); Kerzhner and Jaczewski 1964: 958 (key to species); Wagner and Weber 1964: 94 (key to species); Wagner 1974: 112 (key to species); Muminov 1989: 127 (key to species); Vinokurov and Kanyukova 1995: 98 (key to species); Kerzhner and Josifov 1999: 196 (catalogue).[7]

Diagnosis. Body length in male 6.0–6.6, in female 6.1–7.1; frons protruding above clypeus base (as in Fig. 1C); labium reaching middle coxa, but not surpassing it (as in Fig. 1N); hind femur distinctly tapering towards apex, without spines (Fig. 2B), 6–8× as long as wide; hind tibia curved basally (as in Fig. 2I); swelling on propleura curved (as in Fig. 1H); antennal segment I length/head width ratio in male 1.0, in female 0.8–1.0; antennal segment I/pronotum length ratio 0.6–0.7 in male, 0.6–0.8 in female; antennal segment I not widened ba-

---

[7] For more references and a list of synonyms see Carvalho (1959), Schuh (1995), and Kerzhner and Josifov (1999).

sally, its setae at base as dense as on other parts of this segment; setae in antennal segment I simple; antennal segment II length/head width ratio in male 2.4–2.6; groove on posterior part of mesopleuron absent (as in Fig. 1M); paired pits between calli absent (as in Fig. 1G); setae on posterior margin of hind femur denser than on other parts of femur, shorter than half of hind femur width (Fig. 2B); genital capsule only slightly longer than wide, acute apically, with outgrowth near left paramere socket (Fig. 5R); right paramere ~ 4× as long as wide, its apical part as wide as basal part, apical process bifurcate (Fig. 5E, G); right paramere with apical process acute in posterior view (Fig. 5P), its sensory lobe swollen (Fig. 5F); vesica with four membranous lobes (Fig. 7G–I); membranous swelling on dorsal labiate plate not covering sclerotized rings (Fig. 10C); posterior wall with dorsal structure and sigmoid process between interramal lobes, dorsal structure rounded (Fig. 10D).

Distribution. *Stenodema virens* is widely distributed in Europe, the Near East, and the Caucasus, extending eastwards to Yakutia, Buryatia, Mongolia, and northern China (Kerzhner and Josifov 1999).

Morphological taxonomy

Based on the descriptions and material examined, we could delimit five morphological groups within *Stenodema*.

1. *S. calcarata-pilosa* group (subgenus *Brachystira*). This group has the frons not protruding above the clypeus (Fig. 1I) and hind femur possessing ventroapical spines and not tapering towards apex (Fig. 2A, D). The information on *S. falki* is very scarce, but this species might also belong to this group. According to Kelton (1961), the Nearctic species *S. falki* is very similar to *S. pilosa*, but differs in body ratios and male genitalia, although Schwartz (1987) suspected that these species might be synonymous. Among the species with the female genitalia examined, *S. calcarata* and *S. pilosa* are similar in the absence of the membranous swelling on the dorsal labiate plate and the absence of the dorsal structure between interramal lobes (Fig. 4A, C, E, H).
2. *S. holsata* group includes species with the frons not protruding above the clypeus (Fig. 1H) and hind femur without spines, and non-tapered apical region (Fig. 2E, H). *Stenodema algoviensis*, *S. chinensis*, *S. holsata*, *S. plebeja*, and *S. sericans* possess this set of characters. *Stenodema chinensis* differs from the other four species with the presence of the flattened dorsal setae. *Stenodema plebeja* is longer and differs from other species in the body length/pronotum width ratio equaling 4.9–5.0 in females, while this ratio is < 4.4 in other species. In contrast to other species, *Stenodema sericans* is pale, without dark stripes on pronotum and hemelytron, and has parameres different from S. *algoviensis* and *S. holsata*, with apical half of the right paramere as wide as basal part, and the left paramere without outgrowth or swelling near the apical process (Wagner 1974: fig. 9d–f). Refer to the notes section after the diagnosis of *S. holsata* for the differences between *S. algoviensis* and *S. holsata*.
3. *S. laevigata* group includes species with frons not protruding above clypeus (Fig. 1H) and hind femora without spines and tapered apical region

(Fig. 2E). According to Zheng (1981a), *S. antennata* Zheng, 1981 is close to *S. laevigata*, but much larger, with a female body length of 11. *Stenodema longula* Zheng, 1981 might be close to *S. laevigata* as well (Zheng, 1981a), although this requires further verification.

4. *S. turanica-virens* group includes species with frons protruding above the clypeus base (Fig. 2C) and hind femur lacking spines and apical region tapered (Fig. 2B, C). *Stenodema crassipes* is close to *S. virens* and *S. turanica*. However, it differs from them in the widened hind femur, which is 4–5× as long as wide, and the antennal segment II in female is widened basally with long and dense setae. Based on the drawings of the head and hind tibia in Zheng (1981a), *S. tibeta* Zheng, 1981 also belongs to this group. Nonnaizab and Jorigtoo (1994) compared *S. deserta* Nonnaizab & Jorigtoo, 1994 with *S. virens*, and noted that the former was different in the body structure and the paramere shape. However, those differences can be intraspecific variability, because according to our examinations, the parameres and vesica of *S. virens* are very similar to those depicted in Nonnaizab and Jorigtoo (1994: figs 4–6, 7G–I), and those two species could be conspecific. According to Zheng (1981b), *S. hsiaoi* is similar to *S. virens* and *S. turanica* in the habitus and male genitalia. The same is true for *Stenodema mongolica* Nonnaizab & Jorigtoo, 1994 (Nonnaizab and Jorigtoo 1994: figs 7–12); however, according to the original description it has flattened setae on the antennal segment I. The Nearctic species *S. vicina* (Provancher, 1872), *S. imperii* Bliven, 1858, *S. sequoia* Bliven, 1955, and *S. pilosipes* Kelton, 1961 are allied to the species of *virens-turanica* group (Bliven 1955, 1958; Kelton 1961).
5. *S. sibirica* group includes species with the frons protruding above the clypeus base (as in Fig. 1C), its hind femur does not have spines, and it is not tapering towards apex (Fig. 2F). *Stenodema nippon* is very similar to *S. sibirica* and *S. rubrinervis*, although distinctly differs from them in the salient features and genital structures (Yasunaga 2019). *Stenodema khenteica* is also within this group and differs from *S. nippon*, *S. sibirica*, and *S. rubrinervis* in the antennal segment I shorter than pronotum and distinctly narrower than the eye diameter. Many other species described from China, most probably, belong to this group, and some of them might be conspecific with the species listed above. We had an opportunity to examine the paralectotype of *S. alpestris* Reuter, 1904 preserved at ZISP. In salient features and measurements this species is identical with *S. rubrinervis*. Horváth (1905) did not compare this species with *S. alpestris*, and possibly he was not aware of it. The lectotypes of both species should be examined to draw conclusion on their status. *Stenodema gridellii* Hoberlandt, 1960 has similar parameres to *S. sibirica*, but it has a smaller body (Hoberlandt 1960). Although in the drawings of Hoberlandt (1960) *S. gridellii* is shorter than *S. sibirica*, the provided measurements for the former fit those for *S. sibirica*. Zheng (1981a) compared *S. alticola* Zheng, 1981 with *S. gridellii*, but wrote that the former is longer (males 6.7–6.8, female 7.5–7.6), having the erect setae on antennal segment I and its antennal segment II/I length ratio was 2.5. All those characters correspond to *S. rubrinervis*. Therefore, *S. alticola* and *S. rubrinervis* can be closely related or even synonymous. According to Zheng (1981a), *S. nigricalla* Zheng, 1981 is

similar to *S. chinensis* (from the *turanica-virens* group). Judging from the drawings of the male genitalia, the shape of vesica of *S. nigricalla* is more similar to specimens from Siberia with short ridge on vesica (see Notes for the diagnosis of *S. sibirica*; Zheng 1981a: figs 13D–F, 19). However, the right paramere of this species has a longer apical process, than in those specimens and it is more similar to *S. rubrinervis* (Zheng 1981a: fig. 18; Yasunaga 2019: fig. 8a, e). Zheng (1981a) compared *S. angustata* Zheng, 1981 with *S. nigricalla*. However, the latter is more similar to *S. nippon* in the shape of the right paramere with elongate apical process and the presence of long and narrow vesica lobe at the left hand side (Yasunaga 2019: fig. 7C, F, G; Zheng 1981a: figs 20, 22). Tang (1994) compared *S. qulininginensis* Tang, 1994 with *S. nigricalla*, and, most probably, it also belongs to the *sibirica* group. Zheng (1992) noted that *S. daliensis* Zheng, 1992 is similar to *S. alticola* and *S. gridellii* and differed from them in the body shape and coloration. According to Reuter (1904) *S. elegans* has the hind femur without spines and not tapering apically and its frons is protruded above clypeus, which also corresponds to the *sibirica* group.

We could not place *S dorsalis* (Say, 1832) and *S. parvula* Zheng, 1981 to any group listed above. Kelton (1961) proposed to treat *S. dorsalis* described from the Eastern USA as nomen nudum, because there were no records for it since the original description. *Stenodema parvula* could be close to *S. holsata* or *S. laevigata* because its frons does not protrude above the clypeus; however, the information on the hind femur shape or genitalia structures for this species were not provided (Zheng 1981a).

Phylogenetic relationships between species

The resulted trees from the Bayesian analyses are provided in Figs 14–19, and those resulted from the RaxML analyses are provided in Suppl. material 3.

All analyses show that widely distributed Palearctic species are monophyletic with high supports, as well as *S. rubrinervis* and *S. sericans* (P = 100, BS > 92). The COI sequences of two species from Nearctic, *S. pilosipes* and *S. vicina*, were included in the analyses. *Stenodema vicina* forms a clade (PP = 96 and 94, BS = 89 and 87 for COI and full datasets, respectively). However, *S. pilosipes* forms a clade only in the Bayesian analysis based on the full dataset (PP = 53), and in other cases one of the specimens is closer to *S. vicina* rather than to the second specimen of its species. *Stenodema calcarata* and *S. pilosa* always form sister group relationships (PP = 94–100, BS = 66–83).

The topologies built on COI only and the full dataset comprise the greatest number of specimens and species, and they are very similar. They show that the clade formed by *S. calcarata* and *S. pilosa* (subgenus *Brachystira*) forms sister group relationships with the clade comprising all other *Stenodema* species (nominative subgenus), and the latter has the following supports: PP = 100 and 87, BS = 67 and 70 for COI and full datasets, respectively. Within this clade, *S. holsata*, *S. laevigata*, and *S. sericans* form a clade (PP = 100 and 89, BS = 82 and 75 for COI and full datasets, respectively). In the analyses based on COI only, the relationships between those three species are unresolved. However, in the phylogeny based on the full

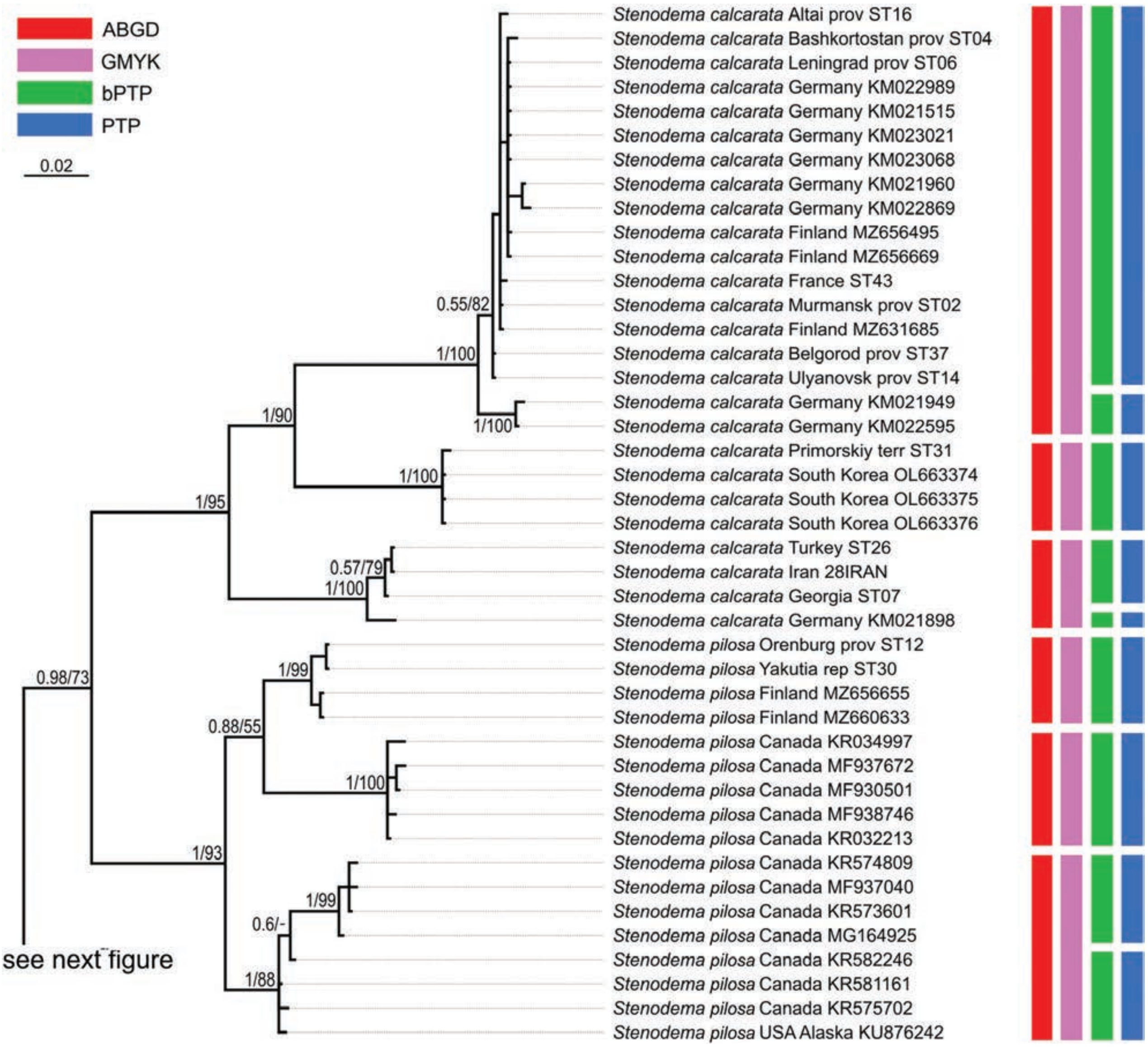

Figure 14. Phylogeny obtained using the Bayesian inference based on the COI dataset, part 1. The supports are provided above the branches. The numbers on the left correspond to PP, the numbers on the right correspond to BS obtained with RAxML. The color stripes correspond to the results of the species delimitation analyses in the following order: ABGD, GMYC, bPTP, PTP.

dataset, *S. sericans* forms a clade with *S. laevigata* although with low supports (PP = 63, BS = 55). *Stenodema pilosipes*, *S. sibirica*, *S. rubrinervis*, *S. turanica*, *S. vicina*, and *S. virens* form a clade (PP = 97 and 100, BS = 77 and 91 for COI and full datasets, respectively). Among those species, *S. turanica* and *S. virens* are sister groups (PP = 100 and 99, BS = 80 and 87 for COI and full datasets, respectively), and *S. pilosipes* and *S. vicina* also form a clade (PP = 100, BS = 98 in both analyses). Those two pairs show reciprocal monophyly (PP = 100 and 99, BS = 77 and 89 for COI and full datasets, respectively). *Stenodema sibirica* and *S. rubrinervis* form a clade in Bayesian analysis (PP = 100 and BS = 62 full dataset), and in the RaxML analysis with COI and 16S rRNA (BS = 90).

The phylogeny based on the reduced dataset with COI and 16S rRNA has the topology corresponding to those obtained based on COI and full datasets.

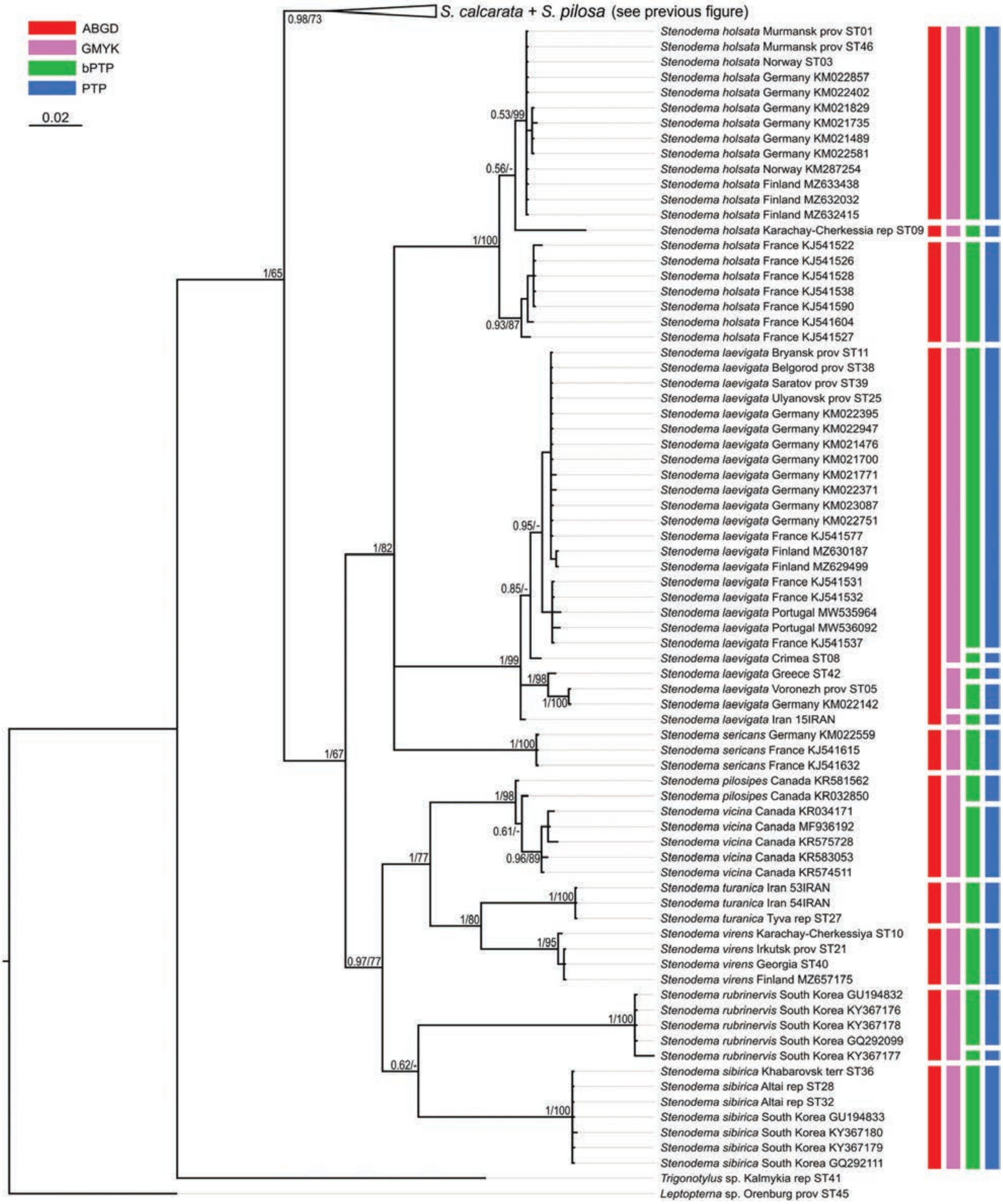

Figure 15. Phylogeny obtained using the Bayesian inference based on the COI dataset, part 2. The supports are provided above the branches. The numbers on the left correspond to PP, the numbers on the right correspond to BS obtained with RAxML. The color stripes correspond to the results of the species delimitation analyses in the following order: ABGD, GMYC, bPTP, PTP.

The results obtained with 16S rRNA have a different topology. In this case, *S. turanica* forms sister group relationships with the clade comprising other species, although with low support (PP = 67). *Stenodema virens* forms sister group relationships with the rest of *Stenodema* species (PP = 89). *Stenodema sibirica*

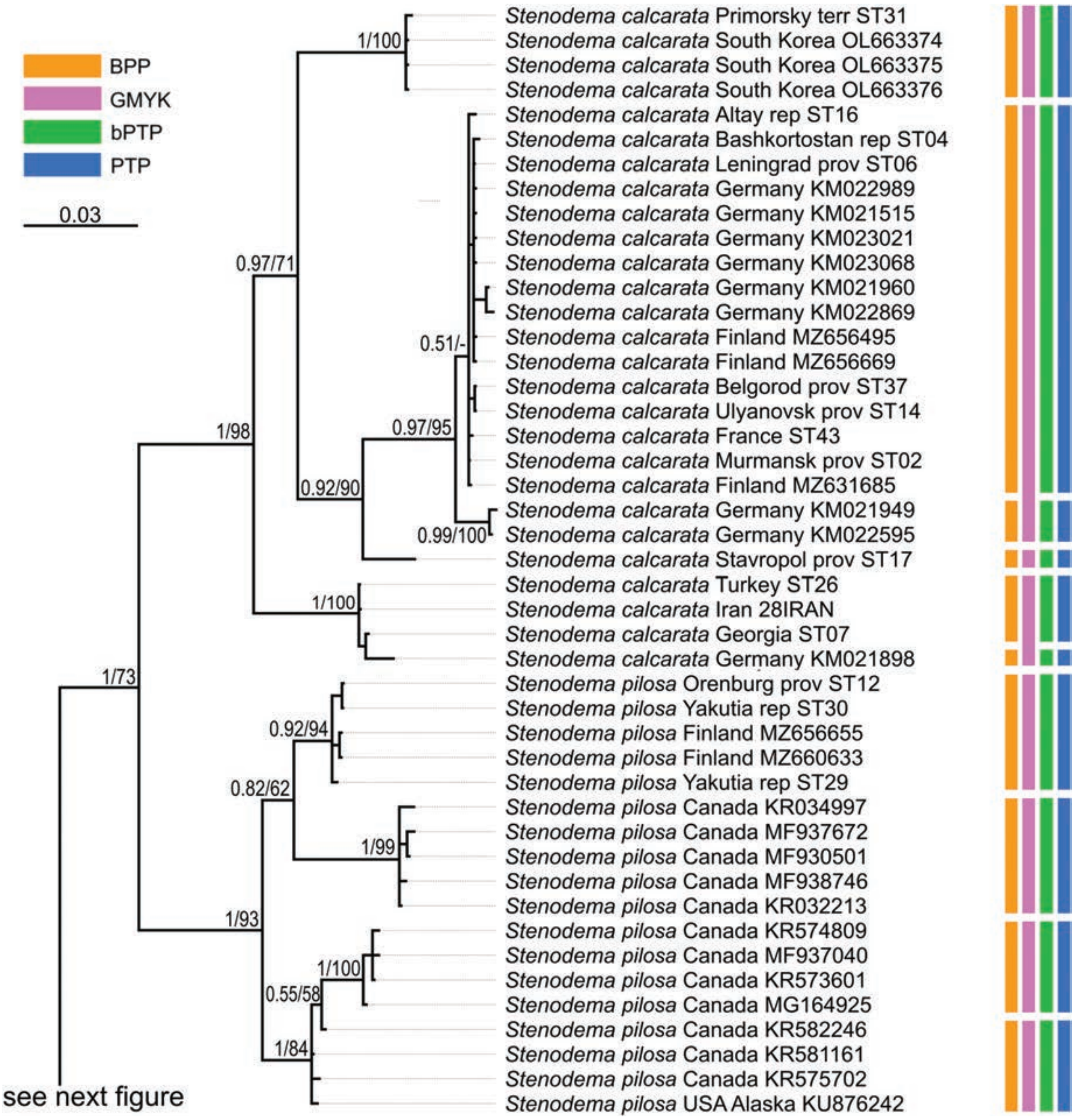

Figure 16. Phylogeny obtained using the Bayesian inference based on the full dataset dataset, part 1. The supports are provided above the branches. The numbers on the left correspond to PP, the numbers on the right correspond to BS obtained with RAxML. The color stripes correspond to the results of the species delimitation analyses in the following order: BPP, GMYC, bPTP, PTP.

and *S. rubrinervis* form a clade (PP = 97, BS = 85), which is a sister group to the clade, formed by *S. calcarata*, *S. holsata*, *S. laevigata*, and *S. pilosa* (PP = 86). *Stenodema laevigata* is a sister group to a clade formed by other three species (PP = 85, BS = 68). *Stenodema holsata* is a sister group to a *S. calcarata*+*S. pilosa* clade (PP = 94, BS = 83).

Intraspecific phylogenetic relationships

At least some analyses show genetic structure within *S. calcarata*, *S. pilosa*, *S. holsata*, and *S. laevigata*. Analyses based on 16S rRNA and reduced dataset do not show the structure within *S. pilosa* and *S. laevigata*.

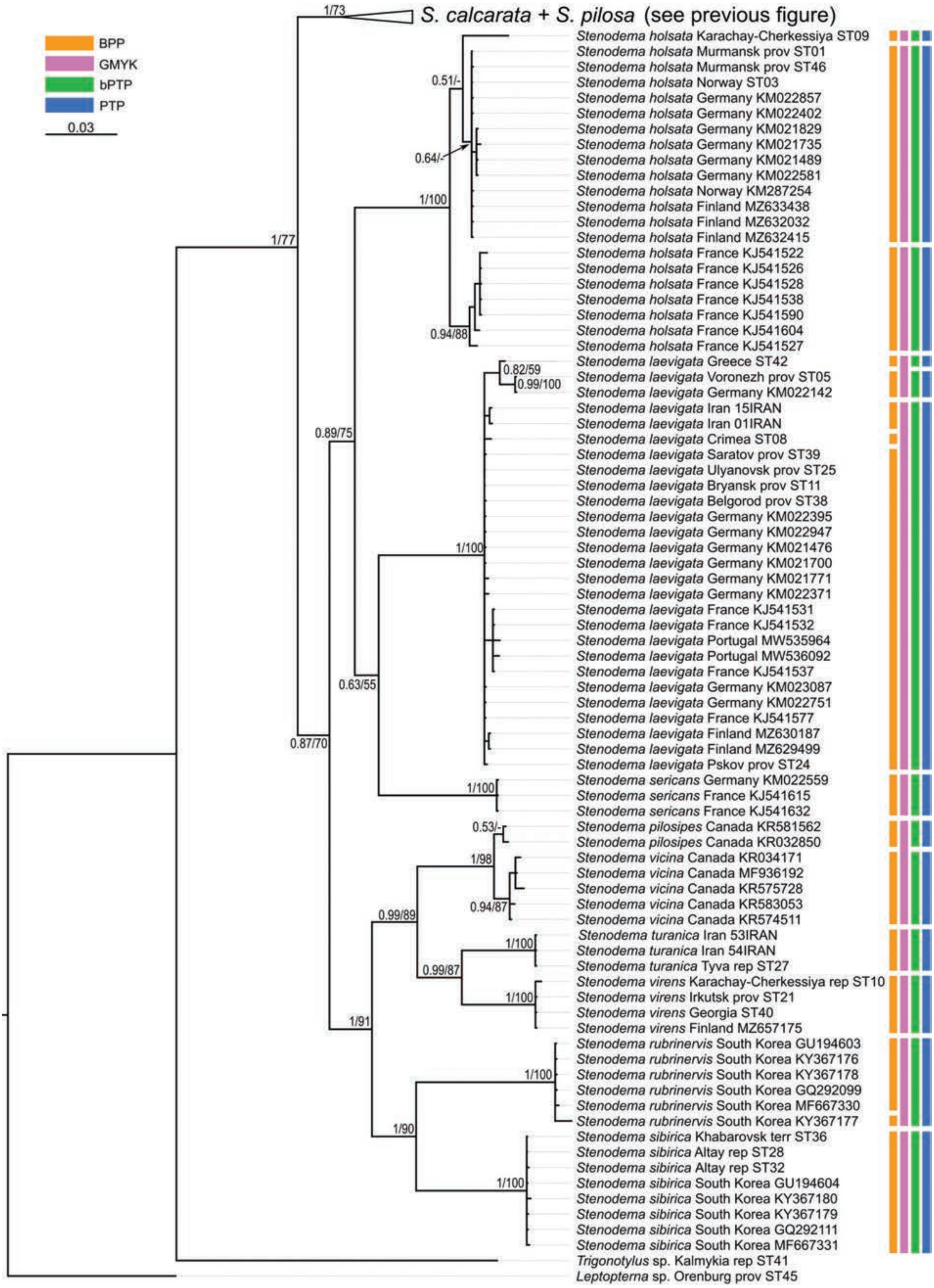

Figure 17. Phylogeny obtained using the Bayesian inference based on the full dataset, part 2. The supports are provided above the branches. The numbers on the left correspond to PP, the numbers on the right correspond to BS obtained with RAxML. The color stripes correspond to the results of the species delimitation analyses in the following order: BPP, GMYC, bPTP, PTP.

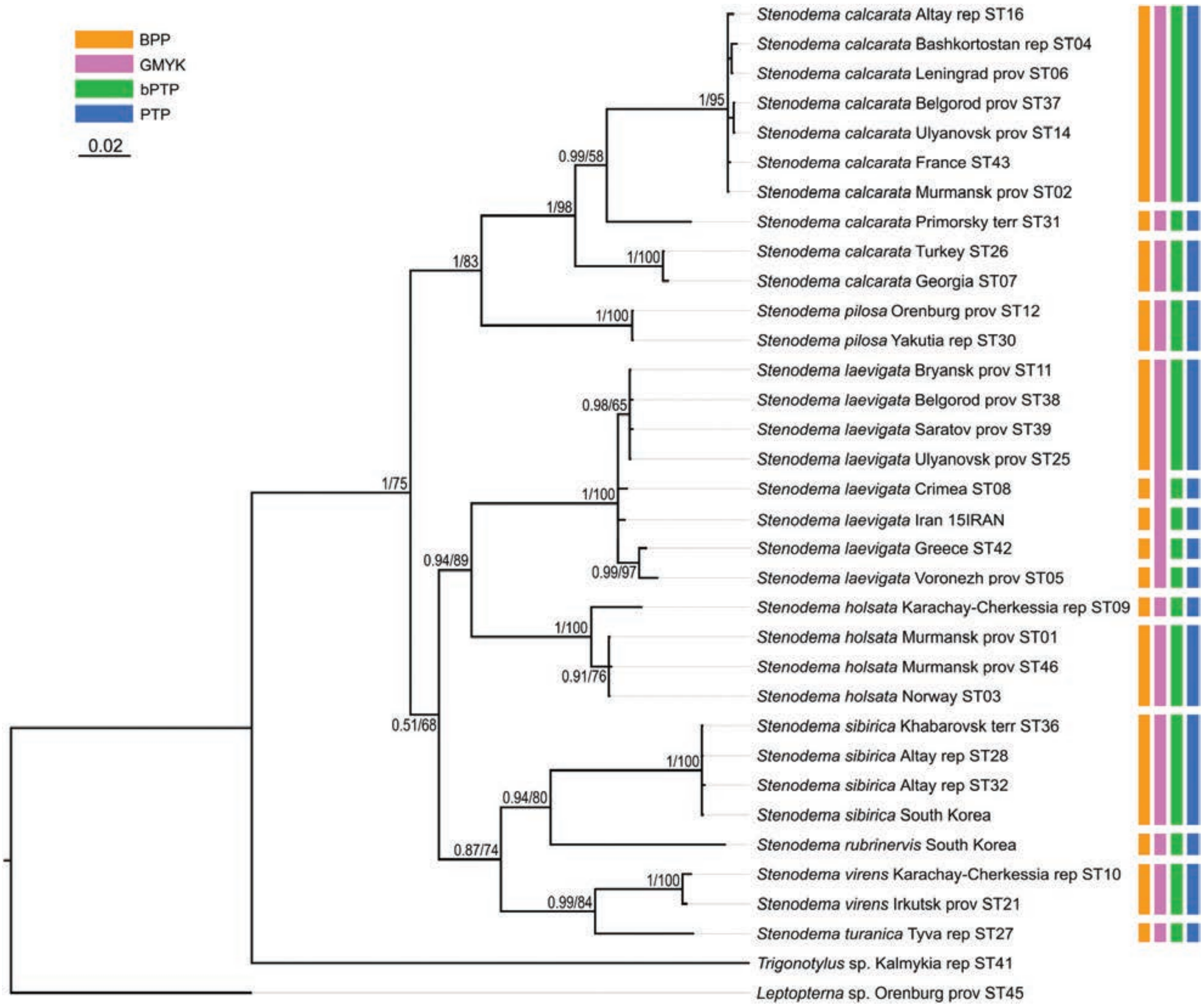

Figure 18. Phylogeny obtained using the Bayesian inference based on the reduced dataset. The supports are provided above the branches. The numbers on the left correspond to PP, the numbers on the right correspond to BS obtained with RAxML. The color stripes correspond to the results of the species delimitation analyses in the following order: BPP, GMYC, bPTP, PTP.

The phylogenetic structure within *Stenodema pilosa* is present only in the results of analyses based on COI and full datasets because Nearctic species are included there. The specimens of this species are split into three main clades: two Nearctic and one Palearctic. One of the Nearctic clades (PP = 100 for both, BS = 88 and 84 or COI and full datasets, respectively) is a sister group to the rest of the specimens. The clade comprising some Nearctic and all Palearctic specimens has low to average supports (PP = 88 and 82, BS = 55 and 62 for COI and full datasets, respectively). This clade splits into two groups: one of them Nearctic (PP = 100 for both, BS = 100 and 99 for COI and full datasets, respectively), and the second one is Palearctic (PP = 100 and 92, BS = 99 and 94 for COI and full datasets, respectively).

In the analyses based on COI and full dataset, representatives of *S. calcarata* from the southern side of Caucasus (Iran, Georgia, Turkey) and a single specimen from Germany form a clade with the highest support, and it is a sister group to the rest of the specimens of this species (PP = 100 and 97, BS = 90 and 71 for COI and full datasets, respectively). Specimens from East Asia (South

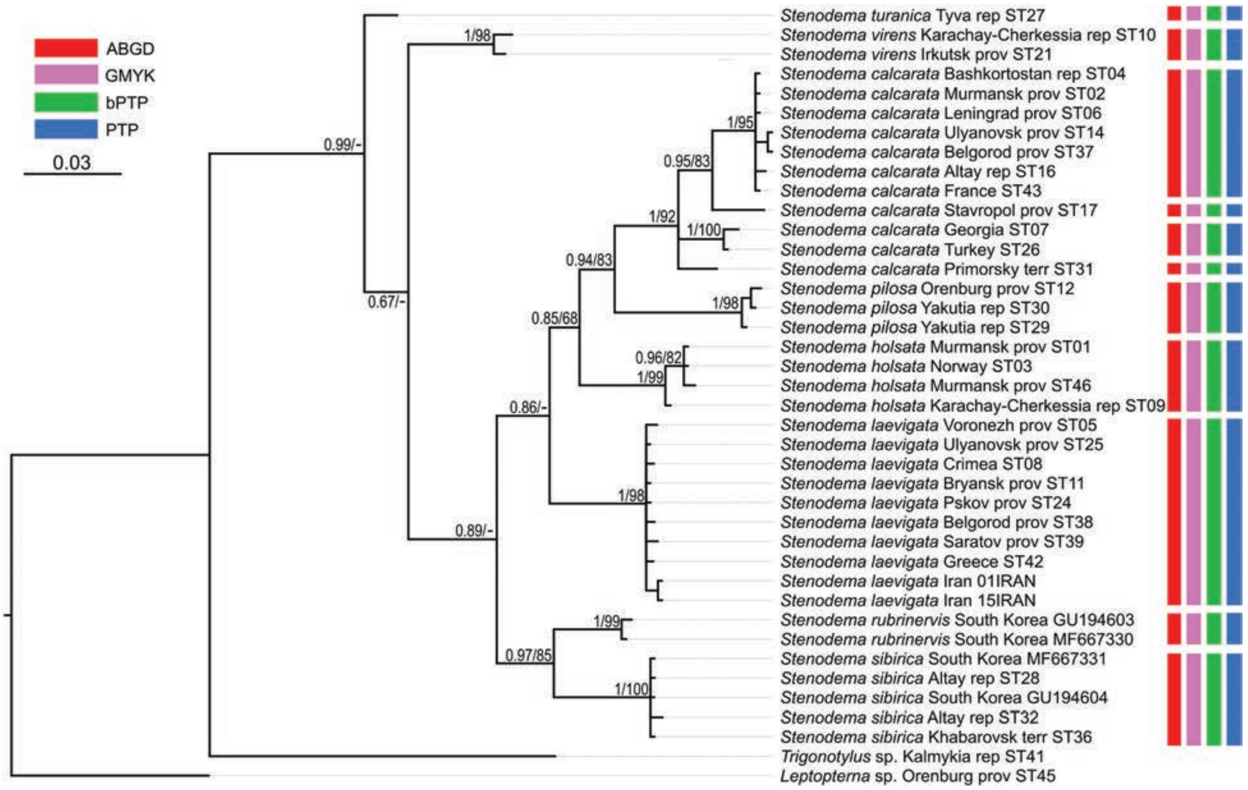

Figure 19. Phylogeny obtained using the Bayesian inference based on the 16S rRNA dataset. The supports are provided above the branches. The numbers on the left correspond to PP, the number on the right correspond to BS obtained with RAxML. The color stripes correspond to the results of the species delimitation analyses in the following order: ABGD, GMYC, bPTP, PTP.

Korea and Primorsky Territory) form a clade with the highest support, which is a sister group to the clade formed by the rest of the specimens (PP = 100 and 92, BS = 100 and 90 for COI and full datasets, respectively). Only 16S rRNA was obtained for the specimen from Stavropol Territory, and in the phylogeny based on the full dataset it is a sister group to the rest of the specimens (PP = 97, BS = 95). Two specimens from Germany form a clade (PP = 100 and 99 for COI and full datasets, respectively, and BS = 100 for both), and they are the sister group to the clade comprising most of the specimens from the Western Palearctic and a specimen from Altay Republic (PP = 55 and 51 COI and full datasets, respectively, BS = 82 for COI).

In the phylogenies based on 16S rRNA and the reduced dataset, specimens of *S. calcarata* from Georgia and Turkey form a clade with the highest supports. In the phylogeny based on 16S rRNA and the reduced dataset, single specimen from the East Asia (Primorsky Territory) included in those analyses has many substitutions. In the analysis based on the 16S rRNA it forms unresolved relationships with the clade, comprising the specimens from Georgia and Turkey (PP = 100, BS = 100) and the clade comprising the rest of the specimens (PP = 95, BS = 83). In the phylogeny based on the reduced dataset, the clade comprising species from Georgia and Turkey forms a reciprocal monophyly with the clade comprising the rest of the specimens including the one from the Primorsky Territory (PP = 99, BS = 58). In the phylogeny based on 16S rRNA specimen from Stavropol Province forms a clade with the clade comprising most of the specimens from the Western Palearctic and Altay Republic (PP = 100, BS = 95 in both datasets).

In the phylogenies based on COI and full dataset all specimens of *S. holsata* from France form a clade (PP = 93 and 94, BS = 87 and 88 for COI and full datasets, respectively), and it is a sister group to the clade formed by the rest of the specimens in the results of the Bayesian analysis (PP = 56 and 51 for COI and full datasets, respectively). Specimen from Karachay-Cherkessia forms a clade with the clade formed by the specimens from Northern and Central Europe (PP = 53 and 64 for COI and full datasets, respectively, BS = 99 for COI dataset). Only four specimens of *S. holsata* are included to the analyses based on 16S rRNA and reduced dataset. The specimen from Karachay-Cherkessia is a sister group to a clade formed by three specimens from northern Europe (PP = 96 and 91, BS = 82 and 76 for COI and full datasets, respectively).

In the phylogenies based on COI and full dataset, there is a clade within *S. laevigata* comprising specimens from Greece, Iran, and Voronezh Province (PP = 100 and 82, BS = 98 and 59 for COI and full datasets, respectively). Within this clade, the specimens from Voronezh Province and Germany are more closely related (PP = 100 and 99 for COI and full datasets, respectively, BS = 100 for both datasets). The results of the analysis based on the full dataset does not show any other clades within this species. The Bayesian inference analysis based on COI dataset also show, that the rest of the specimens except for the three specimens mentioned above and one from Iran, also form a clade (PP = 85). Within this clade, a specimen from Crimea forms sister group relationships with the rest of the specimens (PP = 95).

Species delimitation

All analyses show identical results for the phylogeny built based on 16S rRNA. In the case of COI, ABGD delimits the smallest number of species, followed by GMYC. PTP and bPTP show identical results for this marker. In the analyses based on the combined datasets, GMYC results in the smallest number of species. For the reduced dataset, PTP, bPTP, and BPP show identical results. For the full dataset, BPP results in the largest number of species, and PTP and bPTP showed the identical number of species. All species delimitation analyses do not mix the specimens belonging to different widespread species. *Stenodema sibirica*, *S. turanica*, and *S. virens* each form a single species in all the cases.

All analyses suggested that *S. calcarata* can be a complex of at least three species: (1) Far Eastern clade (2) West Asian clade and a single specimen from Germany, (3) Euro-Siberian clade. Additionally, specimen from Stavropol Province, a clade with two specimens from Germany and specimen from Germany in the West Asian clade form separate clades in some analyses.

Stenodema pilosa also can be a species complex. In the analyses with Nearctic specimens (COI dataset and full dataset) the Palearctic representatives of this species are placed in a single species, and Nearctic sequences are grouped in two or three species.

Stenodema laevigata was subdivided into different number of species depending on the analysis. All analyses based on 16S rRNA, ABGD analysis based on COI and GMYC analysis based on the reduced dataset with both markers, and GMYC, PTP and bPTP analyses for the full dataset place all representatives of this species together. Specimen from Crimea, specimen from Iran and the clade formed by the specimens from Voronezh Province, Greece and Germany are assigned in separated species each by some analyses. Additionally, the specimens from Greece also appeared as a separate species in few cases.

Analyses based on COI and full dataset result in three species within *S. holsata*: (1) all specimens from France, (2) specimen from Karachay-Cherkessia, (3) specimens from northern and Central European areas. Only four specimens (one from Karachay-Cherkessia and three from northern European areas) are included in the analyses based on 16S rRNA and reduced dataset. The analysis based on the reduced dataset shows that the specimen from Karachay-Cherkessia forms a separate species, the analysis based on 16S rRNA places all specimens of *S. holsata* into a single species.

Interspecific genetic distances

Interspecific distances are 6–17% for COI and 5–12% for 16S rRNA, and they are provided in Suppl. material 4. The lowest distances for COI are between *S. turanica* and *S. virens* (6–7%). Those two species also have relatively low genetic differences with Nearctic species *S. pilosipes* and *S. vicina* (~ 7–8%). The highest distances for COI are between *S. pilosa* and *S. rubrinervis* (15–17%). For 16S rRNA, the distances between the two species pairs *S. sibirica* — *S. ribrinerve* and *S. turanica* — *S. viren*s are the lowest (~ 5%), and the highest distances are between *S. pilosa* and *S. virens* (11–12%).

Intraspecific genetic distances

For the COI analysis, seven, three and four specimens are included, respectively for *S. sibirica*, *S. turanica* and *S. virens* (Suppl. material 4). Although the specimens of *S. sibirica* and *S. virens* were collected in different regions (*S. sibirica*: from Altay to South Korea, *S. virens* from Finland, Caucasus, and Irkutsk Province), the diversity of their sequences is very low for both markers (< 0.12%). The COI sequences for *S. turanica* collected in Iran and Tyva Republic are identical. For 16S rRNA, a single specimen of *S. turanic*a is included. There are five specimens of *S. sibirica* and two sequences of *S. virens*, and genetic distances within these species are < 0.1%.

Stenodema holsata and *S. laevigata* have within species mean distance corresponding to 0.8–1.1% for COI and ~ 0.4% for 16S rRNA. The species delimitation analyses resulted in three groups within *S. holsata* for COI, and the distances between them are 1–4%. The largest number of groups delimited within *S. laevigata* is five for COI, and the distances between them are 1–3%.

The interspecific distances within *S. calcarata* and *S. pilosa* are the largest, ~4% for COI for both species, ~ 2% for 16S rRNA of *S. calcarata* and 0.1% for 16S rRNA of *S. pilosa*. The largest number of species resulted from the species delimitation analyses for *S. calcarata* and *S. pilosa* using COI are five and four, respectively. The distances between the groups within S. *calcarata* are 7–9%, and between groups of *S. pilosa* are 2–6%. The species delimitation analysis based on the 16S rRNA dataset showed four groups within *S. calcarata*, and the distances between them are 3–4%.

Discussion

There are 57 species placed within *Stenodema*. In this work we focused on the seven trans-Palearctic species and provided their detailed morphological study. We compared them with other Palearctic and Nearctic species based on the material preserved at ZISP, MZH, and on previous publications. To facilitate the future work on this genus, we placed most of the Palearctic and Nearctic species into five groups based on the set of morphological characters (see Results sections). Among other Palearctic *Stenodema* species, *S. algoviensis*, *S. chinensis*, *S. crassipes*, *S. khentaica*, *S*, *nippon*, *S. plebeja*, and *S. sericans* distinctly differ from widely distributed Palearctic species. Information on other species is scarce. The results of the phylogenetic analyses based on the different datasets are mostly concordant, except for 16S rRNA. However, we consider the latter less reliable, because there is lower nucleotide diversity in this marker in comparison to COI.

We found that most of the species with wide distribution in the Palearctic can be identified using salient features, as well as male and female genitalia. Their monophyly was supported by the phylogenetic analyses. We synonymize *S. trispinosa* with *S. pilosa* (see Results for the details). The subgeneric composition of the genus is supported by the molecular data. Both species with spines on the hind femur, i.e., *S. pilosa* and *S. calcarata*, are contained in the subgenus *Brachystira*. They can be separated by many characters in external view, as well as male and female genitalia, and they form a well-supported clade. This group forms a reciprocal monophyly with the clade formed by all other species (subgenus *Stenodema*) in the analyses based on COI and combined datasets, although the analyses based on 16S rRNA do not support those results. In the phylogenies, *S. holsata* is close to *S. laevigata* and *S. sericans*. However, morphologically it is very similar to *S. algoviensis*, and the molecular data for the latter are needed to confirm those relationships. There are also some species from China, which might be close to either *S. holsata* or *S. laevigata*.

The species with the protruding frons (*S. rubrinervis*, *S. sericans*, *S. sibirica*, *S. turanica*, *S. vicina*, *S. virens*) form a clade in all phylogenies, except for the one, based on 16S rRNA.

Stenodema turanica and *S. virens* have minor differences in the external view, however, they differ in the male and female genitalia, and they form sister groups in the phylogenies. Most Nearctic *Stenodema* species are similar to those two species morphologically. This is also confirmed by the molecular based phylogenies based on COI and combined datasets, where *S. vicina* and *S. pilosipes* form a clade with *S. turanica* and *S. virens*. Some species described from China also might be part of this group.

Stenodema sibirica is very similar to *S. rubrinervis*, their differences in external view are also minor, and we could not find any reliable difference in the genitalia structures. Molecular studies show that those two species distinctly diverged from each other. Most of the species known from Asia (Hoberlandt 1960; Zheng 1981a; Tang 1994; Yasunaga 2019) can be closer to *S. sibirica* rather than to other widely distributed Palearctic species, and some of them might be synonymous with it.

The species delimitation analyses never place the specimens belonging to different species together, except for the Nearctic *S. pilosipes* and *S. vicina*. The interspecific distances are relatively high (> 6% for COI and > 4% for 16S rRNA). Although barcoding regions does not always fit for the species delimitation studies, including Miridae groups (e.g., Toews and Brelsford 2012; Jäckel et al. 2013; Namyatova et al. 2023), it can be reliable for those purposes in *Stenodema*. Hybridization is unlikely between the studied species. Another marker, 16S rRNA, shows less diversity than COI, and the phylogenetic results based on those two markers do not entirely correspond. However, 16S rRNA also confirms the monophyly of the widespread Palearctic species.

Stenodema calcarata, *S. holsata*, *S. laevigata*, and *S. pilosa* show intraspecific structure and at least some species delimitation analyses split them into two or more groups. In all those species the morphological evidence to support those lineages were not found. In *S. holsata* and *S. laevigata* the differences between the subclades are much less than intraspecific differences (1–4% and 1–3% in COI, respectively). The differences between some groups of *S. calcarata* and *S. pilosa* might suggest the presence of the cryptic species. The differences in COI between Palearctic and all Nearctic groups of *S. pilosa* is 4–5%, and the differences between Nearctic groups reaches 6–7%, which is comparable to the differences between *S. turanica* and *S. virens* (~ 6–7%), and between *S. virens* and *S. vicina* (~ 7%). The differences between *S. calcarata* groupings are more pronounced and reach 7–8% for COI and 3–4% for 16S rRNA.

In previous works, interspecific differences within widely distributed species of other Mirinae were studied for the *Lygus* species only: *L. gemellatus* (Herrich-Schaeffer, 1835), *L. pratensis* (Linnaeus, 1758), *Lygus rugulipennis* Poppius, 1911, and *L. wagneri* Remane, 1955 (Namyatova et al. 2023). All those taxa are known from Europe and Asia. Among them, only the trans-Holarctic *L. rugulipennis* has significant intraspecific structure.

In *Stenodema* at least *S. calcarata* and *S. pilosa* have deep population structure with the genetic differences between the clades comparable to the intraspecific differences. The structure within *S. holsata* and *S. laeviagata* is also present, but not so pronounced. However, our results are also affected by the geographic range of the specimens included in the analysis. *Stenodema calcarata*, *S. holsata* and *S. pilosa* inhabit East Asia (Kerzhner and Josifov 1999; Yasunaga 2019); however, only specimens of *S. calcarata* from this region were included in the analysis and they form a distinct clade. Specimens from Siberia were included for both *S. calcarata* (Altay Province) and *S. pilosa* (Yakutia), but in both cases they cluster with the European specimens. There is a clade within *L. rugulipennis*, which comprises specimens from the Far East, Siberia, and Northern Europe (Namyatova et al. 2023). Other species with trans-Palearctic distribution (*L. gemellatus*, *L. punctatus*, *L. wagneri*) have very shallow intraspecific structure.

The specimens from Caucasus and East Asia might represent isolated lineages in *Stenodema*. In *S. calcarata* there is a clade, comprising specimens from Georgia, Iran, Turkey, but it also comprises single specimen from Germany. The specimens of *S. holsata* from Karachay-Cherkessia and specimens of *S. laevigata* from Iran have many unique substitutions. Those results might suggest a presence of refugia at least in southern side of Caucasus and East Asia, which was also hypothesized for other insects (e.g., Wahlberg and Saccheri 2007; Eberle et al. 2021).

In *S. holsata*, the specimens from South Europe (France) form a separate lineage. Lineages of the specimens from South Europe were not found in other studied species.

In *S. laevigata*, there is a clade, formed by the specimens from Greece, Voronezh Province, and Germany. Additionally, specimen from Crimea have unique substitutions. In *L. rugulipennis* two specimens from Voronezh Province also distinctly differ from other specimens of their species, however, they do not cluster with the specimens from Germany or southern Europe (Namyatova et al. 2023). Those results might suggest that South Europe, Voronezh Province, and Crimea also could serve as refugia.

We did not find noticeable differences between the sequences within *S. virens*, *S. turanica*, and *S. sibirica*, even though specimens from different regions were included in the analyses. More specimens of those species should be analyzed to draw any conclusions on their intraspecific differences.

Schwartz (2008) provided morphology-based phylogenetic analysis and revision of Stenodemini, where he delimited *Stenodema* group with predominantly Nearctic distribution. Among 10 genera within this group only *Stenodema* inhabits other regions. The fact that *Stenodema* is much more diverse in the Palearctic than in the Nearctic and the phylogenies obtained in this work, suggest that this genus originated in the Palearctic. Its representatives migrated to the Nearctic at least three times. First, the ancestors of the Nearctic species from the clade, comprising *S. pilosipes*, *S. turanica*, *S. vicina*, and *S. virens*, migrated to the Nearctic. Second, the ancestor of *S. pilosa* also migrated to the Nearctic, and, third, some its representatives formed a separate lineage in the Palearctic. Therefore, we hypothesize that in *Stenodema* the migration occurred in both directions. Another Holarctic genus, *Lygus*, most probably, originated in the Nearctic, and then migrated to the Palearctic at least two times (Namyatova et al. 2023). Therefore, the migration routes in Miridae genera occurred in both directions.

Studies on *Lygus* and *Stenodema* showed that the gene flow between the Nearctic and Palearctic lineages of the same or closely related species is unlikely. In other insects with a Holarctic distribution, Nearctic and Palearctic representatives can be genetically separated from each other (e.g., Martin et al. 2002; Maresova et al. 2019; Francuski et al. 2021), or the gene flow can persist between Nearctic and Palearctic populations of the same species (e.g., Kohli et al. 2018, 2021; Zubrii et al. 2022).

Acknowledgements

We thank Heidi Viljanen (FMNH) for providing the last author access to the collection at FMNH. We are grateful to Stefen Roth (University Museum of Bergen, Bergen, Norway), Reza Hosseini (Guilan University, Rasht, Iran), Armand Matocq (Muséum national d'Histoire naturelle, Paris, France), Viktor Golub (Voronezh State University, Voronezh Province, Russia), Dmitry Gapon, Sergey Belokobylskij, Vladimir Lukhtanov (ZISP), Veronica Tyts, and Shamil Davletshin (St Petersburg State University, Russia) for providing the material for this study. We are also grateful for the administration and stuff of the following nature reserves for assisting us and our colleagues with the specimens collecting: Orenburg Nature Reserve (Orenburg Province), Tigirekskiy National Reserve (Altai Territory), Karadag Nature Reserve (Crimea), Belogorye State Nature Reserve

(Belgorod Province), Nora Nature Reserve (Amur Province), Sebezhsky National Park (Pskov Province), Bureinskiy Nature Reserve (Khabarovsk Territory), Teberda Nature Reserve (Karachay-Cherkessia Republic), Pribaykalsky National Park (Irkutsk Province). We thank Alexey Solodovnikov (Natural History Museum of Denmark, University of Copenhagen, Denmark) who organized two expeditions where some specimens for this research were collected. We also thank administration of Murmansk Marine Biological Institute of the Russian Academy of Sciences (Murmansk Province, Russia) for assisting AN with collecting specimens in Dalnie Zelentsy station. We thank Maria Vishnevskaya (St Petersburg State University) and Valeria Khabibulina (ZISP) for assisting with the molecular work. Attilio Carapezza (Università degli Studi di Palermo, Italy) and Michael Schwartz (The Canadian National Collection of Insects, Arachnids and Nematodes of Agriculture and Agri-Food Canada) provided helpful comments that have substantially improved the manuscript.

Additional information

Conflict of interest

The authors have declared that no competing interests exist.

Ethical statement

No ethical statement was reported.

Funding

The study is supported by the Russian Foundation for Basic Research, project number 20-54-56011. We thank Heidi Viljanen (FMNH) for providing access to the collection at FMNH.

Author contributions

A.A. Namyatova and F.V. Konstantinov designed the study. A.A. Namyatova contributed to the laboratory work, completed all the analyses, morphological studies, SEM imaging, drawings and created the first draft of the manuscript. P.A. Dzhelali completed the measurements and tables. A.A. Namyatova and P.A. Dzhelali completed the plates and specimen databasing. F.V. Konstantinov and P.A. Dzhelali completed the photographs. All authors contributed to the manuscript editing.

Author ORCIDs

Anna A. Namyatova https://orcid.org/0000-0001-9678-3430
Polina A. Dzhelali https://orcid.org/0000-0002-0741-3655
Fedor V. Konstantinov https://orcid.org/0000-0002-7013-5686

Data availability

All of the data that support the findings of this study are available in the main text or Supplementary Information.

References

Angulo A, Icochea J (2010) Cryptic species complexes, widespread species and conservation: lessons from Amazonian frogs of the *Leptodactylus marmoratus* group

(Anura: Leptodactylidae). Systematics and Biodiversity 8(3): 357–370. https://doi.org/10.1080/14772000.2010.507264

Aparicio-Puerta E, Gómez-Martín C, Giannoukakos S, Medina JM, Scheepbouwer C, García-Moreno A, Carmona-Saez P, Fromm B, Pegtel M, Keller A, Marchal JA, Hackenberg M (2022) sRNAbench and sRNAtoolbox 2022 update: Accurate miRNA and sncRNA profiling for model and non-model organisms. Nucleic Acids Research 50(W1): 710–717. https://doi.org/10.1093/nar/gkac363

Blair C, Bryson Jr RW (2017) Cryptic diversity and discordance in single-locus species delimitation methods within horned lizards (Phrynosomatidae: Phrynosoma). Molecular Ecology Resources 17(6): 1168–1182. https://doi.org/10.1111/1755-0998.12658

Bliven BP (1955) New phytophagous Hemiptera from Coast Range Mountains (Pentatomidae, Miridae, Cicadellidae, Psyllidae). Studies on Insects of the Redwood Empire 1: 8–14. [Published by the author, Eureka, California.]

Bliven BP (1958) Studies on insects of the Redwood Empire II: New Hemiptera and further notes on the *Colladonus* complex. Occidental Entomologist 1: 8–24.

Bouckaert R, Heled J, Kühnert D, Vaughan T, Wu CH, Xie D, Suchard MA, Rambaut A, Drummond AJ (2014) BEAST 2: A software platform for Bayesian evolutionary analysis. PLoS Computational Biology 10(4): e1003537. https://doi.org/10.1371/journal.pcbi.1003537

Carvalho JCM (1959) A catalogue of the Miridae of the world. Part IV. Arquivos do Museu Nacional, Rio de Janeiro 48: 1–384.

Cassis G, Schuh RT (2012) Systematics, biodiversity, biogeography, and host associations of the Miridae (Insecta: Hemiptera: Heteroptera: Cimicomorpha). Annual Review of Entomology 57(1): 377–404. https://doi.org/10.1146/annurev-ento-121510-133533

Davletshin SZ, Konstantinov FV (2024) Confocal laser scanning microscopy and three-dimensional reconstruction delimit species in a taxonomically challenging group: a revision of the plant bug genus *Anapus* Stål, 1858 (Heteroptera: Miridae). Insect Systematics & Evolution 55(1): 41–92. https://doi.org/10.1163/1876312X-bja10052

Eberle J, Husemann M, Doerfler I, Ulrich W, Müller J, Bouget C, Brin A, Gossner MM, Heilmann-Clausen J, Isacsson G, Krištín A, Lachat T, Larrieu L, Rigling A, Schmidl J, Seibold S, Vanderkerkhove K, Habel JC (2021) Molecular biogeography of the fungus-dwelling saproxylic beetle *Bolitophagus reticulatus* indicates rapid expansion from glacial refugia. Biological Journal of the Linnean Society. Linnean Society of London 133(3): 766–778. https://doi.org/10.1093/biolinnean/blab037

Fieber FX (1858) Criterien zur generischen Theilung der Phytocoriden (Capsini auct.). Wiener entomologische Monatschrift 2: 289–327, 329–347, 388[, 1 pl.].

Francuski L, Ludoški J, Milutinović A, Krtinić B, Milankov V (2021) Comparative phylogeography and integrative taxonomy of *Ochlerotatus caspius* (Dipera: Culicidae) and *Ochlerotatus dorsalis*. Journal of Medical Entomology 58(1): 222–240. https://doi.org/10.1093/jme/tjaa153

Fujisawa T, Barraclough TG (2013) Delimiting species using single-locus data and the Generalized Mixed Yule Coalescent approach: A revised method and evaluation on simulated data sets. Systematic Biology 62(5): 707–724. https://doi.org/10.1093/sysbio/syt033

Hoberlandt L (1960) Spedizione Italiana al Karakorum ed al Hindu-Kush (1954–1955). Primi Risultati dello studio delle Raccolte Zoologiche. Hemiptera-Heteroptera. Atti del museo civico di storia naturale di Trieste 22: 55–65.

Hortal J, de Bello F, Diniz-Filho JAF, Lewinsohn TM, Lobo JM, Ladle RJ (2015) Seven shortfalls that beset large-scale knowledge of biodiversity. Annual Review of Ecology, Evolution, and Systematics 46(1): 523–549. https://doi.org/10.1146/annurev-ecolsys-112414-054400

Horváth G (1905) Hémiptères nouveaux de Japon. Annales Historico-Naturales Musei Nationalis Hungarici 3: 413–423.

Jakovlev VE (1889) Insecta in itinere cl. N. Przewalski novissime lecta. XVI. Hemiptera Heteroptera. Horae Societatis Entomologicae Rossicae 24: 235–243.

Jäckel R, Mora D, Dobler S (2013) Evidence for selective sweeps by *Wolbachia* infections: phylogeny of *Altica* leaf beetles and their reproductive parasites. Molecular Ecology 22(16): 4241–4255. https://doi.org/10.1111/mec.12389

Jung S, Duwal RK, Lee S (2011) COI barcoding of true bugs (Insecta, Heteroptera). Molecular Ecology Resources 11(2): 266–270. https://doi.org/10.1111/j.1755-0998.2010.02945.x

Kelton LA (1961) Synopsis of the Nearctic species of *Stenodema* Laporte, and description of a new species from Western Canada (Hemiptera: Miridae). Canadian Entomologist 93(6): 450–455. https://doi.org/10.4039/Ent93450-6

Kerzhner IM (1988) Infraorder Cimicomorpha. 21. Family Miridae (Capsidae). In: Ler PA (Ed.) Keys to the identification of insects of the Soviet Far East. Vol. 2, Nauka, Leningrad, 778–857 [in Russian].

Kerzhner IM, Jaczewski TL (1964) Family Isometopidae. Family Miridae (Capsidae). In: Bei-Bienko GY (Ed.) Keys to the Insects of the European part of the USSR 1, Nauka, Moskova and Leningrad, 700–765 [In Russian].

Kerzhner IM, Josifov M (1999) Cimicomorpha II. In: Aukema B, Rieger C (Eds) Catalogue of the Heteroptera of the Palearctic Region, Vol. 3, Amsterdam, Netherlands Entomological Society, 577 pp.

Kim J, Jung S (2018) COI barcoding of plant bugs (Insecta: Hemiptera: Miridae). PeerJ 6: e6070. https://doi.org/10.7717/peerj.6070

Knyshov A, Konstantinov FV (2013a) A taxonomic revision of the genus *Hyoidea* (Hemiptera: Heteroptera: Miridae). Acta Entomologica Musei Nationalis Pragae 53(1): 1–32.

Knyshov A, Konstantinov FV (2013b) A taxonomic revision of the genus *Platycranus* Fieber, 1870 (Hemiptera: Heteroptera: Miridae: Orthotylinae). Zootaxa 3637(3): 201–253. https://doi.org/10.11646/zootaxa.3637.3.1

Kohli MK, Sahlén G, Kuhn WR, Ware JL (2018) Extremely low genetic diversity in a circumpolar dragonfly species, *Somatochlora sahlbergi* (Insecta: Odonata: Anisoptera). Scientific Reports 8(1): 15114. https://doi.org/10.1038/s41598-018-32365-7

Kohli M, Djernæs M, Herrera MS, Sahlen G, Pilgrim E, Simonsen TJ, Olsen K, Ware J (2021) Comparative phylogeography uncovers evolutionary past of Holarctic dragonflies. PeerJ 9: e11338. https://doi.org/10.7717/peerj.11338

Konstantinov FV (2000) Structure of the male genitalia in plant bugs (Heteroptera: Miridae) and its significance for suprageneric classification. Dissertation, St. Petersburg State University. [in Russian]

Konstantinov FV (2003) Male genitalia in Miridae (Heteroptera) and their significance for suprageneric classification of the family. Part I: General review, Isometopinae and Psallopinae. Belgian Journal of Entomology 5: 3–36.

Konstantinov FV (2008) Review of *Solenoxyphus* Reuter, 1875 (Heteroptera: Miridae: Phylinae). American Museum Novitates 2008(3607): 1–42. https://doi.org/10.1206/0003-0082(2008)3607[1:ROSRHM]2.0.CO;2

Konstantinov FV (2019) Revision of *Agraptocoris* Reuter (Heteroptera: Miridae: Phylinae), with description of five new species and a review of aedeagal terminology. Arthropod Systematics & Phylogeny 77(1): 87–124. https://doi.org/10.26049/ASP77-1-2019-05

Konstantinov FV, Neimorovets VV, Korzeev AI (2016) Review of *Campylomma* from Russia, Caucasus, and Central Asia with description of two new species (Hemiptera: Heteroptera: Miridae: Phylinae). Entomologica Americana (New York, N.Y.) 122(1–2): 115–155. https://doi.org/10.1664/15-RA-046

Lattin JD, Oman P (1983) Where are the exotic insect threats. In: Wilson CL, Graham CL (Eds) Exotic plant pests and North American agriculture. Academic, New York, 93–137. https://doi.org/10.1016/B978-0-12-757880-4.50010-5

Maresova J, Habel JC, Neve G, Sielezniew M, Bartonova A, Kostro-Ambroziak A, Fric ZF (2019) Cross-continental phylogeography of two Holarctic Nymphalid butterflies, *Boloria eunomia* and *Boloria selene*. PLoS ONE 14(3): e0214483. https://doi.org/10.1371/journal.pone.0214483

Martin J, Guryev V, Blinov A (2002) Population variability in *Chironomus* (*Camptochironomus*) species (Diptera, Nematocera) with a Holarctic distribution: Evidence of mitochondrial gene flow. Insect Molecular Biology 11(5): 387–397. https://doi.org/10.1046/j.1365-2583.2002.00348.x

Matocq A, Pluot-Sigwalt D (2012) Révision des *Amblytylus* et essai de mise au point sur les genres *Amblytylus* Fieber et *Megalocoleus* Reuter (Heteroptera: Miridae: Phylinae). Annales de la Société Entomologique de France 48(1/2): 123–154. https://doi.org/10.1080/00379271.2012.10697760

Menard KL, Schuh RT, Woolley JB (2014) Total-evidence phylogenetic analysis and reclassification of the Phylinae (Insecta: Heteroptera: Miridae), with the recognition of new tribes and subtribes and a redefinition of Phylini. Cladistics 30(4): 391–427. https://doi.org/10.1111/cla.12052

Muminov NN (1989) Species of the genus *Stenodema* (Heteroptera: Miridae) from the USSR and Mongolia. Insects of Mongolia 10: 126–135. [in Russian]

Namyatova AA (2010) Revision of the genus *Pachytomella* (Heteroptera: Miridae: Orthotylinae: Halticini). Acta Entomologica Musei Nationalis Pragae 50(2): 341–368.

Namyatova AA, Konstantinov FV (2009) Revision of the genus *Orthocephalus* Fieber, 1858 (Hemiptera: Heteroptera: Miridae: Orthotylinae). Zootaxa 2316(1): 1–118. https://doi.org/10.11646/zootaxa.2316.1.1

Namyatova AA, Schwartz MD, Cassis G (2021) Determining the position of *Diomocoris*, *Micromimetus* and *Taylorilygus* in the *Lygus*-complex based on molecular data and first records of *Diomocoris* and *Micromimetus* from Australia, including four new species (Insecta: Hemiptera: Miridae: Mirinae). Invertebrate Systematics 35(1): 90–131. https://doi.org/10.1071/IS20015

Namyatova AA, Tyts VD, Bolshakova DS (2023) Identification and delimitation of the trans-Palearctic *Lygus* species (Insecta: Heteroptera: Miridae) using integrative approach. Insect Systematics & Evolution 54(2): 146–192. https://doi.org/10.1163/1876312X-bja10035

Nonnaizab, Jorigtoo (1994) A preliminary study of *Stenodema* Laporte (Hemiptera: Miridae) from Inner Mongolia, China. Entomotaxonomia 16: 85–90.

Pante E, Schoelinck C, Puillandre N (2015) From integrative taxonomy to species description: one step beyond. Systematic Biology 64(1): 152–160. https://doi.org/10.1093/sysbio/syu083

Pons J, Barraclough TG, Gomez-Zurita J, Cardoso A, Duran DP, Hazell S, Kamoun S, Sumlin WD, Vogler AP (2006) Sequence-based species delimitation for the DNA taxonomy of undescribed insects. Systematic Biology 55(4): 595–609. https://doi.org/10.1080/10635150600852011

Puillandre N, Lambert A, Brouillet S, Achaz G (2012) ABGD, Automatic Barcode Gap Discovery for primary species delimitation. Molecular Ecology 21(8): 1864–1877. https://doi.org/10.1111/j.1365-294X.2011.05239.x

Rambaut A, Drummond AJ, Xie D, Baele G, Suchard MA (2018) Posterior niversityon in Bayesian phylogenetics using Tracer 1.7. Systematic Biology 67(5): 901–904. https://doi.org/10.1093/sysbio/syy032

Raupach MJ, Hendrich L, Küchler SM, Deister F, Morinière J, Gossner MM (2014) Building-up of a DNA barcode library for true bugs (Insecta: Hemiptera: Heteroptera) of Germany reveals taxonomic uncertainties and surprises. PLoS ONE 9(9): e106940. https://doi.org/10.1371/journal.pone.0106940

Reid NM, Carstens BC (2012) Phylogenetic estimation error can decrease the accuracy of species delimitation: A Bayesian implementation of the general mixed Yule-coalescent model. BMC Evolutionary Biology 12(1): 1–11. https://doi.org/10.1186/1471-2148-12-196

Reuter OM (1891) Hemiptera Heteroptera fran trakterna kring Sajanska bärgskedjan, insamlade af K. Ehnberg och R. Hammarström, förtecknade. Öfversigt af Finska Vetenskapssocietetens Förhandlingar 33: 166–208.

Reuter OM (1904) Synopsis speciarum *Stenodema*-Arten Lap., m. Öfversigt af Finska Vetenskapssocietetens Förhandlingar 46(15): 1–21.

Ronquist F, Teslenko M, Van Der Mark P, Ayres DL, Darling A, Höhna S, Huelsenbeck JP (2012) MrBayes 3.2: Efficient Bayesian phylogenetic inference and model choice across a large model space. Systematic Biology 61(3): 539–542. https://doi.org/10.1093/sysbio/sys029

Roslin T, Somervuo P, Pentinsaari M, Hebert PD, Agda J, Ahlroth P, Anttonen P, Aspi J, Blagoev G, Blanco S, Chan D, Clayhills T, deWaard J, deWaard S, Elliot T, Elo R, Haapala S, Helve E, Ilmonen J, Hirvonen P, Ho C, Itämies J, Ivanov V, Jakovlev J, Juslén A, Jussila R, Kahanpää J, Kaila L, Jari-PekkaKaitila, Kakko A, Kakko I, Karhu A, Karjalainen S, Kjaerandsen J, Koskinen J, Laasonen EM, Laasonen L, Laine E, Lampila P, Levesque-Beaudin V, Lu L, Lähteenaro M, Majuri P, Malmberg S, Manjunath R, Martikainen P, Mattila J, McKeown J, Metsälä P, Miklasevskaja M, Miller M, Miskie R, Muinonen A, Veli-MattiMukkala, Naik S, Nikolova N, Nupponen K, Ovaskainen O, Österblad I, Paasivirta L, Pajunen T, Parkko P, Paukkunen J, Penttinen R, Perez K, Pohjoismäki J, Prosser S, Raekunnas M, Rahulan M, Rannisto M, Ratnasingham S, Raukko P, Rinne A, Rintala T, Miranda Romo S, Salmela J, Salokannel J, Savolainen R, Schulman L, Sihvonen P, Soliman D, Sones J, Steinke C, Ståhls G, Tabell J, Tiusanen M, Várkonyi G, Vesterinen EJ, Viitanen E, Vikberg V, Viitasaari M, Vilen J, Warne C, Wei C, Winqvist K, Zakharov E, Mutanen M (2022) A molecular-based identification resource for the arthropods of Finland. Molecular Ecology Resources 22(2): 803–822. https://doi.org/10.1111/1755-0998.13510

Sanchez JA, Cassis G (2018) Towards solving the taxonomic impasse of the biocontrol plant bug subgenus *Dicyphus* (*Dicyphus*) (Insecta: Heteroptera: Miridae) using molecular, morphometric and morphological partitions. Zoological Journal of the Linnean Society 184(2): 330–406. https://doi.orgc/10.1093/zoolinnean/zly005

Satler JD, Carstens BC, Garrick RC, Espíndola A (2021) The phylogeographic shortfall in hexapods: A lot of leg work remaining. Insect Systematics and Diversity 5(5): 1. https://doi.org/10.1093/isd/ixab015

Schuh RT (1995) Plant bugs of the world (Insecta: Heteroptera: Miridae). Systematic catalog, distributions, host list, and bibliography. New York Entomological Society, [i–xii,] 1–1329.

Schuh RT (2013) On-line Systematic Catalog of Plant Bugs (Insecta: Heteroptera: Miridae). http://research.amnh.org/pbi/catalog/ [accessed February 15, 2024]

Schwartz MD (1987) Phylogenetic revision of Stenodemini with a review of the Mirinae. PhD thesis. The City University of New York, New York, USA.

Schwartz MD (2008) Revision of the Stenodemini with a review of the included genera (Hemiptera: Heteroptera: Miridae: Mirinae). Proceedings of the Entomological Society of Washington 110(4): 1111–1201. https://doi.org/10.4289/0013-8797-110.4.1111

Stamatakis A (2014) RAxML Version 8: A tool for phylogenetic analysis and post-analysis of large phylogenies. Bioinformatics 30(9): 1312–1313. https://doi.org/10.1093/bioinformatics/btu033

Taberlet P, Zimmermann NE, Englisch T, Tribsch A, Holderegger R, Alvarez N, Niklfeld H, Coldea G, Mirek Z, Moilanen A, Ahlmer W, Marsan PA, Bona E, Bovio M, Choler P, Cieślak E, Colli L, Cristea V, Dalmas J-P, Frajman B, Garraud L, Gaudeul M, Gielly L, Gutermann W, Jogan N, Kagalo AA, Korbecka G, Küpfer P, Lequette B, Letz DR, Manel S, Mansion G, Marhold K, Martini F, Negrini R, Niño F, Paun O, Pellecchia M, Perico G, Piękoś-Mirkowa H, Prosser F, Puşcaş M, Ronikier M, Scheuerer M, Schneeweiss GM, Schönswetter P, Schratt-Ehrendorfer L, Schüpfer F, Selvaggi A, Steinmann K, Thiel-Egenter C, van Loo M, Winkler M, Wohlgemuth T, Wraber T, Gugerli F (2012) Genetic diversity in widespread species is not congruent with species richness in alpine plant communities. Ecology Letters 15(12): 1439–1448. https://doi.org/10.1111/ele.12004

Tamanini L (1982) Gli eterotteri dell'Alto Adige (Insecta: Heteroptera). Studi Trentini di Scienze Naturali. Acta Biologica 59: 65–194.

Tamura K, Stecher G, Kumar S (2021) MEGA11: Molecular evolutionary genetics analysis version 11. Molecular Biology and Evolution 38(7): 3022–3027. https://doi.org/10.1093/molbev/msab120

Tang ZH (1994) Two new species of Stenodemini (Hemiptera: Miridae) from China. Entomotaxonomia 6: 15–18.

Toews DP, Brelsford A (2012) The biogeography of mitochondrial and nuclear discordance in animals. Molecular ecology 21(16): 3907–3930. https://doi.org/10.1111/j.1365-294X.2012.05664.x

Vinokurov NN, Kanyukova EV (1995) Heteroptera of Siberia. Nauka, Novosibirsk, 238 pp. [in Russian]

Vishnevskaya MS, Saifitdinova AF, Lukhtanov VA (2016) Karyosystematics and molecular taxonomy of the anomalous blue butterflies (Lepidoptera, Lycaenidae) from the Balkan Peninsula. Comparative Cytogenetics 10(5): 1–85. https://doi.org/10.3897/CompCytogen.v10i5.10944

Wagner E (1974) Die Miridae Hahn, 1831, des Mitelmeerraumes und der Makaronesischen Inseln (Hemiptera, Heteroptera). Teil. 1. Entomologische Abhandlungen 37 (Supplement): 1–484. https://doi.org/10.1515/9783112653241

Wagner E, Weber HH (1964) Héteroptères Miridae. "MDUL" In "MDNM": Faune de France 67: 1–592.

Wahlberg N, Saccheri I (2007) The effects of Pleistocene glaciations on the phylogeography of *Melitaea cinxia* (Lepidoptera: Nymphalidae). European Journal of Entomology 104(4): 675–684. https://doi.org/10.14411/eje.2007.085

Wheeler AG (2001) Biology of the plant bugs (Hemiptera: Miridae). pests, predators, opportunists. Cornell University Press, Ithaca, NY, 507 pp.

Wheeler AG, Henry TJ (1992) A synthesis of the Holarctic Miridae (Heteroptera): distribution, biology, and origin, with emphasis on North America. Entomological Society of America, The Thomas Say Foundation, Vol. XV, 282 pp.

Yang Z (2015) The BPP program for species tree estimation and species delimitation. Current Zoology 61(5): 854–865. https://doi.org/10.1093/czoolo/61.5.854

Yasunaga T (2019) Taxonomic review of the plant bug genus *Stenodema* in Japan, with description of a new species (Hemiptera: Heteroptera: Miridae). Heteropterus Revista de Entomología 19(2): 295–311.

Zhang J, Kapli P, Pavlidis P, Stamatakis A (2013) A general species delimitation method with applications to phylogenetic placements. Bioinformatics 29(22): 2869–2876. https://doi.org/10.1093/bioinformatics/btt499

Zheng LY (1981a) New species and new records of *Stenodema* Laporte from China (Hemiptera: Miridae). Entomotaxonomia 3: 57–64.

Zheng LY (1981b) Notes on *Stenodema* Laporte from China (Hemiptera: Miridae). Acta Scientiarum Naturalium Universitatis Nankaiensis 1: 92–98. [In Chinese with English summary]

Zheng LY (1992) Hemiptera: Miridae (Stenodemini). Insects of the Hengduan Mountains Region 1: 182–184.

Zheng L, Lu N, Liu G, Xu B (2004) Hemiptera: Miridae: Mirinae. Fauna Sinica. Insecta. Vol. 33. Science Press. Beijing, China, 797 [+ i–viii] pp. [in Chinese, English summary]

Zubrii NA, Filippov BY, Khruleva OA, Kondakov AV, Rybalov LB (2022) Nearctic species in the Palearctic: Trans-Beringian range, phylogeny and phylogeography of *Pterostichus* (*Cryobius*) *mandibularoides* (Coleoptera, Carabidae). Diversity 14(6): 415. https://doi.org/10.3390/d14060415

Supplementary material 1

List of examined non-type specimens of *Stenodema* spp.

Authors: Anna A. Namyatova, Polina A. Dzhelali, Fedor V. Konstantinov
Data type: pdf

Link: https://doi.org/10.3897/zookeys.1209.124766.suppl1

Supplementary material 2

Voucher information for the specimens used for the comparison and phylogenies of the Palearctic species

Authors: Anna A. Namyatova, Polina A. Dzhelali, Fedor V. Konstantinov
Data type: pdf

Link: https://doi.org/10.3897/zookeys.1209.124766.suppl2

Supplementary material 3

RaxML trees for individual and combined datasets

Authors: Anna A. Namyatova, Polina A. Dzhelali, Fedor V. Konstantinov
Data type: pdf

Link: https://doi.org/10.3897/zookeys.1209.124766.suppl3

Supplementary material 4

Genetic distances

Authors: Anna A. Namyatova, Polina A. Dzhelali, Fedor V. Konstantinov
Data type: pdf

Link: https://doi.org/10.3897/zookeys.1209.124766.suppl4

ZooKeys 1209: 295–314 (2024)
DOI: 10.3897/zookeys.1209.124184

Research Article

Description of five larvae of the genus *Gnaptorina* Reitter, 1887 from Xizang, China (Coleoptera, Tenebrionidae, Blaptinae), with molecular species delimitation and diagnoses

Bao-Yue Ji[1], Tong-Yang Guo[1], Mei-Chang Gu[1], Guo-Dong Ren[1], Xiu-Min Li[1]

1 *Key Laboratory of Zoological Systematics and Application of Hebei Province, College of Life Sciences, Institute of Life Science and Green Development, Hebei University, Baoding 071002, China*

Corresponding author: Xiu-Min Li (lixiumin@hbu.edu.cn)

Abstract

With 39 described species in three subgenera, the *Gnaptorina* is the second most species-rich genus in the subtribe Gnaptorinina (Tenebrionidae: Blaptinae). In this study, a phylogeny of *Gnaptorina* was reconstructed based on one nuclear (28S-D2) and three mitochondrial (COI, Cytb, and 16S) gene fragments; multiple molecular species delimitation approaches were also implemented to assess the taxonomic status of larval specimens based on COI gene fragment. Larvae of five known species of the subgenus *Hesperoptorina* are described and illustrated for the first time: *Gnaptorina nigera* Shi, Ren & Merkl, 2007, *Gnaptorina tishkovi* Medvedev, 1998, *Gnaptorina brucei* Blair, 1923, *Gnaptorina himalaya* Shi, Ren & Merkl, 2007, *Gnaptorina kangmar* Shi, Ren & Merkl, 2007. A key to larvae of four genera of the tribe Blaptini and a key to the known larvae of the genus *Gnaptorina* are provided. This study provides valuable morphological data for larval studies of the tribe Blaptini.

Key words: Beetles, Gnaptorinina, immature stage, morphology, species identification

Academic editor: Patrice Bouchard
Received: 29 March 2024
Accepted: 9 July 2024
Published: 14 August 2024

ZooBank: https://zoobank.org/D45D45AB-9525-4911-825D-900982CFE71C

Citation: Ji B-Y, Guo T-Y, Gu M-C, Ren G-D, Li X-M (2024) Description of five larvae of the genus *Gnaptorina* Reitter, 1887 from Xizang, China (Coleoptera, Tenebrionidae, Blaptinae), with molecular species delimitation and diagnoses. ZooKeys 1209: 295–314. https://doi.org/10.3897/zookeys.1209.124184

Introduction

The Gnaptorinina Medvedev, 2001 is a species-rich subtribe of Blaptini Leach, 1815, consisting of 189 species in 12 genera: *Agnaptoria* Reitter, 1887 (36 species and subspecies), *Asidoblaps* Fairmaire, 1886 (56 species), *Blaptogonia* Medvedev, 1998 (five species), *Colasia* Koch, 1965 (seven species), *Gnaptorina* Reitter, 1887 (39 species and subspecies), *Itagonia* Reitter, 1887 (24 species and subspecies), *Montagona* Medvedev, 1998 (three species), *Nepalindia* Medvedev, 1998 (five species), *Pseudognaptorina* Kaszab, 1977 (four species), *Sintagona* Medvedev, 1998 (one species), *Tagonoides* Fairmaire, 1886 (eight species), and *Viettagona* Medvedev & Merkl, 2003 (one species) (Medvedev and Merkl 2002; Medvedev 2004; Ren et al. 2016; Li et al. 2018, 2019; Chigray 2019; Iwan and Löbl 2020; Bai et al. 2020, 2023; Ji et al. 2024). With 39 described species, *Gnaptorina* is the second most species-rich genus in the subtribe Gnaptorinina. The genus *Gnaptorina* is currently subdivided into three subgenera: *Gnaptorina* Reitter, 1887, *Austroptorina* Bai, Li & Ren, 2020, and *Hesperoptorina* Medvedev, 2009 (Medvedev 2009; Li et al. 2021). To date, immature stages of six species in three genera are described within Gnaptorinina: *Gnaptorina* Reitter, 1887 (larvae of three species), *Agnaptoria* Reitter, 1887 (larvae of two species) and *Itagonia* Reitter, 1887 (larva of one species) (Yu et al. 1996, 1999; Medvedev 2006; Zhu and Ren 2014; Ji et al. 2024). Larval morphology is important for understanding the systematics of different groups, and it has been used to support the close relationships of genera (Grebennikov and Scholtz 2004; Lawrence et al. 2011; Kamiński et al. 2019), including for supraspecific classification of the tribe Blaptini (Skopin 1960; Chigray and Kirejtshuk 2023). However, the larvae were described for only a few species of Blaptini.

In this study, we constructed a molecular phylogenetic tree for the genus *Gnaptorina* and a molecular species delimitation, combining them to verify the taxonomic status of larval specimens. These larvae belong to the five known species of the subgenus *Hesperoptorina* of the genus *Gnaptorina*. Larvae of these five species are described and illustrated. The present results will enrich the existing mitochondrial gene library of the tribe Blaptini and lay the foundation for future evolutionary study of the endemic insects on the Qinghai-Xizang Plateau.

Materials and methods

Morphological examination

In total, 170 larval samples of five species were examined for this study, which are deposited at the Museum of Hebei University, Baoding, China (**MHBU**). The larvae used for the description above were inferred to be in their older instar stage based on previous research on the larval biology of the Blaptini.

The photos were taken with the following imaging system: (a) Canon EOS 5D Mark III (Canon Inc., Tokyo, Japan) connected to a Laowa FF 100 mm F2.8 CA-Dreamer Macro 2× or Laowa FF 25 mm F2.8 Ultra Macro 2.5–10× (Anhui Changgeng Optics Technology Co., Hefei, China). (b) A Leica M205A stereomicroscope equipped with a Leica DFC450 camera (Leica Microsystems, Singapore) was controlled using the Leica application suite v. 4.3; (c) JVC KY-F75U (JVC Kenwood, Long Beach, CA, USA) digital camera attached to a Leica Z16 APO dissecting microscope (Leica Microsystems, Buffalo Grove, IL, USA) with an apochromatic zoom objective and motor focus drive, using a Syncroscopy Auto-Montage System (Synoptics, Cambridge, UK) and software. Multiple images were stacked to construct the final figures. Photographed specimens were illuminated with either an LED ring light attached to the end of the microscope column, with incidental light filtered to reduce glare, or by a gooseneck illuminator with bifurcating fibreoptics; image stacks were white-balance corrected using the system software (Synoptics, Cambridge, UK). Montaged images were edited using Adobe Photoshop v. 22.1.0 to form the final figure plates.

Label data are presented verbatim. A slash (/) separates text on different lines of label.

Taxon sampling, DNA extraction, PCR amplification, and sequencing

Larval specimens were collected in the field from Xizang, China. To correlate the different stages, the molecular data were obtained from larval individuals.

DNA was extracted from pygopod tissue of the larva using the Insect DNA Isolation Kit (BIOMI-GA, Hangzhou, China) following the manufacturer's protocols. The DNA extracted was stored at -20 °C. Fragment of mitochondrial molecular marker (cytochrome oxidase subunit I, COI) was amplified with the primers F 2183 and R 3014 (Folmer et al. 1994). The profile of the PCR amplification consisted of an initial denaturation step at 94 °C for 4 min, 35 cycles of denaturation at 94 °C for 45 s, annealing at 47 °C for 1.5 min, an extension at 72 °C for 1 min, and a final 8 min extension step at 72 °C. PCR was performed using TaKaRa Ex Taq (TaKaRa, Dalian, China). PCR products were subsequently checked by 1% agarose gel electrophoresis and sequencing was performed at General Biol Co. (Anhui, China). Finally, we obtained five sequences for five larvae. Detailed information for the new samples in this study is provided in Table 1.

Table 1. List of larvae examined in this study with the corresponding accession number.

Species	Sampling locality	Elevation (m)	Date of collection	Collector(s)	Accession number
G. nigera	Damxung County, Xizang, China (XZDX)		23.VII.2014	G. Ren et al.	PQ013187
G. tishkovi	Qomolangma, Tingri County, Xizang, China (XZDR)	4960	20.VII.2023	X. Bai et al.	PQ013187
G. brucei	Tingri County, Xizang, China (XZDR)	4820	28.VII.2014	G. Ren et al.	PQ013185
G. kangmar	Gyangzê County, Xizang, China (XZJZ)		6.VIII.2014	G. Ren et al.	PQ013184
G. himalaya	Qusum County, Xizang, China (XZSN)	4790	31.VII.2019	X. Li et al.	PQ013185

Phylogenetic analyses

In total, we used 306 sequences from 88 individuals, including 301 published sequences (from 81 adults, one larva, one pupa) and five new sequences from larvae (Li et al. 2021; Ji et al. 2024). We used the previously published sequences of two species of Platyscelidini Lacordaire, 1859 as outgroups, which have been considered as close relatives of the tribe Blaptini (Kamiński et al. 2021).

The phylogenetic tree was constructed based on concatenated datasets of mitochondrial and nuclear DNA sequences (COI, Cytb, 16S, and 28S-D2) by Maximum Likelihood (ML). A best-fit model was tested according to the corrected Akaike's Information Criterion (AIC) using ModelFinder (included in IQ-TREE) with the software PhyloSuite v. 1.2.2 (Zhang et al. 2020). The ML tree search was performed in IQ-TREE v. 1.6.8 (Nguyen et al. 2015) that was also plugged into PhyloSuite. The ML tree was inferred using an edge-linked partition model for 5000 ultrafast bootstraps (1000 replicates) (Minh et al. 2013). Support for each node is represented by ultrafast bootstrap values (uBV).

Molecular species delimitation analyses

Recent studies have shown that some molecular species definition methods may underestimate or overestimate the number of species (Dellicour and Flot 2018; Luo et al. 2018). Hence, it has been advocated to use them in a complementary way to better assess species boundaries. Here, we used a combination of three distinct methods (ASAP, GMYC, and PTP) to assess the boundaries of species within *Gnaptorina*.

We relied on the Assemble Species by Automatic Partitioning (ASAP) approach as implemented on the online web application (https://bioinfo.mnhn.

fr/abi/public/asap/asapweb.html, Puillandre et al. 2021). ASAP analysis was carried out based on COI gene fragment, and outgroups were excluded. In addition to the distance-based ASAP method, we also performed tree-based analyses using two distinct methods: the General Mixed Yule Coalescent (GMYC) model and Poisson-tree-processes (PTP) (Pons et al. 2006; Zhang et al. 2013). Accordingly, GMYC analysis was conducted on an ultrametric tree from the BEAST analysis, with all outgroups removed. The analysis was conducted in R using the package GMYC with default settings (100 trees randomly selected, 250 million generations with a burn-in of 25 million and a thinning parameter of 100). PTP analysis relied on the best-score ML tree from the IQ-TREE analysis and was carried out on the web server of the Exelixis Lab (http://species.h-its.org/ptp/) using default settings.

Results

Phylogenetic relationships and species delimitation

The final, the IQ-TREE analysis yielded a topology based on concatenated dataset (2219 bp), including 306 sequences from 88 individuals (Fig. 1). The individuals of *Gnaptorina* were grouped into three well-supported clades: C1 (*Gnaptorina*, uBV = 76), C2 (*Austroptorina*, uBV = 100), and C3 (*Hesperoptorina*, uBV = 79). The monophyly of each subgenus was supported overall.

The ML tree and three molecular species delimitation methods associate the larvae and adults of different species with consistent results. Larva and known species cluster into a single well-supported clade respectively (uBV = 100). Three molecular species delimitation results showed that the samples XZDX01, XZDR02, XZDR03, XZJZ04, and XZSN05 consistently merged individuals from known species. Therefore, we conclude that the above assumption is correct: the sample XZDX01 is the larva of *G. nigera*, the sample XZDR02 is the larva of *G. tishkovi*, the sample XZDR03 is the larva of *G. brucei*, the sample XZJZ04 is the larva of *G. kangmar*, and the sample XZSN05 is the larva of *G. himalaya*.

Key to larvae of four genera of the tribe Blaptini

1 Epipharynx with six mastoids above the basal spines **2**
– Epipharynx with eight mastoids above the basal spines................ ***Itagonia***
2 Urogomphi conspicuous..**3**
– Urogomphi inconspicuous.. ***Gnaptorina***
3 Labrum with not less than 6 setae on apical part................................***Blaps***
– Labrum with less than 6 setae on apical part .... ***Prosodes***

Larval diagnosis of the genus *Gnaptorina* Reitter, 1887

The last segment is conical in shape; urogomphi are inconspicuous and the apex is truncated; body is brownish yellow, shiny, with ossified body wall and midline is distinct (Yu et al. 1999). Pairs of setae grow on each tergum. Labrum is transverse; apical part with six setae; anterior margin with two discal setae and lateral margin with sparse setae. Clypeus is trapezoidal, with two pairs of setae at apex and margin, respectively. Epicranial stem is Y- or V-shaped.

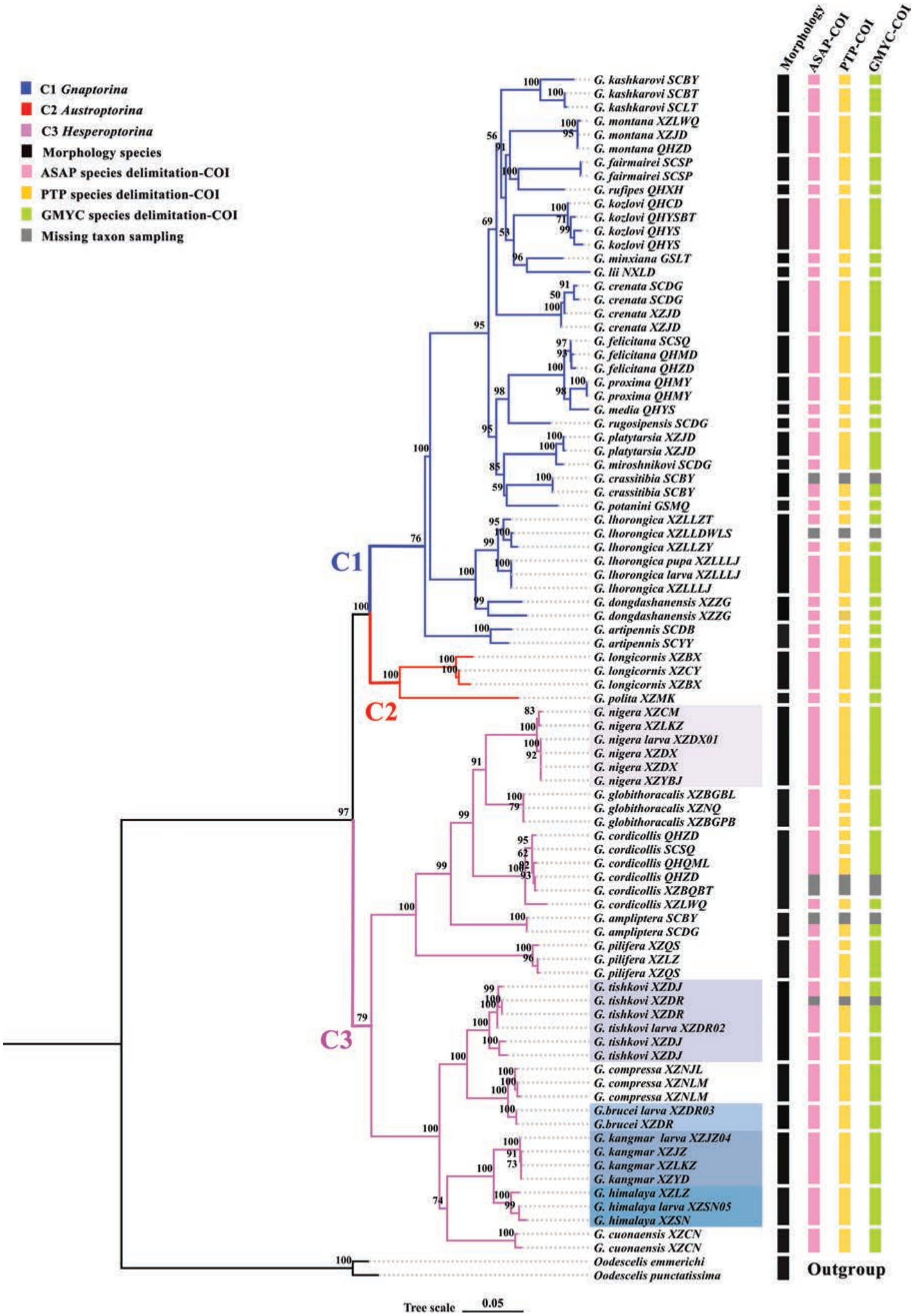

Figure 1. Maximum-likelihood phylogenetic tree based on 2219 bp of mitochondrial and nuclear DNA sequences (COI, Cytb, 16S, and 28S-D2) within the genus *Gnaptorina*. Vertical coloured bars delineate extant morphospecies (black), and the results of three separate molecular analyses delimiting species (pink, yellow. and pale green). For the analysis using COI gene, we used grey colour to delineate specimens for which sequencing failed.

Mandible membranous elevation with two setae. Maxillary palpi are three-segmented, with a seta inside and outside anterior margin of II. Labial palpi are two-segmented, prementum with two setae apically, mentum and submentum with sparse setae. Antennae are three-segmented, the apex of II is dilated and baseball-like, sensation circle C-shaped at apex of II, III is cylindrical, much narrower and shorter than I and II. Prothoracic leg is noticeably stronger, longer, and thicker than meso- and metathoracic legs; each tarsus has differentiated into a highly ossified tarsungulus and a weakly ossified base, with one seta internally at base and one short thick spine laterally; inner margin of each segment with a row of pectinate setae.

Key to the species of known larvae of the genus *Gnaptorina*

1 Mentum trapezoidal (Fig. 2A) **2**
– Mentum elongate hexagonal (Fig. 2B) **3**
2 Median line obvious on pro- and mesonotum .... ***G. kangmar***
– Median line obvious on thorax dorsally and abdominal tergite I ... ***G. himalaya***
3 Ocelli evident (Fig. 2C) **4**
– Ocelli inconspicuous (Fig. 2D) **7**
4 Antennal segment I longer than II **5**
– Antennal segment I shorter than II .... ***G. cylindricollis***
5 Submentum with 10 setae .... ***G. felicitana***
– Submentum with 6 setae **6**
6 Median line obvious on thorax dorsally .... ***G. nigera***
– Median line obvious on thorax dorsally and abdominal tergite I .... ***G. tishkovi***
7 Mentum with 2 setae .... ***G. lhorongica***
– Mentum with 12 setae .... ***G. brucei***

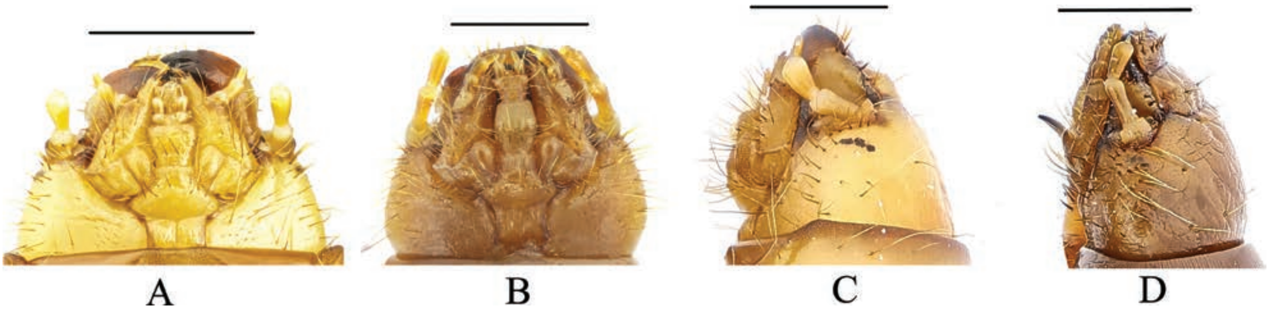

Figure 2. A head of *Gnaptorina himalaya*, ventral view **B** head of *G. brucei*, ventral view **C** head of *G. himalaya*, lateral view **D** head of *G. brucei*, lateral view. Scale bars: 1 mm.

Descriptions of larvae

Gnaptorina nigera Shi, Ren & Merkl, 2007

Examined materials. Larvae. 3 exx. (MHBU): Damxung County, Xizang/ 30°16.05’ N, 90°42.60’ E/ Alt. 4480 m/ 2023-VII-9/ Xiu-Min Li, Tong-Yang Guo leg.; 20 exx. (MHBU): Damxung County, Xizang/ 30°20.78’ N, 91°03.58’ E/ Alt. 4150m/ 2019-VIII-8/ Xiu-Min Li leg.; 31 exx. (MHBU): Yangbajain Township, Damxung County, Xizang/ 2014-VII-23/ Guo-Dong Ren, Xing-Long Bai, Jun-Sheng Shan leg.; 4 exx. (MHBU): Damxung County, Xizang/ 30°32.32’ N, 91°06.42’ E/ Alt. 4350m/

2019-VIII-9/ Xiu-Min Li leg.; 11 exx. (MHBU): Chamda Township, Nagarzê County, Xizang/ 29°00.48’ N, 91°04.87’ E/ Alt. 4540m/ 2019-VIII-8/ Xiu-Min Li leg.; 11 exx. (MHBU): Comai County, Xizang/ 28°50.92' N, 91°22.57' E/ Alt. 4490m/ 2023-VII-8/ Xiu-Min Li leg.; 6 exx. (MHBU): Daglung Township, Nagarzê County, Xizang/ 28°39.48' N, 90°28.10' E/ Alt. 4615m/ 2014-VIII-6/ Guo-Dong Ren, Xing-Long Bai, Jun-Sheng Shan leg.

Description. ***Body*** (Fig. 3A–C). Larvae length 17.2–17.5 mm, width 2.1–2.5 mm. Body subcylindrical; last segment conical; body brownish yellow, shiny, body wall ossified; median line obvious on thorax dorsally; pairs of setae grow on each tergum.

Head (Fig. 3E, D–G). Prognathous, slightly narrower than width of prothorax; labrum transverse; apical part with six setae; anterior margin with two discal and six slender lateral marginal setae; epipharynx with sparse setae on lateral margin, with two basal spines on central area, between the basal spines with four mastoids, with six mastoids above the basal spines (Fig. 3G); mandible left-right unsymmetrical, membranous elevation with two setae; clypeus transverse, trapezoidal, dark brown, with two pairs of setae at apex and margin respectively (Fig. 3D, F). Epicranial stem Y or V-shaped; frons convex, dark brown throughout, with sparse long setae on lateral margins, with four pairs of setae at apex (a pair on anterior margin, a pair on middle margin, two pairs on posterior margin) (Fig. 3D, F). Ocelli evident, two parallel rows arranged transversely (Fig. 3B). Maxillary palpi (Fig. 3E) three-segmented, cylindrical, and conical at apex; **I** widest, **II** longest, **I** as long as **III**. Labial palps two-segmented, short; **II** conical;

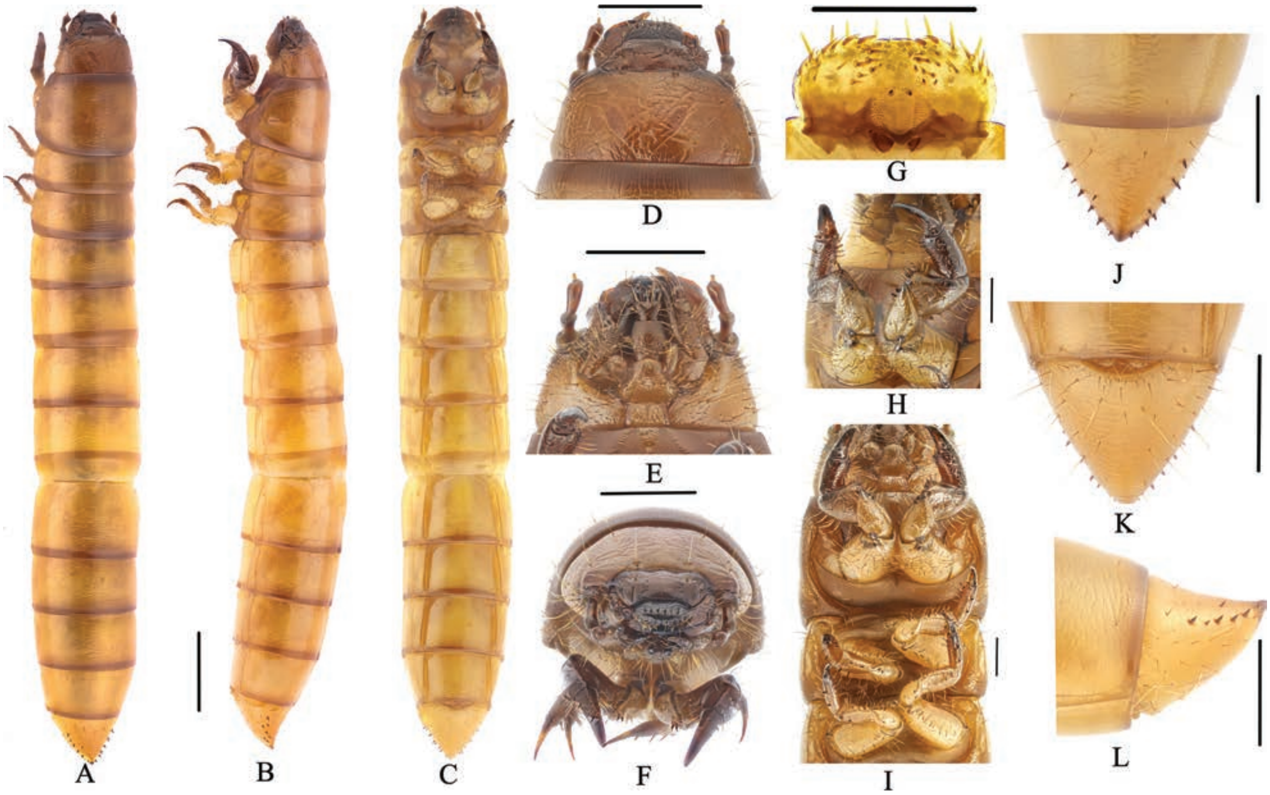

Figure 3. Larva of *Gnaptorina nigera* Shi, Ren & Merkl, 2007 **A** habitus, dorsal view **B** habitus, lateral view **C** habitus, ventral view **D** head, dorsal view **E** head, ventral view **F** head, vertex view **G** epipharynx **H** prothoracic leg **I** legs **J** pygopods, dorsal view **K** pygopods, ventral view **L** pygopods, lateral view. Scale bars: 2 mm (**A–C**); 1 mm (**D–F, J–L**); 0.5 mm (**G, H, I**).

prementum with two setae on anterior margin, apex with two long setae, lateral sides with four or five long setae; mentum convex, hexagonal, base of mentum straight; mentum more slender than prementum, lateral margins with four or five long setae, posterior margin with four setae; submentum with six setae on mid-posterior part (three on left, three on right). Antennae three-segmented, cylindrical at apex; I longest, as wide as II; III shortest and narrowest (Fig. 3B, D–F).

Thorax (Fig. 3A). Thoracic segments parallel-sided, with transverse plicae. Pronotum and mesonotum with two pairs of elongate setae on anterior and posterior margin. Metanotum with two pairs of setae on anterior margin and a pair of setae on posterior margin. Anterior and posterior border of pronotum with brown longitudinal stripes, with pair of irregular brown spots on tergum, posterior border of mesonotum and metanotum with a brown longitudinal stripe. Pronotum longest, 2.40 × as long as mesonotum, 1.70 × as long as metanotum, mesonotum shortest.

Legs (Fig. 3H, I). Protarsungulus strongly sclerotised, sharp, claw-like; protarsungulus with a strong, long seta on inner side and a strong, short spine on outer side at base. Profemora and protibiae gradually narrowing towards apex; inner margin setal formula of prothoracic leg 4(3): 6(3): 2(2); outer margin of tibiae with two setae; outer margin of femora with two setae; trochanter with two setae (Fig. 3G). Mesotarsus with a strong, long seta on inner side and a strong, short spine on outer side at base; inner margin setal formula of mesothoracic leg 3–4(2–3): 4(2): 2(2); outer margin of tibiae with two spines; outer margin of femora with two spines; outer margin of trochanters with two spines. Metatarsus with two short, broad spines at base, inner margin setal formula of metathoracic leg 3(2): 4(2): 2(2), outer margin of tibiae with two short spines, outer margin of femora with two spines, outer margin of trochanters with two spines. Meso- and metathoracic legs shorter than prothoracic one, meso- and metathoracic legs tarsungulus highly ossified, hooked, with dense setae (Fig. 3I).

Abdomen (Fig. 3C, J–L). Approximately 3.10 × as long as thorax; abdominal segments I–VIII subcylindrical, with transverses plicae; ventral side of abdominal segment I with six pairs of setae on each side (five pairs of setae near anterior and a pair of setae near posterior) and 14 setae on anterior margins, ventral side of abdominal segments II–VIII with three pairs of setae on anterior, middle, and posterior margin of lateral margins, respectively (Fig. 3C). Last segment conical, 0.91 × as long as VIII, distinctly narrower than VIII; surface of convex disc with sparse long setae in ventral view, with a row of short spines on each side (six spines on left, seven spines on right); last segment dorsally flattened; urogomphi inconspicuous and apex truncated, with two short spines (Fig. 3J–L).

Spiracles (Fig. 3C). Lateral margins of abdominal segments I–VIII and mesothorax each with a pair of spiracles, mesothoracic spiracles much larger than abdominal one, lateral margins of abdominal segments I–VIII with almost equal-sized spiracles, rounded.

Gnaptorina tishkovi **Medvedev, 1998**

Examined materials. Larvae. 14 exx. (MHBU): Qomolangma, Tingri County, Xizang/ 28°11.33' N, 86°49.80' E/ Alt. 4960m/ 2023-VII-20/ Xing-Long Bai, Quan-Yu Ji, Jian Song leg.; 5 exx. (MHBU): Tingri County, Xizang/ 28°36.68'

N, 87°07.78' E/ Alt. 4270m/ 2014-VII-24/ Guo-Dong Ren, Xing-Long Bai, Jun-Sheng Shan leg.; 5 exx. (MHBU): Tingri County, Xizang/ 28°27.58' N, 87°37.15' E/ Alt. 4480m/ 2019-VIII-16/ Xiu-Min Li leg.; 10 exx. (MHBU): Dinggyê County, Xizang/ 28°08.48' N, 87°42.45' E/ Alt. 4700m/ 2014-VIII-4/ Guo-Dong Ren, Xing-long Bai, Jun-Sheng Shan leg.; 5 exx. (MHBU): Dinggyê County, Xizang/ 2014-VIII-4/ Guo-Dong Ren leg.

Description. ***Body*** (Fig. 4A–C). Larvae length 21.8–23.5 mm, width 2.4–3.0 mm. Body yellowish brown, shiny, body wall ossified; median line obvious on on thorax dorsally and abdominal tergite I.

Head (Fig. 4B, D–G). Labrum transverse; apical part with six setae; anterior margin with two discal and six slender lateral marginal setae; epipharynx with sparse setae on lateral margin, with two basal spines on central area, between the basal spines with four mastoids, with six mastoids above the basal spines (Fig. 4G); mandible left-right unsymmetrical, membranous elevation with two setae (Fig. 4D, F). Epicranial stem Y-shaped, epicranial stem with a pair of pale brown patterns on distal margin; frons convex, with sparse long setae on lateral margins, with four pairs of setae at apex (a pair on upper margin, a pair on middle margin, two pairs on mid-posterior margin) (Fig. 4D, F). Posterior margin of middle part of frontal pale brown covered. Ocelli evident (Fig. 4B). Maxillary palpi (Fig. 4E) three-segmented, cylindrical, and conical at apex; I widest, II longest. Labial palps two-segmented, short; II conical; prementum with two setae on anterior margin, apex with two long setae, lateral sides with two long setae; mentum convex, hexagonal; mentum more slender than prementum, posterior margin with four long setae; submentum with six setae on posterior margin (three on left, three on right). Antennae three-segmented, cylindrical at apex; I longest and widest; III shortest and narrowest (Fig. 4B, D–G).

Thorax (Fig. 4A). Pronotum and metanotum with two pairs of elongate setae on anterior margin and a pair of setae on posterior margin. Mesonotum with a pair of setae on anterior, middle, and posterior margin. Anterior and posterior borders of pronotum with brown longitudinal stripes, posterior border of mesonotum and metanotum with a brown longitudinal stripe. Pronotum longest, 1.96 × as long as mesonotum, 1.61 × as long as metanotum, mesonotum shortest.

Legs (Fig. 4H). Protarsungulus with a strong, long seta on inner side and a strong, short spine on outer side at base. Profemora and protibiae gradually narrowing towards apex; inner margin setal formula of prothoracic leg 3–4(1–2):6(3):2(2); outer margin of tibiae with two strong, short spines; outer margin of femora with two setae; trochanter with two short setae. Mesotarsus with a strong, long seta on inner side and a strong, short spine on outer side at base; inner margin setal formula of mesothoracic leg 4:5(1):2(2); outer margin of tibiae with two spines; outer margin of femora with two spines; outer margin of trochanters with two spines and one seta. Metatarsus with a strong, long seta on inner side and a strong, short spine on outer side at base; inner margin setal formula of metathoracic leg 3–4(2):4(3):2(2), outer margin of tibiae with two spines, outer margin of femora with two spines, outer margin of trochanters with two spines and one seta.

Abdomen (Fig. 4A, C). Not constricted between VIII and IX segments. Approximately 4.20 × as long as thorax; abdominal segments I–VIII

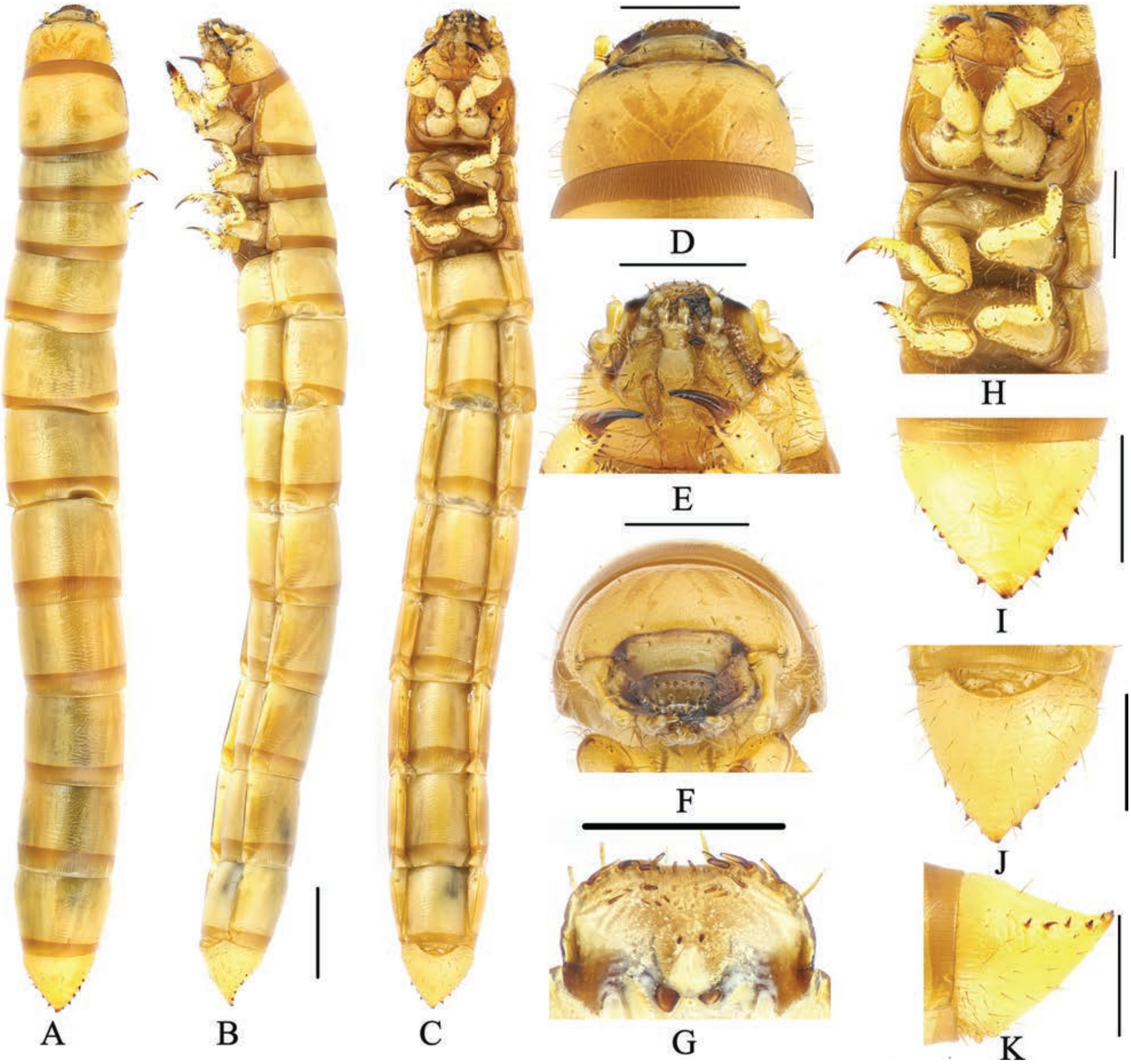

Figure 4. Larva of *Gnaptorina tishkovi* Medvedev, 1998 **A** habitus, dorsal view **B** habitus, lateral view **C** habitus, ventral view **D** head, dorsal view **E** head, ventral view **F** head, vertex view **G** epipharynx **H** legs **I** pygopods, dorsal view **J** pygopods, ventral view **K** pygopods, lateral view. Scale bars: 2 mm (**A–C**); 1 mm (**D–F, H–K**); 0.5 mm (**G**).

subcylindrical, with transverses plicae; ventral side of abdominal segment I with sparse setae on anterior and lateral margins, with four setae on posterior margin (two on left, two on right); ventral side of abdominal segments II–VIII with three pairs of setae on anterior, middle, and posterior margin of lateral margins, respectively. Last segment conical, 0.87 × as long as VIII, distinctly narrower than VIII; surface of convex disc with sparse long setae in ventral view, with a row of short spines on each side (six spines each on left and right); last segment dorsally flattened; urogomphi inconspicuous and apex truncated, with two short spines (Fig. 4I–K).

Spiracles (Fig. 4C). Mesothoracic spiracles are almost twice size of abdominal segment I spiracles; lateral margins of abdominal segments I–VIII and mesothorax each with a pair of oval spiracles, abdominal segment I spiracles largest, abdominal segments I–VIII spiracles gradually shrinking.

Gnaptorina brucei Blair, 1923

Examined materials. Larvae. 2 exx. (MHBU): Rongxar Township, Tingri County, Xizang/ 28°10.92' N, 86°29.25' E/ Alt. 4820m/ 2014-VII-28/Guo-Dong Ren, Xing-Long Bai, Jun-Sheng Shan leg.

Description. ***Body*** (Fig. 5A–C). Larvae length 24.5–25.5 mm, width 2.2–2.5 mm, comparatively thin. Body yellowish brown, shiny, body wall ossified; median line obvious on thorax dorsally and abdominal tergite I.

Head (Fig. 5B, D–H). Labrum transverse; apical part with six setae; anterior margin with two discal and six slender lateral marginal setae; epipharynx with sparse setae on lateral margin, with two basal spines on central area, between the basal spines with four mastoids, with six mastoids above the basal spines (Fig. 5H); mandible left-right unsymmetrical, membranous elevation with two setae (Fig. 5D, E). Epicranial stem Y-shaped; frons convex, frons with densely long setae on lateral margins, with four pairs of setae at apex (a pair on anterior margin, a pair on mid-anterior margin, two pairs on mid-posterior margin) (Fig. 5D). Ocelli inconspicuous (Fig. 5B). Maxillary palpi (Fig. 5E) three-segmented, cylindrical, and conical at apex; I widest, II longest. Labial palps two-segmented, short; II conical; prementum with two setae on anterior margin, apex with two long setae, lateral sides with four long setae; mentum convex, hexagonal; mentum more slender than prementum, lateral margin with five or six long setae, posterior margin with one long setae; submentum with eight setae on posterior margin. Antennae three-segmented, cylindrical at apex; I longest and widest; III shortest and narrowest.

Thorax (Fig. 5A). Each thoracic tergum with two pairs of elongate setae on anterior and posterior margin. Anterior and posterior borders of pronotum with brown longitudinal stripes; posterior border of mesonotum and metanotum with a brown longitudinal stripe. Pronotum longest, 1.70 × as long as mesonotum, 1.45 × as long as metanotum, mesonotum shortest.

Legs (Fig. 5I). Protarsungulus with a strong, long seta on inner side and a strong, short spine on outer side at base. Profemora and protibiae gradually narrowing towards apex; inner margin setal formula of prothoracic leg 5(3): 6–7(4): 2(2); outer margin of tibiae with one short seta and one strong, short spine; outer margin of femora with two setae; trochanter with three setae. Mesotarsus with a strong, long seta on inner side and a strong, short spine on outer side at base; inner margin setal formula of mesothoracic leg 3(3): 5(3): 2(2); outer margin of tibiae with two spines; outer margin of femora with two spines; outer margin of trochanters with one spine and two setae. Metatarsus with a strong, long seta on inner side and a strong, short spine on outer side at base; inner margin setal formula of metathoracic leg 3(2): 5–6(3): 2(2), outer margin of tibiae with two spines, outer margin of femora with two spines, outer margin of trochanters with one spine and two setae.

Abdomen (Fig. 5A, C). Constricted between VIII and IX segments. Approximately 3.54 × as long as thorax; abdominal segments I–VIII subcylindrical, with transverses plicae; ventral side of abdominal segment I with sparse setae on anterior and lateral margins, with two setae on posterior margin; ventral side of abdominal segments II–VIII with two pairs of setae on lateral margin. Last segment conical, 0.79 × as long as VIII, distinctly narrower than VIII; last segment surface of convex disc with sparse long setae in ventral view, with a row

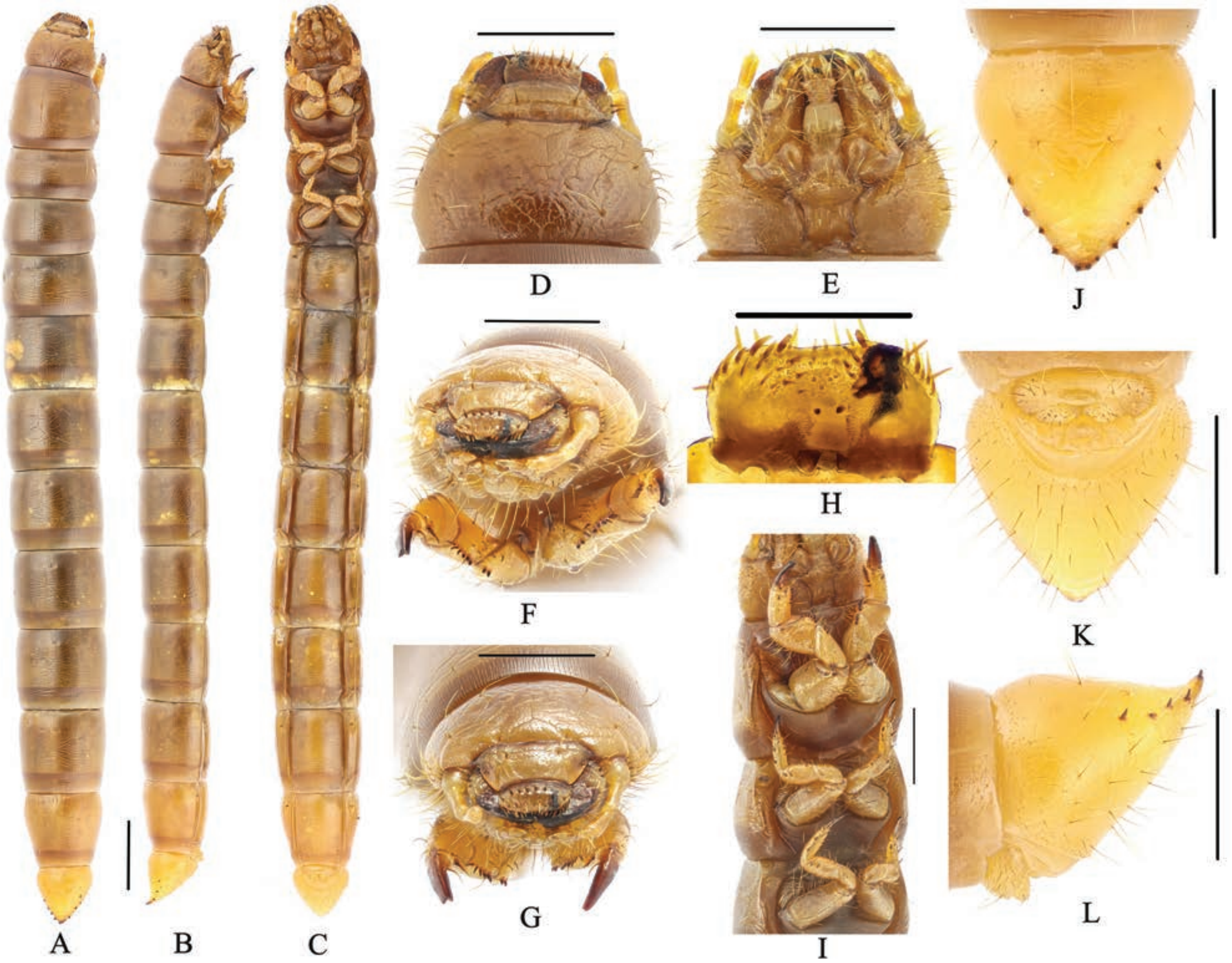

Figure 5. Larva of *Gnaptorina brucei* Blair, 1923 **A** habitus, dorsal view **B** habitus, lateral view **C** habitus, ventral view **D** head, dorsal view **E** head, ventral view **F, G** head, vertex view **H** epipharynx **I** legs **J** pygopods, dorsal view **K** pygopods, ventral view **L** pygopods, lateral view. Scale bars: 2 mm (**A–C**); 1 mm (**D–G, I–L**); 0.5 mm (**H**).

of short spines on each side (four spines on left, six spines on right); urogomphi inconspicuous and upturned slightly, with two short spines (Fig. 5J–L).

Spiracles (Fig. 5C). Lateral margins of abdominal segments I–VIII and mesothorax each with a pair of oval spiracles, mesothoracic spiracles largest, abdominal segments I–VIII spiracles gradually shrinking.

Gnaptorina himalaya Shi, Ren & Merkl, 2007

Examined materials. Larvae. 2 exx. (MHBU): Garyü Countyside, Qusum County, Xizang/ 28°50.25’ N, 91°59.90’ E/ Alt. 4790m/ 2019-VII-31/ Xiu-Min Li leg.; 4 exx. (MHBU): Zag La, Comai County, Xizang/ 2019-VII-31/ Guo-Dong Ren leg.

Description. ***Body*** (Fig. 6A–C). Larvae length 16.8–22.0 mm, width 2.1–2.3 mm, thick. Body yellowish brown, shiny, body wall ossified; median line obvious on thorax dorsally and abdominal tergite I.

Head (Fig. 6B, D–G). Labrum transverse; apical part with six setae; anterior margin with two discal and six slender lateral marginal setae; epipharynx with sparse setae on lateral margin, with two basal spines on central area, between the basal spines with four mastoids, with three pairs of mastoids above the basal spines; mandible left-right unsymmetrical, membranous elevation with two setae (Fig. 6D, F, G). Epicranial stem Y or V-shaped; frons convex, with sparse setae on lateral margins, with four pairs of setae at apex (a pair on anterior margin, a pair on middle margin, two pairs on posterior margin) (Fig. 6D, F). Ocelli evident, three parallel rows arranged transversely (Fig. 6B). Maxillary palpi (Fig. 6E) three-segmented, cylindrical, and conical at apex; I widest, II longest. Labial palps two-segmented, short; II conical; prementum shorter than mentum, with two setae on anterior margin, apex with two long setae; mentum convex, trapezoidal, base of mentum straight; mentum wide and short, posterior margin with 4–6 long setae; submentum with nine setae on middle margin. Antennae three-segmented, cylindrical at apex; I nearly as long as II; III shortest and narrowest (Fig. 6B, D–G).

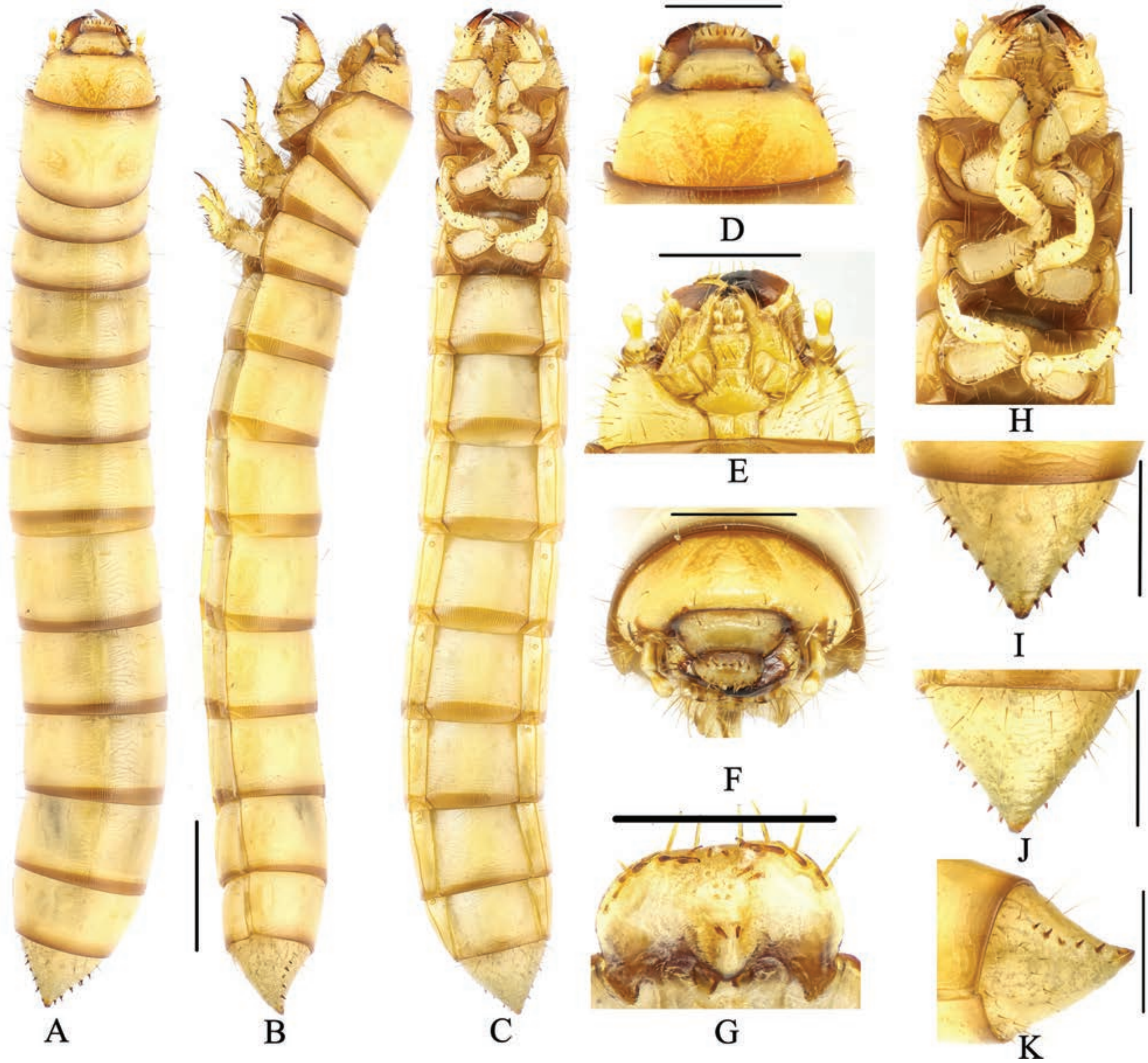

Figure 6. Larva of *Gnaptorina himalaya* Shi, Ren & Merkl, 2007 **A** habitus, dorsal view **B** habitus, lateral view **C** habitus, ventral view **D** head, dorsal view **E** head, ventral view **F** head, vertex view **G** epipharynx **H** legs **I** pygopods, dorsal view **J** pygopods, ventral view **K** pygopods, lateral view. Scale bars: 2 mm (**A–C**); 1 mm (**D–F, H–K**); 0.5 mm (**G**).

Thorax (Fig. 6A). Pronotum with four pairs of setae (two pairs of setae on anterior margin, a pair of setae on middle margin, a pair of setae on posterior margin); mesonotum with three pairs of long setae, a pair on anterior margin, two pairs on middle; metanotum with four pairs of setae, two pairs on anterior margin, two pairs on middle. Anterior and posterior borders of pronotum with brown longitudinal stripes, and a pair of pale brown irregular spots; posterior border of mesonotum and metanotum with a brown longitudinal stripe. Pronotum longest, 2.80 × as long as mesonotum, 2.06 × as long as metanotum, mesonotum shortest.

Legs (Fig. 6H). Protarsungulus with a strong, long seta on inner side and a strong, short spine on outer side at base. Profemora and protibiae gradually narrowing towards apex; inner margin setal formula of prothoracic leg 5(4): 6(2–3): 2(2); outer margin of tibiae with one strong seta and one short spine; outer margin of femora with two setae; trochanter with three setae. Mesotarsus with a strong, long seta on inner side and a strong, short spine on outer side at base; inner margin setal formula of mesothoracic leg 2–4(2–3):5(2–3):2(2); outer margin of tibiae with two spines; outer margin of femora with two spines; outer margin of trochanters with one spine and two setae. Metatarsus with two strong, short spines at base; inner margin setal formula of metathoracic leg 3(2–3): 4(2):2(2), outer margin of tibiae with two spines, outer margin of femora with two spines, outer margin of trochanters with one spine and two setae.

Abdomen (Fig. 6A, C). Not constricted between VIII and IX segments. Approximately 3.91 × as long as thorax; abdominal segments I–VIII subcylindrical, with transverses plicae; ventral side of abdominal segment I with 11 setae on anterior margin and 5–7 on each side, with two pairs of setae on posterior margin; ventral side of abdominal segment II with six pairs of setae (four pairs of setae on lateral margin, two pairs of setae on posterior margin); ventral side of abdominal segments III–VIII with four pairs of setae on lateral margin (two pairs of setae on mid-lateral margin, two pairs of setae on posterior margin). Last segment conical, 0.87 × as long as VIII, distinctly narrower than VIII; last segment surface of convex disc with sparse long setae in ventral view, with a row of short spines each side (five spines on left, five spines on right); last segment dorsally flattened, urogomphi inconspicuous, with one short spines (Fig. 6I–K).

Spiracles (Fig. 6C). Lateral margins of abdominal segments I–VIII and mesothorax each with a pair of oval spiracles, mesothorax spiracles much larger than abdominal spiracles, abdominal segments I–VIII spiracles gradually shrinking.

Gnaptorina kangmar Shi, Ren & Merkl, 2007

Examined materials. Larvae. 27 exx. (MHBU): Nai Chin Kangsang Snow Mountain, Xizang/ 28°53.90’ N, 90°09.85’ E/ Alt. 5030m/ 2014-VIII-6/ Guo-Dong Ren, Xing-Long Bai, Jun-Sheng Shan leg.; 21 exx. (MHBU): Gyangzê County, Xizang/ 2014-VIII-6/ Guo-Dong Ren, Xing-Long Bai, Jun-Sheng Shan leg.

Description. *Body* (Fig. 7A–C). Larvae length 19.2–20.0 mm, width 2.3–2.5 mm, moderately thickened. Body yellowish brown, shiny, body wall ossified; median line obvious on pronotum and mesonotum.

Head (Fig. 7B, D–G). Labrum transverse; apical part with six setae; anterior margin with two discal and six slender lateral marginal setae; epipharynx with sparse setae on lateral margin, with two basal spines on central area, between

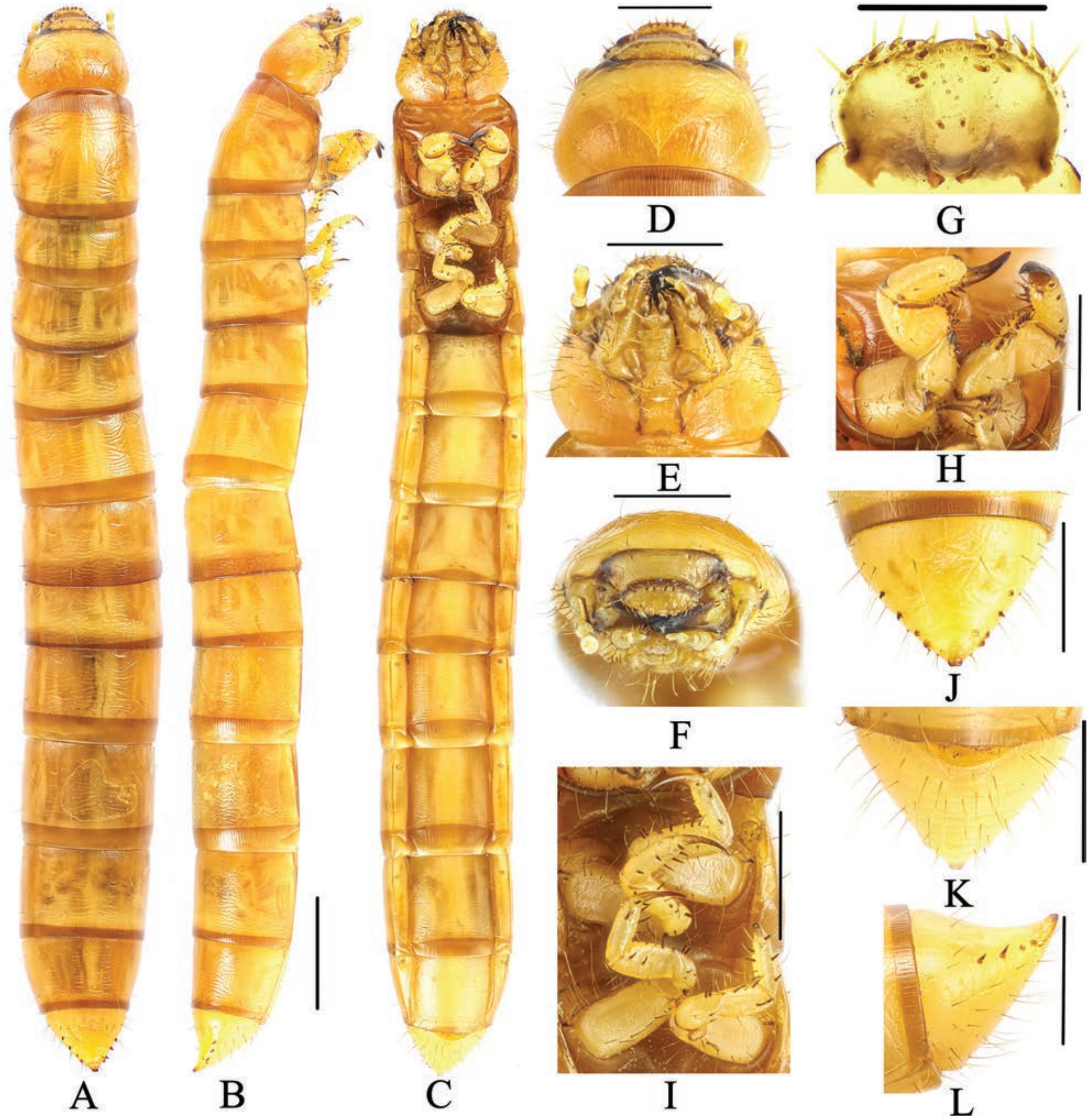

Figure 7. Larva of *Gnaptorina kangmar* Shi, Ren & Merkl, 2007 **A** habitus, dorsal view **B** habitus, lateral view **C** habitus, ventral view **D** head, dorsal view **E** head, ventral view **F** head, vertex view **G** epipharynx **H** prothoracic leg, lateral view **I** mesothoracic and metathoracic legs, lateral view **J** pygopods, dorsal view **K** pygopods, ventral view **L** pygopods, lateral view. Scale bars: 2 mm (**A–C**); 1 mm (**D–F, H–L**); 0.5 mm (**G**).

the basal spines with four mastoids, with six mastoids above the basal spines; mandible left-right unsymmetrical, membranous elevation with two setae (Fig. 7D, E, G). Epicranial stem Y-shaped; frons convex, with sparse setae on lateral margins, with four pairs of setae at apex (a pair on anterior margin, a pair on middle margin, two pairs on mid-posterior margin) (Fig. 7D, F). Ocelli evident, two parallel rows arranged transversely (Fig. 7B). Maxillary palpi (Fig. 7E) three-segmented, cylindrical, and conical at apex; **I** widest, **II** longest. Labial palps two-segmented, short; **II** conical; prementum short, with two setae on anterior margin, apex with two long setae; mentum convex, trapezoidal, base of mentum straight; mentum wide and short, lateral margin with five or six long setae, mid-posterior margin with two long setae; submentum with nine setae on middle margin. Antennae three-segmented, cylindrical at apex; I longest; III shortest and narrowest (Fig. 7B, D–G).

Thorax (Fig. 7A). Pronotum and mesonotum with four pairs of setae (two pairs of setae on anterior margin, two pairs of setae on posterior margin); metanotum with three pairs of long setae, a pair on mid-anterior margin, two pairs on middle. Anterior and posterior borders of pronotum with brown longitudinal stripes; posterior border of mesonotum and metanotum with a brown longitudinal stripe. Pronotum longest, 2.03 × as long as mesonotum, 1.89 × as long as metanotum, mesonotum shortest.

Legs (Fig. 7H, I). Protarsungulus with a strong, long seta on inner side and a strong, short spine on outer side at base. Profemora and protibiae gradually narrowing towards apex; inner margin setal formula of prothoracic leg 5(1): 7(5–6): 2(2); outer margin of tibiae with two strong and short spines; outer margin of femora with two setae; trochanter with three setae. Mesotarsus with a strong, long seta on inner side and a strong, short spine on outer side at base; inner margin setal formula of mesothoracic leg 4(2): 4(2): 2(2); outer margin of tibiae with two spines; outer margin of femora with two spines; outer margin of trochanters with two spines and one seta (Fig. 7H). Metatarsus with a strong, long seta on inner side and a strong, short spine on outer side at base; inner margin setal formula of metathoracic leg 4(3): 5(2): 2(2), outer margin of tibiae with two spines, outer margin of femora with two spines, outer margin of trochanters with two spines and one seta.

Abdomen (Fig. 7A, C). Not constricted between VIII and IX segments Approximately 2.68 × as long as thorax; abdominal segments I–VIII subcylindrical, with transverses plicae; ventral side of abdominal segment I with 12 setae on anterior margin and six setae on each side, with two pairs of setae on posterior margin; ventral side of abdominal segment II with seven pairs of setae (five pairs of setae on lateral margin, two pairs of setae on posterior margin); ventral side of abdominal segments III–VIII with three pairs of setae (two pairs of setae on mid-lateral margin, a pairs of setae on posterior margin); ventral side of abdominal segment VIII with four pairs of setae on lateral margin and two pairs of setae on posterior margin. Last segment conical, 0.91 × as long as VIII, distinctly narrower than VIII; last segment surface of convex disc with sparse long setae in ventral view, with a row of short spines on each side (five spines on left, five spines on right); last segment dorsally flattened, urogomphi inconspicuous, with two short spines (Fig. 7J–L).

Spiracles **(Fig. 7C**). Lateral margins of abdominal segments I–VIII and mesothorax each with a pair of oval spiracles, mesothorax spiracles much larger than abdominal spiracles, abdominal segments I–VIII spiracles gradually shrinking.

Discussion

Molecular species identification has become an important approach in insect taxonomy (Tautz et al. 2002; Hebert et al. 2003; Meier et al. 2006; Rodriguez et al. 2022). These approaches are capable of establishing correlations between larval and adult stages through DNA sequences, and of providing valuable reference information for larval taxonomy (Kamiński et al. 2019). Most

Gnaptorina species are distributed in the high-elevation areas of the Qinghai-Xizang Plateau, where they usually have restricted areas of distribution (Bai et al. 2020; Li et al. 2021; Ji et al. 2024). Therefore, it is usually hard to obtain larvae and pupae through laboratory rearing because of the difficulty in replicating the natural conditions of *Gnaptorina* in the wild. In this study, the larval samples were directly collected from the field, whose classification is challenging due to the lack of larval information on the known species. Our results clearly provided a tool to help associate the larva with known or unknown adults, which successfully resolved the problem of larval taxonomic status. In addition, the results of molecular species delimitation are consistent with previous studies (Li et al. 2021). However, molecular species delimitation was performed based on 88 samples of 32 species (82% of the known species). We did not have a high number of specimens per species on average, which could lead to an increase in the number of inferred MOTUs. Yet molecular species delimitation was performed only based on COI gene fragments per species in this study, requiring a cautious approach to any taxonomic changes. For these taxa, we identified distinctive morphological characters that could support their status as separate species. The molecular phylogenetic results revealed that the larval specimens all belong to the subgenus *Hesperoptorina*. Before the present study, the larval information in only known for three species of the subgenus *Gnaptorina* (*Gnaptorina cylindricollis* Reitter, 1889, *Gnaptorina felicitana* Reitter, 1887, and *Gnaptorina lhorongica* Li, 2024) were recorded. The immature stages of more genera and species need to be properly documented in order to develop an applicable system of the larval and pupal taxonomy in the tribe Blaptini.

Acknowledgements

We would like to thank Prof. Jun-Xia Zhang and Dr. Zhao Pan (College of Life Sciences, Hebei University) for their valuable comments and corrections. We are also very grateful to the editor and anonymous reviewers for their constructive suggestions on the manuscript.

Additional information

Conflict of interest

The authors have declared that no competing interests exist.

Ethical statement

No ethical statement was reported.

Funding

This research was funded by the National Natural Science Foundation of China (32170477) and the Natural Science Foundation of Hebei (C2024201003).

Author contributions

Conceptualisation: B-YJ, X-ML and G-DR. Data curation: X-ML, M-CG and T-YG. Formal analysis: B-YJ, T-YG and X-ML. Writing-original draft: B-YJ and X-ML. Visualisation: B-YJ and T-YG. Funding acquisition: X-ML. Writing-review and editing: B-YJ and T-YG.

Author ORCIDs

Bao-Yue Ji hhttps://orcid.org/0000-0002-9250-5481
Tong-Yang Guo https://orcid.org/0009-0004-1880-7045
Mei-Chang Gu https://orcid.org/0009-0003-6617-4572
Guo-Dong Ren https://orcid.org/0000-0001-5808-9122
Xiu-Min Li https://orcid.org/0000-0003-0575-1869

Data availability

All of the data that support the findings of this study are available in the main text.

References

Bai XL, Li XM, Ren GD (2020) Description of a new subgenus and four new species of *Gnaptorina* Reitter, 1887 (Coleoptera: Tenebrionidae: Blaptini) from China. Zootaxa 4809(1): 165–176. https://doi.org/10.11646/zootaxa.4809.1.10

Bai XL, Liu JZ, Ren GD (2023) *Viettagona vietnamensis*-Newly Recorded Genus and Species from China (Coleoptera: Tenebrionidae: Blaptini). Sichuan Journal of Zoology 42(6): 696–700. http://dx.doi.org/10.11984/j.issn.1000-7083.20230051

Chigray IA (2019) A new genus and species of darkling beetles of the tribe Blaptini (Coleoptera: Tenebrionidae) from Afghanistan and taxonomic changes in the tribe. Entomological Review 99(7): 914–923. https://doi.org/10.1134/S0013873819070054

Chigray IA, Kirejtshuk AG (2023) The supraspecific structure of the subtribe Blaptina Leach, 1815 (Coleoptera, Tenebrionidae: Blaptinae). Acta Zoologica Academiae Scientiarum Hungaricae 69(3): 213–245. https://doi.org/10.17109/AZH.69.3.213.2023

Dellicour S, Flot JF (2018) The hitchhiker's guide to single-locus species delimitation. Molecular Ecology Resources 18(6): 1234–1246. https://doi.org/10.1111/1755-0998.12908

Folmer O, Black M, Hoeh W, Lutz R, Vrijenhoek R (1994) DNA primers for amplification of mitochondrial cytochrome c oxidase subunit I from diverse metazoan invertebrates. Molecular Marine Biology and Biotechnology 3: 294–299.

Grebennikov VV, Scholtz CH (2004) The basal phylogeny of Scarabaeoidea (Insecta: Coleoptera) inferred from larval morphology. Invertebrate Systematics 18(3): 321–348. https://doi.org/10.1071/IS03013

Hebert PDN, Cywinska A, Ball SL, Dewaard JR (2003) Biological identifications through DNA barcodes. Proceedings of the Royal Society B, Biological Sciences 270(1512): 313–321. https://doi.org/10.1098/rspb.2002.2218

Iwan D, Löbl I (2020) Tenebrionoidea. Catalogue of Palaearctic Coleoptera [M]. Volume 5. Koninklijke Brill NV, Leiden, The Netherlands, 945 pp. https://doi.org/10.1163/9789004434998_004

Ji BY, Ma XT, Rong JD, Ren GD, Pan Z, Li XM (2024) The adult, pupa, and larva of a new species of *Gnaptorina* Reitter, 1887 (Coleoptera, Tenebrionidae, Blaptini) from the Tibetan Plateau, with molecular phylogenetic inferences. ZooKeys 1190: 91–106. https://doi.org/10.3897/zookeys.1190.113126

Kamiński MJ, Lumen R, Kubicz Jr M, Steiner Jr W, Kanda K, Iwan D (2019) Immature stages of beetles representing the 'Opatrinoid' clade (Coleoptera: Tenebrionidae): an overview of current knowledge of the larval morphology and some resulting taxonomic notes on Blapstinina. Zoomorphology 138(3): 349–370. https://doi.org/10.1007/s00435-019-00443-7

Kamiński MJ, Lumen R, Kanda K, Iwan D, Johnston MA, Kergoat GJ, Bouchard P, Bai XL, Li XM, Ren GD, Smith AD (2021) Reevaluation of Blapimorpha and Opatrinae: addressing a major phylogeny-classification gap in darkling beetles (Coleoptera: Tenebrionidae: Blaptinae). Systematic Entomology 46(1): 140–156. https://doi.org/10.1111/syen.12453

Lawrence JF, Seago AE, Newton AF, Thayer MK, Marvaldi AE, Slipinski A (2011) Phylogeny of the Coleoptera based on morphological characters of adults and larvae. Annales Zoologici 61(1): 1–217. https://doi.org/10.3161/000345411X576725

Li XM, Bai XL, Ren GD (2018) A new species of the genus *Blaptogonia* from the Himalayas with four DNA markers (Coleoptera, Tenebrionidae, Blaptini). ZooKeys 773: 69–78. https://doi.org/10.3897/zookeys.773.24656

Li XM, Bai XL, Ren GD (2019) Two new species of the genus *Gnaptorina* Reitter from the Hengduan Mountains, China (Coleoptera: Tenebrionidae: Blaptini). Zootaxa 4695(1): 83–89. https://doi.org/10.11646/zootaxa.4695.1

Li XM, Bai XL, Kergoat GJ, Pan Z, Ren GD (2021) Phylogenetics, historical biogeography and molecular species delimitation of *Gnaptorina* Reitter (Coleoptera: Tenebrionidae: Blaptini). Systematic Entomology 46(1): 239–251. https://doi.org/10.1111/syen.12459

Luo A, Ling C, Ho SYW, Zhu CD (2018) Comparison of methods for molecular species delimitation across a range of speciation scenarios. Systematic Biology 67(5): 830–846. https://doi.org/10.1093/sysbio/syy011

Medvedev GS (2004) New species of the darkling-beetle tribe Blaptini (Coleoptera, Tenebrionidae) from India, Nepal and China. Entomologicheskoe Obozrenie 83: 163–189. [In Russian, English translation: Entomological Review 84: 78–99]

Medvedev GS (2006) To the systematics and nomenclature of tenebrionid beetles of the tribes Phaleriini, Lachnogyini, Klewariini, and Blaptini (Coleoptera, Tenebrionidae). Entomological Review 86(7): 820–839. https://doi.org/10.1134/S0013873806070062

Medvedev GS (2009) Composition of the genera *Gnaptorina* Reitter and *Pseudognaptorina* Kaszab of the tribe Blaptini (Coleoptera, Tenebrionidae). Entomological Review 89(4): 451–461. https://doi.org/10.1134/S0013873809040095

Medvedev GS, Merkl O (2002) *Viettagona vietnamensis* Gen. Et Sp. N. From Vietnam (Coleoptera, Tenebrionidae: Blaptini). Acta Zoologica Academiae Scientiarum Hungaricae 48(4): 317–332.

Meier R, Shiyang K, Vaidya G, Ng PKL (2006) DNA barcoding and taxonomy in Diptera: A tale of high intraspecific variability and low identification success. Systematic Biology 55(5): 715–728. https://doi.org/10.1080/10635150600969864

Minh BQ, Nguyen MAT, Von Haeseler A (2013) Ultrafast approximation for phylogenetic bootstrap. Molecular Biology and Evolution 30(5): 1188–1195. https://doi.org/10.1093/molbev/mst024

Nguyen LT, Schmidt HA, Von Haeseler A, Minh BQ (2015) IQ-TREE: A fast and effective stochastic algorithm for estimating maximum-likelihood phylogenies. Molecular Biology and Evolution 32(1): 268–274. https://doi.org/10.1093/molbev/msu300

Pons J, Barraclough TG, Gomez-Zurita J, Cardoso A, Duran DP, Hazell S, Kamoun S, Sumlin WD, Vogler AP (2006) Sequence based species delimitation for the DNA taxonomy of undescribed insects. Systematic Biology 55(4): 595–609. https://doi.org/10.1080/10635150600852011

Puillandre N, Brouillet S, Achaz G (2021) ASAP: Assemble species by automatic partitioning. Molecular Ecology Resources 21(2): 609–620. https://doi.org/10.1111/1755-0998.13281

Ren GD, Ba YB, Liu HY, Niu YP, Zhu XC, Li Z, Shi AM (2016) Coleoptera: Tenebrionidae (I); Fauna Sinica: Insecta, Volume 63. Science Press, Beijing, 532 pp.

Rodriguez EJ, Steck GJ, Moore MR, Norrbom AL, Diaz J, Somma LA, Ruiz-Arce R, Sutton BD, Nolazco N, Muller A, Branham MA (2022) Exceptional larval morphology of nine species of the Anastrepha mucronota speciesgroup (Diptera, Tephritidae). ZooKeys 1127: 155–215. https://doi.org/10.3897/zookeys.1127.84628

Skopin NG (1960) Material on the morphology and the ecology of larvae of the tribe Blaptini (Coleoptera, Tenebrionidae). Trudy Instituta zooologii Akademii nauk Kazakhskoy SSR 11: 36–71. [In Russian]

Tautz D, Arctander P, Minelli A, Thomas RH, Vogler AP (2002) DNA points the way ahead in taxonomy. Nature 418(6897): 479–479. https://doi.org/10.1038/418479a

Yu YZ, Ren GD, Sun QX (1996) Morphology and genus and species key of common Blaptini larvae in Northern China. Entomological Knowledge 4: 198–203.

Yu YZ, Zhang DZ, Wang XP (1999) The larval morphology of five species of the Blaptini-Tribe (Coleoptera: Tenebrionidea). Journal of Ningxia Agricultural College 4: 15–20.

Zhang JJ, Kapli P, Pavlidis P, Stamatakis A (2013) A general species delimitation method with applications to phylogenetic placements. Bioinformatics (Oxford, England) 29(22): 2869–2876. https://doi.org/10.1093/bioinformatics/btt499

Zhang D, Gao FL, Jakovlić I, Zou H, Zhang J, Li WX, Wang GT (2020) PhyloSuite: An integrated and scalable desktop platform for streamlined molecular sequence data management and evolutionary phylogenetics studies. Molecular Ecology Resources 20(1): 348–355. https://doi.org/10.1111/1755-0998.13096

Zhu XC, Ren GD (2014) The larvae of *Gnaptorina felicitana* and *Agnaptoria amdoensis* of the tribe Blaptini from China (Coleoptera:Tenebrionidae). Zoological Systematics 39(02): 275–282.

ZooKeys 1209: 315–330 (2024)
DOI: 10.3897/zookeys.1209.127951

Research Article

Three new spider species of *Belisana* Thorell, 1898 (Araneae, Pholcidae) from karst caves, with a list of *Belisana* species from Guangxi, China

Ludan Zhang[1], Ying Wang[1], Shuqiang Li[2], Xiaoqing Zhang[1], Zhiyuan Yao[1]

1 *College of Life Science, Shenyang Normal University, Shenyang 110034, Liaoning, China*
2 *Institute of Zoology, Chinese Academy of Sciences, Beijing 100101, China*
Corresponding authors: Xiaoqing Zhang (zhangxq@synu.edu.cn); Zhiyuan Yao (yaozy@synu.edu.cn)

Abstract

Three new species of the genus *Belisana* Thorell, 1898 are described from karst caves in Guangxi, China: *Belisana langping* Zhang, Li & Yao, **sp. nov.** (♂♀), *B. lingui* Zhang, Li & Yao, **sp. nov.** (♂♀), and *B. tianyang* Zhang, Li & Yao, **sp. nov.** (♂♀). In addition, a list of all *Belisana* species from Guangxi is also provided.

Key words: Biodiversity, cellar spiders, checklist, invertebrate, morphology, new species, taxonomy

Academic editor: Francesco Ballarin
Received: 20 May 2024
Accepted: 11 July 2024
Published: 14 August 2024

ZooBank: https://zoobank.org/A07CCEE1-C2D5-4993-9437-55E3040E1F79

Citation: Zhang L, Wang Y, Li S, Zhang X, Yao Z (2024) Three new spider species of *Belisana* Thorell, 1898 (Araneae, Pholcidae) from karst caves, with a list of *Belisana* species from Guangxi, China. ZooKeys 1209: 315–330. https://doi.org/10.3897/zookeys.1209.127951

Introduction

Belisana Thorell, 1898, the second largest genus in Pholcidae, includes 157 species (WSC 2024). These species occupy a variety of micro-habitats, e.g., under rocks, in caves, on the underside of leaves, among leaf litter, and amidst foliage in the canopy (Huber 2005; Yao et al. 2015; Zhao et al. 2023a). They are distributed mainly in southern China, as well as in the Indo-Malayan and Australasian regions (Huber 2005; Yao et al. 2013, 2018; Zhu et al. 2020a; Zhu and Li 2021). Southern China exhibits remarkable diversity of this genus, with 71 species (45%) recorded to date. Within southern China, the species count from Yunnan (31 spp.) far outstrips those of Hainan (10 spp.), Guangxi (8 spp.), Guizhou (8 spp.), and Tibet (7 spp.) (Zhang and Peng 2011; Zhu et al. 2020a, b; Zhang et al. 2024). Furthermore, in Fujian, Guangdong and four other provinces, only seven species have been recorded (Zhu et al. 2020a). Recently, a series of surveys of pholcid spiders have been undertaken in China and a large number of new species have been reported (e.g., Yao et al. 2021; Lu et al. 2022; Zhao et al. 2023b; Yang et al. 2024a, b). Nevertheless, these efforts focused on *Pholcus* Walckenaer, 1805 from northern and central China, with relatively few reports on *Belisana* from southern China (Yang et al. 2023; Zhao et al. 2023a; Wang et al. 2024; Zhang et al. 2024).

Guangxi is located in the southwest of China. The karst landform is widely distributed in the northern part of Guangxi. The aim of this work is to describe three new *Belisana* species from karst caves in northern Guangxi (Fig. 1) and provide a list of the species of this genus from Guangxi (Table 1).

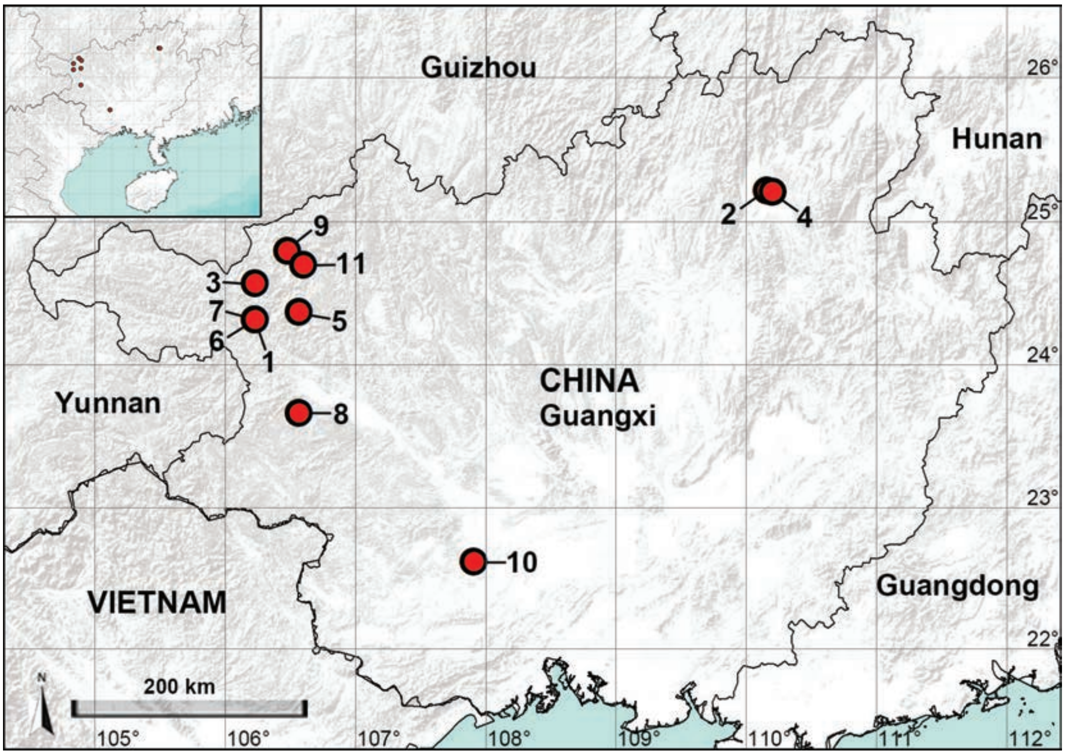

Figure 1. Distribution records of the *Belisana* species from Guangxi, China **1** *Belisana colubrina* Zhang & Peng, 2011 **2** *B. guilin* Yao & Li, 2020 **3** *B. langping* sp. nov. **4** *B. lingui* sp. nov. **5** *B. naling* Yao & Li, 2020 **6** *B. parallelica* Zhang & Peng, 2011 **7** *B. tianlinensis* Zhang & Peng, 2011 **8** *B. tianyang* sp. nov. **9** *B. tongle* Zhang, Chen & Zhu, 2008 **10** *B. xuanguan* Yao & Li, 2020 **11** *B. zhangi* Tong & Li, 2007.

Table 1. A list of all *Belisana* species from Guangxi, China.

Species	Habitat	Reference
B. colubrina Zhang & Peng, 2011	/	Zhang and Peng (2011)
B. guilin Yao & Li, 2020	karst cave	Zhu et al. (2020a)
B. langping sp. nov.	karst cave	this paper
B. lingui sp. nov.	karst cave	this paper
B. naling Yao & Li, 2020	karst cave	Zhu et al. (2020a)
B. parallelica Zhang & Peng, 2011	/	Zhang and Peng (2011)
B. tianlinensis Zhang & Peng, 2011	/	Zhang and Peng (2011)
B. tianyang sp. nov.	karst cave	this paper
B. tongle Zhang, Chen & Zhu, 2008	karst cave	Zhang et al. (2008)
B. xuanguan Yao & Li, 2020	karst cave	Zhu et al. (2020a)
B. zhangi Tong & Li, 2007	karst cave	Tong and Li (2007)

Materials and methods

Specimens were examined and measured with a Leica M205 C stereomicroscope. Left male palps were photographed. Epigynes were photographed before dissection. Vulvae were photographed after treating them in a 10% warm solution of potassium hydroxide (KOH) to dissolve soft tissues. Images were captured with a Canon EOS 750D wide zoom digital camera (24.2 megapixels) mounted on the stereomicroscope mentioned above and assembled using Helicon Focus v.3.10.3 image stacking software (Khmelik et al. 2005). Drawings were done with Procreate v.5.0.2 (Savage Interactive Pty. Ltd.). All measurements are given in millimeters (mm). Leg measurements are shown as total length (femur, patella, tibia, metatarsus and tarsus). Leg segments were measured on their dorsal sides. The distribution map was generated with ArcGIS v. 10.2 (ESRI Inc.). The specimens studied are preserved in 75% ethanol and deposited in the Institute of Zoology, Chinese Academy of Sciences (**IZCAS**) in Beijing, China.

Terminology and taxonomic descriptions follow Huber (2005) and Yao et al. (2015). The following abbreviations are used in the descriptions: **ALE** = anterior lateral eye, **AME** = anterior median eye, **PME** = posterior median eye, **L/d** = length/diameter; used in the illustrations: **aa** = anterior arch, **b** = bulb, **ba** = bulbal apophysis, **da** = distal apophysis, **e** = embolus, **ep** = epigynal pocket, **f** = flap, **pa** = proximo-lateral apophysis, **pp** = pore plate, **pr** = procursus.

Taxonomy

Family Pholcidae C.L. Koch, 1850
Subfamily Pholcinae C.L. Koch, 1850

Genus *Belisana* Thorell, 1898

Type species. *Belisana tauricornis* Thorell, 1898.

Belisana langping Zhang, Li & Yao, sp. nov.

https://zoobank.org/ED94621E-E599-4452-9CD0-7EFB7C35B999

Figs 2, 3, 8A, B, 9A, B

Type material. ***Holotype:*** **China** • ♂; Guangxi, Baise, Tianlin County, Langping Town, Dabao Village, Sanchuantun, Papa Cave; 24°34.226'N, 106°13.675'E; alt. 773 m; 14 Aug. 2011; C Wang leg.; IZCAS-Ar44988. ***Paratypes:*** **China** • 4♀; same data as for holotype; IZCAS-Ar44989–92.

Etymology. The specific name refers to the type locality; noun in apposition.

Diagnosis. The new species resembles *B. phungae* Yao, Pham & Li, 2015 (Yao et al. 2015: 9, figs 19A–D, 20A–G, 21A–E) by having similar male chelicerae and epigyne (Fig. 3A, D), but can be distinguished by procursus with retrolatero-subdistal membranous lamella (arrow in Figs 2D, 8B vs. absent in *B. phungae*), by bulbal apophysis hooked (ba in Fig. 3C vs. distally blunt in *B. phungae*), by cheliceral proximo-lateral apophyses and distal apophyses closer to each other (Fig. 3D vs. widely separated in *B. phungae*), by vulva without sac-like structure (Figs 3B, 9B vs. present in *B. phungae*), and by pore plates nearly triangular (pp in Figs 3B, 9B vs. nearly round in *B. phungae*); also distinguished from *B. zhangi* Tong & Li, 2007 (Tong and Li 2007: 505, figs 1–6) by procursus with sclerotized prolatero-subdistal apophysis (arrow 1 in Figs 2C, 8A vs. spine in *B. zhangi*), prolatero-subdistal membranous lamella (arrow 2 in Figs 2C, 8A vs. absent in *B. zhangi*), and retrolatero-subdistal membranous lamella (arrow in Figs 2D, 8B vs. retrolatero-ventral in *B. zhangi*), by procursus without retrolateral membranous flap (Figs 2D, 8B vs. present in *B. zhangi*), by vulval anterior arch straight (aa in Figs 3B, 9B vs. ridge-shaped in *B. zhangi*), and by pore plates nearly triangular (pp in Figs 3B, 9B vs. long and curved in *B. zhangi*).

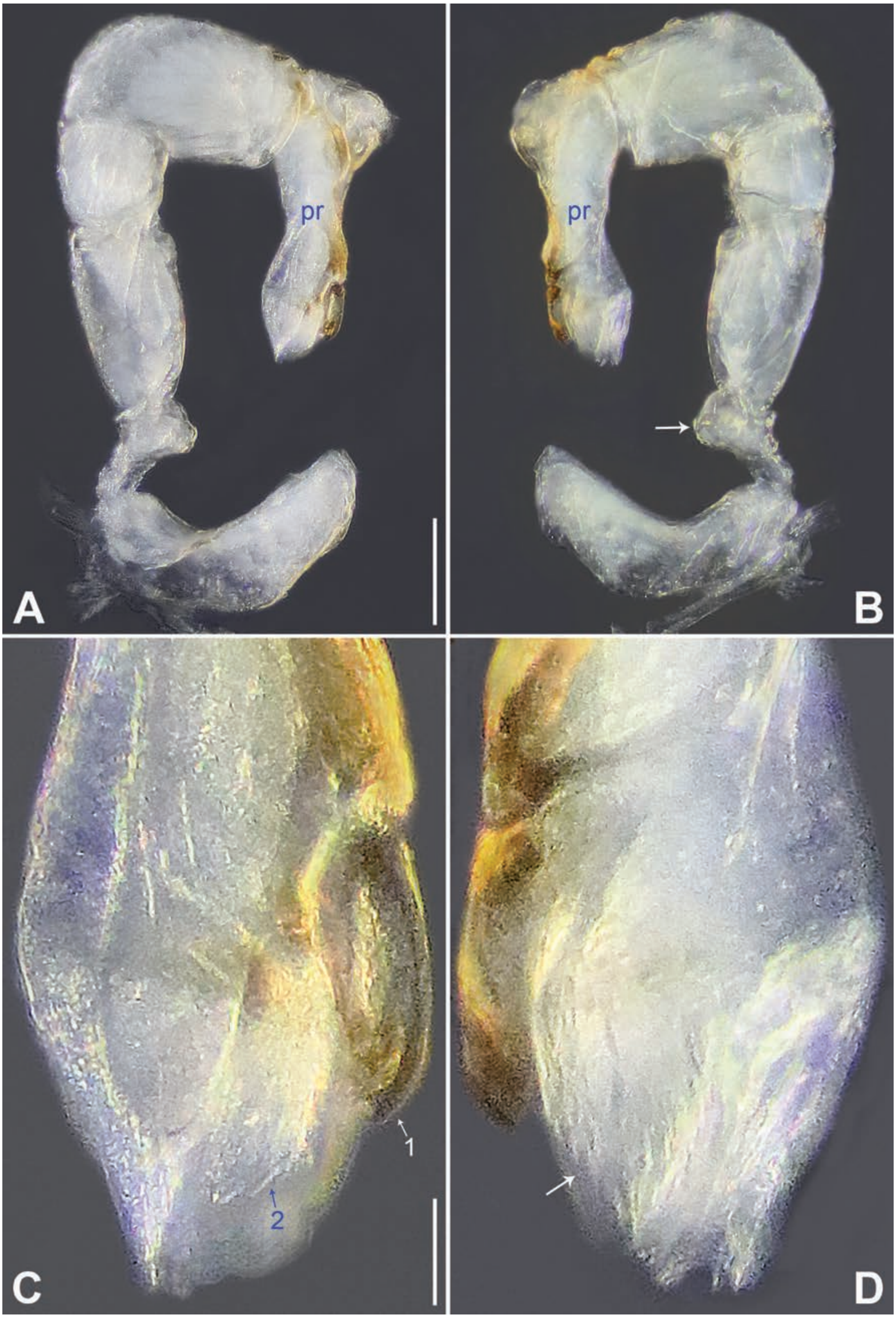

Figure 2. *Belisana langping* sp. nov., holotype male **A, B** palp (**A** prolateral view **B** retrolateral view, arrow points at ventral apophysis) **C, D** distal part of procursus (**C** prolateral view, arrow 1 points at prolatero-subdistal apophysis, arrow 2 points at prolatero-subdistal membranous lamella **D** retrolateral view, arrow points at retrolatero-subdistal membranous lamella). Abbreviation: pr = procursus. Scale bars: 0.10 mm (**A, B**); 0.02 mm (**C, D**).

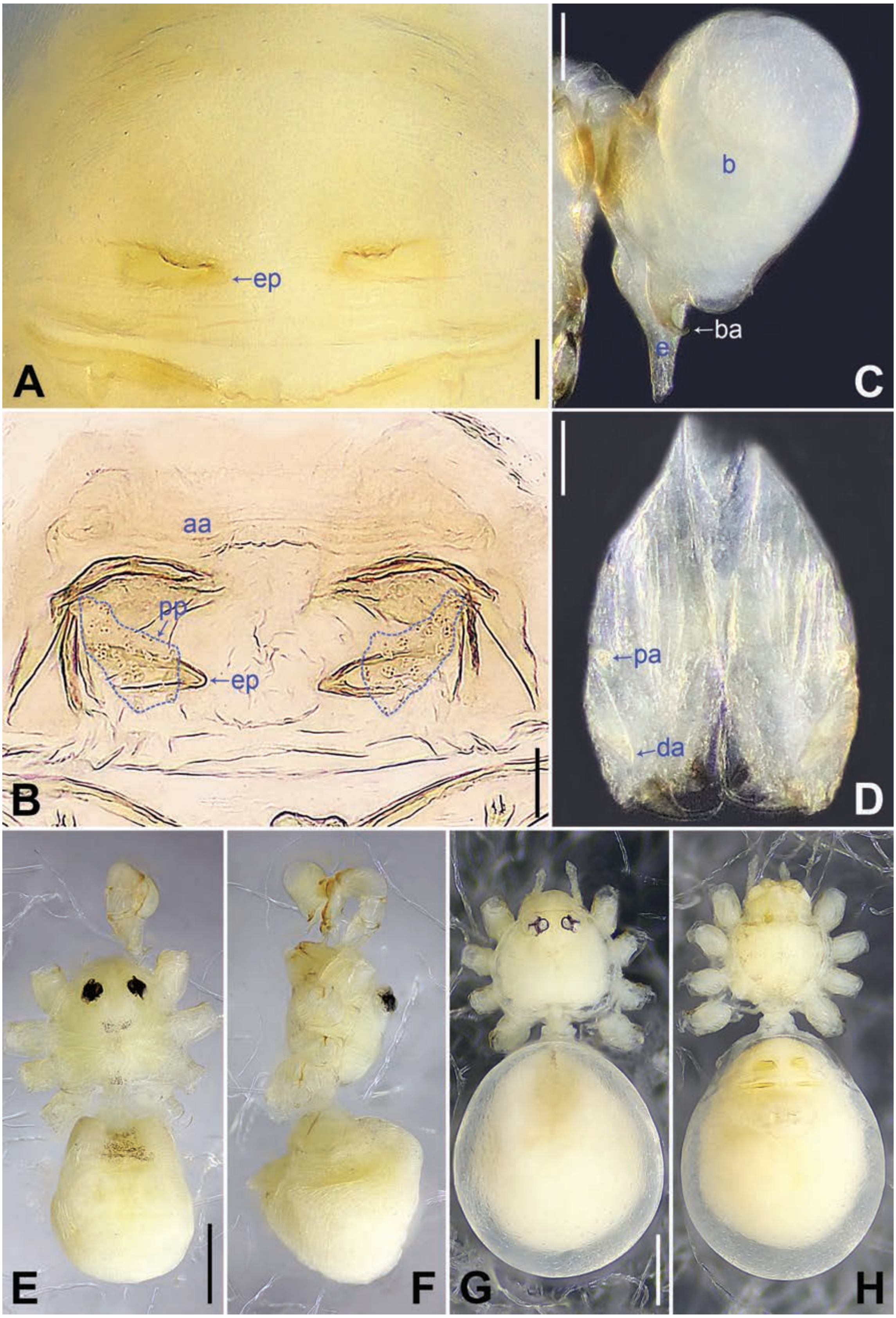

Figure 3. *Belisana langping* sp. nov., holotype male (**C–F**) and paratype female (**A, B, G, H**) **A** epigyne, ventral view **B** vulva, dorsal view **C** bulb, prolateral view **D** chelicerae, frontal view **E–H** habitus (**E, G** dorsal view **F** lateral view **H** ventral view). Abbreviations: aa = anterior arch, b = bulb, ba = bulbal apophysis, da = distal apophysis, e = embolus, ep = epigynal pocket, pa = proximo-lateral apophysis, pp = pore plate. Scale bars: 0.05 mm (**A–D**); 0.30 mm (**E–H**).

Description. Male (***holotype***): Total length 1.11 (1.20 with clypeus), prosoma 0.40 long, 0.53 wide, opisthosoma 0.71 long, 0.54 wide. Leg **I** missing, leg **II**: 4.88 (1.30, 0.20, 1.18, 1.62, 0.58), leg **III**: 3.92 (1.00, 0.19, 0.96, 1.27, 0.50), leg **IV**: 4.76 (1.27, 0.20, 1.17, 1.55, 0.57). Eye interdistances and diameters: PME–PME 0.10, PME 0.06, PME–ALE 0.02, AME absent. Sternum width/length: 0.43/0.33. Habitus as in Fig. 3E, F. Dorsal shield of prosoma yellowish, with indistinct median and posterior marks; sternum yellowish, with indistinct marginal marks. Legs whitish, without darker rings. Opisthosoma yellowish, without spots. Thoracic furrow absent. Clypeus unmodified. Chelicerae with pair of proximo-lateral apophyses (pa in Fig. 3D) and pair of distal apophyses (da in Fig. 3D; distance between tips: 0.11). Palp as in Fig. 2A, B; trochanter with ventral apophysis (arrow in Fig. 2B); procursus simple proximally but complex distally, with sclerotized prolatero-subdistal apophysis (arrow 1 in Figs 2C, 8A), prolatero-subdistal membranous lamella (arrow 2 in Figs 2C, 8A), and retrolatero-subdistal membranous lamella (arrow in Figs 2D, 8B); bulb with hooked apophysis (ba in Fig. 3C) and simple embolus (e in Fig. 3C).

Female (***paratype***, IZCAS-Ar44989): Similar to male, habitus as in Fig. 3G, H. Total length 1.57 (1.66 with clypeus), prosoma 0.43 long, 0.56 wide, opisthosoma 1.14 long, 0.90 wide. Leg **I**: 6.87 (1.86, 0.24, 1.78, 2.16, 0.83); tibia **I** L/d: 36. Eye interdistances and diameters: PME–PME 0.06, PME 0.05, PME–ALE 0.02, AME absent. Sternum width/length: 0.40/0.33. Epigyne simple and flat, with pair of median pockets 0.08 apart (ep in Figs 3A, 9A). Vulva with straight anterior arch (aa in Figs 3B, 9B) and pair of nearly triangular pore plates (pp in Figs 3B, 9B). Retrolateral trichobothria on tibia **I** at 5% proximally; legs with short vertical setae on metatarsi; tarsus **I** with 16 distinct pseudosegments.

Variation. Tibia **I** in other three female paratypes (IZCAS-Ar44990–92): 1.80, 1.93, 1.98.

Habitat. The species was found in the dark zone inside the cave.

Distribution. China (Guangxi, type locality; Fig. 1).

Belisana lingui Zhang, Li & Yao, sp. nov.

https://zoobank.org/1B082AB3-F3BF-4B1D-B26E-E6E90BA19883

Figs 4, 5, 8C, D, 9C, D

Type material. ***Holotype:*** **China** • ♂; Guangxi, Guilin, Lingui County, Yanmendi Village, Shuixianyan Cave; 25°12.819'N, 110°12.050'E; alt. 161 m; 18 Jul. 2009; Z Yao leg.; IZCAS-Ar44993. ***Paratypes:*** **China** • 3♀; same data as for holotype; IZCAS-Ar44994–96.

Etymology. The specific name refers to the type locality; noun in apposition.

Diagnosis. The new species resembles *B. galeiformis* Zhang & Peng, 2011 (Zhang and Peng 2011: 52, fig. 1A–F) by having similar bulbal apophyses and male chelicerae (Fig. 5C, D), but can be distinguished by procursus without prolatero-subdistal sclerite (Figs 4C, 8C vs. present in *B. galeiformis*), by epigyne with posterior pockets (ep in Figs 5A, 9C vs. median in *B. galeiformis*), by pore plates anteriorly narrow and posteriorly wide (pp in Figs 5B, 9D vs. elliptic in *B. galeiformis*), and by dorsal shield of prosoma without marks (Fig. 5E, G vs. with radiating marks in *B. galeiformis*); also distinguished from *B. tongle* Zhang, Chen & Zhu, 2008 (Zhang et al. 2008: 654, figs 1–5) by procursus without prolatero-subdistal sclerite and ventro-subdistal apophysis (Figs 4C, 8C vs. present in *B. tongle*).

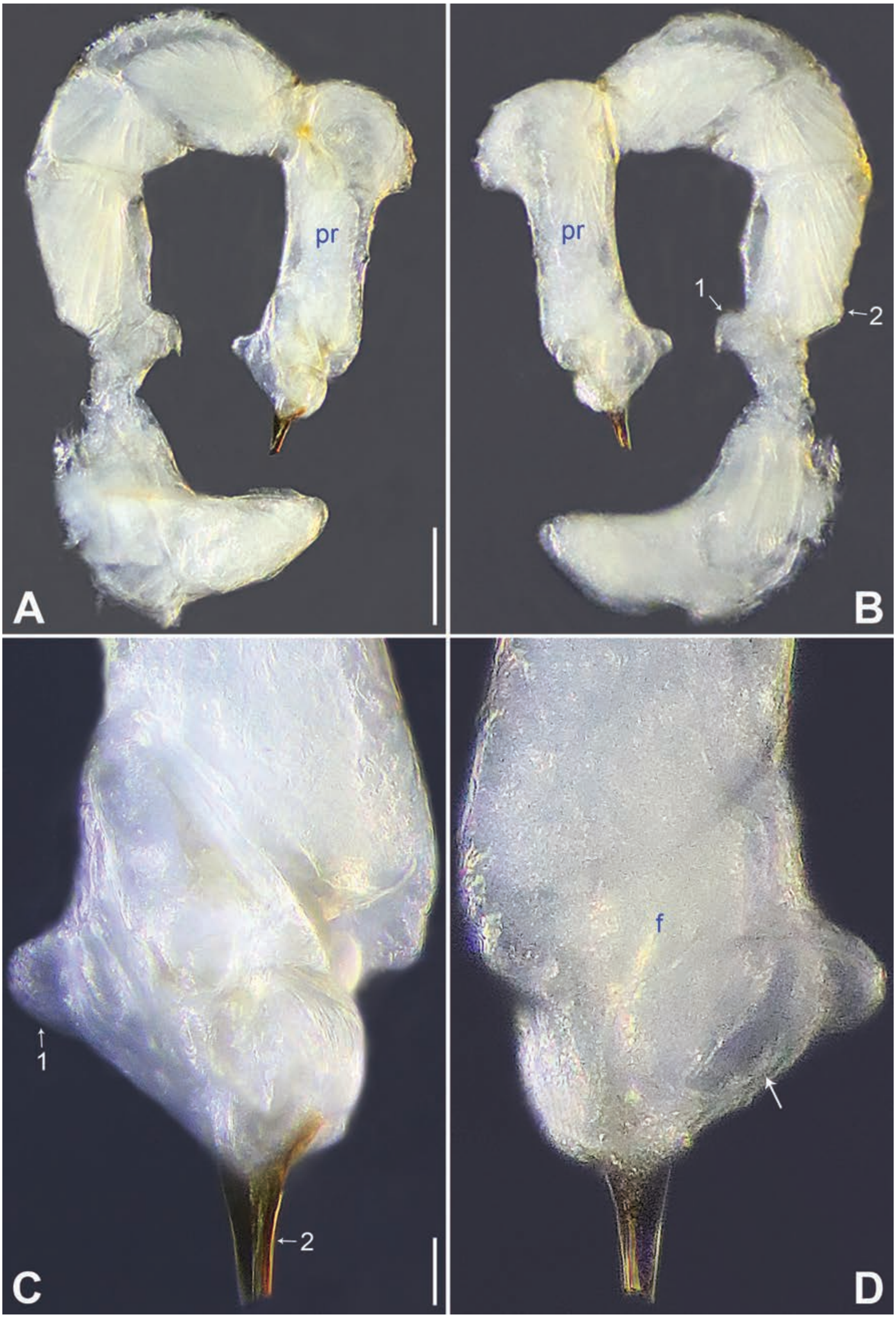

Figure 4. *Belisana lingui* sp. nov., holotype male **A, B** palp (**A** prolateral view **B** retrolateral view, arrow 1 points at ventral apophysis, arrow 2 points at retrolatero-proximal protrusion) **C, D** distal part of procursus (**C** prolateral view, arrow 1 points at ventro-subdistal membranous lamella, arrow 2 points at distal apophysis **D** retrolateral view, arrow points at retrolatero-subdistal membranous lamella). Abbreviations: f = flap, pr = procursus. Scale bars: 0.10 mm (**A, B**); 0.02 mm (**C, D**).

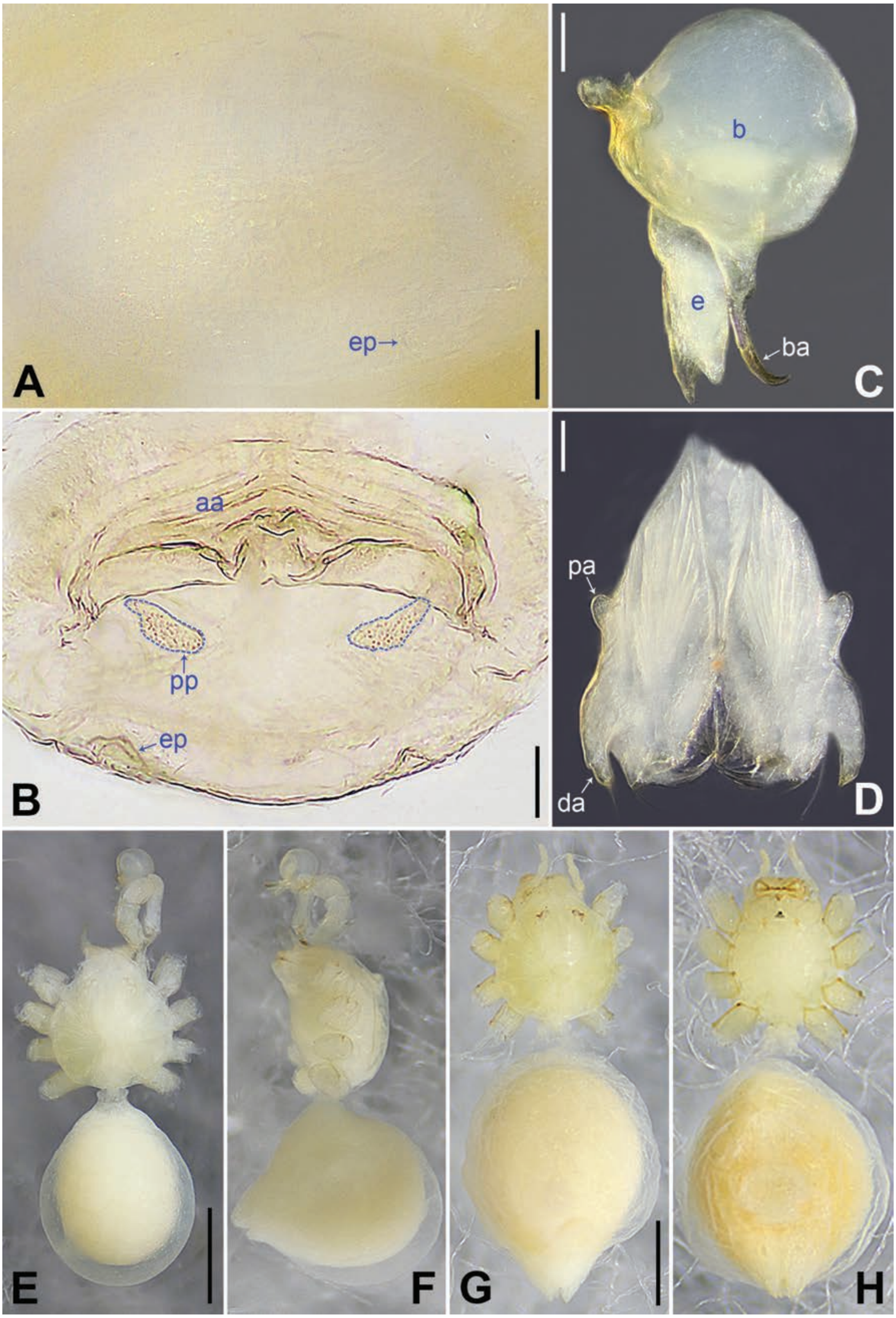

Figure 5. *Belisana lingui* sp. nov., holotype male (**C–F**) and paratype female (**A, B, G, H**) **A** epigyne, ventral view **B** vulva, dorsal view **C** bulb, prolateral view **D** chelicerae, frontal view **E–H** habitus (**E, G** dorsal view **F** lateral view **H** ventral view). Abbreviations: aa = anterior arch, b = bulb, ba = bulbal apophysis, da = distal apophysis, e = embolus, ep = epigynal pocket, pa = proximo-lateral apophysis, pp = pore plate. Scale bars: 0.05 mm (**A–D**); 0.30 mm (**E–H**).

Description. Male (*holotype*): Total length 1.51 (1.59 with clypeus), prosoma 0.56 long, 0.59 wide, opisthosoma 0.95 long, 0.84 wide. Leg I: 20.66 (5.26, 0.33, 5.19, 7.98, 1.90), leg II: 14.16 (3.88, 0.33, 3.64, 5.00, 1.31), leg III: – (2.53, 0.30, 2.25, 3.00, –), leg IV: 11.97 (3.60, 0.30, 3.23, 3.76, 1.08); tibia I L/d: 80. Eye interdistances and diameters: PME–PME 0.12, PME 0.05, PME–ALE 0.02, AME absent. Sternum width/length: 0.49/0.44. Habitus as in Fig. 5E, F. Dorsal shield of prosoma and sternum yellowish, without marks. Legs whitish, without darker rings. Opisthosoma yellowish, without spots. Thoracic furrow absent. Clypeus unmodified. Eyes without pigments, but apparently with small lenses. Chelicerae with pair of proximo-lateral apophyses (pa in Fig. 5D) and pair of distal apophyses (da in Fig. 5D; distance between tips: 0.22). Palp as in Fig. 4A, B; trochanter with ventral apophysis (arrow 1 in Fig. 4B); femur with small retrolatero-proximal protrusion (arrow 2 in Fig. 4B); procursus simple proximally but complex distally, with ventro-subdistal membranous lamella (arrow 1 in Figs 4C, 8C), spine-shaped distal apophysis (tip broken; arrow 2 in Figs 4C, 8C), retrolatero-subdistal membranous lamella (arrow in Figs 4D, 8D), and retrolateral membranous flap (f in Figs 4D, 8D); bulb with hooked apophysis (ba in Fig. 5C) and simple embolus (e in Fig. 5C). Retrolateral trichobothria on tibia I at 4% proximally; legs with short vertical setae on metatarsi; tarsus I with 17 distinct pseudosegments.

Female (*paratype*, IZCAS-Ar44994): Similar to male, habitus as in Fig. 5G, H. Total length 2.00 (2.09 with clypeus), prosoma 0.58 long, 0.63 wide, opisthosoma 1.42 long, 1.01 wide; tibia I: 2.34; tibia I L/d: 39. Eye interdistances and diameters: PME–PME 0.11, PME 0.04, PME–ALE 0.02, AME absent. Sternum width/length: 0.50/0.44. Epigyne simple and flat, with pair of posterior pockets 0.20 apart (ep in Figs 5A, 9C). Vulva with ridge-shaped anterior arch (aa in Figs 5B, 9D) and pair of anteriorly narrow and posteriorly wide pore plates (pp in Figs 5B, 9D).

Variation. Tibia I in the other two female paratypes (IZCAS-Ar44995–96): 2.34, 2.41.

Habitat. The species was found in the dark zone inside the cave.

Distribution. China (Guangxi, type locality; Fig. 1).

Belisana tianyang Zhang, Li & Yao, sp. nov.

https://zoobank.org/4D5E7BF7-2704-4467-9EE5-056C1FFE1D33

Figs 6, 7, 8E, F, 9E, F

Type material. ***Holotype:*** **China** • ♂; Guangxi, Baise, Tianyang County, Dongjing Town, Liangdongyan Cave; 23°40.123'N, 106°33.956'E; alt. 467 m; 7 Aug. 2011; C Wang leg.; IZCAS-Ar44997. ***Paratypes:*** **China** • 3♂; same data as for holotype; IZCAS-Ar44998–45000 • 2♀; same data as for holotype; IZCAS-Ar45001–02.

Etymology. The specific name refers to the type locality; noun in apposition.

Diagnosis. The new species resembles *B. tianlinensis* Zhang & Peng, 2011 (Zhang and Peng 2011: 65, fig. 10A–G) by having similar bulbal apophyses and epigyne (Fig. 7A, C), but can be distinguished by retrolateral flap of procursus strongly curved and wide (4 times wider than long, f in Figs 6D, 8F vs. straight and 2 times wider than long in *B. tianlinensis*), by male cheliceral distal apophyses long (6 times longer than wide) and tips widely separated (da in Fig. 7D vs. 2 times longer than wide and tips closer to each other in *B. tianlinensis*), by pore plates curved, anteriorly pointed and posteriorly wide (pp in Figs 7B, 9F

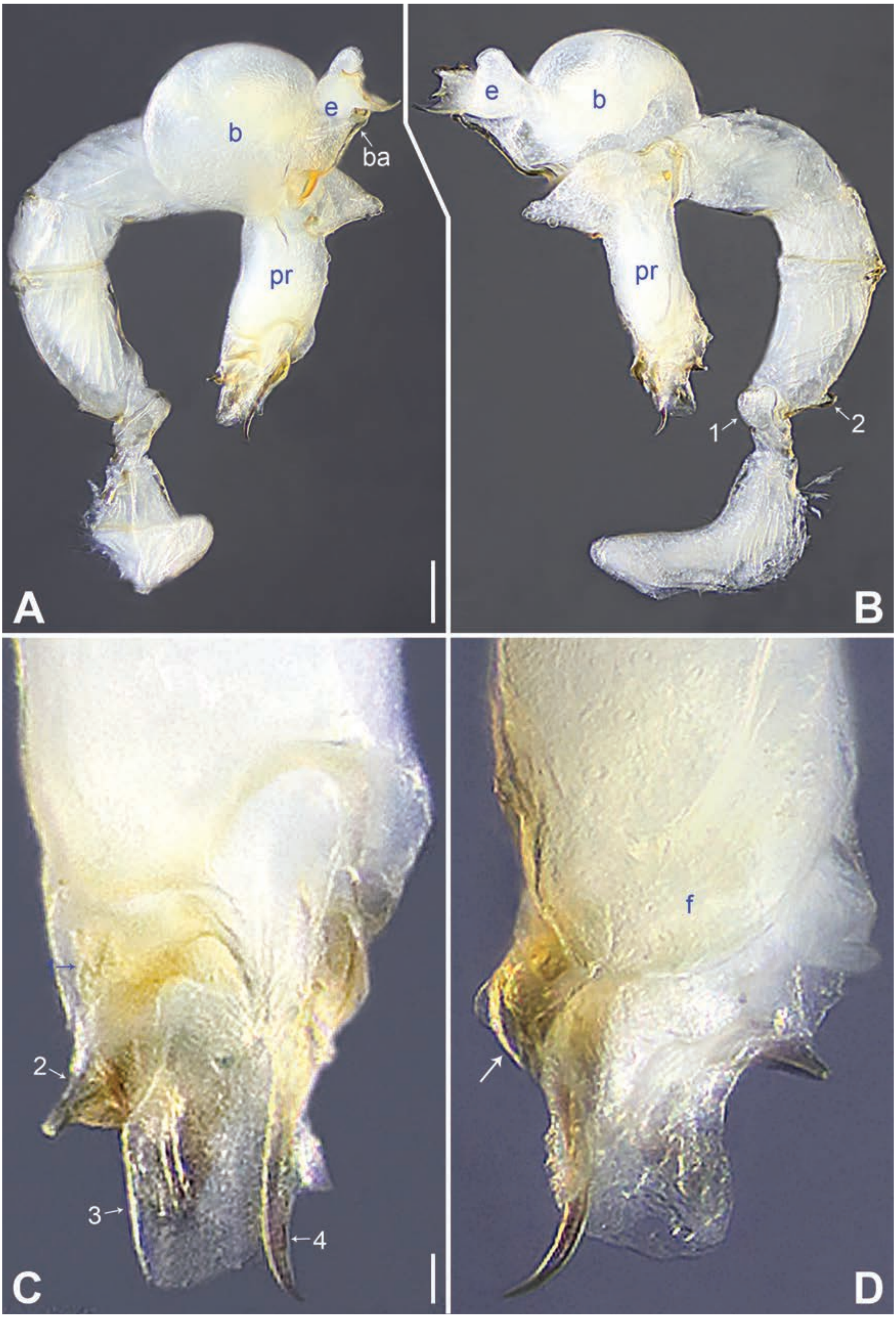

Figure 6. *Belisana tianyang* sp. nov., holotype male **A, B** palp (**A** prolateral view **B** retrolateral view, arrow 1 points at ventral apophysis, arrow 2 points at retrolatero-proximal protrusion) **C, D** distal part of procursus (**C** prolateral view, arrow 1 points at prolatero-subdistal sclerite, arrow 2 points at prolatero-ventral lamella, arrow 3 points at distal membranous lamella, arrow 4 points at distal spine **D** retrolateral view, arrow points at dorso-subdistal apophysis). Abbreviations: b = bulb, ba = bulbal apophysis, e = embolus, f = flap, pr = procursus. Scale bars: 0.10 mm (**A, B**); 0.02 mm (**C, D**).

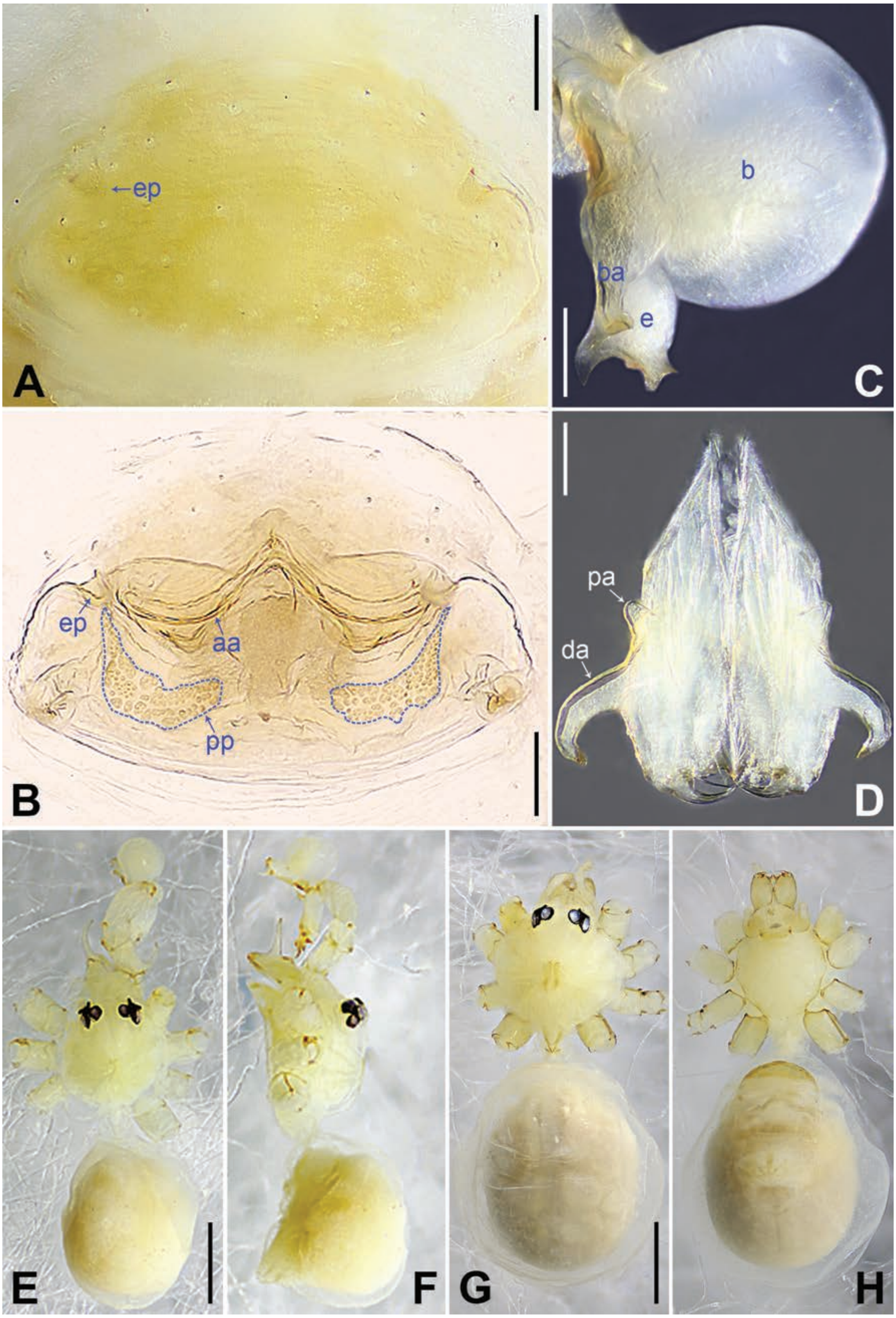

Figure 7. *Belisana tianyang* sp. nov., holotype male (**C–F**) and paratype female (**A, B, G, H**) **A** epigyne, ventral view **B** vulva, dorsal view **C** bulb, prolateral view **D** chelicerae, frontal view **E–H** habitus (**E, G** dorsal view **F** lateral view **H** ventral view). Abbreviations: aa = anterior arch, b = bulb, ba = bulbal apophysis, da = distal apophysis, e = embolus, ep = epigynal pocket, pa = proximo-lateral apophysis, pp = pore plate. Scale bars: 0.10 mm (**A–D**); 0.50 mm (**E–H**).

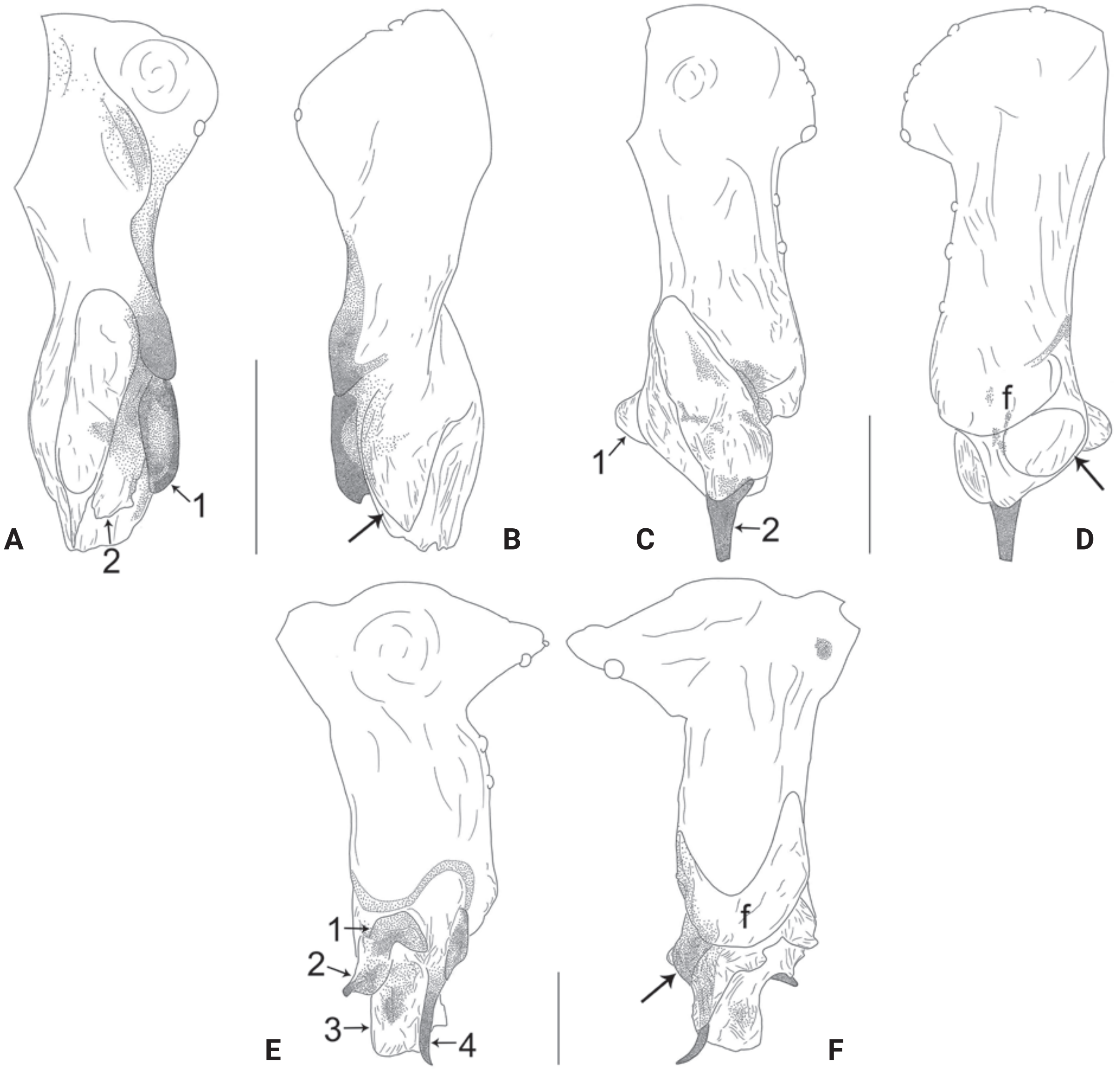

Figure 8. Procursus in prolateral and retrolateral views (arrows point at same structures as photos of each species) **A, B** *Belisana langping* sp. nov. **C, D** *B. lingui* sp. nov. **E, F** *B. tianyang* sp. nov. Abbreviation: f = flap. Scale bars: 0.10 mm.

vs. nearly triangular in *B. tianlinensis*), and by male clypeus unmodified (Fig. 7E vs. with pointed frontal apophysis in *B. tianlinensis*); also distinguished from *B. douqing* Chen, Zhang & Zhu, 2009 (Chen et al. 2009: 59, figs 1–11) by procursus with rectangular distal membranous lamella (arrow 3 in Figs 6C, 8E vs. nearly square in *B. douqing*) and curved retrolateral membranous flap (f in Figs 6D, 8F vs. angular in *B. douqing*) and by pore plates curved, anteriorly pointed and posteriorly wide (pp in Figs 7B, 9F vs. long elliptic in *B. douqing*).

Description. Male (***holotype***): Total length 1.98 (2.08 with clypeus), prosoma 0.74 long, 0.75 wide, opisthosoma 1.24 long, 0.89 wide. Leg **I**: 21.95 (5.51, 0.33, 5.44, 9.17, 1.50), leg **II** missing, leg **III**: 8.82 (2.44, 0.27, 2.25, 3.13, 0.73), leg **IV**: 12.12 (3.60, 0.28, 3.04, 4.45, 0.75); tibia **I** L/d: 68. Eye interdistances and diameters: PME–PME 0.10, PME 0.08, PME–ALE 0.02, AME absent. Sternum width/length: 0.58/0.56. Habitus as in Fig. 7E, F. Dorsal shield of prosoma yellowish, with indistinct median stripe; sternum yellowish, without marks. Legs whitish, without darker rings. Opisthosoma yellowish, without spots. Thoracic furrow absent. Clypeus

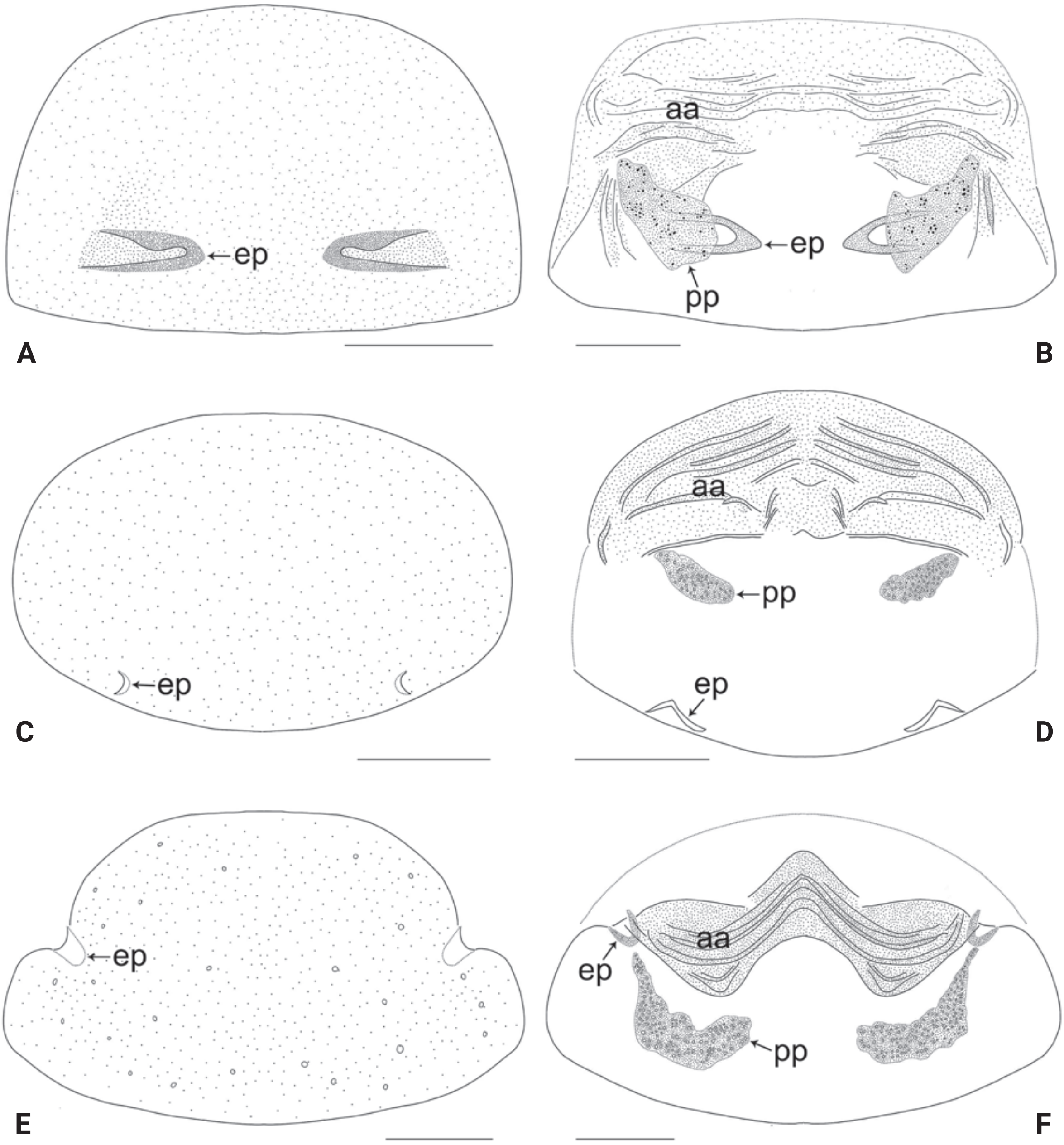

Figure 9. Female genitalia in ventral and dorsal views **A, B** *Belisana langping* sp. nov. **C, D** *B. lingui* sp. nov. **E, F** *B. tianyang* sp. nov. Abbreviations: aa = anterior arch, ep = epigynal pocket, pp = pore plate. Scale bars: 0.10 mm.

unmodified. Chelicerae with pair of proximo-lateral apophyses (pa in Fig. 7D) and pair of distal apophyses (da in Fig. 7D; distance between tips: 0.36). Palp as in Fig. 6A, B; trochanter with ventral apophysis (arrow 1 in Fig. 6B); femur with small retrolatero-proximal protrusion (arrow 2 in Fig. 6B); procursus simple proximally but complex distally, with prolatero-subdistal sclerite (arrow 1 in Figs 6C, 8E), sclerotized prolatero-ventral lamella (arrow 2 in Figs 6C, 8E), distal membranous lamella (arrow 3 in Figs 6C, 8E), curved distal spine (arrow 4 in Figs 6C, 8E), sclerotized dorso-subdistal apophysis (arrow in Figs 6D, 8F), and retrolateral membranous flap (f in Figs 6D, 8F); bulb with hooked apophysis (ba in Fig. 7C) and simple embolus (e in Fig. 7C). Retrolateral trichobothria on tibia I at 5% proximally; legs with short vertical setae on metatarsi; tarsus I with 19 distinct pseudosegments.

Female (***paratype***, IZCAS-Ar45001): Similar to male, habitus as in Fig. 7G, H. Total length 2.14 (2.27 with clypeus), prosoma 0.70 long, 0.79 wide, opisthosoma 1.44 long, 1.32 wide; tibia I: 4.15; tibia I L/d: 52. Eye interdistances and diameters: PME–PME 0.10, PME 0.08, PME–ALE 0.02, AME absent. Sternum width/length: 0.55/0.54. Epigyne simple and flat, with pair of lateral pockets 0.36 apart (ep in Figs 7A, 9E). Vulva with ridge-shaped anterior arch (aa in Figs 7B, 9F) and pair of curved, anteriorly pointed and posteriorly wide pore plates (pp in Figs 7B, 9F).

Variation. Tibia I in three male paratypes (IZCAS-Ar44998–45000): 5.38, 5.64, 5.77. Tibia I in another female paratype (IZCAS-Ar45002) missing.

Habitat. The species was found in the dark zone inside the cave.

Distribution. China (Guangxi, type locality; Fig. 1).

Acknowledgements

The manuscript benefited greatly from comments by Francesco Ballarin, Bernhard Huber, and Jie Liu.

Additional information

Conflict of interest

The authors have declared that no competing interests exist.

Ethical statement

No ethical statement was reported.

Funding

This study was supported by the National Natural Science Foundation of China (NSFC-32170461, 31872193).

Author contributions

ZY and XZ designed the study. LZ, SL, and ZY performed morphological species identification. LZ and YW finished the descriptions and took the photos and drawings. ZY, XZ, SL, and LZ drafted and revised the manuscript.

Author ORCIDs

Ludan Zhang https://orcid.org/0000-0001-5657-751X
Shuqiang Li https://orcid.org/0000-0002-3290-5416
Zhiyuan Yao https://orcid.org/0000-0002-1631-0949

Data availability

All of the data that support the findings of this study are available in the main text.

References

Chen H, Zhang F, Zhu M (2009) Four new troglophilous species of the genus *Belisana* Thorell, 1898 (Araneae, Pholcidae) from Guizhou Province, China. Zootaxa 2092(1): 58–68. https://doi.org/10.11646/zootaxa.2092.1.5

Huber BA (2005) High species diversity, male-female coevolution, and metaphyly in Southeast Asian pholcid spiders: The case of *Belisana* Thorell 1898 (Araneae, Pholcidae). Zoologica 155: 1–126.

Khmelik VV, Kozub D, Glazunov A (2005) Helicon Focus 3.10.3. https://www.heliconsoft.com/heliconsoft-products/helicon-focus/ [Accessed 14 April 2024]

Lu Y, Chu C, Zhang X, Li S, Yao Z (2022) Europe vs. China: *Pholcus* (Araneae, Pholcidae) from Yanshan-Taihang Mountains confirms uneven distribution of spiders in Eurasia. Zoological Research 43(4): 532–534 [& Suppl. 1–78]. https://doi.org/10.24272/j.issn.2095-8137.2022.103

Tong Y, Li S (2007) A new six-eyed pholcid spider (Araneae, Pholcidae) from Karst Tiankeng of Leye County, Guangxi, China. Acta Zootaxonomica Sinica 32: 505–507.

Wang B, Yao Z, Zhang X (2024) A new spider species of *Belisana* Thorell, 1898 (Araneae, Pholcidae) from Guizhou Province, south-western China. Biodiversity Data Journal 12: e125111 [1–7]. https://doi.org/10.3897/BDJ.12.e125111

WSC (2024) World Spider Catalog, Version 25.0. Natural History Museum Bern. https://wsc.nmbe.ch [Accessed 14 April 2024]

Yang L, Zhao F, He Q, Yao Z (2023) A survey of pholcid spiders (Araneae, Pholcidae) from Guiyang, Guizhou Province, China. ZooKeys 1186: 175–184. https://doi.org/10.3897/zookeys.1186.105736

Yang L, Fu C, Zhang Y, He Q, Yao Z (2024a) A survey of *Pholcus* spiders (Araneae, Pholcidae) from the Qinling Mountains of central China, with descriptions of seven new species. Zoosystematics and Evolution 100(1): 199–221. https://doi.org/10.3897/zse.100.116759

Yang L, He Q, Yao Z (2024b) Taxonomic study of four closely-related species of the *Pholcus yichengicus* species group (Araneae, Pholcidae) from China's Qinling Mountains: An integrated morphological and molecular approach. Zoosystematics and Evolution 100(1): 279–289. https://doi.org/10.3897/zse.100.115633

Yao Z, Tavano M, Li S (2013) Notes on four pholcid spiders (Araneae: Pholcidae) described by T. Thorell from Southeast Asia. Zootaxa 3609(3): 302–310. https://doi.org/10.11646/zootaxa.3609.3.4

Yao Z, Pham DS, Li S (2015) Pholcid spiders (Araneae: Pholcidae) from northern Vietnam, with descriptions of nineteen new species. Zootaxa 3909(1): 1–82. https://doi.org/10.11646/zootaxa.3909.1.1

Yao Z, Zhu K, Du Z, Li S (2018) The *Belisana* spiders (Araneae: Pholcidae) from Xishuangbanna Tropical Botanical Garden, Yunnan, China. Zootaxa 4425(2): 243–262. https://doi.org/10.11646/zootaxa.4425.2.3

Yao Z, Wang X, Li S (2021) Tip of the iceberg: species diversity of *Pholcus* spiders (Araneae, Pholcidae) in the Changbai Mountains, Northeast China. Zoological Research 42(3): 267–271 [& Suppl. 1–60]. https://doi.org/10.24272/j.issn.2095-8137.2021.037

Zhang F, Peng Y (2011) Eleven new species of the genus *Belisana* Thorell (Araneae: Pholcidae) from South China. Zootaxa 2989(1): 51–68. https://doi.org/10.11646/zootaxa.2989.1.2

Zhang Y, Chen H, Zhu M (2008) A new troglophilous *Belisana* spider from Guangxi, China (Araneae, Pholcidae). Acta Zootaxonomica Sinica 33: 654–656.

Zhang L, Wu Z, Li S, Yao Z (2024) Eight new spider species of *Belisana* Thorell, 1898 (Araneae, Pholcidae), with an updated overview of *Belisana* species from Yunnan, China. ZooKeys 1202: 255–286. https://doi.org/10.3897/zookeys.1202.121633

Zhao F, Yang L, Li S, Zheng G, Yao Z (2023a) A further study on the *Belisana* spiders (Araneae: Pholcidae) from Xishuangbanna, Yunnan, China. Zootaxa 5351(5): 543–558. https://doi.org/10.11646/zootaxa.5351.5.3

Zhao F, Yang L, Zou Q, Ali A, Li S, Yao Z (2023b) Diversity of *Pholcus* spiders (Araneae: Pholcidae) in China's Lüliang Mountains: an integrated morphological and molecular approach. Insects 14(4): 364 [1–34]. https://doi.org/10.3390/insects14040364

Zhu W, Li S (2021) Six new species of the spider genus *Belisana* (Araneae: Pholcidae) from Southeast Asia. Zootaxa 4963(1): 115–137. https://doi.org/10.11646/zootaxa.4963.1.5

Zhu W, Yao Z, Zheng G, Li S (2020a) Six new species of the spider genus *Belisana* Thorell, 1898 (Araneae: Pholcidae) from southern China. Zootaxa 4810(1): 175–197. https://doi.org/10.11646/zootaxa.4810.1.12

Zhu W, Yao Z, Zheng G, Li S (2020b) The *Belisana* spiders (Araneae: Pholcidae) from Tibet, China. Zootaxa 4802(1): 111–128. https://doi.org/10.11646/zootaxa.4802.1.7

ZooKeys 1209: 331–332 (2024)
DOI: 10.3897/zookeys.1209.130464

Corrigendum

Corrigendum: Addendum to the Acknowledgements: Jirapatrasilp P, Huang C-W, Sutcharit C, Lee C-T (2024) The arboreal snail genus *Amphidromus* Albers, 1850 (Eupulmonata, Camaenidae) of Southeast Asia: 1. Molecular systematics of some Vietnamese species and related species from Cambodia, Indonesia, and Laos. ZooKeys 1196: 15–78. doi: 10.3897/zookeys.1196.112146

Parin Jirapatrasilp[1,2], Chih-Wei Huang[3], Chirasak Sutcharit[1], Chi-Tse Lee[4]

1 *Animal Systematics Research Unit, Department of Biology, Faculty of Science, Chulalongkorn University, Bangkok, Thailand*
2 *Leibniz Institute for the Analysis of Biodiversity Change, Zoological Museum, Martin-Luther-King-Platz 3, Hamburg, Germany*
3 *School of Life Science, National Taiwan Normal University, Taipei, Taiwan*
4 *Department of Life Sciences, National Chung Hsing University, Taichung, Taiwan*
Corresponding authors: Chirasak Sutcharit (jirasak4@yahoo.com, chirasak.s@chula.ac.th); Chi-Tse Lee (leechitse@yahoo.com.tw)

Academic editor: Thierry Backeljau
Received: 25 June 2024
Accepted: 4 July 2024
Published: 14 August 2024

ZooBank: https://zoobank.org/62BCACBC-008F-4780-BB0C-50F26192D845

Citation: Jirapatrasilp P, Huang C-W, Sutcharit C, Lee C-T (2024) Corrigendum: Addendum to the Acknowledgements: Jirapatrasilp P, Huang C-W, Sutcharit C, Lee C-T (2024) The arboreal snail genus *Amphidromus* Albers, 1850 (Eupulmonata, Camaenidae) of Southeast Asia: 1. Molecular systematics of some Vietnamese species and related species from Cambodia, Indonesia, and Laos. ZooKeys 1196: 15–78. doi: 10.3897/zookeys.1196.112146. ZooKeys 1209: 331–332. https://doi.org/10.3897/zookeys.1209.130464

The authors of "The arboreal snail genus *Amphidromus* Albers, 1850 (Eupulmonata, Camaenidae) of Southeast Asia: 1. Molecular systematics of some Vietnamese species and related species from Cambodia, Indonesia, and Laos" missed an acknowledgement to important contributors who collected specimens for this study, and credits to images of living *Amphidromus* specimens in Figure 6. The authors therefore wish to add the following sentence to the Acknowledgements:

We thank Truong Khoa Nguyen, Minh Tuan Nguyen, Ngoc Anh Pham, and K. Vuong for assistance in specimen collection.

The authors also wish to add the credits in the caption of Figure 6 as follows:

Credits: N. A. Pham (**A, C, E–G**), M. T. Nguyen (**B, H**), T. K. Nguyen (**D, I–J**).

We apologize for the previous omission of these important contributors in the Acknowledgements section and the credits in the figure caption.

Additional information

Conflict of interest

The authors have declared that no competing interests exist.

Ethical statement

No ethical statement was reported.

Funding

National Research Council of Thailand and Thailand Research Fund.

Author contributions

Writing - original draft: PJ. Writing - review and editing: CS, CWH, CTL.

Author ORCIDs

Parin Jirapatrasilp https://orcid.org/0000-0002-5591-6724
Chih-Wei Huang https://orcid.org/0000-0002-2921-4294
Chirasak Sutcharit https://orcid.org/0000-0001-7670-9540
Chi-Tse Lee https://orcid.org/0000-0003-2695-0680

Data availability

All of the data that support the findings of this study are available in the main text.